PERSONALIZATION IN MODERN RADIATION ONCOLOGY: PREDICTIONS, PROGNOSIS AND SURVIVAL

EDITED BY: Francesco Cellini, Nicola Silvestris, Felipe A. Calvo, Konstantinos Kamposioras and Milly Buwenge

PUBLISHED IN: Frontiers in Oncology

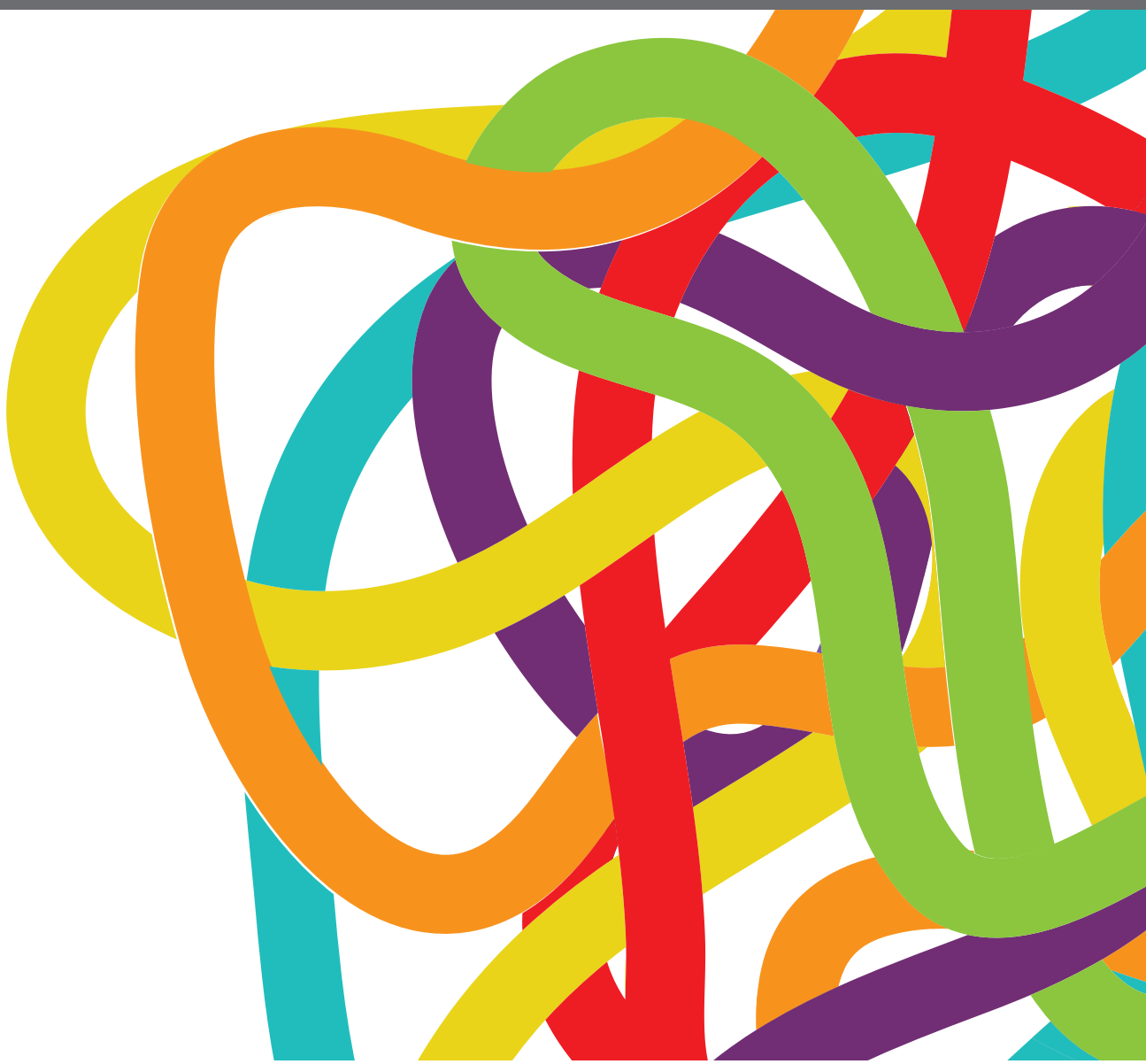

frontiers Research Topics

frontiers

ISSN 1664-8714
ISBN 978-2-83250-823-7
DOI 10.3389/978-2-83250-823-7

About Frontiers

Frontiers is more than just an open-access publisher of scholarly articles: it is a pioneering approach to the world of academia, radically improving the way scholarly research is managed. The grand vision of Frontiers is a world where all people have an equal opportunity to seek, share and generate knowledge. Frontiers provides immediate and permanent online open access to all its publications, but this alone is not enough to realize our grand goals.

Frontiers Journal Series

The Frontiers Journal Series is a multi-tier and interdisciplinary set of open-access, online journals, promising a paradigm shift from the current review, selection and dissemination processes in academic publishing. All Frontiers journals are driven by researchers for researchers; therefore, they constitute a service to the scholarly community. At the same time, the Frontiers Journal Series operates on a revolutionary invention, the tiered publishing system, initially addressing specific communities of scholars, and gradually climbing up to broader public understanding, thus serving the interests of the lay society, too.

Dedication to Quality

Each Frontiers article is a landmark of the highest quality, thanks to genuinely collaborative interactions between authors and review editors, who include some of the world's best academicians. Research must be certified by peers before entering a stream of knowledge that may eventually reach the public - and shape society; therefore, Frontiers only applies the most rigorous and unbiased reviews.
Frontiers revolutionizes research publishing by freely delivering the most outstanding research, evaluated with no bias from both the academic and social point of view. By applying the most advanced information technologies, Frontiers is catapulting scholarly publishing into a new generation.

What are Frontiers Research Topics?

Frontiers Research Topics are very popular trademarks of the Frontiers Journals Series: they are collections of at least ten articles, all centered on a particular subject. With their unique mix of varied contributions from Original Research to Review Articles, Frontiers Research Topics unify the most influential researchers, the latest key findings and historical advances in a hot research area! Find out more on how to host your own Frontiers Research Topic or contribute to one as an author by contacting the Frontiers Editorial Office: frontiersin.org/about/contact

PERSONALIZATION IN MODERN RADIATION ONCOLOGY: PREDICTIONS, PROGNOSIS AND SURVIVAL

Topic Editors:
Francesco Cellini, Università Cattolica del Sacro Cuore, Italy
Nicola Silvestris, University of Messina, Italy
Felipe A. Calvo, Gregorio Marañón Hospital, Spain
Konstantinos Kamposioras, Christie Hospital NHS Foundation Trust, United Kingdom
Milly Buwenge, University of Bologna, Italy

Citation: Cellini, F., Silvestris, N., Calvo, F. A., Kamposioras, K., Buwenge, M., eds. (2022). Personalization in Modern Radiation Oncology: Predictions, Prognosis and Survival. Lausanne: Frontiers Media SA. doi: 10.3389/978-2-83250-823-7

Table of Contents

frontiers in Oncology

REVIEW
published: 24 April 2020
doi: 10.3389/fonc.2020.00628

Precision Medicine and the Role of Biomarkers of Radiotherapy Response in Breast Cancer

James Meehan[1], Mark Gray[1,2], Carlos Martínez-Pérez[1,3], Charlene Kay[1], Lisa Y. Pang[2], Jennifer A. Fraser[4], Amy V. Poole[4], Ian H. Kunkler[5], Simon P. Langdon[5], David Argyle[2] and Arran K. Turnbull[1,3]*

[1] Translational Oncology Research Group, Institute of Genetics and Molecular Medicine, Western General Hospital, University of Edinburgh, Edinburgh, United Kingdom, [2] The Royal (Dick) School of Veterinary Studies and Roslin Institute, University of Edinburgh, Edinburgh, United Kingdom, [3] Breast Cancer Now Edinburgh Research Team, Institute of Genetics and Molecular Medicine, Western General Hospital, University of Edinburgh, Edinburgh, United Kingdom, [4] School of Applied Science, Sighthill Campus, Edinburgh Napier University, Edinburgh, United Kingdom, [5] Cancer Research UK Edinburgh Centre and Division of Pathology Laboratories, Institute of Genetics and Molecular Medicine, University of Edinburgh, Edinburgh, United Kingdom

Radiotherapy remains an important treatment modality in nearly two thirds of all cancers, including the primary curative or palliative treatment of breast cancer. Unfortunately, largely due to tumor heterogeneity, tumor radiotherapy response rates can vary significantly, even between patients diagnosed with the same tumor type. Although in recent years significant technological advances have been made in the way radiation can be precisely delivered to tumors, it is proving more difficult to personalize radiotherapy regimens based on cancer biology. Biomarkers that provide prognostic or predictive information regarding a tumor's intrinsic radiosensitivity or its response to treatment could prove valuable in helping to personalize radiation dosing, enabling clinicians to make decisions between different treatment options whilst avoiding radiation-induced toxicity in patients unlikely to gain therapeutic benefit. Studies have investigated numerous ways in which both patient and tumor radiosensitivities can be assessed. Tumor molecular profiling has been used to develop radiosensitivity gene signatures, while the assessment of specific intracellular or secreted proteins, including circulating tumor cells, exosomes and DNA, has been performed to identify prognostic or predictive biomarkers of radiation response. Finally, the investigation of biomarkers related to radiation-induced toxicity could provide another means by which radiotherapy could become personalized. In this review, we discuss studies that have used these methods to identify or develop prognostic/predictive signatures of radiosensitivity, and how such assays could be used in the future as a means of providing personalized radiotherapy.

Keywords: biomarkers of radiosensitivity, breast cancer, precision medicine, molecular signatures of radiosensitivity, biomarkers of radiation-induced toxicity

OPEN ACCESS

Edited by:
Francesco Cellini, Agostino Gemelli University Polyclinic, Italy

Reviewed by:
Valentina Lancellotta, Agostino Gemelli University Polyclinic, Italy
Michele Fiore, Policlinico Universitario Campus Bio-Medico, Italy

****Correspondence:***
James Meehan
jmeehan@ed.ac.uk

Specialty section:
This article was submitted to Radiation Oncology, a section of the journal Frontiers in Oncology

Received: *05 March 2020*
Accepted: *06 April 2020*
Published: *24 April 2020*

Citation:
Meehan J, Gray M, Martínez-Pérez C, Kay C, Pang LY, Fraser JA, Poole AV, Kunkler IH, Langdon SP, Argyle D and Turnbull AK (2020) Precision Medicine and the Role of Biomarkers of Radiotherapy Response in Breast Cancer. Front. Oncol. 10:628. doi: 10.3389/fonc.2020.00628

RADIOTHERAPY IN BREAST CANCER TREATMENT

In 2018 it was estimated that ∼18 million new cancer cases and 10 million cancer-related deaths occurred worldwide (1). If current trends in global population growth continue, combined with the effects of an aging population, these figures are predicted to increase to 20 million new cases and 13 million deaths per year by 2030 (2). Breast cancer (BC) is the most common female cancer,

with ∼2 million new cases and 0.7 million cancer-related deaths occurring per year (1). Despite the multitude of advances made in both the surgical and systemic treatment of cancer patients, radiotherapy (RT) has a key role in the management of nearly two thirds of all cancers (3).

RT is commonly given to BC patients after surgery. These adjuvant RT treatment plans typically involve the delivery of radiation to the tumor in multiple fractions over a period of several weeks. The most common adjuvant RT fractionation regimen following breast-conserving surgery is 25 fractions of 2 Gy over a 5 week period, or hypofractionated regimens consisting of a total of 40 Gy delivered in 15 fractions over 3 weeks (4). An external beam boost to the tumor bed can also be employed following whole-breast RT or integrated simultaneously with whole-breast irradiation (5) for invasive BCs which have a high risk of local recurrence. This boost procedure typically involves either 10 Gy in 5 fractions or 16 Gy in 8 fractions (6, 7), both delivered over the course of 1 week, or a radiobiologically equivalent dose such as 12 Gy in 4 fractions (8). Local recurrences occur most commonly at the original site of the primary tumor due to remaining microscopic tumor cells left following surgery; the objective of adjuvant and boost RT is to eradicate these tumor cells (7, 9). Accelerated partial breast irradiation (APBI) can be considered as an alternative treatment approach to conventional external beam RT or exclusive hormonal therapy which may be particularly useful for patients with a low-risk of local tumor recurrence or for elderly patients. APBI allows the delivery of higher radiation doses in the area of the tumor bed whilst reducing the dose received by normal breast tissue and adjacent organs at risk. Shorter treatment times and acceptable acute toxicity rates can improve patient quality of life whilst also reducing the total cost of treatment (10–14). Linear accelerators are the most commonly used devices for delivering external beam radiation to patients. In recent years, these machines have undergone significant technology-driven improvements that have culminated in the generation of modern radiation-delivery techniques such as intensity-modulated RT and image-guided RT approaches, which are designed to allow highly conformal and precise distribution of radiation to the tumor. Radiation delivery methods such as "dose painting by numbers" or sculpturing are becoming achievable through the use of these machines, meaning that identified subvolumes can be targeted specifically, limiting the radiation dose received by the nearby normal tissues (15). Although these current radiation planning techniques are largely based on advanced imaging to identify the gross tumor volume, the identification of a biological target volume based on the underlying tumor biology could lead to the development of a more personalized radiation treatment plan.

Of patients diagnosed with BC in England between 2013 and 2014, 63% received curative or palliative RT as part of their primary treatment (16). The Oxford overview shows that adjuvant RT halves the 10-year first risk of recurrence (most of which are local breast recurrences) after breast-conserving surgery and systemic therapy in all risk categories (9) and improves survival in lymph node positive patients receiving adjuvant systemic therapy (17). Studies have suggested that RT can benefit up to 83% of BC patients (18) and that breast-conserving surgery followed by whole-breast RT can provide local control and survival rates equivalent to mastectomy (19–21). These results, combined with the advantages of improved cosmetic outcomes and reduced side effects, have made the incorporation of RT into BC treatment standard practice for a large proportion of patients. Unfortunately, not all BC patients gain therapeutic benefit from RT. Although overall 5-year survival rates after RT are ∼80%, it is estimated that 30% of these patients will develop local recurrences or metastatic disease, the majority of whom will die within 5 years (22). Additionally, others in the neoadjuvant and palliative settings may only experience an initial partial response or may not respond at all. Side effects, which can affect a patient's quality of life, can also occur with RT.

A variety of imaging approaches for measuring tumor response to RT during or after treatment have been developed; these typically analyse how often and by how much a tumor shrinks anatomically. The RECIST (Response Evaluation Criteria in Solid Tumors) criteria have been widely adopted and are commonly used in oncology clinical trials. This categorizes the tumor response into complete (disappearance of tumor lesions for at least 4 weeks), partial (tumor diameter reduction of at least 30% for at least 4 weeks), stable (neither progressive disease nor partial response) or progressive (tumor diameter increase of at least 20%). Imaging techniques used to measure these changes in tumor size include X-ray, X-ray computed tomography, magnetic resonance imaging and positron emission tomography (23). However, as many of these techniques measure changes in tumor size alone to assess response to treatment, they ignore the underlying biology that drives the response to radiation. Additionally, analyzing changes in tumor size is a measurable clinical outcome that is seen only towards the end or after the treatment has finished, with patients who fail to respond to treatment initially going undetected. This delay may contribute to tumor progression, impact long-term survival and ultimately delay the initiation of an alternative treatment strategy. Non-responding patients will also be at risk of developing RT-induced side effects for no therapeutic gain. Despite the significant evidence that RT can benefit BC patients as a whole, there are still no clinically validated biomarkers that can be used to predict whether neoadjuvant/adjuvant RT will improve outcomes for individual patients.

PRECISION MEDICINE, PROGNOSTIC AND PREDICTIVE BIOMARKERS

Precision medicine is defined as the incorporation of disease biomarkers, molecular signatures and phenotypes in combination with patient lifestyle and environment into the prevention, investigation and treatment of diseases (24). Using these criteria, patients can be classified into cohorts according to differences in disease susceptibility, prognosis and likely treatment response rates. To improve clinical outcomes, this type of information can be used to select patients that may require more aggressive treatments and those that are most likely to

benefit from specific treatments (25). Genomic instability is a key feature of cancer that is characterized by genetic and epigenetic heterogeneity (26–28); it is therefore not surprising that patients diagnosed with the same cancer type vary in prognosis and in their responses to treatment. As we improve our understanding of the fundamental processes that control carcinogenesis and pathogenesis, precision medicine will become more and more important in the management of cancer patients. An era of personalized cancer medicine, in which biomarkers can be used to tailor treatment to each specific patient, is a major goal in oncology.

Biomarkers can be defined as characteristics which can be evaluated and measured as indicators of normal biological processes, pathogenesis or response to therapy (29). Cancer biomarkers may be diagnostic, prognostic, predictive, or used to monitor treatment responses. Prognostic biomarkers provide information about a patient's overall cancer outcome, irrespective of therapy. They can identify high-risk patients who may benefit from more aggressive treatments but provide no information on which patients will most likely derive a clinical benefit from a specific therapy. Conversely, predictive biomarkers can indicate the probability of a patient gaining a therapeutic benefit from a specific treatment (30–32). These fundamental prognostic and predictive biomarker concepts have been integrated into the precision medicine initiative.

BC radiomics, an emerging field in precision medicine, is the process of extracting quantitative information from medical images to influence patient treatment. This concept assumes that extracted imaging data are the result of biological processes occurring at a genetic and molecular level, and are therefore associated with the genotypic and phenotypic characteristics of the tumor (33). Radiomic features have been correlated with BC clinical data including stage, lymph node involvement and hormone receptor status (34), and also have the ability to discriminate between malignant and benign lesions (35). While radiomics has the potential to contribute to BC precision medicine in the future, BC molecular classification systems based on microarray gene expression analysis are currently being used clinically. These classification systems have identified several intrinsic BC molecular subtypes which have been shown to differ in treatment responses and predict disease-free survival and overall survival (36–39). Unfortunately, microarray analysis or genome sequencing for individual patients is cost-prohibitive for routine clinical use. To overcome this issue, studies have investigated the potential utility of using smaller gene sets to stratify BC patients, providing prognostic and/or predictive information which can be employed by clinicians to guide the use of adjuvant chemotherapy or endocrine therapy (40). These clinically-available tests include the breast cancer index (41), Endopredict (42), the Oncotype DX 21-gene recurrence score (43), the BreastOncPx 14-gene distant metastasis signature (44), and the MammaPrint 70-gene prognosis signature (45). Finally, a 50-gene signature called PAM50 (now commercialized under the name Prosigna) has improved the ability to predict recurrence of estrogen receptor$^+$/lymph node$^-$ BC patients compared to models using only clinical variables (46, 47). Although these clinically validated genetic tests have made significant changes in the way patients are selected for receiving chemotherapy or endocrine therapy, RT treatment plans still rely upon historically standardized, one-size-fits-all therapeutic approaches.

A move toward more personalized RT treatment, tailored to individual risk and tumor biology, would help improve patient outcomes (48). Many factors are known to influence a tumor's response to irradiation, including total dose, fractionation, tumor doubling time, hypoxia and intrinsic radiosensitivity. If RT is to become part of the precision medicine initiative, we need to identify clinically-validated biomarkers that can predict response to RT before starting treatment or biomarkers that can help clinicians assess a tumor's response to RT during treatment (49). Currently there are no sufficiently validated biomarkers of radiosensitivity for routine application in the clinic (49). These assays/biomarkers might allow the tailoring of radiation dose regimens to individual patients based on tumor biology or the prediction of the risk of localized tissue toxicity. Patients unlikely to benefit from RT could be spared radiation-induced toxicities and associated co-morbidities, whilst allowing more effective therapies to be instigated at an earlier stage of the treatment process (**Figure 1**). As discussed above, molecular signatures have been developed that enable clinicians to more individually tailor systemic therapies for patients with BC. Slower progress is being made to develop tools to predict RT response; in part this is due to radiation oncology vendors not having the financial capacity to support genomic-orientated collaborations with radiation oncology investigators (50). Nonetheless, much work has been performed to try and develop such biomarkers. The aim of this review is to highlight recent developments in this exciting yet under-researched field.

MOLECULAR SIGNATURES OF RADIOSENSITIVITY

Intrinsic Subtypes

Gene expression profiling and histopathological classification using the expression of estrogen receptor (ER), progesterone receptor (PgR) and human epidermal growth factor receptor 2 (HER2) can be used to classify BC into different subtypes. These subtypes can be broadly categorized into luminal, normal-like, HER2-overexpressing and triple negative breast cancer (TNBC) (36–39, 51). Gene expression profiling can stratify BC subtypes to a greater degree than histological assessment; however, as previously mentioned, this is often not feasible for use with large scale patient populations due to financial constraints (52). Both classification methods have confirmed the heterogeneous nature of BC which can lead to substantial differences in biology, pathogenesis, treatment response and patient outcome (39, 53, 54). Luminal subtypes (which correspond to ER$^+$ BC) are associated with a more favorable prognosis, whereas HER2-overexpressing and TNBC subtypes are associated with significantly worse recurrence-free survival and overall survival.

BC subtyping has also been investigated for its use in predicting response to RT. The major advantage of using these subtyping markers in the selection of patients for RT is that testing for these markers using biopsy samples is now mandatory

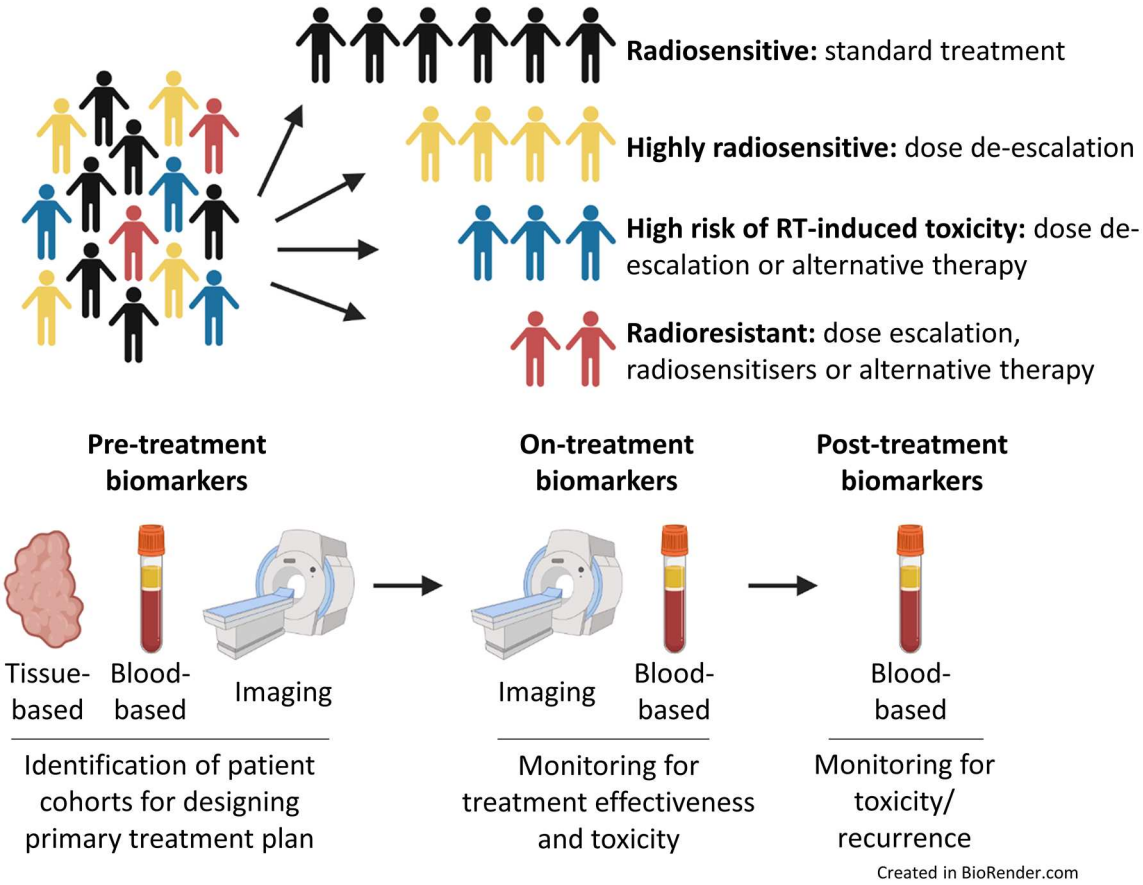

FIGURE 1 | Precision medicine and radiotherapy. Patients could be stratified into different cohorts based on predicted intrinsic radiosensitivity and risk of toxicity. On-treatment monitoring may provide information on response to treatment, enabling adaptive changes to a patient's treatment to be made if necessary. Post-treatment biomarkers could be used to assess for evidence of toxicity, tumor recurrence or the development of metastatic disease.

in the clinics, as they are used for selecting patients for hormonal or targeted therapies. *In vitro* studies using BC cell lines have shown that individual subtypes exhibit differential inherent sensitivities to radiation (55). Multiple clinical analyses have also shown that subtype is related to radiosensitivity; one large study reported that local recurrence for invasive BC treated with breast-conserving surgery followed by RT was 0.8% for luminal A, 1.5% for luminal B, 8.4% for HER2-overexpressing and 7.1% for TNBC (56). HER2-overexpressing and TNBC have also been associated with an increased risk of local recurrence and distant metastasis in combination with reduced overall survival in patients treated with post-mastectomy RT or RT alone (56–58). Improved overall survival after post-mastectomy RT has also been identified in ER^+/ PgR^+/$HER2^-$ patients, whereas no significant overall survival improvement was seen following the same treatment in ER^-/ PgR^-/$HER2^+$ patients (58). Similar results were observed when using the Oncotype DX recurrence score to predict overall survival following post-mastectomy RT; this study suggested that low-risk patients, as determined by low OncotypeDX recurrence scores, had significantly improved overall survival following post-mastectomy RT compared to those low-risk patients that did not receive this treatment. In comparison, post-mastectomy RT was not of significant benefit to intermediate and high-risk patients. The authors suggested that OncotypeDX recurrence score may be a predictor of survival benefit from post-mastectomy RT (59). Furthermore, improved overall survival has been documented in patients with ER^+/ PgR^+/$HER2^-$ tumor who received post-mastectomy RT when compared with those who received no RT (58). This suggests that RT is particularly effective for breast cancers of the luminal phenotype.

Pan-Cancer Genomic Signatures

The first pan-cancer genomic radiosensitivity signature was developed using 35 cancer cell lines from the National Cancer Institute-60 (NCI-60) panel (60). Torres-Roca et al. (60) used gene expression data combined with the survival fraction of cells that received a dose of 2 Gy (SF2), an accepted experimental measure of cellular radiosensitivity, to develop a radiation classifier that could predict inherent radiosensitivity. Their results showed that the classifier successfully predicted SF2 values in 22 of 35 NCI-60 cell lines. The authors then went on to identify three novel genes (*RbAp48*, *RGS19*, and *R5PIA*) whose expression was correlated with radiation sensitivity. These results were the

first to show that gene expression profiles had the potential to predict radiation sensitivity and that genomics could be used to identify novel radiosensitivity molecular markers. Unfortunately, subsequent studies have failed to reproduce these *in vitro* results using modern gene expression techniques; therefore, the validity of this signatures use in cell lines remains open to debate (61).

This pan-cancer genomic radiosensitivity signature has since been developed by the same group to include biological variables such as tissue of origin, p53 and ras status, known influencers of radiosensitivity. Using SF2 values from 48 cancer cell lines from the NCI-60 panel, gene expression analysis was performed to identify a 10 gene signature associated with intrinsic radiosensitivity (*AR*, *cJun*, *STAT1*, *PKC*, *RelA*, *cABL*, *SUMO1*, *CDK1*, *HDAC1*, and *IRF1*). These 10 genes are associated with specific pathways that included cell cycle, DNA damage response, histone deacetylation, proliferation and apoptosis. These results were used to produce a radiosensitivity index (RSI), whereby lower RSI correlates with greater radiosensitivity (62). The RSI has been used in clinical studies; these have shown the signature to be disease-site independent, predicting clinical outcomes in esophageal, rectal, head and neck, prostate, pancreas, colon, glioblastoma and non-small cell lung cancer patients following RT (62–66). However, some of these results were obtained from pilot studies which had low patient numbers, whereas others did not compare the results with non-RT treated controls. The RSI has also been evaluated in 2 independent BC patient cohorts. Results indicated that RT-treated patients classified as radiosensitive by RSI had improved recurrence-free survival or distant metastasis-free survival at 5 years, but there was no difference in recurrence-free survival or distant metastasis-free survival between radiosensitive and radioresistant patients in those not treated with RT. The authors suggested that RSI is RT-specific, because it was not prognostic for patients treated with surgery alone, but importantly can be used as a predictive signature of RT benefit. Furthermore, they demonstrated that the impact of RSI was affected by ER status, with RSI-classified radiosensitive patients having greater distant metastasis-free survival in ER^+ patients (67). RSI has also been integrated with BC molecular subtyping to predict local recurrence; Torres-Roca et al. (68) showed that although RSI did not uniformly predict for local recurrence, it was able to identify a subpopulation of TNBC that had high RSI scores which were classified as radioresistant with the highest risk of local recurrence. They also illustrated that RSI could identify a luminal radioresistant subpopulation that would benefit from radiation dose escalation. They concluded that the combined use of RSI and molecular subtyping could help guide the selection of patients for RT treatment in BC (68).

In an attempt to tailor radiation doses across differing BC subtypes, researchers have integrated the RSI with the linear quadratic model to derive a genomic-adjusted radiation dose (GARD); this aimed to predict which tumors would gain an enhanced therapeutic effect from RT. GARD values were calculated for over 800 tumor samples using data from the prospective, observational Total Cancer Care cohort. The results demonstrated that there was a wide range of GARD values within tumor types and that GARD values could independently predict clinical outcome in lung, pancreatic, glioblastoma and BC patients (69). The limitations of this study included the failure to evaluate the prognostic potential of GARD (no data were evaluated for patients that did not receive RT) and a lack of external validation. However, this GARD-based clinical model could allow for RT personalisation based on radiation dose tailored to tumor radiosensitivity and may provide a means to develop genomically-guided RT-based clinical trials.

A similar approach which used the same NCI-60 cell line panel was undertaken to identify not only genes whose expression profiles were related to intrinsic radiosensitivity, but also genes whose expression changed following radiation treatment and were associated with post-radiation survival. Changes in gene expression induced by radiation were found to be similar between different tumor types and were also associated with p53 status. The authors suggested that there was possibly a conserved set of genes responsible for a specific radiation response (70). However, this work contradicts a more comprehensive study that profiled the radiation response of over 500 cell lines which showed sensitivity to radiation was characterized by significant genetic variation within and between cell line lineages. As well as identifying genes whose expression was associated with response, they also identified somatic copy number alterations and gene mutations that correlated with post-radiation survival (71).

In addition to radiation-induced gene response signatures, other groups have looked at signatures that may predict response to radiation treatment for a range of different cancer types. These gene expression profiles include hypoxia-related signatures (72–74), cell cycle and DNA damage gene-related signatures (75, 76), along with signatures predicting response to radiosensitising drugs (77, 78). As with many of the other *in vitro* derived signatures, none of these has thus far withstood stringent external validation and therefore have yet to be translated into clinical practice.

Breast Cancer Specific Genomic Signatures

With a technique similar to that employed to produce the RSI, a different study used only BC cell lines to develop a BC specific radiation sensitivity signature (RSS) (79). Their aim was to produce a gene signature that could predict the radiation response of BC patients and allow the identification of patients with tumors refractive to conventional RT regimens. To derive their gene signature, intrinsic radiosensitivity was correlated with gene expression using SF2 values from a panel of 16 BC cell lines. Interestingly, Speers et al. (79) found no association between intrinsic radiosensitivity of the BC cell lines and subtype classification, contradicting findings from previous publications. A 51 gene signature, enriched for pathways involved in DNA damage response and cell cycle, was developed from their results. Validation of this gene signature, the most promising to date, was performed in two independent clinical BC datasets in which patients had been treated with breast-conserving surgery and RT. The results showed that the RSS could provide information on which patients were likely to respond poorly to standard RT regimens (79). However, as all patients in the studied cohorts received standard RT, the 51

gene signature could not be validated for its predictive potential. This RSS has subsequently been marketed as RadiotypeDX and is regarded as having potentially similar applications to that of OncotypeDX, which is used for selecting the most appropriate systemic therapies for BC patients. RadiotypeDX is currently undergoing external validation, using tissue and clinical data from a randomized controlled trial evaluating post-operative RT after breast-conserving surgery in patients with early BC, who received appropriate adjuvant systemic therapy according to ER status (80). Although the results are yet to be published, these types of trials, as well as prospective randomized trials or "prospective retrospective" analyses from phase III trials, are essential in order to show that these kinds of signatures have clinical applications and that they could be integrated into clinical practice (81).

More recently a refined version of RadiotypeDX (Adjuvant Radiotherapy Intensification Classifier [ARTIC]) has been validated in a Swedish Conservation trial in which patients were randomized to post-operative whole-breast RT or no RT (82). Of note, a limited number of patients in this trial received systemic therapy. ARTIC was found to be highly prognostic for loco-regional recurrence and predictive of benefit from RT. Patients who had a low ARTIC score derived a substantial benefit from RT; in contrast, patients with high ARTIC scores had less benefit from RT. The authors recognized the requirement to validate ARTIC within a trial of patients treated by breast-conserving therapy, systemic therapy +/– post-operative whole-breast irradiation.

A gene profile called DBCG-RT, predictive for therapeutic benefit from post-mastectomy RT and prognostic for locoregional control, was developed by the Danish Breast Cancer Cooperative Group and has been independently validated (83). The DBCG-RT gene profile can divide patients into those with a high- and low-risk of local recurrence and can identify a subcategory of low-risk patients who obtain no additional benefit from RT. A correlation between patients that were at an increased risk of developing local recurrence and non-luminal, ER^- tumors (basal and HER2-overexpressing) was observed, while the low local recurrence risk group correlated with the luminal A subtype. These findings indicate that intrinsic subtyping and the DBCG-RT profile can identify the same tumor types and their responses to RT treatment.

Others have attempted to develop specific radiation signatures for BC that distinguish patients who require treatment intensification, for whom traditional therapies (surgery, chemotherapy and RT) are inadequate. Gene analysis has been conducted on early stage BC patients, all treated with RT after surgery, to try and distinguish gene signatures prognostic of local recurrence in patients treated with radiation. A radiation signature consisting of 81 genes outperformed pathologic and clinical characteristics for predicting local recurrence (84). A similar study performed gene expression microarray profiling to identify differentially expressed genes between tumors from patients who developed local recurrence after breast-conserving surgery and radiation, and patients who did not; Kreike et al. (85) derived a 111 gene signature, enriched for cell proliferation, which was independently associated with local recurrence. Unfortunately, both of these signatures failed external validation.

The Early Breast Cancer Trialists' Collaborative Group meta-analysis suggested that most early stage BC patients treated with breast-conserving surgery are cured of their disease with both surgery and endocrine therapy alone, without the need for RT (9). Studies have also suggested that RT may be omitted in selected elderly patients with low-risk disease (86). RT omission after breast-conserving surgery has also been explored in several randomized phase III trials; unfortunately, heterogeneous eligibility criteria across the trials has resulted in differing results with confounding interpretations (87). These types of studies have led to an increased interest in the development of radiation omission signatures specific for BC, whereby low-risk patients can be spared RT. An omission signature has yet to be developed; however, different groups are attempting to validate a variety of previously described molecular classifiers for this purpose. Trials are ongoing to assess the potential of OncotypeDx (IDEA trial), Prosigna (PRECISION trial), IHC (LUMINA trial), and IHC4 (PRIMETIME trial) scores as stratification methods for radiation omission (81).

Barriers to Clinical Adoption of Molecular Signatures

Although many molecular signatures have been developed to predict a tumor's response to radiation, most have failed external validation and, as a result, none have gained approval for clinical use. In part, as indicated earlier, the barriers are the high costs of academic-industry collaborations and in part scientific (50). Unfortunately, the gene profiles derived from the studies outlined in this review show little similarity to each other, which suggests that the methods used to produce the signatures may influence which genes and pathways are selected. Like many other cancers, BC is a complex heterogenous disease; differences in pathway activation can lead to different drivers of oncogenesis, even within the same subtype. These significant differences will influence how each tumor reacts to RT; it is possible that gene signatures are unable to account for the complexity of a tumor's radiation response. These issues are likely to be more pronounced in profiles derived from cell lines, as these are clonal populations that cannot account for tumor heterogeneity and the effects of the tumor microenvironment. Validation of the signatures using clinical trial data is also complicated; variations between trials in terms of the radiation treatment regimens used, inclusion of different patient subtypes and inconsistencies between the numbers of treated and control patients included in the studies makes the generation of meaningful data and rigid signature validation challenging. The methods used for RNA extraction and subsequent gene expression analysis can also differ between the original studies which developed the profiles and the clinical trials in which they are being validated. These issues are specific for gene signature validation; there are also more general hurdles that must be overcome if lab-based research is to be successfully translated into a clinically applicable test. These include the development of standard operating procedures and making tests cost effective and easy to use, while also providing evidence that they can improve upon standard practices already in place in the clinics. The combination of these gene signature specific and

general issues are factors that are currently contributing to their lack of clinical translation and use in the clinic.

GENE MUTATIONS, mRNA AND INTRACELLULAR PROTEIN MARKERS

Several studies have looked at individual biomarkers, rather than cohorts of genes, for their potential to correlate with a tumor's response to RT. In BC, expression levels of Holliday junction recognition protein mRNA can be prognostic for disease-free survival and overall survival, thereby predicting patient sensitivity to RT (88). High cytoplasmic expression of peroxiredoxin-I has also been shown to correlate with increased local recurrence after RT (89). Proteasome (prosome, macropain) 26S subunit, non-ATPase, 9 (PSMD9) is another protein whose elevated expression was associated with increased incidence of local recurrence in a cohort of patients that received adjuvant RT, but not in those that did not receive RT; the authors concluded that this protein might therefore be a predictive biomarker for RT response (52).

The *BRCA1/2* genes are part of the granin gene family and function as tumor suppressors; they play critical roles in maintaining genome stability through controlling pathways involved in DNA damage response/repair, cell cycle and transcription (90). Previous studies have shown that *BRCA1/2* gene deregulation is associated with BC carcinogenesis (91), with germline *BRCA1/2* mutations accounting for up to 10% of all cases (92). Inherited *BRCA1/2* mutations are estimated to increase the risk of BC by to 84% (93–95). These tumors exhibit ineffective homologous recombination DNA repair, causing an accumulation of genetic mutations, which can drive carcinogenesis. Although tumors deficient in a DNA repair mechanism may be expected to exhibit radiation sensitivity, they are instead thought to rely upon alternative DNA repair mechanisms that are more effective at repairing radiation-induced DNA damage. PARP enzymes play a key role in the repair of DNA single-strand breaks through the repair of base excisions, a process normally performed by error-free homologous recombination (96). The inhibition of PARPs can result in the accumulation of DNA single-strand breaks, leading to the generation of double-strand breaks at replication forks. Double-strand breaks are usually repaired by error-free homologous recombination, a process that is inhibited in BRCA1/2 mutated tumors; these double-strand breaks can lead to apoptosis of cancer cells within the tumor. The PARP enzyme inhibitor olaparib is currently undergoing trials to assess its clinical usefulness and cost effectiveness in the treatment of BRCA1/2 mutated $HER2^-$ metastatic BC patients following chemotherapy (97). This drug has previously gained clinical approval for use in patients with recurrent, platinum-sensitive, BRCA1/2 mutated ovarian cancers (98). Furthermore, the small molecular PARP inhibitor niraparib has been shown to radiosensitise a variety of human xenograft tumors, including the triple-negative MDA-MB-231 human BC cell line (99). It has therefore been suggested that BRCA status could be a useful biomarker for stratifying patients for the use of PARP inhibitors in combination with RT.

BLOOD-ASSOCIATED BIOMARKERS OF TUMOR RADIOSENSITIVITY

The identification of circulating prognostic or predictive biomarkers in the blood has advantages over tissue-based approaches as it is non-invasive and does not require a biopsy. These liquid biopsies can be taken pre-, post- or on-treatment, allowing for continual patient monitoring with the potential to assess the tumors response to treatment. These biomarkers could hold particular promise in patients with metastatic disease, where monitoring for progression is critical but where repeated biopsy sampling is often unfeasible due to the location of the lesions. Studies have investigated the use of blood based biomarkers, such as carcinoembryonic antigen and carbohydrate antigen 15–3 for primary diagnosis and the detection of metastatic disease (100–105), with others examining the correlation between serum HER2 concentration and tumor HER2 status (106–109). Although the use of blood-based biomarkers to assess tumor pre-treatment radiosensitivity or on-treatment response to RT has been less intensively studied, there is a growing interest in the use of these types of biomarkers for precision RT. Areas of research currently under investigation include exosomes and circulating tumor cells (CTCs).

Exosomes are formed from the inward budding of the membrane of multi-vesicular bodies and are ∼40–100 nm in diameter. The contents of exosomes are released from cells via endocytosis through fusion of their membrane with that of the cell's plasma membrane. Exosomes have been shown to contain nucleic acids, proteins, lipids and enzymes (110). There is increasing evidence that exosomes play roles in tumorigenesis and cancer progression, including immune suppression, angiogenesis, cell migration and invasion (111–115); as a result, their use as liquid biopsy biomarkers through exosomal profiling is being investigated for disease diagnosis and therapy efficacy monitoring. The transfer of exosome contents to local tumor or stromal cells in the tumor microenvironment, or to a distant site within the body, has been shown to be a mechanism through which cancer cells can transmit the malignant phenotype to normal cells and establish a suitable environment for metastatic colonization (113). Exosomes transferred from stromal to BC cells can also contribute to chemotherapy and radiotherapy resistance. Resistance mechanisms mediated by exosomal transfer are thought to involve anti-viral and NOTCH3 pathways (116). Tumor oxygen concentrations at the time of radiation have been shown to influence cell radiosensitivity (117). When exposed to a given dose of radiation, cancer cells in low oxygen states can withstand 2–3 times higher doses than aerobic cells. Known as the oxygen enhancement effect, the role that oxygen plays in RT is described through the oxygen fixation hypothesis (118, 119). Oxygen present at the time of RT can react with radiation-induced DNA radicals producing permanent DNA damage; however, in the absence of oxygen this damage can be repaired

by free radical scavengers such as endogenous thiols (120), giving these hypoxic cells a significant survival advantage. Hypoxia leads to the increased production of exosomes (121, 122), with the transfer of exosomes from stromal to BC cells stimulating signaling pathways related to radiation resistance (116). The tumor-associated exosome profile may also give an indication of the oxygenation status of breast tumors, and therefore could be used to identify radioresistant tumors (122).

CTCs and circulating tumor DNA are cells or DNA that have been shed by the tumor into the systemic circulation; these can be indicators of residual disease following treatment and are likely to represent an important mechanism through which a tumor can metastasise (123, 124). CTCs have been detected in up to 30% of non-metastatic BC patients and their presence (even just one CTC) has been shown to be prognostic for recurrence-free survival and overall survival (125–135). CTC detection is also related to metastasis and poor survival in low-risk patients with lymph node negative disease who did not receive adjuvant therapy (133). Data from the National Cancer Database and SUCCESS (Simultaneous Study of Gemcitabine-Docetaxel Combination Adjuvant Treatment as well as Extended Bisphosphonate and Surveillance) clinical trials have been used to investigate the use of CTC status to predict the benefit of RT in early stage BC (136). The results suggested that CTC status could predict the effectiveness of RT and showed that CTC^+ patients had improved local recurrence-free survival and disease-free survival following RT, whereas CTC^- patients obtained no benefit. Furthermore, CTC^+ patients that received RT had improved overall survival compared with CTC^+ patients who did not receive RT. Pooled analysis using both cohorts who underwent breast-conserving surgery indicated that RT was associated with longer overall survival in CTC^+ patients, but not in CTC^- patients. However, CTC status was not associated with an overall survival benefit in patients who underwent mastectomy and RT. Overall, these results suggested that CTC status may be used as a predictive marker for assessing the potential benefit from incorporating RT into the treatment of early stage BC for patients undergoing breast-conserving surgery (136, 137).

Although circulating tumor biomarkers have the potential to be used for cancer diagnosis, measuring response to treatment and monitoring for recurrence, studies evaluating their clinical usefulness are still limited in number. While advances have been made in this field, circulating tumor biomarkers in BC patients are not yet employed for primary diagnosis, largely due to their low sensitivity and specificity, and also because of a lack of validation through large prospective trials. Such trials are essential to fully evaluate their prognostic or predictive potential in determining tumor radiosensitivity and to enable their use in the future (138).

BIOMARKERS OF RADIATION-INDUCED TOXICITY

In contrast to the relatively limited research involving blood-based biomarkers for tumor radiosensitivity, the use of circulating biomarkers to assess radiation-induced toxicities has attracted much greater interest. Like any cancer treatment, RT has the potential to cause toxic side effects in normal tissues; these ultimately dictate the total dose that can be delivered to a patient, which can influence outcome. In BC, radiation-associated side effects include cardiac and skin toxicities, fibrosis, lymphedema, secondary cancers, rib fractures and brachial plexopathy (139). In some studies the combination of tamoxifen and RT has resulted in an increased risk of fibrosis, hypothesized to be due to a tamoxifen-induced increase in TGF-β (140–144). Even with highly conformal intensity-modulated RT and image-guided RT, which aim to spare regional organs from radiation exposure, these side effects can occur in up to 15% of patients and can seriously affect patients' physiological and physical quality of life (145, 146). Taking into account the high survival rate of BC patients, there is a need to develop tests that can be used either pre-treatment, or at an early stage of the treatment process, to predict which patients are at a higher risk of developing radiation-associated side effects (147). Predicting radiation-induced toxicity could enable better treatment regimens to be devised for individual patients in a range of cancer types. Radiation toxicity is related to treatment schedule (dose and duration), patient specific factors and genetic factors. With these in mind, several tests have been proposed to classify individual patient radiosensitivity based on the induction of DNA damage and radiation-induced apoptosis, in addition to gene expression profiles (148).

One area of research that holds promise in predicting the risk of late radiation-associated toxicity is through assessment of the radiation-induced initial DNA damage response of peripheral blood lymphocytes through DNA double strand break quantification, comet or micronucleus assays (148). A relationship between high rates of double strand breaks in peripheral blood lymphocytes and late grade 3 skin and subcutaneous tissue toxicities in BC patients has suggested that assessing the initial DNA damage could be useful for predicting radiation toxicity (149). Unfortunately, various studies assessing the radiation-induced DNA damage through other methods have shown both negative (150, 151) and positive (152–154) associations with radiation toxicity. Additionally, the clinical usefulness of radiation-induced DNA damage response assays is yet to be fully determined. Determining peripheral blood lymphocyte radiation-induced apoptosis appears to be the most promising assay for determining radiation toxicity. Studies have shown that radiation-induced apoptosis increases with higher doses of radiation; however, elevated levels of radiation-induced apoptosis were associated with reduced risk of late radiation toxicities (155). In BC patients, studies have used a combination of DNA damage assessment and levels of radiation-induced apoptosis to assess radiation-induced toxicity. Henríquez-Hernández et al. (156) demonstrated that patients showing lower levels of initial DNA damage and higher levels of radiation-induced apoptosis were considered resistant to RT. These patients were at a lower risk of suffering severe subcutaneous late toxicities after treatment with high radiation doses.

Although these results were based on a small number of patients, it provided evidence that dose escalation can be achieved in patients that are resistant and tolerant to higher radiation doses.

There is an association between the dose of radiation received by the heart and increased risk of heart disease (157–159); as the dose increases so does the risk of developing heart complications. Cardiovascular side effects are a major concern for clinicians treating BC patients with RT (160, 161), especially for left sided BC or patients with pre-existing cardiovascular disease. Cardiotoxic effects of RT can be seen for several years after RT, and increased risk may remain for at least 2 years post-RT (161). Pericarditis, valvular dysfunction, cardiomyopathy and coronary artery disease are some of the severe late cardiotoxic effects seen in up to 30% of BC cases within 5–10 years following RT (162). Blood biomarkers have been investigated for their roles in detecting and monitoring cardiotoxicity and assessing early signs of cardiovascular dysfunction following RT. Brain natriuretic peptide and its amino terminal fragment are biomarkers produced by ventricular myocytes, with elevated blood levels commonly seen in unstable angina, myocardial infarction and cardiac failure (163). Several studies have shown that levels of these biomarkers increase after RT, suggesting that these may be also be biomarkers of early radiation-induced cardiotoxicity (164–166). Circulating cardiac troponin I and cardiac troponin T are highly sensitive and specific biomarkers for cardiac disease and have been shown to be useful for detecting cardiotoxicity following chemotherapy (167, 168) and, although some studies indicate they do not increase following RT (165, 169), others show that they do (164, 170, 171). While these traditional cardiac biomarkers are the most extensively studied for cardiotoxicity following RT, other blood biomarkers that have been investigated include C-reactive protein and lipopolysaccharide. C-reactive protein, an acute phase protein whose expression is related to inflammatory cytokines, has been proposed as a biomarker of radiation-associated cytotoxicity as studies have highlighted an association between elevated C-reactive protein levels and adverse prognosis in patients with heart failure (172–174). Although Lipshultz et al. (166) found increased levels of C-reactive protein in children following treatment for a variety of cancers with chemotherapy and RT, the majority of studies have failed to find an association between circulating C-reactive protein levels and myocardial damage post-chemotherapy (175–177) or RT (178). Lipopolysaccharide-binding protein has been investigated as a potential biomarker for lung toxicity after chest RT (179). In BC, lipopolysaccharide-binding protein concentrations were observed to increase within 24 h post-RT and remained elevated 1 month after RT. Raised lipopolysaccharide-binding protein levels were also correlated with cardiac dysfunction, which was evaluated up to 3 years following the completion of RT, suggesting that lipopolysaccharide-binding protein could be a potentially useful prognostic biomarker of RT-induced cardiotoxicity (178). Characteristics such as early detection in the blood and persistent kinetics, in combination with concentrations being related to toxicity, have made lipopolysaccharide-binding protein an attractive biomarker for clinical use. Other proposed biomarkers include heart-type fatty acid-binding protein, glycogen phosphorylase isoenzyme BB, myeloperoxidase and nitric oxide (180). Although these biomarkers have yet to be used clinically, they could in the future play key roles in determining which RT patients may require dose de-escalation, or even the provision of alternative treatments if BC patients can be classified as high-risk for developing radiation-induced side effects post-treatment.

TABLE 1 | Techniques used for measuring the response of tumors to RT.

Imaging-based methods
Method: Advanced imaging modalities can provide information on tumor size (X-ray computed tomography, ultrasound, magnetic resonance imaging) and give an estimation of hypoxia and proliferation heterogeneity within different areas of a tumor (positron emission tomography). Imaging can be conducted pre-, during and post-treatment.
Advantages: Non-invasive. Real-time measurements of response can be obtained. Methods, protocols and criteria for visualizing and assessing changes in tumor size are already established within the clinic.
Disadvantages: Changes in tumor size can be gradual and slow which may only be seen towards the end or after the treatment has finished; patients who fail to respond will initially go undetected. Patient safety concerns over repeat exposure to radiation and radioisotopes.
Cancer tissue-based biomarkers
Method: Evaluating the expression levels of genes or proteins using biopsy samples.
Advantages: Pre-treatment biopsies are already taken as part of standard of care treatment, meaning patients do not require an additional procedure. Protein assessment using IHC can identify the location of protein expression and provide information on functional status. Gene signatures may be prognostic and predictive of responses to RT.
Disadvantages: Invasive. Unable to monitor response to treatment without further invasive procedures, which can be difficult to obtain and hard to justify. Some methods of analysis are cost prohibitive. Does not provide real-time measurements of response.
Blood-based biomarkers
Method: Measuring the presence or expression levels of CTCs or proteins using liquid biopsy (blood) samples. Samples can be obtained readily pre-, during and post-treatment.
Advantages: Non-invasive. Real-time measurements of response can be obtained.
Disadvantages: Low sensitivity and specificity of tests developed to date.

Advantages and disadvantages of each method are provided (IHC, immunohistochemistry; RT, radiotherapy; CTCs, circulating tumor cells).

A summary of the techniques used to identify biomarkers of radiosensitivity that have been described in this paper is provided in **Figure 2** and **Table 1**. **Table 1** also outlines the specific advantages and disadvantages associated with each method.

CONCLUSION

Significant advances have been made in the development of molecular signatures to stratify BC patients for more personalized targeted and endocrine therapies; however, similar

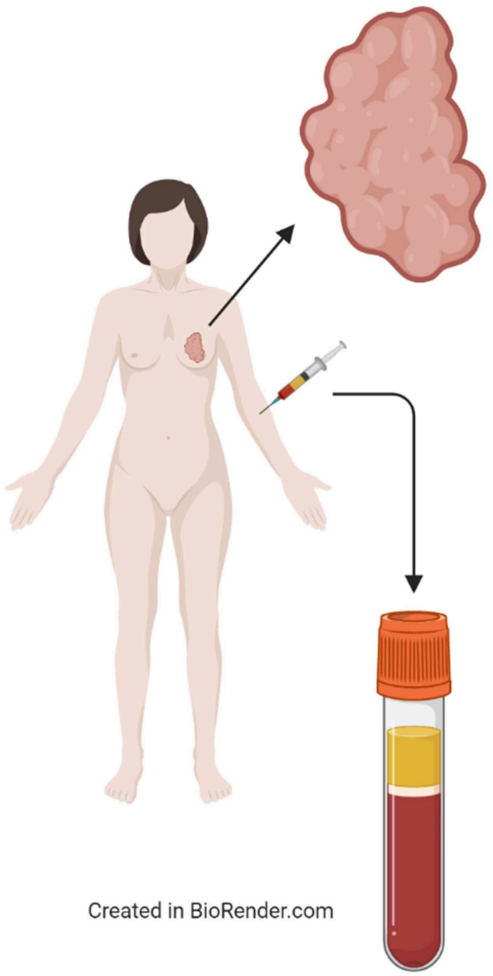

Cancer tissue associated biomarkers

Histopathological classification
- ER/PgR/HER2 (55-59)

Pan-cancer genomic signatures with studies performed in breast
- Radiosensitivity index (RSI) (62, 67-68)
- Genomic-adjusted radiation dose (GARD) (69)
- Cell cycle and DNA damage-related (75-76)
- Predicting response to radiosensitizing drugs (77)

Breast cancer specific genomic signatures
- RadiotypeDX (79-80)
- Adjuvant Radiotherapy Intensification Classifier (ARTIC) (82)
- Danish Breast Cancer Cooperative Group - RT (DBCG-RT) (83)
- Treatment intensification signatures (84-85)
- Radiation omission signatures (81)

Gene mutations, mRNA and intracellular protein markers
- BRCA1/2 genes (99)
- Holliday junction recognition protein mRNA (88)
- Peroxiredoxin-I protein (89)
- Proteasome (prosome, macropain) 26S subunit, non-ATPase, 9 (PSMD9) protein (52)

Blood associated biomarkers

Biomarkers of tumor radiosensitivity
- Exosomes (116, 122)
- Circulating tumor cells (136-137)

Biomarkers of radiation-induced toxicity
- Radiation-induced initial DNA damage response of peripheral blood lymphocytes (148-154)
- Peripheral blood lymphocyte radiation-induced apoptosis (156)
- Brain natriuretic peptide protein (164-166)
- Cardiac troponin I and cardiac troponin T proteins (164-165, 169-171)
- C-reactive protein (172-174)
- Lipopolysaccharide protein (178)
- Myeloperoxidase (180)

FIGURE 2 | Biomarkers of radiotherapy response for breast cancer. An overview of cancer tissue-associated and blood-associated biomarkers of radiotherapy response that have been developed for breast cancer patients (ER, Estrogen receptor; PgR, Progesterone receptor; HER2, human epidermal growth factor receptor 2).

improvements in the field of personalized RT have yet to be adopted in the clinic. Technological developments in the methods used for radiation delivery have allowed radiation oncologists to accurately conform radiation to the tumor; however, only limited methods of analyzing response to treatment are available. To truly achieve personalized RT, we also need to be able to stratify patient's pre-treatment based on individual patient radiosensitivity and through analyzing the tumor's response to RT during treatment. Unfortunately, there are currently no clinically-validated prognostic or predictive signatures/biomarkers that can reliably classify patients into those that would benefit the most from RT, those that could be safely treated with dose escalation or de-escalation, or those that should be treated without RT. While preliminary efforts to develop these signatures/biomarkers have been encouraging, there is still much work to do in order to refine and validate them. Ultimately, for any of these tests to be translated into the clinic, studies will need to demonstrate their accuracy and reproducibility, and perhaps more importantly, exhibit their utility in improving outcomes or refining the selection of patients for RT through clinical trials. While not yet realized, the ongoing development of these signatures and biomarkers holds much promise; the linking of these signatures and biomarkers with other techniques, such as imaging, would help deliver an overall precision medicine package that could greatly enhance the effectiveness of RT. There is confidence within the scientific community that personalized medicine will finally be realized

for BC patients undergoing radiation treatment in the decades to come.

AUTHOR CONTRIBUTIONS

JM, MG, DA, and AT conceptualized the article. JM wrote the majority of the manuscript. Figures and tables were composed by JM and MG. Critical revisions were made by JM, MG, CM-P, CK, LP, JAF, AVP, IK, SPL, DA, and AT. All authors read and approved the final manuscript.

FUNDING

This work was supported by the Breast Cancer Institute Fund (S03181) from the Edinburgh Lothian Health Foundation.

REFERENCES

1. Bray F, Ferlay J, Soerjomataram I, Siegel RL, Torre LA, Jemal A. Global cancer statistics 2018: GLOBOCAN estimates of incidence and mortality worldwide for 36 cancers in 185 countries. *Cancer J Clin*. (2018) 68:394–424. doi: 10.3322/caac.21492
2. Bray F, Jemal A, Grey N, Ferlay J, Forman D. Global cancer transitions according to the Human Development Index (2008–2030): a population-based study. *Lancet Oncol*. (2012) 13:790–801. doi: 10.1016/S1470-2045(12)70211-5
3. Siegel R, DeSantis C, Virgo K, Stein K, Mariotto A, Smith T, et al. Cancer treatment and survivorship statistics, 2012. *Cancer J Clin*. (2012) 62:220–41. doi: 10.3322/caac.21149
4. Haviland JS, Owen JR, Dewar JA, Agrawal RK, Barrett J, Barrett-Lee PJ, et al. The UK standardisation of breast radiotherapy (START) trials of radiotherapy hypofractionation for treatment of early breast cancer: 10-year follow-up results of two randomised controlled trials. *Lancet Oncol*. (2013) 14:1086–94. doi: 10.1016/S1470-2045(13)70386-3
5. Nitsche M, Dunst J, Carl UM, Hermann RM. Emerging role of hypofractionated radiotherapy with simultaneous integrated boost in modern radiotherapy of breast cancer. *Breast Care*. (2015) 10:320–4. doi: 10.1159/000436951
6. Bartelink H, Maingon P, Poortmans P, Weltens C, Fourquet A, Jager J, et al. Whole-breast irradiation with or without a boost for patients treated with breast-conserving surgery for early breast cancer: 20-year follow-up of a randomised phase 3 trial. *Lancet Oncol*. (2015) 16:47–56. doi: 10.1016/S1470-2045(14)71156-8
7. Kindts I, Laenen A, Depuydt T, Weltens C. Tumour bed boost radiotherapy for women after breast-conserving surgery. *Cochrane Database Syst Rev*. (2017) 11:CD011987. doi: 10.1002/14651858.CD011987.pub2
8. Janssen S, Glanzmann C, Lang S, Verlaan S, Streller T, Wisler D, et al. Hypofractionated radiotherapy for breast cancer acceleration of the START A treatment regime: intermediate tolerance and efficacy. *Radiat Oncol*. (2014) 9:165. doi: 10.1186/1748-717X-9-165
9. E.B.C.Group TC. Effect of radiotherapy after breast-conserving surgery on 10-year recurrence and 15-year breast cancer death: meta-analysis of individual patient data for 10 801 women in 17 randomised trials. *Lancet*. (2011) 378:1707–16. doi: 10.1016/S0140-6736(11)61629-2
10. Strnad V, Ott OJ, Hildebrandt G, Kauer-Dorner D, Knauerhase H, Major T, et al. 5-year results of accelerated partial breast irradiation using sole interstitial multicatheter brachytherapy versus whole-breast irradiation with boost after breast-conserving surgery for low-risk invasive and *in-situ* carcinoma of the female breast: a randomised, phase 3, non-inferiority trial. *Lancet*. (2016) 387:229–38. doi: 10.1016/S0140-6736(15)00471-7
11. Livi L, Buonamici FB, Simontacchi G, Scotti V, Fambrini M, Compagnucci A, et al. Accelerated partial breast irradiation with IMRT: new technical approach and interim analysis of acute toxicity in a phase iii randomized clinical trial. *Int J Radiat Oncol Biol Phys*. (2010) 77:509–15. doi: 10.1016/j.ijrobp.2009.04.070
12. Aristei C, Maranzano E, Lancellotta V, Chirico L, Zucchetti C, Italiani M, et al. Partial breast irradiation with interstitial multi-catheter high-dose-rate brachytherapy. Long-term results of a phase II prospective study. *Radiother Oncol*. (2017) 124:208–13. doi: 10.1016/j.radonc.2017.07.015
13. Tagliaferri L, Lancellotta V, Colloca G, Marazzi F, Masiello V, Garganese G, et al. Could a personalized strategy using accelerated partial breast irradiation be an advantage for elderly patients? A systematic review of the literature and multidisciplinary opinion. *J Oncol*. (2020) 2020:3928976. doi: 10.1155/2020/3928976
14. Lancellotta V, Kovács G, Tagliaferri L, Perrucci E, Colloca G, Valentini V, et al. Age is not a limiting factor in interventional radiotherapy (brachytherapy) for patients with localized cancer. *BioMed Res Int*. (2018) 2018:2178469. doi: 10.1155/2018/2178469
15. Baumann M, Krause M, Overgaard J, Debus J, Bentzen SM, Daartz J, et al. Radiation oncology in the era of precision medicine. *Nat Rev Cancer*. (2016) 16:234–49. doi: 10.1038/nrc.2016.18
16. National Cancer Registration & Analysis Service and Cancer Research UK. *Chemotherapy, Radiotherapy and Tumour Resections in England: 2013–2014*. London: NCRAS London (2017).
17. McGale P, Taylor C, Correa C, Cutter D, Duane F, Ewertz M, et al. Effect of radiotherapy after mastectomy and axillary surgery on 10-year recurrence and 20-year breast cancer mortality: meta-analysis of individual patient data for 8135 women in 22 randomised trials. *Lancet*. (2014) 383:2127–2135. doi: 10.1016/S0140-6736(14)60488-8
18. Delaney G, Jacob S, Featherstone C, Barton M. The role of radiotherapy in cancer treatment: estimating optimal utilization from a review of evidence-based clinical guidelines. *Cancer*. (2005) 104:1129–37. doi: 10.1002/cncr.21324
19. Onitilo AA, Engel JM, Stankowski RV, Doi SA. Survival comparisons for breast conserving surgery and mastectomy revisited: community experience and the role of radiation therapy. *Clin Med Res*. (2015) 13:65–73. doi: 10.3121/cmr.2014.1245
20. Cao J, Olson R, Tyldesley S, Comparison of recurrence and survival rates after breast-conserving therapy and mastectomy in young women with breast cancer. *Curr Oncol*. (2013) 20:593–601. doi: 10.3747/co.20.1543
21. Poortmans P. Evidence based radiation oncology: breast cancer. *Radiother Oncol*. (2007) 84:84–101. doi: 10.1016/j.radonc.2007.06.002
22. Allemani C, Sant M, Weir HK, Richardson LC, Baili P, Storm H, et al. Breast cancer survival in the US and Europe: A CONCORD high-resolution study. *Int J Cancer*. (2013) 132:1170–81. doi: 10.1002/ijc.27725
23. Eisenhauer EA, Therasse P, Bogaerts J, Schwartz LH, Sargent D, Ford R, et al. New response evaluation criteria in solid tumours: revised RECIST guideline (version 1.1). *Eur J Cancer*. (2009) 45:228–47. doi: 10.1016/j.ejca.2008.10.026
24. Ghasemi M, Nabipour I, Omrani A, Alipour Z, Assadi M. Precision medicine and molecular imaging: new targeted approaches toward cancer therapeutic and diagnosis. *Am J Nuclear Med Mol Imaging*. (2016) 6:310–27.
25. Penet MF, Krishnamachary B, Chen Z, Jin J, Bhujwalla ZM. Molecular imaging of the tumor microenvironment for precision medicine and theranostics. *Adv Cancer Res*. (2014) 124:235–56. doi: 10.1016/B978-0-12-411638-2.00007-0
26. Burrell RA, McGranahan N, Bartek J, Swanton C. The causes and consequences of genetic heterogeneity in cancer evolution. *Nature*. (2013) 501:338–45. doi: 10.1038/nature12625
27. Hanahan D, Weinberg RA. The Hallmarks of Cancer. *Cell*. (2000) 100:57–70. doi: 10.1016/S0092-8674(00)81683-9
28. Hanahan D, Weinberg RA. Hallmarks of cancer: the next generation. *Cell*. (2011) 144:646–74. doi: 10.1016/j.cell.2011.02.013
29. Atkinson AJ Jr, Colburn WA, DeGruttola VG, DeMets DL, Downing GJ, Hoth DF, et al. Biomarkers and surrogate endpoints: preferred definitions and conceptual framework. *Clin Pharmacol Ther*. (2001) 69:89–95. doi: 10.1067/mcp.2001.113989

30. Mandrekar SJ, Sargent DJ. Clinical trial designs for predictive biomarker validation: theoretical considerations and practical challenges. *J Clin Oncol*. (2009) 27:4027–34. doi: 10.1200/JCO.2009.22.3701
31. Polley MYC, Freidlin B, Korn EL, Conley BA, Abrams JS, McShane LM. Statistical and practical considerations for clinical evaluation of predictive biomarkers. *J Natl Cancer Inst*. (2013) 105:1677–83. doi: 10.1093/jnci/djt282
32. Ludwig JA, Weinstein JN. Biomarkers in cancer staging, prognosis and treatment selection. *Nat Rev Cancer*. (2005) 5:845–56. doi: 10.1038/nrc1739
33. Valdora F, Houssami N, Rossi F, Calabrese M, Tagliafico AS. Rapid review: radiomics and breast cancer. *Breast Cancer Res Treat*. (2018) 169:217–29. doi: 10.1007/s10549-018-4675-4
34. Guo W, Li H, Zhu Y, Lan L, Yang S, Drukker K, et al. Prediction of clinical phenotypes in invasive breast carcinomas from the integration of radiomics and genomics data. *J Med Imaging*. (2015) 2:041007. doi: 10.1117/1.JMI.2.4.041007
35. Bickelhaupt S, Paech D, Kickingereder P, Steudle F, Lederer W, Daniel H, et al. Prediction of malignancy by a radiomic signature from contrast agent-free diffusion MRI in suspicious breast lesions found on screening mammography. *J Magn ResonImaging*. (2017) 46:604–16. doi: 10.1002/jmri.25606
36. Perou CM, Sorlie T, Eisen MB, van de Rijn M, Jeffrey SS, Rees CA, et al. Molecular portraits of human breast tumours. *Nature*. (2000) 406:747–52. doi: 10.1038/35021093
37. Sorlie T, Perou CM, Tibshirani R, Aas T, Geisler S, Johnsen H, et al. Gene expression patterns of breast carcinomas distinguish tumor subclasses with clinical implications. *Proc Natl Acad Sci USA*. (2001) 98:10869–74. doi: 10.1073/pnas.191367098
38. Sorlie T, Tibshirani R, Parker J, Hastie T, Marron JS, Nobel A, et al. Repeated observation of breast tumor subtypes in independent gene expression data sets. *Proc Natl Acad Sci USA*. (2003) 100:8418–23. doi: 10.1073/pnas.0932692100
39. Sotiriou C, Neo SY, McShane LM, Korn EL, Long PM, Jazaeri A, et al. Breast cancer classification and prognosis based on gene expression profiles from a population-based study. *Proc Natl Acad Sci USA*. (2003) 100:10393–8. doi: 10.1073/pnas.1732912100
40. Markopoulos C, van de Velde C, Zarca D, Ozmen V, Masetti R. Clinical evidence supporting genomic tests in early breast cancer: do all genomic tests provide the same information? *Eur J Surg Oncol*. (2017) 43:909–20. doi: 10.1016/j.ejso.2016.08.012
41. Sgroi DC, Sestak I, Cuzick J, Zhang Y, Schnabel CA, Schroeder B, et al. Prediction of late distant recurrence in patients with oestrogen-receptor-positive breast cancer: a prospective comparison of the breast-cancer index (BCI) assay, 21-gene recurrence score, and IHC4 in the TransATAC study population. *Lancet Oncol*. (2013) 14:1067–76. doi: 10.1016/S1470-2045(13)70387-5
42. Dubsky P, Brase J, Jakesz R, Rudas M, Singer C, Greil R, et al. The EndoPredict score provides prognostic information on late distant metastases in ER+/HER2– breast cancer patients. *Br J Cancer*. (2013) 109:2959–64. doi: 10.1038/bjc.2013.671
43. Paik S, Shak S, Tang G, Kim C, Baker J, Cronin M, et al. A multigene assay to predict recurrence of tamoxifen-treated, node-negative breast cancer. *N Engl J Med*. (2004) 351:2817–26. doi: 10.1056/NEJMoa041588
44. Tutt A, Wang A, Rowland C, Gillett C, Lau K, Chew K, et al. Risk estimation of distant metastasis in node-negative, estrogen receptor-positive breast cancer patients using an RT-PCR based prognostic expression signature. *BMC Cancer*. (2008) 8:339. doi: 10.1186/1471-2407-8-339
45. Van De Vijver MJ, He YD, Van't Veer LJ, Dai H, Hart AA, Voskuil DW, et al. A gene-expression signature as a predictor of survival in breast cancer. *N Engl J Med*. (2002) 347:1999–2009. doi: 10.1056/NEJMoa021967
46. Parker JS, Mullins M, Cheang MC, Leung S, Voduc D, Vickery T, et al. Supervised risk predictor of breast cancer based on intrinsic subtypes. *J Clin Oncol*. (2009) 27:1160–7. doi: 10.1200/JCO.2008.18.1370
47. Ellis MJ, Suman VJ, Hoog J, Lin L, Snider J, Prat A, et al. Randomized phase II neoadjuvant comparison between letrozole, anastrozole, and exemestane for postmenopausal women with estrogen receptor–rich stage 2 to 3 breast cancer: clinical and biomarker outcomes and predictive value of the baseline PAM50-based intrinsic subtype—ACOSOG Z1031. *J Clin Oncol*. (2011) 29:2342–9. doi: 10.1200/JCO.2010.31.6950
48. Bernier J. Precision medicine for early breast cancer radiotherapy: opening up new horizons? *Crit Rev Oncol Hematol*. (2017) 113:79–82. doi: 10.1016/j.critrevonc.2017.03.015
49. Forker LJ, Choudhury A, Kiltie A. Biomarkers of tumour radiosensitivity and predicting benefit from radiotherapy. *Clin Oncol*. (2015) 27:561–9. doi: 10.1016/j.clon.2015.06.002
50. Hall WA, Bergom C, Thompson RF, Baschnagel AM, Vijayakumar S, Willers H, et al. Precision oncology and genomically guided radiation therapy: a report from the American Society for radiation oncology/American association of physicists in medicine/national cancer institute precision medicine conference. *Int J Radiat Oncol Biol Phys*. (2018) 101:274–84. doi: 10.1016/j.ijrobp.2017.05.044
51. Brenton JD, Carey LA, Ahmed AA, Caldas C. Molecular classification and molecular forecasting of breast cancer: ready for clinical application? *J Clin Oncol*. (2005) 23:7350–60. doi: 10.1200/JCO.2005.03.3845
52. Langlands F, Horgan K, Dodwell D, Smith L. Breast cancer subtypes: response to radiotherapy and potential radiosensitisation. *Br J Radiol*. (2013) 86:20120601. doi: 10.1259/bjr.20120601
53. Carey LA, Perou CM, Livasy CA, Dressler LG, Cowan D, Conway K, et al. Race, breast cancer subtypes, and survival in the Carolina breast cancer study. *JAMA*. (2006) 295:2492–502. doi: 10.1001/jama.295.21.2492
54. Wang Y, Yin Q, Yu Q, Zhang J, Liu Z, Wang S, et al. A retrospective study of breast cancer subtypes: the risk of relapse and the relations with treatments. *Breast Cancer Res Treat*. (2011) 130:489–98. doi: 10.1007/s10549-011-1709-6
55. Smith L, Qutob O, Watson MB, Beavis AW, Potts D, Welham KJ, et al. Proteomic identification of putative biomarkers of radiotherapy resistance: a possible role for the 26S proteasome? *Neoplasia*. (2009) 11:1194–207. doi: 10.1593/neo.09902
56. Nguyen PL, Taghian AG, Katz MS, Niemierko A, Abi Raad RF, Boon WL, et al. Breast cancer subtype approximated by estrogen receptor, progesterone receptor, and HER-2 is associated with local and distant recurrence after breast-conserving therapy. *J Clin Oncol*. (2008) 26:2373–8. doi: 10.1200/JCO.2007.14.4287
57. Stål O, Sullivan S, Wingren S, Skoog L, Rutqvist L, Carstensen J, et al. c-erbB-2 expression and benefit from adjuvant chemotherapy and radiotherapy of breast cancer. *Eur J Cancer*. (1995) 31:2185–90. doi: 10.1016/0959-8049(95)00344-4
58. Kyndi M, Sørensen FB, Knudsen H, Overgaard M, Nielsen HM, Overgaard J. Estrogen receptor, progesterone receptor, HER-2, and response to postmastectomy radiotherapy in high-risk breast cancer: the Danish Breast Cancer Cooperative Group. *J Clin Oncol*. (2008) 26:1419–26. doi: 10.1200/JCO.2007.14.5565
59. Goodman CR, Seagle BLL, Shahabi S, Strauss JB. Oncotype score and benefit of post-mastectomy radiotherapy in T1–2 N1 breast cancer. *Int J Radiat Oncol Biol Phys*. (2017) 99:S53. doi: 10.1016/j.ijrobp.2017.06.134
60. Torres-Roca JF, Eschrich S, Zhao H, Bloom G, Sung J, McCarthy S, et al. Prediction of radiation sensitivity using a gene expression classifier. *Cancer Res*. (2005) 65:7169–76. doi: 10.1158/0008-5472.CAN-05-0656
61. Hall JS, Iype R, Senra J, Taylor J, Armenoult L, Oguejiofor K, et al. Investigation of radiosensitivity gene signatures in cancer cell lines. *PLoS ONE*. (2014) 9:e86329. doi: 10.1371/journal.pone.0086329
62. Eschrich SA, Pramana J, Zhang H, Zhao H, Boulware D, J.-Lee H, et al. A gene expression model of intrinsic tumor radiosensitivity: prediction of response and prognosis after chemoradiation. *Int J Radiat Oncol Biol Phys*. (2009) 75:489–96. doi: 10.1016/j.ijrobp.2009.06.014
63. Ahmed KA, Chinnaiyan P, Fulp WJ, Eschrich S, Torres-Roca JF, Caudell JJ. The radiosensitivity index predicts for overall survival in glioblastoma. *Oncotarget*. (2015) 6:34414–22. doi: 10.18632/oncotarget.5437
64. Torres-Roca J, Erho N, Vergara I, Davicioni E, Jenkins R, Den R, et al. A molecular signature of radiosensitivity (RSI) is an RT-specific biomarker in prostate cancer. *Int J Radiat Oncol Biol Phys*. (2014) 90:S157. doi: 10.1016/j.ijrobp.2014.05.642
65. Strom T, Hoffe SE, Fulp W, Frakes J, Coppola D, Springett GM, et al. Radiosensitivity index predicts for survival with adjuvant radiation in resectable pancreatic cancer. *Radiother Oncol*. (2015) 117:159–64. doi: 10.1016/j.radonc.2015.07.018
66. Ahmed KA, Fulp WJ, Berglund AE, Hoffe SE, Dilling TJ, Eschrich SA, et al. Differences between colon cancer primaries and metastases using

a molecular assay for tumor radiation sensitivity suggest implications for potential oligometastatic SBRT patient selection. *Int J Radiat Oncol Biol Phys*. (2015) 92:837–42. doi: 10.1016/j.ijrobp.2015.01.036
67. Eschrich SA, Fulp WJ, Pawitan Y, Foekens JA, Smid M, J.Martens WM, et al. Validation of a radiosensitivity molecular signature in breast cancer. *Clin Cancer Res*. (2012) 18:5134–43. doi: 10.1158/1078-0432.CCR-12-0891
68. Torres-Roca JF, Fulp WJ, Caudell JJ, Servant N, Bollet MA, van de Vijver M, et al. Integration of a radiosensitivity molecular signature into the assessment of local recurrence risk in breast cancer. *Int J Radiat Oncol Biol Phys*. (2015) 93:631–8. doi: 10.1016/j.ijrobp.2015.06.021
69. Scott JG, Berglund A, Schell MJ, Mihaylov I, Fulp WJ, Yue B, et al. A genome-based model for adjusting radiotherapy dose (GARD): a retrospective, cohort-based study. *Lancet Oncol*. (2017) 18:202–11. doi: 10.1016/S1470-2045(16)30648-9
70. Amundson SA, Do KT, Vinikoor LC, Lee RA, Koch-Paiz CA, Ahn J, et al. Integrating global gene expression and radiation survival parameters across the 60 cell lines of the National Cancer Institute Anticancer Drug Screen. *Cancer Res*. (2008) 68:415–24. doi: 10.1158/0008-5472.CAN-07-2120
71. Yard BD, Adams DJ, Chie EK, Tamayo P, Battaglia JS, Gopal P, et al. A genetic basis for the variation in the vulnerability of cancer to DNA damage. *Nat Commun*. (2016) 7:11428. doi: 10.1038/ncomms11428
72. Eustace A, Mani N, Span PN, Irlam JJ, Taylor J, Betts GN, et al. A 26-gene hypoxia signature predicts benefit from hypoxia-modifying therapy in laryngeal cancer but not bladder cancer. *Clin Cancer Res*. (2013) 19:4879–88. doi: 10.1158/1078-0432.CCR-13-0542
73. Toustrup K, Sørensen BS, M.Metwally AH, Tramm T, Mortensen LS, Overgaard J, et al. Validation of a 15-gene hypoxia classifier in head and neck cancer for prospective use in clinical trials. *Acta Oncologica*. (2016) 55:1091–8. doi: 10.3109/0284186X.2016.1167959
74. Yang L, Taylor J, Eustace A, Irlam JJ, Denley H, Hoskin PJ, et al. A gene signature for selecting benefit from hypoxia modification of radiotherapy for high-risk bladder cancer patients. *Clin Cancer Res*. (2017) 23:4761–8. doi: 10.1158/1078-0432.CCR-17-0038
75. Oh DS, Cheang MC, Fan C, Perou CM. Radiation-induced gene signature predicts pathologic complete response to neoadjuvant chemotherapy in breast cancer patients. *Radiat Res*. (2014) 181:193–207. doi: 10.1667/RR13485.1
76. Kim HS, Kim SC, Kim SJ, Park CH, Jeung HC, Kim YB, et al. Identification of a radiosensitivity signature using integrative metaanalysis of published microarray data for NCI-60 cancer cells. *BMC Genom*. (2012) 13:348. doi: 10.1186/1471-2164-13-348
77. Feng FY, Speers C, Liu M, Jackson WC, Moon D, Rinkinen J, et al. Targeted radiosensitization with PARP1 inhibition: optimization of therapy and identification of biomarkers of response in breast cancer. *Breast Cancer Res Treat*. (2014) 147:81–94. doi: 10.1007/s10549-014-3085-5
78. Jonsson M, Ragnum HB, Julin CH, Yeramian A, Clancy T, Frikstad KAM, et al. Hypoxia-independent gene expression signature associated with radiosensitisation of prostate cancer cell lines by histone deacetylase inhibition. *Br J Cancer*. (2016) 115:929. doi: 10.1038/bjc.2016.278
79. Speers C, Zhao S, Liu M, Bartelink H, Pierce LJ, Feng FY. Development and validation of a novel radiosensitivity signature in human breast cancer. *Clin Cancer Res*. (2015) 21:3667–77. doi: 10.1158/1078-0432.CCR-14-2898
80. Forrest AP, Stewart HJ, Everington D, Prescott RJ, McArdle CS, Harnett AN, et al. Randomised controlled trial of conservation therapy for breast cancer: 6-year analysis of the Scottish trial. *Lancet*. (1996) 348:708–13. doi: 10.1016/S0140-6736(96)02133-2
81. Speers C, Pierce LJ. Molecular signatures of radiation response in breast cancer: towards personalized decision-making in radiation treatment. *Int J Breast Cancer*. (2017) 2017:4279724. doi: 10.1155/2017/4279724
82. Sjöström M, Chang SL, Fishbane N, Davicioni E, Zhao SG, Hartman L, et al. Clinicogenomic radiotherapy classifier predicting the need for intensified locoregional treatment after breast-conserving surgery for early-stage breast cancer. *J Clin Oncol*. (2019) 37:3340–9. doi: 10.1200/JCO.19.00761
83. Tramm T, Kyndi M, Myhre S, Nord S, Alsner J, Sørensen FB, et al. Relationship between the prognostic and predictive value of the intrinsic subtypes and a validated gene profile predictive of loco-regional control and benefit from post-mastectomy radiotherapy in patients with high-risk breast cancer. *Acta Oncologica*. (2014) 53:1337–46. doi: 10.3109/0284186X.2014.925580
84. Niméus-Malmström E, Krogh M, Malmström P, Strand C, Fredriksson I, Karlsson P, et al. Gene expression profiling in primary breast cancer distinguishes patients developing local recurrence after breast-conservation surgery, with or without postoperative radiotherapy. *Breast Cancer Res*. (2008) 10:R34. doi: 10.1186/bcr1997
85. Kreike B, Halfwerk H, Armstrong N, Bult P, Foekens JA, Veltkamp SC, et al. Local recurrence after breast-conserving therapy in relation to gene expression patterns in a large series of patients. *Clin Cancer Res*. (2009) 15:4181–90. doi: 10.1158/1078-0432.CCR-08-2644
86. Albert JM, Liu DD, Shen Y, Pan IW, Y.-Shih CT, Hoffman KE, et al. Nomogram to predict the benefit of radiation for older patients with breast cancer treated with conservative surgery. *J Clin Oncol*. (2012) 30:2837–43. doi: 10.1200/JCO.2011.41.0076
87. Franco P, De Rose F, De Santis MC, Pasinetti N, Lancellotta V, Meduri B, et al. Omission of postoperative radiation after breast conserving surgery: a progressive paradigm shift towards precision medicine. *Clin Transl Radiat Oncol*. (2020) 21:112–9. doi: 10.1016/j.ctro.2020.02.003
88. Hu Z, Huang G, Sadanandam A, Gu S, Lenburg ME, Pai M, et al. The expression level of HJURP has an independent prognostic impact and predicts the sensitivity to radiotherapy in breast cancer. *Breast Cancer Res*. (2010) 12:R18. doi: 10.1186/bcr2487
89. Woolston CM, Storr SJ, Ellis IO, D.Morgan AL, Martin SG. Expression of thioredoxin system and related peroxiredoxin proteins is associated with clinical outcome in radiotherapy treated early stage breast cancer. *Radiother Oncol*. (2011) 100:308–13. doi: 10.1016/j.radonc.2011.05.029
90. Venkitaraman AR. Cancer susceptibility and the functions of BRCA1 and BRCA2. *Cell*. (2002) 108:171–82. doi: 10.1016/S0092-8674(02)00615-3
91. Söderlund K, Skoog L, Fornander T, Askmalm MS. The BRCA1/BRCA2/Rad51 complex is a prognostic and predictive factor in early breast cancer. *Radiother Oncol*. (2007) 84:242–51. doi: 10.1016/j.radonc.2007.06.012
92. Martin A, Greshock J, Rebbeck T, Weber B. *Allele Frequencies of Cytokine Gene Polymorphisms in Caucasians and African Americans*. Chicago, IL: American Journal Of Human Genetics; Univ Chicago Press 5720 South Woodlawn AVE (2000). p. 318.
93. Ford D, Easton D, Stratton M, Narod S, Goldgar D, Devilee P, et al. Genetic heterogeneity and penetrance analysis of the BRCA1 and BRCA2 genes in breast cancer families. *Am J Hum Genet*. (1998) 62:676–89. doi: 10.1086/301749
94. King MC, Marks JH, Mandell JB. Breast and ovarian cancer risks due to inherited mutations in BRCA1 and BRCA2. *Science*. (2003) 302:643–46. doi: 10.1126/science.1088759
95. Struewing JP, Hartge P, Wacholder S, Baker SM, Berlin M, McAdams M, et al. The risk of cancer associated with specific mutations of BRCA1 and BRCA2 among Ashkenazi Jews. *N Engl J Med*. (1997) 336:1401–8. doi: 10.1056/NEJM199705153362001
96. Dantzer F, de la Rubia G, Ménissier-de Murcia J, Hostomsky Z, de Murcia G, Schreiber V. Base excision repair is impaired in mammalian cells lacking Poly (ADP-ribose) polymerase-1. *Biochemistry*. (2000) 39:7559–69. doi: 10.1021/bi0003442
97. Robson M, Im SA, Senkus E, Xu B, Domchek SM, Masuda N, et al. Olaparib for metastatic breast cancer in patients with a germline BRCA mutation. *N Engl J Med*. (2017) 377:523–33. doi: 10.1056/NEJMoa1706450
98. Tucker H, Charles Z, Robertson J, Adam J. NICE guidance on olaparib for maintenance treatment of patients with relapsed, platinum-sensitive, BRCA mutation-positive ovarian cancer. *Lancet Oncol*. (2016) 17:277–8. doi: 10.1016/S1470-2045(16)00062-0
99. Wang L, Mason KA, Ang KK, Buchholz T, Valdecanas D, Mathur A, et al. MK-4827, a PARP-1/-2 inhibitor, strongly enhances response of human lung and breast cancer xenografts to radiation. *Invest New Drugs*. (2012) 30:2113–20. doi: 10.1007/s10637-011-9770-x
100. Lamerz R, Stieber P, Fateh-Moghadam A. Serum marker combinations in human breast cancer. *In Vivo*. (1993) 7:607–13.
101. Dnistrian AM, Schwartz MK, Greenberg EJ, Smith CA, Schwartz DC. Evaluation of CA M26, CA M29, CA 15–3 and CEA as circulating

tumor markers in breast cancer patients. *Tumor Biol*. (1991) 12:82–90. doi: 10.1159/000217692
102. Ebeling FG, Stieber P, Untch M, Nagel D, Konecny GE, Schmitt UM, et al. Serum CEA and CA 15–3 as prognostic factors in primary breast cancer. *Br J Cancer*. (2002) 86:1217–22. doi: 10.1038/sj.bjc.6600248
103. Stieber P, Nagel D, Ritzke C, Rössler N, Kirsch C, Eiermann W, et al. Significance of bone alkaline phosphatase, CA 15–3 and CEA in the detection of bone metastases during the follow-up of patients suffering from breast carcinoma. *Clin Chem Lab Med*. (1992) 30:809–14. doi: 10.1515/cclm.1992.30.12.809
104. Vizcarra E, Lluch A, Cibrian R, Jarque F, Garcia-Conde J. CA15. 3, CEA and TPA tumor markers in the early diagnosis of breast cancer relapse. *Oncology*. (1994) 51:491–6. doi: 10.1159/000227391
105. Duffy MJ, Evoy D, McDermott EW. CA 15–3: uses and limitation as a biomarker for breast cancer. *Clin Chim Acta*. (2010) 411:1869–74. doi: 10.1016/j.cca.2010.08.039
106. Ludovini V, Gori S, Colozza M, Pistola L, Rulli E, Floriani I, et al. Evaluation of serum HER2 extracellular domain in early breast cancer patients: correlation with clinicopathological parameters and survival. *Ann Oncol*. (2008) 19:883–90. doi: 10.1093/annonc/mdm585
107. Molina R, Augé JM, Escudero JM, Filella X, Zanon G, Pahisa J, et al. Evaluation of tumor markers (HER-2/neu oncoprotein, CEA, and CA 15.3) in patients with locoregional breast cancer: prognostic value. *Tumor Biol*. (2010) 31:171–80. doi: 10.1007/s13277-010-0025-9
108. Asgeirsson KS, Agrawal A, Allen C, Hitch A, Ellis IO, Chapman C, et al. Serum epidermal growth factor receptor and HER2 expression in primary and metastatic breast cancer patients. *Breast Cancer Res*. (2007) 9:R75. doi: 10.1186/bcr1788
109. Leyland-Jones B, Smith BR. Serum HER2 testing in patients with HER2-positive breast cancer: the death knell tolls. *Lancet Oncol*. (2011) 12:286–95. doi: 10.1016/S1470-2045(10)70297-7
110. Vader P, Breakefield XO, Wood MJ. Extracellular vesicles: emerging targets for cancer therapy. *Trends Mol Med*. (2014) 20:385–93. doi: 10.1016/j.molmed.2014.03.002
111. Valadi H, Ekström K, Bossios A, Sjöstrand M, Lee JJ, Lötvall JO. Exosome-mediated transfer of mRNAs and microRNAs is a novel mechanism of genetic exchange between cells. *Nat Cell Biol*. (2007) 9:654–59. doi: 10.1038/ncb1596
112. Iero M, Valenti R, Huber V, Filipazzi P, Parmiani G, Fais S, et al. Tumour-released exosomes and their implications in cancer immunity. *Cell Death Differ*. (2008) 15:80–8. doi: 10.1038/sj.cdd.4402237
113. Greening DW, Gopal SK, Mathias RA, Liu L, Sheng J, Zhu HJ, et al. Emerging roles of exosomes during epithelial–mesenchymal transition and cancer progression. *Semin Cell Dev Biol*. (2015) 40:60–71. doi: 10.1016/j.semcdb.2015.02.008
114. Kahlert C, Kalluri R. Exosomes in tumor microenvironment influence cancer progression and metastasis. *J Mol Med*. (2013) 91:431–7. doi: 10.1007/s00109-013-1020-6
115. Wang J, Hendrix A, Hernot S, Lemaire M, De Bruyne E, Van Valckenborgh E, et al. Bone marrow stromal cell–derived exosomes as communicators in drug resistance in multiple myeloma cells. *Blood*. (2014) 124:555–66. doi: 10.1182/blood-2014-03-562439
116. Boelens MC, Wu TJ, Nabet BY, Xu B, Qiu Y, Yoon T, et al. Exosome transfer from stromal to breast cancer cells regulates therapy resistance pathways. *Cell*. (2014) 159:499–513. doi: 10.1016/j.cell.2014.09.051
117. Gray LH, Conger AD, Ebert M, Hornsey S, Scott OCA. The concentration of oxygen dissolved in tissues at the time of irradiation as a factor in radiotherapy. *Br J Radiol*. (1953) 26:638–48. doi: 10.1259/0007-1285-26-312-638
118. Bertout JA, Patel SA, Simon MC. The impact of O2 availability on human cancer. *Nat Rev Cancer*. (2008) 8:967–75. doi: 10.1038/nrc2540
119. Okunieff P, Fenton B, Chen Y. Past, present, and future of oxygen in cancer research. *Adv Exp Med Biol*. (2005) 566:213–22. doi: 10.1007/0-387-26206-7_29
120. Vos O. Role of endogenous thiols in protection. *Adv Space Res*. (1992) 12:201–7. doi: 10.1016/0273-1177(92)90109-B
121. Eldh M, Ekström K, Valadi H, Sjöstrand M, Olsson B, Jernås M, et al. Exosomes communicate protective messages during oxidative stress; possible role of exosomal shuttle RNA. *PLoS ONE*. (2010) 5:e15353. doi: 10.1371/journal.pone.0015353
122. Thomas SN, Liao Z, Clark D, Chen Y, Samadani R, Mao L, et al. Exosomal proteome profiling: a potential multi-marker cellular phenotyping tool to characterize hypoxia-induced radiation resistance in breast cancer. *Proteomes*. (2013) 1:87–108. doi: 10.3390/proteomes1020087
123. Kallergi G, Papadaki MA, Politaki E, Mavroudis D, Georgoulias V, Agelaki S. Epithelial to mesenchymal transition markers expressed in circulating tumour cells of early and metastatic breast cancer patients. *Breast Cancer Res*. (2011) 13:R59. doi: 10.1186/bcr2896
124. Massagué J, Obenauf AC. Metastatic colonization by circulating tumour cells. *Nature*. (2016) 529:298–306. doi: 10.1038/nature17038
125. Krishnamurthy S, Cristofanilli M, Singh B, Reuben J, Gao H, Cohen EN, et al. Detection of minimal residual disease in blood and bone marrow in early stage breast cancer. *Cancer*. (2010) 116:3330–7. doi: 10.1002/cncr.25145
126. Bidard FC, Mathiot C, Delaloge S, Brain E, Giachetti S, De Cremoux P, et al. Single circulating tumor cell detection and overall survival in nonmetastatic breast cancer. *Ann Oncol*. (2009) 21:729–33. doi: 10.1093/annonc/mdp391
127. Janni WJ, Rack B, Terstappen LW, J.-Pierga Y, Taran FA, Fehm T, et al. Pooled analysis of the prognostic relevance of circulating tumor cells in primary breast cancer. *Clin Cancer Res*. (2016) 22:2583–93. doi: 10.1158/1078-0432.CCR-15-1603
128. Rack B, Schindlbeck C, Jückstock J, Andergassen U, Hepp P, Zwingers T, et al. Circulating tumor cells predict survival in early average-to-high risk breast cancer patients. *J Natl Cancer Inst*. (2014) 106:dju066. doi: 10.1093/jnci/dju066
129. Franken B, De Groot MR, Mastboom WJ, Vermes I, van der Palen J, Tibbe AG, et al. Circulating tumor cells, disease recurrence and survival in newly diagnosed breast cancer. *Breast Cancer Res*. (2012) 14:R133. doi: 10.1186/bcr3333
130. Lucci A, Hall CS, Lodhi AK, Bhattacharyya A, Anderson AE, Xiao L, et al. Circulating tumour cells in non-metastatic breast cancer: a prospective study. *Lancet Oncol*. (2012) 13:688–95. doi: 10.1016/S1470-2045(12)70209-7
131. Bidard FC, Belin L, Delaloge S, Lerebours F, Ngo C, Reyal F, et al. Time-dependent prognostic impact of circulating tumor cells detection in non-metastatic breast cancer: 70-month analysis of the REMAGUS02 study. *Int J Breast Cancer*. (2013) 2013:130470. doi: 10.1155/2013/130470
132. Bidard FC, Hajage D, Bachelot T, Delaloge S, Brain E, Campone M, et al. Assessment of circulating tumor cells and serum markers for progression-free survival prediction in metastatic breast cancer: a prospective observational study. *Breast Cancer Res*. (2012) 14:R29. doi: 10.1186/bcr3114
133. Molloy TJ, Bosma AJ, Baumbusch LO, Synnestvedt M, Borgen E, Russnes HG, et al. The prognostic significance of tumour cell detection in the peripheral blood versus the bone marrow in 733 early-stage breast cancer patients. *Breast Cancer Res*. (2011) 13:R61. doi: 10.1186/bcr2898
134. Hall C, Karhade M, Laubacher B, Anderson A, Kuerer H, DeSynder S, et al. Circulating tumor cells after neoadjuvant chemotherapy in stage I–III triple-negative breast cancer. *Ann Surg Oncol*. (2015) 22:552–8. doi: 10.1245/s10434-015-4600-6
135. Hall CS, Karhade MG, J.Bauldry BB, Valad LM, Kuerer HM, DeSnyder SM, et al. Prognostic value of circulating tumor cells identified before surgical resection in nonmetastatic breast cancer patients. *J Am Coll Surg*. (2016) 223:20–9. doi: 10.1016/j.jamcollsurg.2016.02.021
136. Goodman CR, Seagle BLL, T.Friedl WP, Rack B, Lato K, Fink V, et al. Association of circulating tumor cell status with benefit of radiotherapy and survival in early-stage breast cancer. *JAMA Oncol*. (2018) 4:e180163. doi: 10.1001/jamaoncol.2018.0163
137. Speers C, Rugo HS. Circulating tumors cells as a biomarker of radiation benefit. *JAMA Oncol*. (2018) 4:e180194. doi: 10.1001/jamaoncol.2018.0194
138. Tsé C, Gauchez AS, Jacot W, Lamy PJ. HER2 shedding and serum HER2 extracellular domain: biology and clinical utility in breast cancer. *Cancer Treat Rev*. (2012) 38:133–42. doi: 10.1016/j.ctrv.2011.03.008
139. Shapiro CL, Recht A. Side effects of adjuvant treatment of breast cancer. *N Engl J Med*. (2001) 344:1997–2008. doi: 10.1056/NEJM200106283442607
140. Wazer DE, DiPetrillo T, Schmidt-Ullrich R, Weld L, Smith T, Marchant D, et al. Factors influencing cosmetic outcome and complication risk after conservative surgery and radiotherapy for early-stage breast carcinoma. *J Clin Oncol*. (1992) 10:356–63. doi: 10.1200/JCO.1992.10.3.356

141. Azria D, Gourgou S, Sozzi W, Zouhair A, Mirimanoff R, Kramar A, et al. Concomitant use of tamoxifen with radiotherapy enhances subcutaneous breast fibrosis in hypersensitive patients. *Br J Cancer*. (2004) 91:1251–60. doi: 10.1038/sj.bjc.6602146
142. Collette S, Collette L, Budiharto T, Horiot JC, Poortmans PM, Struikmans H, et al. Predictors of the risk of fibrosis at 10 years after breast conserving therapy for early breast cancer–A study based on the EORTC trial 22881–10882 'boost versus no boost'. *Eur J Cancer*. (2008) 44:2587–99. doi: 10.1016/j.ejca.2008.07.032
143. Colletta A, Wakefield L, Howell F, Van Roozendaal K, Danielpour D, Ebbs S, et al. Anti-oestrogens induce the secretion of active transforming growth factor beta from human fetal fibroblasts. *Br J Cancer*. (1990) 62:405–9. doi: 10.1038/bjc.1990.307
144. Aristei C, Palumbo I, Capezzali G, Farneti A, Bini V, Falcinelli L, et al. Outcome of a phase II prospective study on partial breast irradiation with interstitial multi-catheter high-dose-rate brachytherapy. *Radiother Oncol*. (2013) 108:236–41. doi: 10.1016/j.radonc.2013.08.005
145. Hau E, Browne L, Capp A, Delaney GP, Fox C, Kearsley JH, et al. The impact of breast cosmetic and functional outcomes on quality of life: long-term results from the St. George and Wollongong randomized breast boost trial. *Breast Cancer Res Treat*. (2013) 139:115–23. doi: 10.1007/s10549-013-2508-z
146. Taghian NR, Miller CL, Jammallo LS, O'Toole J, Skolny MN. Lymphedema following breast cancer treatment and impact on quality of life: a review. *Crit Rev Oncol Hematol*. (2014) 92:227–34. doi: 10.1016/j.critrevonc.2014.06.004
147. Back M, Guerrieri M, Wratten C, Steigler A. Impact of radiation therapy on acute toxicity in breast conservation therapy for early breast cancer. *Clin Oncol*. (2004) 16:12–6. doi: 10.1016/j.clon.2003.08.005
148. Henríquez-Hernández LA, Bordón E, Pinar B, Lloret M, Rodríguez-Gallego C, Lara PC. Prediction of normal tissue toxicity as part of the individualized treatment with radiotherapy in oncology patients. *Surg Oncol*. (2012) 21:201–6. doi: 10.1016/j.suronc.2011.12.002
149. Pinar B, Lara PC, Lloret M, Bordón E, Núñez MI, Villalobos M, et al. Radiation-induced DNA damage as a predictor of long-term toxicity in locally advanced breast cancer patients treated with high-dose hyperfractionated radical radiotherapy. *Radiat Res*. (2007) 168:415–22. doi: 10.1667/RR0746.1
150. Rached E, Schindler R, Beer K, Vetterli D, Greiner R. No predictive value of the micronucleus assay for patients with severe acute reaction of normal tissue after radiotherapy. *Eur J Cancer*. (1998) 34:378–83. doi: 10.1016/S0959-8049(97)00373-0
151. Słonina D, Klimek M, Szpytma T, Gasinska A. Comparison of the radiosensitivity of normal-tissue cells with normal-tissue reactions after radiotherapy. *Int J Radiat Biol*. (2000) 76:1255–64. doi: 10.1080/09553000050134483
152. Alapetite C, Thirion P, de la Rochefordière A, Cosset JM, Moustacchi E. Analysis by alkaline comet assay of cancer patients with severe reactions to radiotherapy: defective rejoining of radioinduced DNA strand breaks in lymphocytes of breast cancer patients. *Int J Cancer*. (1999) 83:83–90. doi: 10.1002/(SICI)1097-0215(19990924)83:1<83::AID-IJC16>3.0.CO;2-8
153. Müller WU, Bauch T, Stüben G, Sack H, Streffer C. Radiation sensitivity of lymphocytes from healthy individuals and cancer patients as measured by the comet assay. *Radiat Environ Biophys*. (2001) 40:83–9. doi: 10.1007/s004110000087
154. Widel M, Jedrus S, Lukaszczyk B, Raczek-Zwierzycka K, Swierniak A. Radiation-induced micronucleus frequency in peripheral blood lymphocytes is correlated with normal tissue damage in patients with cervical carcinoma undergoing radiotherapy. *Radiat Res*. (2003) 159:713–21. doi: 10.1667/0033-7587
155. Ozsahin M, Crompton NE, Gourgou S, Kramar A, Li L, Shi Y, et al. CD4 and CD8 T-lymphocyte apoptosis can predict radiation-induced late toxicity: a prospective study in 399 patients. *Clin Cancer Res*. (2005) 11:7426–33. doi: 10.1158/1078-0432.CCR-04-2634
156. Henríquez-Hernández LA, Carmona-Vigo R, Pinar B, Bordón E, Lloret M, Núñez MI, et al. Combined low initial DNA damage and high radiation-induced apoptosis confers clinical resistance to long-term toxicity in breast cancer patients treated with high-dose radiotherapy. *Radiat Oncol*. (2011) 6:60. doi: 10.1186/1748-717X-6-60
157. Carr ZA, Land CE, Kleinerman RA, Weinstock RW, Stovall M, Griem ML, et al. Coronary heart disease after radiotherapy for peptic ulcer disease. *Int J Radiat Oncol Biol Phys*. (2005) 61:842–50. doi: 10.1016/j.ijrobp.2004.07.708
158. Aznar MC, Korreman S, Pedersen AN, Persson GF, Josipovic M, Specht L. Evaluation of dose to cardiac structures during breast irradiation. *Br J Radiol*. (2011) 84:743–46. doi: 10.1259/bjr/12497075
159. Lohr F, El-Haddad M, Dobler B, Grau R, Wertz HJ, Kraus-Tiefenbacher U, et al. Potential effect of robust and simple IMRT approach for left-sided breast cancer on cardiac mortality. *Int J Radiat Oncol Biol Phys*. (2009) 74:73–80. doi: 10.1016/j.ijrobp.2008.07.018
160. van den Bogaard VA, Ta BD, van der Schaaf A, Bouma AB, Middag AM, Bantema-Joppe EJ, et al. Validation and modification of a prediction model for acute cardiac events in patients with breast cancer treated with radiotherapy based on three-dimensional dose distributions to cardiac substructures. *J Clin Oncol*. (2017) 35:1171–8. doi: 10.1200/JCO.2016.69.8480
161. Darby SC, Ewertz M, McGale P, Bennet AM, Blom-Goldman U, Brønnum D, et al. Risk of ischemic heart disease in women after radiotherapy for breast cancer. *N Engl J Med*. (2013) 368:987–98. doi: 10.1056/NEJMoa1209825
162. Carver JR, Shapiro CL, Ng A, Jacobs L, Schwartz C, Virgo KS, et al. American Society of clinical oncology clinical evidence review on the ongoing care of adult cancer survivors: cardiac and pulmonary late effects. *J Clin Oncol*. (2007) 25:3991–4008. doi: 10.1200/JCO.2007.10.9777
163. Mant J, Doust J, Roalfe A, Barton P, Cowie M, Glasziou P, et al. Systematic review and individual patient data meta-analysis of diagnosis of heart failure, with modelling of implications of different diagnostic strategies in primary care. *Health Technol Assess*. (2009) 13:1–207. doi: 10.3310/hta13320
164. Nellessen U, Zingel M, Hecker H, Bahnsen J, Borschke D. Effects of radiation therapy on myocardial cell integrity and pump function: which role for cardiac biomarkers? *Chemotherapy*. (2010) 56:147–52. doi: 10.1159/000313528
165. D'Errico MP, Grimaldi L, Petruzzelli MF, Gianicolo EA, Tramacere F, Monetti A, et al. N-Terminal Pro-B–type natriuretic peptide plasma levels as a potential biomarker for cardiac damage after radiotherapy in patients with left-sided breast cancer. *Int J Radiat Oncol Biol Phys*. (2012) 82:e239–46. doi: 10.1016/j.ijrobp.2011.03.058
166. Lipshultz SE, Landy DC, Lopez-Mitnik G, Lipsitz SR, Hinkle AS, Constine LS, et al. Cardiovascular status of childhood cancer survivors exposed and unexposed to cardiotoxic therapy. *J Clin Oncol*. (2012) 30:1050–7. doi: 10.1200/JCO.2010.33.7907
167. Cardinale D, Sandri MT, Colombo A, Colombo N, Boeri M, Lamantia G, et al. Prognostic value of troponin I in cardiac risk stratification of cancer patients undergoing high-dose chemotherapy. *Circulation*. (2004) 109:2749–54. doi: 10.1161/01.CIR.0000130926.51766.CC
168. Garrone O, Crosetto N, Nigro CL, Catzeddu T, Vivenza D, Monteverde M, et al. Prediction of anthracycline cardiotoxicity after chemotherapy by biomarkers kinetic analysis. *Cardiovasc Toxicol*. (2012) 12:135–42. doi: 10.1007/s12012-011-9149-4
169. Hughes-Davies L, Sacks D, Rescigno J, Howard S, Harris J. Serum cardiac troponin T levels during treatment of early-stage breast cancer. *J Clin Oncol*. (1995) 13:2582–4. doi: 10.1200/JCO.1995.13.10.2582
170. Erven K, Florian A, Slagmolen P, Sweldens C, Jurcut R, Wildiers H, et al. Subclinical cardiotoxicity detected by strain rate imaging up to 14 months after breast radiation therapy. *Int J Radiat Oncol Biol Phys*. (2013) 85:1172–8. doi: 10.1016/j.ijrobp.2012.09.022
171. Skyttä T, Tuohinen S, Boman E, Virtanen V, Raatikainen P, Kellokumpu-Lehtinen PL. Troponin T-release associates with cardiac radiation doses during adjuvant left-sided breast cancer radiotherapy. *Radiat Oncol*. (2015) 10:141. doi: 10.1186/s13014-015-0436-2
172. Mueller C, Laule-Kilian K, Christ A, Brunner–La Rocca HP, Perruchoud AP. Inflammation and long-term mortality in acute congestive heart failure. *Am Heart J*. (2006) 151:845–50. doi: 10.1016/j.ahj.2005.06.046
173. Windram JD, Loh PH, Rigby AS, Hanning I, Clark AL, Cleland JG. Relationship of high-sensitivity C-reactive protein to prognosis and other prognostic markers in outpatients with heart failure. *Am Heart J*. (2007) 153:1048–55. doi: 10.1016/j.ahj.2007.03.044
174. Arruda-Olson AM, Enriquez-Sarano M, Bursi F, Weston SA, Jaffe AS, Killian JM, et al. Left ventricular function and C-reactive protein

levels in acute myocardial infarction. *Am J Cardiol*. (2010) 105:917–21. doi: 10.1016/j.amjcard.2009.11.025

175. Morris PG, Chen C, Steingart R, Fleisher M, Lin N, Moy B, et al. Troponin I and C-reactive protein are commonly detected in patients with breast cancer treated with dose-dense chemotherapy incorporating trastuzumab and lapatinib. *Clin Cancer Res*. (2011) 17:3490–9. doi: 10.1158/1078-0432.CCR-10-1359
176. Lipshultz SE, Miller TL, Scully RE, Lipsitz SR, Rifai N, Silverman LB, et al. Changes in cardiac biomarkers during doxorubicin treatment of pediatric patients with high-risk acute lymphoblastic leukemia: associations with long-term echocardiographic outcomes. *J Clin Oncol*. (2012) 30:1042–9. doi: 10.1200/JCO.2010.30.3404
177. Ky B, Putt M, Sawaya H, French B, Januzzi JL, Sebag IA, et al. Early increases in multiple biomarkers predict subsequent cardiotoxicity in patients with breast cancer treated with doxorubicin, taxanes, and trastuzumab. *J Am Coll Cardiol*. (2014) 63:809–16. doi: 10.1016/j.jacc.2013.10.061
178. Chalubinska-Fendler J, Graczyk L, Piotrowski G, Wyka K, Nowicka Z, Tomasik B, et al. Lipopolysaccharide-binding protein is an early biomarker of cardiac function after radiation therapy for breast cancer. *Int J Radiat Oncol Biol Phys*. (2019) 104:1074–83. doi: 10.1016/j.ijrobp.2019.04.002
179. Chalubinska-Fendler J, Fendler W, Spych M, Wyka K, Luniewska-Bury J, Fijuth J. Lipopolysaccharide-binding protein is efficient in biodosimetry during radiotherapy of lung cancer. *Biomed Rep*. (2016) 5:450–4. doi: 10.3892/br.2016.739
180. Tian S, Hirshfield KM, Jabbour SK, Toppmeyer D, Haffty BG, Khan AJ, et al. Serum biomarkers for the detection of cardiac toxicity after chemotherapy and radiation therapy in breast cancer patients. *Front Oncol*. (2014) 4:277. doi: 10.3389/fonc.2014.00277

Conflict of Interest: The authors declare that the research was conducted in the absence of any commercial or financial relationships that could be construed as a potential conflict of interest.

frontiers in Oncology

ORIGINAL RESEARCH
published: 28 July 2020
doi: 10.3389/fonc.2020.01135

Evaluation of Postoperative Radiotherapy Effect on Survival of Resected Stage III-N2 Non-small Cell Lung Cancer Patients

Fei Gao[1], *Nan Li*[2], *YongMei Xu*[1] *and GuoWang Yang*[1]*

[1] Department of Oncology & Hematology, Beijing Hospital of Traditional Chinese Medicine, Capital Medical University, Beijing, China, [2] Graduate School, China Academy of Chinese Medical Sciences, Beijing, China

Objective: The role of postoperative radiotherapy (PORT) in resected stage IIIA-N2 non-small cell lung cancer (NSCLC) patients remains controversial. This study aimed to explore the effect of PORT on survival of resected stage IIIA-N2 NSCLC patients.

Methods: Resected stage IIIA-N2 NSCLC patients aged 18 years or older were identified from the SEER (Surveillance, Epidemiology, and End Results) database from 2010 to 2015. Cox regression analysis was used to identify factors including PORT associated with survival time. A subgroup analysis of patients stratified by number of lymph node metastases was also performed. Overall survival (OS) and overall mortality were compared among the different groups.

Results: A total of 3,445 patients were included in the study. Multivariate Cox analysis showed that PORT had no significant impact on survival of patients with <6 positive lymph node [hazard ratio (HR) = 1.012, $P = 0.858$, 95% CI: 0.886–1.156]. Postoperative chemotherapy (POCT) (HR = 0.605, $P < 0.001$, 95% CI: 0.468–0.783) and PORT (HR = 0.724, $P = 0.007$, 95% CI: 0.574–0.914) are both favorable prognostic factors for stage IIIA-N2 patients with ≥6 positive lymph nodes. In 2,735 patients who featured <6 number of positive regional lymph nodes, patients who received PORT had better survival and lower 3-years and 5-years overall mortality rate than patients who underwent surgery only (41 vs. 28 months, $P < 0.015$). There was no significant difference in the survival of postoperative patients who underwent POCT in view of whether received PORT (44 vs. 53 months, $P = 0.176$). A total of 710 patients who featured ≥6 number of positive regional lymph node metastasis were divided into two groups by PORT. PORT did not prolong survival for postoperative patients who did not receive chemotherapy (12 vs. 15 months, $P = 0.632$). PORT showed a significant advantage in influencing OS in patients who received PORT combined with POCT as compared with those who received POCT only (32 vs. 25 months, $P = 0.006$).

Conclusions: For IIIA-N2 patients with <6 lymph node metastases, use of PORT can be encouraged to improve survival. For patients with ≥6 positive lymph nodes, PORT combined with POCT significantly improved OS and decreased overall mortality.

Keywords: non-small cell lung cancer, stage IIIA-N2, postoperative radiotherapy, overall survival, SEER database

OPEN ACCESS

Edited by:
Francesco Cellini, Catholic University of the Sacred Heart, Italy

Reviewed by:
Stefano Vagge, IRCCS Ospedale Policlinico San Martino, Italy
Antonella Martino, Agostino Gemelli University Polyclinic, Italy

***Correspondence:**
GuoWang Yang
zyyyzlk@163.com

Specialty section:
This article was submitted to Radiation Oncology, a section of the journal Frontiers in Oncology

Received: *14 April 2020*
Accepted: *05 June 2020*
Published: *28 July 2020*

Citation:
Gao F, Li N, Xu Y and Yang G (2020) Evaluation of Postoperative Radiotherapy Effect on Survival of Resected Stage III-N2 Non-small Cell Lung Cancer Patients. Front. Oncol. 10:1135. doi: 10.3389/fonc.2020.01135

INTRODUCTION

Lung cancer is one kind of the most frequent malignant tumors with the highest morbidity and mortality in the world. Non-small cell lung cancer (NSCLC) is the most common type, accounting for 80–85% of lung cancer (1), among which stage IIIA-N2 patients account for about 20% (2, 3). The benefit of radical surgery is limited for stage IIIA-N2 patients. Previous studies have shown that the 5-years survival rate of patients with stage IIIA-N2 NSCLC after lung cancer radical pneumonectomy was only 15–20% (4). The main cause of postoperative failure was local recurrence or distant metastasis (5, 6). Nearly 40% of patients have local recurrence or regional lymph node metastasis within 5 years after surgery, even if after a complete resection of lung cancer. Therefore, complete surgical resection combined with postoperative adjuvant therapy is still the main treatment mode for stage IIIA-N2 NSCLC patients.

Clinical evidence showed that postoperative chemotherapy (POCT) could improve the long-term survival of patients (7, 8). However, it has been reported that the local failure rate still exists despite complete resection and postoperative adjuvant chemotherapy. Local recurrence indicated the importance of local postoperative adjuvant therapy. Postoperative radiotherapy (PORT), as a kind of local treatment, can theoretically improve the local control rate and improve the survival of patients. However, whether PORT can improve the survival rate of stage IIIA-N2 NSCLC remains controversial. The selection of stage IIIA-N2 patients who can benefit from PORT is confusing for clinicians. Prospective randomized controlled studies of PORT for resected stage IIIA-N2 NSCLC patients are mostly single-center, small-sample-size studies, the radiotherapy technology used is old, and the radiation dose and range are not uniform, which will reduce the effectiveness of the existing clinical evidence. Our study was based on a population-based cohort to provide more evidence for the application of PORT in resected stage IIIA-N2 NSCLC patients.

MATERIALS AND METHODS

This retrospective study, which was approved by Ethics Committee of Beijing Hospital of Traditional Chinese Medicine, Capital Medical University, retrieved data from the SEER (Surveillance, Epidemiology, and End Results) database using SEER*STAT 8.3.6 software. Permission to access the custom data file in the SEER program was obtained, and the reference number was 14026-Nov2018. The SEER database, which aimed to reduce the cancer burden in Americans, recorded the incidence, mortality, and morbidity of millions of cancer patients in the United States over the past 40 years. At present, the number of registration stations has expanded to 18. These registration stations operated with the SEER*STAT software, a powerful computer tool for statistical analysis, and submitted data to NCI twice a year for classification, statistics, and aggregation.

We extracted data of lung cancer patients registered from 2010 to 2015. Patients who met the following criteria were included in this study: (1) adults aged 18 years or older; (2) patients with pathologically confirmed NSCLC (9); their histologic types selected were coded as 8012/3,8013/3, 8022/3, 8031/3, 8032/3, 8033/3, 8035/3, 8046/3, 8050/3, 8052/3, 8070/3, 8071/3, 8072/3, 8074/3, 8082/3, 8083/3, 8084/3, 8123/3, 8140/3,8200/3, 8201/3, 8250/3, 8252/3, 8253/3, 8255/3, 8260/3, 8310/3, 8323/3, 8430/3, 8480/3,8481/3, 8490/3, 8550/3, 8560/3, 8570/3, 8574/3, and 8980/3; (3) patients who were diagnosed with stage IIIA-N2 NSCLC according to the guidelines of the American Joint Committee on Cancer (AJCC, 7th Edition); (4) NSCLC patients who had underwent either lobectomy or pneumonectomy; (5) the number of lymphadenectomy and positive lymph node metastasis was recorded after surgical operation; and (6) complete radiotherapy information record (patients who received postoperative adjuvant radiotherapy or did not receive radiotherapy).

Patients with the following conditions were excluded from this study: (1) patients with incomplete information registration required by the research; and (2) patients whose survival time was <1 month.

Variables extracted from the SEER database include the following: age at diagnosis, year of diagnosis, sex, race recode, primary site (main bronchus, upper lobe, middle lobe, lower lobe, and overlapping lesion of lung), International Classification of Diseases for Oncology (ICD-O) 3 Hist/behave, grade, derived AJCC T, RX summ-surg prim site, regional nodes positive, radiation sequence with surgery, chemotherapy recode, survival months, vital status recode, COD to site recode, SEER cause-specific death classification, and SEER other cause of death classification.

For a better analysis, all variables are converted to categorical variables. The chi-square test was used to evaluate the unadjusted association between the PORT and other clinicopathological categorical variables of interest. The hazard ratio (HR) was determined by univariate and multivariate Cox proportional hazard models. The aforementioned statistical calculations were carried out using SPSS 19.0 software. Overall survival (OS) was defined as the time from the beginning of the diagnosis until death of any cause or until the last follow-up date. The survival analysis was performed using Kaplan–Meier curves with P value determined by log-rank method. Figures of survival curve were drawn by "ggplot2," "survminer," and "survival" packages in R; the version of R was 3.6.0. All statistical tests were two-sided, and $P < 0.05$ was considered statistically significant.

RESULTS

The Correlation Between Clinical Parameters and Postoperative Radiotherapy Use of IIIA-N2 Non-small Cell Lung Cancer Patients

We identified 220,265 lung cancer patients registered in 2010–2015. According to the inclusion criteria, 3,445 patients were

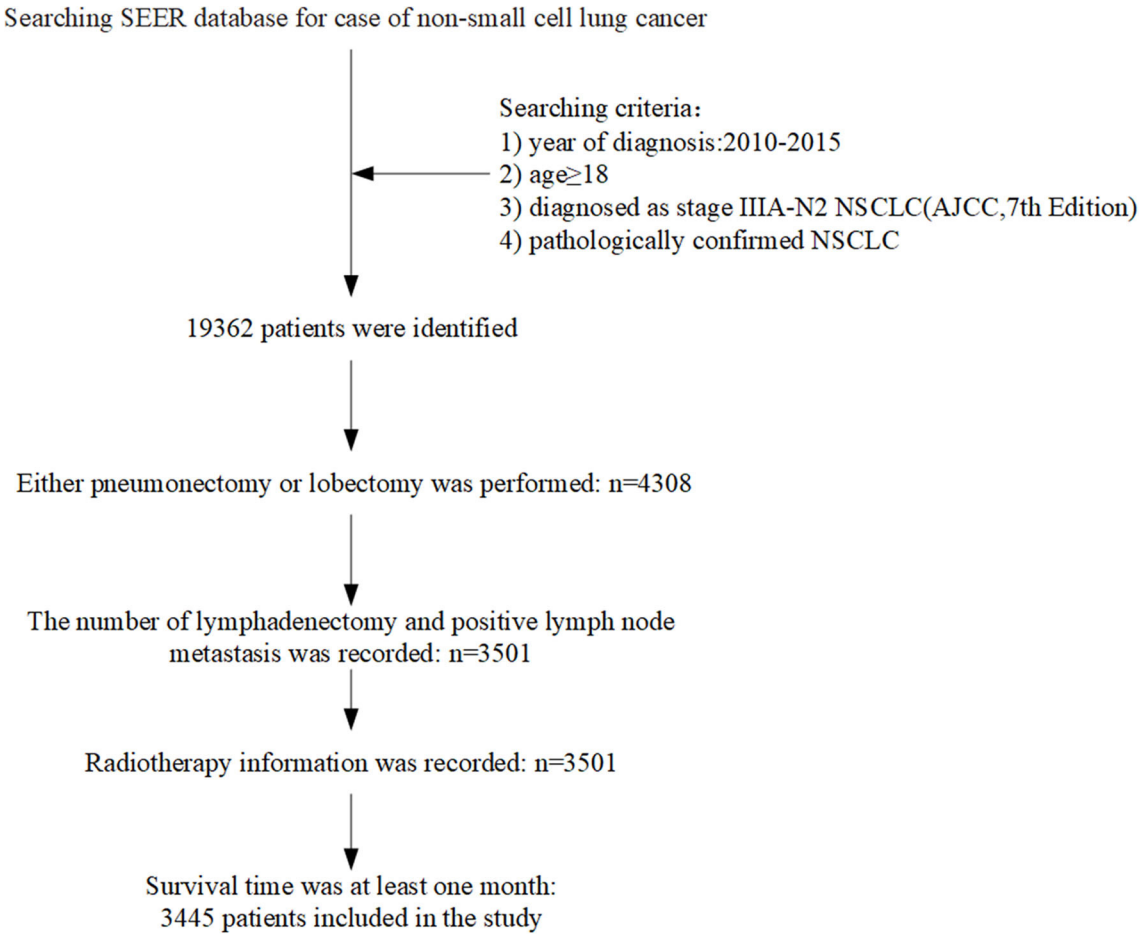

FIGURE 1 | Flow chart showed selection of non-small cell lung cancer (NSCLC) patients registered in the SEER (Surveillance, Epidemiology, and End Results) from 2010 to 2015 in this study.

included in this study. **Figure 1** showed the flow chart of cases selection. The median age at diagnosis was 67 years (age ranging from 19 to 91). A total of 1,568 (45.52%) patients received PORT. The proportion of patients who received radiotherapy differed in age, primary site of tumors, pathological grading of tumors, and whether they were treated with chemotherapy ($P < 0.05$). There was no significant difference in gender, year of diagnosis, race, T stage, number of positive regional lymph nodes, and pathological type between patients who received PORT and those not received PORT. The results are shown in **Table 1**.

Univariate Analysis of Clinical Parameters Affecting the Prognosis of IIIA-N2 Non-small Cell Lung Cancer Patients

PORT and POCT were favorable prognostic factors and associated with better OS in univariate analyses of all IIIA-N2 patients. Adverse prognostic factors included age (≥60 years old), male, non-adenocarcinoma pathological type, higher T stage, and ≥6 number of positive regional lymph nodes. We divided all the patients into two groups according to the number of positive lymph node metastases. The previous prognostic factors were consistent in a univariate survival analysis of IIIA-N2 NSCLC patients with <6 positive lymph node metastases, whereas the pathological type was not the prognostic factor in patients with ≥6 positive lymph node metastases. The results are shown in **Table 2**.

Multivariate Analysis of Clinical Parameters Affecting the Prognosis of IIIA-N2 Non-small Cell Lung Cancer Patients

The multivariate survival analysis of all patients showed that age (≥60 years), being male, non-adenocarcinoma pathological type, higher T stage, and ≥6 number of positive regional lymph nodes were independent risk factors for prognosis, indicating a shorter survival period. POCT were favorable prognostic factors and related to longer survival period.

We conducted a subgroup multivariate survival analysis according to the number of positive lymph node metastases (<6 positive lymph nodes and ≥6 positive lymph nodes). In a

TABLE 1 | The correlation between clinical parameters and PORT use.

Clinical parameters	No. of patients who did not receive PORT	No. of Patients who received PORT	No. of patients	*P*
Age at diagnosis				<0.001
<60	367 (19.6%)	467 (29.8%)	834 (24.2%)	
≥60	1,510 (80.4%)	1,101 (70.2%)	2,611 (75.8%)	
Gender				0.532
Male	934 (49.8%)	797 (50.8%)	1,731 (50.2%)	
Female	943 (50.2%)	771 (49.2%)	1,714 (49.8%)	
Race				0.565
Black	186 (9.9%)	139 (8.9%)	325 (9.4%)	
White	1,534 (81.7%)	1,293 (82.5%)	2,827 (82.1%)	
Others	157 (8.4%)	136 (8.7%)	293 (8.5%)	
Year of diagnosis				0.584
2010	345 (18.4%)	272 (17.3%)	617 (17.9%)	
2011	333 (17.7%)	261 (16.6%)	594 (17.2%)	
2012	309 (16.5%)	277 (17.7%)	586 (17.0%)	
2013	307 (16.4%)	238 (15.2%)	545 (15.8%)	
2014	291 (15.5%)	260 (16.6%)	551 (16.0%)	
2015	292 (15.6%)	260 (16.6%)	552 (16.0%)	
Primary tumor site				0.004
Main bronchus	16 (0.9%)	18 (1.1%)	34 (1.0%)	
Upper lobe	1,045 (55.7%)	921 (58.7%)	1,966 (57.1%)	
Middle lobe	82 (4.4%)	93 (5.9%)	175 (5.1%)	
Lower lobe	671 (35.7%)	508 (32.4%)	1,179 (34.2%)	
Overlapping lesion	47 (2.5%)	21 (1.3%)	68 (2.0%)	
Unknown	16 (0.9%)	7 (0.4%)	23 (0.7%)	
Pathology				0.755
Adenocarcinoma	1,359 (72.4%)	1,153 (73.5%)	2,512 (72.9%)	
Squamous cell	417 (22.2%)	333 (21.2%)	750 (21.8%)	
Others	101 (5.4%)	82 (5.2%)	183 (5.3%)	
Pathological grade				<0.001
I	111 (5.9%)	67 (4.3%)	178 (5.2%)	
II	802 (42.7%)	630 (40.2%)	1,432 (41.6%)	
III	825 (44.0%)	675 (43.0%)	1,500 (43.5%)	
IV	24 (1.3%)	24 (1.5%)	48 (1.4%)	
Unknown	115 (6.1%)	172 (11.0%)	287 (8.3%)	
T				0.320
T1	510 (27.2%)	410 (26.1%)	920 (26.7%)	
T2	1,001 (53.3%)	820 (52.3%)	1,821 (52.9%)	
T3	366 (19.5%)	338 (21.6%)	704 (20.4%)	
POCT				<0.001
No	726 (38.7%)	101 (6.4%)	827 (24.0%)	
Yes	1,151 (61.3%)	1,467 (93.6%)	2,618 (76.0%)	
No. of positive lymph nodes				0.053
<6	1,513 (80.6%)	1,222 (77.9%)	2,735 (79.4%)	
≥6	364 (19.4%)	346 (22.1%)	710 (20.6%)	

Pathological grade I, well-differentiated; II, moderately differentiated; III, poorly differentiated; IV, undifferentiated, anaplastic.
PORT, postoperative radiotherapy; POCT, postoperative chemotherapy.

group of patients with <6 positive lymph node metastases, the results showed that PORT had no significant impact on survival (HR = 1.012, $P = 0.858$, 95% CI: 0.886–1.156). POCT had a positive effect on survival in IIIA-N2 patients with <6 positive lymph node metastases (HR = 0.573, $P < 0.001$, 95% CI: 0.498–0.660). Chemotherapy can prolong the survival of patients. The

TABLE 2 | Univariate analysis of clinical parameters affecting the prognosis of IIIA-N2 NSCLC patients.

Parameters	All patients (n = 3,445)			No. of patients with< 6 positive lymph nodes (n = 2,735)			No. of patients with≥ 6 positive lymph nodes (n = 710)		
	HR	95% CI	*P*	HR	95% CI	*P*	HR	95% CI	*P*
PORT									
No		1.00 (Ref)			1.00 (Ref)			1.00 (Ref)	
Yes	0.793	0.715–0.881	<0.001	0.836	0.741–0.943	0.004	0.623	0.506–0.766	<0.001
Age at diagnosis									
<60		1.00 (Ref)			1.00 (Ref)			1.00 (Ref)	
≥60	1.497	1.316–1.702	<0.001	1.535	1.319–1.786	<0.001	1.492	1.169–1.903	<0.001
Gender									
Male		1.00 (Ref)			1.00 (Ref)			1.00 (Ref)	
Female	0.671	0.605–0.745	<0.001	0.641	0.568–0.723	<0.001	0.791	0.644–0.972	0.026
Race									
Black		1.00 (Ref)			1.00 (Ref)			1.00 (Ref)	
White	1.180	0.983–1.416	0.076	1.215	0.979–1.507	0.077	1.137	0.804–1.607	0.467
Others	0.902	0.649–1.172	0.438	0.846	0.618–1.158	0.296	1.067	0.663–1.718	0.789
Year of diagnosis									
2010		1.00 (Ref)			1.00 (Ref)			1.00 (Ref)	
2011	1.031	0.892–1.191	0.682	1.085	0.916–1.283	0.345	0.898	0.676–1.192	0.456
2012	0.994	0.853–1.158	0.939	1.056	0.884–1.262	0.545	0.848	0.629–1.145	0.282
2013	0.928	0.782–1.102	0.397	0.985	0.808–1.200	0.878	0.847	0.598–1.199	0.348
2014	0.849	0.691–1.044	0.121	0.862	0.075–1.100	0.232	0.828	0.561–1.220	0.339
2015	0.800	0.565–1.133	0.208	0.801	0.527–1.217	0.298	0.770	0.412–1.439	0.413
Primary tumor site									
Main bronchus		1.00 (Ref)			1.00 (Ref)			1.00 (Ref)	
Upper lobe	0.833	0.491–1.412	0.479	0.930	0.463–1.869	0.839	0.840	0.372–1.893	0.673
Middle lobe	0.837	0.471–1.488	0.544	0.950	0.450–2.007	0.894	0.737	0.294–1.846	0.515
Lower lobe	1.039	0.611–1.767	0.887	1.168	0.580–2.353	0.663	0.973	0.430–2.204	0.948
Overlapping lesion	1.259	0.679–2.334	0.465	1.218	0.547–2.711	0.630	1.947	0.729–5.196	0.183
Unknown	0.933	0.414–2.100	0.867	1.642	0.634–4.257	0.307	0.169	0.020–1.407	0.100
Pathology									
Adenocarcinoma		1.00 (Ref)			1.00 (Ref)			1.00 (Ref)	
Squamous cell	1.336	1.184–1.507	<0.001	1.419	1.238–1.625	<0.001	1.227	0.943–1.597	0.127
Others	1.367	1.106–1.691	0.004	1.474	1.165–1.865	0.001	1.177	0.711–1.949	0.526
Pathological grade									
I		1.00 (Ref)			1.00 (Ref)			1.00 (Ref)	
II	0.978	0.766–1.247	0.855	1.023	0.774–1.352	0.873	0.751	0.453–1.244	0.266
III	1.247	0.980–1.587	0.073	1.266	0.961–1.668	0.093	1.045	0.636–1.719	0.861
IV	1.513	0.954–2.399	0.078	1.664	0.979–2.831	0.060	0.936	0.369–2.377	0.889
Unknown	0.945	0.694–1.286	0.718	0.878	0.614–1.255	0.474	1.213	0.655–2.247	0.539
T									
T1		1.00 (Ref)			1.00 (Ref)			1.00 (Ref)	
T2	1.220	1.073–1.386	0.002	1.220	1.055–1.411	0.007	1.092	0.835–1.429	0.519
T3	1.640	1.412–1.905	<0.001	1.640	1.381–1.949	<0.001	1.432	1.056–1.942	0.021
POCT									
No		1.00 (Ref)			1.00 (Ref)			1.00 (Ref)	
Yes	0.558	0.499–0.624	<0.001	0.561	0.494–0.638	<0.001	0.503	0.401–0.631	<0.001
No. of positive lymph nodes									
<6		1.00 (Ref)			—			—	
≥6	1.556	1.382–1.752	<0.001	—	—	—	—	—	—

Pathological grade I, well differentiated; II, moderately differentiated; III, poorly differentiated; IV, undifferentiated, anaplastic.
HR, hazard ratio; Ref, reference; PORT, postoperative radiotherapy; POCT, postoperative chemotherapy; NSCLC, non-small cell lung cancer.

TABLE 3 | Multivariate analysis of clinical parameters affecting the prognosis of IIIA-N2 NSCLC patients.

Parameters	All patients (n = 3,445)			No. of patients with <6 positive lymph nodes (n = 2,735)			No. of patients with ≥6 positive lymph nodes (n = 710)		
	HR	95% CI	*P*	HR	95% CI	*P*	HR	95% CI	*P*
PORT									
No		1.00 (Ref)			1.00 (Ref)			1.00 (Ref)	
Yes	0.931	0.830–1.045	0.226	1.012	0.886–1.156	0.858	0.724	0.574–0.914	0.007
Age at diagnosis									
<60		1.00 (Ref)			1.00 (Ref)			1.00 (Ref)	
≥60	1.322	1.158–1.510	<0.001	1.303	1.114–1.524	0.001	1.356	1.051–1.748	0.019
Gender									
Male		1.00 (Ref)			1.00 (Ref)			1.00 (Ref)	
Female	0.696	0.626–0.775	<0.001	0.667	0.589–0.755	<0.001	0.776	0.627–0.961	0.020
Race									
Black		1.00 (Ref)			1.00 (Ref)			1.00 (Ref)	
White	1.091	0.907–1.312	0.357	1.104	0.889–1.372	0.371	1.090	0.765–1.553	0.632
Other	0.833	0.639–1.085	0.175	0.757	0.551–1.039	0.085	1.084	0.661–1.777	0.749
Year of diagnosis									
2010		1.00 (Ref)			1.00 (Ref)			1.00 (Ref)	
2011	1.028	0.888–1.189	0.713	1.039	0.877–1.232	0.657	0.971	0.725–1.301	0.844
2012	1.026	0.880–1.196	0.745	1.066	0.891–1.276	0.483	0.943	0.693–1.281	0.706
2013	0.964	0.810–1.146	0.675	0.987	0.808–1.206	0.900	0.884	0.619–1.264	0.500
2014	0.871	0.708–1.073	0.194	0.870	0.680–1.111	0.264	0.846	0.572–1.253	0.404
2015	0.799	0.564–1.132	0.207	0.819	0.538–1.246	0.351	0.772	0.413–1.444	0.418
Primary tumor site									
Main bronchus		1.00 (Ref)			1.00 (Ref)			1.00 (Ref)	
Upper lobe	1.073	0.628–1.833	0.797	1.232	0.608–2.498	0.563	0.857	0.372–1.976	0.717
Middle lobe	1.119	0.624–2.006	0.705	1.280	0.600–2.734	0.523	0.831	0.325–2.125	0.699
Lower lobe	1.274	0.744–2.181	0.377	1.461	0.719–2.968	0.295	1.016	0.439–2.353	0.970
Overlapping lesion	1.487	0.799–2.768	0.211	1.523	0.680–3.411	0.306	1.663	0.609–4.536	0.321
Unknown	0.892	0.394–2.020	0.784	1.926	0.737–5.035	0.181	0.148	0.017–1.251	0.079
Pathology									
Adenocarcinoma		1.00 (Ref)			1.00 (Ref)			1.00 (Ref)	
Squamous cell	1.159	1.022–1.316	0.022	1.194	1.035–1.378	0.015	1.037	0.784–1.371	0.800
Others	1.244	0.994–1.558	0.057	1.296	1.009–1.664	0.043	0.999	0.587–1.698	0.996
Pathological grade									
I		1.00 (Ref)			1.00 (Ref)			1.00 (Ref)	
II	0.960	0.750–1.228	0.745	0.950	0.717–1.259	0.722	0.978	0.580–1.650	0.934
III	1.159	0.906–1.483	0.239	1.119	0.845–1.482	0.432	1.291	0.764–2.183	0.341
IV	1.211	0.752–1.950	0.432	1.323	0.763–2.297	0.319	1.021	0.382–2.729	0.967
Unknown	1.029	0.749–1.412	0.861	0.891	0.617–1.285	0.536	1.516	0.790–2.906	0.211
T									
T1		1.00 (Ref)			1.00 (Ref)			1.00 (Ref)	
T2	1.161	1.020–1.322	0.024	1.210	1.044–1.403	0.011	1.021	0.773–1.347	0.886
T3	1.492	1.280–1.738	<0.001	1.531	1.284–1.825	<0.001	1.420	1.035–1.947	0.030
POCT									
No		1.00 (Ref)			1.00 (Ref)			1.00 (Ref)	
Yes	0.573	0.507–0.648	<0.001	0.573	0.498–0.660	<0.001	0.605	0.468–0.783	<0.001
No. of positive lymph nodes									
<6		1.00 (Ref)			—			—	
≥6	1.602	1.420–1.807	<0.001	—	—	—	—	—	—

Pathological grade I, well-differentiated; II, moderately differentiated; III, poorly differentiated; IV, undifferentiated, anaplastic.
HR, hazard ratio; Ref, reference; PORT, post operative radiotherapy; POCT, postoperative chemotherapy; NSCLC, non-small cell lung cancer.

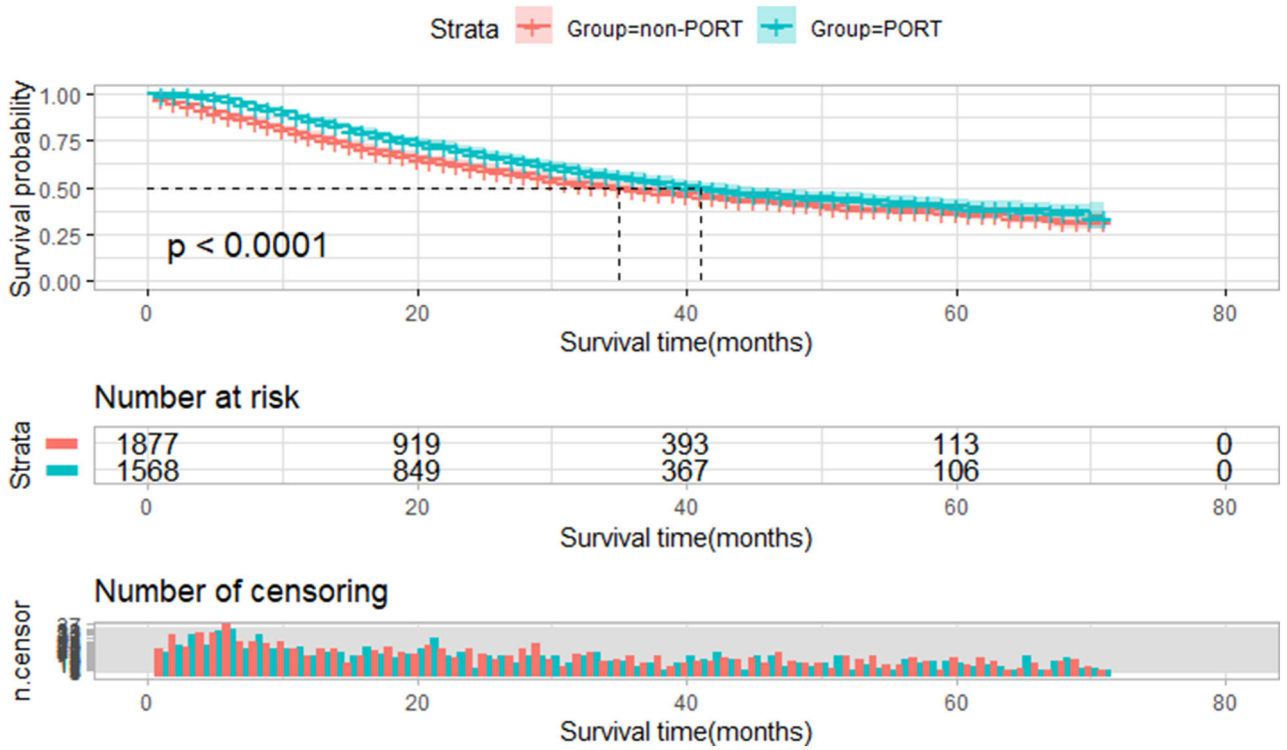

FIGURE 2 | Overall survival of all selected patients stratified by postoperative radiotherapy (PORT). Overall survival of all patients treated with PORT ($n = 1,568$) vs. patients not treated with PORT ($n = 1,877$) ($P < 0.001$).

multivariate survival analysis showed that POCT (HR = 0.605, $P < 0.001$, 95% CI: 0.468–0.783) and PORT (HR = 0.724, $P = 0.007$, 95% CI: 0.574–0.914) are both favorable prognostic factors for stage IIIA-N2 patients with ≥6 positive lymph nodes; POCT and PORT can significantly improve OS. The multivariate analysis results are shown in **Table 3**.

Effect of Postoperative Radiotherapy on Overall Survival of IIIA-N2 Patients Divided by Number of Positive Lymph Node Metastases

Among 3,445 IIIA-N2 NSCLC patients, PORT showed a statistically significant survival advantage relative to non-PORT (41 vs. 35 months, $P < 0.001$, **Figure 2**).

A total of 2,735 patients who featured <6 number of positive regional lymph node metastasis were divided into two groups by PORT. We compared the survival differences between the two groups. There was a significant statistical difference in survival between these two groups; median survival time of patients with PORT was 44 months, longer than the median survival time of those without PORT (41 months, $P = 0.003$, **Figure 3A**). We further conducted a subgroup analysis to explore the impact of PORT on OS. In 2,735 patients without POCT, patients who received PORT had better survival than patients who underwent surgery treatment only (41 vs. 28 months, $P = 0.015$, **Figure 3B**). In 2,060 patients with POCT, there was no significant difference in the survival of postoperative patients who underwent POCT in view of whether received PORT; although the result was not statistically significant, the survival of patients who received POCT combined with PORT seemed to be worse than that of patients who received POCT (44 vs. 53 months, $P = 0.176$, **Figure 3C**).

Similarly, 710 patients who featured ≥6 number of positive regional lymph node metastasis were divided into two groups by PORT. Compared with that of patients who received PORT, the median survival time of patients who did not receive PORT was significantly shortened (32 vs. 22 months, $P < 0.001$, **Figure 4A**). The result of a subgroup analysis showed that for 152 patients without POCT, PORT did not prolong survival for postoperative patients who did not receive chemotherapy (12 vs. 15 months, $P = 0.632$). Kaplan–Meier plot is presented in **Figure 4B**. Among the 328 patients who received PORT combined with POCT and 230 patients who received POCT, PORT showed a significant advantage in influencing OS in these patients compared with those who received POCT only (32 vs. 25 months, $P = 0.006$). The result is shown **Figure 4C**.

Overall Mortality of IIIA-N2 Patients Treated With Different Therapy

We analyzed the death outcomes of IIIA-N2 patients stratified by number of positive regional lymph nodes. In the group of 2,735 patients who featured <6 number of positive regional lymph node metastasis, the 3 and 5-years overall mortality rates

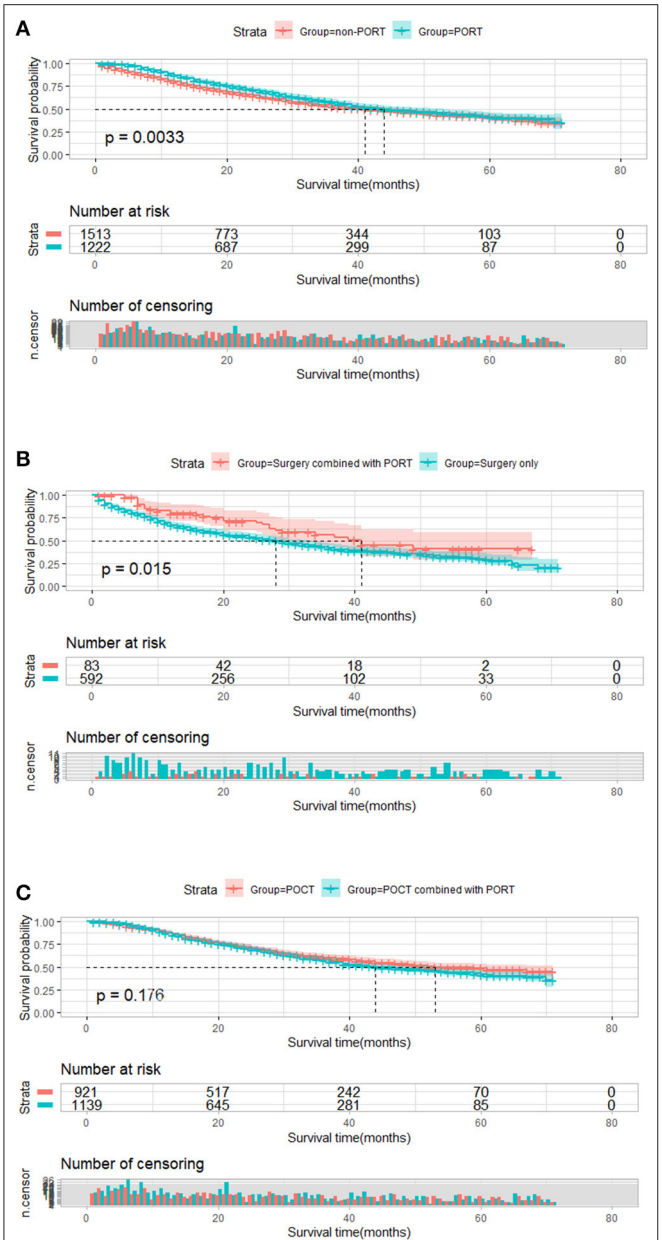

FIGURE 3 | Overall survival of patients who featured <6 number of positive regional lymph node metastasis stratified by postoperative radiotherapy (PORT). **(A)** Overall survival of patients who featured <6 number of positive regional lymph node metastasis treated with PORT ($n = 1,222$) vs. patients not treated with PORT ($n = 1,513$) ($P = 0.003$). **(B)** Overall survival of patients who featured <6 number of positive regional lymph node metastasis treated with surgery combined with PORT ($n = 83$) vs. patients treated with surgery only ($n = 592$) ($P = 0.015$). **(C)** Plot of overall survival for 2,060 patients who featured <6 number of positive regional lymph node metastasis received postoperative chemotherapy (POCT) stratified by PORT use. Patients who received POCT combined with PORT ($n = 1,139$) vs. patients who received POCT ($n = 921$) ($P = 0.176$).

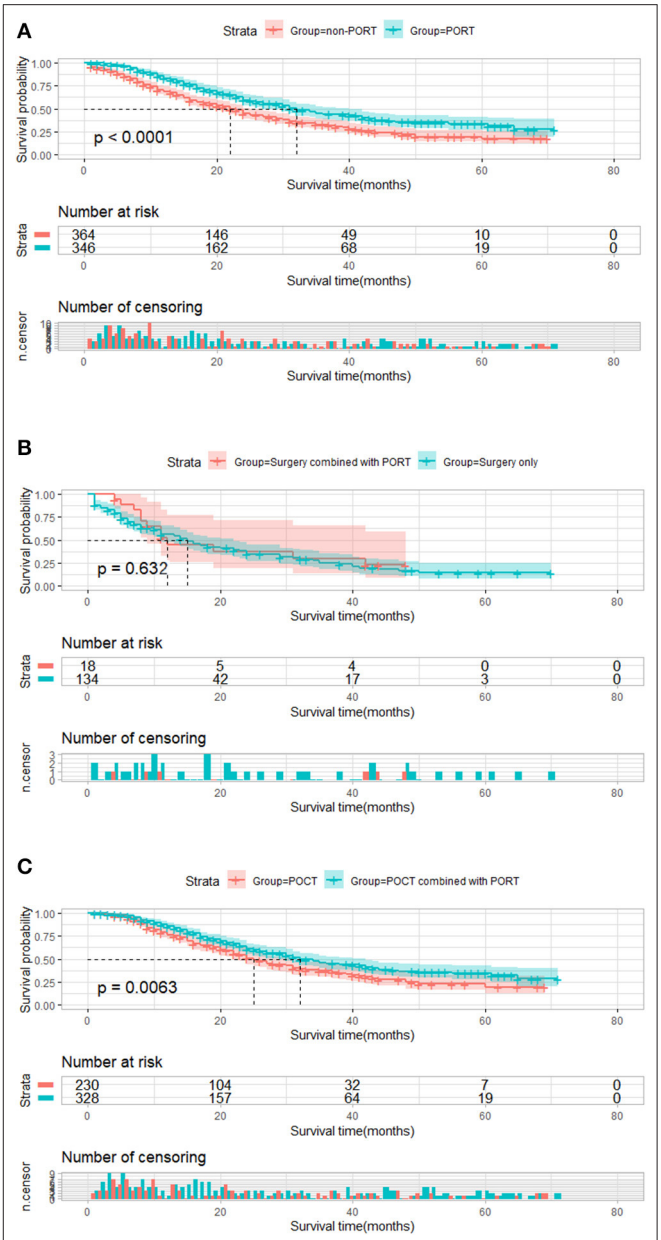

FIGURE 4 | Overall survival of patients who featured ≥6 number of positive regional lymph node metastasis stratified by postoperative radiotherapy (PORT). **(A)** Overall survival of patients who featured ≥6 number of positive regional lymph node metastasis treated with PORT ($n = 346$) vs. patients not treated with PORT ($n = 364$) ($P < 0.001$). **(B)** Overall survival of patients who featured ≥6 number of positive regional lymph node metastasis treated with surgery combined with PORT ($n = 18$) vs. patients treated with surgery only ($n = 134$) ($P = 0.632$). **(C)** Plot of overall survival for 558 patients who featured ≥6 number of positive regional lymph node metastasis received postoperative chemotherapy (POCT) stratified by PORT use. Patients who received POCT combined with PORT ($n = 328$) vs. patients who received POCT ($n = 230$) ($P = 0.0063$).

of patients treated with surgery combined with PORT were significantly lower than those of patients treated with surgery alone ($P = 0.014$); the 3 and 5-years overall mortality rates of patients treated with surgery combined with PORT were 43.55 and 59.25%, respectively; and in patients treated with surgery alone, these rates were 58.53% and 71.06% (**Figure 5A**).

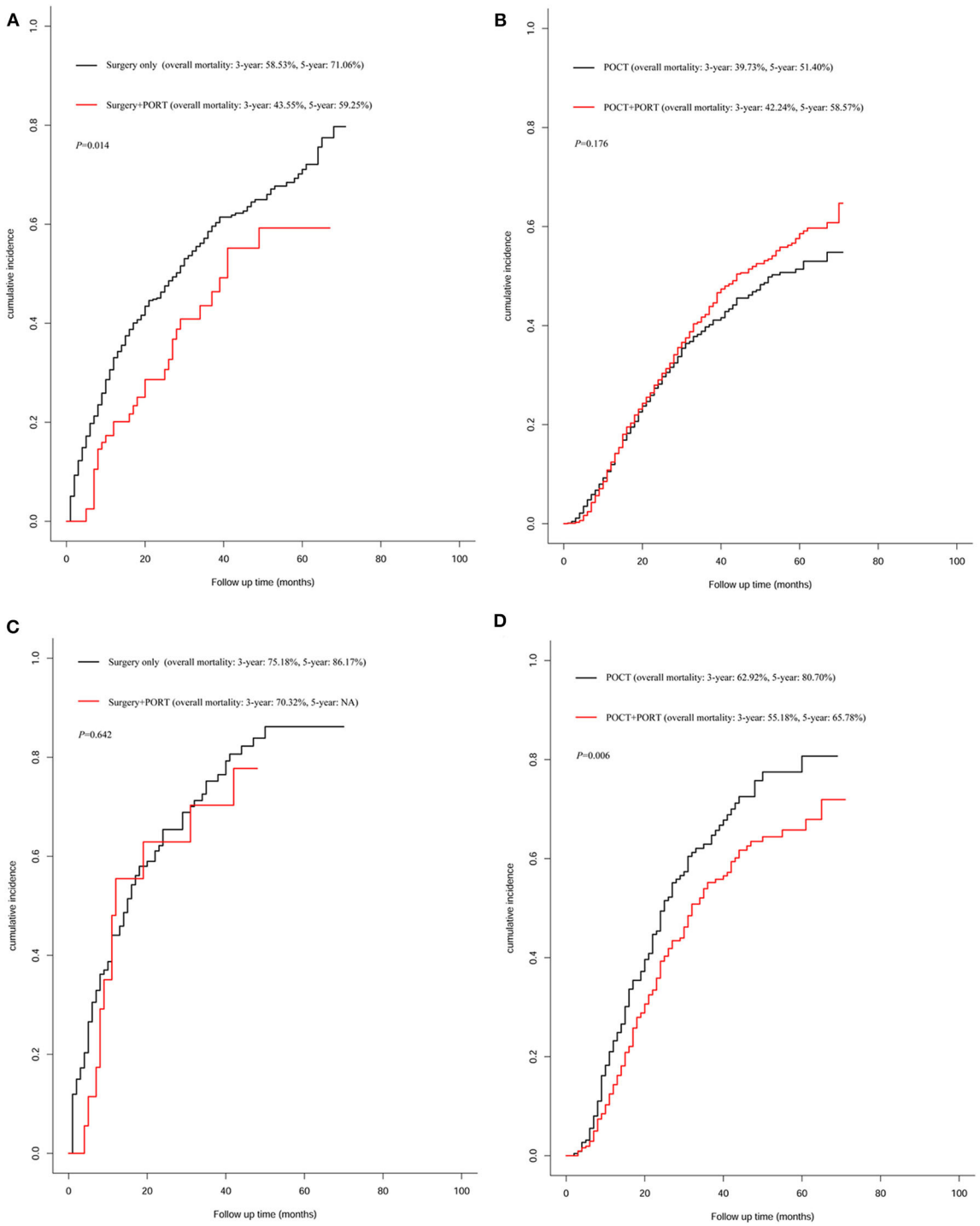

FIGURE 5 | Analysis for overall mortality of patients treated with different therapy. **(A)** Overall mortality of patients who featured <6 number of positive regional lymph node metastasis treated with surgery combined with postoperative radiotherapy (PORT) vs. patients treated with surgery only ($P = 0.014$). **(B)** Overall mortality of patients who featured <6 number of positive regional lymph node metastasis received postoperative chemotherapy (POCT) combined with PORT vs. patients who received POCT ($P = 0.176$). **(C)** Overall mortality of patients who featured ≥6 number of positive regional lymph node metastasis treated with surgery combined with PORT vs. patients treated with surgery only ($P = 0.642$). **(D)** Overall mortality of patients who featured ≥6 number of positive regional lymph node metastasis received POCT combined with PORT vs. patients who received POCT ($P = 0.006$).

Compared with patients who received POCT, the 3 and 5-years overall mortality rates were not different in patients treated with POCT combined with PORT ($P = 0.176$, **Figure 5B**).

In the group of 710 patients who featured ≥6 number of positive regional lymph node metastasis, PORT did not reduce overall mortality compared with mortality of patients who received surgery alone ($P = 0.642$, **Figure 5C**). For patients who received POCT, PORT can significantly reduce mortality; the result showed that the 3-years mortality rate decreased by 7.74% and the 5-years mortality rate decreased by 14.92% caused by PORT ($P = 0.006$, **Figure 5D**).

DISCUSSION

Stage IIIA-N2 NSCLC is a highly heterogeneous disease. The survival rate of stage IIIA-N2 patients after radical surgery was varied in different reported literatures. Even after complete resection, nearly 30% patients will suffer local recurrence or regional lymph node metastasis within 5 years (10). POCT can improve the disease-free survival (DFS) and OS by killing the local residual lesions and micrometastasis. National Comprehensive Cancer Network (NCCN) guidelines recommended POCT as a standard treatment for IIIA-N2 NSCLC patients. PORT, theoretically, can kill the residual tumor cells in the surgical field and significantly reduce the local recurrence rate of IIIA-N2 patients. The impact of the number of positive lymph nodes on the resected IIIA-N2 prognosis has been confirmed by many studies. Different N2 situations determine different prognoses and different treatment strategies. However, owing to the lack of research on the effect of PORT on NSCLC patients with stage IIIA-N2, it is still controversial whether PORT can bring OS benefits to IIIA-N2 patients. And also, owing to the lack of positive lymph node metastasis site records in SEER database and space limitation, we decided to stratify the analysis only for the number of positive nodes. Our study attempted to answer the clinical question: Does the state of N2 affect the PORT effect?

The largest postoperative radiotherapy meta-analysis of NSCLC conducted by PORT Meta-analysis Trialists Group revealed that the effect of PORT on IIIA-N2 patients was not clear (11). Kim et al. (12) evaluated the effect of PORT on stage III A-N2 NSCLC, and they found that PORT significantly improved the local control rate of stage III A-N2 NSCLC but did not prolong the OS period. But several studies have confirmed that PORT can prolong survival and reduce local recurrence in IIIA-N2 patients. Lally et al. (13) demonstrated that PORT increased the 5-years survival rate of pN2 patients from 20% to 27% and reduced the risk of death by 14.5%. The ANITA study (14) showed that PORT increased the 5-years survival rate of stage IIIA-N2 NSCLC from 34% to 47%. Herskovic et al. (15) showed that PORT could improve the survival of IIIA-N2 NSCLC patients, that PORT displayed a 17% reduced hazard of death as compared with non-PORT, and that the median overall survival was 53.1 months for PORT compared with 44.5 months for non-PORT. Based on the above different research conclusions, the 2017 version of American Society of Clinical Oncology (ASCO) guidelines does not recommend the routine use of adjuvant radiotherapy for IIIA-N2 patients; instead, the benefits and risks of adjuvant radiotherapy for each N2 patient should be evaluated in various aspects after operation. But the 2017 version of NCCN guidelines recommend that POCT or concurrent chemotherapy and radiotherapy should be used as adjuvant treatment for N2 patients who underwent complete resection. Corso et al. (16) retrospectively analyzed 30,552 patients with stage II-IIIA NSCLC who underwent R0 resection in the National Cancer Database (NCDB) from 1998 to 2006, 3,430 of whom received postoperative radiotherapy. The results revealed that the 5-years survival rate of stage N2 patients treated with PORT was improved (27.8 vs. 34.1%, $P < 0.001$), and the absolute survival rate was increased by 6.3% compared with that of patients who did not receive PORT. Sakib et al. (17) showed that PORT could significantly improve local control rate and survival of resected stage IIIA-N2 NSCLC patients, regardless of whether they received chemotherapy.

We included surgically resected IIIA-N2 lung cancer patients in the study, and the exact removed number of lymph nodes in all patients was recorded. All postoperative patients met the definition of N2 in the AJCC 7th Edition in SEER database. Therefore, the definition of N2 is not a clinical diagnosis but a postoperative confirmation.

Our results demonstrated for IIIA-N2 NSCLC patients that the survival time of patients who received PORT is significantly longer than that of non-PORT patients, which was similar to the previous research conclusion. However, the survival time of IIIA-N2 NSCLC patients was significantly different, and the number of lymph node metastasis was related to the prognosis of NSCLC. Can all N2 patients benefit from PORT regardless of number of lymph node metastases? Should PORT be a necessary and conventional treatment for all IIIA-N2 patients? We stratified the N2 patients according to the number of lymph node metastases and analyzed the benefits of PORT in different groups.

For patients with <six lymph node metastases, median survival of patients treated with surgery alone was 28 months, and the median survival of patients who received PORT treatment after radical surgery was extended to 41 months. PORT could prolong survival time as compared with no adjuvant therapy after surgery if these patients did not undergo POCT for some reason. PORT reduced the 3 and 5-years mortality rates by 14.98 and 11.81%, respectively. However, for patients with ≥6 number of positive regional lymph nodes metastasis, if they do not receive POCT, PORT did not improve survival and did not reduce mortality. We speculated that PORT can be used as an effective supplement treatment to surgery for patients with <6 lymph node metastases. Compared with surgery alone, use of PORT could be converted into survival benefits by reducing the local recurrence rate. Therefore, we suggested that for patients who cannot tolerate POCT, if their physical condition permits, PORT could be used as a recommended therapy.

Previous studies have confirmed the necessity of POCT in resectable IIIA-N2 patients. Does PORT improve survival on the basis of chemotherapy? Mikell et al. (18) analyzed 2,115 patients with NSCLC in N2 stage who received POCT from 2004 to 2006 in NCDB database, and they concluded that compared with the control group, PORT can improve the 5-years survival rate (39.8 vs. 34.7%, $P = 0.048$). Lei et al. (19) showed that compared with POCT, PORT combined with

TABLE 4 | Strategy for postoperative adjuvant treatment of resected stage III A-N2 NSCLC.

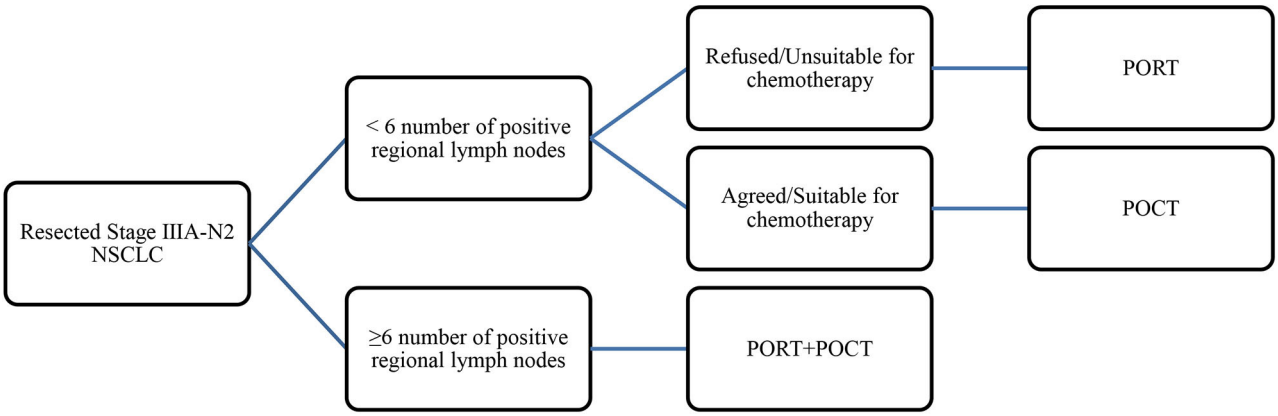

NSCLC, non-small cell lung cancer.

POCT was beneficial to OS of IIIA-N2 NSCLC patients, but not to DFS. Our results revealed that for patients with <6 lymph node metastases, PORT combined with POCT therapy has no significant benefit compared with POCT. Although it is not statistically significant, the median survival time of PORT combined with POCT group seems to be shorter than that of POCT group. But for the patients with ≥6 number of positive regional lymph node metastasis, PORT combined with POCT therapy is necessary. Compared with the median survival time of 25 months in the chemotherapy group, the treatment of PORT combined with POCT can prolong OS and increase the median survival time to 32 months. Meanwhile, PORT combined with POCT therapy can reduce the 3 and 5-years mortality rates by 7.74% and 14.92%, respectively. We speculated that for IIIA-N2 patients with ≥6 positive lymph nodes, the risk of local recurrence and distant metastasis are higher than those of other IIIA patients, so surgery alone is not enough; local and systemic treatment should be strengthened to reduce recurrence and metastasis in order to prolong the survival period. PORT has a beneficial effect on survival by eliminating the local micrometastasis, reducing the local recurrence and cancer-related death rate. POCT can prevent the systemic micrometastasis and recurrence so as to improve the survival period.

Conclusions about the effect of PORT from previous studies were inconsistent, which may be related to the different states of IIIA-N2 patients, as well as different radiotherapy equipment and doses used in studies. Our findings suggested that IIIA-N2 patients should be carefully evaluated according to the number of lymph node metastases before PORT treatment. POCT was necessary and important for all IIIA-N2 NSCLC patients. For patients with <6 lymph node metastases, if patients cannot tolerate POCT, the use of PORT to improve survival can be encouraged. For IIIA-N2 patients with ≥6 positive lymph nodes, if the patients' physical conditions allow, PORT combined with POCT therapy should be applied, because PORT alone did not have survival benefit for this group. The results are shown in **Table 4**.

There are limitations in our research: We did not analyze the dose and range of radiotherapy owing to lack of record in SEER database. It is undeniable that our research was a retrospective study and bias was inevitable. We try to minimize this bias through a large data analysis and statistical method. At present, it is urgent to carry out a multicenter prospective randomized controlled study based on modern precise radiotherapy technology and unified radiotherapy program, so as to provide a higher level of evidence for the application of PORT in the stage IIIA-N2 NSCLC patients and guide the selection of the beneficiary population.

Currently, there is no standard treatment for locally advanced IIIA-N2 NSCLC, and the single treatment is limited. For resectable IIIA-N2 NSCLC, the chance of death from recurrence or metastasis within 5 years after operation is still high regardless of R0 resection. The optimal combination of surgery, chemotherapy, and radiotherapy treatment including perioperative target therapy and immunotherapy for patients with stage IIIA-N2 NSCLC is still to be determined. Each NSCLC patient with stage IIIA-N2 should be carefully evaluated by a multidisciplinary team to develop the best treatment strategy.

CONCLUSION

In patients who featured <6 number of positive regional lymph nodes, patients who received PORT had better survival rate than patients who underwent surgery only. But in this group, there was no significant difference in the survival of postoperative patients who underwent POCT in view of whether received PORT. For patients with ≥6 positive lymph nodes, PORT combined with POCT significantly improved OS and decreased overall mortality. Owing to limitations in our study, a large-cohort, multicenter, and prospective study is needed.

DATA AVAILABILITY STATEMENT

The raw data supporting the conclusions of this article will be made available by the authors, without undue reservation.

ETHICS STATEMENT

The studies involving human participants were reviewed and approved by This retrospective study was approved by Ethics Committee of Beijing Hospital of Traditional Chinese Medicine, Capital Medical University. Written informed consent for participation was not required for this study in accordance with the national legislation and the institutional requirements.

AUTHOR CONTRIBUTIONS

FG collected the data and wrote the original draft. NL provided statistical analysis. YX assisted in providing statistical analysis. GY provided the original idea of the manuscript and reviewed the manuscript. All authors contributed to the article and approved the submitted version.

FUNDING

The research for this manuscript was not financially supported, and none of the authors had any relevant financial relationships.

ACKNOWLEDGMENTS

We would like to give special thanks to the efforts of the SEER tumor registry team.

REFERENCES

1. Bradbury P, Sivajohanathan D, Chan A, Kulkarni S, Ung Y, Ellis PM. Postoperative adjuvant systemic therapy in completely resected non-small-cell lung cancer: a systematic review. *Clin Lung Cancer*. (2017) 18:259–73.e8. doi: 10.1016/j.cllc.2016.07.002
2. Goya T, Asamura H, Yoshimura H, Kato H, Shimokata K, Tsuchiya R, et al. Prognosis of 6644 resected non-small cell lung cancers in Japan: a Japanese lung cancer registry study. *Lung Cancer*. (2005) 50:227–34. doi: 10.1016/j.lungcan.2005.05.021
3. Detterbeck FC, Boffa DJ, Tanoue LT. The new lung cancer staging system. *Chest*. (2009) 136:260–71. doi: 10.1378/chest.08-0978
4. Rusch VW, Crowley J, Giroux DJ, Goldstraw P, Im JG, Tsuboi M, et al. The IASLC lung cancer staging project: proposals for the revision of the N descriptors in the forthcoming seventh edition of the TNM classification for lung cancer. *J Thorac Oncol*. (2007) 2:603–12. doi: 10.1097/JTO.0b013e31807ec803
5. Sawyer TE, Bonner JA, Gould PM, Foote RL, Deschamps C, Trastek VF, et al. The impact of surgical adjuvant thoracic radiation therapy for patients with nonsmall cell lung carcinoma with ipsilateral mediastinal lymph node involvement. *Cancer*. (1997) 80:1399–408. doi: 10.1002/(SICI)1097-0142(19971015)80:8<1399::AID-CNCR6>3.0.CO;2-A
6. Saintigny P, Noel G, Mazeron JJ. [A controlled study of postoperative radiotherapy for patients with completely resected non small cell lung carcinoma]. *Cancer Radiother*. (2000) 4:318–9. doi: 10.1016/S1278-3218(00)80011-6
7. Arriagada R, Auperin A, Burdett S, Higgins JP, Johnson DH, Le Chevalier T, et al. Adjuvant chemotherapy, with or without postoperative radiotherapy, in operable non-small-cell lung cancer: two meta-analyses of individual patient data. *Lancet*. (2010) 375:1267–77. doi: 10.1016/S0140-6736(10)60059-1
8. Arriagada R, Dunant A, Pignon JP, Bergman B, Chabowski M, Grunenwald D, et al. Long-term results of the international adjuvant lung cancer trial evaluating adjuvant cisplatin-based chemotherapy in resected lung cancer. *J Clin Oncol*. (2010) 28:35–42. doi: 10.1200/JCO.2009.23.2272
9. SEER Annotated ICD O 3 Histology List. (2019) Available Online at: https://www.naaccr.org/icdo3/ (accessed December 20, 2017).
10. Veeramachaneni NK, Feins RH, Stephenson BJ, Edwards LJ, Fernandez FG. Management of stage IIIA non-small cell lung cancer by thoracic surgeons in North America. *Ann Thorac Surg*. (2012) 94:922–6; discussion 6–8. doi: 10.1016/j.athoracsur.2012.04.087
11. PORT Meta-analysis Trialists Group. Postoperative radiotherapy in non-small-cell lung cancer: systematic review and meta-analysis of individual patient data from nine randomised controlled trials. PORT Meta-analysis trialists group. *Lancet*. (1998) 352:257–63. doi: 10.1016/S0140-6736(98)06341-7
12. Kim BH, Kim HJ, Wu HG, Kang CH, Kim YT, Lee SH, et al. Role of postoperative radiotherapy after curative resection and adjuvant chemotherapy for patients with pathological stage N2 non-small-cell lung cancer: a propensity score matching analysis. *Clin Lung Cancer*. (2014) 15:356–64. doi: 10.1016/j.cllc.2014.05.005
13. Lally BE, Zelterman D, Colasanto JM, Haffty BG, Detterbeck FC, Wilson LD. Postoperative radiotherapy for stage II or III non-small-cell lung cancer using the surveillance, epidemiology, and end results database. *J Clin Oncol*. (2006) 24:2998–3006. doi: 10.1200/JCO.2005.04.6110
14. Douillard JY, Rosell R, De Lena M, Riggi M, Hurteloup P, Mahe MA. Impact of postoperative radiation therapy on survival in patients with complete resection and stage I, II, or IIIA non-small-cell lung cancer treated with adjuvant chemotherapy: the adjuvant Navelbine International Trialist Association (ANITA) Randomized Trial. *Int J Radiat Oncol Biol Phys*. (2008) 72:695–701. doi: 10.1016/j.ijrobp.2008.01.044
15. Herskovic A, Mauer E, Christos P, Nagar H. Role of postoperative radiotherapy in pathologic stage IIIA (N2) non-small cell lung cancer in a prospective nationwide oncology outcomes database. *J Thorac Oncol*. (2017) 12:302–13. doi: 10.1016/j.jtho.2016.09.135
16. Corso CD, Rutter CE, Wilson LD, Kim AW, Decker RH, Husain ZA. Re-evaluation of the role of postoperative radiotherapy and the impact of radiation dose for non-small-cell lung cancer using the national cancer database. *J Thorac Oncol*. (2015) 10:148–55. doi: 10.1097/JTO.0000000000000406
17. Sakib N, Li N, Zhu X, Li D, Li Y, Wang H. Effect of postoperative radiotherapy on outcome in resectable stage IIIA-N2 non-small-cell lung cancer: an updated meta-analysis. *Nucl Med Commun*. (2018) 39:51–9. doi: 10.1097/MNM.0000000000000764
18. Mikell JL, Gillespie TW, Hall WA, Nickleach DC, Liu Y, Lipscomb J, et al. Postoperative radiotherapy is associated with better survival in non-small cell lung cancer with involved N2 lymph nodes: results of an analysis of the national cancer data base. *J Thorac Oncol*. (2015) 10:462–71. doi: 10.1097/JTO.0000000000000411
19. Lei T, Xu XL, Chen W, Xu YP, Mao WM. Adjuvant chemotherapy plus radiotherapy is superior to chemotherapy following surgical treatment of stage IIIA N2 non-small-cell lung cancer. *Onco Targets Ther*. (2016) 9:921–8. doi: 10.2147/OTT.S95517

Conflict of Interest: The authors declare that the research was conducted in the absence of any commercial or financial relationships that could be construed as a potential conflict of interest.

frontiers in Oncology

ORIGINAL RESEARCH
published: 15 September 2020
doi: 10.3389/fonc.2020.01297

Preoperative Use of Intravenous Contrast Media Is Associated With Decreased Excellent Response Rates in Intermediate-Risk DTC Patients Who Subsequently Receive Total Thyroidectomy and Low-Dose RAI Therapy

Wei Lan[1,2†], *Wang Renjie*[1,2†], *Wan Qichang*[3], *Teng Feiyue*[1,2], *Ma Qingjie*[1,2*] *and Ji Bin*[1,2*]

[1] Department of Nuclear Medicine, China-Japan Union Hospital of Jilin University, Changchun, China, [2] NHC Key Laboratory of Radiobiology, School of Public Health of Jilin University, Changchun, China, [3] Department of Nuclear Medicine, Third Affiliated Hospital of Sun Yat-sen University, Guangzhou, China

OPEN ACCESS

Edited by:
Francesco Cellini,
Catholic University of the Sacred Heart, Italy

Reviewed by:
Monica Mangoni,
University of Florence, Italy
Luca Tagliaferri,
Fondazione Policlinico A. Gemelli IRCCS, Italy

***Correspondence:**
Ji Bin
jibin1983104@163.com
Ma Qingjie
maqingjiejlu@163.com

†These authors have contributed equally to this work

Specialty section:
This article was submitted to Radiation Oncology, a section of the journal Frontiers in Oncology

Received: 04 April 2020
Accepted: 22 June 2020
Published: 15 September 2020

Citation:
Lan W, Renjie W, Qichang W, Feiyue T, Qingjie M and Bin J (2020) Preoperative Use of Intravenous Contrast Media Is Associated With Decreased Excellent Response Rates in Intermediate-Risk DTC Patients Who Subsequently Receive Total Thyroidectomy and Low-Dose RAI Therapy. Front. Oncol. 10:1297. doi: 10.3389/fonc.2020.01297

Purpose: To evaluate the impact of preoperative use of intravenous contrast media (ICM) on the excellent response (ER) rates in a cohort of intermediate-risk differentiated thyroid cancer (DTC) patients who received total thyroidectomy (TT) and low-dose radioactive iodine (RAI) therapy.

Methods: A total of 683 consecutive patients were retrospectively reviewed in a single center between August 2016 and August 2018. Patients were divided into ICM group ($n = 532$) and non-ICM group ($n = 151$). Intravenous contrast media patients were 1:1 propensity matched to non-ICM patients based on T stage, N stage, and urinary iodine. Risk-adjusted logistic regression models were constructed to assess the association between the use of ICM and ER rates.

Results: Intravenous contrast media patients had significantly higher T stage ($P < 0.001$), N stage ($P < 0.001$), urinary iodine ($P < 0.001$), and ps-Tg ($P = 0.042$) than non-ICM patients. Preoperative use of ICM was found to be significantly associated with decreased ER rates in both the primary cohort [odds ratio (OR) = 0.47, 95% confidence interval (CI) = 0.32–0.71; $P < 0.001$] and the matched cohort (OR = 0.48, 95% CI = 0.25–0.94; $P = 0.031$). Subgroup analysis on RAI delay time in the primary cohort revealed that ER rates in ICM patients were significantly lower than that of non-ICM patients for 1–2 months ($P = 0.0245$) and >2–3 months ($P = 0.0221$) subgroups, but not for >3–4 months, >4–5 months, and >5–6 months subgroups (all $P > 0.05$). A delay time of >3–4 months exhibited the highest ER rate (63.08%) within the ICM group.

Conclusions: Preoperative use of ICM is associated with decreased ER rates in intermediate-risk DTC patients who subsequently receive TT and low-dose RAI therapy. For such patients, if ICM has already been received, an RAI delay time of >3–4 months would seem to be more appropriate to achieve better ER rates.

Keywords: differentiated thyroid cancer, intravenous contrast media, radioactive iodine therapy, delay time, excellent response

INTRODUCTION

Post-operative use of radioactive iodine (RAI) continues to be conservative in differentiated thyroid cancer (DTC) patients with low to intermediate recurrence risk. While high dose is considered to be associated with dysfunctions in non-thyroidal organs such as salivary and lachrymal and long-term effects such as second primary cancer, plenty of studies have demonstrated that low dose is as effective as high dose in achieving ablation success and controlling disease recurrence in this patient population (1–3). However, delivering sufficient absorbed doses to the thyroid tissue is still important to ensure therapeutic efficacy.

Iodinated contrast media (ICM) is often used in DTC patients with locally aggressive disease or clinically apparent cervical lymph node to optimize preoperative planning and the completeness of surgery (4). Because ICM contains several 100-fold the recommended daily allowance of iodine and may cause a retention of iodine in the body for years (5, 6), there has long been a concern among nuclear medicine physicians that it could interfere with thyroid RAI uptake. Accordingly, in clinical practice, RAI administration was usually delayed for a certain period to eclipse this effect (7, 8). However, when a low-dose RAI protocol is applied, the interference of preoperative use of ICM may become significantly pronounced. It is possible that the patients' clinical outcome and management strategy will be altered in this scenario.

Response-to-therapy assessment during the first 1–2 years after initial therapy for DTC patients is effective in estimating risk of long-term recurrence and was endorsed by the 2015 American Thyroid Association (ATA) guidelines (4). The most significant impact of this system is in patients with excellent response (ER), in whom the risk of disease recurrence was very low (1–4%), and far less intensive management would be required during follow-up. Thus, it is desirable to ensure that patients have a better chance of ER after RAI therapy.

In the present study, we evaluated whether the ER rates were influenced by preoperative use of ICM in the setting of a low-dose RAI protocol. Patients with initial ATA intermediate risk of recurrence were included, in whom the risk of recurrence is significant and in whom the impact of the response to therapy is most evident in terms of follow-up.

MATERIALS AND METHODS

Patients

The China-Japan Union Hospital is a tertiary-care University teaching center in northeastern China providing comprehensive care for thyroid cancer patients. All DTC patients in our center, except those with primary tumor measuring 1 cm or less confined to the thyroid gland, underwent total thyroidectomy (TT) with central or lateral neck dissection, depending on risk and intraoperative findings. From August 2016 on, the thyroid surgery department began to routinely select DTC patients to perform preoperative contrast CT following the 2015 ATA guidelines. However, because these guidelines also indicated that a 4–8-week interval between the use of ICM and RAI administration, which was defined as "RAI delay time" in this article, would be adequate to eclipse the impact of ICM on RAI

TABLE 1 | Protocol for RAI dosing.

Risk stratification	Aim	Dose
Low and intermediate risk*	Remnant ablation	1,110 MBq
High risk	Adjuvant therapy	3,700–5,550 MBq
	Therapy for persistent disease	3,700–7,400 MBq

**For patients with low risk of recurrence, RAI was administered based on patient's preference, although the ATA guideline did not routinely recommend RAI therapy for these patients.*

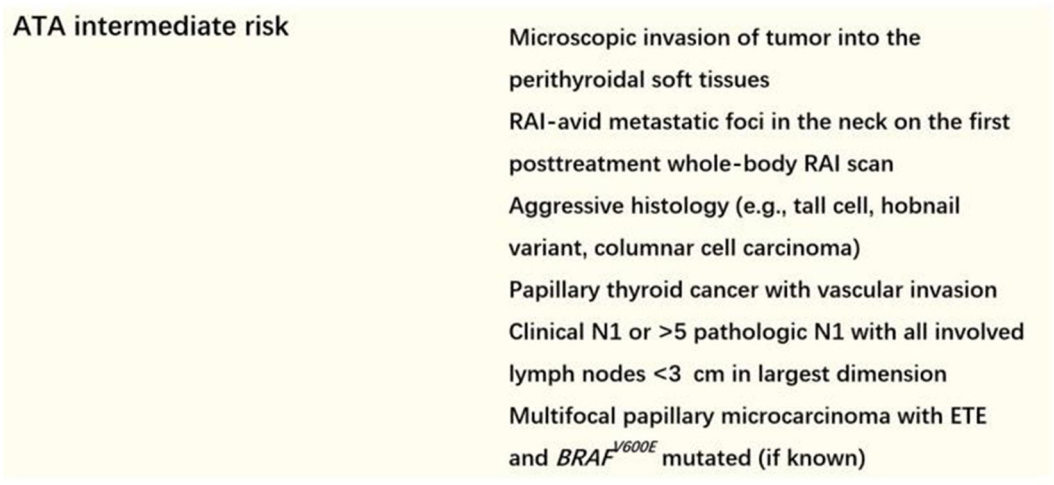

FIGURE 1 | Criteria of 2015 ATA intermediate-risk patients.

therapy, in our department, the RAI delay time for all patients (with or without ICM) in this period were solely determined by the patient's access to medical facilities and availability of RAI for administration.

We screened ATA intermediate-risk patients (detailed definition of intermediate risk in the 2015 ATA recurrence stratification system was shown in **Figure 1**) who had undergone TT and low-dose RAI therapy between August 2016 and August 2018. Patients who met the following criteria were excluded: (1) RAI delay time was more 6 months; (2) suspicion of distant metastases because of elevated serum ps-Tg level, radiological findings including chest computed tomography (CT), or positron emission tomography/CT, or therapeutic RAI scan, or histopathological biopsy; (3) positive or elevated serum Tg antibody (TgAb) level; and (4) patients with incomplete clinical data. Finally, a total of 683 patients were retrospectively enrolled. The study was approved by the local ethics committee.

Preoperative ICM and Measurement of Preablation Urinary Iodine Concentration

Preoperative ICM included iodixanol, iohexol, and iopromide, which are all non-ionic and have an iodine concentration of 320, 350, and 370 mg/mL, respectively. The ICM dose administered was 100 mL for iodixanol or iohexol and 80–100 mL for iopromide per CT scan.

Preablation urinary iodine (UI) concentration was measured using a rapid kit (Zhongsheng Jinyu Diagnostic Technology Company Limited, Beijing, China) developed based on the study of Rendl et al. (9, 10). After sample collection (between 8 and 11 AM), measurement was done within 2 h according to manufacturer's protocol.

RAI Protocol

Patients were prepared by levothyroxine (LT4) withdrawal together with a strict low-iodine diet for at least 2 weeks, with the goal of attaining an appropriate thyroid-stimulating

TABLE 2 | Patients' baseline characteristics.

	Primary cohort (n = 683)			Matched cohort (n = 186)		
	Non-ICM (n = 532)	ICM (n = 151)	P-value	Non-ICM (n = 93)	ICM (n = 93)	P-value
Age at diagnosis [n (%)]	41.5 ± 14.8	41.5 ± 13.0	0.989	38.8 ± 13.9	42.1 ± 13.6	0.105
Gender [n (%)]			0.138			0.213
Female	362 (68.0%)	93 (61.6%)		66 (71.0%)	58 (62.4%)	
Male	170 (32.0%)	58 (38.4%)		27 (29.0%)	35 (37.6%)	
Multifocality [n (%)]			0.228			0.552
No	230 (43.2%)	57 (37.7%)		41 (44.1%)	37 (39.8%)	
Yes	302 (56.8%)	94 (62.3%)		52 (55.9%)	56 (60.2%)	
T stage [n (%)]			<0.001			0.069
T1	335 (63.0%)	55 (36.4%)		47 (50.5%)	55 (59.1%)	
T2	86 (16.2%)	2 (1.3%)		9 (9.7%)	1 (1.1%)	
T3	94 (17.7%)	80 (53.0%)		28 (30.1%)	29 (31.2%)	
T4	17 (3.2%)	14 (9.3%)		9 (9.7%)	8 (8.6%)	
N stage [n (%)]			<0.001			0.247
N0	86 (16.2%)	7 (4.6%)		5 (5.4%)	7 (7.5%)	
N1a	347 (65.2%)	31 (20.5%)		42 (45.2%)	31 (33.3%)	
N1b	99 (18.6%)	113 (74.8%)		46 (49.5%)	55 (59.1%)	
Delay time [n (%)]			0.742			0.883
1–2 months	100 (18.8%)	27 (17.9%)		14 (15.1%)	18 (19.4%)	
2–3 months	211 (39.7%)	54 (35.8%)		35 (37.6%)	31 (33.3%)	
3–4 months	97 (18.2%)	33 (21.9%)		16 (17.2%)	18 (19.4%)	
4–5 months	82 (15.4%)	22 (14.6%)		19 (20.4%)	16 (17.2%)	
5–6 months	42 (7.9%)	15 (9.9%)		9 (9.7%)	10 (10.8%)	
Histologic subtype [n (%)]			0.980			0.601
Papillary	500 (94.0%)	142 (94.0%)		86 (92.5%)	84 (90.3%)	
Follicular	32 (6.0%)	9 (6.0%)		7 (7.5%)	9 (9.7%)	
^{99m}Tc-pertechnetate uptake [n (%)]			0.187			0.240
Negative	253 (47.6%)	81 (53.6%)		40 (43.0%)	48 (51.6%)	
Positive	279 (52.4%)	70 (46.4%)		53 (57.0%)	45 (48.4%)	
TSH (μIU/mL), mean	103.6 ± 34.9	99.1 ± 28.1	0.151	101.1 ± 34.3	100.5 ± 28.5	0.895
Ps-Tg (ng/ml), mean	4.3 ± 4.2	5.1 ± 4.6	0.042	4.6 ± 4.2	5.6 ± 4.7	0.122
UI (μg/L), mean	82.9 ± 30.9	96.5 ± 32.1	<0.001	95.6 ± 36.0	91.1 ± 30.4	0.356

hormone (TSH) level > 30 μIU/mL. Patients who were scheduled to perform an imminent RAI therapy should have a UI concentration of < 200 μg/L. The RAI dose administered was based on the 2015 ATA guidelines according to TNM stage and recurrence risk stratification. For intermediate-risk patients included in this study, a fixed low-dose RAI was administered for successful remnant ablation (**Table 1** shows the protocol for RAI dosing in our department). Thyroxine therapy was resumed on the third day, and a therapeutic RAI scan was performed 3–5 days after RAI therapy.

Response Assessment

Response assessment was performed 16–40 months after RAI therapy. In this study, the response was divided into ER and NER according to the serological examination (suppressed Tg, stimulated Tg, and TgAb) and imaging technique (DxWBS, cervical ultrasound, chest CT, and bone scintigraphic imaging) described in the 2015 ATA guidelines. Excellent response was defined as negative imaging and at the same time either suppressed Tg up to 0.2 ng/mL or ps-Tg up to 1 ng/mL with the absence of TgAb.

Statistical Analysis

We utilized propensity score methods to adjust for difference in the baseline characteristics of patients in the ICM and non-ICM groups. To estimate the propensity score, logistic regression was performed with three variables: T stage, N stage, and UI (all $P < 0.001$ in univariate analyses). After propensity score estimation, the ICM and non-ICM groups were matched according to propensity score in a 1:1 ratio with a caliper of 0.05. Univariate

TABLE 3 | Factors associated with the excellent response.

	Primary cohort ($n = 683$)			Matched cohort ($n = 186$)		
	NER ($n = 256$)	ER ($n = 427$)	*P*-value	NER ($n = 81$)	ER ($n = 105$)	*P*-value
ICM [n (%)]			0.011			0.183
No	186 (72.7%)	346 (81.0%)		36 (44.4%)	57 (54.3%)	
Yes	70 (27.3%)	81 (19.0%)		45 (55.6%)	48 (45.7%)	
Age at diagnosis (years), mean	41.0 ± 15.1	41.8 ± 14.0	0.462	39.3 ± 14.4	41.3 ± 13.3	0.344
Gender [n (%)]			0.360			0.530
Female	176 (68.8%)	279 (65.3%)		52 (64.2%)	72 (68.6%)	
Male	80 (31.2%)	148 (34.7%)		29 (35.8%)	33 (31.4%)	
Multifocality [n (%)]			0.372			0.074
No	102 (39.8%)	185 (43.3%)		28 (34.6%)	50 (47.6%)	
Yes	154 (60.2%)	242 (56.7%)		53 (65.4%)	55 (52.4%)	
T stage [n (%)]			0.958			0.24
T1	146 (57.0%)	244 (57.1%)		51 (63.0%)	51 (48.6%)	
T2	32 (12.5%)	56 (13.1%)		4 (4.9%)	6 (5.7%)	
T3	65 (25.4%)	109 (25.5%)		21 (25.9%)	36 (34.3%)	
T4	13 (5.1%)	18 (4.2%)		5 (6.2%)	12 (11.4%)	
N stage [n (%)]			0.194			0.664
N0	32 (12.5%)	61 (14.3%)		5 (6.2%)	7 (6.7%)	
N1a	134 (52.3%)	244 (57.1%)		29 (35.8%)	44 (41.9%)	
N1b	90 (35.2%)	122 (28.6%)		47 (58.0%)	54 (51.4%)	
Delay time [n (%)]			0.175			0.954
1–2 months	47 (18.4%)	80 (18.7%)		16 (19.8%)	16 (15.2%)	
2–3 months	88 (34.4%)	177 (41.5%)		28 (34.6%)	38 (36.2%)	
3–4 months	48 (18.8%)	82 (19.2%)		14 (17.3%)	20 (19.0%)	
4–5 months	47 (18.4%)	57 (13.3%)		15 (18.5%)	20 (19.0%)	
5–6 months	26 (10.2%)	31 (7.3%)		8 (9.9%)	11 (10.5%)	
Histologic subtype [n (%)]			0.833			0.986
Papillary	240 (93.8%)	402 (94.1%)		74 (91.4%)	96 (91.4%)	
Follicular	16 (6.2%)	25 (5.9%)		7 (8.6%)	9 (8.6%)	
^{99m}Tc-pertechnetate uptake [n (%)]			<0.001			0.002
Negative	99 (38.7%)	235 (55.0%)		28 (34.6%)	60 (57.1%)	
Positive	157 (61.3%)	192 (45.0%)		53 (65.4%)	45 (42.9%)	
TSH (μIU/mL), mean	102.8 ± 33.7	102.5 ± 33.5	0.916	101.2 ± 34.0	100.5 ± 29.5	0.878
Ps-Tg (ng/ml), mean	7.2 ± 4.9	3.6 ± 3.6	<0.001	7.0 ± 4.5	3.6 ± 3.8	<0.001
UI (μg/L), mean	86.7 ± 29.5	85.4 ± 32.9	0.172	91.9 ± 30.2	94.5 ± 35.6	0.595

analyses were performed to compare the clinical characteristics of the patients and ER rates between the two groups. To evaluate the impact of preoperative use of ICM on ER rates, non-adjusted, risk-adjusted, and fully adjusted logistic regression models were constructed for the both primary and the matched cohort. For risk-adjusted analyses, we adjusted for features that were significant in the univariate analyses. The subgroup analyses were performed using R × C χ^2 test. Categorical variables were compared with either χ^2 test or Fisher exact test as appropriate. Student *t*-test was used for normally distributed continuous variables, and the Mann-Whitney *U*-test was used for non-normally distributed continuous variables. Statistical analysis was performed using R software (version 3.4.3; http://www.R-project.org, The R Foundation). $P < 0.05$ was considered to indicate statistical significance.

RESULTS

Patients

For the included patients, five hundred and thirty-two of them underwent preoperative ICM and 151 did not. Patients' baseline characteristics are shown in **Table 2**. As can be seen, T stage ($P < 0.001$), N stage ($P < 0.001$), UI ($P < 0.001$), and ps-Tg ($P = 0.042$) in the ICM group were significantly higher than that of the non-ICM group. After propensity score matching, 93 pairs of patients were successfully matched, and all baseline characteristics were well-balanced between the matched groups.

Impact of Preoperative Use of ICM on ER Rates

The distribution of ER rates for the ICM patients and the non-ICM patients is shown in **Table 3**. Excellent response rates in the ICM group were lower than those of the non-ICM group either in the primary cohort (53.6 vs. 65.0%) or in the matched cohort (45.7 vs. 54.3%).

In univariate analyses, for the primary cohort, significant difference was found between ER group and non-ER group for the use of ICM ($P = 0.011$), ^{99m}Tc-pertechnetate uptake ($P < 0.001$) and ps-Tg ($P < 0.001$); for the matched cohort, significant difference was found between the ER group and non-ER group for the use of ICM ($P = 0.011$), ^{99m}Tc-pertechnetate uptake ($P = 0.002$), and ps-Tg ($P < 0.001$) (**Table 3**). In multivariate analyses, the use of ICM was found to be significantly associated with decreased ER rates in crude model [odds ratio (OR) = 0.61, 95% confidence interval (CI) = 0.43–0.90, $P = 0.011$, in the primary cohort; and OR = 0.67, 95% CI = 0.38–1.21, $P = 0.184$, in the matched cohort], risk-adjusted model (OR = 0.47, 95% CI = 0.32–0.71, $P < 0.001$, in the primary cohort; and OR = 0.48, 95% CI = 0.25–0.94, $P = 0.031$, in the matched cohort), and fully adjusted model (OR = 0.48, 95% CI = 0.29–0.80, $P = 0.005$, in the primary cohort; and OR = 0.51, 95% CI = 0.25–1.04, $P = 0.065$, in the matched cohort) (**Table 4**).

TABLE 4 | Multivariate regression for impact of preoperative ICM on ER rates.

	Crude model		Risk adjusted model		Fully adjusted model	
	OR/β (95%CI)	*P*-value	OR/β (95%CI)	*P*-value	OR/β (95%CI)	*P*-value
Primary cohort						
Non-ICM	Reference		Reference		Reference	
ICM	0.61 (0.43, 0.90)	0.011	0.47 (0.32, 0.71)	<0.001	0.48 (0.29, 0.80)	0.005
Matched cohort						
Non-ICM	Reference		Reference		Reference	
ICM	0.67 (0.38, 1.21)	0.184	0.48 (0.25, 0.94)	0.031	0.51 (0.25, 1.04)	0.065

Crude model: non-adjusted; Risk adjusted model: ^{99m}Tc-pertechnetate uptake and ps-Tg were adjusted in the primary cohort and matched cohort.
Fully adjusted model: all factors were adjusted.

TABLE 5 | Subgroup analysis on RAI delay time in the primary cohort.

RAI delay time		Non-ICM patients	ICM patients	*P*-value
1–2 months	ER	68 (68.00%)	12 (44.44%)	0.024
	NER	32 (32.00%)	15 (55.56%)	
2–3 months	ER	148 (70.14%)	29 (53.70%)	0.022
	NER	63 (29.86%)	25 (46.30%)	
3–4 months	ER	61 (62.89%)	21 (63.64%)	0.939
	NER	36 (37.11%)	12 (36.36%)	
4–5 months	ER	45 (54.88%)	12 (54.55%)	0.978
	NER	37 (45.12%)	10 (45.45%)	
5–6 months	ER	24 (57.14%)	7 (46.67%)	0.484
	NER	18 (42.86%)	8 (53.33%)	

TABLE 6 | UI concentration according to clinical outcomes for the five RAI delay time subgroups in the primary cohort.

RAI delay time	UI in ICM patients			UI in non-ICM patients		
	ER	NER	*P*-value	ER	NER	*P*-value
1–2 months	110.8 ± 39.6	100.7 ± 23.7	0.416	80.3 ± 28.4	80.9 ± 25.4	0.913
>2–3 months	99.0 ± 33.8	98.4 ± 31.2	0.950	84.3 ± 31.0	87.6 ± 27.6	0.457
>3–4 months	98.6 ± 33.4	85.8 ± 31.2	0.289	85.8 ± 35.5	82.1 ± 28.5	0.605
>4–5 months	88.3 ± 32.7	90.0 ± 26.7	0.899	75.3 ± 32.2	81.9 ± 32.0	0.360
>5–6 months	97.1 ± 33.5	82.5 ± 35.4	0.427	79.2 ± 36.3	84.1 ± 29.1	0.509

Subgroup Analysis on RAI Delay Time

The RAI delay time of the 683 patients were categorized into five subgroups, and the number of patients in each group can be seen in **Table 2**. In the primary cohort, the ER rates in ICM patients were significantly lower than those of non-ICM patients for 1–2 months ($P = 0.0245$) and >2–3 months ($P = 0.0221$)

subgroups, but not for >3–4 months, >4–5 months, and >5–6 months subgroups (All $P > 0.05$) (**Table 5**).

Relationship Between UI Concentration and Clinical Outcomes

In univariate and multivariate analyses, UI concentration was found to be not associated with ER rates for either the primary or the matched cohort (All $P > 0.05$). **Table 6** shows UI concentration according to clinical outcomes for the five RAI delay time subgroups in the primary cohort. Still, no association between UI concentration and ER rates was found within each of the five subgroups (All $P > 0.05$).

DISCUSSION

The 2015 ATA guidelines assumed that the use of ICM should not be a major concern for RAI therapy as long as 4–8 weeks' delay time was fulfilled (4). However, this arbitrary cutoff was only inferred based on the clearance time of UI values (11–13). It is unclear whether these values accurately reflect free iodide accumulation by thyroid tissue. Moreover, in a recent study, Vassaux et al. suggested that independent of free iodide, the ICM itself could directly reduce thyroid iodide uptake by decreasing NIS expression in thyroid cells. Besides, they found that ICM induces thyroid stunning to a greater and longer-lasting degree than free iodide found in ICM could explain (14). Thus, the influence of the use of ICM might have been stronger and more enduring than we previously thought. Nevertheless, although the interference of ICM on thyroid RAI uptake is well-documented in the literature (15), as far as we know, there have been no previous studies to directly and systemically evaluate the impact of preoperative use of ICM on patients' clinical outcome after RAI therapy.

In the present study, by analyzing a large cohort of intermediate-risk patients in the setting of a low-dose RAI protocol, which our department had been implementing since August 2015 (16), we evaluated whether preoperative use of ICM significantly impacted the ER rates. We chose ER rates as a clinical endpoint in this study, because in intermediate-risk patients, ER decreases the estimated risk of recurrence from 20 to 30% to < 5%, leading to less intensive follow-up and no need for TSH suppression (17). Propensity score matching was performed to balance the confounding factors in the primary cohort. In multivariate analysis, we found that the use of ICM was significantly associated with decreased ER rates in non-adjusted, risk-adjusted, and fully adjusted models for either the primary or the matched cohort. This implies that the use of ICM has a significant negative impact in terms of patients' clinical outcome, although it might help to improve evaluation of tissue planes and detection of local invasion before surgery. Thus, the negative

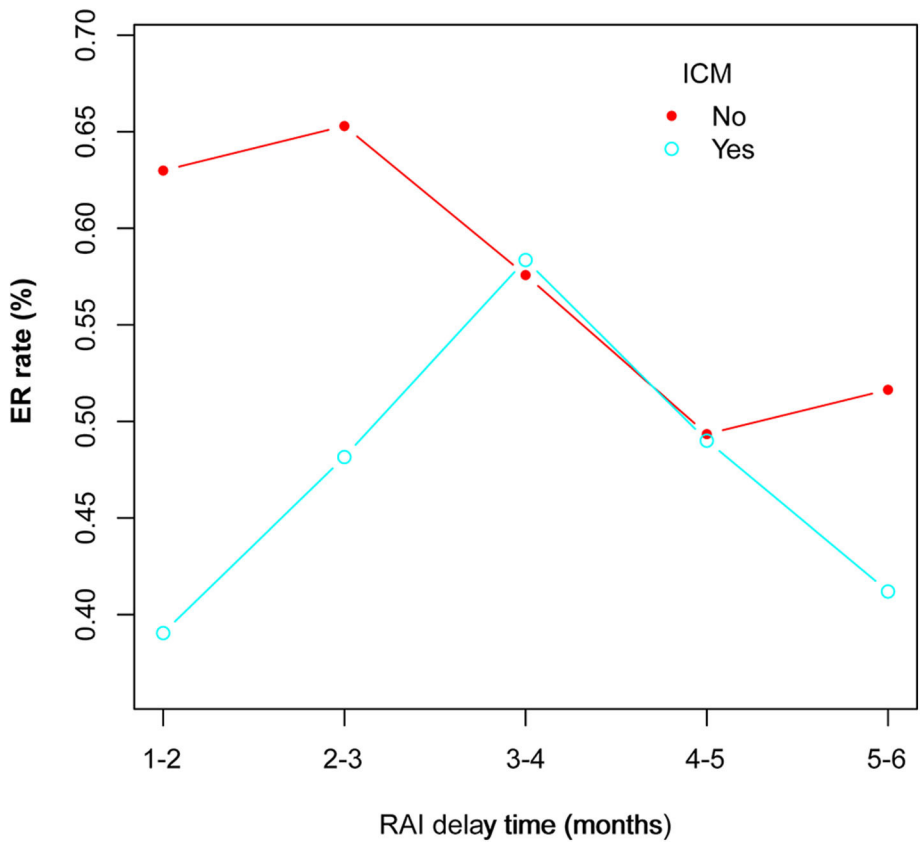

FIGURE 2 | Changes of ER rates as RAI delay time extends in both ICM and non-ICM patients.

impact of ICM on RAI therapy cannot be ignored in this scenario, and decision making of the use of ICM should at least take into account whether the patients are likely to receive low-dose RAI therapy afterward. To go a step further, withholding ICM might be an option in patients with lower tumor burden. As a matter of fact, toward the necessity of preoperative use of ICM, many scholars have already argued that CT without ICM can provide sufficient information regarding tumor and vascular and aerodigestive structures for effective surgical planning (18).

In a subgroup analysis on RAI delay time, we showed that in the primary cohort ER rates in ICM patients were significantly lower than that of non-ICM patients for 1–2 months ($P = 0.0245$) and >2–3 months ($P = 0.0221$) subgroups, but not for >3–4 months, >4–5 months, and >5–6 months subgroups (All $P > 0.05$). This indicated that the would-be negative impact of ICM on RAI therapy might persist until 3 months after surgery. In other words, if the patients had received contrast CT, the RAI delay time should be at least more than 3 months for the ICM not to significantly influence ER rates. Moreover, the RAI delay time itself is believed to impact RAI therapy, and longer delay time usually correlates with worse clinical outcome (19, 20). In our ICM group, the ER rates showed a first increased and then decreased trend among the five delay time subgroups, with the >3–4 months subgroup exhibiting the highest (**Figure 2**). It could be speculated that this time period might be able to better balance the decreasing negative impact of ICM and the increasing negative impact of delay time itself on RAI therapy. Thus, an RAI delay time of >3–4 months seems to be more appropriate for patients to achieve better ER rates in this scenario.

Urinary iodine is an easily obtainable indicator for iodine status and a sensitive marker of iodine intake and changes in iodine status. Previously, several researchers concluded that 1-month delay is sufficient for ICM patients to perform RAI therapy because UI concentration could return to baseline values (before the use of ICM) during this period (11, 12). However, in our study, although the UI concentrations of all included patients were within normal range (<200 μg/L) before RAI therapy, it was found to be not associated with the clinical outcome for either the primary or the matched cohort or within each of the five RAI delay time subgroups in the primary cohort. These results indicated that UI concentration within normal range cannot guarantee the absence of interference from ICM in terms of clinical outcome. This was in accordance with the theory proposed by Vassaux et al. (14) in *in vitro* studies as mentioned previously. Therefore, our study demonstrated in a clinical practice setting that it might be not suitable for using a "normal UI concentration" to decide the initiation of RAI therapy if the patients had received preoperative ICM.

There are some limitations to this study. First, it was a retrospective study performed in a single institution. Although propensity score matching was used to minimize the effect of observed confounders, it cannot address unobserved confounders. For example, preoperative contrast CT was performed at the surgeons' discretion after seeing the result of the neck ultrasound. This could have already led to selection bias. In this regard, a multi-institutional prospective randomized trial with a larger number of patients would be more appropriate. Second, the follow-up duration in our study is relatively short, and continued observations are still needed to evaluate long-term clinical outcomes. Lastly, we used a rapid UI test method that is not completely quantitative, and rather than a period of 24 h, only single-spot urinary was collected. These might undermine the results derived from UI concentration in our study.

CONCLUSIONS

Preoperative use of ICM is associated with decreased ER rates in intermediate-risk DTC patients who subsequently receive TT and low-dose RAI therapy. For such patients, if ICM has already been received, an RAI delay time of >3–4 months would seem to be more appropriate to achieve better ER rates.

DATA AVAILABILITY STATEMENT

The raw data supporting the conclusions of this article will be made available by the authors, without undue reservation.

ETHICS STATEMENT

The studies involving human participants were reviewed and approved by ethics committee of China-Japan Union Hospital. Written informed consent for participation was not required for this study in accordance with the national legislation and the institutional requirements.

AUTHOR CONTRIBUTIONS

JB, MQ, and WL conceived and designed the study. WL, WR, WQ, and TF performed the retrospective study. WR and WQ interpreted the data. WL and JB wrote the paper. JB and MQ supervised the study, reviewed, and edited the manuscript. All authors approved the final manuscript.

REFERENCES

1. Dehbi HM, Mallick U, Wadsley J, Newbold K, Harmer C, Hackshaw A. Recurrence after low-dose radioiodine ablation and recombinant human thyroid-stimulating hormone for differentiated thyroid cancer (HiLo): long-term results of an open-label, non-inferiority randomised controlled trial. *Lancet Diabetes Endocrinol.* (2019) 7:44–51. doi: 10.1016/S2213-8587(18)30306-1
2. Castagna MG, Cevenini G, Theodoropoulou A, Maino F, Memmo S, Claudia C, et al. Post-surgical thyroid ablation with low or high radioiodine activities results in similar outcomes in intermediate risk differentiated thyroid cancer patients. *Eur J Endocrinol.* (2013) 169:23–9. doi: 10.1530/EJE-12-0954
3. Mallick U, Harmer C, Yap B, Wadsley J, Clarke S, Moss L, et al. Ablation with low-dose radioiodine and thyrotropin alfa in thyroid cancer. *N Engl J Med.* (2012) 366:1674–85. doi: 10.1056/NEJMoa1109589
4. Haugen BR, Alexander EK, Bible KC, Doherty GM, Mandel SJ, Nikiforov YE, et al. 2015 American thyroid association management guidelines for adult patients with thyroid nodules and differentiated thyroid cancer: the American thyroid association guidelines task force on thyroid nodules and differentiated thyroid cancer. *Thyroid.* (2016) 26:1–133. doi: 10.1089/thy.2015.0020

5. Costa A, Testori OB, Cenderelli C, Giribone G, Migliardi M. Iodine content of human tissues after administration of iodine containing drugs or contrast media. *J Endocrinol Invest.* (1978) 1:221–5. doi: 10.1007/BF03350384
6. Burman KD, Wartofsky L. Iodine effects on the thyroid gland: biochemical and clinical aspects. *Rev Endocr Metab Disord.* (2000) 1:19–25. doi: 10.1023/A:1010004218052
7. Silberstein EB, Alavi A, Balon HR, Clarke SE, Divgi C, Gelfand MJ, et al. The SNMMI practice guideline for therapy of thyroid disease with 131I 3.0. *J Nucl Med.* (2012) 53:1633–51. doi: 10.2967/jnumed.112.105148
8. Luster M, Clarke SE, Dietlein M, Lassmann M, Lind P, Oyen WJ, et al. Guidelines for radioiodine therapy of differentiated thyroid cancer. *Eur J Nucl Med Mol Imaging.* (2008) 35:1941–59. doi: 10.1007/s00259-008-0883-1
9. Rendl J, Bier D, Groh T, Reiners C. Rapid urinary iodide test. *J Clin Endocrinol Metab.* (1998) 83:1007–12. doi: 10.1210/jcem.83.3.4633
10. Shao HJ, Li J, He XQ, Liu N, Li YH, Yan JJ, et al. Prevalence of nontoxic nodular goiter after a nearly two-decade universial salt iodization in a littoral region of shandong province, China. *Acta Endocrinol.* (2016) 12:43–6. doi: 10.4183/aeb.2016.43
11. Padovani RP, Kasamatsu TS, Nakabashi CC, Camacho CP, Andreoni DM, Malouf EZ, et al. One month is sufficient for urinary iodine to return to its baseline value after the use of water-soluble iodinated contrast agents in post-thyroidectomy patients requiring radioiodine therapy. *Thyroid.* (2012) 22:926–30. doi: 10.1089/thy.2012.0099
12. Sohn SY, Choi JH, Kim NK, Joung JY, Cho YY, Park SM, et al. The impact of iodinated contrast agent administered during preoperative computed tomography scan on body iodine pool in patients with differentiated thyroid cancer preparing for radioactive iodine treatment. *Thyroid.* (2014) 24:872–7. doi: 10.1089/thy.2013.0238
13. Mishra A, Pradhan PK, Gambhir S, Sabaretnam M, Gupta A, Babu S. Preoperative contrast-enhanced computerized tomography should not delay radioiodine ablation in differentiated thyroid carcinoma patients. *J Surg Res.* (2015) 193:731–7. doi: 10.1016/j.jss.2014.07.065
14. Vassaux G, Zwarthoed C, Signetti L, Guglielmi J, Compin C, Guigonis JM, et al. Iodinated contrast agents perturb iodide uptake by the thyroid independently of free iodide. *J Nucl Med.* (2018) 59:121–6. doi: 10.2967/jnumed.117.195685
15. Laurie AJ, Lyon SG, Lasser EC. Contrast material iodides: potential effects on radioactive iodine thyroid uptake. *J Nucl Med.* (1992) 33:237–8.
16. Lan W, Gege Z, Ningning L, Qiang W, Lin B, Qingjie M, et al. Negative remnant (99m)Tc-pertechnetate uptake predicts excellent response to radioactive iodine therapy in low- to intermediate-risk differentiated thyroid cancer patients who have undergone total thyroidectomy. *Ann Nucl Med.* (2019) 33:112–8. doi: 10.1007/s12149-018-1314-4
17. Moreno I, Hirsch D, Duskin-Bitan H, Dicker-Cohen T, Shimon I, Robenshtok E. Response to therapy assessment in intermediate-risk thyroid cancer patients: is thyroglobulin stimulation required? *Thyroid.* (2020) 30:863–70. doi: 10.1089/thy.2019.0431
18. Luster M, Aktolun C, Amendoeira I, Barczynski M, Bible KC, Duntas LH, et al. European perspective on 2015 American thyroid association management guidelines for adult patients with thyroid nodules and differentiated thyroid cancer: proceedings of an interactive international symposium. *Thyroid.* (2019) 29:7–26. doi: 10.1089/thy.2017.0129
19. Li H, Zhang YQ, Wang C, Zhang X, Li X, Lin YS. Delayed initial radioiodine therapy related to incomplete response in low- to intermediate-risk differentiated thyroid cancer. *Clin Endocrinol.* (2018) 88:601–6. doi: 10.1111/cen.13551
20. Higashi T, Nishii R, Yamada S, Nakamoto Y, Ishizu K, Kawase S, et al. Delayed initial radioactive iodine therapy resulted in poor survival in patients with metastatic differentiated thyroid carcinoma: a retrospective statistical analysis of 198 cases. *J Nucl Med.* (2011) 52:683–9. doi: 10.2967/jnumed.110.081059

Conflict of Interest: The authors declare that the research was conducted in the absence of any commercial or financial relationships that could be construed as a potential conflict of interest.

frontiers in Oncology

ORIGINAL RESEARCH
published: 14 October 2020
doi: 10.3389/fonc.2020.569435

Utility of Radiomics for Predicting Patient Survival in Hepatocellular Carcinoma With Portal Vein Tumor Thrombosis Treated With Stereotactic Body Radiotherapy

Kui Wu[1], *Yongjie Shui*[1], *Wenzheng Sun*[1], *Sheng Lin*[2]* *and Haowen Pang*[2]*

[1] *Department of Radiation Oncology, The Second Affiliated Hospital, Zhejiang University School of Medicine, Hangzhou, China,* [2] *Department of Oncology, The Affiliated Hospital of Southwest Medical University, Luzhou, China*

OPEN ACCESS

Edited by:
Francesco Cellini, Catholic University of the Sacred Heart, Italy

Reviewed by:
Alexander F. I. Osman, Al-Neelain University, Sudan
Vinay Sharma, University of the Witwatersrand, South Africa

***Correspondence:**
Sheng Lin
lslinsheng@163.com
Haowen Pang
haowenpang@foxmail.com

Specialty section:
This article was submitted to Radiation Oncology, a section of the journal Frontiers in Oncology

Received: *04 June 2020*
Accepted: *16 September 2020*
Published: *14 October 2020*

Citation:
Wu K, Shui Y, Sun W, Lin S and Pang H (2020) Utility of Radiomics for Predicting Patient Survival in Hepatocellular Carcinoma With Portal Vein Tumor Thrombosis Treated With Stereotactic Body Radiotherapy. Front. Oncol. 10:569435. doi: 10.3389/fonc.2020.569435

Introduction: This study aimed to develop and validate the combination of radiomic features and clinical characteristics that can predict patient survival in hepatocellular carcinoma (HCC) with portal vein tumor thrombosis (PVTT) treated with stereotactic body radiotherapy (SBRT).

Materials and Methods: The prediction model was developed in a primary cohort of 70 patients with HCC and PVTT treated with SBRT, using data acquired between December 2015 and June 2017. The radiomic features were extracted from computed tomography (CT) scans. A least absolute shrinkage and selection operator regression model was used to build the model. Multivariate Cox-regression hazard models were created for analyzing survival outcomes and the radiomic features and clinical characteristics were presented with a nomogram. The area under the receiver operating characteristic curve (AUROC) was used to evaluate the model. Participants were divided into a high-risk group and a low-risk group based on the radiomic features.

Results: A total of four radiomic features and six clinical characteristics were extracted for survival analysis. A combination of the radiomic features and clinical characteristics resulted in better performance for the estimation of overall survival (OS) [area under the curve (AUC) = 0.859 (CI: 0.770–0.948)] than that with clinical characteristics alone [AUC = 0.761 (CI: 0.641–0.881)]. These patients were divided into high-risk and low-risk groups according to the radiomic features.

Conclusion: This study demonstrated that a nomogram of combined radiomic features and clinical characteristics can be conveniently used to assess individualized preoperative prediction of OS in patients with HCC with PVTT before SBRT.

Keywords: hepatocellular carcinoma, portal vein tumor thrombosis, stereotactic body radiotherapy, radiomics, outcome prediction

INTRODUCTION

Hepatocellular carcinoma (HCC) is the sixth most prevalent cancer worldwide, and the third leading cause of cancer-related deaths (1). China accounts for more than 50% of the global incidence of HCC and HCC is the fourth most commonly diagnosed cancer (2). Macrovascular invasion, where tumor cells invade the portal vein, hepatic veins, or the inferior vena cava in the liver (3, 4), is common in HCC. Portal vein tumor thrombosis (PVTT) is one of the most serious complications of HCC and has an incidence ranging from 44 to 62.2% (5). Between 10 and 60% of patients with HCC already have PVTT at the time of diagnosis (6, 7). This condition is strongly correlated with poor prognosis and the natural median survival time of patients with HCC and PVTT is only 2–4 months (8, 9).

Several clinical studies have confirmed that radiotherapy is effective for treating HCC with PVTT (10–12). Shui et al. (13) have shown stereotactic body radiotherapy (SBRT) can be used as the first-line therapy for HCC patients with extensive PVTT originally considered unsuitable for surgical resection or TACE. SBRT has emerged as a new radiotherapy technology that can deliver high doses of radiation to the target area in fewer fractions (14, 15). SBRT can accurately transfer a large dose of multiple beams to the target tumor within 1–5 fractions, owing to technical progress in accurate dose transfer, respiratory movement management, and daily image guidance. The relatively short treatment process can benefit patients by reducing interference with other treatment measures. Hence, we typically recommend SBRT to patients with unresectable HCC with PVTT undergoing multidisciplinary treatment. The purpose of SBRT is to reduce tumor thrombus and retain sufficient portal vein blood flow to allow the beneficial effect of any follow-up treatment.

Studies have also investigated the possibility of using radiomics as a potential prognostic indicator in oncology, specifically to classify patients and assess their risk categories, to develop personalized oncological treatments (16–18). The aim of this study was to develop a combination of radiomic features and clinical characteristics to estimate the overall survival (OS) in patients with HCC with PVTT treated using SBRT. Although numerous studies have been published on the use of radiomics in several cancer-outcome prediction models (19–21), and the correlation between the characteristics of radiation and the results of radiotherapy, few studies have focused on HCC with PVTT treated using SBRT. Therefore, our study aimed to develop and validate the combination of radiomic features and clinical characteristics that can predict patient survival in HCC with PVTT treated with SBRT.

MATERIALS AND METHODS

Patient Selection

All patients ($n = 70$) who were treated at the Second Affiliated Hospital, Zhejiang University School of Medicine from December 2015 to June 2017 were included in the study. Treatment and data analysis were conducted according to the Declaration of Helsinki. Ethical approval for retrospective data analysis was obtained from the Second Affiliated Hospital, Zhejiang University School of Medicine Ethics Committee. The diagnosis of liver cancer was based on the guidelines of the American Association for the Study of Liver Diseases (22). Portal vein invasion was determined by the presence of filling defects in a low attenuation cavity near the primary tumor, as observed on enhanced computed tomography (CT).

In this study, patients received SBRT according to the following criteria: [1] tumor thrombus involving the main portal vein and/or the first portal vein, which was deemed unsuitable for surgery or transarterial chemoembolization; [2] Eastern Cooperative Oncology Group (ECOG) performance status (PS) score of 0–1; [3] absence of refractory ascites; [4] Child-Pugh class A, B, and C; [5] no previous history of radiotherapy for the liver; and [6] availability of more than 700 cm^3 of unaffected liver.

SBRT

The gross tumor volume (GTV) represents the extent of tumor thrombosis visualized on contrast-enhanced CT and magnetic resonance imaging (MRI). If the extent of primary liver disease was small (<5 cm) and adjacent to the PVTT, both were considered to be a part of the GTV. A total dose of 25–50 Gy was prescribed in five fractions over 5–7 days based on the GTV. SBRT plans were generated using the Varian radiation treatment planning system (Eclipse software, Varian Medical Systems, Palo Alto, CA, USA). Treatment was delivered with a Varian Trilogy linear accelerator (Varian Medical Systems, Palo Alto, CA) using a 6-MV photon beam.

Follow-Up

The cutoff date for the last follow-up was February 28, 2018, for censored data analysis. The OS was calculated from the start of SBRT to the date of death or the last follow-up visit.

Image Acquisition

The entire image used for radiomic analysis was obtained from the CT scan acquired prior to SBRT. Contrast-enhanced CT imaging was performed using a LightSpeed RT 16 scanner (GE Healthcare, Chicago, IL, USA). The scanning parameters used in this study were as follows: tube voltage, 120 kVp; field of view, 250–400 mm; pixel size, 512 × 512; slice thickness, 0.25 cm; and average number of slices, 116. The CT images were preprocessed by wavelet-based methods and then analyzed to extract the radiomic features from the GTV that contributed to the SBRT plans. Feature extraction was based on the three-dimensional (3D) slicer platform and performed using the pyradiomics package, which is available at: http://PyRadiomics.readthedocs.io/en/latest/ (accessed on June 30, 2019) (23).

Statistical Analyses

All statistical analyses were performed using R software, version 3.6.3 (R Foundation for Statistical Computing, Vienna, Austria) and X-tile software, version 3.6.1 (Yale University School of Medicine, New Haven, Conn). Least absolute shrinkage and selection operator (LASSO) Cox regression modeling was used for data dimension reduction, feature selection, and radiomic feature building to select the most valuable predictive radiomic features from GTV. Multivariate Cox-regression hazard models were built for the survival outcome, radiomic features,

TABLE 1 | Patient characteristics.

Characteristics	*n* (%)
Age, y	
≥50	48 (68.6)
<50	22 (31.4)
Gender	
Male	59 (84.3)
Female	11 (15.7)
Stage T	
T3	65(92.9)
T4	5(7.1)
Stage N	
N0	48(68.6)
N1	22(31.4)
Stage M	
M0	57(81.4)
M1	13(18.6)
Types of PVTT	
II	42 (60.0)
III	27 (38.6)
IV	1 (1.4)
HBsAg	
Negative	12 (17.1)
Positive	58 (82.9)
Child-Pugh classification	
A	45 (64.3)
B	24 (34.3)
C	1 (1.4)
ECOG	
0	56 (80.0)
1	14 (20.0)
AFP, ng/L	
≤20	13 (18.6)
21∼399	17 (24.3)
≥400	40 (57.1)
PLT, 10^9/L	
≥100	39 (55.7)
<100	31 (44.3)
HGB, g/L	
≥120	42 (60.0)
<120	28 (40.0)
TBIL, μmol/L	
≥20	34 (48.6)
<20	36 (51.4)
ALB, g/L	
≥35	41 (58.6)
<35	29 (41.4)
ALT, U/L	
≥50	25 (35.7)
<50	45 (64.3)
AST, U/L	
≥50	48 (68.6)
<50	22 (31.4)

PVTT, Portal vein tumor thrombus; HBsAg, Hepatitis B surface antigen; PS, Performance status; ECOG, Eastern Cooperative Oncology Group; AFP, Alpha–fetoprotein; PLT, Platelet; HGB, Hemoglobin; TBIL, Total bilirubin; ALB, Albumin; ALT, Alanine aminotransferase; AST, Aspartate aminotransferase.

and clinical characteristics presented with the nomogram. A nomogram is a specific functional representation that graphically displays prediction models using lines with numerical scales based on traditional statistical methods. LASSO was used to select radiomic features to fit the Cox proportion model using the "glmnet" package in R software, and the Multivariate Cox-regression hazards models and nomogram and calibration curve were performed with the "survival" and "rms" packages in R software, respectively. The area under the receiver operating characteristic (AUROC) curve was used to evaluate the nomogram model. The radiomic scores (Rad-scores) were calculated for each patient using a linear combination of selected radiomic features, weighted by their respective coefficients. The cutoff value of the Rad-score was calculated using X-tile software to categorize patients into the high-risk or low-risk groups.

RESULTS

The median follow-up time was 9.5 months. Twenty-five patients (35.7%) were still alive at the time of the current analysis. The median survival time was 10.0 months (95% CI, 7.7–12.3). **Table 1** shows the patients' clinical characteristics. All 851 radiomic features were extracted, including Shape features (which include descriptors of the 2D and 3D size and shape of the region of interest and are independent from the gray level intensity distribution in the region of interest and therefore only calculated on the non-derived image and mask), First Order features (which describe the distribution of voxel intensities within the image region defined by the mask through commonly used and basic metrics), Gray Level Co-occurrence Matrix features (GLCM, which describe the second-order joint probability function of an image region constrained by the mask), Gray Level Dependence Matrix features (GLDM, which quantify gray level dependencies in an image), Gray Level Run Length Matrix features (GLRLM, which quantify gray level runs that are defined as the length in number of consecutive pixels that have the same gray level value), Gray Level Size Zone Matrix features (GLSZM, which quantify gray level zones in an image), and Neighboring Gray Tone Difference Matrix features (NGTDM, which quantify the difference between a gray value and the average gray value of its neighbors within some distance). High-throughput radiomic features were reduced with LASSO regression (**Figure 1**). Four radiomic features and six clinical characteristics were extracted for OS analysis. The radiomic features included Short Run Low Gray Level Emphasis (SRLGLE, which measures the joint distribution of shorter run lengths with lower gray-level values) of the GLRLM of the wavelet-HLL (H = high-frequency band, L = low-frequency band) (feature 1), Inverse Difference Moment Normalized (Idmn, which is a measure of the local homogeneity of an image) of the GLCM of the wavelet-LLL (feature 2), Small Dependence Low Gray Level Emphasis (SDLGLE, which measures the joint distribution of small dependence with lower gray-level values) of the GLDM of the wavelet-HLL (feature 3), and Idmn of the GLCM of the original (feature 4). The clinical characteristics included the ECOG score, type of PVTT, Child-Pugh classification, age, and

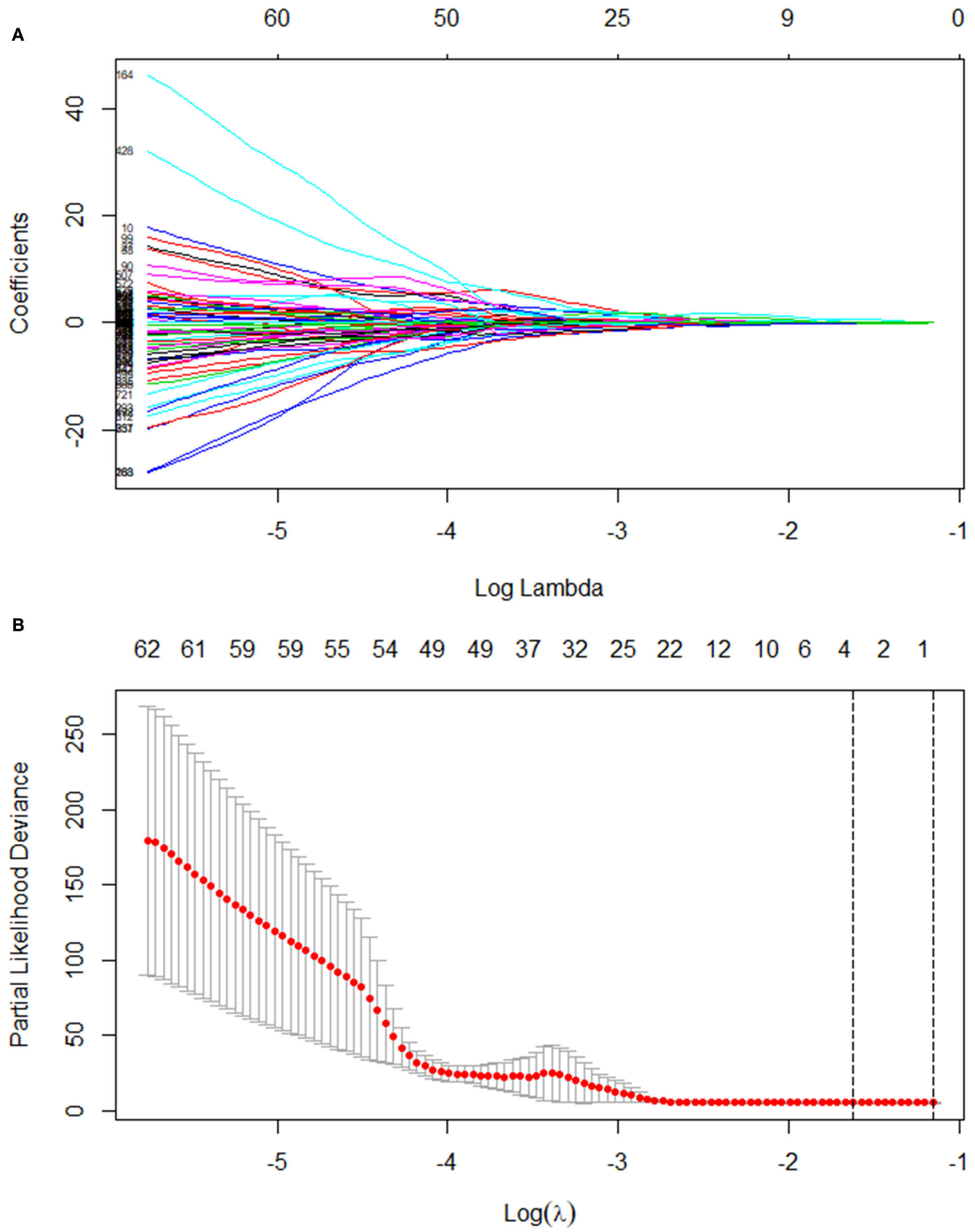

FIGURE 1 | LASSO coefficient profiles of the 851 texture features **(A)** Tuning parameter (λ) selection in the LASSO model used 10-fold cross-validation with minimum criteria **(B)**. LASSO, least absolute shrinkage and selection operator.

albumin and hemoglobin levels. **Table 2** summarizes the results of the univariate log-rank test for clinical characteristics.

The coefficients of the selected radiomic features are shown in **Figure 2**. Features 1–4 consisted of radiomic features and the Rad_score was calculated using the following formula:

$$\text{Rad\_score} = \text{feature 1} \times 1.7386385 - \text{feature 2} \times 1.0795126 + \text{feature 3} \times 0.8927949 + \text{feature 4} \times 0.1599488$$

The cutoff Rad-score value was −0.1, which was used to classify patients into the high-risk group (Rad-score ≥-0.1) and low-risk group (Rad-score < −0.1). The survival curves of both groups are shown in **Figure 3**.

The combination of the radiomic features, clinical characteristics nomogram, and calibration curves is presented in **Figure 4**. The area under the curve (AUC) for the clinical characteristics was 0.761 (CI: 0.641–0.881), and the AUC was 0.859 (CI: 0.770–0.948) when the radiomic features were combined with the clinical characteristics (**Figure 5**). We also compared our findings with those of recent studies (**Table 3**) (24–27).

TABLE 2 | Significant covariates with respect to the survival and related log-rank test *P*-values.

Covariate	HR (95% CI for HR)	*P*-value
Age	1.04 (1.011–1.07)	0.006796
Gender	1.728 (0.8304–3.598)	0.1435
Stage T	0.7244 (0.2225–2.358)	0.5924
Stage N	0.943 (0.5012–1.773)	0.8546
Stage M	0.936 (0.435–2.014)	0.8656
Types of PVTT	0.518 (0.276–0.971)	0.0403
HBsAg	0.989 (0.9302–1.052)	0.7339
Child-Pugh classification	1.914 (1.036–3.537)	0.0243
ECOG	2.342 (1.232–4.453)	0.009441
AFP	1 (1)	0.06224
PLT	1 (0.9963–1.005)	0.8193
HGB	0.9783 (0.9628–0.994)	0.006954
TBIL	1.007 (0.9957–1.018)	0.2332
ALB	0.918 (0.8543–0.9865)	0.01982
ALT	0.997 (0.993–1.002)	0.2326
AST	0.999 (0.9981–1.001)	0.5197

PVTT, Portal vein tumor thrombus; HBsAg, Hepatitis B surface antigen; PS, Performance status; ECOG, Eastern Cooperative Oncology Group; AFP, Alpha–fetoprotein; PLT, Platelet; HGB, Hemoglobin; TBIL, Total bilirubin; ALB, Albumin; ALT, Alanine aminotransferase; AST, Aspartate aminotransferase.

DISCUSSION

The application of radiomics has been extensively studied in esophageal cancer (28, 29), non-small cell lung cancer (30), breast cancer (31), nasopharyngeal carcinoma (32), Glioblastoma (33), and rectal cancer (34), which indicates the potential of radiomics for predicting the efficacy of treatment or patient prognosis. Radiotherapy-orientated CT imaging must be acquired prior to SBRT treatment of HCC with PVTT. Image data analysis of the pre-SBRT CT image is used to predict the OS of patients with HCC and PVTT, to limit examinations and provide guidance for clinical treatment decisions. This knowledge provided the basis for this retrospective study. We developed and validated a nomogram based on a combination of radiomic features and clinical characteristics from localized CT performed prior to SBRT treatment to make individualized OS predictions in patients with HCC with PVTT. The nomogram included four radiological features and six clinical features. The methodology implemented in this study is simple and reproducible because the features were generated from a validated package, which is freely available from the 3D slicer (23).

LASSO regression is suitable for the accurate analysis of large radiological features with relatively small sample sizes and its design can prevent overfitting of the model (35, 36). The regression coefficients of most features are reduced to zero during the model fitting process, making it easier to interpret the model, which allows for the identification of features closely related to OS. Yin et al. (37) compared three feature selection methods (relief, LASSO, and random forest), and concluded that LASSO had the best performance, which could enhance

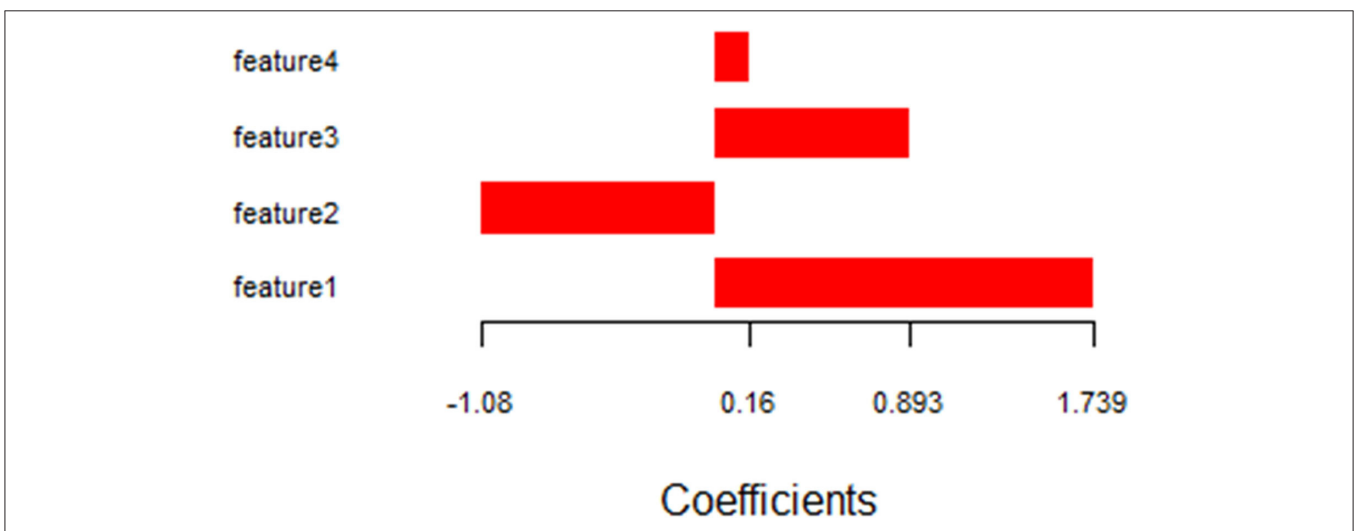

FIGURE 2 | Histograms showing the role of individual features contributing to the radiomic features. Contributing features are plotted on the y-axis and their LASSO analysis coefficients are plotted on the x-axis. LASSO, least absolute shrinkage and selection operator.

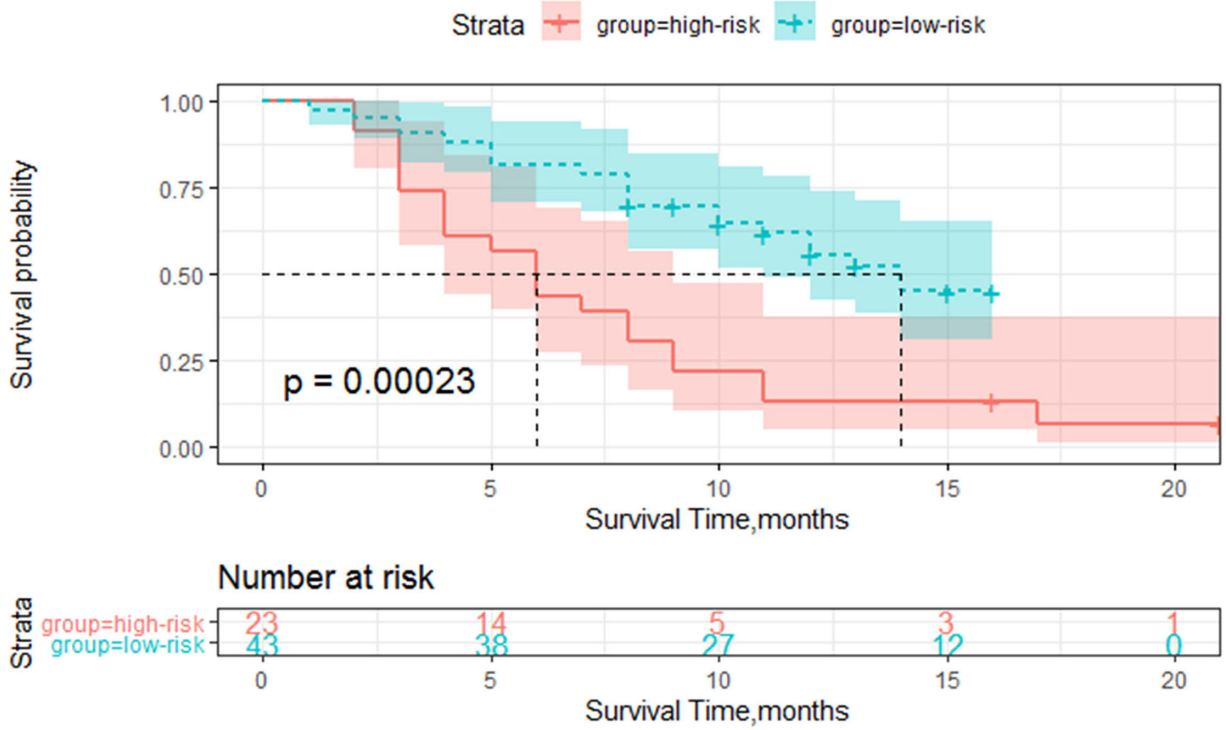

FIGURE 3 | Survival curve of the high and low-risk groups based on the radiomics score classification.

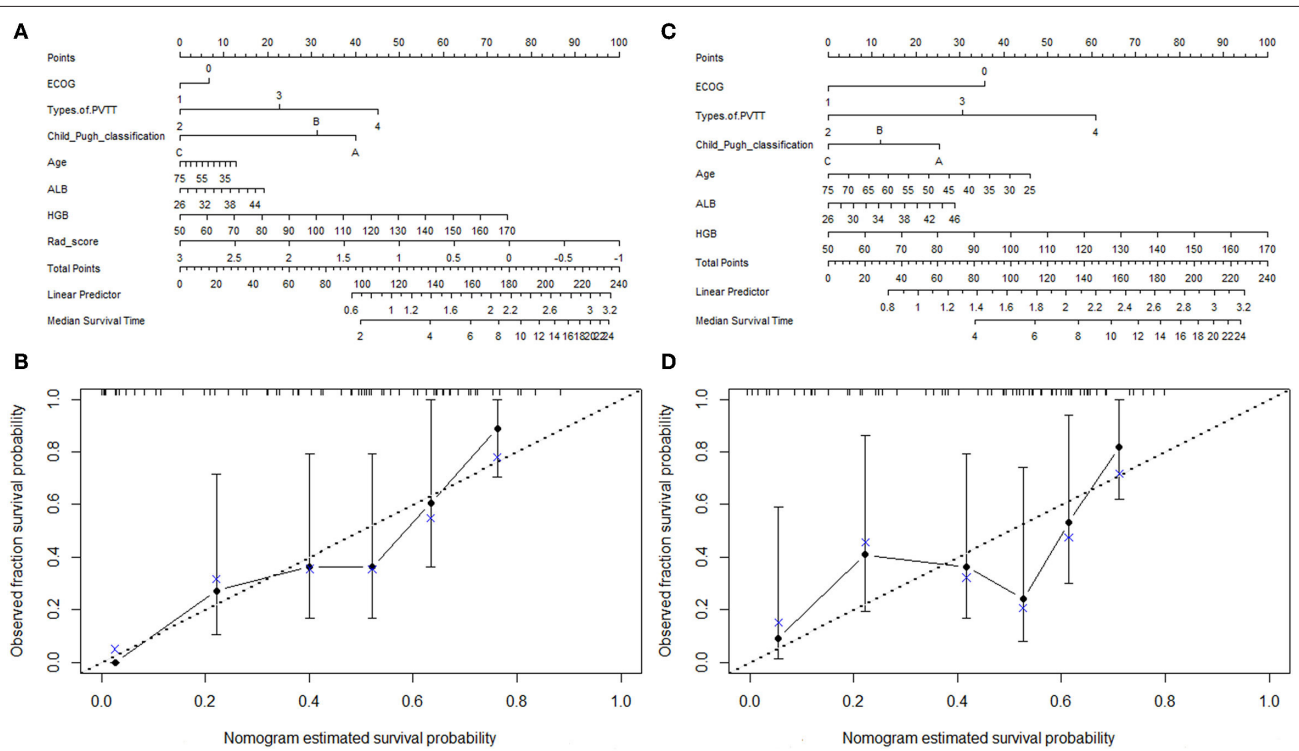

FIGURE 4 | The nomogram of the combination of the radiomic features and clinical characteristics **(A)** and the associated calibration curve for the combination of the radiomic features and clinical characteristics. **(B)** The nomogram of the clinical characteristics **(C)** and the associated calibration curve for clinical characteristics **(D)**.

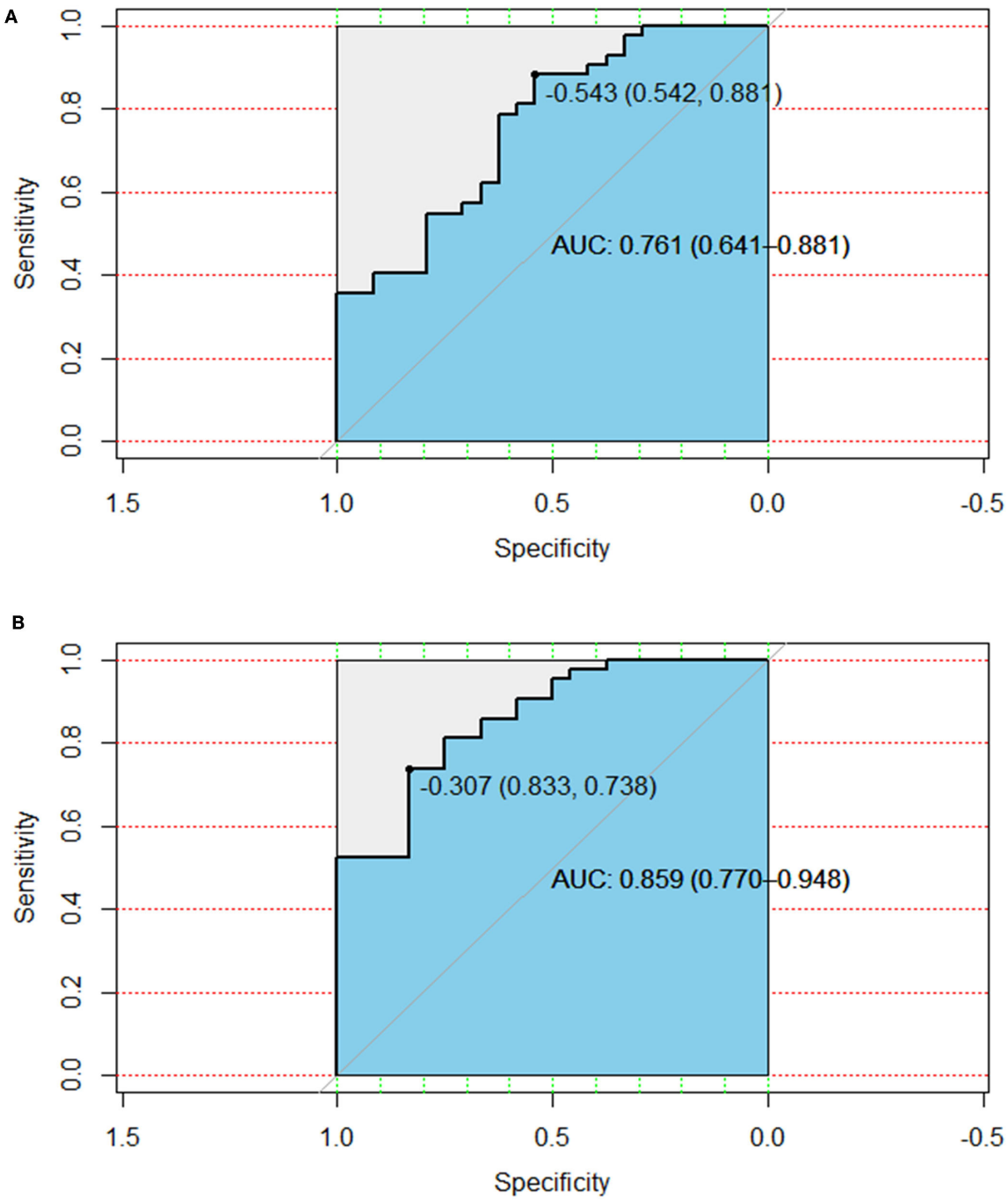

FIGURE 5 | The AUC of clinical characteristics **(A)** and the combined radiomic features and clinical characteristics **(B)**. AUC, area under the curve.

the application of radiomics methods. The radiological features identified successfully classified patients into high-risk and low-risk groups, based on the Rad-scores.

SBRT focusses on treating stage IIIA and IVB HCC with PVTT, which has a relatively short OS. The accurate prediction of the OS of patients with HCC with PVTT undergoing SBRT will typically benefit those with shorter OS periods the most. We aim to develop a new model in a future study, which will include patients with low-stage HCC treated with SBRT. TNM staging was not selected as a clinical feature related to OS in this study because patients with HCC with PVTT belong to the late clinical-stage, which makes it difficult to predict OS using clinical staging since all patients have similar staging information. Alpha-fetoprotein was also not selected as a clinical feature to determine

TABLE 3 | Summary of the studies that evaluated radiomics in the hepatocellular carcinoma.

References	Purposes	Type	Treatment	Imaging modality	Feature selection model	Main results
Ji et al. (24)	RFS	Early Stage HCC	Hepatectomy	Contrast-enhanced CT	LASSO	AUC 0.82
Shan et al. (25)	Predict early recurrence	HCC	Hepatectomy	Contrast-enhanced CT	LASSO	AUC 0.80
Zheng et al. (26)	Predict recurrence and survival	Solitary HCC	Hepatectomy	Contrast-enhanced CT	LASSO	Recurrence AUC 0.64 Survival AUC 0.71
Peng et al. (27)	Prediction of MVI	HBV-related HCC	–	Contrast-enhanced CT	LASSO	c-index 0.846
In this study	Predict survival	HCC with PVTT	SBRT	Contrast-enhanced CT	LASSO	Survival AUC 0.859

RFS, recurrence-free survival; HCC, hepatocellular carcinoma; LASSO, least absolute shrinkage and selection operator; MVI, microvascular invasion; HBV, hepatitis B virus; SBRT, stereotactic body radiotherapy.

OS in this study for the same reason. This probably contributed to the poor predictive value of the clinical parameters in this study. The combination of the radiomic features and clinical characteristics resulted in better performance for the estimation of OS [AUC = 0.859 (CI: 0.770–0.948)] than that with the clinical characteristics alone [AUC = 0.761 (CI: 0.641–0.881)]. The radiomic features effectively compensated for the deficiencies in the clinical characteristics. This model also supported the value of radiomic features for the individual association between the OS of HCC with PVTT treated by SBRT.

The limitations of the study are that genomic characteristics were not considered. In recent years, genetic markers have been used to predict OS in patients with liver cancer in research settings (38). Radiogenomics is a discipline that studies the relationship between image phenotypes and genomics. It has gradually emerged in the field of cancer research and continues to receive more attention (39–41). Further research is necessary with a larger study population to identify the associated genetic characteristics and predict the OS of patients more accurately. Another limitation of this feasibility study is the lack of validation based on independent data sets. For the training sample size, Chalkidou et al. (42) proposed that for multiple regressions, at least 10–15 observations per predictor variable is required to produce reasonably stable estimates. In our study, four features were selected for the final model and the minimum data size was 40–60. Finally, 70 patients were involved in this study as training group, which were enough. Due to the limited sample size, we were unable to divide the survey cohort into testing groups. A separate multi-center validation study is currently underway and will enroll a larger patient population to overcome this limitation.

CONCLUSIONS

This study demonstrated that the use of a nomogram combining radiologic features with clinical risk factors can personalize OS prediction in patients with HCC with PVTT who underwent SBRT.

DATA AVAILABILITY STATEMENT

All datasets generated in this study are included in the article/**Supplementary Material**.

ETHICS STATEMENT

The studies involving human participants were reviewed and approved by treatment and data analysis were conducted according to the Declaration of Helsinki. The studies involving human participants were reviewed and approved by the Second Affiliated Hospital, Zhejiang University School of Medicine Ethics Committee. The patients/participants provided their written informed consent to participate in this study.

AUTHOR CONTRIBUTIONS

HP: guarantor of integrity of entire study. KW and HP: literature research. KW, YS, and HP: statistical analysis and manuscript editing. All authors: study concepts, study design, data acquisition, data analysis and interpretation, manuscript drafting and manuscript revision for important intellectual content, approval of final version of submitted manuscript, agree to ensure any questions related to the work are appropriately resolved, and clinical studies.

SUPPLEMENTARY MATERIAL

The Supplementary Material for this article can be found online at: https://www.frontiersin.org/articles/10.3389/fonc.2020.569435/full#supplementary-material

REFERENCES

1. Siegel RL, Miller KD, Jemal A. Cancer statistics, 2017. *CA Cancer J Clin*. (2017) 67:7–30. doi: 10.3322/caac.21387
2. Chen W, Zheng R, Baade PD, Zhang S, Zeng H, Bray F, et al. Cancer statistics in China, 2015. *CA Cancer J Clin*. (2016) 66:115–32. doi: 10.3322/caac.21338
3. Costentin CE, Ferrone CR, Arellano RS, Ganguli S, Hong ST, Zhu A, et al. Hepatocellular carcinoma with macrovascular invasion: defining the

optimal treatment strategy. *Liver Cancer*. (2017) 6:360–74. doi: 10.1159/000481315
4. Yuan BH, Yuan WP, Li RH, Xiang BD, Gong WF, Li LQ, et al. Propensity score-based comparison of hepatic resection and transarterial chemoembolization for patients with advanced hepatocellular carcinoma. *Tumour Biol*. (2016) 37:2435–41. doi: 10.1007/s13277-015-4091-x
5. Zhang ZM, Lai EC, Zhang C, Yu H, Liu Z, Wan B, et al. The strategies for treating primary hepatocellular carcinoma with portal vein tumor thrombus. *Int J Surg*. (2015) 20:8–6. doi: 10.1016/j.ijsu.2015.05.009
6. Chan SL, Chong CC, Chan AW, Poon DM, Chok KS. Management of hepatocellular carcinoma with portal vein tumor thrombosis: review and update at 2016. *World J Gastroenterol*. (2016) 22:7289–300. doi: 10.3748/wjg.v22.i32.7289
7. Zhong JH, Peng NF, You XM, Ma L, Xiang X, Wang YY, et al. Tumor stage and primary treatment of hepatocellular carcinoma at a large tertiary hospital in China: a real-world study. *Oncotarget*. (2017) 8:18296–302. doi: 10.18632/oncotarget.15433
8. Schöniger-Hekele M, Müller C, Kutilek M, Ferenci P, Gangl A. Hepatocellular carcinoma in Central Europe: prognostic features and survival. *Gut*. (2001) 48:103–9. doi: 10.1136/gut.48.1.103
9. Cabibbo G, Enea M, Attanasio M, Bruix J, Craxì A, Cammà C. A meta-analysis of survival rates of untreated patients in randomized clinical trials of hepatocellular carcinoma. *Hepatology*. (2010) 51:1274–83. doi: 10.1002/hep.23485
10. Koo JE, Kim JH, Lim YS, Park SJ, Won HJ, Sung KB, et al. Combination of transarterial chemoembolization and three-dimensional conformal radiotherapy for hepatocellular carcinoma with inferior vena cava tumor thrombus. *Int J Radiat Oncol Biol Phys*. (2010) 78:180–7. doi: 10.1016/j.ijrobp.2009.07.1730
11. Fujino H, Kimura T, Aikata H, Miyaki D, Kawaoka T, Kan H, et al.Role of 3-D conformal radiotherapy for major portal vein tumor thrombosis combined with hepatic arterial infusion chemotherapy for advanced hepatocellular carcinoma. *Hepatol Res*. (2015) 45:607–17. doi: 10.1111/hepr.12392
12. Kubo K, Kimura T, Aikata H, Takahashi S, Takeuchi Y, Takahashi I, et al. Long-term outcome of stereotactic body radiotherapy for patients with small hepatocellular carcinoma: long-term outcome of SBRT for HCC. *Hepatol Res*. (2018) 48:701–7. doi: 10.1111/hepr.13063
13. Shui Y, Yu W, Ren X, Guo Y, Xu J, Ma T, et al. Stereotactic body radiotherapy based treatment for hepatocellular carcinoma with extensive portal vein tumor thrombosis. *Radiat Oncol*. (2018) 13:188–9. doi: 10.1186/s13014-018-1136-5
14. Kellock T, Liang T, Harris A, Schellenberg D, Ma R, Ho S, et al. Stereotactic body radiation therapy (SBRT) for hepatocellular carcinoma: imaging evaluation post treatment. *Br J Radiol*. (2018) 91:20170118. doi: 10.1259/bjr.20170118
15. Miften M, Vinogradskiy Y, Moiseenko V, et al. Radiation dose-volume effects for liver SBRT. *Int J Radiat Oncol Biol Phys*. (2018) 119:S45. doi: 10.1016/j.ijrobp.2017.12.290
16. Larue R, Defraene G, De Ruysscher D, Lambin P, Elmpt W. Quantitative radiomics studies for tissue characterization: a review of technology and methodological procedures. *Br J Radiol*. (2017) 90:20160665. doi: 10.1259/bjr.20160665
17. Cook GJR, Azad G, Owczarczyk K, Siddique M, Goh V. Challenges and promises of PET radiomics. *Int J Radiat Oncol Biol Phys*. (2018) 102:1083–9. doi: 10.1016/j.ijrobp.2017.12.268
18. Parmar C, Grossmann P, Rietveld D, Rietbergen M, Lambin P, Aerts H. Radiomic machine learning classifiers for prognostic biomarkers of head and neck cancer. *Front Oncol*. (2015) 3:272. doi: 10.3389/fonc.2015.00272
19. Limkin E, Sun R, Dercle L, Zacharaki E, Robert C, Reuzé Z, et al. Promised and challenges for the implementation of computational medical imaging (radiomics) in oncology. *Ann Oncol*. (2017) 28:1191–2006. doi: 10.1093/annonc/mdx034
20. Scalco E, Rizzo G. Texture analysis of medical images for radiotherapy applications. *Br J Radiol*. (2017) 90:20160642. doi: 10.1259/bjr.20160642
21. Sanduleanu S, Woodruff H C, De Jong EEC, van Timmeren JE, Jochems A, Dubois L, et al. Tracking tumor biology with radiomics: a systematic review utilizing a radiomics quality score. *Radiother Oncol*. (2018) 127:349–60. doi: 10.1016/j.radonc.2018.03.033
22. Bruix J, Sherman M. Management of hepatocellular carcinoma. *Hepatology*. (2005) 42:1208–36. doi: 10.1002/hep.20933
23. Fedorov A, Beichel R, Kalpathy-Cramer J, Finet J, Fillion-Robin JC, Pujol S, et al. 3D Slicer as an image computing platform for the Quantitative Imaging Network. *Magn Reson Imaging*. (2012) 30:1323–41. doi: 10.1016/j.mri.2012.05.001
24. Ji GW, Zhu WP, Xu Q, Wang K, Wu MY, Tang WW, et al. Radiomic features at contrast-enhanced CT predict recurrence in early stage hepatocellular carcinoma: a multi-institutional study. *Radiology*. (2020) 294:191470. doi: 10.1148/radiol.2020191470
25. Shan QY, Hu HT, Feng ST, Peng ZP, Chen SL, Zhou Q, et al. CT-based peritumoral radiomics signatures to predict early recurrence in hepatocellular carcinoma after curative tumor resection or ablation. *Cancer Imaging*. (2019) 19:11. doi: 10.1186/s40644-019-0197-5
26. Zheng BH, Liu LZ, Zhang ZZ, Shi JY, Dong LQ, Tian LY, et al. Radiomics score: apotential prognostic imaging feature for postoperative survival of solitary HCC patients. *BMC Cancer*. (2018) 18:1148. doi: 10.1186/s12885-018-5024-z
27. Peng J, Zhang J, Zhang Q, Xu Y, Zhou J, Liu L. A radiomics nomogram for preoperative prediction of microvascular invasion risk in hepatitis B virus-related hepatocellular carcinoma. *Diagn Interv Radiol*. (2018) 24:121–7. doi: 10.5152/dir.2018.17467
28. Shen C, Liu Z, Wang Z, Guo J, Zhang H, Wang Y, et al. Building CT radiomics based nomogram for preoperative esophageal cancer patients lymph node metastasis prediction. *Transl Oncol*. (2018) 11:815–24. doi: 10.1016/j.tranon.2018.04.005
29. Qiu Q, Duan J, Deng H, Han Z, Gu J, Yue NJ, et al. Development and validation of a radiomics nomogram model for predicting postoperative recurrence in patients with esophageal squamous cell cancer who achieved pCR after neoadjuvant chemoradiotherapy followed by surgery. *Front Oncol*. (2020) 10:1398. doi: 10.3389/fonc.2020.01398
30. Pyka T, Bundschuh RA, Andratschke N, Mayer B, Specht H, Papp L, et al. Textural features in pre-treatment [F18]-FDG-PET/CT are correlated with risk of local recurrence and disease-specific survival in early stage NSCLC patients receiving primary stereotactic radiation therapy. *Radiat Oncol*. (2015) 10:100. doi: 10.1186/s13014-015-0407-7
31. Antunovic L, De Sanctis R, Cozzi L, Kirienko M, Sagona A, Torrisi R, et al. PET/CT radiomics in breast cancer: promising tool for prediction of pathological response to neoadjuvant chemotherapy. *Eur J Nucl Med Mol Imag*. (2019) 46:1468–77. doi: 10.1007/s00259-019-04313-8
32. Peng H, Dong D, Fang MJ, Li L, Tang LL, Chen L, et al. Prognostic value of deep learning PET/CT-based radiomics: potential role for future individual induction chemotherapy in advanced nasopharyngeal carcinoma. *Clin Cancer Res*. (2019) 25:4271–9. doi: 10.1158/1078-0432.ccr-18-3065
33. Osman AFI. A multi-parametric MRI-based radiomics signature and a practical ML model for stratifying glioblastoma patients based on survival toward precision oncology. *Front Comput Neurosci*. (2019) 13:58. doi: 10.3389/fncom.2019.00058
34. Giannini V, Mazzetti S, Bertotto I, Chiarenza C, Cauda S, Delmastro E, et al. Predicting locally advanced rectal cancer response to neoadjuvant therapy with (18)F-FDG PET and MRI radiomics features. *Eur J Nucl Med Mol Imag*. (2019) 46:878–88. doi: 10.1007/s00259-018-4250-6
35. Tibshirani R. The LASSO method for variable selection in the Cox model. *Stat Med*. (1997) 16:385–95. doi: 10.1002/(sici)1097-0258(19970228)16:4<385::aid-sim380>3.0.co;2-3
36. Gui J, Li H. Penalized Cox regression analysis in the high-dimensional and low-sample size settings, with applications to microarray gene expression data. *Bioinformatics*. (2005) 21:3001–8. doi: 10.1093/bioinformatics/bti422
37. Yin P, Mao N, Zhao C, Wu J, Sun C, Chen L, et al. Comparison of radiomics machine-learning classifiers and feature selection for differentiation of sacral chordoma and sacral giant cell tumour based on 3D computed tomography features. *Eur Radiol*. (2019) 29:1841–7. doi: 10.1007/s00330-018-5730-6
38. Golobschwarzl N, Krassnig S, Toeglhofer AM, Park YN, Gogg-Kamerer M, Vierlinger K, et al. New liver cancer biomarkers: PI3K/AKT/mTOR pathway members and eukaryotic translation initiation factors. *Eur J Cancer*. (2018) 56:56–70. doi: 10.1016/j.ejca.2017.06.003
39. Hong EK, Choi SH, Shin DJ, Jo S, Yoo RE, Kang K, et al. Radiogenomics correlation between MR imaging features and major genetic profiles

in glioblastoma. *Eur Radiol*. (2018) 28:1–12. doi: 10.1007/s00330-018-5400-8
40. Rattay T, Symonds RP, Shokuhi S, Talbot CJ, Schnur JB. The patient perspective on radiogenomics testing for breast radiation toxicity. *Clin Oncol*. (2018) 30:151–7. doi: 10.1016/j.clon.2017.12.001
41. Rutman AM, Kuo MD. Radiogenomics: creating a link between molecular diagnostics and diagnostic imaging. *Eur J Radiol*. (2009) 70:232–41. doi: 10.1016/j.ejrad.2009.01.050
42. Chalkidou A, O'Doherty MJ, Marsden PK. False discovery rates in PET and CT studies with texture features: a systematic review. *PLoS ONE*. (2015) 10:e124165. doi: 10.1371/journal.pone.0124165

Conflict of Interest: The authors declare that the research was conducted in the absence of any commercial or financial relationships that could be construed as a potential conflict of interest.

frontiers in Oncology

ORIGINAL RESEARCH
published: 27 November 2020
doi: 10.3389/fonc.2020.599907

^{18}F-FDG PET/CT Metrics Are Correlated to the Pathological Response in Esophageal Cancer Patients Treated With Induction Chemotherapy Followed by Neoadjuvant Chemo-Radiotherapy

Nicola Simoni[1], Gabriella Rossi[1], Giulio Benetti[2], Michele Zuffante[3], Renato Micera[1], Michele Pavarana[4], Stefania Guariglia[2], Emanuele Zivelonghi[2], Valentina Mengardo[5], Jacopo Weindelmayer[5], Simone Giacopuzzi[5], Giovanni de Manzoni[5], Carlo Cavedon[2†] and Renzo Mazzarotto[1†]*

[1] Department of Radiation Oncology, University of Verona Hospital Trust, Verona, Italy, [2] Department of Medical Physics, University of Verona Hospital Trust, Verona, Italy, [3] Department of Nuclear Medicine, University of Verona Hospital Trust, Verona, Italy, [4] Department of Oncology, University of Verona Hospital Trust, Verona, Italy, [5] Department of General and Upper G.I. Surgery, University of Verona Hospital Trust, Verona, Italy

Background and Objective: The aim of this study was to assess the ability of Fluorodeoxyglucose Positron Emission Tomography/Computed Tomography (^{18}F-FDG PET/CT) to provide functional information useful in predicting pathological response to an intensive neoadjuvant chemo-radiotherapy (nCRT) protocol for both esophageal squamous cell carcinoma (SCC) and adenocarcinoma (ADC) patients.

Material and Methods: Esophageal carcinoma (EC) patients, treated in our Center between 2014 and 2018, were retrospectively reviewed. The nCRT protocol schedule consisted of an induction phase of weekly administered docetaxel, cisplatin, and 5-fluorouracil (TCF) for 3 weeks, followed by a concomitant phase of weekly TCF for 5 weeks with concurrent radiotherapy (50–50.4 Gy in 25–28 fractions). Three ^{18}F-FDG PET/CT scans were performed: before (PET_1) and after (PET_2) induction chemotherapy (IC), and prior to surgery (PET_3). Correlation between PET parameters [maximum and mean standardized uptake value (SUV_{max} and SUV_{mean}), metabolic tumor volume (MTV), and total lesion glycolysis (TLG)], radiomic features and tumor regression grade (TGR) was investigated.

Results: Fifty-four patients (35 ADC, 19 SCC; 48 cT3/4; 52 cN+) were eligible for the analysis. Pathological response to nCRT was classified as major (TRG1-2, 41/54, 75.9%) or non-response (TRG3-4, 13/54, 24.1%). A major response was statistically correlated with SCC subtype (p = 0.02) and smaller tumor length (p = 0.03). MTV and TLG measured prior to IC (PET_1) were correlated to TRG1-2 response (p = 0.02 and p = 0.02, respectively). After IC (PET_2), SUV_{mean} and TLG correlated with major response (p =

OPEN ACCESS

Edited by:
Francesco Cellini, Catholic University of the Sacred Heart, Italy

Reviewed by:
Chunhao Wang, Duke University Medical Center, United States
Valentina Lancellotta, Catholic University of the Sacred Heart, Italy

***Correspondence:**
Nicola Simoni
nicola.simoni@aovr.veneto.it

†These authors share senior authorship

Specialty section:
This article was submitted to Radiation Oncology, a section of the journal Frontiers in Oncology

Received: *28 August 2020*
Accepted: *27 October 2020*
Published: *27 November 2020*

Citation:
Simoni N, Rossi G, Benetti G, Zuffante M, Micera R, Pavarana M, Guariglia S, Zivelonghi E, Mengardo V, Weindelmayer J, Giacopuzzi S, de Manzoni G, Cavedon C and Mazzarotto R (2020) ^{18}F-FDG PET/CT Metrics Are Correlated to the Pathological Response in Esophageal Cancer Patients Treated With Induction Chemotherapy Followed by Neoadjuvant Chemo-Radiotherapy. Front. Oncol. 10:599907. doi: 10.3389/fonc.2020.599907

0.03 and p = 0.04, respectively). No significance was detected when relative changes of metabolic parameters between PET_1 and PET_2 were evaluated. At textural quantitative analysis, three independent radiomic features extracted from PET_1 images ([JointEnergy and InverseDifferenceNormalized of GLCM and LowGrayLevelZoneEmphasis of GLSZM) were statistically correlated with major response ($p < 0.0002$).

Conclusions: ^{18}F-FDG PET/CT traditional metrics and textural features seem to predict pathologic response (TRG) in EC patients treated with induction chemotherapy followed by neoadjuvant chemo-radiotherapy. Further investigations are necessary in order to obtain a reliable predictive model to be used in the clinical practice.

Keywords: positron emission tomography metrics, pathological response, induction chemotherapy, chemo-radiation, esophageal cancer, radiomic features, neoadjuvant therapy

INTRODUCTION

Esophageal Cancer (EC) is a major health problem worldwide, representing the 7th leading cause of cancer-related mortality (1). In locally advanced stage disease, a preoperative approach (chemotherapy or chemo-radiotherapy) is currently accepted as standard of care (2). In particular, randomized trials evaluating neoadjuvant chemo-radiotherapy (nCRT) followed by surgery, have demonstrated a 10%–15% improvement in long-term survival rate with trimodality therapy as compared with surgery alone (3–5). Notably, Tumor Regression Grade (TRG) of the primary tumor after nCRT is a well-established prognostic factor to predict long-term prognosis in EC (6–8). Hence, in order to identify a subset of patients who would most likely benefit from nCRT, the availability of prognostic and predictive markers for response, is strongly advocated.

In our experience, after the completion of a phase II study, an intensive nCRT protocol consisting of induction chemotherapy (IC), followed by concurrent chemo-radiotherapy (CRT), and thereafter by surgery, was considered the standard approach for both Squamous Cell Carcinoma (SCC) and Adenocarcinoma (ADC) of the esophagus and gastroesophageal junction (EGJ). In our series, 5-year survival rates were 77% for pathological complete response (pCR), 44% for near pCR (microfoci of tumor cells on the primary tumor), and 14% for residual tumor subsets, respectively ($p < 0.001$) (9). It can be hypothesized that the use of induction chemotherapy may allow to screen patients with EC in "good responders", in which CRT following IC may determine an effective survival advantage and therefore should be used, and in "bad responders", in which CRT could be unnecessary or even detrimental due to possible adverse events. In this unfavorable group, surgery should not be further delayed or, alternatively, a change in systemic therapy should be adopted.

Fluorodeoxyglucose Positron Emission Tomography/Computed Tomography (^{18}F-FDG PET/CT), combining functional PET information with anatomical CT images, is routinely used for diagnosis, radiation treatment planning, and response evaluation in various gastrointestinal malignancies (10–13). In particular, the role of ^{18}F-FDG PET/CT for baseline staging, restaging before surgery, and recurrence/distant metastases detection during follow-up in EC is well established (14, 15). Furthermore, it represents a useful, non-invasive tool to assess the response to neoadjuvant chemotherapy and chemo-radiotherapy. Several traditional PET parameters, such as maximum and mean standardized uptake value (SUVmax and SUVmean), metabolic tumor volume (MTV), and total lesion glycolysis (TLG), have demonstrated the ability to provide functional information useful in predicting pathological response to nCRT in EC patients (16–18). More recently, radiomic features are emerging as promising tools to stratify patients in "good" or "bad" responders. Some studies have investigated different first, second and high-order features, in EC patients, demonstrating that PET radiomic parameters can predict the response to nCRT (19–25). In addition, Chen et al. postulated that using a combination of traditional and radiomic PET parameters can provide a better stratification of patients into different prognostic subgroups (26).

Based on this background, we performed a novel analysis to evaluate the ability of ^{18}F-FDG PET/CT metrics to predict histological tumor regression in patients with EC treated with an intensive nCRT protocol.

MATERIAL AND METHODS

Study Design

This is a single-center retrospective analysis of prospectively collected data, approved by the Institutional Review Board of our Hospital. Inclusion criteria were: a) patients treated with an intensive nCRT protocol for locally advanced resectable SCC or ADC of the esophagus or EGJ (Siewert I and II); b) availability of ^{18}F-FDG PET/CT scans performed before and after induction chemotherapy, and before surgery; c) surgical resection; d) availability of resection specimens for pathological analysis. Exclusion criteria were: a) chemo-radiation therapy approaches other than the nCRT protocol (e.g., CROSS scheme); b) Siewert III type (candidates for peri-operative chemotherapy) and SC cervical tumors (treated with definitive CRT); c) upfront resectable (cT1 or cT2N0) or metastatic disease; d) non-execution of at least one of the three ^{18}F-FDG PET/CT scans; e) no surgical resection; f) unavailability of resection specimens.

nCRT Protocol and Surgery

The nCRT protocol consisted of a first phase of induction chemotherapy with docetaxel, cisplatin and 5-fluorouracil (TCF) for 3 weeks (days 1-22), followed by a second phase of concurrent chemotherapy (TCF) and radiotherapy for 5–6 weeks (days 29-63), as previously described (9). Radiation therapy (RT) was delivered with volumetric modulated arc therapy (VMAT), prescribing 50-50.4 Gy in 25-28 fractions. **Figure 1** describes the nCRT protocol schedule. Sample VMAT plans are presented in **Figures S1** and **S2** (**Supplementary Material**).

After restaging, surgery with radical intent was performed 8 weeks after nCRT completion. Tri-incisional subtotal esophagectomy (McKeown procedure), partial esophagectomy (Ivor-Lewis procedure) or total gastrectomy with distal esophagectomy was performed based on tumor characteristics.

^{18}F-FDG PET/CT Method and Metrics

Three ^{18}F-FDG PET/CT scans were performed: the first (PET_1) at baseline, before the start of the induction phase and the second (PET_2) before the concomitant phase (week 4 of nCRT protocol). PET_1 and PET_2 were performed with the patient in RT treatment position, as simulation for volume delineation and treatment planning. The third ^{18}F-FDG PET/CT (PET_3) was performed during restaging prior to surgery. **Figure 2** shows ^{18}F-FDG PET/CT relative time points.

The ^{18}F-FDG PET/CT scan was performed using the Gemini TF Big Bore system (Philips Medical Systems, Eindhoven, The Netherlands) at our Nuclear Medicine Department. All patients were asked to fast for at least 6 h and blood glucose levels were checked before imaging. Patients underwent a whole-body scan, from skull base to mid-thigh, starting 60 ± 10 min after the intravenous injection of 3 MBq/Kg of ^{18}F-FDG. The acquisition parameters for diagnostic CT scan were: 120 kV, 60–80 mAs, pitch 0.813, collimation 16x1,5 mm, field of view (FOV) 600 mm. CT scan images were reconstructed using a filtered back projection with 5 mm thickness and 512x512 matrix. For simulation, CT mAs automatic modulation and 3 mm thickness reconstruction were adopted. The acquisition time of PET scanning was 1.15 min per bed position, with a FOV of 576 mm. PET images were reconstructed using list mode ordered subset expectation maximization (LMOSEM) algorithm (144 x 144 matrix, 4 mm/pixel, 4 mm slice thickness). CT images were used to correct the PET emission data for photon attenuation.

For this analysis, the tumor was segmented on the ^{18}F-FDG PET/CTs dataset using a semi-automatic gradient-based method called "PET Edge" (MIM software, Mim Software Inc., US), which identifies the boundary of the metabolically active tumor based on the surface defined by the maximum gradient of metabolic activity. Quantitative parameters were extracted from the ^{18}F-FDG PET/CT scans at the three time points

		First Phase (Induction Chemotherapy)				Second Phase (Concurrent Chemoradiotherapy)					
Week		1	2	3	4	5	6	7	8	9	10
CHT T	35 mg/m^2	↓	↓	↓		↓	↓	↓	↓	↓	
C	25 mg/m^2	↓	↓	↓		↓	↓	↓	↓	↓	
F	c.i.	180 x 3 weeks				150 x 5 weeks					
RT§						|||||	|||||	|||||	|||||	|||||	||*

FIGURE 1 | Schematic diagram of the neoadjuvant chemo-radiotherapy protocol schedule. CHT, chemotherapy; T, docetaxel; C, cisplatin; F, 5 fluorouracil; c.i., continuous infusion; RT, radiotherapy. Doses of 5 fluorouracil (F) are given as mg/m^2/day. § RT 50-50.4 Gy in 25–28 fractions; * if 28 RT fractions are used.

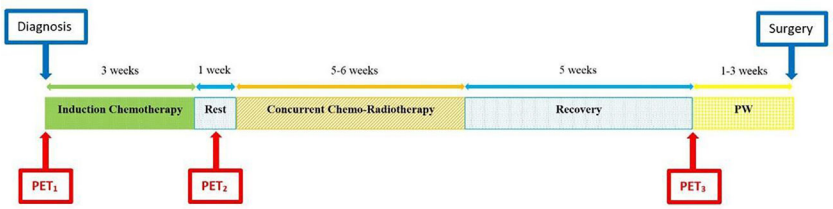

FIGURE 2 | Diagram of total neoadjuvant protocol from diagnosis to surgery, including induction chemotherapy and concomitant chemo-radiotherapy, with ^{18}F-FDG PET/CTs at relative time points. PW, preoperative workup, including restaging.

(PET_1, PET_2, and PET_3) previously reported. These parameters were: maximum and mean standardized uptake value (SUV_{max} and SUV_{mean}), metabolic tumor volume (MTV) and total lesion glycolysis (TLG), defined as the product of MTV and SUV_{mean}.

Radiomic Feature Extraction

Radiomic features were extracted from PET_1 and PET_2 without applying any gray-level normalization nor voxel resampling. Indeed, according to the IBSI guidelines, calibrated gray levels should not be further standardized and the cubic voxel spacing was the same for the whole dataset. The DICOM files (volumes and RT Structures) were converted to the nii format through dcmrtstruct2nii (27). Since the gradient-based contouring algorithm, used to define the VOI, tends to exclude the most peripheral zones of the lesion, with the consequent inclusion of a limited number of voxels, the VOIs were dilated by 1 voxel (4 mm) in each direction. This was performed by using the built-in BinaryDilateImageFilter method of SimpleITK (v1.2.4) (28), implemented in Python (v3.7.6) under conda (v4.8.2) environment. In addition to increasing the number of voxels included in the lesion, dilating the VOI also allows the analysis to be performed on the low-enhancement region of the tumor, potentially adding information on how the uptake decreases on the lesion boundary. Radiomic features were extracted through pyradiomics (v3.0), an open-source python package (29). All the available features implemented in pyradiomics were extracted: Shape, First Order, GLCM, GLDM, GLRLM, GLSZM, and NGTDM [the meaning of these acronyms can be found in Zwanenburg et al. (30)]. For gray-level discretization, a fixed bin-count of 64 bins was adopted. A hundred and five features were extracted from both PET_1 and PET_2.

Pathological Analysis

Postsurgical pathology examination provided macroscopic and microscopic description of the primary tumor and retrieved nodes. Post-resection staging was assessed following ypTNM categories according to the International Union against Cancer (UICC, 7th edition, 2010). The degree of pathologic response was scored using the tumor regression grade (TRG) classification according to a modified Mandard score system: TRG1 = no residual cancer cells; TRG2 = residual cancer cells scattered through fibrosis; TRG3 = increased residual cancer cells with predominant fibrosis and TRG4 = including TRG4, residual cancer predominant fibrosis, and TRG5, no regressive changes within the tumor, of the Mandard score system (6). Patients were grouped according to the pathological response to nCRT in two classes of outcome. Major pathologic response was defined as TRG1–2 while non-response as TRG3–4.

Statistical Analysis

The association between clinical/radiomic data and response to treatment was first analyzed by means of the chi-square test or Fisher's exact test for categorical parameters, and Student's T-test for continuous quantities (age and length of tumor). The association between PET/CT metabolic parameters and response to treatment (defined as a dichotomous variable) was assessed by means of logistic regression and ROC analysis. For logistic regression analysis, quantitative metabolic parameters were logarithmically transformed to meet the assumption of linearity on the logit scale, as in van Rossum et al. (18). Quantitative variables were described as median and interquartile range (IQR) or mean and standard deviation (SD), and categorical variables were summarized as counts and percentages. Statistical analysis was performed using R version 4.0.2 (https://www.R-project.org/) and MATLAB version R2019a (The Mathworks, Inc.; Natick, Massachusetts, USA). The significance level of the radiomic analysis was computed at $p < 0.05/N$, where $N = 210$ is the number of the tested features considering both PET_1 and PET_2 (Bonferroni correction). Two features were considered strongly correlated (*i.e.* redundant) when the pairwise Pearson's correlation coefficient was higher than 0.90; in this case, the feature with the highest average correlation with all the other features was removed. The significance level for all tests was assumed at $p < 0.05$.

RESULTS

Study Population

Ninety-eight patients with biopsy-proven locally advanced esophageal squamous cell carcinoma (SCC) or adenocarcinoma (ADC), who underwent neoadjuvant chemo-radiotherapy at our Institution between January 2014 and December 2018, were retrospectively identified. Forty-four patients were excluded from the study for the following reasons: preoperative approach other than nCRT protocol (n=31); no surgery (n=8); lack of at least one ^{18}F-FDG PET/CT scan (n=5). The remaining 54 patients were considered eligible for analysis. Among them, 41 (75.9%) showed a major pathologic response (TRG1-2) and 13 (24.1%) a non-response (TRG3-4) to nCRT.

All patients completed the nCRT planned program. PET_1 was performed immediately before (median 8.5 days, IQR 6–14) the start of IC, while PET_2 was performed during the 4th week (median 25 days, IQR 22–28) of the nCRT protocol schedule. PET_3 was performed 5 weeks (median 5.1 weeks, IQR 4.0-5.4), and surgery 8 weeks (median 7.9 weeks, IQR 6.6–9.1) after nCRT completion.

At the last follow-up, 33 patients (61.1%) were alive. The median follow-up of the entire cohort was 32.5 months (IQR 26.0–45.0 months). The median overall survival (OS) and disease-free survival (DFS) of the TRG1-2 group at the time of last follow-up were 34.7 months (IQR 27.5–49.7 months) and 30.7 months (IQR 17.1–47.7 months), respectively, while the corresponding figures for the TRG3-4 group were 28.0 months (IQR 23.4–30.8 months) and 18.1 months (IQR 10.4–30.7 months), respectively ($p < 0.01$).

TRG and Baseline Characteristics

Table 1 reports the results of the analysis of the association between baseline parameters and response to the nCRT protocol. Parameters that statistically correlated to outcome were histological subtype ($p = 0.02$) and tumor length ($p = 0.03$). All other parameters evaluated were not statistically linked to treatment outcome.

TABLE 1 | Baseline features with significance of association to treatment outcome.

	Major response (n=41)	Non-response (n=13)	*p* value[§]
Male gender	33 (80.5%)	11 (84.6%)	0.74
Age (years)**	64.3 ± 8.9	59.9 ± 8.9	0.12
Tumor location			0.10
Medial	15 (36.6%)	1 (7.7%)	
Distal	12 (29.3%)	4 (30.8%)	
EGJ	14 (34.1%)	8 (61.5%)	
Histological subtype			0.02*
SCC	18 (43.9%)	1 (7.7%)	
ADK	23 (56.1%)	12 (92.3%)	
Length of tumor (cm)**	5.4 ± 2.1	6.8 ± 1.5	0.03*
Clinical T stage			0.90
T1/T2	5 (12.2%)	1 (7.7%)	
T3	33 (80.5%)	11 (84.6%)	
T4	3 (7.3%)	1 (7.7%)	
Clinical N stage			—
N0	2 (4.9%)	0 (0.0%)	
N+	39 (95.1%)	13 (100.0%)	

[§]*p-value of chi-square test, Fischer's exact test or Student's T-test.*
**statistically significant.*
***mean ± SD.*

TRG and Metabolic Parameters

Table 2 reports the results of the analysis of the association between metabolic parameters of PET_1 and PET_2 with tumor regression grade class (TRG1-2 vs. TRG3-4). Relative differences between the parameters at the two subsequent PET/CT scans are also reported. At baseline, MTV (AUC 0.74) and TLG (AUC 0.69) were statistically correlated to histological tumor regression. In addition, at PET_2, SUVmean (AUC 0.67) and TLG (AUC 0.64) were significantly related to a higher chance of major pathologic response (**Figure 3**). No significance was detected when relative differences were considered. Interestingly, none of the post-CRT PET metrics resulted significantly correlated with the outcome measured (average SUV_{max} was 5.01 vs. 5.09, SUV_{mean} 2.81 vs. 2.75, and MTV 8.74 ml vs. 8.74 ml, in TRG1-2 vs. TRG3-4 patients, respectively; all $p > 0.05$). Therefore, additional analysis, relative to PET_3 metrics, was not conducted. **Figure 4A** reports the boxplot distribution of the MTV at PET_1, the parameter most correlated to treatment outcome at logistic regression analysis.

Radiomic Feature Analysis

Among the 210 radiomic features (105 for each PET scan), 14 resulted significant to the t-test with the adjusted significance threshold $p_{Th} = 0.05/210 = 0.00024$ and none of them were extracted from the PET_2 scan. Since many of these features are strongly correlated, as visible in **Figure 5**, the redundant information was removed resulting in three independent features. The three resulting features, highlighted in **Figure 5** with bold fonts, are representative for the whole cluster and further reported in **Figure 6** with the relative scatterplots and histograms. The boxplot of one of these three features is reported in **Figure 4B** (LowGrayLevelZoneEmphasis).

DISCUSSION

Neoadjuvant chemo-radiotherapy (nCRT) has been widely accepted as the standard of care for the treatment of locally advanced, resectable esophageal cancer. However, a not negligible number of patients show a poor response to neoadjuvant therapy at the time of surgery (residual tumor on the resection specimen), as an expression of pre-existing intrinsic chemo- and radio-resistance. Notably, non-responder patients to nCRT have a significantly worse prognosis than responders

TABLE 2 | Results of the logistic regression and ROC curve analysis of metabolic 18F-FDG parameters before and after induction chemotherapy, with their relative differences.

	Major response median (IQR)	Non-response median (IQR)	OR (95% C.I.)	p value	AUC
SUV_{max}					
PET_1	13.3 (9.3, 16.1)	13.3 (10.5, 15.1)	0.69 (0.02 - 22.66)	0.84	0.44
PET_2	5.8 (4.5, 7.2)	6.6 (6.3, 9.8)	0.03 (0.00 - 1.08)	0.05	0.65
PET_1-PET_2 relative difference [Δ SUV_{max} (%)]	-43.3 (-65.9, -24.7)	-40.3 (-52.8, -24.4)	0.98 (0.96 – 1.01)	0.20	0.56
SUV_{mean}					
PET_1	6.1 (5.1, 7.1)	6.2 (4.6, 8.6)	1.55 (0.03 - 93.97)	0.83	0.43
PET_2	3.1 (2.5, 4.0)	3.7 (3.4, 5.0)	0.01 (0.00 – 0.59)	**0.03***	0.67
PET_1-PET_2 relative difference [Δ SUV_{mean} (%)]	-40.8 (-59.1, -29.4)	-38.6 (-44.2, -14.6)	0.98 (0.96 – 1.01)	0.19	0.54
MTV (mL)					
PET_1	17.7 (7.7, 41.4)	38.6 (35.4, 44.2)	0.03 (0.00 - 0.51)	**0.02***	0.74
PET_2	10.8 (6.6, 16.2)	13.9 (10.8, 19.3)	0.15 (0.02 – 1.41)	0.10	0.62
PET_1-PET_2 relative difference [D MTV (%)]	-44.2 (-72.4, -22.4)	-63.6 (-70.8, -55.6)	1.02 (0.99 – 1.04)	0.15	0.62
TLG					
PET_1	112.3 (54.1, 265.5)	216.8 (178.3, 300.8)	0.07 (0.01 – 0.63)	**0.02***	0.69
PET_2	30.2 (18.1, 61.5)	51.1 (30.8, 93.5)	0.11 (0.01 – 0.94)	**0.04***	0.64
PET_1-PET_2 relative difference [Δ TLG (%)]	-72.7 (-88.0, -48.8)	-73.2 (-86.6, -62.7)	1.01 (0.99 – 1.03)	0.34	0.47

**statistically significant.*

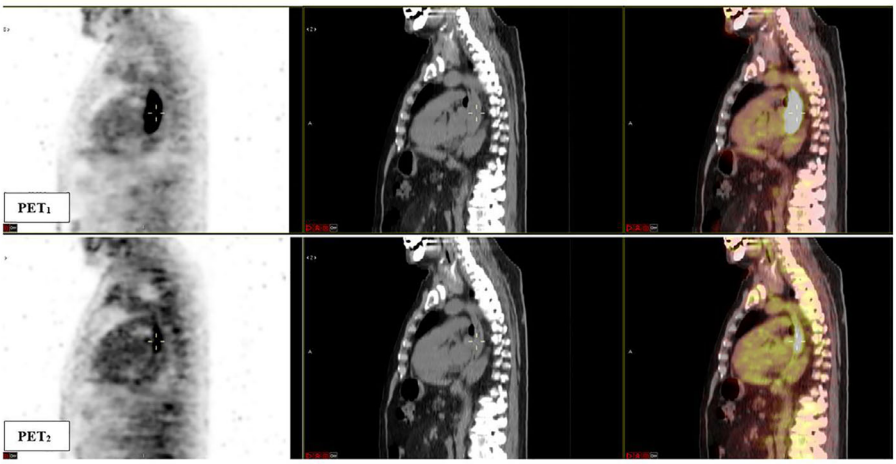

FIGURE 3 | Sagittal fused ^{18}F-FDG PET/CT images obtained at baseline (PET_1) and after induction chemotherapy (PET_2). A significant response to induction chemotherapy (reduction in metabolic parameters) of the esophageal lesion can be observed. The patient was classified as TRG1 at final pathological examination. PET_1 parameters: SUV_{max} 26.9, SUV_{mean} 12.7, MTV 43.7 ml, TLG 553.9; PET_2 parameters: SUV_{max} 6.7, SUV_{mean} 3.2, MTV 15.9 ml, TLG 50.5.

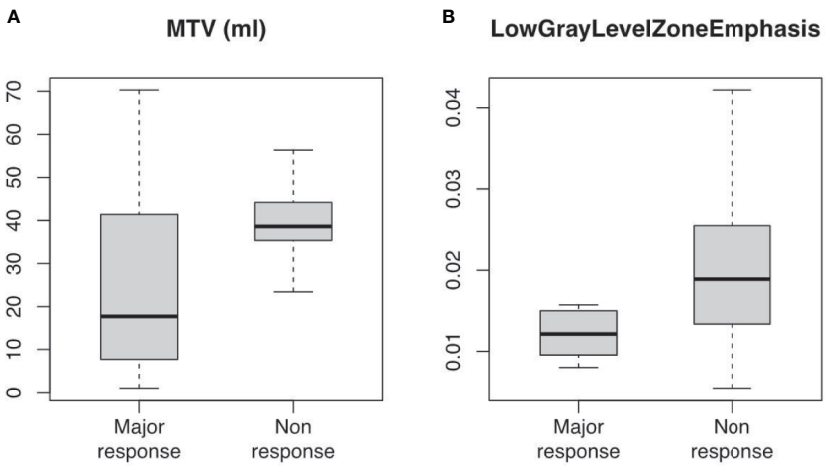

FIGURE 4 | Boxplot distribution of **(A)** MTV (ml) and **(B)** LowGrayLevelZoneEmphasis (GLCM) radiomic feature at ^{18}F-FDG PET/CT scan taken before induction chemotherapy (PET_1). Classes are divided between major (TRG1-2) and non (TRG3-4) response (median, interquartile and full range are displayed).

(6–8, 31). Thus, there is an urgent need to early identify patients who could benefit or not from preoperative treatment, using prognostic and predictive tumor biology markers. This study demonstrated that ^{18}F-FDG PET/CT metrics may be able to predict the degree of pathologic response, according to a modified Mandard tumor regression grade (TRG) score system, in patients undergoing induction chemotherapy (IC) followed by chemo-radiotherapy as an intensive neoadjuvant protocol.

Metabolic parameters, that were statistically correlated to treatment outcome, were the MTV ($p = 0.02$) at PET_1, and SUV_{mean} ($p = 0.03$) at PET_2. The TLG was also significant at both time-points ($p = 0.02$ and $p = 0.04$, respectively). This can be interpreted as a consequence of the above, as TLG is defined as the product between MTV and SUV_{mean}. These results might suggest that the lesion volume, as determined before IC, and the average metabolic activity, as determined after IC, should be considered significant. In addition, at textural quantitative analysis, three independent radiomic features extracted from PET_1 images (JointEnergy and InverseDifferenceNormalized of GLCM and LowGrayLevelZoneEmphasis of GLSZM) were statistically correlated with major response ($p < 0.0002$). This indication could be important in view of a possible early prediction of outcome, with potential advantages to patients believed to benefit from the three-stage treatment. However, further investigations are necessary in order to obtain a reliable predictive model to be used in the clinical practice, especially if

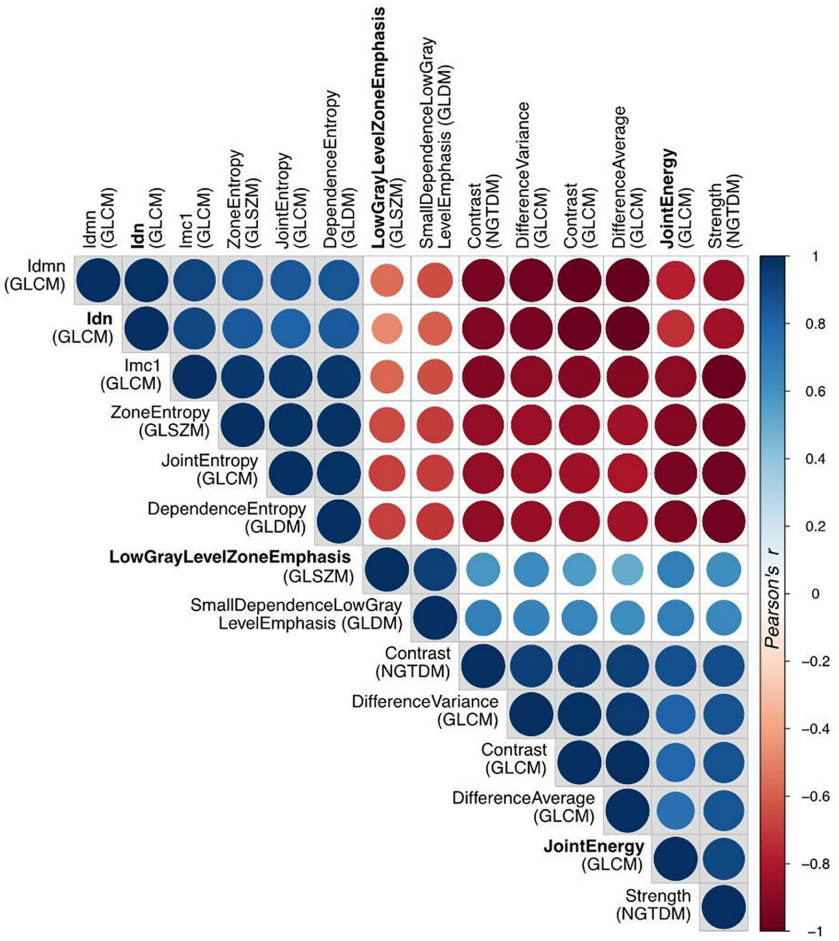

FIGURE 5 | Correlation matrix of all the radiomic features with high significance (p<0.0002) in t-test for patient response. The Pearson's correlation coefficient identifies three disjointed clusters, in which the three representatives (Idn=InverseDifferenceNormalized, JointEnergy and LowGrayLevelZoneEmphasis) are highlighted in bold.

the inclusion of radiomic features in the model is foreseen. In fact, additional validation is mandatory in the latter case since predictive models, based on radiomics, are more prone to overfitting compared to models based on conventional PET parameters.

The results of the present study could lead to different considerations. Metabolic tumor volume (MTV) combines the information of SUV uptake and tumor volume, corresponding to the volume of tumor tissues with increased glycolytic activity. In our study, MTV in poor responders was significantly higher than in good responders (38.6 ml vs. 17.7 ml, p = 0.02). Since SUV_{max} and SUV_{mean} did not differ significantly between the two groups (TRG1-2 vs. 3-4) at PET_1, this figure appears to be consensual to the greater extent of the primary tumor in non-responder patients at the time of diagnosis (tumor length 6.8 cm vs. 5.4 cm in good responders, p = 0.02). This result is consistent with previous experiences reported in the literature, showing a link between tumor length and outcome in EC patients (32, 33). This could suggest that the MTV of the primary tumor has the potential to become a valuable prognostic biomarker for response at baseline in EC patients. The other baseline parameter, significantly correlated with TRG class after nCRT, was squamous histological subtype (p = 0.02). This confirms the greater sensitivity to nCRT of the squamous histology compared to ADC, as reported in the literature (34). In this regard, whether surgery on demand is advisable in selected complete responder SCC patients after nCRT is currently under evaluation in the randomized SANO trial (35).

At PET_2 evaluation, SUV_{mean} represents the main predictor for pathological response (p = 0.03). The SUV_{mean} provides information about intrinsic lesion characteristics, related to tumor grading, biological factors, and the presence of hypoxic or necrotic areas. Thus, it is reasonable to hypothesize that SUV_{mean} after IC might be an effective predictor of the final response to nCRT. This post-induction chemotherapy assessment could help to guide a PET-adapted preoperative

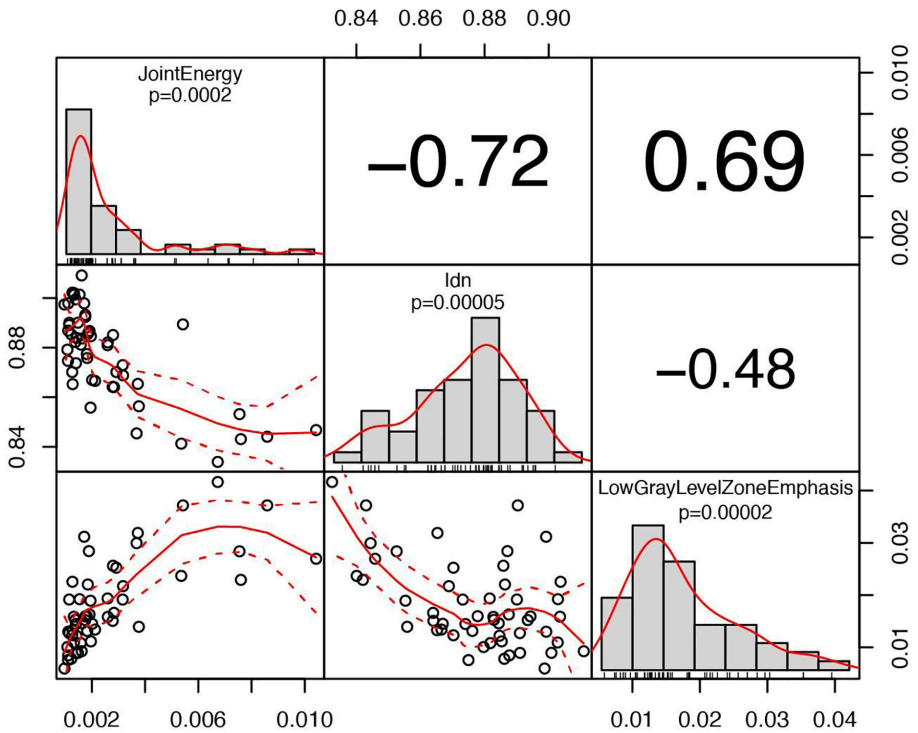

FIGURE 6 | Correlation chart between the selected radiomic features with a high significance for predicting patient response. The name of the feature, the significance level and the distribution are displayed on the diagonal. In the top triangular part, the absolute value of the Pearson's correlation coefficient is reported. In the bottom, the bivariate scatterplot is visible together with the fitted line according to a second order local polynomial regression.

strategy in EC. Recently, a Memorial Sloan Kettering Cancer Center series tested the impact of changing concurrent chemotherapy, during radiotherapy, in PET non-responders after IC: no survival benefit was seen from this change in therapeutic strategy (36). On the other hand, in the MUNICON trial, after 2 weeks of IC, ^{18}F-FDG PET/CT poor responders were referred to immediate surgery, while good responders continued with preoperative chemo-radiotherapy (37). The results of this trial suggested no decrement in survival outcomes with early termination of ineffective chemotherapy in PET non-responders, supporting a possible early discontinuation of preoperative treatment in this subset of patients. In the near future, the integration of ^{18}F-FDG PET/CT metabolic parameters, magnetic resonance imaging (MRI) data, and genomic and molecular information (e.g. liquid biopsies), could lead to a more individualized treatment approach for non-responder patients (38).

The value of metabolic parameters, to predict response to nCRT in EC, has been obtained from heterogeneous studies with remarkable differences in the adopted protocols and outcomes measured. Possible predictive valuable metrics are: the percentage decrease in TLG (36), the SUV_{max} (39), the percentage decrease in MTV and TLG (40), the MTV and TLG at PET performed on day 21 of nCRT (41), or the relative changes in MTV and SUV_{mean} at PET performed after 11 fractions of RT (42). Differently from other authors (36, 42), we did not observe any significant correlation with the metabolic parameters measured when relative differences were evaluated. Therefore, considering the aforementioned differences between the present and other studies, the role of ^{18}F-FDG PET/CT traditional metrics as a predictor of response is undoubtedly intriguing, but requires further investigation.

The analysis of radiomic features revealed that textural characteristics of PET_1 were more significantly correlated to treatment response compared to PET_2, confirming the possible predictive value of PET_1. Many radiomic features were correlated to each other, suggesting a redundancy of information that should be carefully taken into account if using radiomics in a predictive model. To this regard, extensive validation is necessary. However, the textural metrics, that correlate to treatment outcome, are associated to micro-variations of local metabolic activity thus indicating a possible role of spatial intra-tumor heterogeneity in predicting response (19). Relatively few studies have investigated the role of PET radiomic features in predicting response to nCRT in EC. As a whole, the results have highlighted a possible contribution of radiomic in the prognostic stratification of these patients (**Table 3**).

The predictive value of post-CRT ^{18}F-FDG PET/CT functional informations has been largely evaluated, with conflicting results. Indeed, the utility of PET metrics after

TABLE 3 | Recent findings on the application of PET radiomics for the prediction of response in esophageal cancer patients treated with neoadjuvant chemo-radiotherapy (summary).

Study, year (ref)	Sample size	nCRT protocol	PET time point	Main features evaluated	Results
Tixier et al. (19)	41 (ADC 10, SCC 31)	60 Gy + C or carboplatin/F	Pre-CRT	First order statistics GLCM RLM GLSZM NGTDM	Tumor textural analysis (GLCM homogeneity, GLCM entropy, RLM intensity variability and GLSZM size zone variability) can identify NR, PR and CR with higher sensitivity (76%–92%) than any SUV measurement
Tan et al. (20)	20 (ADC 17, SCC 3)	50.4 Gy + C/F	Pre & Post-CRT	First order statistics GLCM	SUV_{max} decline, SUV_{mean} decline and skewness, GLCM inertia, correlation and cluster prominence, are predictors of CR (AUC 0.76–0.85)
Van Rossum et al. (21)	217 ADC	45–50.4 Gy + fluoropyrimidine/ platinum or taxane	Pre & Post-CRT	First order statistics Geometry GLCM NGTDM	At multivariate analysis baseline cluster shade, Δrun percentage, ΔICM entropy, and post-CRT roundness, correlates with CR
Yip et al. (22)	45 (ADC 44, SCC 1)	45–50.4 Gy + C, F, irinotecan/ paclitaxel or carboplatin/ paclitaxel	Pre & Post-CRT	GLCM: homogeneity, entropy RLM: high gray run emphasis, short-run high gray run emphasis GLSZM: high gray zone emphasis, short-zone high-gray emphasis	Change in run length and size zone matrix parameters differentiate CR/PR from NR (AUC 0.71–0.76)
Beukinga et al. (23)	97 (ADC 88, SCC 9)	41.4 Gy + carboplatin/paclitaxel	Pre-CRT	First order statistics Geometry GLCM NGTDM	Long runs (coarse texture) with low gray levels and homogeneity of runs (fine texture) higher in patients with CR
Nakajo et al. (24)	52 SCC	41–70 Gy + C/F	Pre-CRT	GLCM: Entropy, homogeneity, dissimilarity; GLSZM: Intensity variability, Size-zone variability, zone percentage	Texture features (GLSZM intensity variability and GLSZM size-zone variability), and volumetric parameters (MTV and TLG) can predict tumor response
Beukinga et al. (25)	70 (ADC 65, SCC 8)	41.4 Gy + carboplatin/paclitaxel	Pre & Post-CRT	First order statistics Geometry Local intensity GLCM GLSZM NGTDM	The combination of clinical T-stage and post-nCRT joint maximum predict CR
Chen et al. (26)	44 SCC	50 Gy + platinum-based regimen	Pre-CRT	SUV variance, standard deviation, skewness, kurtosis, and entopy NGLCM TFCCM NGTDM	Pre-CRT primary tumor histogram entropy ≥ 3.69 predicts unfavorable response

nCRT, neoadjuvant chemo-radiotherapy; C, cisplatin; F, 5 fluorouracil; NR, non response; PR, partial response; CR, complete response.

radiotherapy remains controversial due to difficulties in distinguishing post-treatment inflammation from residual viable tumor (43, 44). In the present study, none of the PET_3 metrics resulted significantly correlated with the pathological response to nCRT, confirming that metabolic parameters relative to post-CRT PET are poorly evaluable and potentially inaccurate, mostly due to post-radiation inflammatory-related uptake or the disappearance of detectable metabolic activity, both considered as confounding factors. On the other hand, the use of ^{18}F-FDG PET/CT imaging before surgery, in appropriate combination with other restaging modalities, remains essential for the early detection of loco-regional and distant progression to nCRT.

Our study presents some limitations, including its retrospective nature. This is a single-center analysis; thus the results should be interpreted with caution. Moreover, different histologies (SCC and ADC) were considered, which potentially add heterogeneity to the outcomes measured. On the other hand, these limitations are counterbalanced by the analysis of one of the most homogeneous sample sizes for this topic so far, with patients undergoing the same intensive nCRT protocol, using a prospectively collected database, a standardized ^{18}F-FDG PET/CT acquisition modality and a modern metabolic and radiomic parameter analysis.

In conclusion, our observations confirm that ^{18}F-FDG PET/CT metrics are correlated with pathological response in EC. The analysis of PET traditional metrics and radiomic features may provide a new imaging perspective, moving from tumor staging to a promising role in disease stratification and prognostication. However, further studies are needed to justify a PET-guided strategy in the neoadjuvant approach to locally advanced EC. The integration with MRI data, as well as genomic and molecular analysis, might be useful as prognostic and predictive biomarkers for the selection of a tailored strategy improving the efficiency of neoadjuvant treatment for EC patients.

DATA AVAILABILITY STATEMENT

The datasets presented in this article are not readily available because the datasets generated for this study are available on request to the corresponding author, subject to approval by the Institutional Review Board. Requests to access the datasets should be directed to NS, nicola.simoni@aovr.veneto.it.

ETHICS STATEMENT

The studies involving human participants were reviewed and approved by Comitato etico per la Sperimentazione Clinica (CESC) delle Province di Verona e Rovigo. Written informed consent for participation was not required for this study in accordance with the national legislation and the institutional requirements.

AUTHOR CONTRIBUTIONS

Conceptualization, NS and CC. Methodology, NS, GB, and CC. Data curation, MZ, RMi, MP, EZ, and VM. Statistical analysis and radiomics, GR, GB, and CC. Validation, SGu, JW, and SGi. Writing—original draft preparation, NS, MZ, and CC. Writing—review and editing, GR, RMi, JW, and SGi. Supervision, GD and RMa. All authors contributed to the article and approved the submitted version.

SUPPLEMENTARY MATERIAL

The Supplementary Material for this article can be found online at: https://www.frontiersin.org/articles/10.3389/fonc.2020.599907/full#supplementary-material

REFERENCES

1. Siegel R, Ma J, Zou Z, Jemal A. Cancer statistics, 2014. CA. *Cancer J Clin* (2014) 64:9–29. doi: 10.3322/caac.21208
2. Network NCC. *Esophageal and Esophagogastric Junction Cancers Version 1.2020. NCCN Guidelines*. (2020). Available at: https://www.nccn.org/professionals/physician_gls/pdf/esophageal.pdf.
3. Tepper J, Krasna MJ, Niedzwiecki D, Hollis D, Reed CE, Goldberg R, et al. Phase III trial of trimodality therapy with cisplatin, fluorouracil, radiotherapy, and surgery compared with surgery alone for esophageal cancer: CALGB 9781. *J Clin Oncol* (2008) 26:1086–92. doi: 10.1200/JCO.2007.12.9593
4. van Hagen P, Hulshof MC, van Lanschot JJ, Steyerberg EW, van Berge Henegouwen MI, Wijnhoven BPL, et al. Preoperative Chemoradiotherapy for Esophageal or Junctional Cancer. *N Engl J Med* (2012) 366:2074–84. doi: 10.1016/S1470-2045(15)00040-6
5. Yang H, Liu H, Chen Y, Zhu C, Fang W, Yu Z, et al. Neoadjuvant Chemoradiotherapy Followed by Surgery Versus Surgery Alone for Locally Advanced Squamous Cell Carcinoma of the Esophagus (NEOCRTEC5010): A Phase III Multicenter, Randomized, Open-Label Clinical Trial. *J Clin Oncol* (2018) 36:2796–803. doi: 10.1200/JCO.2018.79.1483
6. Mandard AM, Dalibard F, Mandard JC, Marnay J, Henry-Amar M, Petiot JF, et al. Pathologic assessment of tumor regression after preoperative chemoradiotherapy of esophageal carcinoma. Clinicopathologic correlations. *Cancer* (1994) 73:2680–6. doi: 10.1002/1097-0142(19940601)73:11<2680::aid-cncr2820731105>3.0.co;2-c
7. Davies AR, Gossage JA, Zylstra J, Mattsson F, Lagergren J, Maisey N, et al. Tumor Stage After Neoadjuvant Chemotherapy Determines Survival After Surgery for Adenocarcinoma of the Esophagus and Esophagogastric Junction. *J Clin Oncol* (2014) 32:2983–90. doi: 10.1200/JCO.2014.55.9070
8. Lerttanatum N, Tharavej C, Chongpison Y, Sanpavat A. Comparison of tumor regression grading system in locally advanced esophageal squamous cell carcinoma after preoperative radiochemotherapy to determine the most accurate system predicting prognosis. *J Gastrointest Oncol* (2019) 10:276–82. doi: 10.21037/jgo.2018.12.01
9. Pasini F, de Manzoni G, Zanoni A, Grandinetti A, Capirci C, Pavarana M, et al. Neoadjuvant therapy with weekly docetaxel and cisplatin, 5 fluorouracil continuous infusion, and concurrent radiotherapy in patients with locally advanced esophageal cancer produced a high percentage of long-lasting pathological complete response: a phase 2 study. *Cancer* (2013) 119:939–45. doi: 10.1002/cncr.27822
10. Bang JI, Ha S, Kang SB, Lee KW, Lee HS, Kim JS, et al. Prediction of neoadjuvant radiation chemotherapy response and survival using pretreatment [(18)F]FDG PET/CT scans in locally advanced rectal cancer. *Eur J Nucl Med Mol Imaging* (2016) 43:422–31. doi: 10.1007/s00259-015-3180-9
11. Lovinfosse P, Polus M, Van Daele D, Martinive P, Daenen F, Hatt M, et al. FDG PET/CT radiomics for predicting the outcome of locally advanced rectal cancer. *Eur J Nucl Med Mol Imaging* (2018) 45:365–75. doi: 10.1007/s00259-017-3855-5
12. Jones M, Hruby G, Solomon M, Rutherford N, Martin J. The role of FDG-PET in the initial staging and response assessment of anal Cancer: a systematic review and meta-analysis. *Ann Surg Oncol* (2015) 22:3574–81. doi: 10.1245/s10434-015-4391-9
13. Schwarz JK, Siegel BA, Dehdashti F, Myerson RJ, Fleshman JW, Grigsby PW. Tumor response and survival predicted by post-therapy FDG-PET/CT in anal cancer. *Int J Radiat Oncol Biol Phys* (2008) 71:180–6. doi: 10.1016/j.ijrobp.2007.09.005
14. Flamen P, Lerut A, Van Cutsem E, De Wever W, Peeters M, Stroobants S, et al. Utility of positron emission tomography for the staging of patients with potentially operable esophageal carcinoma. *J Clin Oncol* (2000) 18:3202–10. doi: 10.1200/JCO.2000.18.18.3202
15. Cremonesi M, Garibaldi C, Timmerman R, Ferrari M, Ronchi S, Grana CM, et al. Interim (18)F-FDG-PET/CT during chemo-radiotherapy in the management of oesophageal cancer patients. A systematic review. *Radiother Oncol* (2017) 125:200–12. doi: 10.1016/j.radonc.2017.09.022
16. Westerterp M, van Westreenen HL, Reitsma JB, Hoekstra OS, Stoker J, Fockens P, et al. Esophageal cancer: CT, endoscopic US, and FDG PET for assessment of response to neoadjuvant therapy– systematic review. *Radiology* (2005) 236:841–51. doi: 10.1148/radiol.2363041042
17. Elliott JA, O'Farrell NJ, King S, Halpenny D, Malik V, Muldoon C, et al. Value of CT-PET after neoadjuvant chemoradiation in the prediction of histological tumour regression, nodal status and survival in oesophageal adenocarcinoma. *Br J Surg* (2014) 101:1702–11. doi: 10.1002/bjs.9670
18. van Rossum PSN, Fried DV, Zhang L, Hofstetter WL, Ho L, Meijer GJ, et al. The value of 18F-FDG PET before and after induction chemotherapy for the early prediction of a poor pathologic response to subsequent preoperative chemoradiotherapy in oesophageal adenocarcinoma. *Eur J Nucl Med Mol Imaging* (2017) 44:71–80. doi: 10.2967/jnumed.117.192591
19. Tixier F, Le Rest CC, Hatt M, Albarghach N, Pradier O, Metges JP, et al. Intratumor heterogeneity characterized by textural features on baseline 18F-FDG PET images predicts response to concomitant radiochemotherapy in esophageal cancer. *J Nucl Med* (2011) 52:369–78. doi: 10.2967/jnumed.110.082404
20. Tan S, Kligerman S, Chen W, Lu M, Kim G, Feigenberg S, et al. Spatial-temporal [^{18} F]FDG-PET features for predicting pathologic response of esophageal cancer to neoadjuvant chemoradiation therapy. *Int J Radiat Oncol Biol Phys* (2013) 85:1375–82. doi: 10.1016/j.ijrobp.2012.10.017
21. van Rossum PS, Fried DV, Zhang L, Hofstetter WL, van Vulpen M, Meijer GJ, et al. The Incremental Value of Subjective and Quantitative Assessment of 18F-FDG PET for the Prediction of Pathologic Complete Response to Preoperative Chemoradiotherapy in Esophageal Cancer. *J Nucl Med* (2016) 57:691–700. doi: 10.2967/jnumed.115.163766
22. Yip SS, Coroller TP, Sanford NN, Huynh E, Mamon H, Aerts HJ, et al. Use of registration-based contour propagation in texture analysis for esophageal

cancer pathologic response prediction. *Phys Med Biol* (2016) 61:906–22. doi: 10.1088/0031-9155/61/2/906
23. Beukinga RJ, Hulshoff JB, van Dijk LV, Muijs CT, Burgerhof JGM, Kats-Ugurlu G, et al. Predicting Response to Neoadjuvant Chemoradiotherapy in Esophageal Cancer with Textural Features Derived from Pretreatment 18F-FDG PET/CT Imaging. *J Nucl Med* (2017) 58:723–9. doi: 10.2967/jnumed.116.180299
24. Nakajo M, Jinguji M, Nakabeppu Y, Nakajo M, Higashi R, Fukukura Y, et al. Texture analysis of 18F-FDG PET/CT to predict tumour response and prognosis of patients with esophageal cancer treated by chemoradiotherapy. *Eur J Nucl Med Mol Imaging* (2017) 44:206–14. doi: 10.1007/s00259-016-3506-2
25. Beukinga RJ, Hulshoff JB, Mul VEM, Noordzij W, Kats-Ugurlu G, Slart RHJA, et al. Prediction of Response to Neoadjuvant Chemotherapy and Radiation Therapy with Baseline and Restaging 18F-FDG PET Imaging Biomarkers in Patients with Esophageal Cancer. *Radiology* (2018) 287:983–92. doi: 10.1148/radiol.2018172229
26. Chen YH, Lue KH, Chu SC, Chang BS, Wang LY, Liu DW, et al. Combining the radiomic features and traditional parameters of 18F-FDG PET with clinical profiles to improve prognostic stratification in patients with esophageal squamous cell carcinoma treated with neoadjuvant chemoradiotherapy and surgery. *Ann Nucl Med* (2019) 33:657–70. doi: 10.1007/s12149-019-01380-7
27. Phil T. dcmrtstruct2nii: Convert DICOM RT-Struct to nii. [Computer software]. Zenodo (2020). doi: 10.5281/ZENODO.4037865
28. *SimpleITK - Home*. Available at: https://simpleitk.org/ (Accessed Jul 28, 2020).
29. van Griethuysen JJM, Fedorov A, Parmar C, Hosny A, Aucoin N, Narayan V, et al. Computational Radiomics System to Decode the Radiographic Phenotype. *Cancer Res* (2017) 77:e104–7. doi: 10.1158/0008-5472.CAN-17-0339
30. Zwanenburg A, Leger S, Vallières M, Löck S. Image biomarker standardisation initiative - feature definitions. *Radiology* (2016) 295:328–38. doi: 10.1148/radiol.2020191145
31. Blum Murphy M, Xiao L, Patel VR, Maru DM, Correa AM, Amlashi FG, et al. Pathological complete response in patients with esophageal cancer after the trimodality approach: The association with baseline variables and survival-The University of Texas MD Anderson Cancer Center experience. *Cancer* (2017) 123:328–38. doi: 10.1002/cncr.30953
32. Gaur P, Sepesi B, Hofstetter WL, Correa AM, Bhutani MS, Watson TJ, et al. M. D. Anderson Esophageal Cancer Group and University of Rochester School of Medicine and Dentistry Foregut Group: Endoscopic esophageal tumor length: A prognostic factor for patients with esophageal cancer. *Cancer* (2011) 117:63–9. doi: 10.1002/cncr.25373
33. Wang BY, Liu CY, Lin CH, Hsu PK, Hsu WH, Wu YC, et al. Endoscopic tumor length is an independent prognostic factor in esophageal squamous cell carcinoma. *Ann Surg Oncol* (2012) 19:2149–58. doi: 10.1245/s10434-012-2273-y
34. Bollschweiler E, Metzger R, Drebber U, Baldus S, Vallböhmer D, Kocher M, et al. Histological type of esophageal cancer might affect response to neo-adjuvant radiochemotherapy and subsequent prognosis. *Ann Oncol* (2009) 20:231–8. doi: 10.1093/annonc/mdn622
35. Noordman BJ, Wijnhoven BPL, Lagarde SM, Boonstra JJ, Coene PPLO, Dekker JWT, et al. Neoadjuvant chemoradiotherapy plus surgery versus active surveillance for oesophageal cancer: a stepped-wedge cluster randomised trial. *BMC Cancer* (2018) 18:142. doi: 10.1186/s12885-018-4034-1
36. Greally M, Chou JF, Molena D, Rusch VW, Bains MS, Park BJ, et al. Positron-Emission Tomography Scan-Directed Chemoradiation for Esophageal Squamous Cell Carcinoma: No Benefit for a Change in Chemotherapy in Positron-Emission Tomography Nonresponders. *J Thorac Oncol* (2019) 14:540–6. doi: 10.1016/j.jtho.2018.10.152
37. Lordick F, Ott K, Krause BJ, Weber WA, Becker K, Stein HJ, et al. PET to assess early metabolic response and to guide treatment of adenocarcinoma of the oesophagogastric junction: the MUNICON phase II trial. *Lancet Oncol* (2007) 8:797–805. doi: 10.1016/S1470-2045(07)70244-9
38. Defize LI, van Hillegersberg R, Mook R, Meijer GJ, Lin SH, Ruurda JP, et al. Restaging after chemoradiotherapy for locally advanced esophageal cancer. *Ann Transl Med* (2019) 7:S288. doi: 10.21037/atm.2019.11.57
39. Ishihara R, Yamamoto S, Iishi H, Nagai K, Matui F, Kawada N, et al. Predicting the effects of chemoradiotherapy for squamous cell carcinoma of the esophagus by induction chemotherapy response assessed by positron emission tomography: toward PET-response-guided selection of chemoradiotherapy or esophagectomy. *Int J Clin Oncol* (2012) 17:225–32. doi: 10.1007/s10147-011-0278-3
40. Roedl JB, Colen RR, Holalkere NS, Fischman AJ, Choi NC, Blake MA. Adenocarcinomas of the esophagus: response to chemoradiotherapy is associated with decrease of metabolic tumor volume as measured on PET-CT. Comparison to histopathologic and clinical response evaluation. *Radiother Oncol* (2008) 89:278–86. doi: 10.1016/j.radonc.2008.06.014
41. Palie O, Michel P, Menard JF, Rousseau C, Rio E, Bridji B, et al. The predictive value of treatment response using FDG PET performed on day 21 of chemoradiotherapy in patients with oesophageal squamous cell carcinoma. A prospective, multicentre study (RTEP3). *Eur J Nucl Med Mol Imaging* (2013) 40:1345–55. doi: 10.1007/s00259-013-2450-7
42. Kim N, Cho H, Yun M, Park KR, Lee CG. Prognostic values of mid-radiotherapy 18F-FDG PET/CT in patients with esophageal cancer. *Radiat Oncol* (2019) 14:27. doi: 10.1186/s13014-019-1232-1
43. Konski AA, Cheng JD, Goldberg M, Li T, Maurer A, Yu JQ, et al. Correlation of molecular response as measured by 18-FDG positron emission tomography with outcome after chemoradiotherapy in patients with esophageal carcinoma. *Int J Radiat Oncol Biol Phys* (2007) 69:358–63. doi: 10.1016/j.ijrobp.2007.03.053
44. Jayachandran P, Pai RK, Quon A, Graves E, Krakow TE, La T, et al. Postchemoradiotherapy positron emission tomography predicts pathologic response and survival in patients with esophageal cancer. *Int J Radiat Oncol Biol Phys* (2012) 84:471–7. doi: 10.1016/j.ijrobp.2011.12.029

Conflict of Interest: The authors declare that the research was conducted in the absence of any commercial or financial relationships that could be construed as a potential conflict of interest.

The handling editor declared a past co-authorship with one of the authors with several of the authors [NS, RMa].

frontiers in Oncology

ORIGINAL RESEARCH
published: 08 January 2021
doi: 10.3389/fonc.2020.603994

The Role of Multiparametric Magnetic Resonance in Volumetric Modulated Arc Radiation Therapy Planning for Prostate Cancer Recurrence After Radical Prostatectomy: A Pilot Study

Angela Sardaro[1], Barbara Turi[2], Lilia Bardoscia[3], Cristina Ferrari[4], Giuseppe Rubini[4], Angela Calabrese[5], Federica Ammirati[1], Antonietta Grillo[2], Annamaria Leo[2], Filomenamila Lorusso[6], Antonio Santorsola[2], Antonio Amato Stabile Ianora[1] and Arnaldo Scardapane[1]*

[1] Interdisciplinary Department of Medicine, Section of Radiology and Radiation Oncology, University of Bari "Aldo Moro", Bari, Italy, [2] Radiation Oncology Unit, Azienda Ospedaliero-Universitaria Policlinico, Bari, Italy, [3] Radiation Therapy Unit, Department of Oncology and Advanced Technology, Azienda USL-IRCCS di Reggio Emilia, Reggio Emilia, Italy, [4] Nuclear Medicine Unit, Interdisciplinary Department of Medicine, University of Bari Aldo Moro, Bari, Italy, [5] Department of Radiology, IRCCS Istituto Tumori "Giovanni Paolo II", Bari, Italy, [6] Department of Radiology, "Di Venere" Hospital of Bari, Bari, Italy

OPEN ACCESS

Edited by:
Francesco Cellini,
Catholic University of the Sacred Heart, Italy

Reviewed by:
Joshua Pohyun Kim,
Henry Ford Health System, United States
Luciana Caravatta,
SS Annunziata Polyclinic Hospital, Chieti, Italy

***Correspondence:**
Lilia Bardoscia
liliabardoscia@gmail.com

Specialty section:
This article was submitted to Radiation Oncology, a section of the journal Frontiers in Oncology

Received: 08 September 2020
Accepted: 26 November 2020
Published: 08 January 2021

Citation:
Sardaro A, Turi B, Bardoscia L, Ferrari C, Rubini G, Calabrese A, Ammirati F, Grillo A, Leo A, Lorusso F, Santorsola A, Stabile Ianora AA and Scardapane A (2021) The Role of Multiparametric Magnetic Resonance in Volumetric Modulated Arc Radiation Therapy Planning for Prostate Cancer Recurrence After Radical Prostatectomy: A Pilot Study. Front. Oncol. 10:603994. doi: 10.3389/fonc.2020.603994

Background and Purpose: Volumetric modulated arc radiotherapy (RT) has become pivotal in the treatment of prostate cancer recurrence (RPC) to optimize dose distribution and minimize toxicity, thanks to the high-precision delineation of prostate bed contours and organs at risk (OARs) under multiparametric magnetic resonance (mpMRI) guidance. We aimed to assess the role of pre-treatment mpMRI in ensuring target volume coverage and normal tissue sparing.

Material and Methods: Patients with post-prostatectomy RPC eligible for salvage RT were prospectively recruited to this pilot study. Image registration between planning CT scan and T2w pre-treatment mpMRI was performed. Two sets of volumes were outlined, and DWI images/ADC maps were used to facilitate precise gross tumor volume (GTV) delineation on morphological MRI scans. Two rival plans (mpMRI-based or not) were drawn up.

Results: Ten patients with evidence of RPC after prostatectomy were eligible. Preliminary data showed lower mpMRI-based clinical target volumes than CT-based RT planning (p = 0.0003): median volume difference 17.5 cm^3. There were no differences in the boost volume coverage nor the dose delivered to the femoral heads and penile bulb, but median rectal and bladder V_{70Gy} was 4% less (p = 0.005 and p = 0.210, respectively) for mpMRI-based segmentation.

Conclusions: mpMRI provides high-precision target delineation and improves the accuracy of RT planning for post-prostatectomy RPC, ensures better volume coverage

with better OARs sparing and allows non-homogeneous dose distribution, with an aggressive dose escalation to the GTV. Randomized phase III trials and wider datasets are needed to fully assess the role of mpMRI in optimizing therapeutic strategies.

Keywords: prostate cancer recurrence, multiparametric magnetic resonance, radiotherapy, CT simulation, treatment planning system, dose–volume parameters, imaging registration

INTRODUCTION

Prostate cancer (PC) is the second most frequent tumor diagnosis in men, accounting for 1,276,106 new cases reported worldwide in 2018, with a higher prevalence in developed countries (1, 2).

In Italy, PC has been estimated to account for 9.6% of all tumors diagnosed in the whole population and 18.5% of those in males in the last year (3).

Several factors may affect the risk of developing prostate cancer, such as age, black race, given the reported higher levels of androgens, dihydrotestosterone (DHT) and 5-alpha reductase than in Caucasian men (4); hormonal and genetic factors; a family history of PC (on both the paternal and maternal side); metabolic syndrome (although there is insufficient evidence to justify recommending lifestyle changes or a modified diet to lower this risk), and smoking (5).

In recent years, screening and early detection of PC by prostate-specific antigen (PSA) blood test has become one of the most controversial topics in the Uro-Oncology community due to increasing evidence of some cases of overdiagnosis. Despite this, PSA remains a better predictor of cancer than either clinical rectal examination or transrectal ultrasound; therefore, an individualised risk-adapted strategy for early detection is recommended (6).

PSA is also crucial in the follow-up after prostatectomy. Six weeks after primary surgery, PSA is expected to drop to undetectable values; consequently, PSA levels higher than 0.2 ng/ml in at least two subsequent samples are conventionally taken to define the condition of post-prostatectomy biochemical recurrence (BCR) of PC (7, 8).

Radiation therapy (RT) has become pivotal in the treatment of PC. It may represent a radical, exclusive approach for organ-confined or locally advanced disease, and may also be performed as adjuvant or salvage treatment following radical prostatectomy, in cases with adverse pathological features (pT3a-pT3b-pT4 staging high- and very high-risk PC, positive surgical margins), biochemical failure and/or macroscopic evidence of disease recurrence (8, 9).

In the field of External Beam Radiotherapy (EBRT), advances in rotational, intensity-modulated delivery techniques with volumetric modulated arc irradiation (VMAT) have made it possible to individualize the radiation dose distribution to the prostate volume while sparing the surrounding normal tissues and organs, thus optimizing treatment efficacy and minimizing genitourinary (GU) and gastrointestinal (GI) toxicity (10, 11).

Magnetic resonance imaging (MRI) has gained increasing interest for the pre-treatment assessment of prostate cancer. Advances in diagnostic procedures, improving diagnostic reliability for primary and recurrent PC (RPC), have allowed a more accurate detection of prostatic lesions (6). In particular, given the better soft tissue contrast provided by anatomic MRI, the accuracy of prostate tumor identification, anatomic location and characterization in terms of extraprostatic extension and seminal vesicle involvement now ranges from 69 to 90% (12, 13). The addition of functional sequences, such as diffusion-weighted imaging (DWI), dynamic contrast-enhanced (DCE) imaging and MR spectroscopy has further improved the performance of MRI imaging in tumor detection (12, 13).

In this scenario, multiparametric MR imaging (mpMRI) has emerged as helpful in the precise identification of tumor site and extent, extraprostatic and/or seminal vesicles involvement. mpMRI is also reported to allow the precise location of a recurrent prostate tumor, and so to assess if the disease relapse is strictly limited to the prostate bed since it appears as a T2-weighted (T2w) isointense to hyperintense lesion close to the surgical scar, with rapid early enhancement and washout on DCE MR sequences (14). Such a highly accurate delineation of the prostate contours under mpMRI guidance has also given rise to radiation treatment optimization: so-called dose-painting, that is targeting prostate tumor sites with a higher radiation dose, with or without a dose gradient on the lower-risk prostate/prostate bed areas, while guaranteeing maximum sparing of the bladder and rectum (13, 15). Most of the available literature is focused on the identification of dominant, intraprostatic lesions to define dose-escalation protocols in the radical setting (16, 17). On the contrary, data on the identification of post-prostatectomy RPC lesions to be safely boosted for an ablative eradication treatment protocol are still lacking. We carried out a prospective pilot study with the aim of assessing the role of pre-treatment mpMRI in target volume delineation and treatment planning for recurrent prostate cancer after radical prostatectomy, in terms of target volume coverage and normal tissue sparing.

MATERIALS AND METHODS

Patient Selection and Treatment

Patients with post-prostatectomy BCR as per Phoenix criteria (7), and with macroscopic evidence of RPC, presenting at our Institution and eligible for salvage EBRT, were prospectively recruited to the study. A staging workup with 11C-Choline PET-CT was performed in cases with two consecutive PSA values ≥1 ng/ml, to exclude nodal and/or systemic metastatization.

Radiation treatment was performed using Image-guided radiotherapy (IGRT), VMAT technique, with daily cone beam CT scans for monitoring.

All the recruited patients underwent pelvic mpMRI before EBRT planning, regardless of any other morphological and/or functional workup already performed for diagnostic purposes. Then, planning pelvic CT scan with 3 mm slice was acquired, both for mpMRI and CT, in conventional, supine position.

The present study was carried out in accordance with the principles of Good Clinical Practice, conforming to the ICH GCP guidelines and the ethical principles contained in the Helsinki declaration.

Since the recruitment period started during the rapid COVID-19 spread in Italy, all the diagnostic and treatment procedures described below were performed in accordance with the Italian Government official recommendation statements and Italian Association of Radiotherapy and Clinical Oncology (AIRO) tips for the management of oncological patients in the context of the COVID-19 pandemic (18, 19).

mpMRI Protocol and Image Interpretation

The mpMRI was performed with a 1.5 T scanner (Philips Achieva 1.5), using a 16-channel surface coil in supine position according to the PIRADS 2.1 protocol.

The inhibition of intestinal peristalsis was guaranteed through the intramuscular injection of 10 ml/mg of N-butyl scopolamine (Buscopan, Boehringer Ingelheim, Germany), before the MRI test.

The imaging protocol consisted of the following sequences:

- T2-weighted Turbo Spin Echo (TSE), on the axial, coronal and sagittal planes.
- Axial FOV (AP 160, RL 160 mm, FH 82 mm), matrix 212 × 206 × 25 slices, NSA (number of signals) three;
- Coronal FOV (AP 66 mm, RL 160 mm, FH 160), matrix 200 × 195 × 20 slices, NSA (number of signals) two;
- Sagittal FOV (AP 160, RL 82 mm, FH 160 mm), matrix 200 × 199 × 25 slices, NSA (number of signals) two;
- TE 110 ms, TR shortest, section thickness 3 mm, 24–30 sections, acquisition time 3–3.5 min.
- T2-weighted Turbo Spin Echo (TSE), on the axial planes with wide view to evaluate lymph node involvement, FOV (AP 300, RL 300 mm, FH 258 mm), matrix 332 × 299 × 40 slices, NSA (number of signals) one;
- Dynamic THRIVE SPAIR, on the axial plane, FOV (FH 75mm, RL 200, AP 200 mm), matrix 112 × 171 × 25 slices, NSE (number of signals) one; TE/TR shortest, thickness 6 mm, 20 acquisition (10 s for each acquisition).
- DWI, on the axial plane, TE/TR shortest, section thickness 3 mm, with B value of 0.700, 1000 and 1400, FOV (RL 160, AP 160mm, F H 99 mm), matrix 64 × 56 × 25 slices, NSE (number of signals) one; ADC maps were subsequently calculated.

All the images were reviewed and interpreted by two radiologists (with 20 and 4 years' experience, respectively).

The RPC diagnosis was based on the presence of solid nodules on T2w scan, with close evaluation of the most frequent location on the vesicourethral anastomosis, discretely vascularized after the injection of contrast agent, showing signal restriction in the DWI sequences and a low signal on the ADC (apparent diffusion coefficient) map.

The presence of any other pelvic tumor mass and enlarged hypogastric, obturator, iliac and sacral lymph nodes (diameter > 5 mm) was checked.

Areas of signal intensity restriction on DWI/ADC images, as well as enhancing areas with no visible pathologic tissue on morphologic T2w images, were also recorded.

Planning Computed Tomography Acquisition Protocol

Before CT simulation, all patients underwent rectal emptying (using an enema 2–3 h before the procedure) and comfortable bladder filling (complete urination 30 min before CT scan, then drinking 500 ml of water until CT execution), in order to ensure inter-fraction setup reproducibility during treatment delivery and improved sparing of organs at risk (OARs).

CT simulation was acquired with patients in supine position, hands over the chest, using foot lock and kneefix support systems. Longitudinal alignment along the sternum and navel and transverse alignment at the level of the pubic symphysis were ensured, while the field depth was defined at the patient's hemi-thickness. Skin reference points were marked at the laser crossings, with corresponding placement of three radiopaque markers.

A control scan was first performed to assess the correct alignment of the patient on the CT table, and the longitudinal alignment was checked on the anterior topogram. Once the patient's position had been verified, CT scan with 3 mm slices was acquired. At the end of the procedure, the correct position of the radiopaque markers on the zero slice, adequate bladder filling, and rectal emptying were checked.

Radiation Treatment Planning

Target volume delineation and RT planning were performed using the Monaco® HD Treatment Planning System (TPS) 5,11,03 by Elekta. In cases of MR evidence of RPC lesions, image registration between the planning CT scan and T2w plus DWI mpMRI images was performed. Two sets of volumes were contoured, with and without mpMRI-guidance. Gross tumor volume (GTV) was outlined in both the CT simulation and the T2w MR scan, DWI images and related apparent diffusion coefficient (ADC) maps were used to facilitate the precise GTV contouring onto the morphological MR scans. Clinical target volume (CTV) was defined as the prostate fossa, and contoured as per the Kirsty et al. consensus definition for the anatomic boundaries of the prostate bed (20): the superior boundary was the superior surgical clips (if present) or 5 mm above the inferior border of the vas deferens; the inferior boundary was 8 mm below the vesicourethral anastomosis or the top of the penile bulb; the posterior 15 mm of the bladder wall was taken as the anterior, cranial boundary; the posterior edge of the pubis symphysis up to the top of the pubis symphysis as the anterior, caudal boundary; the lateral, cranial boundary

was the sacrorectogenitopubic fascia, lateral to the neurovascular structures; the posterior, cranial boundary was the mesorectal fascia; the lateral, caudal boundary was the medial border of the levator ani and obturator internus muscles; the anterior border of the rectal wall and levator ani muscle was the posterior, caudal boundary; a 10-mm extension of the outlined boundaries was made beyond the GTV and the visible surgical clips located outside the boundaries, if present, except for high lymphadenectomy vessel clips. An isotropic, 5 mm expansion was applied to the CTV to obtain the Planning treatment volume (PTV) (prostate bed), and to the GTV to obtain the PTV (boost). OARs (bladder, rectum, penile bulb, femoral heads) were delineated in both mpMRI and planning CT scan.

Two rival plans were drawn up, one per each set of volumes, taking into account the dose constraints for limiting normal tissue toxicity based on the quantitative Analysis of Normal Tissue Effects in the Clinic (QUANTEC) (21) and the Radiation Therapy Oncology Group (RTOG) GU consensus (22). The GU OAR dose constraints applied for VMAT inverse treatment planning are summarized in **Table 1**. Dose prescription, dose recording and reporting were performed as per ICRU Report 83 (23). We ensured that the same target volumes coverage was obtained in the rival plans.

The prescribed dose was 70 Gy in 35 daily fractions on the prostate lodge, with a sequential boost or higher doses targeting any macroscopic evidence of RPC at the pre-treatment mpMRI.

Statistical Analysis

A sample size of at least 10 RPC patients was arbitrarily defined, since this was a pilot, prospective trial and no similar study designs with which to compare accrual evaluation have been reported in literature. Statistical analysis is intended as descriptive for future findings and data integration. For the same purpose, the size of the obtained CTV (prostate bed) (cm^3), the dose covering 98% of the PTV (boost) ($D_{98\%}$), the volume (%) of rectum receiving 50, 65, and 70 Gy (V_{50Gy}, V_{65Gy} and V_{70Gy}), the volume (%) of bladder receiving 55, 65 and 70 Gy (V_{55Gy}, V_{65Gy} and V_{70Gy}), the volume (%) of femoral heads receiving 50 Gy (V_{50Gy}), the mean dose to 95%, and the dose delivered to 70% of the penile bulb volume ($D_{70\%}$) were chosen as referral parameters for statistical comparison between the rival mpMRI and non-mpMRI plans.

Statistical analysis was performed using SPSS statistical software v25.0. To describe the data, median and ranges were used and proportions and percentages for categorical variables. Differences between two-sample central tendencies were assessed with two independent samples t-test. A p value of <0.05 was considered statistically significant.

RESULTS

From April 2020 to October2020, a total of 17 patients fitted the selection criteria.

Choline-PET restaging was negative in all the patients who performed it.

Negative pre-treatment mpMRI confirmed biochemical recurrence in 7 (41.2%) patients.

Ten (58.8%) patients showed macroscopic disease recurrence at the pre-EBRT mpMRI, PSA values ranging from 0.52 to 6.9 ng/ml. Among these, all but one underwent a total dose of 70 Gy —2-Gy/fraction on the prostate fossa, then a sequential boost on the RPC lesion(s) was delivered according to the following schedules: additional 2 Gy per five fractions (80 Gy in total) for 3 patients (30%), 6 Gy in three fractions (total 76 Gy) for two (20%) patients, and 2 Gy per four fractions (total 78 Gy) for four (40%) of them; one (10%) patient underwent a total dose of 80 Gy on the entire prostate bed.

An example of CT-based target volume and OAR delineation with and without mpMRI co-registration in our series is reported in **Figure 1** and **Figure 2**.

Preliminary dosimetric comparison between mpMRI-based and non-mpMRI-based treatment plans was made in the 10 enrolled patients with macroscopic RPC. The results obtained are reported in **Table 2** and **Table 3**. Median delineated CTV (prostate bed) was 15.7 cm^3 in size (range 5.6–30.7) on the T2w MRI scan, compared to median 33.4 cm^3 (range 19.5–51.0) for those outlined on the CT simulation only, with a median difference of 17.5 cm^3 (range 8.3–26.7) between the two contour sets (p = 0.0003). No substantial differences were found in terms of the boost volume coverage, median $D_{98\%}$ for PTV (boost) was 76.3 Gy (range 74–78.5) for mpMRI-based delineation and 76.1 Gy (range 73.8–77.2) for CT-based delineation only (p = 0.376).

TABLE 1 | QUANTEC dose constraints for inverse treatment planning (21, 22).

Organs at Risk	Volume segmented	Dose (Gy) or dose/volume parameters
Rectum	Whole organ	V_{50Gy} <50% V_{65Gy} <25% V_{70Gy} <20%
Bladder	Whole organ	V_{55Gy} <50% V_{65Gy} <50% V_{70Gy} <35%
Penile bulb	Whole organ	Mean dose to 95% of gland <50 Gy $D_{60\text{-}70\%}$ <70 Gy
Femoral heads	Whole organ	V_{50Gy} <5%

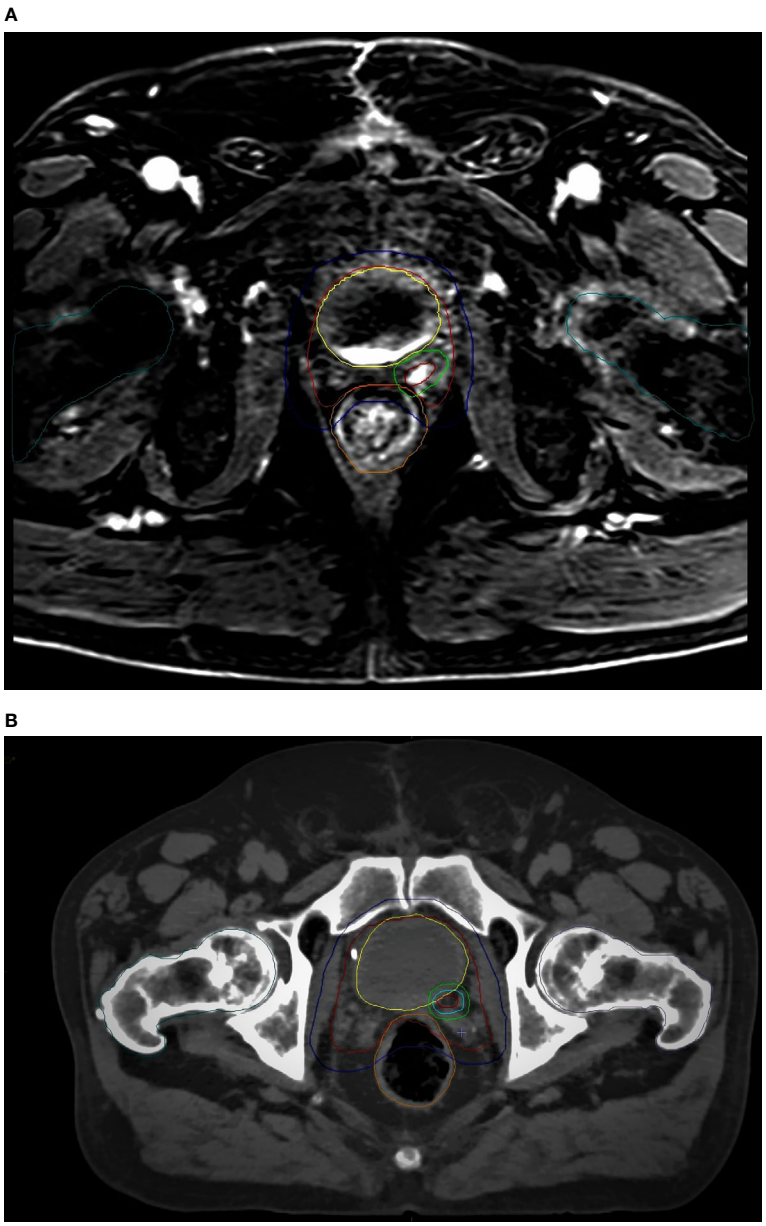

FIGURE 1 | mpMRI-based **(A)** *vs* CT-based **(B)** CTV/PTV (prostate bed) and OARs delineation: red, CTV (prostate bed); blue, PTV (prostate bed); yellow, bladder; orange, rectum; dark green, femoral heads.

As to OARs, no differences were found in terms of femoral heads and penile bulb sparing, nor differences in rectum V_{50Gy} and V_{65Gy}, bladder V_{55Gy} and V_{65Gy}, respectively (data not shown). However, we recorded a median rectal V_{70Gy} 4% (range 0.2–5.7) smaller for treatment delineation on T2w MRI scans, with a median V_{70Gy} of 9.2% (range 4.9–13.8) for mpMRI-based RT plans, and of 13.5% (range 5.1–16.7) for non-mpMRI based RT plans ($p = 0.005$). Likewise, there was a median bladder V_{70Gy} of 22.6% (range 10.3–35) for mpMRI-based RT plans, compared to median 27.6% (range 14.5–37.3) for CT-based RT plans, with a median bladder V_{70Gy} difference of 4% (range 0.3–5.8) between the two rival plans ($p = 0.210$).

DISCUSSION

The addition of image registration with pre-treatment mpMRI to CT-based target volume delineation has dramatically improved the accuracy of treatment planning for prostate cancer. MR imaging is well known to provide better soft tissue contrast

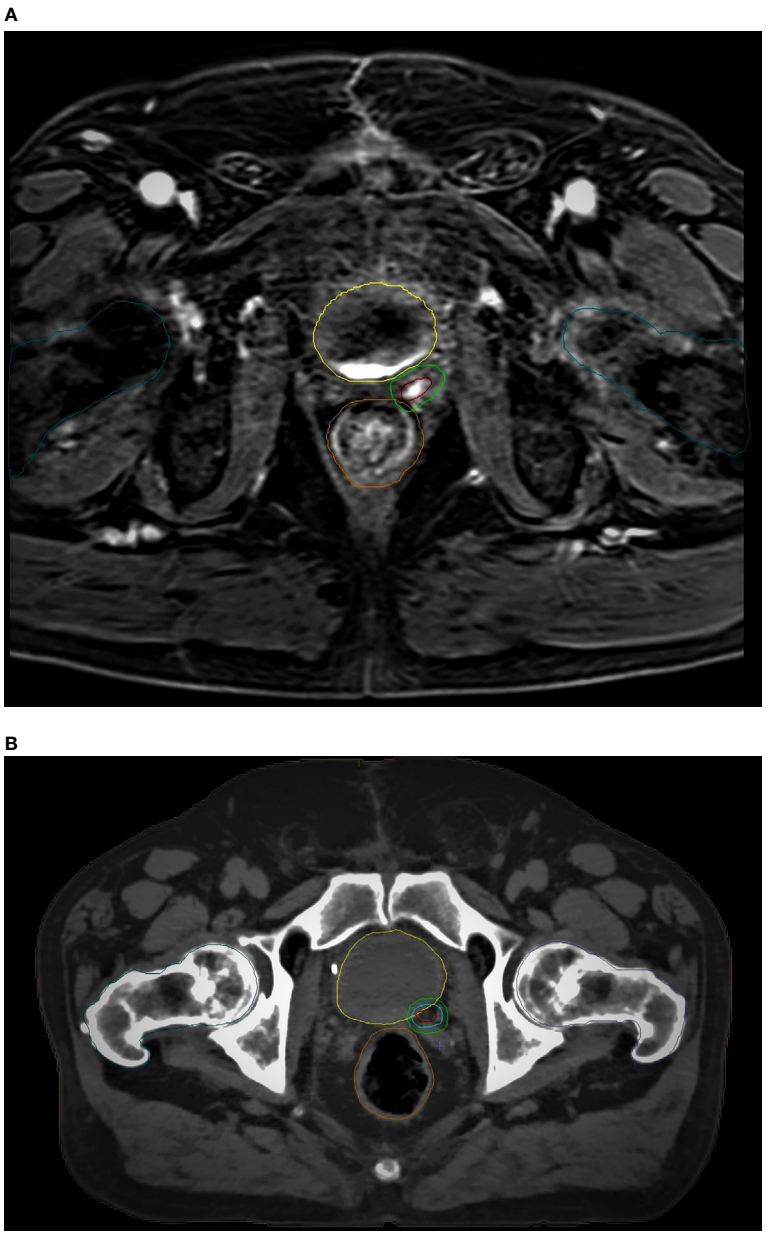

FIGURE 2 | mpMRI-based **(A)** *vs* CT-based **(B)** GTV/PTV (boost) and OARs delineation: brown, GTV; light green, PTV (boost); yellow, bladder; orange, rectum; dark green, femoral heads.

than conventional morphological imaging techniques such as ultrasound or computed tomography (CT). For this reason, mpMRI may ensure a proper definition of the pelvic organs anatomy, of the prostate and prostate bed boundaries, so that several publications have highlighted a smaller prostate volume delineated on MRIs than on CTs (13–17). Moreover, the addition of functional sequences like DWI, DCE, and MR spectroscopy further improved the precise location and characterization of primary and recurrent prostate tumor lesions, even in the post-prostatectomy setting (14). Such findings, together with the possibility of dose-painting and advances in stereotactic EBRT and VMAT delivery techniques, have opened out a new era allowing highly non-homogeneous dose distributions, with aggressive dose escalation to the GTV while contemporarily reducing the dose to lower-risk areas of the prostate, and improving OARs sparing (13, 15).

Post-prostatectomy recurrent tumors may be found at the urethrovesical anastomosis, seminal vesicles bed, bladder posterior wall or rectal anterior wall. Boonsirikamchai et al. retrospectively showed >90% accuracy of DCE MR scans in the

TABLE 2 | Dosimetric comparison between mpMRI-based and non-mpMRI-based RT plans: target volume coverage (significant correlations shown in bold).

	CT-based RT plan	mpMRI-based RT plan	Difference	P value
CTV (prostate bed) (cm^3)				
Patient 1	19.50	11.20	8.30	
Patient 2	34.70	8.00	26.70	
Patient 3	51.00	30.72	20.28	
Patient 4	24.30	5.64	18.66	
Patient 5	32.22	21.08	11.14	**0.0002**
Patient 6	32.35	15.20	17.15	
Patient 7	34.40	16.30	18.10	
Patient 8	30.30	12.40	17.90	
Patient 9	43.60	27.00	16.60	
Patient 10	35.70	19.30	16.40	
PTV (boost) $D_{98\%}$ (Gy)				
Patient 1	74.10	74.90	0.80	
Patient 2	74.00	74.90	0.90	
Patient 3	75.70	76.00	0.30	
Patient 4	73.80	74.00	0.20	
Patient 5	76.36	78.5	2.14	0.376
Patient 6	76.10	76.20	0.10	
Patient 7	76.10	76.40	0.30	
Patient 8	77.20	77.30	0.10	
Patient 9	76.90	77.20	0.30	
Patient 10	77.00	78.10	1.10	

TABLE 3 | Dosimetric comparison between mpMRI-based and non-mpMRI-based RT plans: high-doses OAR sparing (significant correlations shown in bold; outrange values highlighted).

	CT-based RT plan	mpMRI-based RT plan	Difference	*P* value
Rectum V_{70Gy} (%)				
Patient 1	5.10	4.90	0.20	
Patient 2	14.50	9.80	4.70	
Patient 3	16.70	13.80	2.90	
Patient 4	13.40	7.70	5.70	
Patient 5	13.00	9.50	3.50	**0.005**
Patient 6	13.30	8.10	5.20	
Patient 7	14.40	9.00	5.40	
Patient 8	12.60	8.70	3.90	
Patient 9	15.30	11.12	4.18	
Patient 10	13.60	10.30	3.30	
Bladder V_{70Gy} (%)				
Patient 1	**37.30**	**35.00**	2.30	
Patient 2	14.50	10.30	4.20	
Patient 3	33.30	33.00	0.30	
Patient 4	24.90	22.90	2.00	
Patient 5	28.00	22.70	5.30	0.210
Patient 6	25.20	21.30	3.90	
Patient 7	27.20	22.50	4.70	
Patient 8	24.20	20.40	3.80	
Patient 9	28.20	23.30	4.90	
Patient 10	28.20	22.40	5.80	

detection of prostate bed recurrences (14). Currently, mpMRI is the only imaging technique recommended by the European Society of Urogenital Radiology (ESUR) for the detection of pelvic post-prostatectomy RPC in patients with PSA rising to conventional biochemical relapse values (0.2–2 ng/ml) (24, 25), given its higher sensitivity in detecting local lesions, especially small ones (<10 mm) with low blood PSA levels (26). Detection rates of 84–95% have been reported using endorectal coil-mpMRI for PSA values >1 ng/ml, while other retrospective studies and a metanalysis reported recurrence rates ranging from 24 to 91%. This variability is due to the retrospective nature of the study designs and extremely heterogeneous sample sizes and procedures (15).

The addition of functional DWI and DCE perfusion scans to the morphological T2w imaging dramatically improved the performance of MRI in detecting malignant lesions, with their

typical, albeit relatively variable, early uptake and early washout of the contrast material (15).

DWI imaging is also powerful in detecting tumor masses since they appear as highly cellular tissues. However, in the prostate setting, the ADC alone, derived for absolute quantification, may be vague and difficult to interpret. mpMRI can overcome the problem of the unavoidable heterogeneity of the ADC maps due to the well-known highly heterogeneous cell density between malignant and benign prostate areas, which may obscure small lesions or part of tumor masses (27).

The precise location and segmentation of a tumor mass have given rise to better patient selection for focal therapy (28). In the field of EBRT, Stoyanova and colleagues analyzed mpMRI of 65 planned and treated prostate cancer patients and found they could detect the tumor burden by including ADC and DCE-MRI information, imported in a DICOM-RT ready format, into the radiotherapy TPS (29). They subsequently created an automated, mpMRI-based, quantitative method to guide dose-escalation to more aggressive prostate tumor masses, referenced to the prostatectomy Gleason score (30). This means that mpMRI-guided, precise delineation of tumor boundaries may allow the complete eradication of disease through highly-escalated dose delivery, leading to radiation doses of up to 80 Gy on the high-risk GTVs while ensuring lower doses to the low-risk, less aggressive prostate areas, with better OARs dose saving and hence limited treatment-related toxicity. In this regard, the ongoing prospective, phase II trials, hypo-FLAME Trial and DELINEATE Trial, both reached their primary endpoint in terms of acceptable acute toxicity with simultaneous focal boosting to the mpMRI-detected macroscopic tumor(s) in addition to whole gland prostate irradiation (31, 32). Thus, in the setting of salvage RT for macroscopic, local recurrence of PC after radical prostatectomy, such findings are likely to improve the efficacy and safety of radiotherapy: firstly, thanks to a dose-escalated boost over the mpMRI-delineated RPC lesions, in addition to the 64 to 70 Gy-standard irradiation of the prostate fossa (33, 34); secondly, thanks to the precise segmentation of prostate bed recurrent masses with the help of mpMRI co-registration, enabling stereotactic salvage treatments to be performed in the attempt to provide a better local control than the conventional, normofractionated RT protocols (35).

On the other hand, there are some intrinsic limitations due to the non-linear information content of the registered MR images compared to planning CT scan, as the former is usually performed regardless of the radiation treatment position, with a different appearance of the surrounding hollow OARs, often with the use of an endorectal coil which is helpful in the correct delimitation of prostate boundaries from the rectal wall, but in contrast with the EBRT patients setup requiring an empty rectum and comfortable bladder filling (36). In this regard, Couñago and colleagues first found a significantly higher probability of radiological evidence of local recurrence at the pre-treatment mpMRI without endorectal coil in patients undergoing salvage EBRT for biochemical relapse after prostatectomy with PSA doubling time >14 months (adjusted Odds ratio (OR) 7.12, p = 0.01) and/or PSA levels >0.5 ng/ml (adjusted OR 6.25, p = 0.02) (37). Ciardo et al. also described a multimodal, voxel-based and contrast enhancement-based deformable registration procedure, with acceptable accuracy despite varying setups in MRI (17).

Despite the limitation of the few analyzed cases and intrinsic biases due to the pilot study design, our results are in line with the scarce available literature, and support the use of pre-treatment mpMRI to better assess the prostate tumor phenotype and personalize radiation treatment segmentation and dose prescription. In our series, mpMRI was acquired without an endorectal coil, in view of the patient treatment position. The possibility of EBRT treatment planning with the help of image registration with pre-treatment mpMRI allowed high-precision matching and target volume delineation. This made it possible to deliver doses up to 80 Gy to the RPC lesions or to the whole prostate bed without compromising treatment safety and tolerability, possibly improving the sparing of the surrounding normal tissues and OARs.

Another limitation of our study is the unavoidable, intrinsic variability of the CTVs and GTVs due to the extension of the RPC lesions and patients anatomy, affecting the outlined volumes. However, the mpMRI-based CTV (prostate bed) were significantly smaller than the CT-based ones in all the recruited patients, with a significant median reduction of 17.5 cm^3. These findings support the more accurate identification and delineation of the volumes of interest through the better soft tissue contrast provided by mpMRI, together with the possible better dose saving to the surrounding normal tissues.

Equally importantly, dosimetric evaluation showed that rectum and bladder sparing were most evident in the analysis of high doses. Since the macroscopic RPC is the volume of interest, receiving the higher radiation dose up to 76–80 Gy, the greatest difference in terms of normal tissues sparing is reasonably expected at the highest dose levels. Our results seem to confirm this trend.

International guidelines recommend rectum V_{70Gy} <20% and bladder V_{70Gy} <35% (21, 22). These dose constraints were respected in both rival plans for all the recruited patients, except for one case of bladder V_{70Gy} 37.3% in the non-mpMRI-based RT plan, which we could reduce to below threshold (V_{70Gy} 35%) with the help of mpMRI registration (**Table 3**). Our series revealed a median 4% reduction in rectum and bladder V_{70Gy}, although the latter was not statistically significant. Such differences may be relevant to prevent exceeding or not the recommended dose constraints, and this may have a non-negligible impact on treatment tolerance and toxicity. Therefore, if such results should be confirmed in a wider series, it may be reasonable to define the percentage of OAR volume receiving more than a 70 Gy dose as the most useful parameter to ensure dose saving to the rectum and bladder during post-prostatectomy prostate bed irradiation.

Further studies are warranted to fully assess the role of mpMRI in optimizing therapeutic strategies, especially in the field of post-prostatectomy recurrent PC, as well as the ability of combined anatomic and functional MR scans to provide biological and pathophysiological information on prostate cancer behavior, and so radiation resistance (38).

The completion of our statistical analysis on a wider dataset will strengthen the statistical power of our series and possibly provide a definitive validation of our promising findings.

Noteworthily, in the era of next-generation IGRT, where MR-Linac EBRT has been gaining increasing interest in the field of prostate cancer (39–41), radiation treatment planning with mpMRI appears as a cost-effective procedure and may contribute to ensure quality oncological healthcare in the South of Italy.

In conclusion, mpMRI may improve the accuracy of radiation treatment planning in the setting of salvage EBRT for recurrent prostate cancer after prostatectomy, provide high precision target volumes and OAR delineation, thus ensuring better target volume coverage with better OAR sparing. The addition of mpMRI to conventional, CT-based EBRT planning may also improve the optimization of dose distribution, as it allows a dose reduction to lower-risk areas of the prostate fossa, together with an aggressive dose escalation to the macroscopic RPC lesions, while reducing the dose delivered to the surrounding normal tissues.

In the future perspective of patient-tailored medicine, prospective, randomized, phase III studies, and validation of our findings on a wider dataset are needed to complete the assessment of the power of T2w/ADC-based target volume segmentation and dose prescription in improving the accuracy and precision, hence safety and effectiveness, of radiation treatment delivery for primary and recurrent prostate cancer.

DATA AVAILABILITY STATEMENT

The datasets presented in this article are not readily available because the present prospective study is currently ongoing. Requests to access the datasets should be directed to Angela Sardaro, angela.sardaro@uniba.it.

AUTHOR CONTRIBUTIONS

AnS developed the project, analyzed the data, and edited the manuscript. BT edited the manuscript. LB reviewed the literature and wrote the manuscript. CF edited the manuscript. GR analyzed the data, performed accuracy check, and edited the manuscript. AC wrote the manuscript. FA collected the data. AG collected the data and edited the manuscript. AL collected and managed the data. FL edited the manuscript. AS analyzed the data. AI interpreted the data and edited the manuscript. ArS developed the project, checked the data integrity, checked the data analysis accuracy, and edited the manuscript. All authors contributed to the article and approved the submitted version.

ACKNOWLEDGMENTS

The authors acknowledge Mary Victoria Pragnell for assisting in revising and editing the English manuscript.

REFERENCES

1. Bray F, Ferlay J, Soerjomataram I, Siegel RL, Torre LA, Jemal A. Global cancer statistics 2018: GLOBOCAN estimates of incidence and mortality worldwide for 36 cancers in 185 countries. *CA Cancer J Clin* (2018) 68(6):394–424. doi: 10.3322/caac.21492
2. Arnold M, Karim-Kos HE, Coebergh JW, Byrnes G, Antilla A, Ferlay J, et al. Recent trends in incidence of five common cancers in 26 European countries since 1988: Analysis of the European Cancer Observatory. *Eur J Cancer* (2015) 51(9):1164–87. doi: 10.1016/j.ejca.2013.09.002
3. AIOM - AIRTUM SIAPEC-IAP. *I Numeri del Cancro in Italia 2020*. Intermedia EDITORE (2020). Available at: https://www.aiom.it/wp-content/uploads/2020/10/2020_Numeri_Cancro-operatori_web.pdf.
4. Dess RT, Hartman HE, Mahal BA, Soni PD, Jackson WC, Cooperberg MR, et al. Association of Black Race With Prostate Cancer-Specific and Other-Cause Mortality. *JAMA Oncol* (2019) 5(7):975–83. doi: 10.1001/jamaoncol.2019.0826
5. Merriel SWD, Funston G, Hamilton W. Prostate Cancer in Primary Care. *Adv Ther* (2018) 35(9):1285–94. doi: 10.1007/s12325-018-0766-1
6. Mottet N, Bellmunt J, Bolla M, Briers E, Cumberbatch MG, De Santis M, et al. EAU-ESTRO-SIOG Guidelines on Prostate Cancer. Part 1: Screening, Diagnosis, and Local Treatment with Curative Intent. *Eur Urol* (2017) 71(4):618–29. doi: 10.1016/j.eururo.2016.08.003
7. Amling CL, Bergstralh EJ, Blute ML, Slezak JM, Zincke H. Defining prostate specific antigen progression after radical prostatectomy: what is the most appropriate cut point? *J Urol* (2001) 165(4):1146–51.
8. Cornford P, van den Bergh RCN, Briers E, Van den Broeck T, Cumberbatch MG, De Santis M, et al. EAU-EANM-ESTRO-ESUR-SIOG Guidelines on Prostate Cancer. Part II—2020 Update: Treatment of Relapsing and Metastatic Prostate Cancer. *Eur Urol* (2020). doi: 10.1016/j.eururo.2020.09.046
9. Pisansky TM, Thompson IM, Valicenti RK, D'Amico AV, Selvarajah S. Adjuvant and Salvage Radiotherapy after Prostatectomy: ASTRO/AUA Guideline Amendment 2018-2019. *J Urol* (2019) 202(3):533–8. doi: 10.1097/JU.0000000000000029510
10. Kuban DA, Tucker SL, Dong L, Starkschall G, Huang EH, Cheung MR, et al. Long-term results of the M. D. Anderson randomized dose-escalation trial for prostate cancer. *Int J Radiat Oncol Biol Phys* (2008) 70(1):67–74. doi: 10.1016/j.ijrobp.2007.06.054
11. Peeters ST, Heemsbergen WD, Koper PC, van Putten WL, Slot A, Dielwart MF, et al. Dose-response in radiotherapy for localized prostate cancer: results of the Dutch multicenter randomized phase III trial comparing 68 Gy of radiotherapy with 78 Gy. *J Clin Oncol* (2006) 24(13):1990–6. doi: 10.1200/JCO.2005.05.2530
12. Delongchamps NB, Rouanne M, Flam T, Beuvon F, Liberatore M, Zerbib M, et al. Multiparametric magnetic resonance imaging for the detection and localization of prostate cancer: combination of T2-weighted, dynamic contrast-enhanced and diffusion-weighted imaging. *BJU Int* (2011) 107(9):1411–8. doi: 10.1111/j.1464-410X.2010.09808.x
13. Boonsirikamchai P, Choi S, Frank SJ, Ma J, Elsayes KM, Kaur H, et al. MR imaging of prostate cancer in radiation oncology: what radiologists need to know. *Radiographics* (2013) 33(3):741–61. doi: 10.1148/rg.333125041
14. Boonsirikamchai P, Kaur H, Kuban DA, Jackson E, Hou P, Choi H. Use of maximum slope images generated from dynamic contrast-enhanced MRI to detect locally recurrent prostate carcinoma after prostatectomy: a practical approach. *AJR Am J Roentgenol* (2012) 198(3):W228–36. doi: 10.2214/AJR.10.6387
15. Counago F, Sancho G, Catala V, Hernandez D, Recio M, Montemuino S, et al. Magnetic resonance imaging for prostate cancer before radical and salvage radiotherapy: What radiation oncologists need to know. *World J Clin Oncol* (2017) 8(4):305–19. doi: 10.5306/wjco.v8.i4.305
16. Steenbergen P, Haustermans K, Lerut E, Oyen R, De Wever L, Van den Bergh L, et al. Prostate tumor delineation using multiparametric magnetic resonance imaging: Inter-observer variability and pathology validation. *Radiother Oncol* (2015) 115(2):186–90. doi: 10.1016/j.radonc.2015.04.012
17. Ciardo D, Jereczek-Fossa BA, Petralia G, Timon G, Zerini D, Cambria R, et al. Multimodal image registration for the identification of dominant

intraprostatic lesion in high-precision radiotherapy treatments. *Br J Radiol* (2017) 90(1079):20170021. doi: 10.1259/bjr.20170021
18. *COVID-19, raccomandazioni per i pazienti oncologici*. Available at: http://www.salute.gov.it/portale/nuovocoronavirus/dettaglioNotizieNuovoCoronavirus.jsp?lingua=italiano&menu=notizie&p=dalministero&id=4200 (Accessed April 1, 2020).
19. Filippi AR, Russi E, Magrini SM, Corvò R. Letter from Italy: First practical indications for radiation therapy departments during COVID-19 outbreak. *Int J Radiat Oncol Biol Phys* (2020) 107(3):597–9. doi: 10.1016/j.ijrobp.2020.03.007
20. Wiltshire KL, Brock KK, Haider MA, Zwahlen D, Kong V, Chan E, et al. Anatomic boundaries of the clinical target volume (prostate bed) after radical prostatectomy. *Int J Radiat Oncol Biol Phys* (2007) 69(4):1090–9. doi: 10.1016/j.ijrobp.2007.04.068
21. Marks LB, Yorke ED, Jackson A, Ten Haken RK, Constine LS, Eisbruch A, et al. Use of normal tissue complication probability models in the clinic. *Int J Radiat Oncol Biol Phys* (2010) 76(3 Suppl):S10–9. doi: 10.1016/j.ijrobp.2009.07.1754
22. Lawton CAF, Michalski J, El-Naqa I, Buyyounouski MK, Lee WR, Menard C, et al. RTOG GU Radiation oncology specialists reach consensus on pelvic lymph node volumes for high-risk prostate cancer. *Int J Radiat Oncol Biol Phys* (2009) 74(2):383–7. doi: 10.1016/j.ijrobp.2008.08.002
23. ICRU. ICRU report Vol. 83. Bethesda: International Commission on Radiation Units and Measurements. Prescribing, recording, and reporting photon-beam intensity-modulated radiation therapy (IMRT). *J ICRU* (2010) 10(1). doi: 10.1093/jicru/ndq001
24. Buyyounouski MK, Hanlon AL, Eisenberg DF, Horwitz EM, Feigenberg SJ, Uzzo RG, et al. Defining biochemical failure after radiotherapy with and without androgen deprivation for prostate cancer. *Int J Radiat Oncol Biol Phys* (2005) 63(5):1455–62. doi: 10.1016/j.ijrobp.2005.05.053
25. Barentsz JO, Richenberg J, Clements R, Choyke P, Verma S, Villeirs G, et al. ESUR prostate MR guidelines 2012. *Eur Radiol* (2012) 22(4):746–57. doi: 10.1007/s00330-011-2377-y
26. Panebianco V, Sciarra A, Lisi D, Galati F, Buonocore V, Catalano C, et al. Prostate cancer: 1HMRS-DCEMR at 3T versus [(18)F]choline PET/CT in the detection of local prostate cancer recurrence in men with biochemical progression after radical retropubic prostatectomy (RRP). *Eur J Radiol* (2012) 81(4):700–8. doi: 10.1016/j.ejrad.2011.01.095
27. Borren A, Moman MR, Groenendaal G, Boeken Kruger AE, van Diest PJ, van der Groep P, et al. Why prostate tumour delineation based on apparent diffusion coefficient is challenging: an exploration of the tissue microanatomy. *Acta Oncol* (2013) 52(8):1629–36. doi: 10.3109/0284186X.2013.787164
28. Wysock JS, Lepor H. Multi-parametric MRI imaging of the prostate-implications for focal therapy. *Transl Androl Urol* (2017) 6(3):453–63. doi: 10.21037/tau.2017.04.29
29. Stoyanova R, Sandler K, Pollack A. Delineation and visualization of prostate cancer in multiparametric MRI. *Pract Radiat Oncol* (2013) 3(2 Suppl 1):S30–1. doi: 10.1016/j.prro.2013.01.105
30. Stoyanova R, Chinea F, Kwon D, Reis IM, Tschudi Y, Parra NA, et al. An Automated Multiparametric MRI Quantitative Imaging Prostate Habitat Risk Scoring System for Defining External Beam Radiation Therapy Boost Volumes. *Int J Radiat Oncol Biol Phys* (2018) 102(4):821–9. doi: 10.1016/j.ijrobp.2018.06.003
31. Draulans C, van der Heide UA, Haustermans K, Pos FJ, van der Voort van Zyp J, De Boer H, et al. Primary endpoint analysis of the multicentre phase II hypo-FLAME trial for intermediate and high risk prostate cancer. *Radiother Oncol* (2020) 147:92–8. doi: 10.1016/j.radonc.2020.03.015
32. Murray JR, Tree AC, Alexander EJ, Sohaib A, Hazell S, Thomas K, et al. Standard and Hypofractionated Dose Escalation to Intraprostatic Tumor Nodules in Localized Prostate Cancer: Efficacy and Toxicity in the DELINEATE Trial. *Int J Radiat Oncol Biol Phys* (2020) 106(4):715–24. doi: 10.1016/j.ijrobp.2019.11.402
33. Shelan M, Odermatt S, Bojaxhiu B, Nguyen DP, Thalmann GN, Aebersold DM, et al. Disease Control With Delayed Salvage Radiotherapy for Macroscopic Local Recurrence Following Radical Prostatectomy. *Front Oncol* (2019) 9:12. doi: 10.3389/fonc.2019.00012
34. Dirix P, van Walle L, Deckers F, Van Mieghem F, Buelens G, Meijnders P, et al. Proposal for magnetic resonance imaging-guided salvage radiotherapy for prostate cancer. *Acta Oncol* (2017) 56(1):27–32. doi: 10.1080/0284186X.2016.1223342
35. Francolini G, Jereczek-Fossa BA, Di Cataldo V, Simontacchi G, Marvaso G, Zerella MA, et al. Stereotactic radiotherapy for prostate bed recurrence after prostatectomy, a multicentric series. *BJU Int* (2020) 125(3):417–25. doi: 10.1111/bju.14924
36. Hanvey S, Sadozye AH, McJury M, Glegg M, Foster J. The influence of MRI scan position on image registration accuracy, target delineation and calculated dose in prostatic radiotherapy. *Br J Radiol* (2012) 85(1020):e1256–62. doi: 10.1259/bjr/26802977
37. Counago F, del Cerro E, Recio M, Diaz AA, Marcos FJ, Cerezo L, et al. Role of 3T multiparametric magnetic resonance imaging without endorectal coil in the detection of local recurrent prostate cancer after radical prostatectomy: the radiation oncology point of view. *Scand J Urol* (2015) 49(5):360–5. doi: 10.3109/21681805.2015.1004643
38. Zamboglou C, Eiber M, Fassbender TR, Eder M, Kirste S, Bock M, et al. Multimodal imaging for radiation therapy planning in patients with primary prostate cancer. *Phys Imaging Radiat Oncol* (2018) 8:8–16. doi: 10.1016/j.phro.2018.10.001
39. McPartlin AJ, Li XA, Kershaw LE, Heide U, Kerkmeijer L, Lawton C, et al. MR-Linac consortium: MRI-guided prostate adaptive radiotherapy - A systematic review. *Radiother Oncol* (2016) 119(3):371–80. doi: 10.1016/j.radonc.2016.04.014
40. Mannerberg A, Persson E, Jonsson J, Gustafsson CJ, Gunnlaugsson A, Olsson LE. Dosimetric effects of adaptive prostate cancer radiotherapy in an MR-linac workflow. *Radiat Oncol* (2020) 15(1):168. doi: 10.1186/s13014-020-01604-5
41. Dunlop A, Mitchell A, Tree A, Barnes H, Bower L, Chick J, et al. Daily adaptive radiotherapy for patients with prostate cancer using a high field MR-linac: Initial clinical experiences and assessment of delivered doses compared to a C-arm linac. *Clin TranslRadiat Oncol* (2020) 23:35–42. doi: 10.1016/j.ctro.2020.04.011

Conflict of Interest: The authors declare that the research was conducted in the absence of any commercial or financial relationships that could be construed as a potential conflict of interest.

frontiers in Oncology

REVIEW
published: 08 January 2021
doi: 10.3389/fonc.2020.604965

Prediction of Response in Head and Neck Tumor: Focus on Main Hot Topics in Research

Liliana Belgioia[1,2]*, *Silvia Daniela Morbelli*[2,3] *and Renzo Corvò*[1,2]

[1] Radiation Oncology Department, IRCCS Ospedale Policlinico San Martino, Genoa, Italy, [2] Health Science Department (DISSAL), University of Genoa, Genoa, Italy, [3] Nuclear Medicine Department, IRCCS Ospedale Policlinico San Martino, Genoa, Italy

Radiation therapy is a cornerstone in the treatment of head and neck cancer patients; actually, their management is based on clinical and radiological staging with all patients at the same stage treated in the same way. Recently the increasing knowledge in molecular characterization of head and neck cancer opens the way for a more tailored treatment. Patient outcomes could be improved by a personalized radiotherapy beyond technological and anatomical precision. Several tumor markers are under evaluation to understand their possible prognostic or predictive value. In this paper we discuss those markers specific for evaluate response to radiation therapy in head and neck cancer for a shift toward a biological personalization of radiotherapy.

Keywords: head and neck cancer, radiation therapy, biomarkers, prognostic factors, predictive factors, precision medicine

OPEN ACCESS

Edited by:
Francesco Cellini, Catholic University of the Sacred Heart, Italy

Reviewed by:
Francesco Micciche', Fondazione Policlinico A. Gemelli IRCCS, Italy
Jon Cacicedo, Cruces University Hospital, Spain

***Correspondence:**
Liliana Belgioia
liliana.belgioia@unige.it

Specialty section:
This article was submitted to Radiation Oncology, a section of the journal Frontiers in Oncology

Received: *10 September 2020*
Accepted: *26 November 2020*
Published: *08 January 2021*

Citation:
Belgioia L, Morbelli SD and Corvò R (2021) Prediction of Response in Head and Neck Tumor: Focus on Main Hot Topics in Research. Front. Oncol. 10:604965. doi: 10.3389/fonc.2020.604965

INTRODUCTION

Squamous cell carcinoma of the head and neck (SCCHN) accounts for about 4% of all malignant disease in adults. According to SEER data the 5-year OS is approximately 60% (1). Radiation therapy is a cornerstone in the treatment of these patients, and prognosis is influenced by several clinical factors as disease stage, site, HPV/EBV positivity, age and co-morbidity. About 50% of patients with head and neck cancer (HNC) present a locally advanced stage at diagnosis and are treated with multimodality therapy but the prognosis of these patients is still not satisfactory (2).

The evolution of treatments in oncology is moving towards precision medicine that is the cross from the so-called "one-size-fit-all medicine" to stratified treatments on certain subpopulations of patients based, for example, on disease subtypes, risk profiles, demographic, socio-economic characteristics, biomarkers and molecular subpopulations, to arrive at the possible proposal of a "precision" treatment, specific to the individual patient so that this can benefit from the treatment itself by limiting the risk of toxicity related to it. All of this, in part, is alreadily applied in daily clinical practice in oncology, but it is still a challenge in radiotherapy (RT) treatments (3).

On the one hand, in fact, the field of radiation therapy has substantially evolved over the last decades; in particular technological advances have led to the development of various high-precision techniques such as modulated intensity radiotherapy (IMRT), radiotherapy guided by image (IGRT), stereotactic radiotherapy (SBRT), particle therapies and brachytherapy, which allow for delivering the radiation dose more accurately, by administering high doses to the tumor and limiting those to surrounding organs (4). In HNC this has resulted, from a clinical point of view, in

the reduction of acute and late severe toxicities and in a better quality of life (3). Despite this, currently, RT treatments are planned on the anatomy of the individual patient but are not modulated according to the biological characteristics of that patient's specific neoplasm; patients with tumors at the same stage and site are considered similar and then treated at the same way (5).

The implementation of precision medicine in oncology and, especially, in RT therefore requires a precise understanding of the behavior of the disease, even at the molecular level aiming at a biology-driven radiotherapy approach. In this context, the identification of prognostic and predictive factors is of considerable interest. Specifically, the prognostic factor is defined as that factor that describes the natural progression of the disease with or without a therapeutic intervention; by predictive factor, on the other hand, we define the factor that describes the response to a specific therapeutic regimen, so in fact it describes the response or absence of response (if we are referring to the effectiveness of the treatment) or the development of toxicity. In literature several data underline the importance and the potential impact of some biomarker; in radiation oncology those that have been shown to influence response to treatment are focused on some biological characteristics.

In this review we try to describe which novel prognostic and predictive factor in HNC are developed and which of those might be specific for evaluated radiation response in clinical practice (**Table 1**).

BIOLOGY DETERMINANTS

EBV-DNA

Several data reported on patients with nasopharyngeal cancer show that pre-treatment plasma concentrations of EBV-DNA and the presence or absence of viral DNA in plasma after RT are statistically significant correlate with overall survival (2-year OS: 56.3% in patients with detectable EBV-DNA *vs* 96.7% in patients with undetectable EBV-DNA after RT) and with relapse-free survival (RFS) (6). Data revealed that several months before recurrence high serum EBV-DNA could be detected demonstrating its potential as a biomarker of subclinical disease. Moreover, the presence of high pre-treatment plasma viral levels also correlates with the risk of developing distant metastases (7). High post-treatment EBV-DNA is a recognized negative prognostic factor that a phase II–III trial has incorporated serum EBV-DNA to personalized treatment in stage II–IV nasopharyngeal cancer (NCT02135042). All the 924 planned patients of this randomized trial will first undergo concurrent chemo-radiotherapy and then are randomized according to plasma EBV-DNA. If plasma EBV-DNA is not detectable patients are randomized to standard adjuvant chemotherapy or observation. Instead if plasma EBV-DNA is detectable patients will be randomized to standard cisplatin and fluorouracil chemotherapy *versus* gemcitabine and paclitaxel (8).

TABLE 1 | Overview on the main points described in the review.

Potential biomarker		
Biological	Viral factors	
	Hypoxia	RSI
		GARD
Immunological	TILs	
	Treg cells	
Imaging	PET/CT	
	MRI	

RSI, radiosensitivity index; GARD, genomic-adjusted radiation dose; TILs, tumor infiltrating lymphocytes; PET/CT, positron emission tomography/computed tomography; MRI, magnetic resonance imaging.

HPV Infection

Another particularly important example in oropharyngeal squamous cell carcinoma (OPSCC) is represented by HPV infection; it is widely demonstrated that patients with HPV-related head and neck neoplasia have better outcomes than HPV negative patients; specifically, HPV positivity is the strongest prognostic factor for survival (9). This factor is so significant that the classification of oropharyngeal tumors has been changed, initially leading to a classification into three risk groups (low, intermediate, and high) based on the combination with other parameters (HPV, smoking, and stage of disease) (9) and in 2018, the TNM staging was modified.

Considering these better outcomes, the identification of biomarkers of HPV driven disease is extremely important; actually p16 expression is considered a surrogate for HPV+ OPSCC; however, the association of p16 with HPV DNA positivity is more accurate in predicting recurrence free survival (10). Currently other factors as HPV oncoproteins and serum E6 and E7 proteins are under evaluation in order to documenting biologically active HPV infections rather than mere HPV DNA detection (11).

Some data suggest that HPV-driven OPSCC are associated with serum antibodies to the HPV oncoproteins E6 and E7; it seems that pre-treatment levels of these antibodies are related to disease-free survival in HPV+ OPSCC, indicating that a highly immunogenic response to these proteins before treatment can be detected (12). Moreover further data demonstrated that clearance of E6 and E7 antibodies is lower in patients who develop recurrence after chemoradiotherapy compared to those who do not recur; thus E6 and E7 antibodies might be potential biomarkers in HPV OPSCC (13). Considering the better outcome of HPV-positive OPSCC, a large number of trials are evaluating a de-escalation approach for this subset of patients; de-intensification strategies could be several and regard both chemotherapy and radiation therapy. Here we concentrated on RT approaches that could consider a reduction of RT doses or volumes. Several studies have been conducted and others are on-going to investigate this option: the ECOG1308 trial, a non-randomized phase II trial, enrolled 90 HPV16 and/or p16-positive, stage III–IV OPSCC patients. They received three cycles of induction chemotherapy (IC) with cisplatin, paclitaxel, and cetuximab and, according to IC response, received intensity modulated radiation therapy (IMRT) 54 Gy with cetuximab in case of a clinical complete response (cCR) or IMRT 69.3 Gy and cetuximab in those patients with less than cCR to IC.

The oncological outcomes were interesting with 2-year progression-free survival (PFS) and OS rates of 80 and 94% respectively, for patients with primary-site cCR treated with 54 Gy of radiation; the authors concluded de-intensification of treatment in selected patients with HPV related OPSCC could be explored in further study; moreover it should be considered that RT dose reduction improved significantly swallowing and nutritional status (14).

The Quarterback trial, a phase III non-inferiority randomized trial, evaluated the oncological results of reduced RT dose (56 *versus* 70 Gy concomitant to carboplatin) after induction chemotherapy (three cycles of TPF) in 20 HPV+ locally advanced OPSCC. The 3 yy PFS and the OS were 87.5% for standard CRT and 83.3% for reduced CRT for both endpoints, respectively (15). At the 2019 ASTRO annual meeting the preliminary results of NRG-HN002 trial were presented: it is a randomized phase II trial that compared accelerated IMRT (60 Gy in 5 weeks) *versus* IMRT (60 Gy in 6 weeks) plus weekly CDDP in p16+ OPSCC; both arms could be considered testing some form of de-escalation (the former provides omission of chemotherapy but accelerated RT, the last reduction in RT dose −60 Gy *versus* standard 70 Gy). It was designed to select the schedule that achieve acceptable PFS and swallowing function for further trial, this was met by IMRT plus CDDP arm (16).

Other two on-going phase II trials evaluate reduced RT doses associated with standard chemotherapy (NCT03215719–NCT01088802) in favorable risk HPV positive OPSCC (17, 18). Moreover another on-going trial is evaluating volume (level IB lymph node is excluded from the elective nodal volumes) and dose de-intensified RT (60 Gy to gross tumor volume and 54 Gy to region at risk of subclinical disease in 30 fractions) for p16+ squamous cell carcinoma of the oropharynx with CDDP based chemotherapy (19).

The biological rationale for these approaches is based on the fact that the best outcomes of HPV-positive OPSCC may be linked to response to radiation therapy. *In vitro* studies showed that HPV positive cells presented an increase in cell thickness and motility after RT; this suggests that they undergo apoptotic death and are more radiosensitive than HPV negative cells (20). These preclinical data are confirmed by retrospective analysis of several clinical trials. The critical point is that all patients with HPV-positive tumors and with defined clinical characteristics are treated in the same way. Although some results support de-escalation approaches, some concerns were raised as they can result in detrimental outcomes for patients (in RTOG 1016, a randomized non-inferiority trial that compared RT plus cetuximab *versus* RT plus cisplatin, a reduced LRC and OS with de-escalation was detected) (21, 22). This could probably be due to lack of adequate risk stratification system to identify the most suitable HPV+ patients for de-intensification trial; in fact the development of more accurate treatment response classifiers is needed. The next step that should be integrated is a more personalized approach based on the biology of the tumor that might help to develop criteria to better define lower risk HPV+ subpopulations. On this concept an interesting ongoing trial is a non-inferiority phase II study (NCT03323463) which randomized patients with HPV positive and hypoxia negative T1–2, N1–2c (AJCC, 7th ed) OPSCC to descalated RT associated with two cycles of chemotherapy *versus* standard chemoradiotherapy. RT schedule provides a total dose of 30 Gy in 3 weeks (2 Gy per fraction, 5 days per week), deliver to GTV, postoperative bed and all area at microscopic risk of disease. The estimated enrollment is of 300 patients (23). The most interesting point of this trial is that it is specific for patients with HPV+ but hypoxia negative tumors.

Hypoxia

Hypoxia is another parameter widely studied in head and neck neoplasms; it is present in many solid tumors and is well known to be related to radioresistance and therefore indicative of an unfavorable prognosis. Several studies tried to identify biomarker of tumor hypoxia. The methods for detecting intratumoral hypoxia have continuously evolved over the years but their application in clinical practice is still difficult; more recently the attempt is to identify gene expression of hypoxia as endogenous biomarker (24, 25). Specifically, in HNC, gene expression signatures (a group of gene instead of a single one) were developed (26).

Toustrupt et al. identified a method for characterizing the hypoxic state of a tumor based on the quantification of hypoxia-specific genes within the tumor biopsy and generated a model that could improve the ability to individualize treatment according to this characterization. This classification, based on the evaluation of 15 hypoxia-sensitive genes assessed as the best to be able to discriminate between "plus" and "less" hypoxic HNC, was applied to 323 biopsies of patients enrolled in the DAHANCA 5 study (a clinical trial that randomized patients to placebo *versus* hypoxic modification with nimorazole plus RT). The classifier categorized 114 tumors as "more" hypoxic and 209 as "less" hypoxic. In the group "more" hypoxic, patients treated with nimorazole and RT presented a better locoregional control failure rate at 5 years when compared to patients treated with RT alone (79 *vs* 46%). No difference was detected between treatments in the group classified as "less" hypoxic suggesting that hypoxic modification of RT could be useful only in a subgroup of patients with gene expression classified "more" hypoxic tumors. Therefore, this 15-gene hypoxia classifier attains both prognostic and predictive potential (25).

Radiosensitivity Index

Eschrich et al., considering the expression of 10 genes, developed a new model of intrinsic tumor radiosensitivity, to create the radiosensitivity index (RSI) that is directly proportional to tumor radioresistance. The lower is this index, the higher is the tumor's radiosensitivity. The use of this model has been clinically validated on two separate cohorts of patients and subsequently in HNC patients treated with radical chemo-radiotherapy; what emerges is that, by classifying the tumors into "more" radiosensitive and "less" radiosensitive on the basis of the RSI, it is possible to distinguish subgroup of patients with different outcomes. In HNC the radiosensitive group presented an

improved 2-year locoregional control (2-year LRC 86 *vs.* 61%, $p = 0.05$), underling that this model is able to identify biological similarities strictly linked to tumor radiosensitivity across disease sites (27). Another extremely interesting thing of this index is that seems to have a predictive value only in patients treated with RT, and not for other treatments as surgery or chemotherapy. Therefore, RSI can be considered an independent predictor of response to RT alone (27). Based on these data, the concept that the benefit of RT is not uniform in all patients and that it varies in genomically distinct subpopulations is increasingly evident.

Genomic-Adjusted Radiation Dose

A further potential of this index, however, arises from its combination with linear-quadratic model to create the GARD "genomic-adjusted radiation dose", a clinical model that represents a molecular estimate of the fraction of cells surviving at 2 Gy and could allow individualizing the dose of radiation therapy based on the radiosensitivity of the individual tumor. GARD model was prospectively validated by Scott et al. in 2017 and is associated with outcomes in five clinical cohorts. The GARD varies widely among the various tumor histotypes, a high GARD value provides a high therapeutic effect for RT. In fact, lower median GARD values for HPV negative oropharyngeal cancer and higher for HPV positive oropharynx have been detected, therefore in line with the superior clinical results that are normally obtained in HPV related OPSCC (28). GARD should not be considered a predictive factor but rather a tool that allows to personalized treatment on the specific tumor of the single patient. This could be obtained in different way as: 1—a modulation (increase or reduction) of radiation dose based on GARD value, 2—a combined treatment with drugs modifier of hypoxia, 3—change in treatment modality, for example in less radiosensitive tumors, GARD might suggest that RT dose required is beyond the tolerance of normal tissue so the patients might be treated with surgery/chemotherapy. Obviously, these represent hypothetic potentiality of GARD model, moreover it should be considered some limits of GARD as that it accounts only for tumor radiosensitivity and no other important biological parameters as proliferation, DNA repair or patients characteristics.

HEAD AND NECK AND IMMUNE SYSTEM

The immune response to tumors is a recent studied factor; it is extremely complex with the involvement of different cell types both of the adaptive and innate immune systems, and it plays an important role in neoplastic progression (29). The immune system stimulates the elimination of tumor cells and the control of tumor growth; moreover, the tumor microenvironment is highly suppressive and hinders the physiological activity of T cells (29). Generally, HNC is considered a cold tumor capable of creating evasion effect and being less attacked by natural and adaptive immunity. In the context of head and neck neoplasms, patients with high T lymphocytes infiltrated (TILs) tumors appear to have better OS, PFS, and distant metastasis-free survival compared to patients with poorly infiltrated tumors (30, 31). The major correlation with oncological outcome has been demonstrated for CD8+ effector lymphocytes, in fact their rate is higher in HPV-positive cancers, and this could partially explain the better outcome of this subpopulation (32). The CD3 + and CD8 + TILs represent strong prognostic and also predictive markers capable of identifying a subset of HNC patients who have a greater probability of progression and shorter survival after radical chemoradiotherapy (30). The use of TILs as biomarkers to predict recurrence and death from cancer is very interesting especially in advanced diseases; in fact in this setting the implementation of immunotherapy combined with chemoradiotherapy could be particularly advantageous. This association could have a double effect, from one side immunotherapy can enhance the efficacy of RT as a locoregional treatment but RT could work also as an *in situ* vaccination to increase the efficacy of immunotherapy (33); in fact RT is able to upregulate programmed death ligand 1 (PD-L1) on tumor cells, which may increase the response to some immunotherapies.

Furthermore regulatory T cells (Tregs) have the role to suppress immune system and they act inhibiting the action of cytotoxic T cells (34). Several data demonstrated a higher Treg rate in peripheral blood of HNC patients compared to healthy controls, and it seems that patients with high Treg infiltrates cancer present a worse prognosis (35). Also dendritic cells play an important role T cell responses as they present tumor antigens on MHC-I; this leads to activation of CD4+ and CD8+ naïve T cells and to differentiate in effector T cells. Some data showed that tumor with high rate of dendritic cell tumor lead to better outcome in HNC patient (36).

ROLE OF MOLECULAR IMAGING IN RESEARCH

Another strategy that has been explored is the integration of imaging into precision care. To date the 2-deoxy-2-[18F]fluoro-D-glucose (FDG) positron emission tomography/computed tomography (PET/CT) is a standard diagnostic methodic used in HNC patients for staging, restaging, RT planning, and outcome evaluation (37, 38). Several data published in literature underline how changes of neoplastic glucose metabolism, evaluated by FDG PET, are able to predict tumor response rates and oncological outcomes in several solid cancer (39). In particular as regards PET in HNC the major data are validated for SCCHN and nasopharyngeal cancer.

In this settings, PET/CT could help radiation oncologist for target delineation and in radiation planning (39). Moreover, it has been suggested that FDG is able to detect primary tumor site in about 25% of patients with unknown disease (40) and at baseline, it allows quantification of the tumor tracer uptake thus producing semiquantitative values that can be indicative of prognosis. The prognostic role of these parameters in HNC is under active investigation.

In fact, the possibility to identify pre-treatment biomarkers correlated with outcome could be of particular interest in some

subgroups of patients with the aim to intensify treatment (41). The most widely used semiquantitative parameter in oncology is the so-called maximum standardized uptake value (SUVmax). The SUV is a semiquantitative measure of the tracer uptake in a region of interest that normalizes the lesion activity to the injected activity and a measure of the volume of distribution (usually total body weight or lean body mass). Some studies of patients with HNC have shown no predictive value (42, 43), while others have suggested a potential prognostic significance of SUVmax of the primary lesion is (44, 45).

Of note, SUV and SUVmax lack of reproducibly between different PET scanners (also in terms of its uptake time dependence) and thus might be not suitable for the multicenter research settings (46).

It has been suggested that the use of uptake time normalized tumor-to-blood SUV ratio (standardized uptake ratio, SUR) might remove most of these shortcomings improving test–retest stability and providing significantly better prognostic value compared to tumor SUV (39). However, more recently, other PET-based parameters have emerged as potentially valuable for the prognostic stratification in several oncologic diseases including HNC. In particular data are already available with respect to the predictive value of metabolic tumor volume (MTV) and total lesion glycolysis (TLG) (47). MTV is defined as the sum of the volume of voxels with SUV exceeding a certain threshold value in a tumor, reflecting the volume of FDG activity in a tumor assessed by automated volume of interest delineation, while TLG is obtained by multiplying MTV and the mean SUV of the MTV. Romesser et al. found in patients treated and submitted to chemoradiation that a lower MTV is related to improved local control, PFS and OS (42). Similarly, Hanamoto and colleagues found that high metabolic burden in terms of TLG and MTV can independently predict treatment failure more accurately than SUVmax or SUVmean (48). Suzuki and colleagues demonstrated that a TLG ≥5.4 was significantly linked with shorter disease-specific survival, distant metastasis-free survival, and lung metastasis-free survival in laryngeal or pharyngeal cancer patients treated with salvage surgery (49). Finally, recent systematic reviews (one of them including also a meta-analytic analysis) evaluated the relationship between semiquantitative metabolic parameters and outcomes of patients with HNC. These data demonstrated that higher pre-treatment MTV is linked to worse OS, PSF, and locoregional control (50, 51).

Moreover the distribution of FDG uptake in tumors has been studied by other groups as potential prognostic factor of complex heterogeneity parameters such as entropy or textures (52). In particular, Meyer et al. evaluated the relationships between histogram analysis of apparent diffusion coefficient (ADC) values and FDG PET-derived parameters in SCCHN (53). In fact, also functional imaging MRI, such as diffusion-weighted imaging (DWI) can be added to provide further insight into tumor microstructure (54). DWI measures random water movement and can be quantified by the ADC. Previously, various studies identified an inverse relationship between ADC values, cellularity, and proliferation thus suggesting that ADC values mirror tumor microstructure (55). Meyer et al. showed that entropy derived from ADC maps is strongly associated with MTV and TLG in HNC (53). This correlation demonstrated to be stronger in G1/2 tumors and entropy; SUVmax, SUVmean, TLG, and MTV were statistically significantly higher in T3/4 tumors in comparison to T1/2 carcinomas (53). Some trials compared MRI to PET/CT with the aim to evaluate advantages and disadvantages of both methods. Cao et al., in 54 patients with locally advanced SCCHN, investigated p16+ effects on imaging parameters, differences between imaging biomarkers of tumors with local, regional or distant progression and the predictive values of MRI and PET biomarkers. They found that the p16– primary tumors had elevated ADC values pre-RT and low early response rates compared to p16+ tumors; also, high mean apparent diffusion coefficient (ADC) value pre-RT is a hazard for local and regional failure of p16– tumors. Moreover multiple MRI and PET imaging parameters predicted regional and distant failure, but the nodal GTV defined on anatomic MRI was the strongest predictor. They concluded that the performance of MRI related parameters is stronger than PET parameters and that MRI could play an important role from treatment planning, to early response assessment, and boost target definition with different but complementary information (56). Moreover, a comparison between MRI and PET/CT was done by Wong et al. in predicting the response to definitive treatment after induction chemotherapy in locally advanced SCCHN. Firstly, they detected that changes in functional and molecular imaging parameters with both modalities after first induction chemotherapy cycle are representative of its full effects. They did not find pre-treatment ADC to be predictive of treatment outcome; this datum, that is partially in contradiction with other data literature, is explained by authors with the high prevalence of HPV related tumors in their cohort of patients, as HPV related OPSCC often presented unique histologic features as micronecrosis (57). Instead in the context of radical chemo-radiotherapy, increase in ADC has been demonstrated in responders and a lower increase or decrease 1–3 weeks into radiotherapy in non-responders (58, 59). To conclude both PET/CT than MRI could give complementary information to try to identify patients with better or worse prognosis.

Besides the role in the potential intensification of therapy, FDG PET might also have a role in therapy de-intensification. In patients with HNC, viral-related mechanisms have a relevant role in developing a robust personalized medicine associated with specific tumor characteristics at individual level thus guiding appropriate treatment selection. In particular, HPV and EBV provide robust prognostic biomarkers in SCCHN and nasopharyngeal carcinoma respectively and are now being incorporated into clinical trials (60). In this setting FDG PET might help to categorize patients according to risk of recurrence and then to tailor treatment. Floberg et al. in 153 HPV related OPSCC patients demonstrated that the optimum MTV (identified as 24 cm^3) is significantly related to freedom from recurrence, freedom from distant metastasis and OS; these data support the use of MTV as prognostic marker in patients treated with surgery as well as definitive radiotherapy (61).

Another parameter that has been investigated is the heteroneity index (HI) that is a quantitative measure of the intratumoral heterogeneity of 18F-FDG uptake although HI has

been reported as a prognostic factor in locally advanced nasopharyngeal carcinoma (62).

Moreover Kimura et al. evaluated HI in patients with oral cavity SCC and showed that it is a statistically significant prognostic factor for OS in patients with OSCC treated with primary surgery (63). Finally, although 18F-FDG is by far the most frequently used radiopharmaceutical in HNC, glycolysis is not the only metabolic process or biochemical pathway that can be visualized.

In particular, PET technology is able to track the presence of tumor hypoxia (39). As mentioned above, tumor hypoxia is related with worse outcomes and is a major driver in treatment resistance (39, 64). In fact the possibility to track hypoxia *in vivo* is of interest to guide the use of hypoxia sensitizers or of specific IMRT. Most studied evaluated [18F]Fluoromisonidazole (18F-FMISO) PET/CT as it was the first hypoxia tracer (39, 65); it is a 2-nitroimidazole molecule and is well known that imidazole derivates are trapped in hypoxic cells. Studies aiming to evaluate features of patients' non-responders to RT by means of 18F-FMISO PET have suggested that around a half of locoregional failures in SCCHN occur because of hypoxia. Despite this 18F-FMISO is not normally used in the clinical practice, this is due mainly to its high lipophilicity and slow clearance from normal tissues (39) with subsequent difficult in hypoxia identification. Another imidazole derived tracer is [18F] Fluoroazomycin Arabinoside (FAZA) that is characterized by a faster clearance from blood and non-target tissues (39).

Finally, the emerging role of immunotherapy and in particular of immune checkpoints inhibitors (ICPIs) in several cancers, including HNC have further stimulated the development of PET-based prognostic biomarkers (66). RT can modify the expression of some receptor (as PD1/PD-L1) on cancer cells or on myeloid cells, which may affect response to PD-1-based immunotherapy. On these basis novel and promising non-FDG PET tracers have been developed with the aim of predicting response to ICPIs (67, 68).

In fact, PD-L1 expression by immunohistochemistry has been correlated with response and survival following PD-(L)1 monoclonal antibody therapy. However, a lack of response has also been demonstrated in patients with PD-L1 expression and has been linked to heterogeneity of PD-L1 expression within tumors. PET studies in preclinical models have tested this hypothesis.

Some preliminary data on PET imaging with 18F-BMS-986192, 89Zr-Nivolumab, and 89Zr atezolizumab performed in patients with different tumor types before treatment with ICPIs detected a tumor tracer uptake heterogeneity in different patients and in different lesions of the same patient (67, 68).

To conclude both PET/CT could give complementary information to try to identify patients with better or worse prognosis than MRI.

A prognostic effectiveness of baseline FDG PET parameters as biomarkers of OS, DFS, and DM among patients with HNC has increasingly been recognized. Parameters (MTV and TLG) measuring metabolic tumor burden seemed relevant for identifying patients with a higher risk of treatment failure and early disease progression. However, further large-scale studies including patients stratified according to localization and further analysis of the textural indices are required to define a reliable FDG PET-based prognostic model of mortality and recurrence risk for HNC patients. Finally, while FDG remains by far the most frequently used radiopharmaceutical in HNC, novel PET radiotracers especially tracking hypoxia as well as immunoPET imaging might be of further value in the baseline and early prognostic stratification of HNC.

CONCLUSIONS

At present only HPV can be considered a novel prognostic biomarker and must be used in clinical practice to stratify patients among those with better or worse prognosis. The role of the HPV should be integrated with other parameters related to the patient and the tumor that modulate the outcome of the treatments. Unfortunately, even if HPV is the strongest available biomarker, it does not yet allow us to modify the treatment approach outside clinical trials.

Moreover, a prognostic effectiveness of baseline FDG PET parameters as biomarkers of OS, DFS, and DM among patients with HNC has increasingly been recognized.

Despite the increase in the number of studies that investigate possible predictive biomarker in HNC, currently there are no biomarkers of response to RT used as standard of care in clinical practice; certainly some are promising, in particular to understand when to use innovative immunological drugs associated with RT, but further evaluations are needed.

AUTHOR CONTRIBUTIONS

All authors contributed to the study conception and design. LB and SM wrote the paper and reviewed the final manuscript. RC reviewed and edited the final manuscript. All authors contributed to the article and approved the submitted version.

REFERENCES

1. Zhai T-T, van Dijk LV, Huang B-T, Lin Z-X, Ribeiro CO, Brouwer CL, et al. Improving the prediction of overall survival for head and neck cancer patients using image biomarkers in combination with clinical parameters. *Radiother Oncol* (2017) 124:256–62. doi: 10.1016/j.radonc.2017.07.013
2. Rampino M, Bacigalupo A, Russi E, Schena M, Lastrucci L, Iotti C, et al. Efficacy and Feasibility of Induction Chemotherapy and Radiotherapy plus Cetuximab in Head and Neck Cancer. *Anticancer Res* (2012) 32:195–9.
3. Caudell JJ, Torres-Roca JF, Gillies RJ, Enderling H, Kim S, Rishi A, et al. The future of personalised radiotherapy for head and neck cancer. *Lancet Oncol* (2017) 18:e266–73. doi: 10.1016/S1470-2045(17)30252-8
4. Corradini S, Alongi F, Andratschke N, Belka C, Boldrini L, Cellini F, et al. MR-guidance in clinical reality: current treatment challenges and future perspectives. *Radiat Oncol* (2019) 14:92. doi: 10.1186/s13014-019-1308-y
5. Baumann M, Krause M, Overgaard J, Debus J, Bentzen SM, Daartz J, et al. Radiation oncology in the era of precision medicine. *Nat Rev Cancer* (2016) 16:234–49. doi: 10.1038/nrc.2016.18

6. Lin J-C, Wang W-Y, Chen KY, Wei Y-H, Liang W-M, Jan J-S, et al. Quantification of Plasma Epstein–Barr Virus DNA in Patients with Advanced Nasopharyngeal Carcinoma. *N Engl J Med* (2004) 350:2461–70. doi: 10.1056/NEJMoa032260
7. Leung S, Chan ATC, Zee B, Ma B, Chan LYS, Johnson PJ, et al. Pretherapy quantitative measurement of circulating Epstein–Barr virus DNA is predictive of posttherapy distant failure in patients with early-stage nasopharyngeal carcinoma of undifferentiated type. *Cancer* (2003) 98:288–91. doi: 10.1002/cncr.11496
8. *Individualized Treatment in Treating Patients With Stage II-IVB Nasopharyngeal Cancer Based on EBV DNA - Full Text View - ClinicalTrials.gov*. Available at: https://clinicaltrials.gov/ct2/show/NCT02135042 (Accessed September 8, 2020).
9. Ang KK, Harris J, Wheeler R, Weber R, Rosenthal DI, Nguyen-Tân PF, et al. Human Papillomavirus and Survival of Patients with Oropharyngeal Cancer. *N Engl J Med* (2010) 363(1):24–35. doi: 10.1056/NEJMoa0912217
10. Deng Z, Hasegawa M, Aoki K, Matayoshi S, Kiyuna A, Yamashita Y, et al. A comprehensive evaluation of human papillomavirus positive status and p16INK4a overexpression as a prognostic biomarker in head and neck squamous cell carcinoma. *Int J Oncol* (2014) 45:67–76. doi: 10.3892/ijo.2014.2440
11. Holzinger D, Wichmann G, Baboci L, Michel A, Höfler D, Wiesenfarth M, et al. Sensitivity and specificity of antibodies against HPV16 E6 and other early proteins for the detection of HPV16-driven oropharyngeal squamous cell carcinoma. *Int J Cancer* (2017) 140:2748–57. doi: 10.1002/ijc.30697
12. Spector ME, Sacco AG, Bellile E, Taylor JMG, Jones T, Sun K, et al. E6 and E7 Antibody Levels Are Potential Biomarkers of Recurrence in Patients with Advanced-Stage Human Papillomavirus–Positive Oropharyngeal Squamous Cell Carcinoma. *Clin Cancer Res* (2017) 23:2723–9. doi: 10.1158/1078-0432.CCR-16-1617
13. Khanal S, Joh J, Kwon AM, Zahin M, Perez CA, Dunlap NE, et al. Human papillomavirus E7 serology and association with p16 immunohistochemistry in squamous cell carcinoma of the head and neck. *Exp Mol Pathol* (2015) 99:335–40. doi: 10.1016/j.yexmp.2015.06.018
14. Marur S, Li S, Cmelak AJ, Gillison ML, Zhao WJ, Ferris RL, et al. E1308: Phase II Trial of Induction Chemotherapy Followed by Reduced-Dose Radiation and Weekly Cetuximab in Patients With HPV-Associated Resectable Squamous Cell Carcinoma of the Oropharynx—ECOG-ACRIN Cancer Research Group. *J Clin Oncol* (2016) 35(5):490–7. doi: 10.1200/JCO.2016.68.3300
15. Misiukiewicz K, Gupta V, Miles BA, Bakst R, Genden E, Selkridge I, et al. Standard of care vs reduced-dose chemoradiation after induction chemotherapy in HPV+ oropharyngeal carcinoma patients: The Quarterback trial. *Oral Oncol* (2019) 95:170–7. doi: 10.1016/j.oraloncology.2019.06.021
16. Yom SS, Torres-Saavedra P, Caudell JJ, Waldron JN, Gillison ML, Truong MT, et al. NRG-HN002: A Randomized Phase II Trial for Patients With p16-Positive, Non-Smoking-Associated, Locoregionally Advanced Oropharyngeal Cancer. *Int J Radiat Oncol Biol Physics* (2019) 105:684–5. doi: 10.1016/j.ijrobp.2019.08.038
17. NYU Langone Health. Adaptive Treatment De-escalation in Favorable Risk HPV-Positive Oropharyngeal Carcinoma. clinicaltrials.gov (2020). Available at: https://clinicaltrials.gov/ct2/show/NCT03215719 (Accessed September 7, 2020).
18. Sidney Kimmel Comprehensive Cancer Center at Johns Hopkins. A Phase II Study on Treatment De-Intensification in Favorable Squamous Cell Carcinoma of the Oropharynx. clinicaltrials.gov (2019). Available at: https://clinicaltrials.gov/ct2/show/NCT01088802 (Accessed September 7, 2020).
19. p16+ Oropharyngeal Cancer Radiation Optimization Trial Reducing Elective Treatment Volumes (PROTEcT) - Full Text View - ClinicalTrials.gov. Available at: https://clinicaltrials.gov/ct2/show/NCT04104945 (Accessed September 8, 2020).
20. Zhang M, Hong AM. The human papillomavirus confers radiosensitivity in oropharyngeal cancer cells by enhancing DNA double strand break. *Oncotarget* (2020) 11:1417–26. doi: 10.18632/oncotarget.27535
21. Gillison ML, Trotti AM, Harris J, Eisbruch A, Harari PM, Adelstein DJ, et al. Radiotherapy plus cetuximab or cisplatin in human papillomavirus-positive oropharyngeal cancer (NRG Oncology RTOG 1016): a randomised, multicentre, non-inferiority trial. *Lancet* (2019) 393:40–50. doi: 10.1016/S0140-6736(18)32779-X
22. Maddalo M, Borghetti P, Tomasini D, Corvò R, Bonomo P, Petrucci A, et al. Cetuximab and Radiation Therapy Versus Cisplatin and Radiation Therapy for Locally Advanced Head and Neck Cancer: Long-Term Survival and Toxicity Outcomes of a Randomized Phase 2 Trial. *Int J Radiat Oncol Biol Physics* (2020) 107:469–77. doi: 10.1016/j.ijrobp.2020.02.637
23. Memorial Sloan Kettering Cancer Center. A Prospective Single Arm Non-inferiority Trial of Major Radiation Dose De-Escalation Concurrent With Chemotherapy for Human Papilloma Virus Associated Oropharyngeal Carcinoma (Major De-escalation to 30Gy for Select Human Papillomavirus Associated Oropharyngeal Carcinoma). clinicaltrials.gov (2020). Available at: https://clinicaltrials.gov/ct2/show/NCT03323463 (Accessed September 7, 2020).
24. Horsman MR, Mortensen LS, Petersen JB, Busk M, Overgaard J. Imaging hypoxia to improve radiotherapy outcome. *Nat Rev Clin Oncol* (2012) 9:674–87. doi: 10.1038/nrclinonc.2012.171
25. Toustrup K, Sørensen BS, Lassen P, Wiuf C, Alsner J, Overgaard J. Gene expression classifier predicts for hypoxic modification of radiotherapy with nimorazole in squamous cell carcinomas of the head and neck. *Radiother Oncol* (2012) 102:122–9. doi: 10.1016/j.radonc.2011.09.010
26. Harris BHL, Barberis A, West CML, Buffa FM. Gene Expression Signatures as Biomarkers of Tumour Hypoxia. *Clin Oncol* (2015) 27:547–60. doi: 10.1016/j.clon.2015.07.004
27. Eschrich SA, Pramana J, Zhang H, Zhao H, Boulware D, Lee J-H, et al. A Gene Expression Model of Intrinsic Tumor Radiosensitivity: Prediction of Response and Prognosis After Chemoradiation. *Int J Radiat Oncol Biol Physics* (2009) 75:489–96. doi: 10.1016/j.ijrobp.2009.06.014
28. Scott JG, Berglund A, Schell MJ, Mihaylov I, Fulp WJ, Yue B, et al. A genome-based model for adjusting radiotherapy dose (GARD): a retrospective, cohort-based study. *Lancet Oncol* (2017) 18:202–11. doi: 10.1016/S1470-2045(16)30648-9
29. Bhardwaj N. Harnessing the immune system to treat cancer. *J Clin Invest* (2007) 117:1130–6. doi: 10.1172/JCI32136
30. Balermpas P, Michel Y, Wagenblast J, Seitz O, Weiss C, Rödel F, et al. Tumour-infiltrating lymphocytes predict response to definitive chemoradiotherapy in head and neck cancer. *Br J Cancer* (2014) 110:501–9. doi: 10.1038/bjc.2013.640
31. Ward MJ, Thirdborough SM, Mellows T, Riley C, Harris S, Suchak K, et al. Tumour-infiltrating lymphocytes predict for outcome in HPV-positive oropharyngeal cancer. *Br J Cancer* (2014) 110:489–500. doi: 10.1038/bjc.2013.639
32. Näsman A, Romanitan M, Nordfors C, Grün N, Johansson H, Hammarstedt L, et al. Tumor Infiltrating CD8+ and Foxp3+ Lymphocytes Correlate to Clinical Outcome and Human Papillomavirus (HPV) Status in Tonsillar Cancer. *PLoS One* (2012) 7:e38711. doi: 10.1371/journal.pone.0038711
33. Belgioia L, Desideri I, Errico A, Franzese C, Daidone A, Marino L, et al. Safety and efficacy of combined radiotherapy, immunotherapy and targeted agents in elderly patients: A literature review. *Crit Rev Oncol Hematol* (2019) 133:163–70. doi: 10.1016/j.critrevonc.2018.11.009
34. Wolf AM, Wolf D, Steurer M, Gastl G, Gunsilius E, Grubeck-Loebenstein B. Increase of Regulatory T Cells in the Peripheral Blood of Cancer Patients. *Clin Cancer Res* (2003) 9:606–12.
35. Lechner A, Schlößer H, Rothschild SI, Thelen M, Reuter S, Zentis P, et al. Characterization of tumor-associated T-lymphocyte subsets and immune checkpoint molecules in head and neck squamous cell carcinoma. *Oncotarget* (2017) 8:44418–33. doi: 10.18632/oncotarget.17901
36. Palucka K, Banchereau J. Cancer immunotherapy via dendritic cells. *Nat Rev Cancer* (2012) 12:265–77. doi: 10.1038/nrc3258
37. Grégoire V, Lefebvre J-L, Licitra L, Felip E. Squamous cell carcinoma of the head and neck: EHNS–ESMO–ESTRO Clinical Practice Guidelines for diagnosis, treatment and follow-up. *Ann Oncol* (2010) 21:v184–6. doi: 10.1093/annonc/mdq185
38. Chan ATC, Grégoire V, Lefebvre J-L, Licitra L, Hui EP, Leung SF, et al. Nasopharyngeal cancer: EHNS–ESMO–ESTRO Clinical Practice Guidelines for diagnosis, treatment and follow-up†. *Ann Oncol* (2012) 23:vii83–5. doi: 10.1093/annonc/mds266
39. Hohenstein NA, Chan JW, Wu SY, Tahir P, Yom SS. Diagnosis, Staging, Radiation Treatment Response Assessment, and Outcome Prognostication of Head and Neck Cancers Using PET Imaging: A Systematic Review. *PET Clinics* (2020) 15:65–75. doi: 10.1016/j.cpet.2019.08.010

40. Lee JR, Kim JS, Roh J-L, Lee JH, Baek JH, Cho K-J, et al. Detection of Occult Primary Tumors in Patients with Cervical Metastases of Unknown Primary Tumors: Comparison of 18F FDG PET/CT with Contrast-enhanced CT or CT/MR Imaging—Prospective Study. *Radiology* (2014) 274:764–71. doi: 10.1148/radiol.14141073
41. Differding S, Hanin F-X, Grégoire V. PET imaging biomarkers in head and neck cancer. *Eur J Nucl Med Mol Imaging* (2015) 42:613–22. doi: 10.1007/s00259-014-2972-7
42. Romesser PB, Lim R, Spratt DE, Setton J, Riaz N, Lok B, et al. The relative prognostic utility of standardized uptake value, gross tumor volume, and metabolic tumor volume in oropharyngeal cancer patients treated with platinum based concurrent chemoradiation with a pre-treatment [18F] fluorodeoxyglucose positron emission tomography scan. *Oral Oncol* (2014) 50:802–8. doi: 10.1016/j.oraloncology.2014.06.018
43. Schinagl DAX, Span PN, Oyen WJ, Kaanders JHAM. Can FDG PET predict radiation treatment outcome in head and neck cancer? Results of a prospective study. *Eur J Nucl Med Mol Imaging* (2011) 38:1449–58. doi: 10.1007/s00259-011-1789-x
44. Apostolova I, Steffen IG, Wedel F, Lougovski A, Marnitz S, Derlin T, et al. Asphericity of pretherapeutic tumour FDG uptake provides independent prognostic value in head-and-neck cancer. *Eur Radiol* (2014) 24:2077–87. doi: 10.1007/s00330-014-3269-8
45. Kim SY, Roh J-L, Kim MR, Kim JS, Choi S-H, Nam SY, et al. Use of 18F-FDG PET for Primary Treatment Strategy in Patients with Squamous Cell Carcinoma of the Oropharynx. *J Nucl Med* (2007) 48:752–7. doi: 10.2967/jnumed.107.039610
46. Boellaard R, Delgado-Bolton R, Oyen WJG, Giammarile F, Tatsch K, Eschner W, et al. FDG PET/CT: EANM procedure guidelines for tumour imaging: version 2.0. *Eur J Nucl Med Mol Imaging* (2015) 42:328–54. doi: 10.1007/s00259-014-2961-x
47. Castelli J, De Bari B, Depeursinge A, Simon A, Devillers A, Roman Jimenez G, et al. Overview of the predictive value of quantitative 18 FDG PET in head and neck cancer treated with chemoradiotherapy. *Crit Rev Oncol/Hematol* (2016) 108:40–51. doi: 10.1016/j.critrevonc.2016.10.009
48. Hanamoto A, Tatsumi M, Takenaka Y, Hamasaki T, Yasui T, Nakahara S, et al. Volumetric PET/CT parameters predict local response of head and neck squamous cell carcinoma to chemoradiotherapy. *Cancer Med* (2014) 3:1368–76. doi: 10.1002/cam4.295
49. Suzuki H, Tamaki T, Nishio M, Nakata Y, Hanai N, Nishikawa D, et al. Total lesion glycolysis on FDG-PET/CT before salvage surgery predicts survival in laryngeal or pharyngeal cancer. *Oncotarget* (2018) 9:19115–22. doi: 10.18632/oncotarget.24914
50. Bonomo P, Merlotti A, Olmetto E, Bianchi A, Desideri I, Bacigalupo A, et al. What is the prognostic impact of FDG PET in locally advanced head and neck squamous cell carcinoma treated with concomitant chemo-radiotherapy? A systematic review and meta-analysis. *Eur J Nucl Med Mol Imaging* (2018) 45:2122–38. doi: 10.1007/s00259-018-4065-5
51. Creff G, Devillers A, Depeursinge A, Palard-Novello X, Acosta O, Jegoux F, et al. Evaluation of the Prognostic Value of FDG PET/CT Parameters for Patients With Surgically Treated Head and Neck Cancer: A Systematic Review. *JAMA Otolaryngol Head Neck Surg* (2020) 146:471–9. doi: 10.1001/jamaoto.2020.0014
52. El Naqa I, Grigsby P, Apte A, Kidd E, Donnelly E, Khullar D, et al. Exploring feature-based approaches in PET images for predicting cancer treatment outcomes. *Pattern Recognit* (2009) 42:1162–71. doi: 10.1016/j.patcog.2008.08.011
53. Meyer H-J, Purz S, Sabri O, Surov A. Relationships between histogram analysis of ADC values and complex 18F-FDG-PET parameters in head and neck squamous cell carcinoma. *PLoS One* (2018) 13:e0202897. doi: 10.1371/journal.pone.0202897
54. Galgano SJ, Marshall RV, Middlebrooks EH, McConathy JE, Bhambhvani P. PET/MR Imaging in Head and Neck Cancer: Current Applications and Future Directions. *Magnetic Resonance Imaging Clinics North America* (2018) 26:167–78. doi: 10.1016/j.mric.2017.08.010
55. Surov A, Meyer HJ, Wienke A. Associations between apparent diffusion coefficient (ADC) and KI 67 in different tumors: a meta-analysis. Part 1: ADC mean. *Oncotarget* (2017) 8:75434–44. doi: 10.18632/oncotarget.20406
56. Cao Y, Aryal M, Li P, Lee C, Schipper M, Hawkins PG, et al. Predictive Values of MRI and PET Derived Quantitative Parameters for Patterns of Failure in Both p16+ and p16- High Risk Head and Neck Cancer. *Front Oncol* (2019) 9:1118. doi: 10.3389/fonc.2019.01118
57. Wong KH, Panek R, Welsh L, Mcquaid D, Dunlop A, Riddell A, et al. The Predictive Value of Early Assessment After 1 Cycle of Induction Chemotherapy with 18F-FDG PET/CT and Diffusion-Weighted MRI for Response to Radical Chemoradiotherapy in Head and Neck Squamous Cell Carcinoma. *J Nucl Med* (2016) 57:1843–50. doi: 10.2967/jnumed.116.174433
58. Vandecaveye V, Dirix P, De Keyzer F, de Beeck KO, Vander Poorten V, Roebben I, et al. Predictive value of diffusion-weighted magnetic resonance imaging during chemoradiotherapy for head and neck squamous cell carcinoma. *Eur Radiol* (2010) 20:1703–14. doi: 10.1007/s00330-010-1734-6
59. Matoba M, Tuji H, Shimode Y, Toyoda I, Kuginuki Y, Miwa K, et al. Fractional change in apparent diffusion coefficient as an imaging biomarker for predicting treatment response in head and neck cancer treated with chemoradiotherapy. *AJNR Am J Neuroradiol* (2014) 35:379–85. doi: 10.3174/ajnr.A3706
60. Mena E, Thippsandra S, Yanamadala A, Redy S, Pattanayak P, Subramaniam RM. Molecular Imaging and Precision Medicine in Head and Neck Cancer. *PET Clinics* (2017) 12:7–25. doi: 10.1016/j.cpet.2016.08.009
61. Floberg JM, DeWees TA, Chin R-I, Garsa AA, Dehdashti F, Nussenbaum B, et al. Pretreatment metabolic tumor volume as a prognostic factor in HPV-associated oropharyngeal cancer in the context of AJCC 8th edition staging. *Head Neck* (2018) 40:2280–7. doi: 10.1002/hed.25337
62. Yang Z, Shi Q, Zhang Y, Pan H, Yao Z, Hu S, et al. Pretreatment (18)F-FDG uptake heterogeneity can predict survival in patients with locally advanced nasopharyngeal carcinoma–a retrospective study. *Radiat Oncol* (2015) 10:4. doi: 10.1186/s13014-014-0268-5
63. Kimura M, Kato I, Ishibashi K, Shibata A, Nishiwaki S, Fukumura M, et al. The prognostic significance of intratumoral heterogeneity of 18F-FDG uptake in patients with oral cavity squamous cell carcinoma. *Eur J Radiol* (2019) 114:99–104. doi: 10.1016/j.ejrad.2019.03.004
64. Löck S, Linge A, Seidlitz A, Bandurska-Luque A, Nowak A, Gudziol V, et al. Repeat FMISO-PET imaging weakly correlates with hypoxia-associated gene expressions for locally advanced HNSCC treated by primary radiochemotherapy. *Radiother Oncol* (2019) 135:43–50. doi: 10.1016/j.radonc.2019.02.020
65. Choi W, Lee S, Park SH, Ryu JS, Oh SJ, Im KC, et al. Planning study for available dose of hypoxic tumor volume using fluorine-18-labeled fluoromisonidazole positron emission tomography for treatment of the head and neck cancer. *Radiother Oncol* (2010) 97:176–82. doi: 10.1016/j.radonc.2010.04.012
66. Donegani MI, Ferrarazzo G, Marra S, Miceli A, Raffa S, Bauckneht M, et al. Positron Emission Tomography-Based Response to Target and Immunotherapies in Oncology. *Medicina* (2020) 56:373. doi: 10.3390/medicina56080373
67. Bensch F, van der Veen EL, Lub-de Hooge MN, Jorritsma-Smit A, Boellaard R, Kok IC, et al. 89 Zr-atezolizumab imaging as a non-invasive approach to assess clinical response to PD-L1 blockade in cancer. *Nat Med* (2018) 24:1852–8. doi: 10.1038/s41591-018-0255-8
68. Niemeijer AN, Leung D, Huisman MC, Bahce I, Hoekstra OS, van Dongen GAMS, et al. Whole body PD-1 and PD-L1 positron emission tomography in patients with non-small-cell lung cancer. *Nat Commun* (2018) 9:4664. doi: 10.1038/s41467-018-07131-y

Conflict of Interest: The authors declare that the research was conducted in the absence of any commercial or financial relationships that could be construed as a potential conflict of interest.

frontiers in Oncology

ORIGINAL RESEARCH
published: 08 January 2021
doi: 10.3389/fonc.2020.590722

The Distribution of Pelvic Nodal Metastases in Prostate Cancer Reveals Potential to Advance and Personalize Pelvic Radiotherapy

*Irina Filimonova[1], Daniela Schmidt[2], Sina Mansoorian[1], Thomas Weissmann[1], Hadi Siavooshhaghighi[1], Alexander Cavallaro[3], Torsten Kuwert[2], Christoph Bert[1], Benjamin Frey[1], Luitpold Valentin Distel[1], Sebastian Lettmaier[1], Rainer Fietkau[1] and Florian Putz[1]**

[1] Department of Radiation Oncology, Universitätsklinikum Erlangen, Friedrich-Alexander-Universität Erlangen-Nürnberg, Erlangen, Germany, [2] Department of Nuclear Medicine, Universitätsklinikum Erlangen, Friedrich-Alexander-Universität Erlangen-Nürnberg, Erlangen, Germany, [3] Institute of Radiology, Universitätsklinikum Erlangen, Friedrich-Alexander-Universität Erlangen-Nürnberg, Erlangen, Germany

OPEN ACCESS

Edited by:
Francesco Cellini,
Catholic University of the Sacred Heart, Italy

Reviewed by:
Alessandro Nini,
Saarland University Hospital, Germany
Thomas Zilli,
Université de Genève, Switzerland

***Correspondence:**
Florian Putz
florian.putz@uk-erlangen.de

Specialty section:
This article was submitted to Radiation Oncology, a section of the journal Frontiers in Oncology

Received: 02 August 2020
Accepted: 16 November 2020
Published: 08 January 2021

Citation:
Filimonova I, Schmidt D, Mansoorian S, Weissmann T, Siavooshhaghighi H, Cavallaro A, Kuwert T, Bert C, Frey B, Distel LV, Lettmaier S, Fietkau R and Putz F (2021) The Distribution of Pelvic Nodal Metastases in Prostate Cancer Reveals Potential to Advance and Personalize Pelvic Radiotherapy. Front. Oncol. 10:590722. doi: 10.3389/fonc.2020.590722

Background: Traditional clinical target volume (CTV) definition for pelvic radiotherapy in prostate cancer consists of large volumes being treated with homogeneous doses without fully utilizing information on the probability of microscopic involvement to guide target volume design and prescription dose distribution.

Methods: We analyzed patterns of nodal involvement in 75 patients that received RT for pelvic and paraaortic lymph node metastases (LNs) from prostate cancer in regard to the new NRG-CTV recommendation. Non-rigid registration-based LN mapping and weighted three-dimensional kernel density estimation were used to visualize the average probability distribution for nodal metastases. As independent approach, the mean relative proportion of LNs observed for each level was determined manually and NRG and non-NRG levels were evaluated for frequency of involvement. Computer-automated distance measurements were used to compare LN distances in individual patients to the spatial proximity of nodal metastases at a cohort level.

Results: 34.7% of patients had pelvic LNs outside NRG-consensus, of which perirectal was most common (25.3% of all patients) followed by left common iliac nodes near the left psoas major (6.7%). A substantial portion of patients (13.3%) had nodes at the posterior edge of the NRG obturator level. Observer-independent mapping consistently visualized high-probability hotspots outside NRG-consensus in the perirectal and left common iliac regions. Affected nodes in individual patients occurred in highly significantly closer proximity than at cohort-level (mean distance, 6.6 cm vs. 8.7 cm, $p < 0.001$).

Conclusions: Based on this analysis, the common iliac level should extend to the left psoas major and obturator levels should extend posteriorly 5 mm beyond the obturator internus. Incomplete coverage by the NRG-consensus was mostly because of perirectal involvement. We introduce three-dimensional kernel density estimation after non-rigid

registration-based mapping for the analysis of recurrence data in radiotherapy. This technique provides an estimate of the underlying probability distribution of nodal involvement and may help in addressing institution- or subgroup-specific differences. Nodal metastases in individual patients occurred in highly significantly closer proximity than at a cohort-level, which supports that personalized target volumes could be reduced in size compared to a "one-size-fits-all" approach and is an important basis for further investigation into individualized field designs.

Keywords: prostate cancer, lymph node metastases, mapping, patterns of recurrence, pelvic radiotherapy

INTRODUCTION

The benefit of elective pelvic radiotherapy in prostate cancer has been repeatedly called into question. The well-known RTOG-9413 trial showed a significant benefit in progression-free survival for prophylactic whole-pelvic radiotherapy with prostate boost and neoadjuvant androgen deprivation therapy (ADT) compared to prostate-only radiotherapy with neoadjuvant ADT (1). However, there was no significant difference between whole-pelvic radiotherapy with neoadjuvant ADT and prostate-only radiotherapy with adjuvant ADT (2). The subsequently conducted randomized GETUG-01 trial also failed to unequivocally prove the superiority of pelvic irradiation in comparison to prostate-only radiotherapy (3). Suboptimal clinical target volume (CTV) definition that missed a substantial proportion of microscopically involved nodes is an important explanation for the lack of clear benefit of pelvic radiotherapy in past randomized trials in the primary setting. At the same time, there is a rising practice of treating nodal oligorecurrent prostate cancer with local ablative therapy (i.e., lymph node dissection or radiotherapy) (4, 5). In case of radiotherapy for oligorecurrent nodal disease, current target volume concepts include involved node stereotactic body radiotherapy (SBRT), involved site SBRT to involved field RT and elective whole pelvic RT without a clear standard having been established yet (4). To clarify the role of elective pelvic radiotherapy in nodal recurrence from prostate cancer, two important multicenter prospective phase II trials including patients with up to five pelvic nodal metastases have been initiated. The STORM trial assesses the benefit of whole pelvic radiotherapy in addition to 6 months of ADT and metastases-directed therapy (salvage lymph node dissection or SBRT) in a randomized fashion (6) and the OLIGOPELVIS-GETUG P07 investigated the impact of pelvic radiotherapy with a simultaneous integrated boost to PET positive nodes plus 6 months of ADT in a single arm phase II design (7).

So far, several attempts have been undertaken to improve CTV design for pelvic radiotherapy in prostate cancer. In 2009, the RTOG-GU radiation oncology specialists published a consensus recommendation on pelvic lymph node volumes for high-risk intact node-negative prostate cancer (8). Furthermore, a variety of studies have investigated nodal recurrence patterns providing valuable insights into the distribution of malignant lymph nodes in prostate cancer (9–14). Several of these studies showed a lack of coverage at important sites of pelvic nodal recurrence especially in the common iliac region above L5/S1 (12–14). For this very reason, the NRG recently put forth an updated international consensus atlas on pelvic nodal volumes for intact node negative as well as node positive and postoperative prostate cancer taking into account critical findings of the last ten years and raising the cranial border to the aortic bifurcation as the most important modification to the previous RTOG consensus recommendation (15). As of yet, patterns of nodal involvement have not been evaluated in regard to this new NRG CTV consensus recommendation.

Moreover, CTV definition for elective pelvic radiotherapy in prostate cancer still largely consists of large volumes being treated with homogeneous doses potentially without fully utilizing information on the probability of microscopic nodal involvement to guide target volume design and prescription dose distribution.

To visualize the average probability distribution for pelvic nodal metastases in prostate cancer, we introduce three-dimensional kernel density estimation after non-rigid registration-based mapping for the analysis of recurrence data in radiotherapy and evaluate results in regard to the newly proposed NRG CTV recommendation. As complementary method, we manually determine the frequency of binary involvement as well as the relative proportion of lymph node metastases for NRG and non-NRG levels and critically analyze coverage of lymph node metastases by the new NRG level definitions. Moreover, we explore preconditions for a potential individualization of target volumes by assessing if nodal metastases in individual patients are more spatially confined than metastases at a cohort-level and by comparing patterns of involvement in patients with and without upfront surgery.

MATERIALS AND METHODS

Ethics

Ethical review and approval was not required for this study on human participants in accordance with the local legislation and institutional requirements (BayKrG Art. 27). Written informed consent to participate in this study was provided by the patients.

Patient Population

Patients receiving local curative stereotactic radiotherapy of pelvic and/or paraaortic lymph node metastases from prostate cancer in the overall context of a curative or oligometastatic

treatment concept between January 2009 to September 2018 were included in this study.

Curative or oligometastatic treatment concept was defined as locally curative treatment (16) of all tumor sites with local curative doses being defined as exceeding an equivalent total dose in 2 Gy fractions (EQD2, alpha/beta = 2) of 50 Gy. Patients who had disseminated disease and those treated with palliative intent were excluded. The treatment indication for radiotherapy of each specific lymph node was based on an interdisciplinary review by experts in diagnostic radiology, nuclear medicine, urology, and radiation oncology after considering the clinical history and all available imaging in each patient case. In general lymph nodes were considered malignant that had significant tracer uptake, a short-axis diameter of ≥1 cm or were enlarging in the context of a rising PSA. Each lymph node included in this study was specifically treated with stereotactic radiotherapy in local ablative intent.

Seventy-five patients treated at our institution fulfilled the abovementioned criteria and were included. Of these 75 cases, 6 patients had paraaortic nodes exclusively and were excluded from analyses investigating the distribution of pelvic nodal metastases, for which the remaining 69 cases were used. Concerning overall tumor stage, 52.0% (39/75) had involved regional lymph nodes only, i.e., cN1 disease located exclusively below the bifurcation of the common iliac arteries. In addition, 36.0% (27/75) had cM1a disease, of which 74.1% (20/27) had paraaortic disease, 51.9% (14/27) had common iliac involvement, 11.1% (3/27) had inguinal metastases, and one patient had a singular mediastinal lymph node in addition to pelvic nodal metastases (3.7%). Only 12.0% (9/75) of patients had cM1b disease, because of additional limited bone metastases. Most patients received conventionally fractionated stereotactic radiotherapy in single doses of 1.8 Gy (97.3%, 73/75). Median EQD2$\alpha/\beta = 2$ to involved lymph nodes was 65.0 Gy (range, 53.0–68.4). Lymph node metastases had been identified in most cases by PSMA-PET/CT (42.7%, 32/75) or Choline-PET/CT (30.7%, 23/75), whereas PSMA-SPECT/CT (6.7%, 5/75) and contrast CT (20.0%, 15/75) had been used in the remaining cases (**Table 1**). Importantly, all nodal lesions included in this study went on to receive stereotactic radiotherapy underpinning that the overall clinical certainty in malignant involvement of each lymph node in this analysis was high. There was no significant difference in lymph node region involvement between patients diagnosed with Choline/PSMA-imaging vs. CT alone (**Supplemental Table 1**). In patients who received two series of radiotherapy (17.3%, 13/75), lymph node locations from both treatments were used for analysis.

TABLE 1 | Patients' characteristics.

Patient characteristic	Total cohort (N = 75)
D'Amico risk group at first diagnosis, n (%)	
High risk	60 (80.0%)
Intermediate risk	14 (18.7%)
Low risk	1 (1.3%)
Gleason score at first diagnosis, n (%)	
5	2 (2.7%)
6	6 (8.0%)
7	30 (40.0%)
8	18 (24.0%)
9	15 (20.0%)
10	4 (5.3%)
iPSA at first diagnosis, ng/ml	
Median (range)	12.7 (3.3–431)
T stage at first diagnosis, n (%)	
T1a	2 (2.7%)
T1b	2 (2.7%)
T1c	3 (4.0%)
T2a	4 (5.3%)
T2b	4 (5.3%)
T2c	21 (28.0%)
T3a	19 (25.3%)
T3b	18 (24.0%)
T4	2 (2.7%)
Primary treatment, n (%)	
Prior radical prostatectomy	55 (73.3%)
Prior antiandrogenic therapy	18 (24.0%)
Prior radiotherapy	10 (13.3%)
prostatic fossa only	8 (10.7%)
prostatic fossa and elective RT of pelvic lymph node levels	2 (2.7%)
R-Status (resected patients only)	
R0	34 (61.8%)
R1	11 (20.0%)
Unknown	10 (18.2%)
Number of initially resected nodes (resected patients only)	
Median (range)	16 (3–55)
Initial pN stage (resected patients only)	
pN0	42 (76.4%)
pN1	13 (23.6%)
Time interval between primary treatment and RT for nodal recurrence, years	
Median (IQR)	4.8 (1.4–9.1)
Age at start of RT for nodal metastases, years	
Median (range)	70 (43–85)
M stage at start of RT for nodal metastases, n (%)	
cM0	39 (52.0%)
cM1a	27 (36.0%)
cM1b	9 (12.0%)
Imaging technique for detection of nodal metastases, n (%)	
PSMA-PET/CT	32 (42.7%)
Choline-PET/CT	23 (30.7%)
PSMA-SPECT/CT (99mTc-MIP-1404)	5 (6.7%)
Contrast CT	15 (20.0%)

PSMA-PET, prostate specific membrane antigen positron emission tomography; CT, computed tomography; RT, Radiotherapy; IQR, Interquartile range.

Mapping Analysis

In all patients with pelvic nodal metastases (n = 69), verified GTV segmentations were exported from the treatment planning system (Iplan, Brainlab Feldkirchen Germany) and imported into 3DSlicer (v.4.10.2) (17). Geometric centers of every lymph node segmentation were calculated and in every patient, the Euclidean distance between all pelvic lymph node center coordinates was computed using the function cdist of the Python library SciPy (18) (401 distances in total) before mapping.

A patient CT dataset that best represented the average anatomy of the cohort served as common template and mapping target. Non-rigid registration was performed with the 3DSlicer SlicerRT Plastimatch B-spline deformable registration

module (17, 19, 20). After a first rigid registration step (subsampling 2 × 2 × 1, maximum of 100 iterations), a 3-stage B-Spline deformable registration (stage 1: subsampling 2,2,1, grid 25 mm, regularization 0.01, landmark penalty 0.005, maximum iterations 100, stage 2: subsampling 2,2,1, grid 10 mm, regularization 0.01, landmark penalty 0.005, maximum iterations 100, stage 3: subsampling 1,1,1, grid 2 mm, regularization 0.01, landmark penalty 0.005, maximum iterations 100) with Mean Squared Error as cost function empirically provided the best results and was used in all cases. The resulting deformation vector fields were used to map the lymph node center locations from each patient into the common template anatomy. The quality of the non-rigid registration and the resulting mapping locations were reviewed by a radiation oncologist and accepted in all cases. After mapping, the Euclidean distances between all 210 mapped pelvic lymph node center locations were computed using SciPy (18) (21,945 unique distances in total) and compared to the lymph node distances obtained *via* intra-patient measurements (401 distances).

Kernel density estimation was applied to convert the mapped lymph node center locations into an estimate of the underlying average probability distribution for metastatic lymph node involvement. Kernel density estimation is a widely used and accepted statistical technique to estimate the underlying probability density function from a limited set of observations (21). Three-dimensional kernel density estimation based on the mapped lymph node center locations was performed using the Python library KDEpy (22) (rectangular kernel, bandwidth 1.25 cm, p-norm 2), which results in a spherical representation of mapped nodal locations. To avoid bias toward patients with a high number of lymph nodes, weighting was applied, so that each patient contributed equally to the estimate irrespective of the number of positive nodes. To facilitate visualization the resulting spatial distribution was smoothened using the ITK recursive gaussian filter (sigma 2.5) (23). Three-dimensional renderings and a CT atlas of the average distribution of pelvic nodal metastases were created with 3DSlicer (17).

Expert-Based Assessment and Statistical Analysis

Independent from the mapping technique, the patterns of lymph node involvement were analyzed by expert-based assessment as a complementary method. For every patient dataset, a radiation oncologist evaluated the number of metastatic lymph nodes in all pelvic levels as well as in the paraaortic region. The results were reviewed by a second radiation oncologist and confirmed in all cases. For the definition of lymph node levels, the NRG consensus recommendations were used except for perirectal and inguinal regions, where the RTOG consensus for anorectal cancer was employed as these regions are not included in the NRG consensus for prostate cancer (15, 24).

The frequency of binary involvement was calculated for every region at a patient-level. Differences between patients with and without prior surgery were evaluated using Fisher's exact test with Bonferroni adjustment for multiple testing.

In addition to binary involvement, the varying extent of metastatic involvement was quantified for pelvic lymph node levels. To avoid bias toward patients with a high number of lymph nodes, calculations were not carried out at the level of individual lymph nodes. Instead, the relative contribution of each pelvic lymph node level to the total amount of positive nodes was first determined in each patient and this patient-level metric was subsequently evaluated for the whole population. The relative proportion of lymph nodes observed for each level was normalized by the level volume to identify possible hotspot regions. Analysis was limited to NRG and perirectal lymph node regions. Level volumes were determined *via* segmentation in the template dataset. In addition, we statistically tested if the mean relative proportion of lymph node metastases observed for each level was significantly different from the value theoretically expected by a homogeneous distribution of nodal metastases. A bootstrapped one-sample T-test and a bootstrapped 95% CI of the mean (BCa-based bootstrapping, 10,000 bootstrap samples) was used as normality could not be assumed. Time-to-event metrics were estimated using the Kaplan-Meier method and calculated from the start of stereotactic radiotherapy to local progression of irradiated nodal metastases (local control), local or distant progression (freedom from progression) or death from prostate cancer (disease-specific survival) with patients being censored at last follow-up or death, respectively. Median follow-up of this cohort was 58.9 months. Statistics were calculated using IBM SPSS 21. Graphs were created using GraphPad Prism 7 and SPSS.

RESULTS

In total, 92.0% (69/75) of patients had pelvic lymph node involvement, while in 8.0% (6/75), only paraaortic nodes were present. In addition, 24.0% of patients (18/75) suffered from both pelvic and paraaortic lymph node metastases. The median number of involved lymph node regions per patient was 2 (range, 1–9 and interquartile range, 1–2), differentiating left and right levels, respectively. Pelvic lymph node involvement was strictly unilateral in 76.8% of patients (53/69), whereas 23.2% (16/69) had metastatic pelvic nodes in left as well as right lymph node levels. The median number of malignant pelvic nodes in each patient was 2 (range, 1–11) and 36.2% (25/69) had only one metastatic pelvic lymph node. In patients with at least two positive pelvic nodes, the median of the maximum intra-patient lymph node distance was 7.8 cm, the 75th%ile was 11.0 cm and the 95th%ile was 17.0 cm. The external iliac lymph node region was most frequently involved (37.3%, 28/75) followed by the paraaortic (32.0%, 24/75), internal iliac and perirectal (25.3%, 19/75 each), common iliac (22.7%, 17/75), obturator (20.0%, 15/75), and the presacral region (10.7%, 8/75). The inguinal and prevesical lymph node region, not included in the new NRG CTV recommendation, each only harbored metastatic lymph nodes in 4.0% of patients (3/75). One of the most important additions in the new NRG consensus CTV is the inclusion of common iliac nodal levels above L5/S1 that had not been part of the previous RTOG-GU consensus volume. 18.7% of patients (14/75) had positive nodes in the common iliac region that were located above L5/S1 and thus outside the previous

RTOG-GU consensus recommendation. However, when carefully analyzing the location of left common iliac metastases, we observed that a fraction of these lymph nodes also was located outside the new NRG CTV recommendation in between the left boundary of the NRG consensus CTV and the medial surface of the left psoas major muscle (**Figure 1**). In addition, 50% (5/10) of patients with left common iliac metastases had nodal metastases outside the NRG consensus recommendation corresponding to 6.7% (5/75) of all patients, when using a standard margin of 7 mm around the vessels. The NRG consensus recommendation gives the option to increase this margin to 10 mm particularly anterior to vessels, if clinically indicated (15). However, even when using this more generous margin, still 20% (2/10) of patients with left common iliac involvement or 2.7% (2/75) of all patients had common iliac metastases outside the NRG consensus CTV volume, respectively. Importantly, all common iliac nodal metastases would have been covered if the left CTV boundary had extended to the medial surface of the left psoas major muscle (**Figure 1**). An additional important observation was made regarding obturator nodes. Despite no obturator node was indisputably located outside the NRG consensus CTV, 10 patients had obturator metastases located right near the posterior edge of the NRG consensus CTV corresponding to 66.7% (10/15) of patients with obturator level involvement and 13.3% (10/75) of all patients (**Figure 2**). In total, excluding paraaortic involvement, 34.7% of patients (26/75) had metastatic lymph nodes not included in the new NRG consensus, of which perirectal was the most frequent (25.3%, 19/75 patients) (**Table 2**).

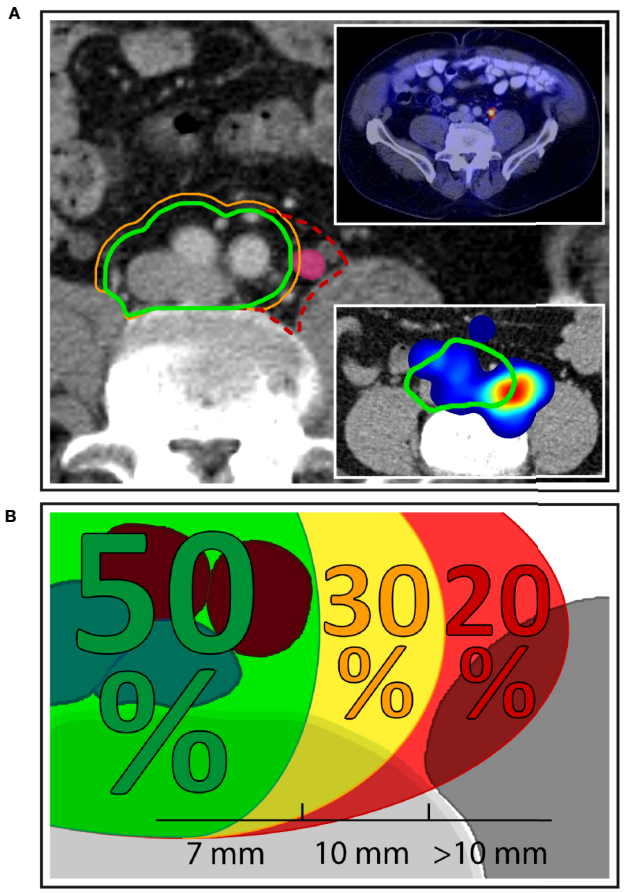

FIGURE 1 | Left common iliac nodal metastases outside NRG consensus CTV. **(A)** Exemplary patient case with a left common iliac nodal metastasis outside the NRG CTV recommendation using margin options of 7 mm (green contour) and 10 mm (orange contour), respectively. Dashed red contour: proposed extension of the CTV to the medial surface of the left major psoas muscle. Top right inset: PSMA-PET/CT of the same patient demonstrating PSMA uptake. Bottom right inset: Corresponding anatomic location in the independent mapping analysis showing a high-probability hotspot that extends beyond the left boundary of the NRG CTV recommendation. **(B)** Overall, 50.0% of patients with left common iliac nodal involvement had all common iliac metastases covered using a margin of 7 mm around the vessels. A 10 mm margin encompassed all nodal metastases in an additional 30.0% of patients, while 20.0% of patients with left common iliac metastases had lymph node metastases that extended even beyond the 10-mm margin.

Interestingly, right external iliac involvement was significantly reduced in patients with previous prostatectomy and pelvic lymph node dissection compared to patients without prior surgery (10.9% vs. 45.0%, p = 0.002, p adjusted for multiple testing 0.022, **Table 3**). All nodal metastases included in this study received stereotactic radiotherapy in local ablative intent. Local control of nodal metastases following stereotactic radiotherapy was 90.7% at 5 years. Disease-specific survival of this cohort was 86.6% and freedom from local and distant progression was 44.5% at 5 years post radiotherapy (**Figure 3**).

Lymph Node Mapping and Kernel Density Estimation

The geometric centers of pelvic nodes from all patients were mapped into a common template CT using an observer-independent non-rigid registration-based mapping technique (**Figure 4**). After mapping, distances between all lymph nodes from all patients were calculated (210 lymph nodes, 21945 unique distances) and compared to the lymph node distances obtained *via* intra-patient measurements (401 distances). The mean distance between involved pelvic lymph nodes was highly significantly smaller in individual patients than at a cohort-level (6.6 cm vs. 8.7 cm, $p < 0.001$), i.e., metastatic nodes were significantly closer. This was equally true, if distances between lymph nodes in individual patients were measured after being mapped into the common anatomy of the template dataset (6.1 cm vs. 8.7 cm, $p < 0.001$) showing that the increase in mean lymph node distance at a cohort-level was not artificially introduced by the mapping procedure.

For the mapping analysis, weighted three-dimensional kernel density estimation was used to assess the underlying average probability distribution of pelvic lymph node metastases. The CT atlas and three-dimensional renderings illustrate the estimated three-dimensional probability density function of pelvic nodal metastases in ‰ per cm^3 for the whole cohort in a common reference CT with weighting being applied so that each patient contributes equally to the estimate irrespective of the amount of positive nodes. Hotspots of lymph node involvement outside NRG consensus are visualized especially in the perirectal region (**Figures 5** and **6**, **Supplemental Video S1**). Consistent with the manual

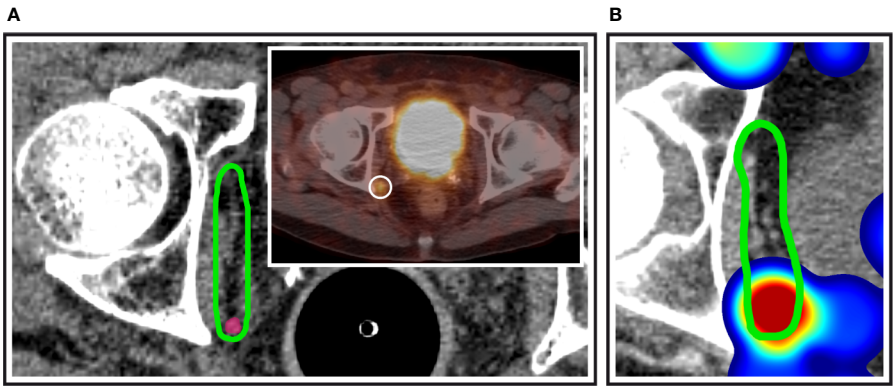

FIGURE 2 | Obturator nodes at the posterior edge of the NRG consensus CTV. **(A)** Exemplary patient case with a PSMA-avid nodal metastasis (inset) right at the posterior edge of the NRG obturator level. **(B)** Corresponding anatomic location in the independent mapping analysis showing a high-probability hotspot near the posterior edge of the NRG CTV recommendation.

TABLE 2A | Frequency of lymph node involvement.

Lymph node region n (%)	Total cohort (N = 75)
External iliac	28 (37.3%)
Paraaortic	**24 (32.0%)**
Internal iliac	19 (25.3%)
Perirectal	**19 (25.3%)**
Common iliac	17 (22.7%)
Left common iliac outside NRG (7/10 mm)	**5 (6.7%)/2 (2.7%)**
Obturator	15 (20.0%)
Presacral	8 (10.7%)
Inguinal	**3 (4.0%)**
Prevesical	**3 (4.0%)**

Regions indicated in bold are not part of the NRG consensus recommendation.

TABLE 2B | Frequency of lymph node involvement with discrimination of left and right lymph node groups.

Lymph node region n (%)	Left	Right
External iliac	19 (25.3%)	15 (20.0%)
Paraaortic	20 (26.7%)	19 (25.3%)
Internal iliac	15 (20.0%)	7 (9.3%)
Perirectal	11 (14.7%)	8 (10.7%)
Common iliac	10 (13.3%)	11 (14.7%)
Obturator	5 (6.7%)	10 (13.3%)
Inguinal	1 (1.3%)	3 (4.0%)
Prevesical	2 (2.7%)	1 (1.3%)

assessment, the independent mapping analysis also revealed a high-probability hotspot extending beyond the NRG consensus volume in the left common iliac region and high risk for malignant nodes near the posterior edge of the NRG obturator level (**Figures 1** and **2**).

Expert-Based Assessment

As an independent approach to the mapping technique, the relative distribution of lymph node metastases was determined by a radiation oncologist for every patient.

TABLE 3 | Differences in lymph node region involvement in patients with and without prior prostatectomy with pelvic lymph node dissection.

Lymph Node Region	Resection part of primary treatment		
	No	Yes	P
Common iliac, left	5.0%	16.4%	0.272
Common iliac, right	25.0%	10.9%	0.150
Internal iliac, left	25.0%	18.2%	0.526
Internal iliac, right	10.0%	9.1%	1.000
External iliac, left	35.0%	21.8%	0.368
External iliac, right	**45.0%**	**10.9%**	**0.002**
Obturator, left	5.0%	7.3%	1.000
Obturator, right	10.0%	14.5%	1.000
Perirectal, left	10.0%	16.4%	0.717
Perirectal, right	10.0%	10.9%	1.000
Presacral	0.0%	14.5%	0.100

P, Fishers exact test.
The observed difference in right external iliac involvement remained significant after Bonferroni correction for multiple testing (p = 0.022).

To avoid bias toward patients with many positive nodes, the relative contribution of a lymph node level to the total amount of positive nodes was first determined in every individual patient and this patient-level metric was subsequently evaluated for the whole population.

The mean proportion of metastatic lymph nodes per level volume was highest for the obturator levels (3.58‰/cm³), followed by external iliac (2.34‰/cm³), perirectal (1.47‰/cm³), internal (1.43‰/cm³), and common iliac (1.33‰/cm³). The proportion of involved lymph nodes for the presacral level was lowest (mean 1.01‰/cm³), significantly lower than expected by a homogeneous spatial distribution of lymph node metastases ($p = 0.047$). When differentiating by side, the right obturator (4.01‰/cm³), left obturator (3.14‰/cm³), left external iliac (2.60‰/cm³), and left internal iliac (2.08‰/cm³) levels showed the highest mean relative lymph node involvement per cm³ (**Figure 7**).

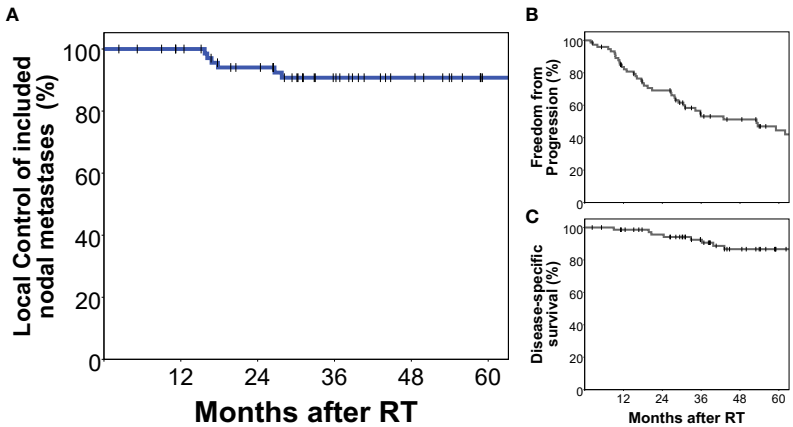

FIGURE 3 | Treatment outcomes of the analyzed cohort. All nodal metastases included in this analysis had been specifically treated with stereotactic radiotherapy in local ablative intent. Local control of included nodal metastases was 90.7% at 5 years **(A)**. Freedom from local and distant progression **(B)** as well as prostate cancer-specific survival **(C)** of this cohort are also shown.

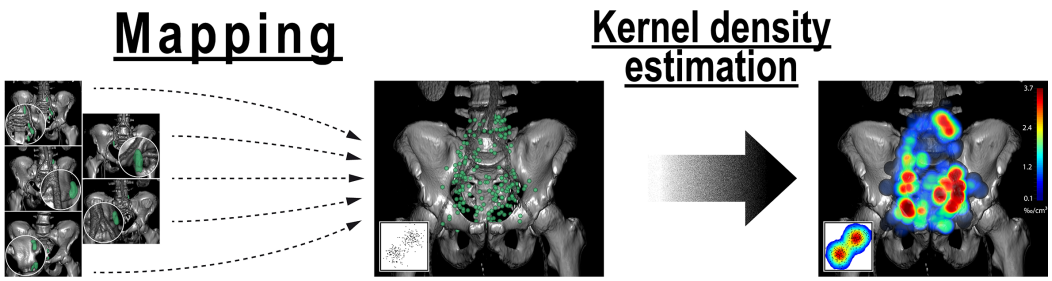

FIGURE 4 | Analysis of the average probability distribution for nodal metastases by observer-independent mapping and three-dimensional kernel density estimation. First, lymph node center locations from all patients were mapped into a common template CT (left). Weighted three-dimensional kernel density estimation was then applied to convert the mapped lymph node center locations into an estimate of the underlying average probability distribution for lymph node metastases (right). Weighting was applied so that each patient case contributed equally to the estimate irrespective of the number of positive nodes. Kernel density estimation is a widely used and accepted statistical technique to estimate the underlying probability density function from a limited set of observations that is most commonly applied for one- and two-dimensional data (inset). Note: Kernel density estimation helps in visually identifying regions with high density of nodal involvement without the need to restrict the analysis to predetermined level boundaries.

DISCUSSION

Renewed interest in the distribution of pelvic nodal metastases has been sparked by recent evidence that pelvic nodal recurrence represents an important site of treatment failure in prostate cancer (25). Suboptimal CTV design is an important explanation for the lack of clear benefit of pelvic radiotherapy in past randomized trials for intact prostate cancer (2, 3). On the other hand, there is rising use of local ablative approaches in the treatment of nodal oligorecurrent prostate cancer with radiotherapy target volumes varying from involved-node SBRT over involved site and involved field approaches to elective pelvic radiotherapy (4, 5).

A variety of studies have investigated patterns of recurrence after radical prostatectomy and/or radiotherapy, some of them in relation to the previous RTOG-GU consensus recommendation, and have provided important information for the optimization of radiotherapy field design and the extent of surgical dissection (9–14). Because of this new evidence, an updated NRG international consensus atlas on pelvic lymph node volumes for pelvic radiotherapy in prostate cancer was recently published taking into account critical findings of the last ten years of published research. To obtain a new consensus for CTV design in pelvic radiotherapy 18 international experts had contoured the nodal CTV for an intact node-negative, intact node-positive as well as a postoperative prostate cancer case after a systematic literature review. Regions of controversy were subsequently identified by evaluating nodal CTVs from all experts and a consensus was reached. The inclusion of all common iliac nodes up to the aortic bifurcation in the new NRG CTV certainly is the most significant modification over the previous RTOG-GU recommendation (15). To the best of our knowledge, the present study is the first to analyze the coverage of pelvic nodal metastases according to the new NRG consensus recommendation.

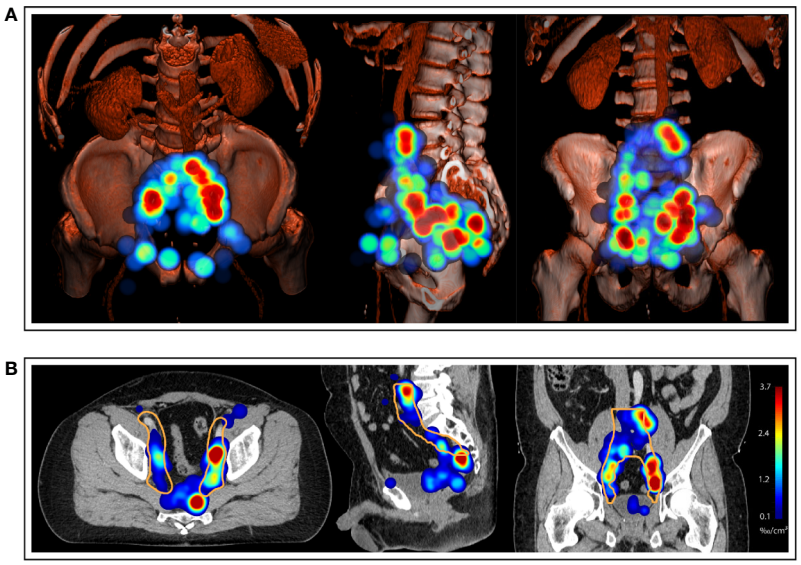

FIGURE 5 | **(A)** Three-dimensional renderings visualize the estimated three-dimensional probability density function of pelvic nodal metastases (maximum intensity projection) for the whole cohort in a common reference CT (composite with shading). **(B)** CT atlas reconstructions (Solid orange contour: Clinical target volume defined according to the recent NRG recommendation). Left column: superior/axial view, middle column: left-side view/sagittal reconstruction, right column: anterior view/coronal reconstruction. Weighting was applied so that each patient case contributed equally to the estimate irrespective of the number of positive nodes.

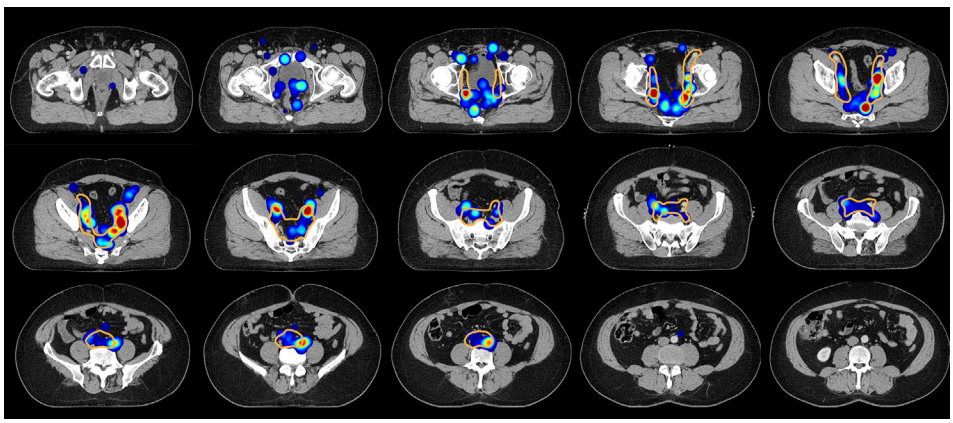

FIGURE 6 | Axial slices of the created CT atlas visualize the estimated three-dimensional probability density function of pelvic nodal metastases for the whole cohort in a common reference CT. Weighting was applied so that each patient case contributed equally to the estimate irrespective of the amount of positive nodes. Slice spacing is 15 mm. Solid orange contour: Clinical target volume defined according to the recent NRG recommendation.

We found that 34.7% of patients harbored metastatic pelvic nodes outside the recently published NRG consensus recommendation for prostate cancer. Perirectal lymph nodes were most frequent (25.3% of all patients) followed by left common iliac nodes in between the left boundary of the NRG consensus CTV and the medial surface of the left psoas major muscle (6.7%), whereas inguinal and prevesical involvement only occurred in 4.0% of patients each. Recommendations for an expansion of the previous RTOG-GU consensus CTV definition had been derived from multiple studies. Spratt et al. found increasing coverage when raising the cranial CTV border with a coverage of 33.3% at S1/S2, 41.7% at L5/S1, and 93.4% at L4/L5 (13). In a large recent study of 82 patients, De Bruycker et al. obtained compatible findings and found that by raising the cranial field border from L5/S1 to the aortic bifurcation an additional 22.8% (36/158) out of all pelvic and paraaortic lesions analyzed in the study could be covered (14). The cranial border also was a crucial factor in our analysis to completely cover all common iliac metastases. These results are very important for the interpretation of past randomized trials

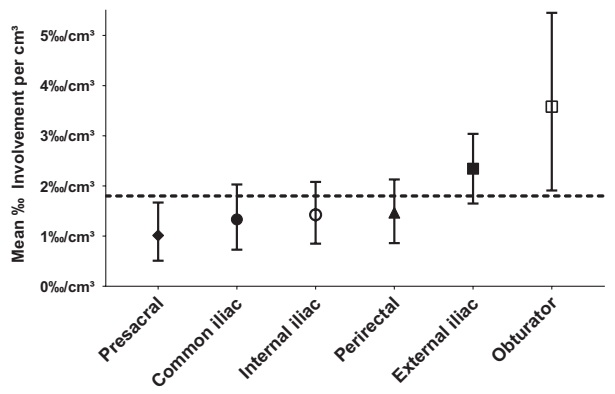

FIGURE 7 | Mean relative proportion of lymph node metastases per cm³ in typical pelvic lymph node levels (n = 66). Error bars indicate 95% CI obtained by BCa-based bootstrapping using 10,000 bootstrap samples. The dashed reference line indicates the mean relative proportion expected by a homogeneous spatial distribution of lymph node metastases.

investigating the benefit of pelvic radiotherapy: The partially positive RTOG 9413 used L5/S1 as cranial border (1), whereas the negative GETUG-01 study used S1/S2 (3). Considering the results from the aforementioned trials and those from our own investigation, it seems evident why it was not possible to achieve a positive effect with a S1/S2 cranial border setting (3).

As an elevation of the cranial field border up to the aortic bifurcation is the most significant addition in the new NRG consensus CTV, it was a particularly important finding that left common iliac nodes were not completely covered by the new NRG CTV in a substantial portion of patients in the present study. In addition, 50.0% (5/10) of patients with left common iliac involvement had metastases in between the left boundary of the NRG consensus CTV and the medial surface of the psoas major muscle using the recommended standard margin of 7 mm around the vessels. Based on this observation, we recommend completely covering the space from the common iliac vessels to the left psoas major muscle when delineating common iliac nodal levels using the medial surface of the psoas major as left-side boundary.

An additional noteworthy observation was made in regard to obturator nodes. Despite none of them was undoubtedly outside the NRG consensus CTV, the majority of patients (66.7%, 10/15) with obturator involvement had lymph node metastases right at the posterior boundary of the NRG obturator level, i.e., near the posterior edge of the obturator internus muscle and were endangered of being missed by a restricted application of the NRG contouring guidelines.

However, by far the most common reason for incomplete NRG coverage of nodal metastases was perirectal involvement. Consistent with our finding that the perirectal level was the most frequently involved region outside the NRG consensus, the largest share of lesions missed by the previous RTOG-GU CTV recommendation (10/20) was also located in the perirectal region in a PSMA-PET–based patterns of failure analysis by Schiller and coauthors (12). While NRG GU experts thoroughly discussed the inclusion of perirectal levels especially for T4 tumors, the majority of experts had opted against routinely including these lymph nodes in view of the corresponding increase in treatment volume (15). As the perirectal region has been a frequent site of nodal recurrence in multiple studies (12, 14, 26), it would be highly beneficial to identify reliable predictive factors for perirectal involvement to include perirectal nodes in high-risk patients but to avoid unnecessary toxicity in others.

It is important to note that care has to be taken when interpreting the results from patterns of involvement studies. First, the diagnostic methods used for the detection of nodal metastases may have an important influence, as the major role of PSMA-PET imaging on radiotherapy treatment planning has already been shown (12, 27). In the cohort by Spratt et al., lymph node metastases were detected in 92.3% *via* CT/MRI imaging and in only 7.7% *via* PET-CT (13), which could explain differences in lymph node involvement. In our cohort, PSMA-PET/CT and Choline-PET/CT were the most common imaging methods for detecting lymph node metastases (73.3%, 55/75), but some were detected by PSMA-SPECT/CT or contrast CT alone. However, the fact that all lymph node metastases were specifically treated with stereotactic radiotherapy after interdisciplinary review underpins that the overall clinical certainty of the malignant involvement of included nodes was high in our series.

The definition of lymphatic regions in patterns of recurrence studies generally is governed by the overall study setting, be it centered on surgical, diagnostic or radiotherapeutic objectives. In the atlas of patterns of spread of prostate cancer, Barbosa et al. describe a diagnostic view of lymph node regions (9). Then again, Spratt et al. analyzed patterns of nodal failure according to Morón et al. using 34 abdomino-pelvic stations (13, 28). These circumstances can lead to possible misinterpretation of study results. In the present analysis, NRG consensus lymph node level definitions were used wherever possible to allow for optimal interpretation of results in regard to radiotherapy field design (15). For the same reason, if metastatic nodal involvement extended beyond the recent NRG consensus, e.g., to inguinal and perirectal regions, we chose RTOG compartment definitions from other cancer types. Concerning NRG consensus levels, the external and internal iliac levels were most commonly involved in our series (37.3% and 25.3% of patients, respectively), whereas the presacral region was only involved in 10.7% of patients.

Furthermore, previous treatments and therefore patient selection might also determine patterns of involvement. Comparing our results to the literature, our observed distribution of pelvic nodal metastases has evident similarities with studies consisting mostly of patients with upfront surgery. Thus, our findings show similarities to the study of Calais et al., which included patients with biochemical recurrence after prostatectomy, as well as to the analysis of McClinton et al., in which the majority of patients had prior resection (64.8% in the study by McClinton et al., 73.3% in our series) (10, 11). In the study from Calais et al., PSMA-PET/CT mapping was performed in a cohort of 270 patients with biochemical recurrence after radical prostatectomy and a PSA < 1.0 ng/ml. In the 83 patients with

positive nodes on PSMA-PET/CT, the most frequent site of nodal recurrence was external iliac (45.8%), followed by internal iliac (32.5%) and obturator level nodes (22.9%) (10). Our finding of significantly different nodal involvement patterns in patients with and without upfront surgery generally supports this notion that prior surgery could influence the distribution of lymph node recurrences. Whereas our observation of reduced right external iliac involvement in patients with prior prostatectomy and pelvic lymph node dissection must not be generalized, it could reflect a preferential dissection of these lymph node levels by referring surgeons in the present series. Interestingly, Meijer et al. had observed a high occurrence of aberrant nodal metastases, especially perirectal involvement, with magnetic resonance lymphography following radical prostatectomy also affirming the hypothesis that prior surgery may influence nodal recurrence patterns. Interestingly, 43% of patients in the study by Meijer et al. harbored perirectal nodes followed by 36% with metastatic lymph nodes in the left common and left internal iliac region each (29).

Finally, De Bruycker et al. analyzed nodal recurrence patterns in patients with biochemical failure and ≤ 5 nodal metastases on choline-PET/CT with most patients (82.9%) having initially been treated with radical prostatectomy or a combination of radical prostatectomy and postoperative radiation (14). Most nodal metastases in the work by De Bruycker et al. were located in the external iliac region (28.5%), followed by common iliac (24.1%) and paraaortic (13.3%) metastases, whereas only 6.3% of positive nodes were located in the perirectal area (14).

It is important to note, that De Bruycker et al. analyzed coverage of nodal metastases not only for radiotherapeutic but also for surgical approaches. The results show that the superextended salvage lymph node dissection included more lesions compared to the new extended, limited or standard lymph node dissection but had a comparable coverage to elective pelvic radiotherapy using the top of L4 as superior border. However, lymph node metastases in at least 31% of patients, especially all perirectal lesions, would still have been missed by all the surgical dissection templates as well as the extended radiotherapy field design (14).

Urological series that analyze the topographic distribution of positive lymph nodes in primary lymphadenectomy are also an important source of evidence for nodal dissemination patterns especially for patients presenting with intact prostate cancer. In 74 patients with primary node negative prostate cancer, Joniau et al. analyzed the patterns of lymph node involvement obtained *via* a sentinel node procedure and superextended lymphadenectomy. Most, histologically proven, lymph node metastases were located in the internal iliac region (35%), followed by the external iliac (26%) and obturator region (25%) (30).

Optimal target volume design is also a pressing question in the context of nodal oligorecurrent prostate cancer, as there is a rising practice of treating nodal oligorecurrent prostate cancer with salvage lymph node dissection and/or radiotherapy (5). In retrospective case series and phase II trials, these metastasis-directed therapies have shown promising progression-free survival with limited toxicity (5, 28). In case of radiotherapy for oligorecurrent nodal disease, current target volume concepts vary from involved node SBRT, involved site SBRT to involved field RT and elective whole pelvic RT without a clear standard having been established yet (4). As most patients treated with SBRT for nodal recurrence alone, however, relapse in adjacent lymph node regions within 24 months there is a good rationale for the exploration of more generous radiotherapy target volume concepts (6). In a systematic review of the mostly retrospective literature, Achard et al. found improved progression-free survival with elective nodal radiotherapy compared to involved-node SBRT in nodal oligorecurrent prostate cancer (4). Following the urgent need for better evidence, two important prospective trials have been initiated to evaluate the oncologic efficacy and toxicity of pelvic radiotherapy in nodal oligorecurrent prostate cancer. De Bruycker et al. are assessing the benefit of whole pelvic radiotherapy in addition to ADT plus salvage lymph node dissection or SBRT for pelvic nodal oligorecurrence (≤ 5 nodes) from prostate cancer in the randomized phase II STORM trial (6). The second trial, the OLIGOPELVIS-GETUG P07 investigated the impact of salvage pelvic radiation therapy plus ADT with a simultaneous integrated boost to a maximum of 5 pelvic metastases in a single-arm phase II design (7).

Notably, both prospective oligorecurrence trials employ the RTOG-GU consensus CTV but with an elevated cranial field border (L4/L5 in the STORM and aortic bifurcation in the OLIGOPELVIS-GETUG P07 trial) (6, 7). The main concern with an elevated cranial field border is of course a higher toxicity rate. However, the already completed OLIGOPELVIS-GETUG P07 trial was able to show a limited toxicity rate (10% urinary and 2% intestinal ≥ grade 2 toxicity at 2 years). Most importantly demonstrating a 2-year progression-free survival of 77.6% the single-arm phase II OLIGOPELVIS-GETUG P07 trial also met its prespecified primary endpoint providing a clear efficacy signal for whole pelvic radiotherapy in the oligorecurrent setting (28). The results of the randomized STORM study are expected for 2024 and are eagerly awaited (6). We performed distance measurements between metastatic pelvic lymph nodes in individual patients and found a median maximum intra-patient lymph node distance of 7.8 cm with a 75th%ile of 11.0 cm and a 95th%ile of 17.0 cm suggesting the need for larger field sizes to adequately cover microscopic nodal involvement in a majority of patients.

As microscopically involved lymph nodes cannot be detected *via* imaging, they only exist as probabilities at the time of pelvic radiotherapy. Aside from analyzing the frequency of binary involvement for NRG lymph node regions and beyond, an important aim of this study was to provide an estimate for these probabilities to gain further insights into how to optimize radiotherapy field design and prescription dose distribution.

We did this using two independent but complementary methods. First, we used lymph node mapping based on an observer-independent non-rigid registration technique and kernel density estimation to create a voxel-level visualization of the average distribution of nodal metastases. While mapping studies in prostate cancer have employed observer-dependent mapping or even rigid registration techniques (10, 12, 13), this is the first study to use an observer-independent non-rigid registration-based mapping technique for the analysis of nodal involvement in

prostate cancer. Three-dimensional kernel density estimation was employed to convert the mapped lymph node locations into an estimate of the underlying three-dimensional probability density function for metastatic lymph node involvement. Weighting was applied so that each patient contributed equally to the estimate irrespective of the number of positive nodes. To the best of our knowledge, this is the first study to introduce three-dimensional kernel density estimation for the analysis of recurrence data. Kernel density estimation is a widely used and accepted statistical technique to estimate the underlying probability density function from a limited set of observations (21). This non-parametric method is widely used in the one-dimensional and two-dimensional setting, e.g., to analyze geographic patterns of disease incidence from a limited number of observations in two dimensional maps (31, 32). By improving visualization and analysis of recurrence data, kernel density estimation could ultimately aid in deriving meaningful insights for optimal CTV design. As these methods can be easily automated, software solutions could be developed that allow fast and convenient patterns of failure analyses in routine clinical practice. This could be especially important, as the average distribution of nodal involvement may vary for different radiotherapy treatment centers, because of local surgical preferences, among others.

The developed mapping and kernel density estimation technique also provided valuable insights in the present study by visualizing the average probability of nodal involvement in reference to the consensus-based NRG CTV recommendation and helped identify regions of suboptimal coverage in the common iliac and obturator region.

Frequently, patterns of recurrence analyses are performed at the level of individual lymph nodes without correction, which might introduce a bias toward the patterns of metastatic spread of patients with many metastatic nodes (11, 12, 14, 33). In our series, lymph node metastases in individual patients occurred in more spatially confined clusters than at a cohort-level, which suggests that the probability distribution of nodal metastases might vary between individual patients. Consequently, the overall pattern obtained when assessing individual lesions without correction will be biased toward patients with an above-average amount of metastatic nodes and misrepresents the pattern for an average patient case. In addition, tumors with a large amount of lymph node metastases may have an unusual underlying biology, which might also affect the pattern of lymph node involvement. In the present analysis, we assessed the spatially varying quantitative extent of metastatic involvement in such a way that every patient case was weighted equally irrespective of the number of involved nodes.

As an independent approach to the observer-independent mapping analysis, the varying quantitative extent of metastatic involvement was quantified manually for all pelvic lymph node levels. We found that the proportion of metastatic lymph nodes was highest for the obturator and external iliac levels (mean of 3.58‰/cm^3 and 2.34‰/cm^3, respectively) followed by the perirectal level (mean 1.47‰/cm^3), whereas the mean proportion of lymph node metastases was lowest for the presacral level (1.01‰/cm^3), significantly lower than expected by a homogeneous distribution of nodal metastases. Our findings collectively support the notion that lymph node metastases are not distributed uniformly across pelvic levels but that the average probability of nodal involvement varies regionally. Based on our findings, obturator and external iliac levels could serve as candidate levels for dose escalation, while the presacral level could be considered for sparing. The perirectal level also was an important region of involvement in this study suggesting that inclusion of perirectal lymph nodes could be beneficial for a subgroup of patients.

These are important findings that warrant confirmation as a validated description of the regionally varying average probability of microscopic lymph node involvement could not only inform the setting of boundaries of radiotherapy target volumes but could even be translated into a non-uniform prescription dose distribution to allow for local dose-escalation and -sparing.

Moreover, the unprecedented finding that nodal metastases were highly significantly more spatially confined in individual patients than at a cohort-level indicates that pelvic radiotherapy in prostate cancer could be substantially improved, if it could be individualized on an individual patient basis compared to a "one-size-fits-all" approach. While advances in machine learning could enable highly-individualized target volumes in the future, it is equally important to compare patterns of involvement for major patient subgroups and to assess institution-specific differences in the location of high-risk regions. Observer-independent mapping and three-dimensional kernel density estimation could be helpful tools in these investigations toward more personalized radiotherapy field designs.

Limitations

Limitations of this study are the sample size that precluded some subgroup analyses. While the retrospective nature of this study increased heterogeneity in included patients, strict prospective patient selection could also have introduced biases and misrepresented nodal involvement for an average patient case in clinical practice. The majority but not all included patients were diagnosed with PSMA- or Choline-PET/CT. However, the fact that all nodes did receive radiotherapy underpins that the clinical certainty in the malignant involvement of included nodes was high.

CONCLUSION

This is the first study to investigate patterns of nodal involvement in regard to the new NRG CTV consensus recommendation. 34.7% of patients had pelvic nodal involvement outside NRG CTV consensus in this study, of which perirectal was the most common. An important observation was that the NRG consensus CTV missed left common iliac nodes in a considerable fraction of patients that could easily be covered by extending the CTV to the medial surface of the left major psoas muscle. In addition, as obturator nodes in many patients were located near the posterior edge of the NRG consensus CTV, we recommend to consider extending the obturator level 5 mm beyond the posterior edge of the obturator internus muscle.

Furthermore, we introduced three-dimensional kernel density estimation after non-rigid registration-based mapping for the analysis of recurrence data in radiotherapy. This technique provides an estimate of the underlying probability distribution of nodal involvement, can be fully automated and thus may help in addressing institution- or subgroup-specific differences. In this study, the developed mapping technique provided valuable insights for analysis of the new NRG consensus CTV. We propose considering analyses that weight every patient case equally in patterns of recurrence studies, as unadjusted analyses at the level of individual lesions could introduce bias toward patients with many metastases. In our study, the relative proportion of involved nodes was highest for the obturator and external iliac levels while it was lowest for the presacral level making these candidate regions for dose-escalation and sparing, respectively. Prior surgery and local surgical preferences could influence the distribution of nodal recurrences and warrant further study. Nodal metastases in individual patients occurred in highly significantly closer proximity than at a cohort-level, which supports that personalized target volumes could be reduced in size compared to a "one-size-fits-all" approach and is an important basis for further investigation into individualized field designs.

DATA AVAILABILITY STATEMENT

The raw data supporting the conclusions of this article will be made available by the authors, without undue reservation.

ETHICS STATEMENT

Ethical review and approval was not required for the study on human participants in accordance with the local legislation and institutional requirements. The patients/participants provided their written informed consent to participate in this study.

AUTHOR CONTRIBUTIONS

IF conducted the manual experiments and contributed with the development of the mapping and kernel density estimation technique and the other employed analyses. FP developed the mapping and kernel density estimation technique, developed the other employed analyses, was responsible for the statistical analyses, and conducted the 3DSlicer and Python based analyses including writing the necessary program code. IF, FP, DS, SM, TW, HS, AC, TK, CB, BF, LD, SL, and RF contributed to writing the manuscript. IF, FP, SL, CB, and RF conceptualized this work. FP, AC, TK, CB, and RF provided the resources. DS and TK provided nuclear medicine and AC provided radiologic expertise for conducting this work. All authors contributed to the article and approved the submitted version.

FUNDING

FP was supported by a grant from the Interdisciplinary Center for Clinical Research (IZKF) Erlangen: rotation program for physician scientists (https://www.izkf.med.fau.de/).

ACKNOWLEDGMENTS

The present work was performed in fulfillment of the requirements for obtaining the degree "Dr. med."

SUPPLEMENTARY MATERIAL

The Supplementary Material for this article can be found online at: https://www.frontiersin.org/articles/10.3389/fonc.2020.590722/full#supplementary-material

REFERENCES

1. Roach M, Moughan J, Lawton CAF, Dicker AP, Zeitzer KL, Gore EM, et al. Sequence of hormonal therapy and radiotherapy field size in unfavourable, localised prostate cancer (NRG/RTOG 9413): long-term results of a randomised, phase 3 trial. *Lancet Oncol* (2018) 19(11):1504–15. doi: 10.1016/s1470-2045(18)30528-x
2. Roach M,3, DeSilvio M, Lawton C, Uhl V, Machtay M, Seider MJ, et al. Phase III trial comparing whole-pelvic versus prostate-only radiotherapy and neoadjuvant versus adjuvant combined androgen suppression: Radiation Therapy Oncology Group 9413. *J Clin Oncol* (2003) 21(10):1904–11. doi: 10.1200/jco.2003.05.004
3. Pommier P, Chabaud S, Lagrange JL, Richaud P, Lesaunier F, Le Prise E, et al. Is there a role for pelvic irradiation in localized prostate adenocarcinoma? Preliminary results of GETUG-01. *J Clin Oncol* (2007) 25(34):5366–73. doi: 10.1200/JCO.2006.10.5171
4. Achard V, Bottero M, Rouzaud M, Lancia A, Scorsetti M, Filippi AR, et al. Radiotherapy treatment volumes for oligorecurrent nodal prostate cancer: a systematic review. *Acta Oncol* (2020) 59(10):1224–34. doi: 10.1080/0284186x.2020.1775291
5. Ost P, Bossi A, Decaestecker K, De Meerleer G, Giannarini G, Karnes RJ, et al. Metastasis-directed therapy of regional and distant recurrences after curative treatment of prostate cancer: a systematic review of the literature. *Eur Urol* (2015) 67(5):852–63. doi: 10.1016/j.eururo.2014.09.004
6. De Bruycker A, Spiessens A, Dirix P, Koutsouvelis N, Semac I, Liefhooghe N, et al. PEACE V - Salvage Treatment of OligoRecurrent nodal prostate cancer Metastases (STORM): a study protocol for a randomized controlled phase II trial. *BMC Cancer* (2020) 20(1):406. doi: 10.1186/s12885-020-06911-4
7. Supiot S, Rio E, Pacteau V, Mauboussin MH, Campion L, Pein F. OLIGOPELVIS - GETUG P07: a multicentre phase II trial of combined salvage radiotherapy and hormone therapy in oligometastatic pelvic node relapses of prostate cancer. *BMC Cancer* (2015) 15:646. doi: 10.1186/s12885-015-1579-0
8. Lawton CA, Michalski J, El-Naqa I, Buyyounouski MK, Lee WR, Menard C, et al. RTOG GU Radiation oncology specialists reach consensus on pelvic lymph node volumes for high-risk prostate cancer. *Int J Radiat Oncol Biol Phys* (2009) 74(2):383–7. doi: 10.1016/j.ijrobp.2008.08.002
9. Barbosa FG, Queiroz MA, Nunes RF, Viana PCC, Marin JFG, Cerri GG, et al. Revisiting Prostate Cancer Recurrence with PSMA PET: Atlas of Typical and Atypical Patterns of Spread. *Radiographics* (2019) 39(1):186–212. doi: 10.1148/rg.2019180079
10. Calais J, Czernin J, Cao M, Kishan AU, Hegde JV, Shaverdian N, et al. (68)Ga-PSMA-11 PET/CT Mapping of Prostate Cancer Biochemical Recurrence After Radical Prostatectomy in 270 Patients with a PSA Level of Less Than 1.0 ng/mL:

Impact on Salvage Radiotherapy Planning. *J Nucl Med* (2018) 59(2):230–7. doi: 10.2967/jnumed.117.201749
11. McClinton C, Niroumand M, Sood S, Shah V, Hill J, Dusing RW, et al. Patterns of lymph node positivity on (11)C-acetate PET imaging in correlation to the RTOG pelvic radiation field for prostate cancer. *Pract Radiat Oncol* (2017) 7(5):325–31. doi: 10.1016/j.prro.2017.03.002
12. Schiller K, Sauter K, Dewes S, Eiber M, Maurer T, Gschwend J, et al. Patterns of failure after radical prostatectomy in prostate cancer - implications for radiation therapy planning after (68)Ga-PSMA-PET imaging. *Eur J Nucl Med Mol Imaging* (2017) 44(10):1656–62. doi: 10.1007/s00259-017-3746-9
13. Spratt DE, Vargas HA, Zumsteg ZS, Golia Pernicka JS, Osborne JR, Pei X, et al. Patterns of Lymph Node Failure after Dose-escalated Radiotherapy: Implications for Extended Pelvic Lymph Node Coverage. *Eur Urol* (2017) 71 (1):37–43. doi: 10.1016/j.eururo.2016.07.043
14. De Bruycker A, De Bleser E, Decaestecker K, Fonteyne V, Lumen N, De Visschere P, et al. Nodal Oligorecurrent Prostate Cancer: Anatomic Pattern of Possible Treatment Failure in Relation to Elective Surgical and Radiotherapy Treatment Templates. *Eur Urol* (2019) 75(5):826–33. doi: 10.1016/j.eururo.2018.10.044
15. Hall WA, Paulson E, Davis BJ, Spratt DE, Morgan TM, Dearnaley D, et al. NRG Oncology Updated International Consensus Atlas on Pelvic Lymph Node Volumes for Intact and Postoperative Prostate Cancer. *Int J Radiat Oncol Biol Phys* (2020). doi: 10.1016/j.ijrobp.2020.08.034
16. Nicosia L, Franzese C, Mazzola R, Franceschini D, Rigo M, D'Agostino G, et al. Recurrence pattern of stereotactic body radiotherapy in oligometastatic prostate cancer: a multi-institutional analysis. *Strahlentherapie und Onkologie Organ der Deutschen Rontgengesellschaft [et al]* (2019) 196:213–21. doi: 10.1007/s00066-019-01523-9
17. Fedorov A, Beichel R, Kalpathy-Cramer J, Finet J, Fillion-Robin JC, Pujol S, et al. 3D Slicer as an image computing platform for the Quantitative Imaging Network. *Magnetic Resonance Imaging* (2012) 30(9):1323–41. doi: 10.1016/j.mri.2012.05.001
18. Virtanen P, Gommers R, Oliphant TE, Haberland M, Reddy T, Cournapeau D, et al. SciPy 1.0: fundamental algorithms for scientific computing in Python. *Nat Methods* (2020) 17(3):261–72. doi: 10.1038/s41592-019-0686-2
19. Pinter C, Lasso A, Wang A, Jaffray D, Fichtinger G. SlicerRT: radiation therapy research toolkit for 3D Slicer. *Med Phys* (2012) 39(10):6332–8. doi: 10.1118/1.4754659
20. Shackleford J, Kandasamy N, Sharp G. Chapter 6 - Plastimatch—An Open-Source Software for Radiotherapy Imaging. In: J Shackleford, N Kandasamy, G Sharp, editors. *High Performance Deformable Image Registration Algorithms for Manycore Processors*. Boston: Morgan Kaufmann (2013). p. 107–14.
21. Silverman BW. *Density Estimation for Statistics and Data Analysis*. London: Chapman and Hall (1986).
22. Odland T. KDEpy: Kernel Density Estimation in Python v0.9.10. (2018). Available at: https://github.com/tommyod/KDEpy.
23. McCormick M, Liu X, Jomier J, Marion C, Ibanez L. ITK: enabling reproducible research and open science. *Front Neuroinform* (2014) 8:13. doi: 10.3389/fninf.2014.00013
24. Myerson RJ, Garofalo MC, El Naqa I, Abrams RA, Apte A, Bosch WR, et al. Elective clinical target volumes for conformal therapy in anorectal cancer: a radiation therapy oncology group consensus panel contouring atlas. *Int J Radiat Oncol Biol Phys* (2009) 74(3):824–30. doi: 10.1016/j.ijrobp.2008.08.070
25. Brand DH, Parker JI, Dearnaley DP, Eeles R, Huddart R, Khoo V, et al. Patterns of recurrence after prostate bed radiotherapy. *Radiother Oncol* (2019) 141:174–80. doi: 10.1016/j.radonc.2019.09.007
26. Meijer HJ, Fortuin AS, van Lin EN, Debats OA, Alfred Witjes J, Kaanders JH, et al. Geographical distribution of lymph node metastases on MR lymphography in prostate cancer patients. *Radiother Oncol* (2013) 106 (1):59–63. doi: 10.1016/j.radonc.2012.10.021
27. Walacides D, Meier A, Knochelmann AC, Meinecke D, Derlin T, Bengel FM, et al. Comparison of (68)Ga-PSMA ligand PET/CT versus conventional cross-sectional imaging for target volume delineation for metastasis-directed radiotherapy for metachronous lymph node metastases from prostate cancer. *Strahlentherapie und Onkologie Organ der Deutschen Rontgengesellschaft [et al]* (2019) 195(5):420–9. doi: 10.1007/s00066-018-1417-9
28. Supiot S, Pasquier D, Buthaud X, Magné N, Beckendorf V, Sargos P, et al. Oligopelvis-GETUG P07: A multicenter phase II trial of combined salvage radiotherapy and hormone therapy in oligorecurrent pelvic node relapses of prostate cancer. *J Clin Oncol* (2020) 38(6suppl):93–. doi: 10.1200/JCO.2020.38.6_suppl.93
29. Meijer HJ, van Lin EN, Debats OA, Witjes JA, Span PN, Kaanders JH, et al. High occurrence of aberrant lymph node spread on magnetic resonance lymphography in prostate cancer patients with a biochemical recurrence after radical prostatectomy. *Int J Radiat Oncol Biol Phys* (2012) 82(4):1405–10. doi: 10.1016/j.ijrobp.2011.04.054
30. Joniau S, Van den Bergh L, Lerut E, Deroose CM, Haustermans K, Oyen R, et al. Mapping of pelvic lymph node metastases in prostate cancer. *Eur Urol* (2013) 63(3):450–8. doi: 10.1016/j.eururo.2012.06.057
31. Rushton G, Peleg I, Banerjee A, Smith G, West M. Analyzing geographic patterns of disease incidence: rates of late-stage colorectal cancer in Iowa. *J Med Syst* (2004) 28(3):223–36. doi: 10.1023/b:joms.0000032841.39701.36
32. Carlos HA, Shi X, Sargent J, Tanski S, Berke EM. Density estimation and adaptive bandwidths: a primer for public health practitioners. *Int J Health Geographics* (2010) 9:39. doi: 10.1186/1476-072x-9-39
33. Mattei A, Fuechsel FG, Bhatta Dhar N, Warncke SH, Thalmann GN, Krause T, et al. The template of the primary lymphatic landing sites of the prostate should be revisited: results of a multimodality mapping study. *Eur Urol* (2008) 53(1):118–25. doi: 10.1016/j.eururo.2007.07.035

Conflict of Interest: CB reports grants from Siemens Healthineers, outside the submitted work. RF reports grants and personal fees from Merck Serono, grants and personal fees from Astra Zenica, grants and personal fees from MSD, grants and personal fees from Novocure, personal fees from Brainlab, personal fees from Fresenius Kabi, personal fees from Bristol Meyers Sqibb, and personal fees from Sennewald GmbH, outside the submitted work. FP reports grants and personal fees from Siemens Healthineers, outside the submitted work.

The remaining authors declare that the research was conducted in the absence of any commercial or financial relationships that could be construed as a potential conflict of interest.

frontiers in Oncology

ORIGINAL RESEARCH
published: 20 January 2021
doi: 10.3389/fonc.2020.625184

Development of a Comorbidity-Based Nomogram to Predict Survival After Salvage Reirradiation of Locally Recurrent Nasopharyngeal Carcinoma in the Intensity-Modulated Radiotherapy Era

Run-Da Huang[1,2,3,4†], Zhuang Sun[1,2,3,4†], Xiao-Hui Wang[1,2,3,4†], Yun-Ming Tian[5], Ying-Lin Peng[1,2,3,4], Jing-Yun Wang[1,2,3,4], Wei-Wei Xiao[1,2,3,4], Chun-Yan Chen[1,2,3,4], Xiao-Wu Deng[1,2,3,4*] and Fei Han[1,2,3,4*]*

[1] Department of Radiation Oncology, Sun Yat-sen University Cancer Center, Guangzhou, China, [2] State Key Laboratory of Oncology in South China, Guangzhou, China, [3] Collaborative Innovation Center for Cancer Medicine, Guangzhou, China, [4] Guangdong Key Laboratory of Nasopharyngeal Carcinoma Diagnosis and Therapy, Guangzhou, China, [5] Department of Radiation Oncology, Hui Zhou Municipal Centre Hospital, Huizhou, China

Purpose: To assess the impact of comorbidity on treatment outcomes in patients with locally recurrent nasopharyngeal carcinoma (lrNPC) using intensity-modulated radiotherapy (IMRT) and to develop a nomogram that combines prognostic factors to predict clinical outcome and guide individual treatment.

Methods: This was a retrospective analysis of patients with lrNPC who were reirradiated with IMRT between 2003 and 2014. Comorbidity was evaluated by Adult Comorbidity Evaluation-27 grading (ACE-27). The significant prognostic factors ($P < 0.05$) by multivariate analysis using the Cox regression model were adopted into the nomogram model. Harrell concordance index (C-index) calibration curves were applied to assess this model.

Results: Between 2003 and 2014, 469 lrNPC patients treated in our institution were enrolled. Significant comorbidity (moderate or severe grade) was present in 17.1% of patients by ACE-27. Patients with no or mild comorbidity had a 5-year overall survival (OS) rate of 36.2 *versus* 20.0% among those with comorbidity of moderate or severe grade ($P < 0.0001$). The chemotherapy used was not significantly different in patients with lrNPC ($P > 0.05$). For the rT3–4 patients, the 5-year OS rate in the chemotherapy + radiation therapy (RT) group was 30.0 *versus* 16.7% for RT only ($P = 0.005$). The rT3–4 patients with no or mild comorbidity were associated with a higher 5-year OS rate in the chemotherapy + RT group than in the RT only group (32.1 and 17.1%, respectively; P=0.003). However, for the rT3–4 patients with a comorbidity (moderate or severe grade), the 5-year OS rate in the chemotherapy + RT group *vs*. RT alone was not significantly

OPEN ACCESS

Edited by:
Nicola Silvestris,
University of Bari Aldo Moro, Italy

Reviewed by:
Sufang Qiu,
Fujian Provincial Cancer Hospital, China
Jun-Lin Yi,
Chinese Academy of Medical Sciences and Peking Union Medical College, China

***Correspondence:**
Fei Han
hanfei@sysucc.org.cn
Xiao-Wu Deng
dengxw@mail.sysu.edu.cn
Chun-Yan Chen
chenchuny@sysucc.org.cn

†These authors have contributed equally to this work

Specialty section:
This article was submitted to Radiation Oncology, a section of the journal Frontiers in Oncology

Received: *02 November 2020*
Accepted: *26 November 2020*
Published: *20 January 2021*

Citation:
Huang R-D, Sun Z, Wang X-H, Tian Y-M, Peng Y-L, Wang J-Y, Xiao W-W, Chen C-Y, Deng X-W and Han F (2021) Development of a Comorbidity-Based Nomogram to Predict Survival After Salvage Reirradiation of Locally Recurrent Nasopharyngeal Carcinoma in the Intensity-Modulated Radiotherapy Era. Front. Oncol. 10:625184. doi: 10.3389/fonc.2020.625184

different (15.7 *vs*. 15.0%, respectively; p > 0.05). Eight independent prognostic factors identified from multivariable analysis were fitted into a nomogram, including comorbidity. The C-index of the nomogram was 0.715. The area under curves (AUCs) for the prediction of 1-, 3-, and 5-year overall survival were 0.770, 0.764, and 0.780, respectively.

Conclusion: Comorbidity is among eight important prognostic factors for patients undergoing reirradiation. We developed a nomogram for lrNPC patients to predict the probability of death after reirradiation and guide individualized management.

Keywords: comorbidity, recurrent, nasopharyngeal carcinoma, reirradiation, prognostic nomogram

INTRODUCTION

Nasopharyngeal carcinoma (NPC) is a type of head and neck cancer. Globally, there were 129,079 new cases of NPC and 72,987 deaths reported worldwide in 2018 (1). Nevertheless, the geographical distribution is extremely unbalanced, and it is considered to be epidemic in East and Southeast Asia, and North Africa, and approximately >70% of new cases are in East and Southeast Asia (1, 2). Due to the concealed location and radiosensitivity of nasopharyngeal carcinoma, radiation therapy (RT) is the first-line treatment modality for primary NPC patients (3).

With the advancement of radiotherapy technology, the diagnostic imaging of nasopharyngeal carcinoma and the improvement of combined chemotherapy, the treatment effect and disease control rate have been improved significantly (4). Nevertheless, approximately 5–10% of patients experience locally recurrent nasopharyngeal carcinoma (lrNPC) after intensity-modulated radiotherapy (IMRT) (5–8). In patients with local recurrence, a repeat course of RT or nasopharyngectomy presents the only treatment options; however, to date, nasopharyngectomy is still challenging owing to its small space and previously irradiated anatomic space, which is often considered when feasible, or reirradiation for patients not eligible for surgery (9, 10). The emergence of IMRT has helped to overcome the technical limitations of conventional two- and three-dimensional RT and improved the therapeutic ratio of salvage RT; nevertheless, severe RT-related toxic reactions occur frequently and account for a large portion of mortality after IMRT treatment (up to 50%) (11, 12).

Hence, it has become evident that risk appropriately stratified *a priori* is warranted if individualized management is to be pursued for patients with lrNPC to avoid overtreatment. Sun et al. and Li et al. investigated robust prognostic models for risk stratification in lrNPC (13, 14). Nevertheless, Sun et al. only considered diabetes mellitus and hypertension among comorbidities, and Li et al. did not consider comorbidity as a prognostic factor. To address this issue, more accurate and comprehensive models are needed to identify individual risks by combining patient characteristics to assist with treatment recommendations in this patient subgroup with different risks. The ACE-27 is a modified Kaplan-Feinstein Index that assesses the severity of 27 different items related to cancer. A number of reports documenting the grading have shown reliability and validity in head and neck cancers as a cause of death, which have also been linked to predicting survival in head and neck cancers (15–18). In this study, we aimed to construct a nomogram that includes independent predictors. Moreover, we incorporated the ACE-27 into the nomogram to help clinicians predict patient survival outcomes and identify optimal candidates for local treatment with IMRT.

MATERIALS AND METHODS

Patient Characteristics

A retrospective review of case records for patients with lrNPC who were reirradiated using a full-course IMRT technique was conducted at Sun Yat-sen University Cancer Center (SYSUCC) from January 2003 to December 2014. The inclusion criteria were as follows: a) pathology confirmed or evidence of local recurrence by at least one imaging study with a consistent clinical process, b) no evidence of distant metastasis, and c) using the IMRT technique for treatment. The exclusion criteria were a) pregnancy or lactation and b) secondary malignancy. The Clinical Research Ethics Committee of Sun Yat-sen University Cancer Center approved this study.

Diagnosis and Comorbidity Assessment

Patients had undergone pretreatment evaluation comprising a complete medical history, nasopharynx and neck magnetic resonance imaging (MRI) or computed tomography (CT), chest X-ray or CT, abdominal CT or ultrasonography, CT whole-body bone scan single photon emission, or ^{18}F-fluorodeoxyglucose (^{18}F-FDG) PET/CT. ACE-27 was performed for comorbid disease severity at diagnosis, which includes the assessment of 27 elements from twelve different organ systems. The ACE-27 grades comorbidities into one of four scores: none 0), mild 1), moderate 2), or severe 3). The total score for each patient's comorbidities is based on the highest-ranked single disease. When two or more moderate diseases occur in different organ systems, the total comorbidity score is considered severe (18–20).

Clinical Treatment

A similar IMRT planning protocol was used as previously described (11, 21), and the total dosage for reirradiation therapy was 50–70 Gy at 1.80–2.50 Gy/fraction, five times a

week on workdays, delivered by the IMRT technique. In this study, most patients received intravenous chemotherapy every 3 weeks. Treatment regimens included concomitant chemoradiotherapy plus induction chemotherapy (CCRT + IC), CCRT plus adjuvant chemotherapy (CCRT + AC), CCRT, RT, IC + RT, and RT + AC.

Follow-Up and Endpoint

Follow-up was measured from the first day of therapy to the last follow-up or death. A range of assessments were carried out every 3 months for the first year, and then follow-up examinations were performed every 6 months thereafter until death. At each follow-up visit, routine assessments included head and neck physical examination, nasopharyngoscopy, nasopharynx and neck MRI with contrast, chest X-ray or CT, abdominal ultrasound or CT, whole-body bone scan, or (^{18}F-FDG) PET/CT. The primary endpoint of our study was OS. OS was defined as the time from the first day of therapy to death from any cause or follow-up endpoint.

Statistical Methods

Based on patient survival status, the optimal cut-off value of the continuous variables that generated the largest χ^2 value in the Mantel-Cox test assessed by X-tile software (version 3.6.3; Yale University, New Haven, CT, USA), the lrNPC patients were stratified into subgroups (22). Life-table estimation was performed according to the Kaplan-Meier method. The log-rank test was used to examine the difference in survival between groups.

Multivariable regression analyses were performed using Cox proportional hazards modeling, which was used to estimate hazard ratios (HR) and 95% confidence intervals (CI), and formed the basis for the survival prediction model. Covariates in this study included comorbidity, age, sex, hemoglobin (HB), Karnofsky performance status (KPS), and prior RT-induced grade ≥ 3 toxicity variables (late RT-induced toxicities were noted and graded according to the Radiation Therapy Oncology Group radiation morbidity scoring scheme), DNA fragmentation index (DFI), recurrent gross tumor volume (GTV), rT stage, rN stage, treatment regimen, and re-RT equivalent dose in 2-Gy fractions [EQD2]. Those variables with a 2-tailed $P < 0.05$ in multivariable regression analyses were considered to create a nomogram based on their contribution to the accuracy of prediction. Statistical analyses were conducted using IBM SPSS Statistics software version 25, R version 3.6.1 (R Core Team, Vienna, Austria) and GraphPad Prism version 8.

RESULTS

Patient Characteristics, Survival, and Toxicities

A total of 469 patients treated from January 2003 to December 2014 were retrospectively enrolled. The median age was 47 years old (range: 21–79), and 378 (80.6%) patients were male. A total of 19.6, 45.2, and 35.2% of the patients had stage rT1–2, rT3, and rT4, respectively, whereas 81.0 and 19.0% had stage rN0 and rN1–3, respectively, and 80 (17.1%) patients had prior RT-induced grade ≥ 3 toxicity. Comorbidity (moderate or severe grade) was present in 80 (17.1%) patients, and chemotherapy was delivered to 328 patients (69.9%). The median delivered EQD2 was 64 Gy [interquartile range (IQR): 61.10–67.10 Gy]. The other characteristics of the patients are detailed in **Table 1**.

All patients completed the IMRT treatment successfully, and the median follow-up was 36 months (range 3–193 months). The 3-year OS, locoregional relapse-free survival (LRRFS), and distant metastasis-free survival (DMFS) rates were 51.3, 70.0, and 90.0%, respectively; the 5-year OS, LRRFS, and DMFS rates were 33.4, 63.3, and 84.6%, respectively.

Treatment was not interrupted because of severe acute side effects in any patient. However, most patients experienced mild acute toxicities, including mucositis and xerostomia. Only 37 patients (7.9%) developed grade-3 acute toxicities. After reirradiation, 163 patients (34.8%) had one of the common late complications, including trismus, xerostomia, and hearing loss. A total of 141 patients (30.1%) had mucosal necrosis, 93 patients (19.8%) had temporal lobe necrosis, and 66 patients (14.1%) had cranial nerve palsy.

The Impact of Comorbidity and Chemotherapy on Survival Outcomes

By the ACE-27 grading, of the 469 lrNPC patients, 188 (40.1%) had one or more comorbidities; 108 (23.0%) patients had ACE-27 scores of 1, 65 (13.9%) had scores of 2, and 15 (3.2%) had scores of 3. Patients with no or mild comorbidity had a 5-year OS rate of 36.2 *versus* 20.0% among those with comorbidity of moderate or severe grade ($P<0.0001$; **Figure 1**).

The prognosis of chemotherapy used was not significant in patients with lrNPC disease ($P>0.05$). Nevertheless, for the rT3–4 patients, the 5-year OS rate in the chemotherapy + RT group was 30.0 *versus* 16.7% for RT only ($P=0.005$). For rT3–4 patients with a comorbidity (ACE ≥ 2), the 5-year OS rate in the chemotherapy + RT group *vs*. for RT alone (15.7 *vs*. 15.0%, respectively; $P>0.05$) failed to confirm the positive association of chemotherapy. However, rT3–4 patients with an ACE-27 score of 0–1 had a higher 5-year OS rate in the chemotherapy + RT group than in the RT only group (32.1 and 17.1%, respectively; $P=0.003$). The results are presented in **Supplemental Figure S1**.

A total of 141/469 (30.1%) lrNPC patients only received RT, 113/469 (24.1%) received IC + RT, 93/469 (19.8%) received IC + CCRT, 116/469 (24.7%) received CCRT, and only 6/469 (1.3%) received AC, including 5/469 (1.1%) who received RT + AC and 1/469 (0.2%) who received CCRT + AC. Due to the small number of AC patients, they were excluded following survival analysis. There was no significant difference between RT only and other treatment regimens (all $P>0.05$). However, for the rT3–4 patients, the 5-year OS rate in the RT group was 16.7 *vs*. 30.4% for CCRT ($P=0.011$), 38.6% for CCRT + IC ($P = 0.001$), and 20.7% for IC + RT ($P>0.05$). For rT3–4 patients with a comorbidity (ACE < 2), the 5-year OS rate in the RT group was 17.1 *vs*. 35.2% for CCRT ($P=0.003$), 38.8% for CCRT + IC ($P=0.002$), and 22.5% for IC + RT ($P>0.05$). However, for rT3–

TABLE 1 | Clinical characteristics of 469 patients with locally recurrent nasopharyngeal carcinoma.

Characteristic	No. of patients (%) (n=469)
Sex	
Male	378 (80.6)
Female	91 (19.4)
Age (years)	
Media age	47
<60	399 (85.1)
≥60	70 (14.9)
Prior RT-induced grade ≥3 toxicity	
No	390 (83.2)
Yes	79 (16.8)
ACE-27 comorbidity grade	
0 or 1	389 (82.9)
2 or 3	80 (17.1)
KPS	
>70	453 (96.6)
≤70	16 (3.4)
HB (g/L)	
≥130	264 (56.3)
<130	205 (43.7)
Repeat IMRT EQD2,Gy	
Media Repeat IMRT EQD2,Gy	64
< 65	285 (60.8)
≥ 65	184 (39.2)
DFI (months)[a]	
≥60	104 (22.2)
<60	365 (77.8)
Recurrent T stage[b]	
rT1-2	92 (19.6)
rT3	212 (45.2)
rT4	165 (35.2)
Recurrent N stage[b]	
rN0	380 (81.0)
rN1-3	89 (19.0)
Volume of GTV-nx (cm3)	
<26	164 (35.0)
26-46	125 (26.7)
≥46	180 (38.4)
Target therapy[b]	
No	416 (88.7)
Yes	53 (11.3)
Chemotherapy	
No	141 (30.1)
Yes	328 (69.9)
IC alone	113 (24.1)
CCT alone	116 (24.7)
IC + CCT	93 (19.8)
AC alone	5 (1.1)
CCT + AC	1 (0.2)
IC + AC	0 (0)
IC + CCT + AC	0 (0)

RT, radiotherapy; ACE-27, Adult Comorbidity Evaluation-27; KPS, Karnofsky Performance Status; HB, hemoglobin; IMRT, intensity-modulated radiotherapy EQD2, equivalent dose in 2-Gy fractions; DFI, disease-free interval; GTV, gross tumor volume; AC, adjuvant chemotherapy; CCT, concurrent chemotherapy; IC, induction chemotherapy.

[a]*DFI, disease-free interval was defined as the duration between the end of first RT and diagnosis of recurrence of > 6 months to exclude partial responders to the first course of RT.*

[b]*Target therapy includes cetuximab, nimotuzumab, and endostar.*

4 patients with a comorbidity (ACE ≥ 2), the 5-year OS rate in the RT group was 15.0 *vs.* 7.2% for CCRT, 37.5% for CCRT + IC, and 14.0% for IC + RT (all P>0.05) (**Supplemental Table S1** and **Supplemental Figure S2**). More details are shown in **Figure 2**.

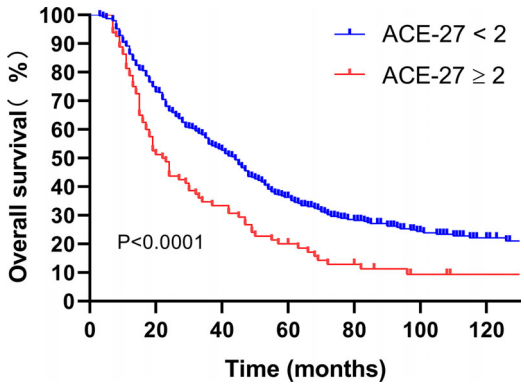

FIGURE 1 | Kaplan-Meier analysis of overall survival is stratified by ACE-27. ACE-27, Adult Comorbidity Evaluation 27.

Univariate Analysis and Multivariate Analysis

Next, it was necessary to assess the prognostic significance of continuous variables and avoid any predetermined cutoff points. The X-tile analysis identified 1 optimal cut-off point, and the age, HB, EQD2, and DFI were 59 years, 128 g/L, 64.69 Gy, and 59 months, respectively. The analysis identified two optimal GTV cut-off points, 25.65 and 46 cc. For the use of minimum P statistics by Miller-Siegmund P-value correction, the best cut-off value is obtained (22). To optimize the cutoff value for its potential acceptance and clinical application, we rounded to the nearest integer in further analysis. Age (< 60 *versus* ≥ 60 years); HB (≤ 130 *versus* > 130 g/L); EQD2 (< 65 *versus* ≥ 65 Gy); and DFI (< 60 *versus* ≥ 60 months) were investigated. Similarly, the nearest integers of 26 and 46 cc were selected. In addition, based on clinical practice, a score of 70 was the cut-off value of KPS. Thus, we performed a univariable analysis on those variables that may be potential prognostic factors (**Table 2**). These variables were analyzed for association with OS by using Cox proportional hazards regression model hazard ratios (HRs), and the univariable P < 0.1 was included in the multivariable analysis. From the results of univariable analysis, age, prior RT-induced grade ≥ 3 toxicity, ACE-27, GTV, KPS, DFI, rT stage, and rN stage were significant survival predictors. On multivariate analysis, we found that age (P < 0.001), prior RT-induced grade ≥ 3 toxicity (P<0.001), KPS (P=0.003), ACE-27 (P=0.002), DFI (P=0.001), rT stage (P<0.001), rN stage (P=0.011), and GTV (P<0.001) remained independent prognostic factors.

Establishment and Evaluation of a Nomogram Model for Overall Survival

Based on the eight independent prognostic factors, a nomogram was established for predicting the 1-, 3-, and 5-year OS for lrNPC (**Figure 3**). Each variable has a corresponding score according to the point scale, and we obtained the total score by calculating the score of each variable. Next, by mapping the total score on the probability scale, the OS probabilities could be estimated at the 1-, 3-, and 5-year time points (**Figure 4**)

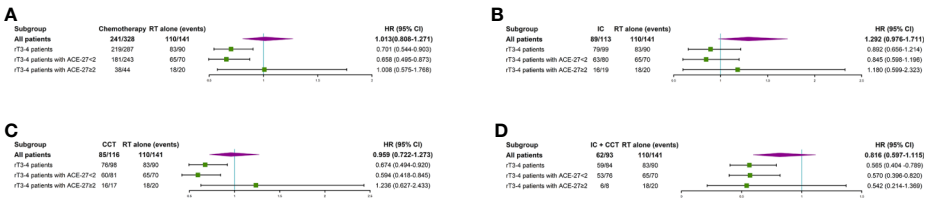

FIGURE 2 | Subgroup analyses of overall survival for patients with radiotherapy only or chemotherapy plus radiotherapy **(A)**, overall survival for patients with radiotherapy only or induction chemotherapy plus radiotherapy **(B)**, overall survival for patients with radiotherapy only or concurrent chemotherapy plus radiotherapy **(C)**, and overall survival for patients with radiotherapy only or induction chemotherapy plus concurrent chemotherapy plus radiotherapy **(D)**. IC, induction chemotherapy; CCT, concurrent chemotherapy; CI, confidence interval; HR, hazard ratio.

By bootstrap correction, the Harrell C index was 0.715 in the nomogram. The area under curves (AUCs) for the prediction of 1-, 3-, and 5-year OS were 0.770, 0.764, and 0.780, respectively. The results exhibited satisfactory accuracy for predicting the 1-, 3-, and 5-year OS for lrNPC. The calibration curves showed that the nomogram predictions were well correlated with the actual observations for 1-, 3-, and 5-year OS (**Supplemental Figures S3–S5**).

DISCUSSION

In general, ACE-27 in patients with primary NPC has been reported, and it has been explained to be a major determinant of survival outcome in patients with NPC (16, 23, 24). To our knowledge, the value of ACE-27 in patients with lrNPC has not yet been analyzed, and this study is the first to describe ACE-27 in patients diagnosed with lrNPC and to assess the prognostic value of ACE-27 on the survival of patients with lrNPC. In this study, comorbidity was present in 40.1% of patients. The incidence of comorbidity in lrNPC patients is similar to that in primary NPC patients (17). However, patients with moderate and severe comorbidities were observed to have higher rates of comorbidity than primary NPC. The reason may be that the patients become susceptible to disease or the original comorbidity has been aggravated after the initial radiotherapy and chemotherapy. The patients with an ACE-27 score of 0–1 had a better survival than those patients with an ACE-27 score of 2–3. This result is similar to that previously reported in primary NPC (24). In addition, patients who had rT3–4 patients with ACE-27 scores of 0–1 who received chemotherapy had better survival than those with RT only. Nevertheless, there was no significant difference between RT only and RT + chemotherapy in patients who had rT3–4 patients with ACE-27 scores of 2–3. Our findings suggest that patients with ACE-27 scores of 2–3 cannot benefit from chemotherapy. The reason may be that those patients have a shorter median survival time, and the benefits of chemotherapy have not been observed; furthermore, comorbidity increases the risk of death from other diseases. It can explain the negative impact of rT3–4 with comorbidities (moderate or severe) on survival.

Although various chemotherapy regimens and targeted agents have been used, there is still a lack of effective clinical evidence for the use of chemotherapy in lrNPC patients (25–27). A meta-analysis did not demonstrate that the addition of chemotherapy had an impact on local failure-free survival (LFFS), DMFS, and OS (28). In our study, however, we found that rT3–4 patients who received CCRT + IC or CCRT had better survival than those who received RT only, but those who received IC + RT had no significant OS benefit compared to those who received RT alone. In particular, rT3–4 patients with a comorbidity (ACE < 2) have similar outcomes. The reason may be that concurrent chemotherapy can improve radiosensitivity, thereby improving local tumor control. Nevertheless, patients with larger GTVs often choose to have increased IC. In addition, IC related to increased associated late toxicities should also be considered. The results show that CCRT may be a preferential therapeutic regimen. It is still worth exploring whether IC can benefit lrNPC patients. Ng WT et al. reported that IC followed by CCRT and weekly cetuximab could achieve a better treatment outcome (3-year PFS and OS rates of 36 and 64%, respectively) in lrNPC (T3–T4, N0–N1, M0) patients than reported in previous studies (29). The sample size in this study is small. To obtain high-level evidence, a prospective, multicenter, phase III clinical trial should be implemented. In addition, some studies have reported that immunotherapy has acquired promising results in recurrent or metastatic nasopharyngeal carcinoma patients (30–32). Nevertheless, the studies included only a small number of lrNPC patients. The effect of immunotherapy deserves more exploration by a large-scale clinical trial of lrNPC.

Some recent studies have shown that the dose of reirradiation by IMRT is an essential prognostic factor in patients with lrNPC (11, 14, 33, 34). In a prognostic model proposed by Li et al. (14), the dose of reirradiation by IMRT (EQD2 ≥ 68 Gy) is a poor prognostic factor. It is combined with the other four factors to form a prognostic index (PI). Tian et al. demonstrated that decreasing the total dose and increasing the fraction size can achieve local control similar to that achieved with a higher dose after IMRT, and it can improve OS by reducing the incidence of severe late complications (33). However, there are small samples in this study. Another study by Ng WT et al. (34) reported that a reirradiation dose equivalent to 60 Gy (EQD2) appears to be the optimal dose for achieving the best survival outcome while balancing the probability of local control and fatal complications. Those studies indicated that 60 Gy may be an

TABLE 2 | Univariable and multivariable analyses.

Characteristic	Univariable		Multivariable	
	Hazard ratio (95% CI)	P[a] value	Hazard ratio (95% CI)	P[a] value
Sex				
Male	reference			
Female	0.859 (0.657–1.124)	0.268		
Age (years)				
<60	Reference		Reference	
≥60	2.106 (1.606–2.763)	<0.001	2.189 (1.646-2.911)	<0.001
Prior RT-induced grade ≥3 toxicity				
No	Reference		Reference	
Yes	2.295 (1.765–2.986)	<0.001	1.923 (1.468–2.519)	<0.001
ACE-27 comorbidity grade				
0 or 1	Reference		Reference	
2 or 3	1.682 (1.293–2.188)	<0.001	1.553 (1.180–2.045)	0.002
KPS				
>70	Reference		Reference	
≤70	2.514 (1.521–4.155)	<0.001	2.213 (1.314–3.727)	0.003
HB (g/L)				
≥130	Reference			
<130	1.216 (0.985–1.501)	0.068		
Repeat IMRT EQD2, Gy				
<65	Reference			
≥65	1.186 (0.958–1.467)	0.117		
DFI (months)[b]				
≥60	Reference		Reference	
<60	1.348 (1.037–1.752)	0.026	1.585 (1.210–2.076)	0.001
Recurrent T stage				
rT1-2	Reference		Reference	
rT3	2.133 (1.543–2.948)	<0.001	1.692 (1.198–2.391)	0.003
rT4	3.238 (2.331–4.498)	<0.001	2.095 (1.429–3.070)	<0.001
Recurrent N stage				
rN0	Reference		Reference	
rN1-3	1.365 (1.058–1.761)	0.017	1.405 (1.082–1.824)	0.011
Volume of GTV-nx (cm^3)				
<26	Reference		Reference	
26-46	1.947 (1.466–2.584)	<0.001	1.638 (1.210–2.216)	0.001
≥46	3.094 (2.384–4.015)	<0.001	2.295 (1.698–3.103)	<0.001
Target therapy[c]				
No	Reference			
Yes	1.321 (0.961–1.816)	0.087		
Chemotherapy				
No	Reference	0.908		
Yes	1.013 (0.808–1.271)			

RT, radiotherapy; ACE-27, Adult Comorbidity Evaluation-27; KPS, Karnofsky Performance Status; HB, hemoglobin; IMRT, intensity-modulated radiotherapy EQD2, equivalent dose in 2-Gy fractions; DFI, disease-free interval; GTV, gross tumor volume; CI, confidence interval.

[a]P values were calculated using Cox proportional hazards model.

[b]DFI, disease-free interval was defined from the date of completion of treatment to diagnosis of recurrence or final follow-up if sooner.

[c]Target therapy includes cetuximab, nimotuzumab and endostar.

The following variables were included in the Cox proportional hazards model with forword LR elimination: the age (≥ 60 vs. < 60); KPS (≤ 70 vs. > 70); HB (≥ 130 vs. < 130); DFI (≥ 60 vs. < 60), prior RT-induced grade ≥ 3 toxicity (yes or no); recurrent T stage (T1–2 vs. T3 vs. T4); recurrent N stage (N0 vs. N1–3); GTV (< 26 vs. 26–46 vs. ≥ 46).

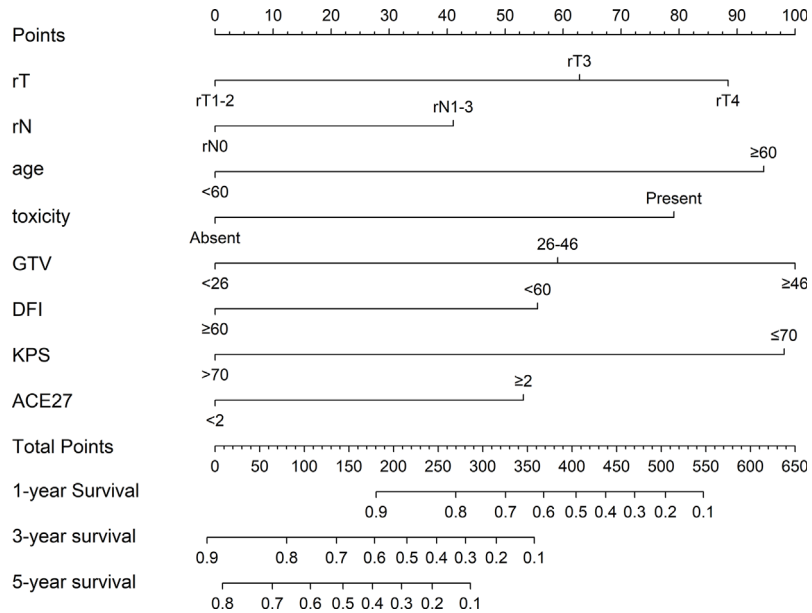

FIGURE 3 | Prognostic nomogram for locally recurrent nasopharyngeal carcinoma (lrNPC) patients: a line was drawn straight down to predict the 1-, 3-, or 5-year overall survival. rT, recurrent T stage; rN, recurrent N stage; toxicity, prior RT-induced grade ≥ 3 toxicity; GTV, gross tumor volume; DFI, disease-free interval; KPS, Karnofsky Performance Status; ACE-27, Adult Comorbidity Evaluation-27.

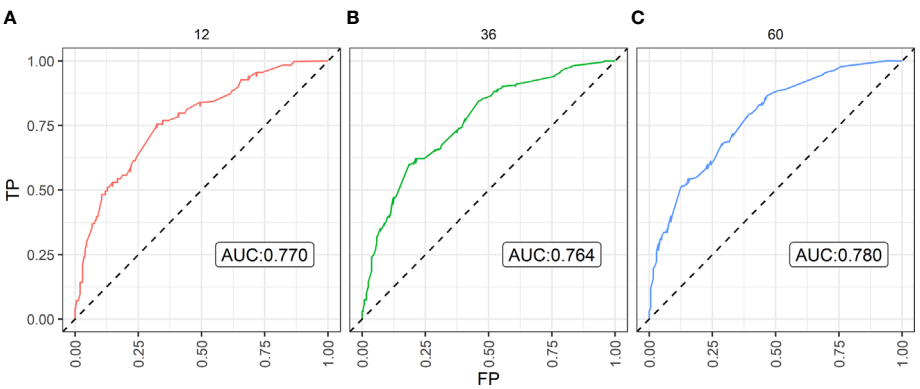

FIGURE 4 | The Area Under Curve (AUC) of the prediction nomogram on **(A)** 1-year, **(B)** 3-year, and **(C)** 5-year overall survival. TP, true positive; FP, false positive.

optimal dose for lrNPC patients, but these studies are based on the analysis of small samples, and the patients in the study by Ng WT reported came from multiple centers. There are great differences in treatment strategies and dose limitation standards. Moreover, in our retrospective study, EQD2 (< 65 *versus* ≥ 65 Gy) had no significant effect on survival; however, the incidence of mucosal necrosis in the higher EDQ2 group was higher than that in the lower EQD2 group (40.2 *versus* 23.5%; respectively, P<0.001) and temporal lobe necrosis (25.5 *versus* 16.1%; respectively, P=0.013). This means that the high reirradiation dose increases the occurrence of complications. We consider that, with dose escalation, the survival benefit is potentially offset by survival detriment because of increased late complications. A meta-analysis by Leong YH found that DFI ≥ 36 months can obtain a higher rate of LFFS, but there is no benefit in OS and DMFS (28). In our study, DFI was an important prognostic factor. The cut-off time was 60 months, and the longer DFI may allow the patient's previously irradiated organs to recover better and reduce the degree of damage by radiotherapy.

In addition, age, rT stage, and GTV were the most important predictors of OS in previous reports (11, 14, 28). We can obtain similar results in this study. To distinguish the impact of GTV on prognosis, we obtained two cutoff values using X-tile software, and the results showed that the different GTV groups had significantly different survival prognoses. The cut-

off value of hemoglobin in this study was obtained using the software X-tile and the value was 128 g/L. However, in order to facilitate the application of the nomogram in clinical practice, we selected 130 g/L as the cut-off value finally. There are great variations between the selected cut-off value of hemoglobin in the previous studies, and there is no uniform standard so far (35–37). Some reports showed that relatively low levels of hemoglobin is a poor prognostic factor for nasopharyngeal carcinoma (35, 36). However, in our study, we fail to get the similar results.

Moreover, the present study has several limitations that deserve further discussion. First, plasma Epstein-Barr virus (EBV) DNA was regarded as an adverse prognostic biomarker in primary NPC (38). In this study, we excluded EBV DNA from the nomogram. We considered the positive rate of pretreatment plasma EBV DNA in the detection of lrNPC to be relatively low, and the prognostic significance of EBV DNA, which lacks prospective data in lrNPC, was uncertain. In addition, the method of plasma EBV DNA measurement lacked standardization, and the EBV DNA polymerase chain reaction assay is susceptible due to changes in experimental conditions (39). Second, it is a single-center retrospective study in an endemic area, and some amount of selection bias is unavoidable. Finally, our proposed models were not validated in an external cohort, and the C-indices of the nomogram showed an imperfect discrimination ability, which indicated that more factors should be considered. Nonetheless, we acknowledge these limitations of our model. The focus of this study is that it is the first large-scale study to evaluate the importance of ACE-27 and its value in predicting survival for lrNPC.

CONCLUSION

In summary, our study is a large-scale study of lrNPC treated with IMRT. In this study, eight prognostic factors are worth investigating before reirradiation. For patients with favorable risk factors, reirradiation should be strongly recommended because it may have better survival benefits. However, for patients with high-risk factors, palliative chemotherapy or immunotherapy should be considered.

DATA AVAILABILITY STATEMENT

The raw data supporting the conclusions of this article will be made available by the authors, without undue reservation.

ETHICS STATEMENT

Written informed consent was obtained from the individual(s) for the publication of any potentially identifiable images or data included in this article.

AUTHOR CONTRIBUTIONS

FH, X-WD, and C-YC provided the study concepts. R-DH, ZS, and X-HW designed the study. R-DH, ZS, and X-HW acquired the data. Y-MT, Y-LP, J-YW, and W-WX conducted the quality control of the data and algorithms. R-DH, ZS, and X-HW analyzed and interpreted the data. R-DH, ZS, and X-HW conducted the statistical analysis. R-DH, ZS, and X-HW prepared the manuscript, R-DH, ZS, and X-HW edited the manuscript. FH, X-WD, and C-YC reviewed the manuscript. All authors contributed to the article and approved the submitted version.

FUNDING

This work was supported by the National Natural Science Foundation of China (12005316), Cancer Precision Radiotherapy Spark Program of China International Medical Foundation (2019-N-11-20), and Medical Scientific Research Foundation of Guangdong Province, China (Granted No. A2016197).

SUPPLEMENTARY MATERIAL

The Supplementary Material for this article can be found online at: https://www.frontiersin.org/articles/10.3389/fonc.2020.625184/full#supplementary-material

REFERENCES

1. Bray F, Ferlay J, Soerjomataram I, Siegel RL, Torre LA, Jemal A. Global cancer statistics 2018: GLOBOCAN estimates of incidence and mortality worldwide for 36 cancers in 185 countries. *CA-Cancer J Clin* (2018) 68(6):394–424. doi: 10.3322/caac.21492
2. Ferlay J, Colombet M, Soerjomataram I, Mathers C, Parkin DM, Pineros M, et al. Estimating the global cancer incidence and mortality in 2018: GLOBOCAN sources and methods. *Int J Cancer* (2019) 144(8):1941–53. doi: 10.1002/ijc.31937
3. Chen Y-P, Chan ATC, Le Q-T, Blanchard P, Sun Y, Ma J. Nasopharyngeal carcinoma. *Lancet* (2019) 394(10192):64–80. doi: 10.1016/s0140-6736(19)30956-0
4. Ng WT, Lee MCH, Hung WM, Choi CW, Lee KC, Chan OSH, et al. Clinical Outcomes and Patterns of Failure After Intensity-Modulated Radiotherapy for Nasopharyngeal Carcinoma. *Int J Radiat Oncol Biol Phys* (2011) 79 (2):420–8. doi: 10.1016/j.ijrobp.2009.11.024
5. Setton J, Han J, Kannarunimit D, Wuu YR, Rosenberg SA, DeSelm C, et al. Long-term patterns of relapse and survival following definitive intensity-modulated radiotherapy for non-endemic nasopharyngeal carcinoma. *Oral Oncol* (2016) 53:67–73. doi: 10.1016/j.oraloncology.2015.11.015
6. Lee AWM, Ng WT, Chan LLK, Hung WM, Chan CCC, Sze HCK, et al. Evolution of treatment for nasopharyngeal cancer - Success and setback in the intensity-modulated radiotherapy era. *Radiother Oncol* (2014) 110(3):377–84. doi: 10.1016/j.radonc.2014.02.003
7. Sun XM, Su SF, Chen CY, Han F, Zhao C, Xiao WW, et al. Long-term outcomes of intensity-modulated radiotherapy for 868 patients with nasopharyngeal carcinoma: An analysis of survival and treatment toxicities. *Radiother Oncol* (2014) 110(3):398–403. doi: 10.1016/j.radonc.2013.10.020
8. Wang RS, Wu F, Lu HM, Wei B, Feng GS, Li GS, et al. Definitive intensity-modulated radiation therapy for nasopharyngeal carcinoma: long-term outcome of a multicenter prospective study. *J Cancer Res Clin Oncol* (2013) 139(1):139–45. doi: 10.1007/s00432-012-1313-0

9. Chan JYW, Tsang RKY, Wei WI. Morbidities after maxillary swing nasopharyngectomy for recurrent nasopharyngeal carcinoma. *Head Neck-J Sci Spec Head Neck* (2015) 37(4):487–92. doi: 10.1002/hed.23633
10. Chan JYW, Wei WI. Impact of resection margin status on outcome after salvage nasopharyngectomy for recurrent nasopharyngeal carcinoma. *Head Neck-J Sci Spec Head Neck* (2016) 38:E594–E9. doi: 10.1002/hed.24046
11. Han F, Zhao C, Huang SM, Lu LX, Huang Y, Deng XW, et al. Long-term Outcomes and Prognostic Factors of Re-irradiation for Locally Recurrent Nasopharyngeal Carcinoma using Intensity-modulated Radiotherapy. *Clin Oncol* (2012) 24(8):569–76. doi: 10.1016/j.clon.2011.11.010
12. Perri F, Scarpati GD, Caponigro F, Ionna F, Longo F, Buonopane S, et al. Management of recurrent nasopharyngeal carcinoma: current perspectives. *OncoTarg Ther* (2019) 12:1583–91. doi: 10.2147/ott.S188148
13. Sun XS, Liang YJ, Jia GD, Liu SL, Liu LT, Guo SS, et al. Establishment of a prognostic nomogram to identify optimal candidates for local treatment among patients with local recurrent nasopharyngeal carcinoma. *Oral Oncol* (2020) 106:7. doi: 10.1016/j.oraloncology.2020.104711
14. Li YQ, Tian YM, Tan SH, Liu MZ, Kusumawidjaja G, Ong EHW, et al. Prognostic Model for Stratification of Radioresistant Nasopharynx Carcinoma to Curative Salvage Radiotherapy. *J Clin Oncol* (2018) 36(9):891–+. doi: 10.1200/jco.2017.75.5165
15. Tanvetyanon T, Padhya T, McCaffrey J, Zhu WW, Boulware D, DeConti R, et al. Prognostic Factors for Survival After Salvage Reirradiation of Head and Neck Cancer. *J Clin Oncol* (2009) 27(12):1983–91. doi: 10.1200/jco.2008.20.0691
16. Sommat K, Yit NLF, Wang FQ, Lim JHC. Impact of comorbidity on tolerability and survival following curative intent intensity modulated radiotherapy in older patients with nasopharyngeal cancer. *J Geriatr Oncol* (2018) 9(4):352–8. doi: 10.1016/j.jgo.2018.01.006
17. Guo R, Mao YP, Chen L, Tang LL, Zhou GQ, Liu LZ, et al. Implication of comorbidity on the initiation of chemotherapy and survival outcomes in patients with locoregionally advanced nasopharyngeal carcinoma. *Oncotarget* (2017) 8(6):10594–601. doi: 10.18632/oncotarget.8621
18. Paleri V, Wight RG, Silver CE, Haigentz M, Takes RP, Bradley PJ, et al. Comorbidity in head and neck cancer: A critical appraisal and recommendations for practice. *Oral Oncol* (2010) 46(10):712–9. doi: 10.1016/j.oraloncology.2010.07.008
19. Piccirillo JF. Importance of comorbidity in head and neck cancer. *Laryngoscope* (2015) 125(10):2242. doi: 10.1002/lary.25278
20. Schimansky S, Lang S, Beynon R, Penfold C, Davies A, Waylen A, et al. Association between comorbidity and survival in head and neck cancer: Results from Head and Neck 5000. *Head Neck* (2019) 41(4):1053–62. doi: 10.1002/hed.25543
21. Tian YM, Huang WZ, Yuan X, Bai L, Zhao C, Han F. The challenge in treating locally recurrent T3-4 nasopharyngeal carcinoma: the survival benefit and severe late toxicities of re-irradiation with intensity-modulated radiotherapy. *Oncotarget* (2017) 8(26):43450–7. doi: 10.18632/oncotarget.15896
22. Camp RL, Dolled-Filhart M, Rimm DL. X-tile: A new bio-informatics tool for biomarker assessment and outcome-based cut-point optimization. *Clin Cancer Res* (2004) 10(21):7252–9. doi: 10.1158/1078-0432.Ccr-04-0713
23. Jin YN, Zhang WJ, Cai XY, Li MS, Lawrence WR, Wang SY, et al. The Characteristics and Survival Outcomes in Patients Aged 70 Years and Older with Nasopharyngeal Carcinoma in the Intensity-Modulated Radiotherapy Era. *Cancer Res Treat* (2019) 51(1):34–42. doi: 10.4143/crt.2017.551
24. Guo R, Chen XZ, Chen L, Jiang F, Tang LL, Mao YP, et al. Comorbidity predicts poor prognosis in nasopharyngeal carcinoma: Development and validation of a predictive score model. *Radiother Oncol* (2015) 114(2):249–56. doi: 10.1016/j.radonc.2014.12.002
25. Koutcher L, Lee N, Zelefsky M, Chan K, Cohen G, Pfister D, et al. Reirradiation of locally recurrent nasopharynx cancer with external beam radiotherapy with or without brachytherapy. *Int J Radiat Oncol Biol Phys* (2010) 76(1):130–7. doi: 10.1016/j.ijrobp.2009.01.055
26. Poon D, Yap SP, Wong ZW, Cheung YB, Leong SS, Wee J, et al. Concurrent chemoradiotherapy in locoregionally recurrent nasopharyngeal carcinoma. *Int J Radiat Oncol Biol Phys* (2004) 59(5):1312–8. doi: 10.1016/j.ijrobp.2004.01.037
27. Chua DTT, Sham JST, Au GKH. Induction chemotherapy with cisplatin and gemcitabine followed by reirradiation for locally recurrent nasopharyngeal carcinoma. *Am J Clin Oncol-Cancer Clin Trials* (2005) 28(5):464–71. doi: 10.1097/01.coc.0000180389.86104.68
28. Leong YH, Soon YY, Lee KM, Wong LC, Tham IWK, Ho FCH. Long-term outcomes after reirradiation in nasopharyngeal carcinoma with intensity-modulated radiotherapy: A meta-analysis. *Head Neck-J Sci Spec Head Neck* (2018) 40(3):622–31. doi: 10.1002/hed.24993
29. Ng WT, Ngan RKC, Kwong DLW, Tung SY, Yuen KT, Kam MKM, et al. Prospective, Multicenter, Phase 2 Trial of Induction Chemotherapy Followed by Bio-Chemoradiotherapy for Locally Advanced Recurrent Nasopharyngeal Carcinoma. *Int J Radiat Oncol Biol Phys* (2018) 100(3):630–8. doi: 10.1016/j.ijrobp.2017.11.038
30. Hsu C, Lee SH, Ejadi S, Even C, Cohen RB, Le Tourneau C, et al. Safety and Antitumor Activity of Pembrolizumab in Patients With Programmed Death-Ligand 1-Positive Nasopharyngeal Carcinoma: Results of the KEYNOTE-028 Study. *J Clin Oncol* (2017) 35(36):4050–+. doi: 10.1200/jco.2017.73.3675
31. Ma BBY, Lim WT, Goh BC, Hui EP, Lo KW, Pettinger A, et al. Antitumor Activity of Nivolumab in Recurrent and Metastatic Nasopharyngeal Carcinoma: An International, Multicenter Study of the Mayo Clinic Phase 2 Consortium (NCI-9742). *J Clin Oncol* (2018) 36(14):1412–+. doi: 10.1200/jco.2017.77.0388
32. Fang WF, Yang YP, Ma YX, Hong SD, Lin LZ, He XH, et al. Camrelizumab (SHR-1210) alone or in combination with gemcitabine plus cisplatin for nasopharyngeal carcinoma: results from two single-arm, phase 1 trials. *Lancet Oncol* (2018) 19(10):1338–50. doi: 10.1016/s1470-2045(18)30495-9
33. Tian YM, Zhao C, Guo Y, Huang Y, Huang SM, Deng XW, et al. Effect of Total Dose and Fraction Size on Survival of Patients With Locally Recurrent Nasopharyngeal Carcinoma Treated With Intensity-Modulated Radiotherapy: A Phase 2, Single-Center, Randomized Controlled Trial. *Cancer* (2014) 120(22):3502–9. doi: 10.1002/cncr.28934
34. Ng WT, Lee MCH, Fung NTC, Wong ECY, Cheung AKW, Chow JCH, et al. Dose volume effects of re-irradiation for locally recurrent nasopharyngeal carcinoma. *Head Neck-J Sci Spec Head Neck* (2020) 42(2):180–7. doi: 10.1002/hed.25988
35. Gao J, Tao YL, Li G, Yi W, Xia YF. Involvement of difference in decrease of hemoglobin level in poor prognosis of Stage I and II nasopharyngeal carcinoma: implication in outcome of radiotherapy. *Int J Radiat Oncol Biol Phys* (2012) 82(4):1471–8. doi: 10.1016/j.ijrobp.2011.05.009
36. Tang LQ, Li CF, Li J, Chen WH, Chen QY, Yuan LX, et al. Establishment and Validation of Prognostic Nomograms for Endemic Nasopharyngeal Carcinoma. *J Natl Cancer Inst* (2016) 108(1):djv291. doi: 10.1093/jnci/djv291
37. Topkan E, Ekici NY, Ozdemir Y, Besen AA, Yildirim BA, Mertsoylu H, et al. Baseline hemoglobin <11.0 g/dL has stronger prognostic value than anemia status in nasopharynx cancers treated with chemoradiotherapy. *Int J Biol Markers* (2019) 34(2):139–47. doi: 10.1177/1724600818821688
38. Liu TB, Zheng ZH, Pan J, Pan LL, Chen LH. Prognostic role of plasma Epstein-Barr virus DNA load for nasopharyngeal carcinoma: a meta-analysis. *Clin Invest Med* (2017) 40(1):E1–E12. doi: 10.25011/cim.v40i1.28049
39. Kim KY, Le QT, Yom SS, Pinsky BA, Bratman SV, Ng RHW, et al. Current State of PCR-Based Epstein-Barr Virus DNA Testing for Nasopharyngeal Cancer. *JNCI-J Natl Cancer Inst* (2017) 109(4):7. doi: 10.1093/jnci/djx007

Conflict of Interest: The authors declare that the research was conducted in the absence of any commercial or financial relationships that could be construed as a potential conflict of interest.

frontiers in Oncology

ORIGINAL RESEARCH
published: 10 February 2021
doi: 10.3389/fonc.2020.600525

Prognosis and Prophylactic Regional Nodal Irradiation in Breast Cancer Patients With the First Isolated Chest Wall Recurrence After Mastectomy

Xu-Ran Zhao[1†], Liang Xuan[2†], Jun Yin[1], Yu Tang[1], Hui-Ru Sun[2], Hao Jing[1], Yong-Wen Song[1], Jing Jin[1], Yue-Ping Liu[1], Hui Fang[1], Hua Ren[1], Bo Chen[1], Yuan Tang[1], Ning Li[1], Shu-Nan Qi[1], Ning-Ning Lu[1], Yong Yang[1], Ye-Xiong Li[1], Bing Sun[2], Shi-Kai Wu[2,3*] and Shu-Lian Wang[1*]*

[1] Department of Radiation Oncology, National Cancer Center/National Clinical Research Center for Cancer/Cancer Hospital, Chinese Academy of Medical Sciences and Peking Union Medical College, Beijing, China, [2] Department of Radiation Oncology, The Fifth Medical Center, Chinese People's Liberation Army (PLA) General Hospital, Beijing, China, [3] Department of Medical Oncology, Peking University First Hospital, Beijing, China

Background and Purpose: Optimal radiation target volumes for breast cancer patients with their first isolated chest wall recurrence (ICWR) after mastectomy are controversial. We aimed to analyze the regional failure patterns and to investigate the role of prophylactic regional nodal irradiation (RNI) for ICWR.

Materials and Methods: Altogether 205 patients with ICWR after mastectomy were retrospectively analyzed. Post-recurrence progression-free survival (PFS) and overall survival (OS) rates were calculated by Kaplan-Meier method and the differences were compared with Log-rank test. Competing risk model was used to estimate the subsequent regional recurrence (sRR) and locoregional recurrence (sLRR) rates, and the differences were compared with Gray test.

Results: The 5-year sRR rate was 25.2% with median follow-up of 88.6 months. Of the 52 patients with sRR, 30 (57.7%) recurred in the axilla, 29 (55.8%) in supraclavicular fossa (SC), and five (9.6%) in internal mammary nodes. Surgery plus radiotherapy was independently associated with better sLRR and PFS rates ($p<0.001$). The ICWR interval of ≤ 4 years was associated with unfavorable sRR ($p=0.062$), sLRR ($p=0.014$), PFS ($p=0.001$), and OS ($p=0.005$). Among the 157 patients who received radiotherapy after ICWR, chest wall plus RNI significantly improved PFS ($p=0.004$) and OS ($p=0.021$) compared with chest wall irradiation alone. In the 166 patients whose ICWR interval was ≤ 4 years, chest wall plus RNI provided the best PFS ($p<0.001$) and OS ($p=0.022$) compared with chest wall irradiation alone or no radiotherapy.

Conclusion: Patients with ICWR have a high-risk of sRR in SC and axilla. Chest wall plus RNI is recommended.

Keywords: breast neoplasm, chest wall recurrence, regional failure patterns, radiotherapy, regional nodal irradiation

OPEN ACCESS

Edited by:
Francesco Cellini, Catholic University of the Sacred Heart, Italy

Reviewed by:
Ruijie Yang, Peking University Third Hospital, China
Jian-Guo Zhou, University of Erlangen Nuremberg, Germany
Jee Suk Chang, Yonsei University, South Korea

***Correspondence:**
Shu-Lian Wang
wsl20040118@yahoo.com
Bing Sun
sunice116@163.com
Shi-Kai Wu
skywu4923@sina.com

†These authors have contributed equally to this work and share first authorship

Specialty section:
This article was submitted to Radiation Oncology, a section of the journal Frontiers in Oncology

Received: *30 August 2020*
Accepted: *14 December 2020*
Published: *10 February 2021*

Citation:
Zhao X-R, Xuan L, Yin J, Tang Y, Sun H-R, Jing H, Song Y-W, Jin J, Liu Y-P, Fang H, Ren H, Chen B, Tang Y, Li N, Qi S-N, Lu N-N, Yang Y, Li Y-X, Sun B, Wu S-K and Wang S-L (2021) Prognosis and Prophylactic Regional Nodal Irradiation in Breast Cancer Patients With the First Isolated Chest Wall Recurrence After Mastectomy. Front. Oncol. 10:600525. doi: 10.3389/fonc.2020.600525

INTRODUCTION

Breast cancer is a common malignancy in women worldwide, and mastectomy is one important surgical procedure. With multimodality management, approximately 5 to 30% of breast cancer patients recurred at locoregional sites after mastectomy. Among them, 2/3 developed an isolated locoregional recurrence (LRR) without concomitant distant metastasis (DM) (1–4). The chest wall is a frequent site for isolated LRR. Several previous studies have demonstrated that the prognosis of isolated chest wall recurrence (ICWR) is better than isolated LRR involving regional lymph nodes, and a substantial proportion of patients with ICWR can enjoy a long-term survival after curative therapy (5–8).

Patients with ICWR are often treated with multimodality approaches, including excision of the recurrent tumor, radiotherapy, and systemic therapy. However, controversy exists as to the optimal radiation target volumes for isolated LRR, with most advocating irradiation of all local and regional areas (9), whereas others recommending elective irradiation of the chest wall and selected nodal regions (5, 10), or involved field radiotherapy only (11). The value of prophylactic regional nodal irradiation (RNI) for patients with ICWR has not been fully assessed, and the results have been hampered either by the research population or by the time period studied. Further, modern systemic therapy has not only decreased the risk of DM, but has also decreased the risk of LRR, which has raised the question concerning the value of RNI in the contemporary era.

The present retrospective study aimed to assess the prognosis and the incidence and patterns of subsequent locoregional recurrence in breast cancer patients with ICWR, and to evaluate the role of prophylactic RNI.

MATERIALS AND METHODS

A total of 928 breast cancer patients with chest wall recurrence following mastectomy were treated at the National Cancer Center and Chinese PLA General Hospital from October 1998 to April 2018. ICWR was defined as any relapse within the ipsilateral chest wall without prior or concomitant relapse in other sites, and all recurrences were confirmed by pathologic or radiographic evidence. Upon review of the patients we identified, 205 eligible patients with ICWR met the following criteria: no prior relapse in other sites, no regional (axillary, supraclavicular, or internal mammary lymph node) recurrence or DM within 1 month of chest wall recurrence, no postmastectomy radiotherapy, no supraclavicular or internal mammary nodal metastasis at initial diagnosis, and no second malignancies (**Figure 1**). The complete medical records of eligible patients were reviewed, and follow-up data were obtained from hospital records or from correspondence directly with the patient or their family. Computed tomography and nodal ultrasound were routinely used for follow-up. The present study was approved by the Institutional Review Board of Cancer Hospital, Chinese Academy of Medical Sciences (approval number 15-057/984) and the Institutional Review Board of the Fifth Medical Center, Chinese PLA General Hospital (approval number ky-2020-5-8).

The ICWR interval was defined as the time from mastectomy to the date of diagnosis of ICWR. The endpoints included subsequent regional recurrence (sRR), subsequent locoregional recurrence (sLRR), progression-free survival (PFS), and overall survival (OS). sRR was defined as any recurrence within the ipsilateral axillary, supraclavicular fossa (SC), or internal mammary nodes (IMN) after salvage treatment for ICWR. sLRR was defined as the disease progression within the chest wall and/or sRR. PFS event was defined as sLRR, DM, or death attributed to any cause. OS event was defined as death attributed to any cause. Time to survival and/or failure was calculated from the date of diagnosis of ICWR.

The Kaplan-Meier method was used to calculate the survival rates, and the differences were compared using the Log-rank test. The competing risk model was used to estimate the sRR, sLRR, and DM rates, and the differences were compared using the Gray test. Competing risk events for sRR, sLRR, and DM were death without sRR, death without sLRR and death without DM, respectively. Multivariate analysis was performed using Cox logistic and Fine–Gray regression. In addition, we used the Maxstat method to identify the optimal cut-off value of ICWR interval for outcomes (12). The characteristics of the subjects were compared using the Fisher exact or $\chi 2$ test. Statistical analyses were performed using cmprsk (https://cran.r-project.org/web/packages/cmprsk/) and Maxstat (https://cran.r-project.org/web/packages/maxstat/index.html) package in R v3.6.0 (http://www.r-project.org/) and SPSS Statistics v24.0 (IBM Corp., Armonk, NY, USA). All P values were two-sided, and a value of less than 0.05 was considered to be significant.

RESULTS

Patient Characteristics

Of the 205 patients, 200 (97.6%) patients were pathologically confirmed with ICWR from surgical specimens (n=151) or fine needle aspirations (n=49), and five (2.4%) were diagnosed clinically. The median age at the initial diagnosis of breast cancer was 47 years old (range of 20–90 years old). All patients received a mastectomy. Axillary lymph node dissection was performed in 203 (99.0%) patients, and two (1.0%) patients with pN0 disease underwent sentinel node biopsy alone. The median number of nodes examined was 15 (range of 3–40). The patient, tumor, and treatment characteristics are summarized in **Table 1**. The median interval from mastectomy to ICWR was 20.9 months (range of 1.5–152.7 months). The median size of the ICWR was 1.5 cm (range of 0.3–20.0 cm). After ICWR, 147 (71.7%) patients received chemotherapy, 97 (47.3%) received endocrine therapy, and nine (4.4%) received anti-HER2 targeted therapy. A total of 151 (73.7%) patients received surgery; among them, 82 (54.3%) had R0, three (1.9%) R1, six (4.0%) R2, 59 (39.1%) Rx chest wall tumor resection alone, and one (0.7%) had Rx chest wall tumor resection plus axillary lymph node dissection. A total of 157 (76.6%) patients received irradiation

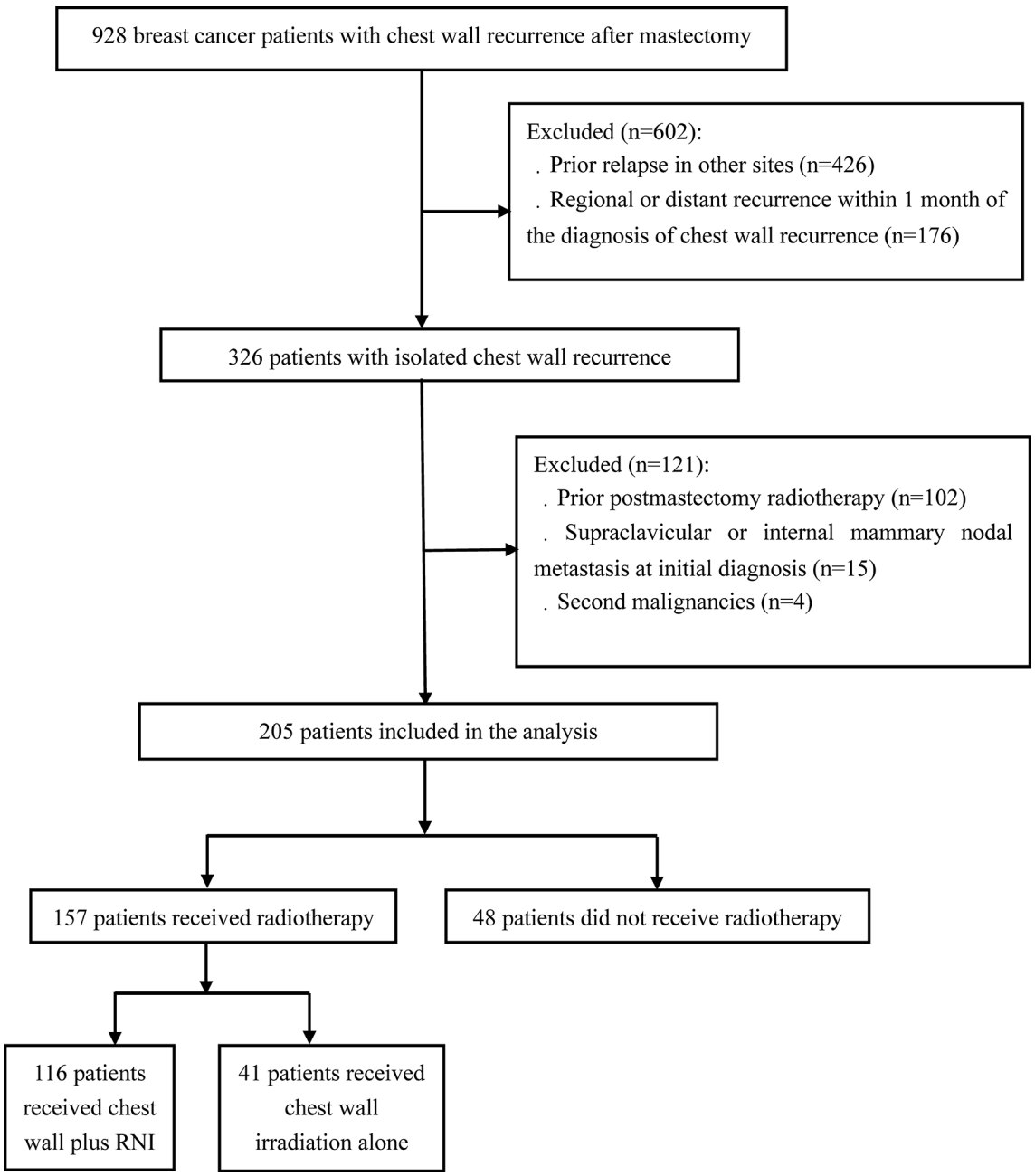

FIGURE 1 | Flow diagram of breast cancer patients included in the study.

to the chest wall ± regional nodes with conventional fractionation. CT-based radiotherapy technique has not been used until 2016, and most patients were treated with two-dimensional radiotherapy technique. A large field encompassing the entire chest wall was used in all patients to deliver a median total dose of 50 Gy (range of 10–73.5 Gy). A local "boost" therapy was used in 80 (51.0%) patients, and the median total dose to recurrent tumor or tumor bed after resection was 65 Gy (range of 50–76 Gy). Bolus was routinely used for at least 60% course of radiotherapy to the chest wall. Among the 116 (73.9%) patients who received RNI, 115 (99.1%) were given SC irradiation, 16 (13.8%) received axillary irradiation, and five (4.3%) received IMN irradiation. The nodal sites were treated to a median dose of 50 Gy (range of 20–64 Gy).

Outcomes and Failure Patterns of the Entire Cohort

Following a median follow-up of 88.6 months (range of 1.6–220.6 months) after ICWR, there were 160 (78.0%) patients that

TABLE 1 | Patient, tumor, and treatment characteristics of 205 breast cancer patients with ICWR.

Characteristics	No. of Patients (%)
Age at initial diagnosis (years)	
≤50	134 (65.4)
>50	71 (34.6)
Initial Location	
Inner/central quadrant	49 (23.9)
Other quadrants	99 (48.3)
Unknown	57 (27.8)
Initial staging*	
I–II	161 (78.5)
III	37 (18.0)
Unknown	7 (3.4)
Initial histological grade	
I–II	77 (37.6)
III	33 (16.1)
Unknown	95 (46.3)
Initial chemotherapy	
Yes	190 (92.7)
No	15 (7.3)
Initial endocrine therapy†	
Yes	100 (75.2)
No	32 (24.1)
Unknown	1 (0.8)
Initial anti-HER2 target therapy‡	
Yes	2 (5.6)
No	33 (91.7)
Unknown	1 (2.8)
ICWR interval (years)	
≤4	166 (80.9)
>4	39 (19.1)
No. of ICWRs	
1	169 (82.4)
2	11 (5.4)
≥3	20 (9.8)
Unknown	5 (2.4)
Molecular subtype#	
Luminal-HER2 negative	100 (48.8)
Luminal-HER2 positive	22 (10.7)
HER2-enriched	16 (7.8)
Triple-negative	48 (23.4)
Unknown	19 (9.3)
Treatment modalities for ICWR	
Locoregional treatment alone	26 (12.7)
Systemic treatment alone	22 (10.7)
Locoregional + systemic treatment	157 (76.6)
Locoregional treatment for ICWR	
Surgery + radiotherapy	125 (61.0)
Radiotherapy alone	32 (15.6)
Surgery alone	26 (12.7)
None	22 (10.7)

HER2, human epidermal growth factor receptor 2.

**For the 17 patients that received neoadjuvant chemotherapy, we used the stage that was higher (clinical or pathological) to reflect the initial tumor burden; †Only hormone-receptor positive patients were included; ‡Only HER2 positive patients were included. # For the 92 patients who had sufficient information for determination of the molecular subtype of ICWR, we used the molecular subtypes of ICWR. For the 94 patients who only had sufficient information for determination of the molecular subtype at initial diagnosis, we used the initial molecular subtypes.*

experienced subsequent recurrence. The results of the first failure were as follows: locoregional in 63 (39.4%) patients, distant in 73 (45.6%) patients, and simultaneous locoregional and distant in 24 (15.0%) patients. A total of 103 (50.2%) patients developed sLRR. The 5-year cumulative sLRR rate was 49.0%, and the median interval from ICWR to sLRR was 12.5 months (range of 1.2–118.7 months). A total of 52 (25.4%) patients developed sRR. The 5-year cumulative sRR rate was 25.2%, and the median interval from ICWR to sRR was 13.8 months (range to 1.9–117.3 months). A total of 138 (67.3%) patients developed DM and 103 (50.2%) patients died. The 5-year cumulative PFS rate was 22.7%, and the median PFS after ICWR was 16.1 months (range of 1.2–117.3 months). The 5-year cumulative OS rate was 53.9%, and the median OS after ICWR was 65.9 months (range of 7.6–162.6 months).

Among 103 patients who developed sLRR, 31 (30.1%) had regional node recurrence only, 21 (20.4%) had both regional node and chest wall recurrences, and 51 (49.5%) had chest wall recurrence only. Of the 52 patients with sRR, 30 (57.7%) recurred in the axilla, 29 (55.8%) in the SC, and five (9.6%) in the IMN (**Figure 2**).

There were 186 patients who had sufficient information for determination of the molecular subtype of breast cancer (**Table 1**). For sLRR patients with luminal-HER2 negative, luminal-HER2 positive, HER2-enriched, and triple-negative tumors, 16 (31.4%), 6 (54.5%), 2 (20.0%), 3 (15.0%) had regional node recurrence only, 10 (19.6%), 1 (9.1%), 4 (40.0%), 4 (20.0%) had both regional node and chest wall recurrences, and 25 (49.0%), 4 (36.4%), 4 (40.0%), 13 (65.0%) had chest wall recurrence only. For sRR patients with luminal-HER2 negative, luminal-HER2 positive, HER2-enriched, and triple-negative tumors, 13 (50.0%), 3 (42.9%), 5 (83.3%), 5 (71.4%) recurred in the axilla, 14 (53.8%), 4 (57.1%), 4 (66.7%), 4 (57.1%) in the SC, and 2 (7.7%), 0 (0.0%), 2 (33.3%), 1 (14.3) in the IMN (**Figure 3**).

The Role of Locoregional Treatment for ICWR of the Entire Cohort

A total of 125 (61.0%) patients received surgery plus radiotherapy, and 80 (39.0%) patients received either surgery or radiotherapy alone, or no locoregional therapy (**Table 1**). The characteristics were well balanced between the four groups (surgery + radiotherapy, surgery alone, radiotherapy alone and none) (**Supplementary Table 1**). Surgery plus radiotherapy was associated with better sLRR and PFS compared with other therapies, and there was a nonsignificant trend toward improved OS with surgery plus radiotherapy compared with other therapies, and there was no difference in sRR between the two groups (**Figure 4**).

Maxstat analysis showed that as an sRR prognostic factor, the optimal cut-off value of ICWR interval was 4.0 years. The univariate analysis showed that an ICWR interval of ≤ 4 years was an unfavorable prognostic factor for sRR, sLRR, PFS, and OS (**Supplementary Table 2**). The multivariate analysis included the most relevant prognostic variables identified from univariate analysis (initial age, initial staging, molecular subtype, ICWR interval ≤ 4 years, locoregional treatment and treatment modalities for ICWR). Surgery plus radiotherapy was an independent favorable prognostic factor for PFS. Locoregional plus systemic treatment was independent favorable prognostic

factors for both PFS and OS. ICWR interval of > 4 years was an independent favorable prognostic factor for sRR, sLRR, PFS, and OS. Initial stage and molecular subtype were independent prognostic factors for OS (**Table 2**).

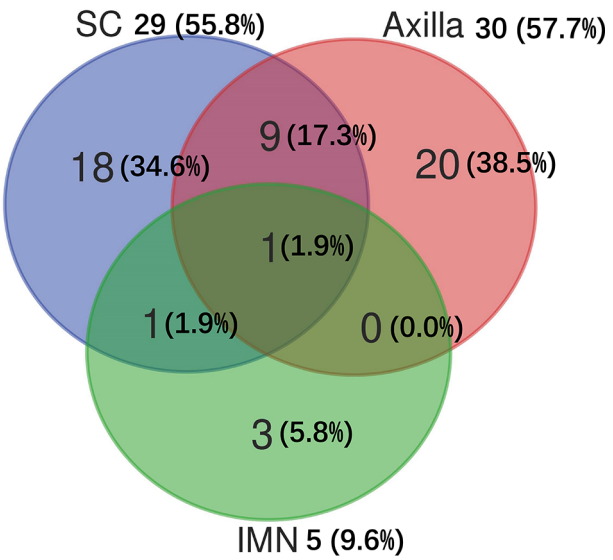

FIGURE 2 | Distribution of subsequent regional recurrences in 52 breast cancer patients. IMN, Internal mammary nodes; SC, Supraclavicular fossa.

Effect of Regional Nodal Irradiation on the Prognosis

Among the 157 patients who received radiotherapy after ICWR, 41 (26.1%) patients received chest wall irradiation alone, and 116 (73.9%) patients received chest wall plus RNI. The characteristics of the two groups are shown in **Supplementary Table 3**. The characteristics were well balanced between the two groups; however, the chest wall plus RNI group had more patients who were >50 years old (p = 0.020) and had ≥ 2 sites of ICWR (p = 0.017). The chest wall plus RNI group showed significantly better PFS and OS than the chest wall irradiation alone group, and there were no differences in sRR or sLRR between the two groups (**Figure 5**). The chest wall plus RNI group showed significantly lower DM than that of the chest wall irradiation alone group (59.0% vs. 79.2% at 5 years, p = 0.003).

The ICWR interval of ≤ 4 years was the variable most strongly predictive of adverse sRR, and the 5-year sRR rate was 28.8% and 9.0% for patients whose ICWR interval of ≤ 4 years and >4 years (p = 0.019), therefore, the influence of RNI was evaluated in 166 patients whose ICWR interval was ≤ 4 years. Chest wall plus RNI (n=94) provided the best OS and PFS compared with patients who received chest wall irradiation alone (n=36) or no radiotherapy (n=36). There was a nonsignificant trend toward reduced sLRR with chest wall plus RNI compared with chest wall irradiation alone or no radiotherapy, but no differences in sRR were detected among the three groups (**Figure 6**). Chest wall plus RNI significantly reduced the risk of DM as compared with chest wall irradiation alone or no radiotherapy (59.1 vs. 77.8 vs. 75.0% at 5 years, p = 0.004).

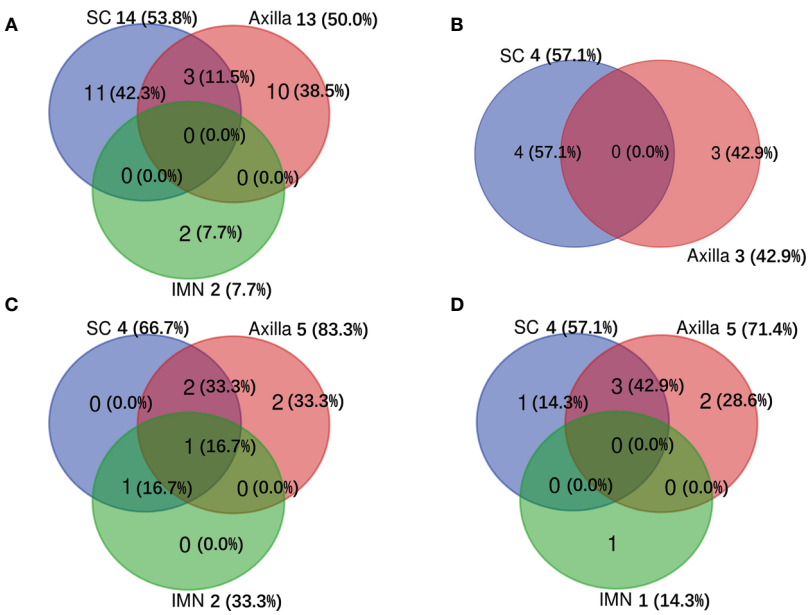

FIGURE 3 | Distribution of subsequent regional recurrences among different molecular subtypes of breast cancer. **(A)** for luminal-HER2 negative, **(B)** for luminal-HER2 positive, **(C)** for HER2-enriched, and **(D)** for triple-negative tumors. IMN, Internal mammary nodes; SC, Supraclavicular fossa.

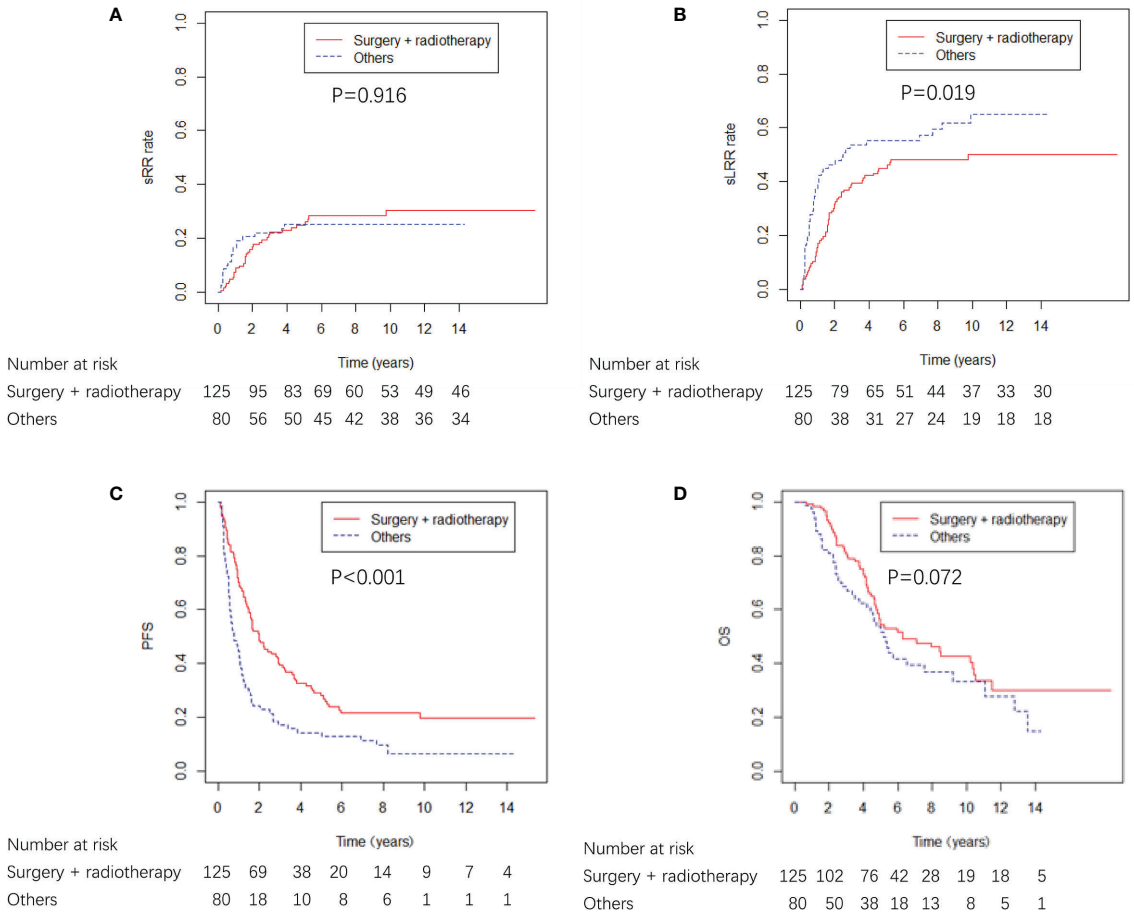

FIGURE 4 | sRR, sLRR, PFS, and OS curves from locoregional treatment given to breast cancer patients with ICWR.

DISCUSSION

In the present study, we found that the sLRR risk was high in patients with ICWR, which indicates the indispensability of locoregional treatment, including both surgery and radiotherapy. Surgical excision is generally the preferred initial treatment. Thus, not only the tumor burden is reduced, but also histological and immunohistochemical diagnosis of the recurrence can be established to help determine systemic-treatment decisions. Early reports have revealed that excision alone results in sLRR rates of 60–75% (13, 14), which indicates the need for adjuvant radiotherapy. In previous studies, surgery plus radiotherapy has been demonstrated to achieve better survival outcome than either surgery or radiotherapy alone (8, 14, 15). Our results showed that surgery plus radiotherapy was an independent favorable prognostic factor for PFS but not for OS in the multivariate analysis. The failure of surgery plus radiotherapy to improve OS could be attributable to the insufficient number of patients analyzed in our study, or the improvements in the effectiveness of systemic therapy as salvage therapy for the subsequent recurrence after the ICWR. Since there was a significant improved PFS (HR 1.89, 95%CI 1.32–2.70; p = 0.001) and a nonsignificant trend toward improved OS with surgery plus radiotherapy (HR 1.27, 95%CI 0.82–1.97; p = 0.279), comprehensive locoregional treatment, including both surgery and radiotherapy, was recommended for these patients.

Previous reports have shown that sLRR not only reduced the quality of life, but also portended an unfavorable survival outcome (5, 16). Our results showed that 50.2% of patients developed sLRR, among which sRR accounted for 50.5%. Multivariate analysis demonstrated that ICWR interval was an important non-treatment-related prognostic factor for sRR (HR 2.9), sLRR (HR 2.3), PFS (HR 2.0) and OS (HR 2.3), which indicated the discrepancy in biological aggressiveness between patients whose ICWR interval was >4 years and those with earlier recurrence. Previous studies have shown that the survival following locoregional and systemic therapies for isolated LRR might be adversely affected by short interval from mastectomy to recurrence (6, 17), some showed that the disease-free interval of less than 1 year was significantly associated with worse OS (18, 19), while most studies observed the disease-free interval of less than 2 years was significantly associated with worse locoregional

TABLE 2 | Multivariate analysis of sRR, sLRR, PFS, and OS in 205 breast cancer patients with ICWR.

Variable	sRR		sLRR		PFS		OS	
	HR (95% CI)	P	HR (95% CI)	P	HR (95% CI)	P	HR (95% CI)	P
Age at initial diagnosis		0.500		0.900		0.455		0.180
≤50 years	1.00		1.00		1.00		1.00	
>50 years	1.23 (0.67–2.25)		0.97 (0.61–1.54)		0.87 (0.61–1.25)		1.34 (0.87–2.06)	
Initial stage		0.210		0.910		0.235		0.021
I–II	1.00		1.00		1.00		1.00	
III	0.55 (0.21–1.42)		1.03 (0.58–1.85)		1.30 (0.84–2.02)		1.86 (1.10–3.14)	
Molecular subtype#		0.230		0.360		0.283		0.002
Luminal-HER2 negative	1.00		1.00		1.00		1.00	
Luminal-HER2 positive	1.17 (0.53–2.57)		0.74 (0.39–1.40)		1.19 (0.71–1.99)		1.49 (0.80–2.79)	
HER2-enriched	1.49 (0.57–3.86)		1.16 (0.56–2.41)		1.36 (0.77–2.41)		3.36 (1.69–6.67)	
Triple-negative	0.51 (0.21–1.23)		0.72 (0.40–1.29)		0.78 (0.50–1.20)		0.86 (0.51–1.44)	
ICWR interval		0.034		0.008		0.003		0.012
>4 years	1.00		1.00		1.00		1.00	
≤4 years	2.94 (1.08–7.99)		2.31 (1.25–4.27)		1.99 (1.26–3.15)		2.25 (1.20–4.24)	
Locoregional treatment for recurrence		0.540		0.150		0.001		0.279
Surgery + radiotherapy	1.00		1.00		1.00		1.00	
Others	0.81 (0.42–1.56)		1.39 (0.88–2.18)		1.89 (1.32–2.70)		1.27 (0.82–1.97)	
Treatment modalities for recurrence		0.680		0.300		0.004		<0.001
Locoregional + systemic treatment	1.00		1.00		1.00		1.00	
Locoregional or systemic treatment alone	1.18 (0.54–2.55)		1.33 (0.78–2.29)		1.86 (1.22–2.81)		2.73 (1.69–4.39)	

HER2, human epidermal growth factor receptor 2.

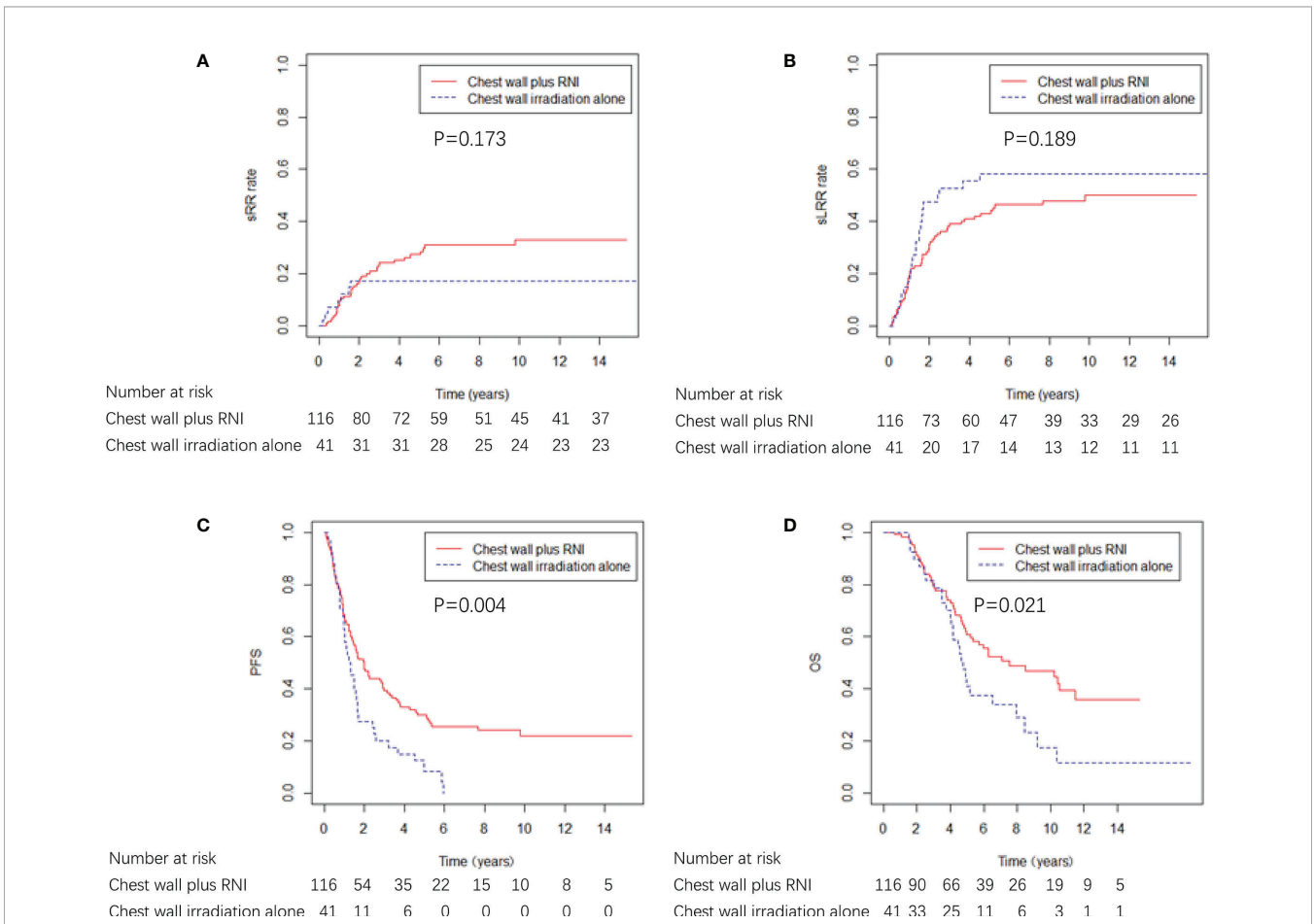

FIGURE 5 | sRR, sLRR, PFS, and OS curves by radiation volume in 157 breast cancer patients that received radiotherapy.

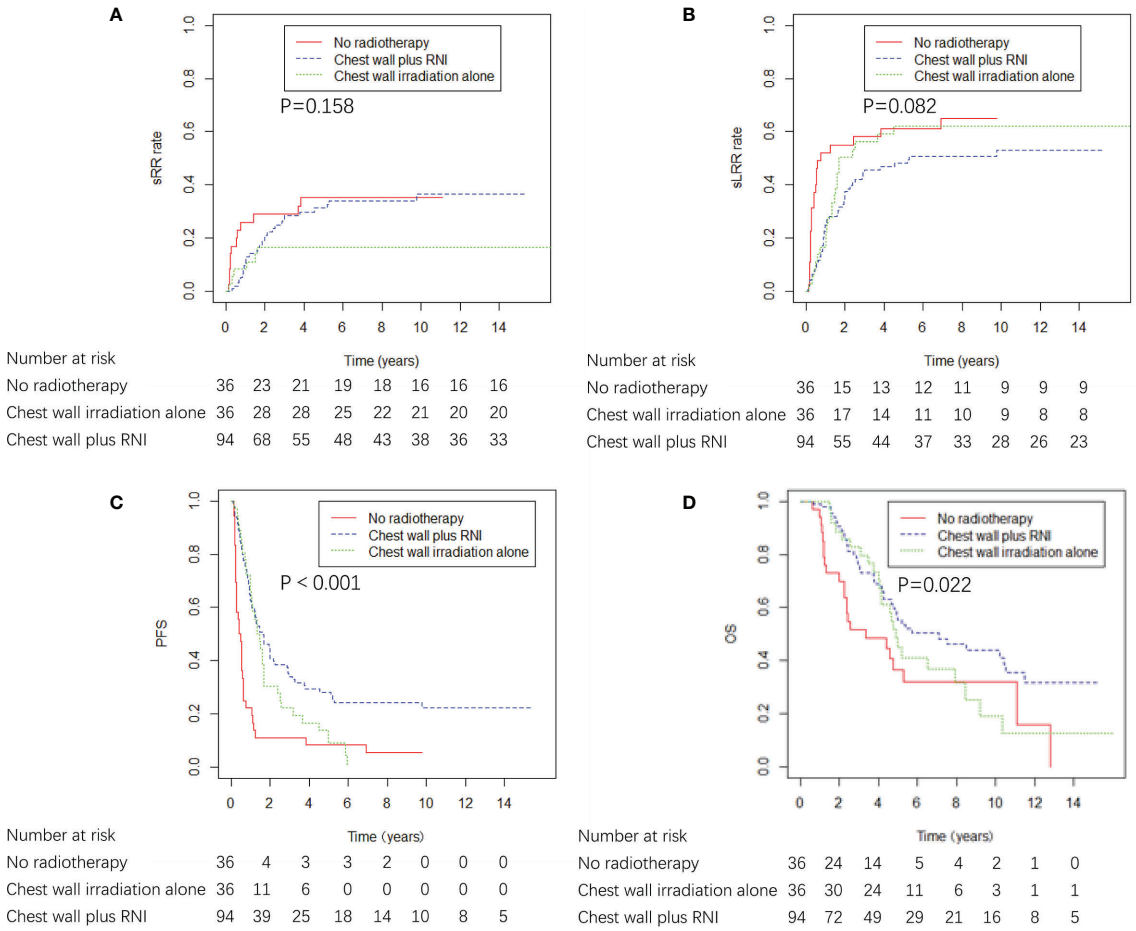

FIGURE 6 | sRR, sLRR, PFS, and OS curves by radiation volume in 166 breast cancer patients whose ICWR interval was ≤ 4 years.

control (14), distant metastasis-free survival (20, 21), PFS (15, 21) or OS (14, 15, 19–23). However, the interval they used as a cut-off was generally defined according to their experience. To the best of our knowledge, our study is the first one to use sRR as a primary endpoint in order to evaluate the effect of RNI on the prognosis for patients with ICWR. In addition, we used the Maxstat method to identify the optimal cut-off value of ICWR interval for outcomes, which is more reasonable. Early isolated LRR events represent biologically aggressive disease, whereas late recurrences indicate indolent disease (24). Thus, more effective local treatment, such as chest wall plus RNI, may be warranted in patients with early isolated LRR. Only a few previous studies have analyzed prognostic factors for sLRR and sRR by multivariate analysis, and showed that ER status of the recurrent tumor (14, 21, 25), lymphovascular invasion of the recurrent tumor (25), and initial staging (24) were associated with sLRR. In addition, ER status along with lymphovascular invasion of the recurrent tumor (25) were associated with sRR. The differences between the previous reports and the present study is explained by the type of patient population. Most previous studies have included patients with various LRR patterns rather than only ICWR (14, 21, 24), and some studies have only analyzed patients with ipsilateral breast tumor recurrence after breast-conserving surgery (25). Furthermore, the use of a more effective systemic therapy in our study possibly effected the prognosis.

There was no consistent plan with regard to irradiation volume for either inclusion or exclusion of uninvolved regions in patients with ICWR. Our results showed that chest wall plus RNI significantly improved PFS and OS compared no RNI in patients who received radiotherapy and in patients whose ICWR interval was ≤ 4 years, which indicates the necessity for RNI in these patients. The effect of RNI on survival may be due to decreased risk of both sLRR and DM by irradiation of subclinical disease in regional sites, thus preventing the dissemination of neoplastic cells. A recently published study revealed that 85.8% of patients with *de novo* metastatic breast cancer harbor regional lymph node disease at presentation (26), which is consistent with the hypothesis that regional involvement may precede metastatic dissemination. That is a possible explanation for our results and

the previous findings that RNI reduces distant recurrences (27–30). The value of prophylactic RNI has been a topic of debate; some studies have suggested that the risk of developing subsequent failures in uninvolved sites is low after involved-field radiotherapy only encompassing the recurrence sites (14, 19). However, Chen et al. reported that the percentage of sRR was 20% in patients with ICWR after chest wall irradiation alone (5). Toonkel et al. reported a survival advantage with prophylactic RNI (9), but Deutsch et al. reported a better 5-year OS for patients receiving chest wall irradiation alone for ICWR compared with patients receiving chest wall plus RNI (11). Similar results were observed by Willner et al., whose findings showed a significant survival advantage with recurrence-site irradiation alone over total locoregional irradiation for patients with isolated LRR (18). Two previous studies showed that the second recurrence rate in the SC was reduced in patients that received prophylactic SC irradiation (10, 13). Patients treated with radiotherapy to a limited target volume probably had less tumor burden than those treated more extensively (11, 18), thus the advantage of recurrence-site irradiation alone should be interpreted with reservation. Most previous studies included patients with various LRR patterns and some did not exclude patients with initial post-mastectomy radiotherapy. Moreover, the sample size was quite small and the follow-up time maybe not long enough to observe the distinction between different patient groups. Systemic treatments as adjuvant or salvage therapies varied considerably due to the different time period studied. Whereas our study included a large number of patients with pure ICWR, mainly treated with modern systemic therapies, which have decreased the incidence of subsequent distant dissemination and made it possible for enlarging irradiation volume to provide superior outcomes.

In our cohort, 56.6% of the patients had received prophylactic RNI, and the 5-year sRR rate was 25.2%. The studies on the LRR patterns after ICWR were scarce. The failure patterns were associated with both disease status and upfront treatment. In the studies evaluating the patterns of nodal involvement for patients with *de novo* metastatic breast cancer, or the first LRR after adjuvant radiotherapy in patients who had undergone breast conservation surgery or mastectomy, axilla was the most common involved site, followed by SC and IMN (26, 31). In contrast, we found that axilla and SC were the most common sites of sRR after ICWR. Notably, among 116 patients who received RNI in our study, 99.1% included SC, whereas only 13.8% included axilla. The high-risk of sRR may be attributed to inadequate regional target volume. Additionally, most patients in the present study were treated with traditional two-dimensional radiotherapy techniques, such as a single anterior field or opposed anterior-posterior/posterior-anterior fields to SC and/or axilla, which may result in an inadequate dose delivered to these regions. Previous dosimetric evaluations have shown that conventional radiotherapy techniques exhibited inferior target volume coverage compared with intensity-modulated radiation therapy (32, 33). Additionally, a high sRR rate may be due to radiation-resistant subclinical disease existing in regional sites. A previous study from MD Anderson Cancer Center reported that radiation dose escalation to at least 66 Gy was not sufficient to achieve a detectable improvement in locoregional control rates among patients with LRR, which suggests the intrinsic radiation resistance of the recurrent disease (34). Prior reports observed the relatively low frequency of relapse in the axilla and increased incidence of arm edema caused by axillary irradiation, which concluded that the axilla should not be routinely included in the treatment volume (10, 13). Thus, mapping the anatomic location of sRR in axilla and SC deserves additional study, and the value of RNI should be examined in a prospective randomized trial using modern radiotherapy technique based on CT imaging.

The limitations of our study should be acknowledged. Because this study was retrospective and spanned a long period of time, systemic treatment, such as adjuvant or salvage therapy, varied considerably and confounding factors likely were present in this series. There was a possible underestimate of sLRR because of the limitations of the follow up images and the retrospective nature of this study. Despite these limitations, our study included a large number of patients with ICWR treated in two institutions, and the follow-up time was lengthy. To the best of our knowledge, the present study is the first to identify the prognostic factors and failure patterns of sRR in patients with ICWR, and it provides a direction for prospective studies to improve the treatment of these patients.

CONCLUSIONS

ICWR after mastectomy poses a challenge for clinicians; comprehensive locoregional treatment, including both surgery and radiotherapy, provide the best outcomes for patients with ICWR. The high-risk of sRR in the SC and axilla indicates the possible important role of prophylactic RNI.

DATA AVAILABILITY STATEMENT

The data analyzed in this study is subject to the following licenses/restrictions: The datasets for this article are not publicly available because of ethical restrictions placed on patient data. Requests to access these datasets should be directed to S-LW, wsl20040118@yahoo.com.

ETHICS STATEMENT

The studies involving human participants were reviewed and approved by The Institutional Review Board of Cancer Hospital, Chinese Academy of Medical Sciences and the Institutional Review Board of the Fifth Medical Center, Chinese PLA General Hospital. Written informed consent for participation

was not required for this study in accordance with the national legislation and the institutional requirements.

AUTHOR CONTRIBUTIONS

X-RZ and LX: Formal analysis, investigation, data collection, methodology, and writing original draft. JY and H-RS: Investigation, data collection, review original draft and editing. YuT: Data collection, patients care, review original draft and editing. HJ, Y-WS, JJ, Y-PL, HF, HR, BC, YuaT, NL, S-NQ, N-NL, and YY: Patients care, review original draft and editing. Y-XL: Statistics guidance, project administration, patients care, review original draft and editing. BS: Formal analysis and data collection, validation, statistics guidance, patients care, and writing original draft and editing. S-KW: Formal analysis and data collection, validation, statistics guidance, patients care, and writing original draft and editing. S-LW: Formal analysis and data collection, validation, statistics guidance, project administration, patients care, and writing original draft and editing. All authors contributed to the article and approved the submitted version.

FUNDING

This work was supported by National Key Projects of Research and Development of China (grant number 2016YFC0904600), Beijing Marathon of Hope, Cancer Foundation of China (grant number LC2016A09), National Natural Science Foundation of China (grant number 81972860).

SUPPLEMENTARY MATERIAL

The Supplementary Material for this article can be found online at: https://www.frontiersin.org/articles/10.3389/fonc.2020.600525/full#supplementary-material

REFERENCES

1. Jacobson JA, Danforth DN, Cowan KH, d'Angelo T, Steinberg SM, Pierce L, et al. Ten-year results of a comparison of conservation with mastectomy in the treatment of stage I and II breast cancer. *N Engl J Med* (1995) 332:907–11. doi: 10.1056/nejm199504063321402
2. Katz A, Strom EA, Buchholz TA, Thames HD, Smith CD, Jhingran A, et al. Locoregional recurrence patterns after mastectomy and doxorubicin-based chemotherapy: implications for postoperative irradiation. *J Clin Oncol* (2000) 18:2817–27. doi: 10.1200/jco.2000.18.15.2817
3. Pierce LJ. The use of radiotherapy after mastectomy: a review of the literature. *J Clin Oncol* (2005) 23:1706–17. doi: 10.1200/jco.2005.08.109
4. Buchanan CL, Dorn PL, Fey J, Giron G, Naik A, Mendez J, et al. Locoregional recurrence after mastectomy: incidence and outcomes. *J Am Coll Surg* (2006) 203:469–74. doi: 10.1016/j.jamcollsurg.2006.06.015
5. Chen KK, Montague ED, Oswald MJ. Results of irradiation in the treatment of locoregional breast cancer recurrence. *Cancer* (1985) 56:1269–73. doi: 10.1002/1097-0142(19850915)56:6<1269::aid-cncr2820560608>3.0.co;2-y
6. Halverson KJ, Perez CA, Kuske RR, Garcia DM, Simpson JR, Fineberg B. Survival following locoregional recurrence of breast cancer: univariate and multivariate analysis. *Int J Radiat Oncol Biol Phys* (1992) 23:285–91. doi: 10.1016/0360-3016(92)90743-2
7. Hsi RA, Antell A, Schultz DJ, Solin LJ. Radiation therapy for chest wall recurrence of breast cancer after mastectomy in a favorable subgroup of patients. *Int J Radiat Oncol Biol Phys* (1998) 42:495–9. doi: 10.1016/s0360-3016(98)00254-5
8. Nielsen HM, Overgaard M, Grau C, Jensen AR, Overgaard J. Loco-regional recurrence after mastectomy in high-risk breast cancer–risk and prognosis. An analysis of patients from the DBCG 82 b&c randomization trials. *Radiother Oncol* (2006) 79:147–55. doi: 10.1016/j.radonc.2006.04.006
9. Toonkel LM, Fix I, Jacobson LH, Wallach CB. The significance of local recurrence of carcinoma of the breast. *Int J Radiat Oncol Biol Phys* (1983) 9:33–9. doi: 10.1016/0360-3016(83)90205-5
10. Bedwinek JM, Fineberg B, Lee J, Ocwieza M. Analysis of failures following local treatment of isolated local-regional recurrence of breast cancer. *Int J Radiat Oncol Biol Phys* (1981) 7:581–5. doi: 10.1016/0360-3016(81)90369-2
11. Deutsch M, Parsons JA, Mittal BB. Radiation therapy for local-regional recurrent breast carcinoma. *Int J Radiat Oncol Biol Phys* (1986) 12:2061–5. doi: 10.1016/0360-3016(86)90002-7
12. Hothorn T, Lausen B. On the exact distribution of maximally selected rank statistics. *Comput Stat Data Anal* (2003) 43:121–37. doi: 10.1016/S0167-9473(02)00225-6
13. Halverson KJ, Perez CA, Kuske RR, Garcia DM, Simpson JR, Fineberg B. Isolated local-regional recurrence of breast cancer following mastectomy: radiotherapeutic management. *Int J Radiat Oncol Biol Phys* (1990) 19:851–8. doi: 10.1016/0360-3016(90)90004-4
14. Schwaibold F, Fowble BL, Solin LJ, Schultz DJ, Goodman RL. The results of radiation therapy for isolated local regional recurrence after mastectomy. *Int J Radiat Oncol Biol Phys* (1991) 21:299–310. doi: 10.1016/0360-3016(91)90775-y
15. Kuo SH, Huang CS, Kuo WH, Cheng AL, Chang KJ, Chia-Hsien Cheng J. Comprehensive locoregional treatment and systemic therapy for postmastectomy isolated locoregional recurrence. *Int J Radiat Oncol Biol Phys* (2008) 72:1456–64. doi: 10.1016/j.ijrobp.2008.03.042
16. Wapnir IL, Gelber S, Anderson SJ, Mamounas EP, Robidoux A, Martin M, et al. Poor Prognosis After Second Locoregional Recurrences in the CALOR Trial. *Ann Surg Oncol* (2017) 24:398–406. doi: 10.1245/s10434-016-5571-y
17. Halverson KJ, Perez CA, Kuske RR, Garcia DM, Simpson JR, Fineberg B. Locoregional recurrence of breast cancer: a retrospective comparison of irradiation alone versus irradiation and systemic therapy. *Am J Clin Oncol* (1992) 15:93–101. doi: 10.1097/00000421-199204000-00001
18. Willner J, Kiricuta IC, Kolbl O. Locoregional recurrence of breast cancer following mastectomy: always a fatal event? Results of univariate and multivariate analysis. *Int J Radiat Oncol Biol Phys* (1997) 37:853–63. doi: 10.1016/s0360-3016(96)00556-1
19. Chen J, Feng Y. Radiotherapy for chest wall recurrence of breast cancer after mastectomy. *Chin J Radiat Oncol* (2004) 13:196–200. doi: 10.3760/j.issn:1004-4221.2004.03.012
20. Chagpar A, Meric-Bernstam F, Hunt KK, Ross MI, Cristofanilli M, Singletary SE, et al. Chest wall recurrence after mastectomy does not always portend a dismal outcome. *Ann Surg Oncol* (2003) 10:628–34. doi: 10.1245/aso.2003.01.004
21. Wang X, Ma J, Mei X, Yang Z, Yu X, Guo X, et al. Outcomes Following Salvage Radiation and Systemic Therapy for Isolated Locoregional Recurrence of Breast Cancer after Mastectomy: Impact of Constructed Biologic Subtype. *J Oncol* (2018) 2018:4736263. doi: 10.1155/2018/4736263
22. Bedwinek JM, Lee J, Fineberg B, Ocwieza M. Prognostic indicators in patients with isolated local-regional recurrence of breast cancer. *Cancer* (1981) 47:2232–5. doi: 10.1002/1097-0142(19810501)47:9<2232::aid-cncr2820470921>3.0.co;2-r
23. Wang Y, Sun H, Meng X, Sun B, Song S, Wu S. Analysis of radiotherapy strategy for 110 breast cancer patients after R0 resection of local recurrence after radical mastectomy. *Chin J Radiol Med Protect* (2018) 38:670–4. doi: 10.3760/cma.j.issn.0254-5098.2018.09.006
24. van Tienhoven G, Voogd AC, Peterse JL, Nielsen M, Andersen KW, Mignolet F, et al. Prognosis after treatment for loco-regional recurrence after mastectomy or breast conserving therapy in two randomised trials (EORTC 10801 and DBCG-82TM). EORTC Breast Cancer Cooperative Group and the Danish Breast Cancer Cooperative Group. *Eur J Cancer* (1999) 35:32–8. doi: 10.1016/s0959-8049(98)00301-3

25. Ishitobi M, Matsushita A, Nakayama T, Motomura K, Koyama H, Tamaki Y. Regional lymphatic recurrence after salvage surgery for ipsilateral breast tumor recurrence of breast cancer without local treatment for regional lymphatic basin. *J Surg Oncol* (2014) 110:265–9. doi: 10.1002/jso.23642
26. Bitencourt A, Rossi Saccarelli C, Morris EA, Flynn J, Zhang Z, Khan A, et al. Regional Lymph Node Involvement Among Patients With De Novo Metastatic Breast Cancer. *JAMA Netw Open* (2020) 3:e2018790. doi: 10.1001/jamanetworkopen.2020.18790
27. Poortmans PM, Collette S, Kirkove C, Van Limbergen E, Budach V, Struikmans H, et al. Internal Mammary and Medial Supraclavicular Irradiation in Breast Cancer. *N Engl J Med* (2015) 373:317–27. doi: 10.1056/NEJMoa1415369
28. Whelan TJ, Olivotto IA, Parulekar WR, Ackerman I, Chua BH, Nabid A, et al. Regional Nodal Irradiation in Early-Stage Breast Cancer. *N Engl J Med* (2015) 373:307–16. doi: 10.1056/NEJMoa1415340
29. Thorsen LB, Offersen BV, Danø H, Berg M, Jensen I, Pedersen AN, et al. DBCG-IMN: A Population-Based Cohort Study on the Effect of Internal Mammary Node Irradiation in Early Node-Positive Breast Cancer. *J Clin Oncol* (2016) 34:314–20. doi: 10.1200/jco.2015.63.6456
30. Dodwell D, Taylor CW, Mcgale P, Coles CE, Whelan T. Abstract GS4-02: Regional lymph node irradiation in early stage breast cancer: An EBCTCG meta-analysis of 13,000 women in 14 trials. *Cancer Res* (2019) 79:GS4–02-GS04-02. doi: 10.1158/1538-7445.SABCS18-GS4-02
31. Chang JS, Lee J, Chun M, Shin KH, Park W, Lee JH, et al. Mapping patterns of locoregional recurrence following contemporary treatment with radiation therapy for breast cancer: A multi-institutional validation study of the ESTRO consensus guideline on clinical target volume. *Radiother Oncol* (2018) 126:139–47. doi: 10.1016/j.radonc.2017.09.031
32. Cavey ML, Bayouth JE, Endres EJ, Pena JM, Colman M, Hatch S. Dosimetric comparison of conventional and forward-planned intensity-modulated techniques for comprehensive locoregional irradiation of post-mastectomy left breast cancers. *Med Dosim* (2005) 30:107–16. doi: 10.1016/j.meddos.2005.02.002
33. Yang B, Wei XD, Zhao YT, Ma CM. Dosimetric evaluation of integrated IMRT treatment of the chest wall and supraclavicular region for breast cancer after modified radical mastectomy. *Med Dosim* (2014) 39:185–9. doi: 10.1016/j.meddos.2013.12.008
34. Skinner HD, Strom EA, Motwani SB, Woodward WA, Green MC, Babiera G, et al. Radiation dose escalation for loco-regional recurrence of breast cancer after mastectomy. *Radiat Oncol* (2013) 8:13. doi: 10.1186/1748-717x-8-13

Conflict of Interest: The authors declare that the research was conducted in the absence of any commercial or financial relationships that could be construed as a potential conflict of interest.

frontiers in Oncology

ORIGINAL RESEARCH
published: 17 March 2021
doi: 10.3389/fonc.2021.639909

Pretreatment Inflammatory-Nutritional Biomarkers Predict Responses to Neoadjuvant Chemoradiotherapy and Survival in Locally Advanced Rectal Cancer

*Yijun Wang[1], Lejun Chen[1], Biyun Zhang[1], Wei Song[1], Guowei Zhou[2], Ling Xie[3] and Dahai Yu[1]**

[1] Department of Radiation Oncology, Jiangsu Province Hospital of Chinese Medicine, Affiliated Hospital of Nanjing University of Chinese Medicine, Nanjing, China, [2] Department of General Surgery, Jiangsu Province Hospital of Chinese Medicine, Affiliated Hospital of Nanjing University of Chinese Medicine, Nanjing, China, [3] Department of Pathology, Jiangsu Province Hospital of Chinese Medicine, Affiliated Hospital of Nanjing University of Chinese Medicine, Nanjing, China

OPEN ACCESS

Edited by:
Nicola Silvestris, University of Bari Aldo Moro, Italy

Reviewed by:
Michael Vickers, Ottawa Hospital, Canada
Patricia Tang, University of Calgary, Canada

***Correspondence:**
Dahai Yu
yudahaipumc@hotmail.com

Specialty section:
This article was submitted to Radiation Oncology, a section of the journal Frontiers in Oncology

Received: *10 December 2020*
Accepted: *03 February 2021*
Published: *17 March 2021*

Citation:
Wang Y, Chen L, Zhang B, Song W, Zhou G, Xie L and Yu D (2021) Pretreatment Inflammatory-Nutritional Biomarkers Predict Responses to Neoadjuvant Chemoradiotherapy and Survival in Locally Advanced Rectal Cancer. Front. Oncol. 11:639909. doi: 10.3389/fonc.2021.639909

Background: To evaluate the value of pretreatment inflammatory-nutritional biomarkers in predicting responses to neoadjuvant chemoradiotherapy (nCRT) and survival in patients with locally advanced rectal cancer (LARC).

Methods: Patients with LARC who underwent nCRT and subsequent surgery between October 2012 and December 2019 were considered for inclusion. Neutrophil to lymphocyte ratio (NLR), platelet to lymphocyte ratio (PLR), lymphocyte to monocyte ratio (LMR), and prognostic nutritional index (PNI) were calculated from according to routine laboratory data within 1 week prior to nCRT. The correlations between baseline inflammatory-nutritional biomarkers and responses were analyzed using Chi-square test or Fisher's exact test, and multivariate logistic regression analysis was performed to identify the independent predictors of pathological responses to nCRT. Univariate and multivariate Cox proportional hazard models were used to assess the correlations of predictors with disease-free survival (DFS) and overall survival (OS).

Results: A total of 273 patients with LARC were enrolled in this study. Higher LMR and PNI were observed in the good-response group, meanwhile higher NLR and PLR were observed in the poor-response group. Multivariate logistic regression analysis results revealed that PLR and PNI independently predicted responses to nCRT. Multivariable Cox regression analysis determined that PNI was an independent predictor of DFS and OS in patients with LARC. The value of pretreatment PNI in predicting responses and survival was continuously superior to those of NLR, PLR, and LMR. The optimal cutoff value of the PNI was approximate 45. Subgroup analyses indicated that the pathological responses and survival in the high PNI group (≥ 45) were significantly better than those in the low PNI group (< 45), especially in patients with clinical stage III rectal cancer.

Conclusion: The pretreatment PNI can serve as a promising predictor of response to nCRT and survival in patients with LACR, which is superior to NLR, PLR, and LMR, and the patients with clinical stage III rectal cancer who have a higher PNI are more likely to benefit from nCRT.

Keywords: rectal cancer, prognostic nutritional index, systemic inflammatory response, pathological response, survival

INTRODUCTION

Standard treatment for patients with clinical locally advanced rectal cancer (LARC) includes neoadjuvant chemoradiation therapy (nCRT) followed by total mesorectal excision (TME) and adjuvant chemotherapy (1). This intensive tri-modal therapy is associated with increased local control and sphincter preservation rates and reducing toxicity compared with the postoperative therapy (2). However, individual response to nCRT is variable. Most primary tumors respond well to nCRT, and about 20% of patients even show a pathological complete response (pCR), which may indicate a favorable prognosis (3). Nonetheless, up to one third of patients exhibit resistance to nCRT and the use of nCRT in these patients may result in fatal outcomes because of disease progression or delayed surgery (4). Pathological response to CRT is highly correlated with prognosis in these patients (5). Therefore, there is a need to identify pretreatment factors that can predict the possible therapeutic response and long-term survival, thus aiding in the optimal personalized management of patients with LARC.

Currently, the tumor node metastasis (TNM) staging classification has been recognized as the most powerful prognostic indicator (6). The treatment with or without neoadjuvant therapy in rectal cancer is determined based on the TNM classification (7). Nevertheless, TNM staging classification is far from optimal, because the patients with the same stage tumors may present with different clinical outcomes despite receiving the same standardized treatment (8). Additional markers have been reported with the intention of predicting the prognosis of patients more accurately, including demographic factors such as gender, age, or performance status and clinicopathological tumor-related factors such as carcinoembryonic antigen (CEA) level, perineural invasion, tumor deposits, and circumferential resection margin (9–12). In addition, the treatment outcomes are also driven by host-related factors, especially the pretreatment systemic inflammatory response (SIR) and individual immune-nutritional condition. Various pretreatment biomarkers have been explored. SIR markers such as increased neutrophil to lymphocyte ratio (NLR) and platelet to lymphocyte ratio (PLR) may predict unfavorable prognosis in different types of malignant tumors, meanwhile increased lymphocyte to monocyte ratio (LMR) may be related to better survival outcomes (13–15). The prognostic nutritional index (PNI) is calculated by combining the serum albumin level and lymphocyte count in peripheral blood, and it is an easily measurable index to reflect both nutrition and immune status of the patient (16). Recently, studies also have shown that preoperative PNI is correlated with long-term outcomes, especially for tumors originating from the digestive system (17).

The correlation between SIR and nutrition-immune status can be complex and possibly synergistic for tumor progression. Although previous studies have suggested the potential predictive or prognostic value of these biomarkers, a combined use of SIR markers and immune-nutritional status has never been simultaneously examined in LARC patients as far as we know. Therefore, this study aimed to perform a comprehensive analysis and explore the correlation of pretreatment inflammatory-nutritional biomarkers with responses to nCRT and long-term survival outcomes, thus aiding in the optimal individualized management of patients with LARC.

MATERIALS AND METHODS

Patients

Patients with LARC who underwent nCRT and subsequent TME in our institution between October 2012 and December 2019 were preliminarily screened for this retrospective study. The inclusion criteria were as follows: (1) patient age, 18 to 75 years; (2) pathologically confirmed rectal adenocarcinoma located < 10 cm from anal verge by endoscopic biopsy specimens; (3) radiologically identified clinical staging T3-T4 or lymph node-positive rectal cancer, absence of metastasis, by computed tomography (CT) scan or magnetic resonance imaging (MRI), according to the 7th edition of the American Joint Committee on Cancer-TNM classification; (4) performance status scale of 0–1 according to Eastern Cooperative Oncology Group (ECOG) criteria; (5) no history of prior chemotherapy or pelvic radiotherapy; and (6) complete clinical records, including therapeutic interventions, pathological characteristics of the tumor, and laboratory data within 7 days before nCRT initiation. The exclusion criteria were (1) resections with macro- or microscopically positive pathological margins (R2 or R1); (2) with "watch-and-wait" strategy; (3) with primary malignancies of other organs; (4) with clinical evidence of acute or chronic infection; (5) with hematology or immunology diseases. This study was approved by the Ethics Committee of our institution.

Data Collection and Definitions

Pretreatment blood biomarkers were calculated from routine laboratory data within 1 week prior to nCRT, including neutrophil, lymphocyte, platelet and monocyte counts, serum albumin, and CEA.

$$\text{NLR} = \text{neutrophil count/lymphocyte count};$$

$$\text{PLR} = \text{platelet count/lymphocyte count};$$

$$\text{LMR} = \text{lymphocyte count/monocyte count};$$

$$\text{PNI} = 10 \times \text{serum albumin (g/dL)} + 0.005 \times \text{total lymphocyte count (per mm}^3\text{)}$$

Treatment

Patients with LARC in this study underwent nCRT and subsequent TME. Radiotherapy was delivered to the pelvic area with a prescribed dose of 45 Gy in 25 fractions and the primary tumor with a boost dose of 5.4 Gy in three fractions, up to a total dose of 50.4 Gy (18). The intensity-modulated radiation therapy (IMRT) was implemented by using 6-MV Clinac iX linear accelerator (Varian, Palo Alto, CA, USA) in seven to nine equally spaced coplanar fields. Capecitabine was administered at a dose of 825 mg/m^2 twice daily from Monday to Friday throughout IMRT. One cycle of CapeOX (Oxaliplatin 130 mg/m^2, day 1, and Capecitabine 1000 mg/m^2, twice daily, days 1–14) was permitted during the interval from the completion of nCRT to surgery All patients underwent surgery according to the principle of TME at 4 to 8 weeks after nCRT. The postoperative chemotherapy regimen was prescribed as eight cycles of FOLFOX (Oxaliplatin, Leucovorin, and 5-Fluorouracil) or six cycles of CapeOX over approximately 4 months, which was defined as full-dose adjuvant chemotherapy.

Assessment of Response to nCRT and Follow-Up

Pathological response to nCRT was assessed according to postoperative specimen histopathologic examinations using the tumor regression grade (TRG) system (19). The TRG system was defined as follows: TRG 0 was defined as no remaining viable cancer cells; TRG 1 was defined as single cells or rare residual cancer cells; TRG 2 was defined as residual cancer with a desmoplastic response; TRG 3 was defined as minimal evidence of tumor response. The pCR was defined as TRG 0, and the others were defined as non-pCR. The good-response was defined as TRG 0 and TRG 1, and the poor-response was defined as TRG 2 and TRG 3. Patients were routinely followed up for 5 years according to the following protocol in our institution: 2–4 weeks after discharge, once every 3 months for 1 year, once every 6 months for 2 years, and yearly thereafter. Physical examinations and laboratory tests, including serum CEA levels, were performed at each follow-up visit. The chest and abdominopelvic CT scan was performed every 6 months, and colonoscopy was performed annually or when there was a suspicion of recurrence. Non-routine MRI was performed at the clinician's discretion. In addition, rigid rectoscopy was performed at each follow-up visit, except when the colonoscopy was performed. Disease-free survival (DFS) was defined as the time from the initiation of nCRT to the development of local recurrence, distant metastasis, or death from any cause (whichever occurred first). Overall survival (OS) was defined as the time from the initiation of nCRT to the date of death or the final follow-up.

Statistical Analyses

Statistical analyses were performed using the Statistical Package for the Social Sciences, version 23.0 (SPSS Inc., Chicago, IL, USA). Categorical variables were compared using Chi-square test or Fisher's exact test (if the expected frequencies were <5). Continuous variables were analyzed by using Student's t-test for normally distributed variables or Mann-Whitney U test for skewed distributed variables. A multivariate logistic regression analysis was performed on statistically significant variables in the univariate analysis using a forward stepwise procedure to examine the final predictors of pathological responses to nCRT. Statistically significant variables in the univariate analysis were further analyzed in the multivariate analysis by using the Cox proportional hazards regression model in a forward stepwise procedure to assess the correlations of predictors with DFS and OS. The X-tile analysis was performed to determine the optimal cutoff value of the statistically significant biomarker to predict total DFS and OS (20). Survival curves were estimated using the Kaplan–Meier method and compared between groups using the log-rank test. The threshold for statistical significance was $P < 0.05$. In univariable Cox regression analyses of DFS and OS, $P < 0.0026$ was considered statistically significant (Bonferroni correction).

RESULTS

Patient Characteristics

This study enrolled 356 patients with LARC who underwent nCRT and subsequent TME from October 2012 to December 2019. Patients treated only with neoadjuvant CRT and "watch-and-wait" strategy (n = 14), those who did not complete the course of chemoradiotherapy (n = 4), those who received concurrent oxaliplatin (n = 21) during CRT, those who did not complete the full-dose adjuvant chemotherapy postoperatively (n = 20), those with macroscopically (R2, n = 1) or microscopically (R1, n = 4) positive pathological resection margin, those with incomplete baseline laboratory results (n = 4), those who had no available postoperative histopathology samples (n = 3) and those who were lost to follow-up (n=12) were excluded from this study. Finally, 273 eligible patients were included in this study to maintain homogeneity of the population, especially concerning tumor treatment. Among these patients, 241 (88%) patients underwent pelvic MRI examination for clinical staging assessment, and the other 32 (12%) patients underwent CT scan and endorectal ultrasound to confirm clinical staging because of contraindications to MRI or patients' willingness. Patient characteristics are summarized in **Table 1**. The median pretreatment levels of NLR, PLR, LMR, and PNI were 3.08 (range, 2.02–6.60), 207.69 (range, 102.31–310.00), 4.33 (range, 2.13–7.00), and 46.00 (range, 36.70–58.55), respectively.

TABLE 1 | Patient characteristics and response to nCRT.

Variables	Number (%) (n = 273)	Good response (n = 177)	Poor response (n = 96)	*P*
Gender				
Male	177 (64.8%)	116	61	0.742
Female	96 (35.2%)	61	35	
Age (years)				
≥60	154 (56.4%)	89	65	**0.006**
<60	119 (43.6%)	88	31	
ECOG performance status				
0	131 (48.0%)	91	40	0.124
1	142 (52.0%)	86	56	
Distance from the anal verge (cm)				
≥5	153 (56.0%)	104	49	0.220
<5	120 (44.0%)	73	47	
Pretreatment CEA (μg/L)				
≥5	139 (50.9%)	70	69	**0.000**
<5	134 (49.1%)	107	27	
Clinical T stage				
T1-2	19 (7.0%)	16	3	0.067
T3-4	254 (93.0%)	161	93	
Clinical N stage				
N (–)	119 (43.6%)	90	29	**0.001**
N (+)	154 (56.4%)	87	67	
Chemotherapy during the interval between nCRT and surgery				
Yes	139 (50.9%)	104	35	**0.000**
No	134 (49.1%)	73	61	
Pretreatment biomarker levels [median (range)]				
Neutrophil count	4.39 (1.72–12.88)	4.45 (2.13–12.88)	4.34 (1.72–8.11)	**0.032**
Platelet count	310.15 (130.61–478.58)	310.70 (132.88–478.58)	308.19 (130.61–452.82)	0.815
Lymphocyte count	1.40 (0.60–3.20)	1.50 (0.80–3.20)	1.30 (0.60–2.10)	**0.000**
Monocyte count	0.33 (0.18–0.89)	0.33 (0.19–0.89)	0.33 (0.18–0.58)	0.851
Serum albumin	39.10 (31.20–50.55)	39.40 (31.46–50.55)	38.53 (31.20–49.45)	**0.004**
NLR	3.08 (2.02–6.60)	2.97 (2.02–4.89)	3.20 (2.04–6.60)	**0.025**
PLR	207.69 (102.31–310.00)	197.54 (102.31–304.29)	220.34 (114.55–310.00)	**0.000**
LMR	4.33 (2.13–7.00)	4.58 (2.13–7.00)	3.85 (2.20–6.39)	**0.000**
PNI	46.00 (36.70–58.55)	48.00 (42.12–58.55)	45.25 (36.70–57.60)	**0.000**

nCRT, neoadjuvant chemoradiotherapy; ECOG, Eastern Cooperative Oncology Group; CEA, carcinoembryonic antigen; NLR, neutrophil to lymphocyte ratio; PLR, platelet to lymphocyte ratio; LMR, lymphocyte to monocyte ratio; PNI, prognostic nutritional index. Bold values mean that P-value is significant.

Correlations Between Pretreatment Biomarkers and Pathological Responses (TRG) to nCRT

Among 273 patients, TRG 0 (pCR) was achieved in 53 (19.4%) patients, TRG 1 in 124 (45.4%), TRG 2 in 50 (18.3%) and TRG 3 in 46 (16.8%), respectively. Totally, 177 (64.8%) patients achieved good-response (TRG 0-1) and 96 (35.2%) patients achieved poor-response (TRG 2-3) to nCRT. The correlations of patient demographic, tumor characteristics, and pretreatment biomarker levels with pathological responses are also available in **Table 1**. In general, higher LMR and PNI were observed in the good-response group, meanwhile higher NLR and PLR were observed in the poor-response group. Multivariate logistic regression analysis results (**Table 2**) revealed that PLR and PNI could independently predict responses to nCRT in patients with LARC.

Correlations Between Pretreatment Biomarkers and Survival

Median follow-up time was 42 (range, 10–78) months, while median DFS was 38 (range, 10–78) months. The 5-year DFS and OS rates were 73.1% and 78.9% for the entire cohort, respectively. The patients with good-response had a significantly better 5-year DFS (81.2% vs. 58.5%, $\boldsymbol{P = 0.000}$) and OS (83.6% vs. 70.9%, $\boldsymbol{P = 0.001}$) rates compared with those with poor-response. The univariate analysis results revealed that the lymphocyte count,

TABLE 2 | Multivariate logistic regression analysis for response to nCRT.

Variables	Hazard Ratio (95% CI)	*P*
Chemotherapy during the interval between nCRT and surgery		
Yes	1.837 (1.047–3.224)	**0.034**
No		
Pretreatment CEA (μg/L)		
≥5	0.424 (0.236–0.761)	**0.004**
<5		
Pretreatment biomarkers		
PLR	0.992 (0.987–0.998)	**0.013**
PNI	1.181 (1.071–1.300)	**0.001**

nCRT, neoadjuvant chemoradiotherapy; CEA, carcinoembryonic antigen; PLR, platelet to lymphocyte ratio; PNI, prognostic nutritional index. Bold values mean that P value is significant.

serum albumin, PLR, and PNI were significantly correlated with DFS, as well as yp T stage, yp N stage, and pathological responses (**Figure 1**), and the serum albumin, PLR, and PNI were significantly correlated with OS, as well as yp N stage and pathological responses (**Figure 2**). Multivariate Cox regression analysis determined that pathological responses and PNI were independent predictors of DFS, and yp N stage and pretreatment PNI were independent predictors of OS in patients with LARC (**Table 3**).

Subgroup Analysis to Assess the Clinical Utility of the Pretreatment PNI in Predicting Pathological Responses to nCRT and Survival

X-tile analysis determined that the optimal cutoff value of the PNI was 44.9 for total DFS and 44.8 for total OS. Considering that the optimized cutoff value of PNI was 45 in the initial pivotal study of Onodera et al. (21), we determined the PNI cutoff value as 45 in the present study. Patients were dichotomized into high PNI group [PNI ≥ 45; n = 177 (64.8%)] and low PNI group [PNI < 45; n = 96 (35.2%)]. The good-response rate in the high PNI group was significantly higher than that in the low PNI group (69.5% vs. 56.3%, ***P*=0.029**). The DFS and OS rates in the high PNI group were also significantly better than those in the low PNI group (5-year DFS: 77.9% vs. 59.7%, ***P*=0.009**, **Figure 3A**; 5-year OS: 82.5% vs. 68.8%, ***P*=0.011**, **Figure 3B**).

We further analyzed the utility of PNI in predicting pathological responses to nCRT and survival based on the clinical TNM stage in patients with LARC. Among patients with clinical stage II rectal cancer (n = 119), higher good-response rate and better survival outcomes were observed in the high PNI group compared with the low PNI group (good-response rate: 77.5% vs. 71.8%, *P* = 0.496; 5-year DFS: 81.3% vs.

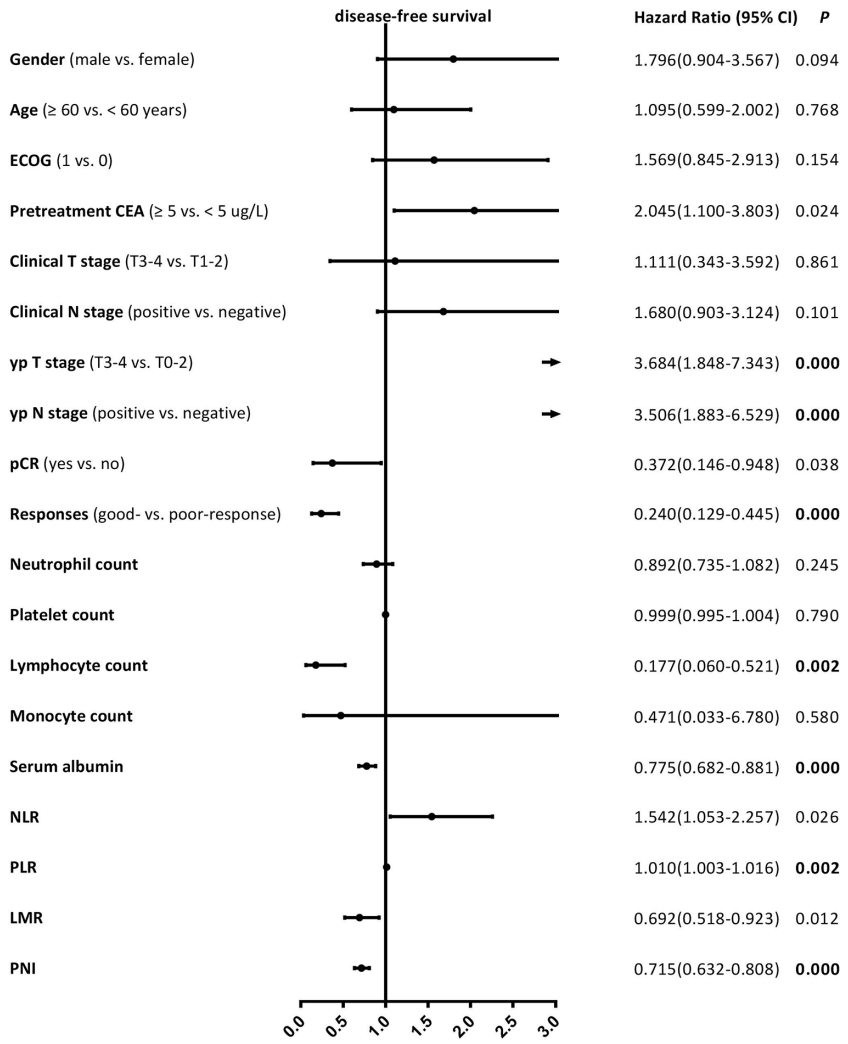

FIGURE 1 | Univariate Cox proportional hazard regression analyses of disease-free survival in patients with locally advanced rectal cancer. Bold value means that P < 0.0026 and it is considered statistically significant after Bonferroni correction.

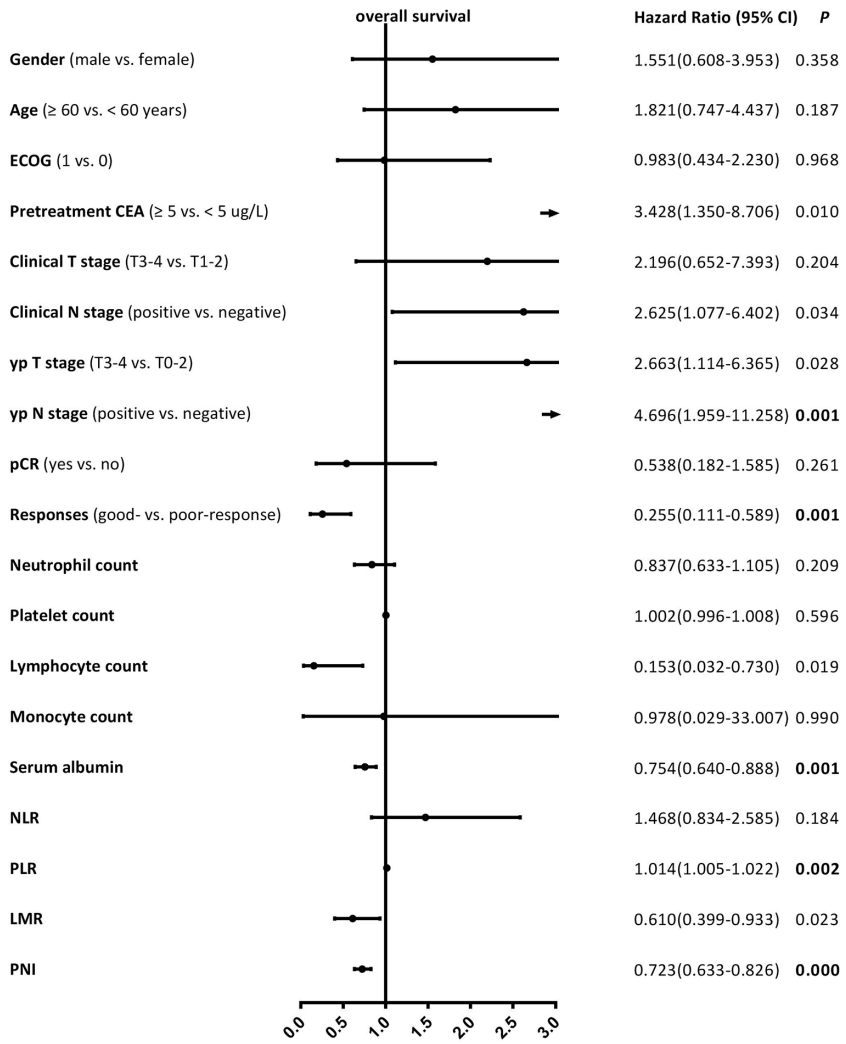

FIGURE 2 | Univariate Cox proportional hazard regression analyses for overall survival in patients with locally advanced rectal cancer. Bold value means that P < 0.0026 and it is considered statistically significant after Bonferroni correction.

TABLE 3 | Multivariate Cox proportional hazard regression analyses of DFS and OS.

Variables	DFS		OS	
	Hazard Ratio (95% CI)	***P***	**Hazard Ratio (95% CI)**	***P***
Pathological responses				
Good-response vs. poor-response	0.357 (0.188–0.678)	**0.002**	–	–
yp N stage				
Positive vs. negative	–		2.880 (1.118–7.422)	**0.028**
Pretreatment biomarkers				
PNI	0.750 (0.663–0.849)	**0.000**	0.767 (0.672–0.876)	**0.000**

DFS, disease-free survival; OS, overall survival; NLR, neutrophil to lymphocyte ratio; PNI, prognostic nutritional index. Bold values mean that P value is significant.

66.7%, $P = 0.559$, **Figure 3C**; 5-year OS: 88.3% vs. 86.4%, $P = 0.481$, **Figure 3D**), but the differences were not statistically significant. Among patients with clinical stage III rectal cancer (n = 154), comparable results were observed between the high and low PNI groups, and the differences were statistically significant (good-response rate: 62.9% vs. 45.6%, $\boldsymbol{P = 0.037}$; 5-year DFS: 73.4% vs. 56.5%, $\boldsymbol{P = 0.004}$, **Figure 3E**; 5-year OS: 75.2% vs. 49.9%, $\boldsymbol{P = 0.008}$, **Figure 3F**).

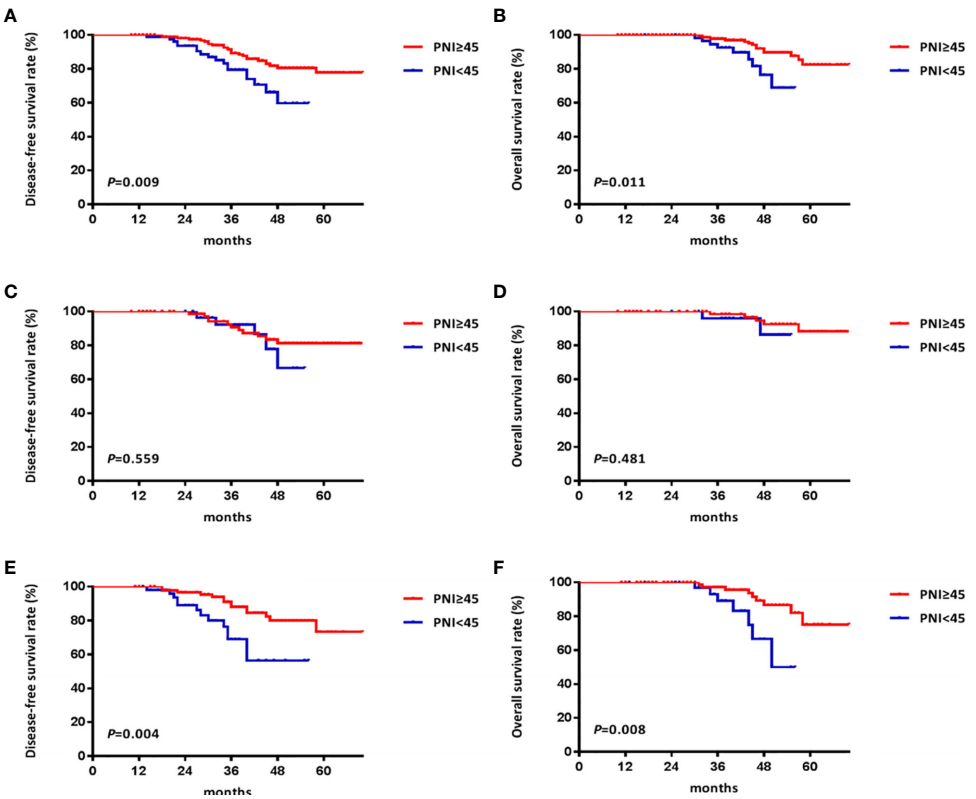

FIGURE 3 | Kaplan Meier survival curves of patients with locally advanced rectal cancer grouped by prognostic nutritional index (PNI) and stratified by clinical stage. **(A)** the disease-free survival (DFS) curves of all patients; **(B)** the overall survival (OS) curves of all patients; **(C)** the DFS curves of patients with clinical stage II rectal cancer; **(D)** the OS curves of patients with clinical stage II rectal cancer; **(E)** the DFS curves of patients with clinical stage III rectal cancer; **(F)** the OS curves of patients with clinical stage III rectal cancer.

DISCUSSION

To the best of our knowledge, this is the first time to evaluate the predictive and prognostic values of these four pretreatment inflammatory and nutritional factors for LARC in one study. The findings suggested that a higher pretreatment PNI is correlated with better pathological responses and prognosis in patients with LARC undergoing nCRT, superior to the established SIR markers such as NLR, PLR, and LMR. Moreover, pretreatment PNI can be used as a supplemental tool in predicting responses to nCRT and survival based on TNM classification for LARC.

It is increasingly recognized that the initiation and progressions of rectal cancer are not solely determined by the inherent characteristics of the tumor but also by host-related factors (22). There may be substantial cross-talk between the systemic inflammation and immune responses against cancer cells and the surrounding microenvironment, and the interaction mechanism is far from being fully understood (23). Although the independent utility of the NLR, PLR, LMR, and PNI as predictors of responses to treatment or patient prognosis have achieved promising results in the published literature, including rectal cancer (24–27), the results have often been controversial when these biomarkers are evaluated simultaneously in the same patient cohort (28). What is more, previous studies usually attempted to identify factors correlated with response to neoadjuvant therapy or long-term survival as two separate entities, the persistence forecasting abilities of these biomarkers remain unknown. Therefore, this study was conducted to investigate the correlations of a range of biomarkers with not only responses to nCRT but also long-term outcomes such as DFS and OS in patients with LARC.

TRG is recommended as the preferred grading method of rectal cancer response to treatment by the AJCC Staging Manual and the College of American Pathologists Guidelines (29). Therefore, TRG was selected to assess the correlation between these biomarkers and the responses to nCRT in this study. Furthermore, although tumor pathological response to nCRT is considered to be correlated with prognosis, the final endpoint should still be long-term outcomes to evaluate the predictive value of these biomarkers (30). Previous literature achieved mixed results regarding the correlation of SIR markers with tumor response or prognosis. Kim et al. reported that NLR, LMR, and PLR could not be used to distinguish total tumor regression from the residual disease after nCRT; while higher PLR was correlated with improved recurrence-free survival (31). Michael

et al. found that NLR and PLR are neither independent predictors of response nor prognostic factors in LARC patients undergoing nCRT followed by radical surgery (32). However, the data from William et al. showed that baseline lower levels of LMR and higher levels of NLR and PLR were correlated with decreased OS (25). The superior indicator value of PNI on the prognosis of patients with LARC has been validated, but there are limited studies on the correlation between PNI and responses (17, 33). In this study, PNI showed a better, more consistent, and independent predictive ability for treatment response and prognosis in univariate and multivariate analyses, other SIR markers such as NLR, PLR, and LMR did not show an independent predictive ability in multivariate analysis, which may be related to the inherent correlation between such indicators and PNI, and this phenomenon has been described in some studies (34, 35), but it still needs to be further explored.

Serum albumin is a broadly recognized indicator for nutrition status, and initial studies documented that the albumin can be used to assess disease progression and prognosis (36, 37). However, there is increasing evidence to suggest that the prognostic value of albumin may be subordinate to an ongoing SIR, so the albumin should be used in combination with other markers to enhance prognostic value (38, 39). Lymphocytes play a crucial role in the host immune response to cancer, which is associated with improved outcomes in solid tumors according to previous reports (40). The results of this study showed that the lymphocytes and serum albumin were significantly correlated with responses to nCRT and survivals in univariate analysis but not in multivariate analysis. PNI is composed of serum albumin level and peripheral lymphocyte count, and it may reflect both the nutritional and immunological status of a patient (21). The multivariate analysis in this study determined that the PNI was an independent predictor of response and prognosis in patients with LARC undergoing nCRT.

Several explanations could contribute to the correlation of PNI with treatment response and prognosis in patients with LARC. Firstly, Capecitabine, the oral fluorinated pyrimidine prodrug, is recommended concomitantly with radiotherapy as a radiation sensitizer. Capecitabine is readily absorbed in the gastrointestinal tract and it requires the presence of thymidine phosphorylase for its conversion into the active form of 5-fluorouracil within the cells (41). Low albumin concentrations may result in abnormal pharmacokinetics and inferior bioavailability, and continuing inflammation at baseline also had significantly decreased metabolic activities of chemotherapy drugs and increased their toxicities, thus leading to unfavorable response and clinical outcomes (42). What is more, LARC patients often develop malnutrition as a result of insufficient food intake, malabsorption, and increased metabolic demands. It has been proposed that malnutrition is related to cytokine-driven inflammation and may lead to the immunosuppressed condition, which can be reflected by hypoalbuminemia and low lymphocyte counts (43). This immunosuppressed condition might be responsible for the insufficient anti-tumor immune response and provide an advantageous microenvironment for tumor progression in low-PNI patients (44). Additionally, patients with decreased PNI may have an enhanced SIR (45). The excessive inflammatory components can further lead to increased depletion of fat stocks, as well as protein degradation in skeletal muscle and other host tissue. The absence of albumin can lead to immune regulation dysfunction by affecting the stabilized cell growth, DNA replication, and antioxygenation *in vivo*, and the albumin degradation products may serve as source of nutrient substrates for accelerating tumor growth and proliferation (46). Inflammation is also an important regulator of tumor progression through suppression of albumin synthesis, recruitment of T lymphocytes and tumor-associated macrophages, and upregulation of angiogenic growth factors (47). The precise mechanisms underlying the correlation between PNI and treatment outcomes may be complex and our understanding of this process remains unclear. Nevertheless, the potential predictive and prognostic values of PNI exist in providing an inexpensive, non-invasive and effective supplemental tool.

Of note, this study differed from previous studies in methodology. A common feature of previous studies was to dichotomize continuous biomarkers primitively to stratify patients into different subgroups to explore the correlations of these biomarkers with response or prognosis, and thus the cut off values of these biomarkers are various in different literature (17, 24–28, 31–35). In this study, we choose not to dichotomize these biomarkers primitively, because the forecasts of continuous variables have enormous advantages from a statistical standpoint. This allowed us to minimize false-positive results and establish a much more accurate forecast model by using Cox proportional hazard model. Our findings suggested that increased PNI was correlated with higher good-response and better long-term outcomes across the continuous range of PNI. If this finding is further confirmed and thus PNI can be considered as a routine test during the first clinical visit, interventions to improve PNI will produce an additive benefit on treatment outcomes in LARC patients, not just those with a PNI above a predefined cut off value. Interestingly, the predictive and prognostic values of pre-treatment PNI were greater in patients with clinical stage III rectal cancer. This finding could be mainly attributed to the fact that the patients with clinical stage III rectal cancer were more likely to suffer from high tumor burden and long-term nutritional consumption, which might up-regulate the expressions of cytokines and inflammatory mediators, leading to immunosuppressed host and decreased local immune response, thus affecting the sensitivity of nCRT and the long-term survival (23).

Currently, available data recommends nCRT followed by TME as the standard treatment for patients with LARC. However, not all LARC patients respond to nCRT, which subgroup population would benefit from nCRT remains unclear. In the present study, we observed the differences in response to nCRT and survival between high and low PNI groups. Patients with a higher PNI are more likely to benefit from nCRT. These findings indicate that the baseline inferior immunonutritional status may impair the efficacy of nCRT. At present, the prospective clinical evidence of immunonutritional intervention during oncological treatment remains limited and our present knowledge about these is still at a rudimentary stage.

However, there may exist potential therapeutic target that can alter the disease course (48). Therefore, it is necessary to pay more attention to the assessment of the immunonutritional status, to provide better guidance for clinical treatment, especially in patients with clinical stage III rectal cancer, who might need additional supportive interventions to further improve their prognoses. In this context, the use of PNI as a surrogate marker of inherent immunological status in a host can provide a new perspective on optimizing strategies for individualized management of patients with LARC.

Following prior studies, we found that chemotherapy during the interval between nCRT and surgery and the pretreatment CEA were independently correlated with responses to nCRT in patients with LARC (9, 49, 50). We also found that responses to nCRT and yp N stage were independent predictors of DFS and OS, respectively (4, 35, 51, 52). In addition, the 5-year DFS and OS rates in the present study are similar to those previously reported in several landmark trials of nCRT in patients with LARC (2, 53, 54). These findings confirm that the current cohort is truly representative of patients with LACR undergoing nCRT and thus support the validity and generalizability of our results.

There are several limitations in this study. The retrospective nature of this type of analysis is subject to shortcomings such as potential data collection and selection bias. This was a single-center and single-race study and the optimal cutoff values for these biomarkers may fluctuate in other heterogenous patient cohorts. Additionally, the PNI is a non-specific biomarker that can be affected by various pathophysiologic conditions and thus will vary from time to time. In this study, we mainly focused on the correlation between baseline inflammatory-nutritional factors and clinical outcomes to aid in the optimal individualized management of patients with LARC. However, the impact of changes in these markers over time has yet to be determined. Therefore, further studies are required to confirm the results of this current study. Finally, C-reactive protein (CRP) was not a preoperative routine examination in our center, so the predictive value of CRP or CRP-based indicator such as Glasgow prognostic score (55) was not analyzed in this study. However, the lack of available CRP data reminds us that currently inflammatory marker detection has not entered clinical practice and it needs to be further explored in the future.

CONCLUSION

In summary, this study confirmed that PNI can serve as a promising predictor of response to nCRT and survival in patients with LACR, and patients with a higher PNI are more likely to benefit from nCRT, especially for patients with clinical stage III rectal cancer. Whilst these results are required to be re-validated in prospective trials, PNI routinely collected before treatment may assist in better risk-stratifying patients and thus aid in the determination of an optimal individual treatment plan for a patient with LARC.

DATA AVAILABILITY STATEMENT

The original contributions presented in the study are included in the article/**Supplementary Material**. Further inquiries can be directed to the corresponding author.

ETHICS STATEMENT

The studies involving human participants were reviewed and approved by the Ethics Committee of Jiangsu Province Hospital of Chinese Medicine. The patients/participants provided their written informed consent to participate in this study.

AUTHOR CONTRIBUTIONS

DY: study design and guidance, critical revision of the manuscript, and study supervision. YW: data acquisition and analysis, statistical evaluation of the results, and drafting of the manuscript. LC, BZ, WS, and LX: data acquisition, analysis, and interpretation. GZ: software application. All authors contributed to the article and approved the submitted version.

FUNDING

This work was partly supported by the Traditional Chinese Medicine Science and Technology Planning Project of Jiangsu Province (No. JD201801).

SUPPLEMENTARY MATERIAL

The Supplementary Material for this article can be found online at: https://www.frontiersin.org/articles/10.3389/fonc.2021.639909/full#supplementary-material

REFERENCES

1. Sauer R, Becker H, Hohenberger W, Rödel C, Wittekind C, Fietkau R, et al. Preoperative versus postoperative chemoradiotherapy for rectal cancer. *N Engl J Med* (2004) 351:1731–40. doi: 10.1056/NEJMoa040694
2. Sauer R, Liersch T, Merkel S, Fietkau R, Hohenberger W, Hess C, et al. Preoperative versus postoperative chemoradiotherapy for locally advanced rectal cancer: results of the German CAO/ARO/AIO-94 randomized phase III trial after a median follow-up of 11 years. *J Clin Oncol* (2012) 30:1926–33. doi: 10.1200/JCO.2011.40.1836
3. van der Valk MJM, Hilling DE, Bastiaannet E, Meershoek-Klein Kranenbarg E, Beets GL, Figueiredo NL, et al. Long-term outcomes of clinical complete responders after neoadjuvant treatment for rectal cancer in the International Watch & Wait Database (IWWD): an international multicentre registry study. *Lancet* (2018) 391:2537–45. doi: 10.1016/S0140-6736(18)31078-X
4. Park IJ, You YN, Agarwal A, Skibber JM, Rodriguez-Bigas MA, Eng C, et al. Neoadjuvant treatment response as an early response indicator for patients

with rectal cancer. *J Clin Oncol* (2012) 30:1770–6. doi: 10.1200/JCO.2011.39.7901
5. Das P, Skibber JM, Rodriguez-Bigas MA, Feig BW, Chang GJ, Hoff PM, et al. Clinical and pathologic predictors of locoregional recurrence, distant metastasis, and overall survival in patients treated with chemoradiation and mesorectal excision for rectal cancer. *Am J Clin Oncol* (2006) 29:219–24. doi: 10.1097/01.coc.0000214930.78200.4a
6. Gunderson LL, Jessup JM, Sargent DJ, Greene FL, Stewart AK. Revised TN categorization for colon cancer based on national survival outcomes data. *J Clin Oncol* (2010) 28:264–71. doi: 10.1200/JCO.2009.24.0952
7. Lin AY, Wong WD, Shia J, Minsky BD, Temple LK, Guillem JG, et al. Predictive clinicopathologic factors for limited response of T3 rectal cancer to combined modality therapy. *Int J Colorectal Dis* (2008) 23:243–9. doi: 10.1007/s00384-007-0406-8
8. Nitsche U, Maak M, Schuster T, Künzli B, Langer R, Slotta-Huspenina J, et al. Prediction of prognosis is not improved by the seventh and latest edition of the TNM classification for colorectal cancer in a single-center collective. *Ann Surg* (2011) 254:793–801. doi: 10.1097/SLA.0b013e3182369101
9. Park YA, Sohn SK, Seong J, Baik SH, Lee KY, Kim NK, et al. Serum CEA as a predictor for the response to preoperative chemoradiation in rectal cancer. *J Surg Oncol* (2006) 93:145–50. doi: 10.1002/jso.20320
10. Knijn N, Mogk SC, Teerenstra S, Simmer F, Nagtegaal ID. Perineural Invasion is a Strong Prognostic Factor in Colorectal Cancer: A Systematic Review. *Am J Surg Pathol* (2016) 40:103–12. doi: 10.1097/PAS.0000000000000518
11. Gopal P, Lu P, Ayers GD, Herline AJ, Washington MK. Tumor deposits in rectal adenocarcinoma after neoadjuvant chemoradiation are associated with poor prognosis. *Mod Pathol* (2014) 27:1281–7. doi: 10.1038/modpathol.2013.239
12. Taylor FG, Quirke P, Heald RJ, Moran BJ, Blomqvist L, Swift IR, et al. Preoperative magnetic resonance imaging assessment of circumferential resection margin predicts disease-free survival and local recurrence: 5-year follow-up results of the MERCURY study. *J Clin Oncol* (2014) 32:34–43. doi: 10.1200/JCO.2012.45.3258
13. Hu B, Yang XR, Xu Y, Sun YF, Sun C, Guo W, et al. Systemic immune-inflammation index predicts prognosis of patients after curative resection for hepatocellular carcinoma. *Clin Cancer Res* (2014) 20:6212–22. doi: 10.1158/1078-0432.CCR-14-0442
14. Szkandera J, Pichler M, Absenger G, Stotz M, Arminger F, Weissmueller M, et al. The elevated preoperative platelet to lymphocyte ratio predicts decreased time to recurrence in colon cancer patients. *Am J Surg* (2014) 208:210–4. doi: 10.1016/j.amjsurg.2013.10.030
15. Stotz M, Pichler M, Absenger G, Szkandera J, Arminger F, Schaberl-Moser R, et al. The preoperative lymphocyte to monocyte ratio predicts clinical outcome in patients with stage III colon cancer. *Br J Cancer* (2014) 110:435–40. doi: 10.1038/bjc.2013.785
16. Hua X, Long ZQ, Huang X, Deng JP, He ZY, Guo L, et al. The value of prognostic nutritional index (pni) in predicting survival and guiding radiotherapy of patients with T1-2N1 breast cancer. *Front Oncol* (2020) 9:1562. doi: 10.3389/fonc.2019.01562
17. Okugawa Y, Toiyama Y, Oki S, Ide S, Yamamoto A, Ichikawa T, et al. Feasibility of assessing prognostic nutrition index in patients with rectal cancer who receive preoperative chemoradiotherapy. *JPEN J Parenter Enteral Nutr* (2018) 42:998–1007. doi: 10.1002/jpen.1041
18. Roels S, Duthoy W, Haustermans K, Penninckx F, Vandecaveye V, Boterberg T, et al. Definition and delineation of the clinical target volume for rectal cancer. *Int J Radiat Oncol Biol Phys* (2006) 65:1129–42. doi: 10.1016/j.ijrobp.2006.02.050
19. Ryan R, Gibbons D, Hyland JM, Treanor D, White A, Mulcahy HE, et al. Pathological response following long-course neoadjuvant chemoradiotherapy for locally advanced rectal cancer. *Histopathology* (2005) 47:141–6. doi: 10.1111/j.1365-2559.2005.02176.x
20. Camp RL, Dolled-Filhart M, Rimm DL. X-tile: a new bio-informatics tool for biomarker assessment and outcome-based cut-point optimization. *Clin Cancer Res* (2004) 10:7252–9. doi: 10.1158/1078-0432.CCR-04-0713
21. Onodera T, Goseki N, Kosaki G. Prognostic nutritional index in gastrointestinal surgery of malnourished cancer patients. *Nihon Geka Gakkai Zasshi* (1984) 85:1001–5.
22. Roxburgh CS, Salmond JM, Horgan PG, Oien KA, McMillan DC. The relationship between the local and systemic inflammatory responses and survival in patients undergoing curative surgery for colon and rectal cancers. *J Gastrointest Surg* (2009) 13:2011–9. doi: 10.1007/s11605-009-1034-0
23. Diakos CI, Charles KA, McMillan DC, Clarke SJ. Cancer-related inflammation and treatment effectiveness. *Lancet Oncol* (2014) 15:e493–503. doi: 10.1016/S1470-2045(14)70263-3
24. Pine JK, Morris E, Hutchins GG, West NP, Jayne DG, Quirke P, et al. Systemic neutrophil-to-lymphocyte ratio in colorectal cancer: the relationship to patient survival, tumour biology and local lymphocytic response to tumour. *Br J Cancer* (2015) 113:204–11. doi: 10.1038/bjc.2015.87
25. Ward WH, Goel N, Ruth KJ, Esposito AC, Lambreton F, Sigurdson ER, et al. Predictive value of leukocyte- and platelet-derived ratios in rectal adenocarcinoma. *J Surg Res* (2018) 232:275–82. doi: 10.1016/j.jss.2018.06.060
26. Xiao WW, Zhang LN, You KY, Huang R, Yu X, Ding PR, et al. A low lymphocyte-to-monocyte ratio predicts unfavorable prognosis in pathological T3N0 rectal cancer patients following total mesorectal excision. *J Cancer* (2015) 6:616–22. doi: 10.7150/jca.11727
27. Nozoe T, Kohno M, Iguchi T, Mori E, Maeda T, Matsukuma A, et al. The prognostic nutritional index can be a prognostic indicator in colorectal carcinoma. *Surg Today* (2012) 42:532–5. doi: 10.1007/s00595-011-0061-0
28. Dayde D, Tanaka I, Jain R, Tai MC, Taguchi A. Predictive and prognostic molecular biomarkers for response to neoadjuvant chemoradiation in rectal cancer. *Int J Mol Sci* (2017) 18:573. doi: 10.3390/ijms18030573
29. Trakarnsanga A, Gönen M, Shia J, Nash GM, Temple LK, Guillem JG, et al. Comparison of tumor regression grade systems for locally advanced rectal cancer after multimodality treatment. *J Natl Cancer Inst* (2014) 106:dju248. doi: 10.1093/jnci/dju248
30. Ryan JE, Warrier SK, Lynch AC, Ramsay RG, Phillips WA, Heriot AG. Predicting pathological complete response to neoadjuvant chemoradiotherapy in locally advanced rectal cancer: a systematic review. *Colorectal Dis* (2016) 18:234–46. doi: 10.1111/codi.13207
31. Jung SW, Park IJ, Oh SH, Yeom SS, Lee JL, Yoon YS, et al. Association of immunologic markers from complete blood counts with the response to preoperative chemoradiotherapy and prognosis in locally advanced rectal cancer. *Oncotarget* (2017) 8:59757–65. doi: 10.18632/oncotarget.15760
32. Dudani S, Marginean H, Tang PA, Monzon JG, Raissouni S, Asmis TR, et al. Neutrophil-to-lymphocyte and platelet-to-lymphocyte ratios as predictive and prognostic markers in patients with locally advanced rectal cancer treated with neoadjuvant chemoradiation. *BMC Cancer* (2019) 19:664. doi: 10.1186/s12885-019-5892-x
33. Tokunaga R, Sakamoto Y, Nakagawa S, Izumi D, Kosumi K, Taki K, et al. Comparison of systemic inflammatory and nutritional scores in colorectal cancer patients who underwent potentially curative resection. *Int J Clin Oncol* (2017) 22:740–8. doi: 10.1007/s10147-017-1102-5
34. Li A, He K, Guo D, Liu C, Wang D, Mu X, et al. Pretreatment blood biomarkers predict pathologic responses to neo-CRT in patients with locally advanced rectal cancer. *Future Oncol* (2019) 15:3233–42. doi: 10.2217/fon-2019-0389
35. Peng J, Zhang R, Zhao Y, Wu X, Chen G, Wan D, et al. Prognostic value of preoperative prognostic nutritional index and its associations with systemic inflammatory response markers in patients with stage III colon cancer. *Chin J Cancer* (2017) 36:96. doi: 10.1186/s40880-017-0260-1
36. Noble F, Hopkins J, Curtis N, Kelly JJ, Bailey IS, Byrne JP, et al. The role of systemic inflammatory and nutritional blood-borne markers in predicting response to neoadjuvant chemotherapy and survival in oesophagogastric cancer. *Med Oncol* (2013) 30:596. doi: 10.1007/s12032-013-0596-6
37. Hanahan D, Weinberg RA. Hallmarks of cancer: the next generation. *Cell* (2011) 144:646–74. doi: 10.1016/j.cell.2011.02.013
38. Garcia-Martinez R, Andreola F, Mehta G, Poulton K, Oria M, Jover M, et al. Immunomodulatory and antioxidant function of albumin stabilises the endothelium and improves survival in a rodent model of chronic liver failure. *J Hepatol* (2015) 62:799–806. doi: 10.1016/j.jhep.2014.10.031
39. Petrelli F, Barni S, Coinu A, Bertocchi P, Borgonovo K, Cabiddu M, et al. The modified glasgow prognostic score and survival in colorectal cancer: a pooled analysis of the literature. *Rev Recent Clin Trials* (2015) 10:135–41. doi: 10.2174/1574887110666150317121413
40. Schmidt MA, Förtsch C, Schmidt M, Rau TT, Fietkau R, Distel LV. Circulating regulatory T cells of cancer patients receiving radiochemotherapy may be useful to individualize cancer treatment. *Radiother Oncol* (2012) 104:131–8. doi: 10.1016/j.radonc.2012.05.003

41. O'Connell MJ, Colangelo LH, Beart RW, Petrelli NJ, Allegra CJ, Sharif S, et al. Capecitabine and oxaliplatin in the preoperative multimodality treatment of rectal cancer: surgical end points from National Surgical Adjuvant Breast and Bowel Project trial R-04. *J Clin Oncol* (2014) 32:1927–34. doi: 10.1200/JCO.2013.53.7753
42. Slaviero KA, Clarke SJ, Rivory LP. Inflammatory response: an unrecognised source of variability in the pharmacokinetics and pharmacodynamics of cancer chemotherapy. *Lancet Oncol* (2003) 4:224–32. doi: 10.1016/s1470-2045(03)01034-9
43. Grivennikov SI, Greten FR, Karin M. Immunity, inflammation, and cancer. *Cell* (2010) 140:883–99. doi: 10.1016/j.cell.2010.01.025
44. Colotta F, Allavena P, Sica A, Garlanda C, Mantovani A. Cancer-related inflammation, the seventh hallmark of cancer: links to genetic instability. *Carcinogenesis* (2009) 30:1073–81. doi: 10.1093/carcin/bgp127
45. Geng Y, Qi Q, Sun M, Chen H, Wang P, Chen Z. Prognostic nutritional index predicts survival and correlates with systemic inflammatory response in advanced pancreatic cancer. *Eur J Surg Oncol* (2015) 41:1508–14. doi: 10.1016/j.ejso.2015.07.022
46. Kratz F. Albumin as a drug carrier: design of prodrugs, drug conjugates and nanoparticles. *J Control Release* (2008) 132:171–83. doi: 10.1016/j.jconrel.2008.05.010
47. Condeelis J, Pollard JW. Macrophages: obligate partners for tumor cell migration, invasion, and metastasis. *Cell* (2006) 124:263–6. doi: 10.1016/j.cell.2006.01.007
48. Lu Z, Fang Y, Liu C, Zhang X, Xin X, He Y, et al. Early interdisciplinary supportive care in patients with previously untreated metastatic esophagogastric cancer: a phase iii randomized controlled trial. *J Clin Oncol* (2021) 39:748–56. doi: 10.1200/JCO.20.01254
49. Yang J, Ling X, Tang W, Hu D, Zhou H, Yin G. Analyses of predictive factors for pathological complete remission in neoadjuvant therapy for locally advanced rectal cancer. *J BUON* (2019) 24:77–83.
50. Garcia-Aguilar J, Chow OS, Smith DD, Marcet JE, Cataldo PA, Varma MG, et al. Effect of adding mFOLFOX6 after neoadjuvant chemoradiation in locally advanced rectal cancer: a multicentre, phase 2 trial. *Lancet Oncol* (2015) 16:957–66. doi: 10.1016/S1470-2045(15)00004-2
51. Quah HM, Chou JF, Gonen M, Shia J, Schrag D, Saltz LB, et al. Pathologic stage is most prognostic of disease-free survival in locally advanced rectal cancer patients after preoperative chemoradiation. *Cancer* (2008) 113:57–64. doi: 10.1002/cncr.23516
52. Yeo SG, Kim DY, Kim TH, Chang HJ, Oh JH, Park W, et al. Pathologic complete response of primary tumor following preoperative chemoradiotherapy for locally advanced rectal cancer: long-term outcomes and prognostic significance of pathologic nodal status (KROG 09-01). *Ann Surg* (2010) 252:998–1004. doi: 10.1097/SLA.0b013e3181f3f1b1
53. Roh MS, Colangelo LH, O'Connell MJ, Yothers G, Deutsch M, Allegra CJ, et al. Preoperative multimodality therapy improves disease-free survival in patients with carcinoma of the rectum: NSABP R-03. *J Clin Oncol* (2009) 27:5124–30. doi: 10.1200/JCO.2009.22.0467
54. Hofheinz RD, Wenz F, Post S, Matzdorff A, Laechelt S, Hartmann JT, et al. Chemoradiotherapy with capecitabine versus fluorouracil for locally advanced rectal cancer: a randomised, multicentre, non-inferiority, phase 3 trial. *Lancet Oncol* (2012) 13:579–88. doi: 10.1016/S1470-2045(12)70116-X
55. Proctor MJ, Morrison DS, Talwar D, Balmer SM, Fletcher CD, O'Reilly DS, et al. A comparison of inflammation-based prognostic scores in patients with cancer. A Glasgow Inflammation Outcome Study. *Eur J Cancer* (2011) 47:2633–41. doi: 10.1016/j.ejca.2011.03.028

Conflict of Interest: The authors declare that the research was conducted in the absence of any commercial or financial relationships that could be construed as a potential conflict of interest.

frontiers in Oncology

ORIGINAL RESEARCH
published: 29 March 2021
doi: 10.3389/fonc.2021.621690

The Multidimensional Assessment for Pediatric Patients in Radiotherapy (M.A.P.-RT) Tool for Customized Treatment Preparation: RADAR Project

Silvia Chiesa[1], Elisa Marconi[1,2], Nicola Dinapoli[1], Maria Zoe Sanfilippo[3], Antonio Ruggiero[3,4], Angela Mastronuzzi[5], Giulia Panza[3], Annalisa Serra[5], Mariangela Massaccesi[1], Antonella Cacchione[5], Francesco Beghella Bartoli[1], Daniela Pia Rosaria Chieffo[2], Maria Antonietta Gambacorta[1,3], Vincenzo Valentini[1,3] and Mario Balducci[1,3]*

[1] UOC di Radioterapia Oncologica, Dipartimento Diagnostica per Immagini, Radioterapia Oncologica ed Ematologia, Fondazione Policlinico Universitario Agostino Gemelli IRCCS, Rome, Italy, [2] UOS di Psicologia Clinica, Fondazione Policlinico Universitario Agostino Gemelli IRCCS, Rome, Italy, [3] Università Cattolica del Sacro Cuore, Rome, Italy, [4] UOC Pediatric Oncology, Department of Woman and Child Health and Public Health, Fondazione Policlinico Universitario A. Gemelli IRCCS, Rome, Italy, [5] Department of Paediatric Haematology/Oncology, IRCCS Bambino Gesù Children's Hospital, Rome, Italy

OPEN ACCESS

Edited by:
Nicola Silvestris,
University of Bari Aldo Moro, Italy

Reviewed by:
Yuanpeng Zhang,
Nantong University, China
Corrado Spatola,
University of Catania, Italy

***Correspondence:**
Maria Zoe Sanfilippo
zoesanfilippo@gmail.com

Specialty section:
This article was submitted to Radiation Oncology, a section of the journal Frontiers in Oncology

Received: 26 October 2020
Accepted: 22 February 2021
Published: 29 March 2021

Citation:
Chiesa S, Marconi E, Dinapoli N, Sanfilippo MZ, Ruggiero A, Mastronuzzi A, Panza G, Serra A, Massaccesi M, Cacchione A, Beghella Bartoli F, Chieffo DPR, Gambacorta MA, Valentini V and Balducci M (2021) The Multidimensional Assessment for Pediatric Patients in Radiotherapy (M.A.P.-RT) Tool for Customized Treatment Preparation: RADAR Project. Front. Oncol. 11:621690. doi: 10.3389/fonc.2021.621690

Aims: Pediatric patients may experience considerable distress during radiotherapy. Combining psychological interventions with standard therapies can reduce the need for sedation. The RADAR Project aims to use a systematic method of recording data that can reveal patients' difficulties and fragility during treatment.
In this context, the aim of our study was to investigate the ability of a multidimensional assessment tool (M.A.P.-RT schedule) to predict the need for sedation during radiotherapy. The schedule, which is administered during the first evaluation, was created to collect information on patients and their families in a standardized way.

Materials and Methods: The study enrolled pediatric patients (aged 0–18 years or 18–21 with cognitive impairment). Data were collected by means of the M.A.P.-RT module; this explores various thematic areas, and is completed by the radiation oncologist, psychologist and nurse during their first evaluation. Features were selected by means of the Boruta method (random forest classifier), and the totals of the significant partial scores on each subsection of the module were inserted into a logistic model in order to test for their correlation with the use of anesthesia and with the frequency of psychological support. The results of logistic regression (LR) were used to identify the best predictors. The AUC was used to identify the best threshold for the scores in the evaluation.

Results: A total of 99 patients were considered for this analysis. The feature that best predicted both the need for anesthesia and the frequency of psychological support was the total score (TS), the AUC of the ROC being 0.9875 for anesthesia and 0.8866 for psychological support.

Conclusion: During the first evaluation, the M.A.P.-RT form can predict the need for anesthesia in pediatric patients, and is a potential tool for personalizing therapeutic and management procedures.

Keywords: radiotherapy, distress, anesthesia, pediatrics, psychological support, children

INTRODUCTION/BACKGROUND

From 2001 to 2010, the worldwide incidence of cancer in subjects aged 0–19 years was 155.8 per million/year (1). In Italy, the AITRUM has estimated that 5-year survival improved among 11,000 children and adolescents newly diagnosed between 2016 and 2020 (2).

A current aim of medicine is to offer therapeutic responses in accordance with the international recommendations, while at the same time enrolling young patients in centralized clinical research protocols in order to guarantee homogeneous, high-quality treatment.

Radiotherapy (RT) is one of the therapeutic options for pediatric neoplasms. In order to ensure the accuracy of radiation treatment, it is necessary to create an *ad-hoc* immobilization system that is personalized according to the site of the tumor. Pediatric patients are required to cooperate closely, first during treatment preparation (by remaining motionless during the preparation of the immobilization system and the phase of image acquisition) and then in the phase of treatment delivery.

Therefore, RT is not only a challenge for children but also for parents and healthcare professionals (3–7). When patients are unable to maintain a fixed and reproducible position, sedation or general anesthesia (GA) becomes necessary. This means that children and adolescents undergo numerous changes in their lifestyle, daily activities, and school and social activities (8). Moreover, numerous sedation treatments can have an impact on eating habits, in that patients have to fast for several hours. Finally, repeated sedation, high doses of sedatives, the use of multiple drugs and general anesthesia can increase the risk of medical complications (9).

In the literature, several studies have described the benefit of combining psychological support interventions with standard therapies for reducing the number of sedations (6, 9, 10). In pediatric RT, recent research has revealed the importance of both pharmacological and non-pharmacological interventions. However, the approaches adopted vary markedly and few assessment tools are available for doctors and researchers. For example, there is, as yet, no assessment tool that can quickly select the type of intervention needed.

In this regard, it has been ascertained that a multi-disciplinary approach implemented by a specialized team (4, 11) can identify the individual patient's needs and enable targeted interventions to be undertaken in order to facilitate treatment preparation and improve patient compliance, thereby avoiding sedation whenever possible.

The RADAR project aims to increase the level of personalization of radiotherapy for the pediatric patient through a multidimensional approach. The project utilizes a standardized tool (Multidimensional Assessment for Pediatric Patients in Radiotherapy M.A.P.-RT schedule) to collect information on patients and their families during the first clinical evaluation; the results obtained allow clinicians to predict the need for sedation and the intensity of specific psychological preparation, and to plan supportive treatment.

MATERIALS AND METHODS

Design, Setting, and Inclusion Criteria

This pilot observational study enrolled pediatric patients with an oncological diagnosis for which radiation treatment had been prescribed. During the patient's first examination, the radiation oncologist, the nurse and the psychologist filled in the M.A.P.-RT form (**Table 1**), a multidimensional assessment form covering a selection of items and standardized tests.

A preliminary set of data were collected from patients who accessed our center last year.

The form was administered to two groups of patients: one aged between 0 and 18 years and the other between 18 and 21 years with cognitive impairment. The M.A.P.-RT form provides for the calculation of several partial scores and of a final score, which could be useful in order to understand the various patients' RT-related needs. However, in this phase, the patient's care pathway did not undergo changes following the scoring of the instrument; patients underwent the preparation phase of the treatment with or without specific interventions and sedation, according to their needs.

Multidimensional Assessment for Pediatric Patients in Radiotherapy, M.A.P.-RT Schedule

The crucial areas in the preparation of children for radiotherapy were identified after 2 years of clinical observations by RT care providers and a psychologist, and on the basis of the literature.

Six areas of interest were identified (**Table 1** and **Figure 1**):

A. **Pain distress-Nursing observations:** data collected when the patient enters the Unit for RT examination for the first time. These data are collected by the first nurse who meets and welcomes the child (Wong Baker Scale WBS—observer: 0–10); maximum value: 10;
B. **Development-Discomfort age score:** this score indicates the potential impact of age on the overall score in children from 0 to 10 years, due to the characteristics of the development and growth of children; maximum value: 10;
C. **Medical-First Medical Evaluation:** this area collects data on the amount of information provided and on the degree of collaboration and distress/pain noted by the RT specialist

TABLE 1 | M.A.P.-RT scoring and items details.

	Dimension	Contents	Score
A	**Pain/distress**	**Nursing observation**	**0–10**
B	**Age**	**Discomfort/age scoring**	**0–10**
C	**Medical**	**First medical evaluation**	**0–22**
		C1: Family information on diagnosis	0–2
		C2: Information on the purpose of RT	0–2
		C3: Information shared with the patient	0–2
		C4: Collaboration of the patient with previous radiography	0–2
		C5: Collaboration with requests from parents/health workers	0–2
		C6: Collaboration in separation from parents	0–2
		C7: Distress/pain level detected during the visit	0–10
D	**Physical**	**Report on skills for RT**	**0–26**
		D1: Physical difficulties	0–2
		D2: Cognitive difficulties	0–2
		D3: Language difficulties	0–2
		D4: Minutes required for the RT	5–20
E	**Emotional distress**	**First Entry to Linac Room (CEMS Scale: Children's Emotional Manifestation Scale)**	**0–25**
		E1: Facial expression	1–5
		E2: Vocalization	1–5
		E3: Activity	1–5
		E4: Interaction	1–5
		E5: Level of cooperation	1–5
F	**Psychological**	**Psychological interview**	**0–30**
		F1: Psychological difficulties before diagnosis	0–3
		F2: Recent loss of mobility/autonomy	0–3
		F3: Patient distress reactive to diagnosis	0–3
		F4: Patient externalizing problem	0–3
		F5: Patient internalizing problem	0–3
		F6: Patient's fear/anxiety (last 2 weeks)	0–3
		F7: Parent's fear/anxiety (last 2 weeks)	0–3
		F8: Parenting difficulties	0–3
		F9: Family/Social/Work difficulties	0–3
		F10: Traumatic events before diagnosis	0–3
		Total Score M.A.P.-RT	**0–123**

The values without bold are the ranges of the scores of the single items. The values in bold are the ranges of the total scores of the contents A–F.

while taking the medical history and performing clinical evaluation; maximum value: 22;

D. **Physical-Skills for RT:** these are the specific skills required for the planned RT treatment, with particular regard to positioning and maintenance of posture during the RT fraction; maximum value: 26;
E. **Emotional Distress-First entry to LINAC room (CEMS):** behavioral and emotional reactions of the child on first entering the bunker; technician records by means of the Children's Emotional Manifestation Scale—CEMS; maximum value: 25;
F. **Psychological-Psychological interview:** this area reports scores assigned by the psychologist following the assessment of psychological areas that are deemed to influence the patient's compliance with RT in both the preparation and treatment phases; for example, past or current mental disorders, previous traumatic events, patient's tendency to implement internalizing or externalizing strategies in the management of distress/pain, family difficulties, etc. maximum value: 30.

Statistical Analysis

We defined two outcomes: anesthesia and psychological support. *Anesthesia* was defined as a binary outcome (patients who needed anesthesia and patients who did not); *psychological support* was defined as a binary outcome (patients who needed an *intensive* course of psychological support and patients who did not); psychological support was defined as "intensive" or "standard" according to a threshold value of 1 support session every 3 days, which was calculated by dividing the median number of psychological sessions during the period of treatment by the number of RT fractions.

Modeling process was assessed in two phases: (12) we performed the feature selection among all the items of M.A.P. report using the Boruta method, which is a novel feature-selection algorithm for identifying all significant variables, designed as a wrapper around a random forest classification algorithm. This test iteratively removes those features which prove to be less significant than random probes, thereby yielding a series of graphs that contain a z-score. The p-value of the z-test is 0.01. All features (items in the M.A.P. report) were tested against the two outcomes listed above (13). The model chosen was the Elastic Net, a regularized generalized linear model; it was used because it enables to discriminate among the items more accurately and to pick out the most significant covariates, even in the presence of cross-correlation. With regard to the outcome "*anesthesia*," our statistical model showed the population classified by a score related to the most significant items found in the M.A.P.-RT schedule: negative scores, i.e., lower than 0, were related to "no anesthesia," while positive ones were found to be mostly associated to "yes anesthesia." The value of each item, when multiplied by the coefficients and added together (linear predictor), returns a score that indicates the actual correlation between patients' characteristics and their need for anesthesia. The same process was used to identify patients who needed *intensive* psychological support and those who did

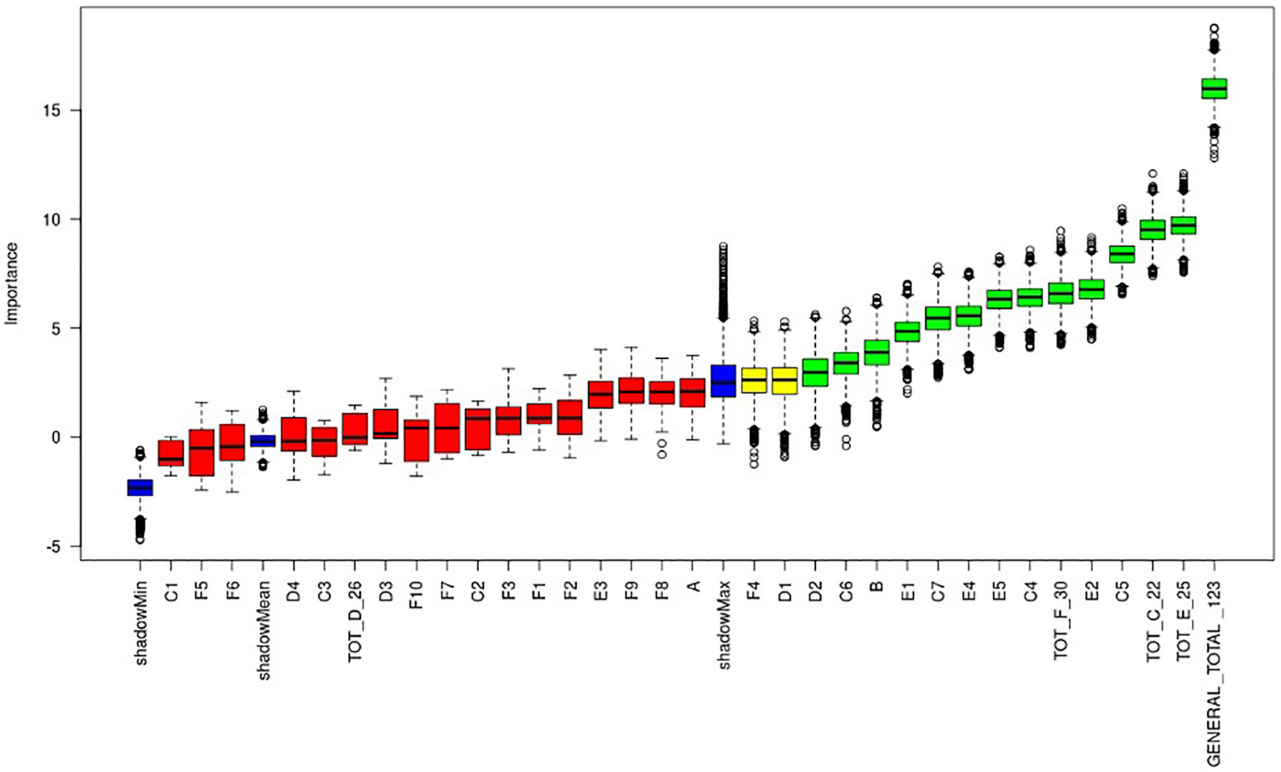

FIGURE 1 | Plot of Boruta feature selection process for the "anesthesia" outcome: the red boxes represent the not relevant items, the yellow are the uncertain ones, the green are the relevant items. Blue boxes are calculated as reference levels during the run of Boruta algorithm.

not. The validation of the models has been performed by using area under the receiver operating characteristic curve (AUC) and confusion matrix statistics computing accuracy, McNemar's test *p*-value, 95% C.I. *p*-value, *k* statistic and *P*-value of binomial test to see if the accuracy is better than "no information rate" (accuracy > NIR).

Ethics Approval

This study was approved by the ethics committee of Agostino Gemelli Polyclinic, Rome.

RESULTS

The study involved 99 consecutive pediatric cancer patients (M.51; F:48), who underwent 99 RT courses (n° RT Fractions: 2097) between January and December 2019.

The M.A.P.-RT form was administered to all patients and data were collected for each area; 20 children who underwent retreatment were excluded from the study. Twenty-two patients needed sedation during radiation treatment. One patient (age 21) presented cognitive impairment. The median age was 7.5 years (range 1–21). Patients' characteristics are reported in **Table 2**.

The team involved in data collection was made up of two oncological radiotherapists, a child psychologist, a nurse, a technician and a resident.

Fourteen items proved to be predictive of the need for anesthesia: B, C4, C5, C6, C7, TOT C, D2, E1, E2, E4, E5, TOT E, TOT F, GENERAL TOT (**Figure 1**). The general total score, and, in particular, the total score of the first clinical medical evaluation and of emotional distress seemed to be the most predictive dimensions of the schedule. The single items that proved predictive were: patient age (see point B **Table 1**), level of collaboration of the patient during previous diagnostic tests (see point C4 **Table 1**), level of the patient's collaboration with the requests of parents and health workers (see point C5 **Table 1**), level of collaboration during separation from the parent (see point C6 **Table 1**), level of distress/pain detected during the first visit (see point C7 **Table 1**), and cognitive difficulties and/or deficits (see point D2 **Table 1**). Other variables that proved to be highly predictive were those related to the patient's psycho-physical attitudes at the time of first entry to the therapy room, specifically: the patient's facial expression (see point E1 **Table 1**), vocal expressions such as crying and screaming (see point E2 **Table 1**), the patient's interaction through verbal or non-verbal responses or possible absence of interaction (see point E4 **Table 1**), the patient's level of cooperation, i.e., whether the child actively participates or is indifferent to external requests (see point E5 **Table 1**).

With regard to the TS, the AUC of the ROC was 0.9875 (sensitivity = 0.91, specificity = 0.97) with a *p*-value = 7.986−12

TABLE 2 | Descriptive statistics and epidemiology of patients population.

	Total	%
Total number patients	99	100%
Sex		
Male	51	51.5%
Female	48	48.5%
Histological diagnosis		
Brain neoplasm	42	42.4%
Hematological neoplasm	24	24.2%
Sarcomas	14	14.1%
Wilms tumor	2	2.0%
Nephroblastoma	2	2.0%
Neuroblastoma	15	15.2%
RT site		
Brain	45	45.5%
Abdomen	15	15.2%
Thorax	9	9.1%
Pelvis	6	6.1%
ACS (Spinal-Skull-Axis)	8	8.1%
TBI (Total Body Irradiation)	11	11.1%
Other	5	5.1%
Immobilization system		
Thermoplastic mask	53	53.5%
VAC-LOC (Vacuum Locked)	21	21.2%
Wing board	9	9.1%
Other	16	16.2%

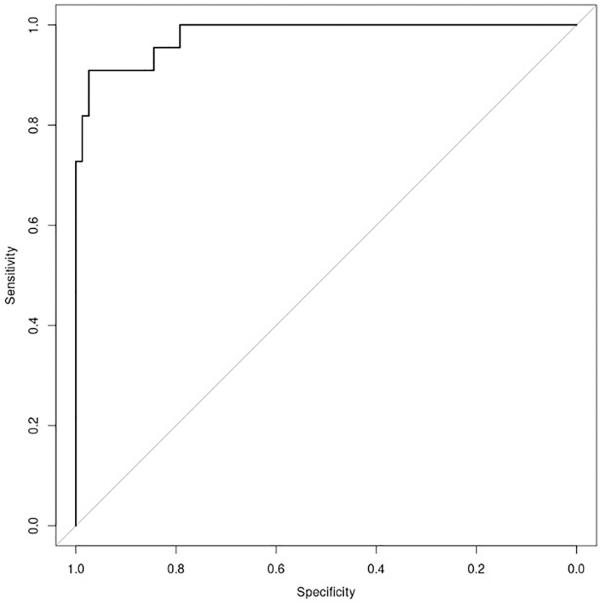

FIGURE 2 | Plot of ROC curve for the "anesthesia" model (AUC = 0.9875), showing possibility to identify patients who need anesthesia support with regards to the total score, achieved putting into the model the value of relevant items of M.A.P.-RT.

(**Figures 2**, **3**). Negative results in **Figure 3** identified patients who underwent treatment without sedation, and positive results identified patients undergoing anesthesia. Confusion matrix statistics are summarized in **Tables 3**, **4**.

We also analyzed the intensity and frequency of psychological support provided for patients. During 99 RT Courses, corresponding to 2097 fractions, 766 psycho-educational interventions were implemented (median: 6, range: 1–20). Moreover, 46 patients received intensive psychological support (>1/3) and 53 standard support (<1/3). In this secondary analysis, the items displaying a predictive value regarding the intensity of the psychological support to be provided were: B, C3, C5, C6, C7, TOT C, D1, D4, TOT D, E2, E3, E5, TOT E, GENERAL TOT (**Figure 4**). The information obtained from points C4–C7, which concern the patient's collaboration, detachment from the caregiver and level of distress/pain, seemed to correlate more closely than the others (C1–C3) with the need for psychological support. Age was also confirmed as a fundamental parameter.

In this case, the model was less accurate; the AUC of the ROC was 0.8866, (sensitivity = 0.91, specificity = 0.84) with a *p*-value = 2.122−07, therefore indicating a higher risk of false negatives or false positives (**Figures 5**, **6**).

DISCUSSION

In pediatric oncology, RT, alone or in combination with surgery or chemotherapy, has become an important treatment option for several kinds of neoplasms. Although it does not cause any pain, the young patient must remain alone and motionless for several minutes during the time of irradiation, a situation that frequently causes distress reactions. Distress reactions are also aggravated by previous traumatic events experienced by patients and their families, such as painful experiences in hospital or at the hands of other healthcare personnel. Such conditions can make the new treatment even more traumatic for the child. Changes in the child's routine, owing to the need to attend the hospital daily, can also constitute an additional source of distress, which may determine the need for sedation. In the literature, some studies have described the experience of anxiety and distress of patients and parents in Pediatric Hematology/Oncology Units, while few studies have described the situation in RT units (7).

In children undergoing radiotherapy, anesthesia ensures adequate immobilization during verification of the patient's position and therapy delivery. With regard to acute and late risks, daily treatment under sedation (14) is associated with major changes in the child's daily routine, such as the need to fast for several hours (15).

Carrying out radiation treatment under sedation also involves specific and careful organization of the treatment room and the presence of the anesthesiologist and the nurse for the entire duration of the treatment; this increases the occupation time of the room and inevitably raises healthcare costs (9).

Some studies in the literature have shown the benefit of combining psychological interventions with standard therapies (11), while others have analyzed the specific activities that can be planned in order to help children to cooperate with RT (16);

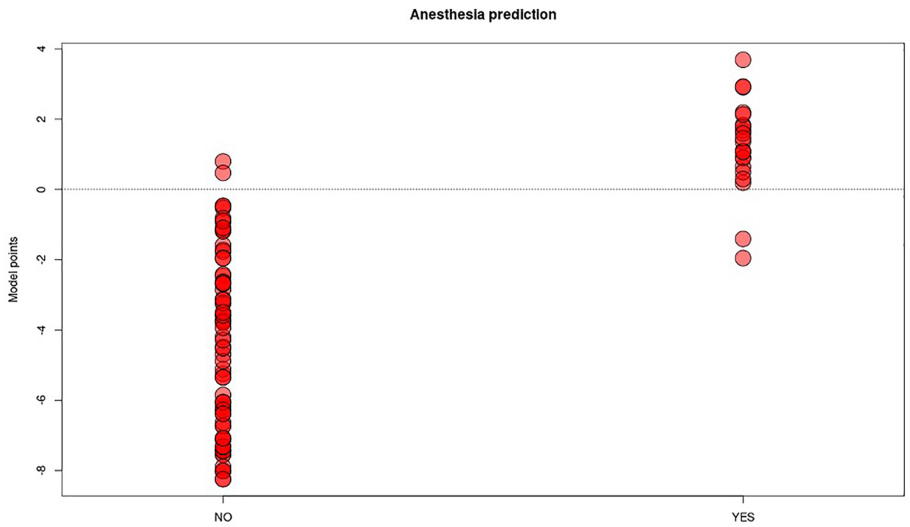

FIGURE 3 | Distribution plot of "anesthesia" predictive model score (y axis) in the two groups of patients undergoing (YES) or not (NO) to anesthesia procedure. The red dots represent each patient in the two groups, the threshold line chosen to best split the two categories is the score 0.

TABLE 3 | Model "anesthesia" performance table: the model shows very high accuracy (0.96), sensitivity (0.91), and specificity (0.97).

Confusion matrix and statistics for anesthesia prediction model			
	Outcome +	**Outcome -**	**Total**
Test +	20	2	22
Test -	2	75	7
Total	22	77	99
No information rate: 0.78			
P-value [Acc > NIR]: 4.567e-07			
Kappa: 0.88			
Mcnemar's Test *P*-value: 1			
Point estimates and 95 % Cis			
Accuracy		0.96 (0.90, 0.99)	
Apparent prevalence		0.22 (0.14, 0.32)	
True prevalence		0.22 (0.14, 0.32)	
Sensitivity		0.91 (0.71, 0.99)	
Specificity		0.97 (0.91, 1.00)	
Positive predictive value		0.91 (0.71, 0.99)	
Negative predictive value		0.97 (0.91, 1.00)	
Positive likelihood ratio		35.00 (8.86, 138.31)	
Negative likelihood ratio		0.09 (0.02, 0.35)	

TABLE 4 | Model "psychological support" performance table: the model shows fair accuracy (0.88), optimal sensitivity (0.91), and specificity (0.94). Overall performance is slightly lower than the "anesthesia" model.

Confusion matrix and statistics for psychological support prediction model			
	Outcome +	**Outcome –**	**Total**
Test +	50	7	57
Test -	5	37	42
Total	55	44	99
No information rate: 0.56			
P-value [Acc > NIR]: 4.078e-12			
Kappa: 0.75			
Mcnemar's test *P*-value: 1			
Point estimates and 95 % Cis			
Accuracy		0.88 (0.80, 0.94)	
Apparent prevalence		0.58 (0.47, 0.67)	
True prevalence		0.56 (0.45, 0.66)	
Sensitivity		0.91 (0.80, 0.97)	
Specificity		0.84 (0.70, 0.93)	
Positive predictive value		0.88 (0.76, 0.95)	
Negative predictive value		0.88 (0.74, 0.96)	
Positive likelihood ratio		5.71 (2.88, 11.33)	
Negative likelihood ratio		0.11 (0.05, 0.25)	

indeed, personalizing the child's preparation can reduce the need for sedation during radiation treatment (10). This problem has often been addressed in the literature, which has highlighted the need for specific scales that can record the levels of pain, anxiety and anguish of pediatric patients and their approach to radiation treatment under sedation. Several instruments have been used to predict pediatric distress in radiotherapy: the Behavioral Distress Observation Scale (OSBD) (8), parent report (7), and qualitative interview (17); other instruments have been applied more generally in the context of sedation (18) or during invasive medical procedures (19).

These tools have made it possible to carry out interventions to reduce emotional distress or monitor the sedation of the pediatric patient. Specifically, some studies have shown that adequate preparation through play activities and the presence of

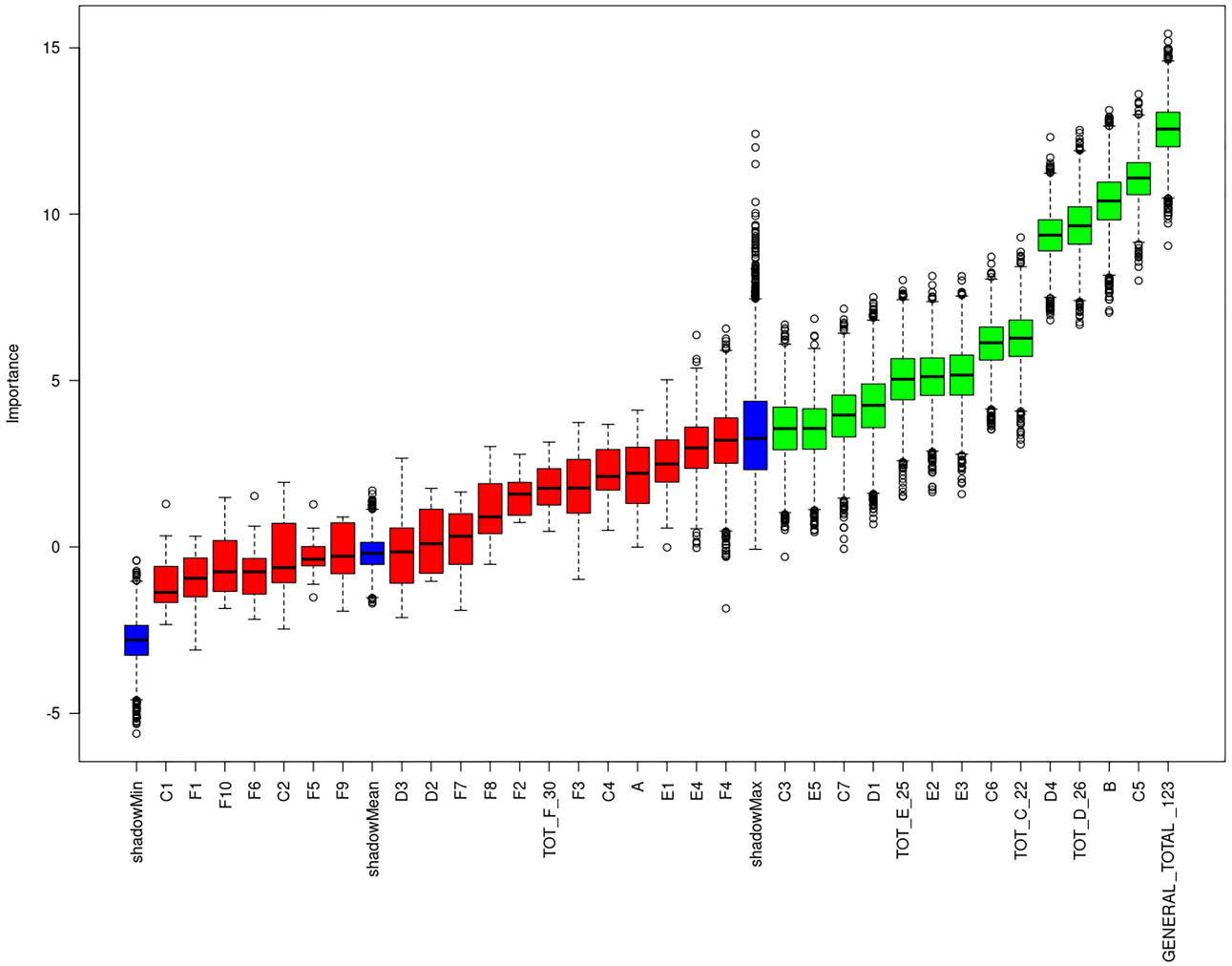

FIGURE 4 | Plot of Boruta feature selection process for the "intensive psychological support" outcome: the red boxes represent the not relevant items, the yellow are the uncertain ones, the green are the relevant items. Blue boxes are calculated as reference levels during the run of Boruta algorithm.

a child psychologist are effective in reducing anxiety and negative emotions (10, 20). For example, some authors have reported that engaging the patient in play activities at the hospital reduces negative emotions and lowers anxiety levels in comparison with normal care (21, 22). Moreover, psychological interventions have proved effective in reducing RT-related distress (as measured by heart rate) and have also been seen to be useful specifically in pediatric radiotherapy (23).

However, few studies have provided clinicians with effective tools to guide the therapeutic and care pathway of pediatric cancer patients undergoing RT. Inspired by the universally used bio-psychosocial model proposed by A. E. Kazak (24), the RADAR project aims to monitor and collect information on pediatric patients undergoing RT and to provide a rapid assessment tool that can identify the needs and risks of these patients.

In our center, the child psychologist, when required, plans psycho-educational intervention before the simulation of radiation treatment. The support plan includes weekly psychological sessions during the period of treatment. Patients defined as more complex, or who have crises during treatment, undergo several interventions per week, daily if necessary.

The introduction of the M.A.P.-RT schedule facilitates multidisciplinary assessment in the initial stages of treatment. To our knowledge, this is the first schedule to collect data in a standardized way in pediatric RT, in order to identify patients' needs; it can therefore optimize and personalize psychological support.

The results of our study identified those items that were predictive of the need for sedation during radiotherapy and for intensive psychological support. Some items were found to be common to both analyses, and proved to be fundamental parameters. For example, age (point B **Table 1**) was confirmed as a fundamental parameter; in our study, we did not establish an age cut-off, but younger children are usually those who most need to be sedated during treatment. In the literature,

the study by Linda Scott, Fiona Langton and Joan O'Donoghue (25) considered 63 children aged between 2 and 5 years; their outcome data suggested that sedation could be minimized in this age-group through the implementation of an effective play preparation program.

Other predictive items were found in group C ("first medical evaluation"): the patient's degree of cooperation, the degree of cooperation in separation from parents, and the distress/pain level detected during the visit. In addition, the total score of F ("psychological interview" and the items in group E, the CEMS scale, had a strong impact on our schedule. The CEMS has been validated (26) and is already used in the field of pediatric radiotherapy (27). Recording patients' distress on entering the bunker for the first time helps the clinician and psychologist to immediately ascertain the complexity of the individual patient.

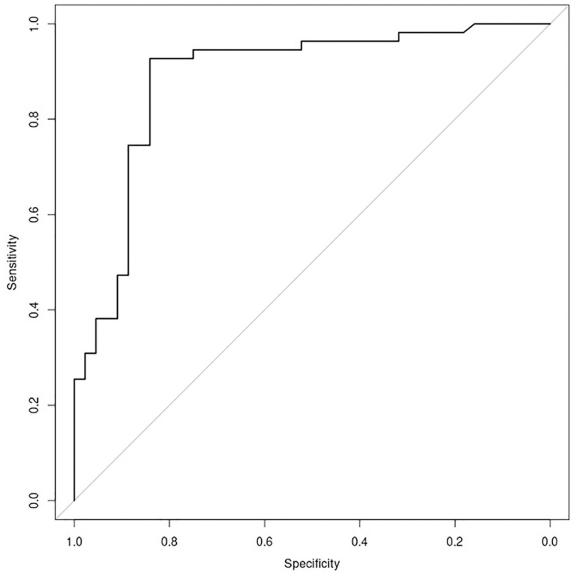

FIGURE 5 | Plot of ROC curve for the "psychological support" model (AUC = 0.8866), showing possibility to identify patients who need intensive support with regards to the total score, achieved putting into the model the value of relevant items of M.A.P.-RT.

Patients who have initially cooperated may experience new side-effects, such as fatigue or crises, during treatment, and may therefore need subsequent psychological support and increased occupancy machine time. By contrast, patients who have difficulty in the preparation phases may rapidly overcome their initial fears or difficulties and require fewer interventions by the child psychologist.

To our knowledge, the M.A.P.-RT schedule is the first tool that has proved to be accurate in predicting, during the first clinical evaluation, the need for sedation during radiation treatment. In addition, it is well-known that administering RT to children requires a great deal of cooperation and that a specialized multidisciplinary team is necessary; the M.A.P.-RT schedule could allow quick, simple and codified communication among the members of this team.

Indeed, the use of the M.A.P.-RT schedule would enable the radiotherapist, child psychologist, residents, nurse and RT technician to understand the specific needs of the patient and to tailor their interventions during treatment preparation and delivery.

Another achievement of this first phase of modeling is that we were able to discern which items in the M.A.P.-RT schedule were the most important. Indeed, some items were not effective in predicting the need for anesthesia during treatment. Therefore, in the future, the form could be modified in such a way as to include only those items with the greatest predictive capability. This would reduce the time needed for its compilation, making

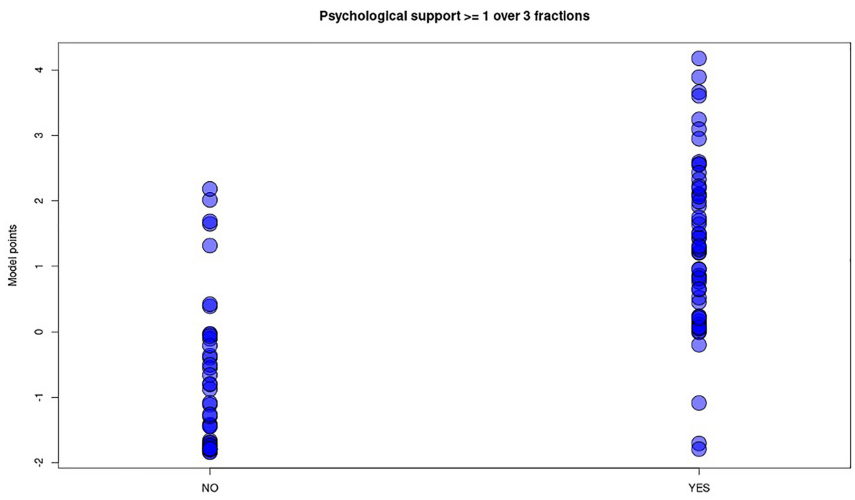

FIGURE 6 | Distribution plot of "psychological support" predictive model score (y axis) in the two groups of patients undergoing (YES) or not (NO) to intensive psychological support. The blue dots represent each patient in the two groups. Differently from "anesthesia" model no threshold line has been plotted, being wide overlapping between the two categories of patients despite fair model performances.

it more manageable by the various professionals involved. Of course, the shorter version would need to be validated on a larger sample of patients, such as the sample that we are currently enrolling prospectively.

A limitation of our study is the fact that the tool does not accurately predict the intensity of the psychological support to be provided; this is partly because, during RT, the need for psychological support may change over time, owing to sideeffects, the influence of other sources of distress, interactions with drugs, clinical or family difficulties, etc. For this reason, psychological support during RT must be modulated over time and personalized, in terms of both type and frequency, according to the patients needs.

In the light of these observations, other scales or tools could be used to evaluate the evolution of patients' needs over time. In this regard, the Radar Project envisions the use of other tools that allow further evaluations during RT (daily evaluation by RT technicians; medical evaluation during RT, psychological scales, etc.). We think that, if the M.A.P.-RT schedule were integrated with data subsequently collected during RT, it would be possible to further customize psychological support, adjust it over time and verify its effectiveness.

CONCLUSIONS

The study shows that multidimensional assessment is an optimal strategy during the procedures of radiation oncology setup and RT delivery in pediatric patients. In particular, the M.A.P.-RT schedule proved to be a good and appropriate work tool capable of predicting, even at the time of the first visit, the pediatric patient's need for sedation. Moreover, its use could also improve cooperation among the specialists of the pediatric team.

DATA AVAILABILITY STATEMENT

The raw data supporting the conclusions of this article will be made available by the authors, without undue reservation.

ETHICS STATEMENT

The studies involving human participants were reviewed and approved by Ethics Committee - Fondazione Policlinico Universitario Agostino Gemelli, IRCCS. Written informed consent to participate in this study was provided by the participants' legal guardian/next of kin.

AUTHOR CONTRIBUTIONS

MB, SC, EM, and MS conceived of the presented idea. ND processed the experimental data, performed the analysis, and designed the figures. MS collected data and drafted the manuscript, while SC and EM reviewed the text. MB provided final approval of the version to publish. All authors discussed the results and commented on the manuscript.

REFERENCES

1. Steliarova-Foucher E, Colombet M, Ries LAG, Moreno F, Dolya A, Bray F, et al. International incidence of childhood cancer, 2001–10: a population-based registry study. *Lancet Oncol*. (2017) 18:719–31. doi: 10.1016/S1470-2045(17)30186-9
2. Pisani P, Buzzoni C, Crocetti E, Dal Maso L, Rondelli R, Alessi D. Italian Cancer Figures - Report 2012 Cancer in children and adolescents AIRTUM Working Group and AIEOP Working Group. *Epidemiol Prev*. (2013) 37:1–296.
3. O'Connor M, Halkett GK. A systematic review of interventions to reduce psychological distress in pediatric patients receiving radiation therapy. *Patient Educ Couns*. (2019) 102:275–83. doi: 10.1016/j.pec.2018.09.023
4. Filin A, Treisman S, Peles Bortz A. Radiation therapy preparation by a multidisciplinary team for childhood cancer patients aged 3/(2) to 6 years. *J Pediatr Oncol Nurs*. (2009) 26:81–5. doi: 10.1177/1043454208328766
5. Sehlen S, Hollenhorst H, Schymura B, Herschbac P, Aydemir U, Firsching M. Psychosocial stress in cancer patients during and after radiotherapy. *Strahlenther Onkol*. (2003) 179:175–80. doi: 10.1007/s00066-003-1018-z
6. Haeberli S, Grotzer MA, Niggli FK, Landolt MA, Linsenmeier C, Ammann RA, et al. A psychoeducational intervention reduces the need for anesthesia during radiotherapy for young childhood cancer patients. *Radiat Oncol*. (2008) 6:1–6. doi: 10.1186/1748-717X-3-17
7. Ångström-Brännström C, Lindh V, Mullaney T, Nilsson K, Johansson G, Svard A. Parents' experiences and responses to an intervention for psychological preparation of children and families during the child's radiotherapy. *J Pediatr Oncol Nurs*. (2018) 35:132–48. doi: 10.1177/1043454217741876
8. Klosky JL, Tyc VL, Tong X, Srivastava DK, Kronenberg M, Armendi A. Predicting pediatric distress during radiation therapy procedures: the role of medical, psychosocial, and demographic factors. *Pediatrics*. (2007) 119:e1159 LP−66. doi: 10.1542/peds.2005-1514
9. Scott MT, Todd KE, Oakley H, Bradley JA, Rotondo RL, Morris AG. Reducing anesthesia and health care cost through utilization of child life specialists in pediatric radiation oncology. *Int J Radiat Oncol Biol Phys*. (2016) 96:401–5. doi: 10.1016/j.ijrobp.2016.06.001
10. Bokun J, Klikovac T, Vujic D, Nikitovic M. The role of the psychologist in the preparation of young children for radiotherapy: short review. *J BUON*. (2011) 16:561–4.
11. Elsner K, Mrt B, Naehrig D, Georgia KB, Halkett, Dhillon H. Reduced patient anxiety as a result of radiation therapist-led psychosocial support : a systematic review. *J Med Radiat Sci*. (2017) 64:220–31. doi: 10.1002/jmrs.208
12. Kursa MB, Rudnicki WR. Feature selection with the boruta package. *J Statist Softw*. (2010) 36:1–13. doi: 10.18637/jss.v036.i11
13. Zou H, Hastie T. Regularization and variable selection *via* the elastic net. *J R Stat Soc Series B Stat Methodol*. (2005) 67:301–20. doi: 10.1111/j.1467-9868.2005.00503.x
14. Anghelescu DL, Burgoyne LL, Liu W, Hankins GM, Cheng C, Beckham PA. Safe anesthesia for radiotherapy in pediatric oncology: St. Jude Children's Research Hospital Experience, 2004–2006. *Int J Radiat Oncol Biol Phys*. (2008) 71:491–7. doi: 10.1016/j.ijrobp.2007.09.044
15. Engvall G, Lindh V, Mullaney T, Nyholm T, Lindh J, Ångström-brännström C. Children' s experiences and responses toward an intervention for psychological preparation for radiotherapy. *Radiat Oncol*. (2018) 13:9. doi: 10.1186/s13014-017-0942-5
16. Grissom S, Boles J, Bailey K, Cantrell K, Kennedy A, Sykes A. Play-based procedural preparation and support intervention for cranial radiation. *Support Care Cancer*. (2016) 24:2421–7. doi: 10.1007/s00520-015-3040-y
17. Shrimpton BJM, Willis DJ, Tongs CD, Rolfo AG. Movie making as a cognitive distraction for paediatric patients receiving radiotherapy treatment: qualitative interview study. *BMJ Open*. (2013) 3:1666. doi: 10.1136/bmjopen-2012-001666
18. Berghmans JM, Poley JM, Ende J, Weber F, Velde MV, Adriaenssens P. A Visual Analog Scale to assess anxiety in children during anesthesia induction

(VAS-I): results supporting its validity in a sample of day care surgery patients. *Paediatr Anaesth*. (2017) 27:955–61. doi: 10.1111/pan.13206
19. Bachanas, Pamela J., Blount, Ronald L. The behavioral approach-avoidance and distress scale: An investigation of reliability and validity during painful medical procedures. *J Pediatr Psychol*. (1996) 21:671–81. doi: 10.1093/jpepsy/21.5.671
20. Mizumoto M, Oshiro Y, Ayuzawa K, Miyamoto T, Okumura T. Preparation of pediatric patients for treatment with proton beam therapy. *Radiother Oncol*. (2015) 114:245–8. doi: 10.1016/j.radonc.2015.01.007
21. Li WHC, Chung JOK, Ho KY, Kwok BMC. Play interventions to reduce anxiety and negative emotions in hospitalized children. *BMC Pediatr*. (2016) 16:63. doi: 10.1186/s12887-016-0570-5
22. Bumin AG, Yüksel S, Ergil J. The effect of play distraction on anxiety before premedication administration: a randomized trial. *J Clin Anesth*. (2016) 36:27–31. doi: 10.1016/j.jclinane.2016.04.044
23. Klosky JL, Tyc VL, Srivastava DK, Tong X, Kronenberg M, Booker ZJ. Brief report: evaluation of an interactive intervention designed to reduce pediatric distress during radiation therapy procedures. *J Pediatr Psychol*. (2004) 29:621–6. doi: 10.1093/jpepsy/jsh064
24. Kazak AE, Abrams AN, Banks J, Christofferson J, DiDonato S, Grootenhuis MA. Psychosocial assessment as a standard of care in pediatric cancer. *Pediatr Blood Cancer*. (2015) 62(Suppl.5):S426–59. doi: 10.1002/pbc.25730
25. Scott L, Langton F, O'Donoghue J. Minimising the use of sedation/anaesthesia in yung children receiving radiotherapy through an effective play preparation programme. *Eur J Oncol Nurs*. (2002) 6:15-22. doi: 10.1054/ejon.2001.0162
26. Cheung H, Li W, Lopez V. Children's Emotional Manifestation Scale: development and testing. *J Clin Nurs*. (2005) 14:223–9. doi: 10.1111/j.1365-2702.2004.01031.x
27. Gårdling J, Törnqvist E, Månsson ME, Hallström IK. Age-appropriate preparations for children with cancer undergoing radiotherapy: a feasibility study. *J Child Health Care*. (2017) 21:370–80. doi: 10.1177/1367493517727070

Conflict of Interest: The authors declare that the research was conducted in the absence of any commercial or financial relationships that could be construed as a potential conflict of interest.

frontiers in Oncology

ORIGINAL RESEARCH
published: 30 June 2021
doi: 10.3389/fonc.2021.578934

Longitudinal Grouping of Target Volumes for Volumetric-Modulated Arc Therapy of Multiple Brain Metastases

*Yingjie Xu, Junjie Miao, Qingfeng Liu, Peng Huang, Pan Ma, Xinyuan Chen, Kuo Men, Jianping Xiao and Jianrong Dai**

Department of Radiation Oncology, National Cancer Center/National Clinical Research Center for Cancer/Cancer Hospital, Chinese Academy of Medical Sciences and Peking Union Medical College, Beijing, China

OPEN ACCESS

Edited by:
Francesco Cellini, Dipartimento di Radioterapia Oncologica, Fondazione Policlinico A. Gemelli (IRCCS), Italy

Reviewed by:
Yulin Song, Memorial Sloan Kettering Cancer Center, United States
Mengying Shi, University of Massachusetts Lowell, United States

***Correspondence:**
Jianrong Dai
dai_jianrong@cicams.ac.cn

Specialty section:
This article was submitted to Radiation Oncology, a section of the journal Frontiers in Oncology

Received: *01 July 2020*
Accepted: *07 June 2021*
Published: *30 June 2021*

Citation:
Xu Y, Miao J, Liu Q, Huang P, Ma P, Chen X, Men K, Xiao J and Dai J (2021) Longitudinal Grouping of Target Volumes for Volumetric-Modulated Arc Therapy of Multiple Brain Metastases. Front. Oncol. 11:578934. doi: 10.3389/fonc.2021.578934

Purpose: Treatment of multiple brain metastases with single-isocenter volumetric modulated arc therapy causes unnecessary exposure to normal brain tissue. In this study, a longitudinal grouping method was developed to reduce such unnecessary exposure.

Materials and Methods: This method has two main aspects: grouping brain lesions longitudinally according to their longitudinal projection positions in beam's eye view, and rotating the collimator to 90° to make the multiple leaf collimator leaves conform to the targets longitudinally group by group. For 11 patients with multiple (5–30) brain metastases, two single-isocenter volumetric modulated arc therapy plans were generated using a longitudinal grouping strategy (LGS) and the conventional strategy (CVS). The prescription dose was 52 Gy for 13 fractions. Dose normalization to 100% of the prescription dose in 95% of the planning target volume was adopted. For plan quality comparison, Paddick conformity and the gradient index of the planning target volume, and the mean dose, the $V_{100\%}$, $V_{50\%}$, $V_{25\%}$, and $V_{10\%}$ volumes of normal brain tissue were calculated.

Results: There were no significant differences between the LGS and CVS plans in Paddick conformity ($p = 0.374$) and the gradient index ($p = 0.182$) of the combined planning target volumes or for $V_{100\%}$ ($p = 0.266$) and $V_{50\%}$ ($p = 0.155$) of the normal brain. However, the $V_{25\%}$ and $V_{10\%}$ of the normal brain which represented the low-dose region were significantly reduced in the LGS plans ($p = 0.004$ and $p = 0.003$, respectively). Consistently, the mean dose of the entire normal brain was 12.04 and 11.17 Gy in the CVS and LGS plans, respectively, a significant reduction in the LGS plans ($p = 0.003$).

Conclusions: The longitudinal grouping method can decrease unnecessary exposure and reduces the low-dose range in normal brain tissue.

Keywords: longitudinal-grouping, multiple brain metastases, VMAT, single-isocenter, decrease unnecessary exposure

INTRODUCTION

Brain metastases (BMs) are the most common type of intracranial tumors. About 20–40% of patients with cancer develop BMs in their tumor history (1), and multiple BMs are present in approximately 70% of patients with BMs. With recent advances in medical care, chemotherapy, and targeted therapies, overall survival has improved in patients with cancer. With advances in the control of systemic disease, treatment of BMs has become a greater challenge for oncologists (2).

With the continuous development of stereotactic radiosurgery (SRS) and hypofractionated stereotactic radiotherapy (HFSRT) technologies, several studies have found that patients with 5–10 BMs showed similar overall survival to patients with two to four BMs who were treated with SRS (3–5). The SRS and HFSRT has been an effective choice for patients with five or more BMs, especially those who have previously been treated with whole brain radiotherapy.

Traditionally, multiple BMs have been treated individually with SRS or HFSRT. For each lesion, the plan employs one isocenter with several arcs or static beams from a linac or uses several focuses with Gamma Knife shots. When the number of BMs reaches five, the duration of a complete treatment can be many hours. Furthermore, planning is more difficult and requires more care with an increased number of BMs.

Volumetric modulated arc therapy (VMAT), which has been developed in the past decade, has been widely used in tumor treatment at various sites because it produces highly conformal dose distributions and has short treatment delivery times (6). Clark GM et al. (7) contended that single-isocenter VMAT plans can deliver conformity equivalent to that of multiple-isocenter VMAT techniques. In recent years, many studies (8–11) have verified the quality of single-isocenter VMAT plans, and they have been an option in SRS or HFSRT for the treatment of multiple BMs.

However, two problems are introduced by employing single-isocenter VMAT in the treatment of multiple BMs using SRS or HFSRT. One problem is how to manage the rotational uncertainties of the patient setup. Many studies (12–15) have focused on this problem and provided advice to address it. Faught AM et al. (13) suggested that clinical medical physicists revisit the quality assurance tolerances of gantry and multi-leaf collimator (MLC) angles. Miao J et al. (15) proposed the method of expanding the nonuniform gross target volume (GTV) or clinical target volume by adding a planning target volume (PTV) margin. The other problem is how to reduce unnecessary exposure of normal brain tissue. In multiple-target single-isocenter VMAT treatment planning, it is common for a pair of targets to share MLC leaf pairs when they are aligned along the direction of MLC leaf travel [i.e., the "island-blocking" problem proposed by Jun Kang (16)]. The island-blocking problem and the larger jaw openings used in VMAT plans result in increased leakage of the dose between the leaves, which is the main reason for the increase in unnecessary exposure of normal brain tissue. Some researchers (16, 17) have proposed some new algorithms to select the optimal couch and collimator angles to reduce the island-blocking problem. However, those methods require couch rotation during treatment, which would not only increase treatment time but also introduce new errors during the patient setup procedure. If such methods are employed, the problem of increased dose leakage between the leaves caused by the larger jaw openings in single-isocenter VMAT plans still exists. Therefore, the existing methods have limitations.

Helical tomotherapy (HT) employs a small 6-MV linac mounted on a ring gantry. It benefits from its binary MLC, which is perpendicular to the transverse plane of the body and the helical treatment mode. It has excellent dose modulation ability and can deliver a complex dose distribution. The island-blocking problem and the larger jaw opening issue no longer exist when patients with multiple BMs undergo helical tomotherapy.

Inspired by the treatment mode of HT, we developed a longitudinal grouping method to reduce unnecessary exposure of normal brain tissue without couch rotation in single-isocenter VMAT technology for treatment of multiple BMs by SRS or HFSRT. The method can reduce the low-dose range of normal brain tissue, and it is easy to implement.

MATERIALS AND METHODS

Method Description

In this study, we developed a longitudinal grouping method to reduce the impact of the island-blocking problem and the larger jaw opening problem in single-isocenter VMAT treatment of multiple BMs. In this method, multiple BMs were divided into several groups according to their locations. Then, treatment arcs were added, and dose optimization was performed. One therapeutic arc was added to each group. The number of therapeutic arcs depended only on the group number, not on the number of BMs in each group. The grouping technique is the most important aspect of this method. In general, the longitudinal positions of the targets on the beam's eye views (BEVs) throughout all 360° of beam angles are the primary consideration. If the targets' longitudinal projections overlap when the gantry rotates, they can be grouped together. If a target is located between two groups, and the two groups have targets that overlap with it, group assignment is more difficult. In such cases, the target can be viewed on CT images to observe its relationship to adjacent targets, and then it can be classified into the group that is closest to it on the CT images. After the grouping process, it should be verified that the distance between the adjacent surfaces of the longitudinal projections of any two lesions in the same group does not exceed 1 cm. **Figure 1** is a grouping example shown in BEV. Then, the collimator can be rotated to 90° to align the MLC conformal to the targets in the longitudinal direction group by group, analogously to the treatment mode of HT. The difference is that in this method, the MLC leaf can stay in any position in the field, whereas the MLC leaves have only on and off modes in HT.

The method has four planning steps. First, all of the multiple BMs are grouped. For each patient, all BMs are composited as a structure named PTVall, and they are divided into several groups longitudinally according to the above grouping method. The associated lesions in each group are combined into a structure

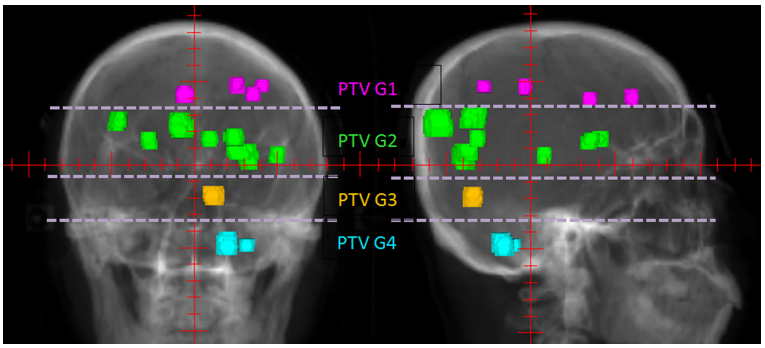

FIGURE 1 | An example of PTV groups in 0° and 90° BEVs. The patient had 14 BMs, which were longitudinally divided into four groups marked by different colors according to their longitudinal projections.

named PTV Gnumber, where PTVall is divided into PTV G1, PTV G2, PTV G3, etc. (**Figure 1**). Each PTV group corresponds to a prescription, and the prescriptions are also named according to the corresponding numbers of the PTV groups (e.g., prescription1, prescription2). **Figure 2** shows four prescriptions for an example patient. Second, the isocenter is set, and the first arc is added. The isocenter is positioned at the centroid of all the targets. After the isocenter is set, the first full arc is added and combined with the first prescription in either the clockwise or counter-clockwise direction. The collimator of the arc is set to 90° to ensure that the MLC leaves longitudinally conform to the lesions in the first group. Third, the first arc is optimized. Only the lesions in the first group are added as the target objects. The organs-at-risk (OARs), the rings (i.e., the rings around PTVall), and normal tissue are set as constrained objects. Fourth, another arc is added and optimized group by group. After the optimization of the first lesion group, the second arc is added, the collimator is rotated to 90°, the second group of lesions replaces the first lesion group as the new target objects, and the constrained objects are adjusted according to the new situation. This process is repeated until all lesion groups are added and optimized.

Patient Selection and Treatment Planning

To evaluate the method's effectiveness, 11 patients with 5–30 previously treated BMs were retrospectively studied in this work.

According to our clinical practice, patients were treated with HFSRT, and the prescription dose was 52 Gy delivered in 13 fractions for each patient. The CT images were acquired on a Somatom Definition AS 40 (Siemens Healthcare, Forchheim, Germany) or Brilliance CT Big Bore (Philips Healthcare, Best, Netherlands) system with 2-mm slice thickness. The MR images were fused with the CT images for GTV contouring, and the PTVs were derived using a 2-mm expansion from the GTVs. Each patient's PTVs were combined into a PTVall for plan evaluation. The mean volume of PTVall was 24.49 cm^3 (2.93–62.51 cm^3).

In each patient, two VMAT plans were generated for comparison to verify the method's ability to reduce the low-

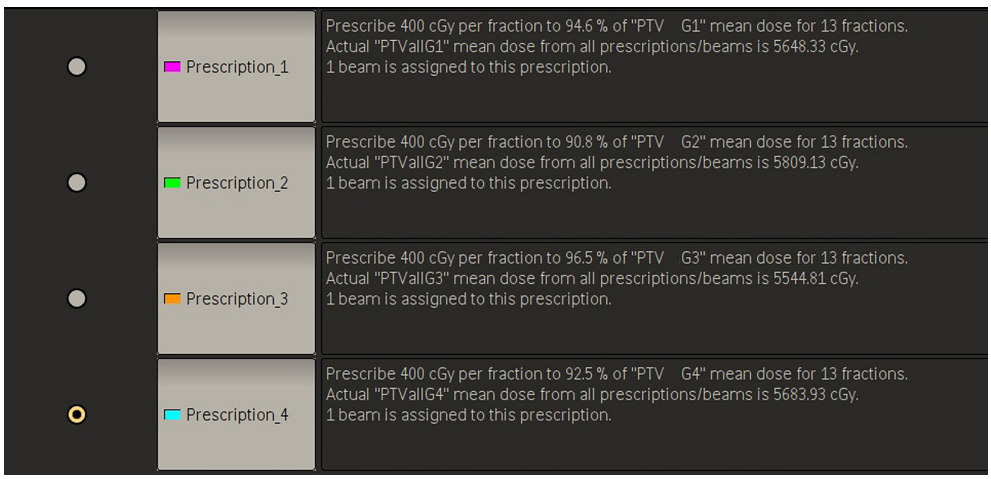

FIGURE 2 | Example prescription settings.

dose range of exposure to normal brain tissue. One plan was designed using the longitudinal grouping strategy devised in this work (named the LGS plan), and the other plan was developed using the conventional strategy, in which all lesions were optimized simultaneously (named the CVS plan). The isocenter and number of VMAT arcs were identical between the CVS and LGS plans. Except for the fact that PTVall was set as the target of optimization, the other constraint objectives were consistent with the final optimization objectives in the LGS plan, and the structures of the constrains were the same in the two planning methods. All plans were designed using the Pinnacle version 16.2 (Philips Healthcare, Best, Netherlands) treatment planning system and the adaptive convolution algorithm. We used a 6-MV flattening filter-free photon beam with a maximum dose rate of 1,400 MU/min. The MLC with 2.5-mm leaves (Varian HD120) was used for planning and delivery, and each plan was calculated with high-resolution dose grid spacing of 2 mm. All plans were normalized so that 95% of the PTVall volume received 100% of the prescription dose.

Plan Evaluation and Comparison

The dosimetric parameters of PTVall and the OARs were derived from the dose volume histograms for plan evaluation. According to International Commission on Radiation Units and Measurements reports 83 (18) and 91 (19), the conformity index (CI) and gradient index (GI) were quantitatively assessed as tumor evaluation parameters. The CI represents the degree to which the prescription dose region conforms to the surface of PTVall, and it is calculated using the Paddick formula (20): $(TVPV)^2/(TV \times PV)$, where TVPV represents the volume of PTVall, which is covered by the prescription dose; TV represents the volume of PTVall; and PV represents the prescription isodose volume. The GI is used to evaluate the dose falloff, and it was defined as PV_{half}/PV, where PV_{half} denotes the volume enclosed by the isodose surface of half the prescription dose, and PV is the volume enclosed by the prescription isodose surface. The median absorbed dose ($D_{50\%}$), the near maximum dose ($D_{2\%}$), and the near-minimum dose ($D_{98\%}$) of PTVall were recorded for target evaluation.

To evaluate the method's effectiveness at minimizing unnecessary exposure to normal brain tissue, the dose received by normal brain tissue was also recorded for statistical analysis, including $V_{100\%}$, $V_{50\%}$, $V_{25\%}$, $V_{10\%}$, and D_{mean} of normal brain. The decreased proportions of $V_{25\%}$ ($1 - V_{25\%,\ LGS\ plan}/V_{25\%,\ CVS\ plan}$), $V_{10\%}$ ($1 - V_{10\%,\ LGS\ plan}/V_{10\%,\ CVS\ plan}$), and D_{mean} ($1 - D_{mean,\ LGS\ plan}/D_{mean,\ CVS\ plan}$) of normal brain in LGS plans were calculated, and the relationships between the decreased proportions and the number of lesions were analyzed.

Statistical Analysis

Paired Wilcoxon signed rank two-sided tests were performed on all datasets with IBM SPSS Statistics 19 (SPSS, Inc., Chicago, IL, USA). Individual comparisons between dosimetric parameters were performed, and p-values of <0.05 were considered significant.

RESULTS

All plans achieved 95% coverage of PTVall. **Figure 3** shows representative axial, sagittal, and coronal dose distributions for the two plans. The LGS plan achieved better low-dose distribution. By checking the BEV of each arc (see **Figure 4**), we found that all of the control points of the LGS plan were shaped like narrow strips and did not have the island-blocking problem, whereas the jaw opening was much larger for the control points of the CVS plan, and the island-blocking problem could not be avoided in the CVS plan. **Table 1** contains a summary of the plan evaluation parameters and the respective descriptive statistics.

The LGS plans achieved a similar level of conformity to that of the CVS plans (CI = 0.80 ± 0.05 and 0.79 ± 0.06, respectively; p = 0.374). There was also no significant difference in GI between the plans (LGS: 6.35 ± 1.15; CVS: 6.53 ± 1.24; p = 0.182). **Figures 5** and **6** show the relationship between CI value, GI value, and lesion number: there was no significant correlation between CI, GI, and the number of BMs. There was also no significant difference in the near-maximum dose ($D_{2\%}$) of PTVall between the two plans (p = 0.534). However, the near-minimum dose ($D_{98\%}$) of the LGS plan was slightly higher than that of the CVS plan, and the median absorbed dose ($D_{50\%}$) of the LGS plan was slightly but significantly lower than that of the CVS plan (p = 0.006 and p = 0.041, respectively).

Consistently with the equivalence in GI values, no significant difference between the two plans resulted for $V_{100\%}$ and $V_{50\%}$ of normal brain: 1.61 ± 2.17 cm^3 and 129.72 ± 109.82 cm^3, respectively, for LGS plans and 2.13 ± 3.26 cm^3 and 139.26 ± 121.21 cm^3, respectively, for CVS plans (p = 0.266 and p = 0.155, respectively). Statistically significant improvement in favor of LGS plans was achieved for $V_{25\%}$ and $V_{10\%}$ of normal brain: the value decreased from (543.72 ± 353.44 cm^3, 1015.68 ± 366.79 cm^3), respectively, for CVS plans to (511.37 ± 342.54 cm^3, 928.45 ± 385.76 cm^3), respectively, for LGS plans (p = 0.004 and p = 0.003, respectively). Consistently, the LGS plans' mean dose of normal brain tissue (1116.68 cGy) was significantly lower than that of CVS plans in statistics (1,204.35 cGy; p = 0.003).

As we mainly focused on evaluating the reduction of unnecessary exposure of normal brain tissue, we determined the relationships between the decreasing proportion of $V_{25\%}$, $V_{10\%}$, and D_{mean} of normal brain and the number of lesions in the two plans. **Figures 7** and **8** show that there was no particular relationship between the decreased proportions of $V_{25\%}$, $V_{10\%}$, and D_{mean} of normal brain in the LGS plans and the number of lesions, but the decreased proportions in the D_{mean} value of normal brain tended to decrease with an increased number of lesions.

DISCUSSION

In this work, we developed a practical method for application in single-isocenter VMAT treatment planning for multiple BMs. This method's strategy is to mimic the treatment mode of HT in single-isocenter VMAT plans. In our department, HT has been used in multiple BMs radiotherapy and has obtained good

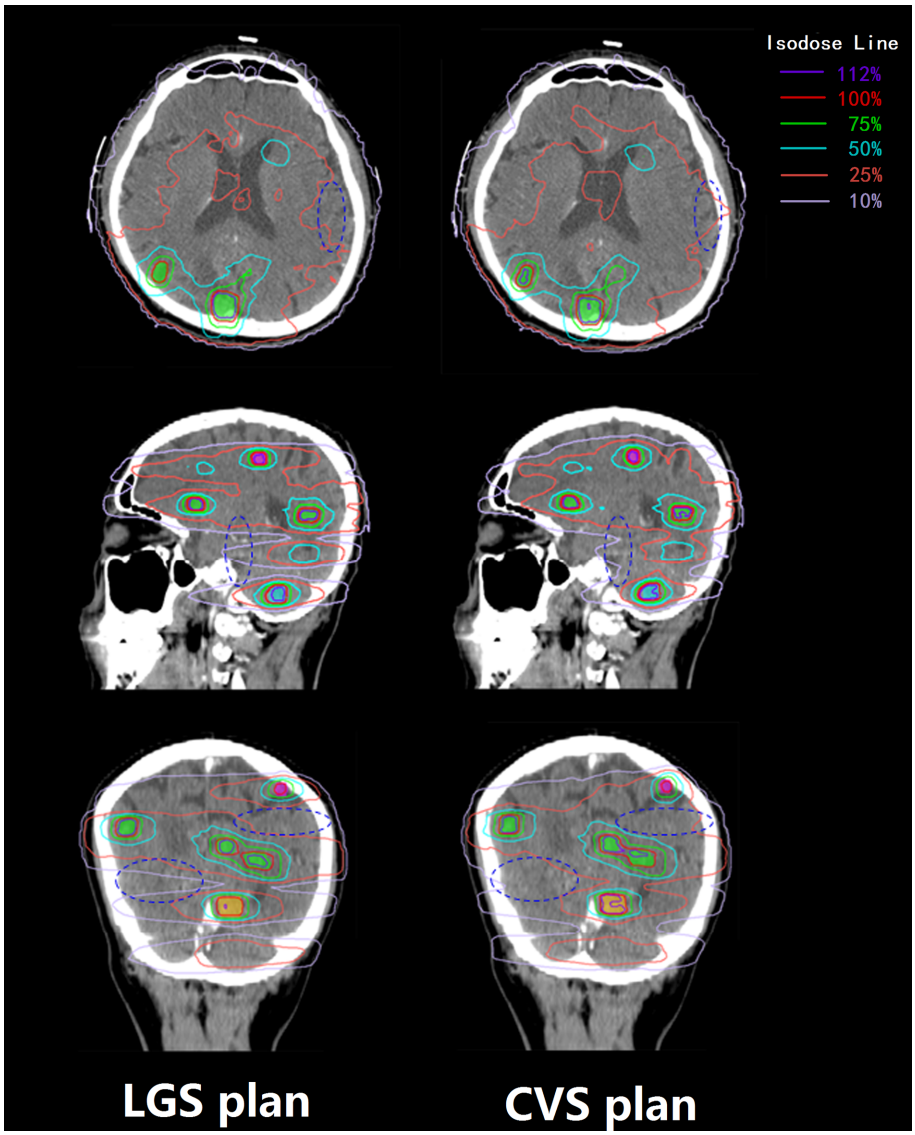

FIGURE 3 | Transverse, sagittal, and coronal dose distributions of two plans for an example patient. The patient had 14 BMs, which were divided into four groups. The 100, 75, and 50% prescription isodose lines did not show much difference between the two plans, but the differences between the 25 and 10% prescription isodose lines between the two plans were obvious. The dark blue ovals mark the areas where there is a significant difference in dose distribution between the two plans.

clinical results (21). Accordingly, if the collimator setting of the C-arm linac is maintained at 90°, the motion of the MLC leaves would be similar to the motion of binary MLC in HT, but more flexible when the optimized target objective is limited to a group of lesions. Since the maximum adjacent surface distance between the longitudinal projections of lesions in the same group did not exceed 1 cm, even when two or more lesions shared the same MLC leaf pairs, there was no unnecessary exposure to normal brain because there was only a narrow exposure gap between the lesions. Furthermore, each VMAT arc only covered lesions in the same group, which indirectly mitigates the deleterious effects of large jaw-defined field sizes. This reduces the island-blocking problem, and reducing the area of the jaw opening also decreases the leakage dose between the leaves, is which caused by the large jaw opening. The present study's results verify this reasoning.

The results of comparisons between the two plan types showed no differences in conformity or gradient between the two methods. This may be because except for the first VMAT arc, the other VMAT arcs were optimized with the previously optimized dose, which may affect the optimization results of the current arc. Although there was no statistical difference between the two plan types' average values of CI and GI, the conformity and gradient of the LGS plan were slightly better than those of the CVS plan.

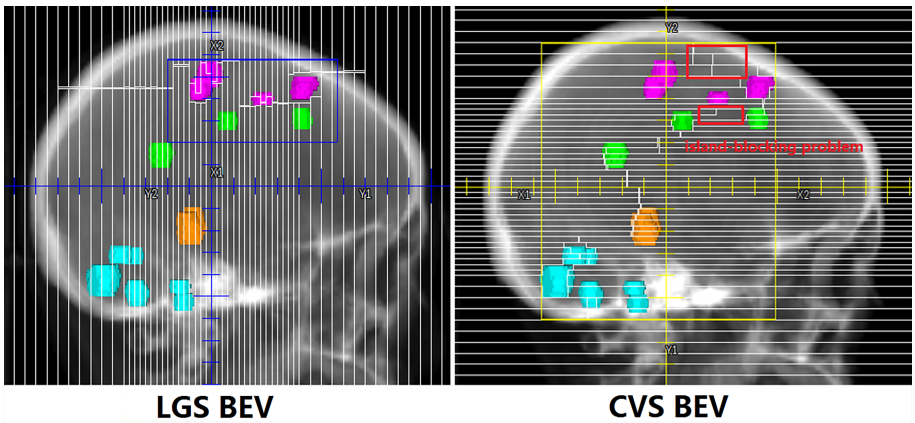

FIGURE 4 | One segment of LGS and CVS in BEV. The control points in the LGS plan are shaped like narrow strips that do not have the island-blocking problem. However, in the CVS plan, the issues of the island-blocking problem and large jaw opening inevitably arise.

TABLE 1 | Statistics of plan evaluation parameters for the two plan types.

		LGS plan			CVS plan			P
		Range	Median	Mean	Range	Median	Mean	
PTVall	D2%	6,026–6,365	6,229	6,210.55	5,820–6,506	6,253	6,236.82	0.534
	D98%	5,048–5,103	5,072	5,074.36	4,983–5,119	5,035	5,037.45	0.006
	D50%	5,583–5,805	5,689	5,690.91	5,569–5,950	5,755	5,760.82	0.041
	CI	0.69–0.86	0.80	0.80	0.65–0.86	0.79	0.79	0.374
	GI	5.08–8.53	6.04	6.35	4.95–8.80	6.22	6.53	0.182
Normal brain	V100%	0.24–7.81	1.02	1.61	0.20–11.28	1.11	2.13	0.266
	V50%	18.85–367.44	91.95	129.72	18.92–383.79	91.07	139.26	0.155
	V25%	87.81–1,047.50	434.11	511.37	100.48–1,048.71	505.99	543.72	0.004
	V10%	348.24–1,389.17	921.81	928.45	403.40–1,414.54	1,154.37	1,015.68	0.003
	Dmean	398.50–1,829.70	1,079.80	1,116.68	475.50–1,954.50	1,184.90	1,204.35	0.003

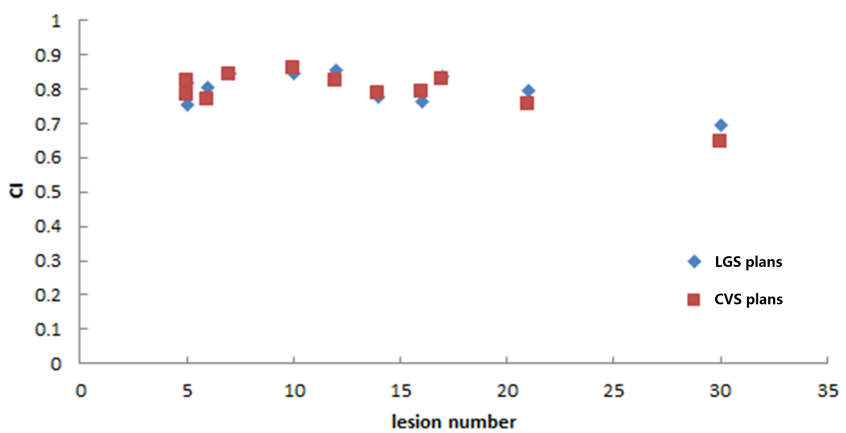

FIGURE 5 | Conformity values of the two plans for the 11 patients.

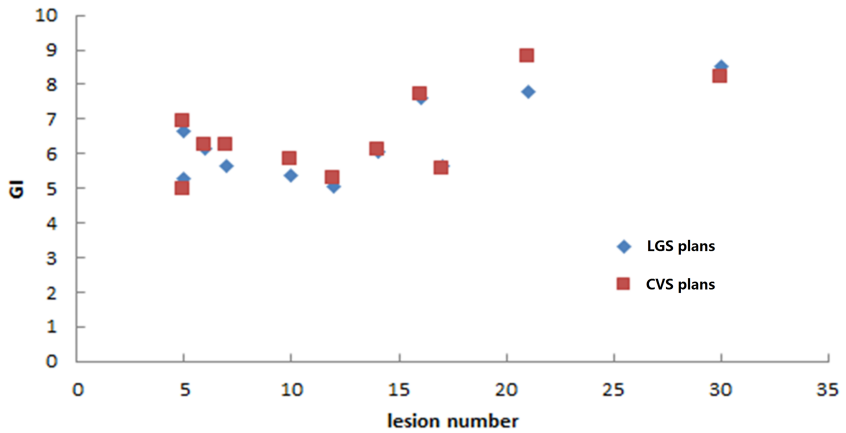

FIGURE 6 | Gradient index values of the two plans for the 11 patients.

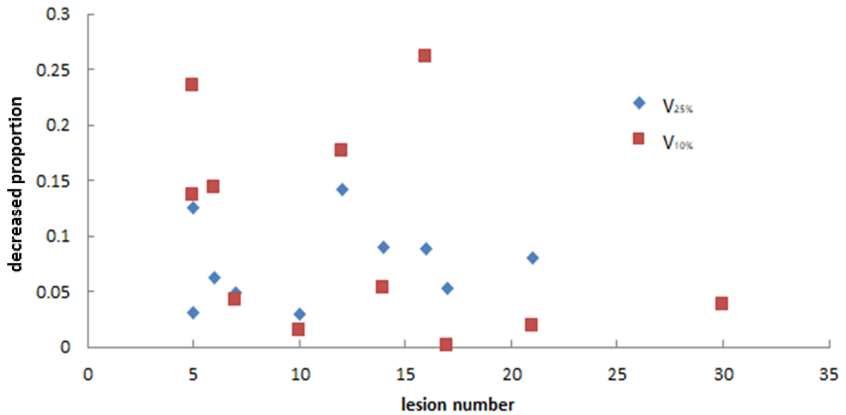

FIGURE 7 | The relationship between the decreased proportion of $V_{25\%}$ and $V_{10\%}$ of normal brain in LGS plans and the number of lesions. There was no obvious correlation between the two factors.

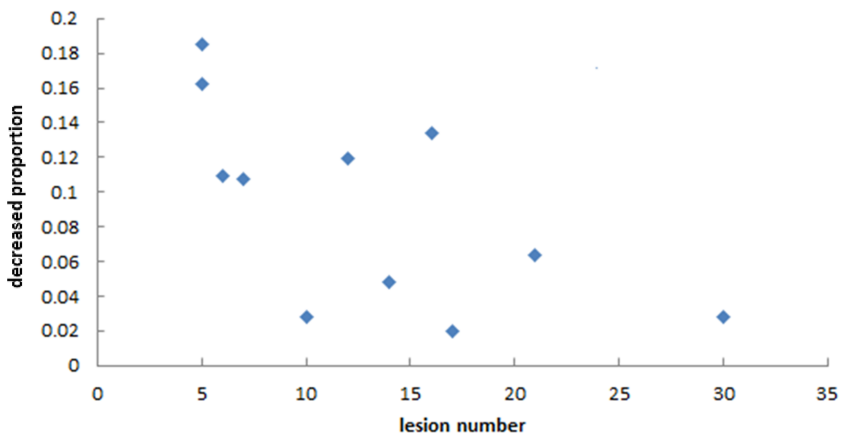

FIGURE 8 | The relationship between the decreased proportion of D_{mean} of normal brain in LGS plans and the number of lesions. It seemed that the decreased proportions in the D_{mean} value of normal brain tended to decrease with an increased number of lesions.

The method proposed in this study decreased the low-dose region of normal brain tissue in some patients, but in some patients, the magnitude of the decrease was small. We can analyze this method's effectiveness according to the number and location distribution of the BMs. First, **Figure 8** shows that this method's effectiveness may decrease with an increased number of BMs, in line with our expectations. When the number of BMs increased, most BMs were adjacent to each other on BEVs. Even if the VMAT plan is created by conventional methods, this reduces the island-blocking problem, and most of the leakage between MLC leaves is also irradiated into tumors, reducing the impact on the low-dose range of normal brain tissue. The locations of BMs are also an influencing factor. The distribution of targets in BEVs can fall into the following three categories: (a) very concentrated; (b) very scattered; (c) partly concentrated, partly scattered. If the targets are very concentrated (i.e., all BMs show closely adjacent status on BEVs), there is no need to use this method because the impact of the problems mentioned above is very small. Thus, the longitudinal grouping method is mainly useful for the other two categories. Furthermore, if there is a large distance between the BMs in the cephalo-caudal direction, a large area of normal brain tissues between those targets may be exposed to low-dose irradiation if the VMAT plan is devised by conventional methods. In addition, the low dose region may be larger if the jaw is fixed during optimization. The longitudinal grouping method would be more advantageous in the latter situation.

Although the proposed method was applied to multiple BMs treated with VMAT, it can also be applied to other situations in which multiple target volumes are treated by either VMAT or IMRT.

In the current method, tumors are grouped manually. This makes the planning process more complicated and time-consuming than the conventional method, in which all of the lesions are planned at the same time. Automatic grouping could solve this limitation, but such methods would require cooperation from the vendors of treatment planning systems. This method can also be applied to non-coplanar situations, but the effects of that specific application require further research.

In conclusion, the longitudinal grouping method can decrease unnecessary exposure and reduces the low-dose range of exposure to normal brain tissue.

DATA AVAILABILITY STATEMENT

The original contributions presented in the study are included in the article/supplementary material; further inquiries can be directed to the corresponding author.

ETHICS STATEMENT

The studies involving human participants were reviewed and approved by Ethics Committee of National Cancer Center/ Cancer Hospital, Chinese Academy of Medical Sciences and Peking Union Medical College. Written informed consent for participation was not required for this study in accordance with the national legislation and the institutional requirements. Written informed consent was obtained from the individual(s) for the publication of any potentially identifiable images or data included in this article.

AUTHOR CONTRIBUTIONS

Conception and design: YX and JD. Financial support: JD. Provision of study materials or patients: QL and JX. Collection and assembly of data: YX, JM, PH, PM, XC, and KM. Data analysis and interpretation: YX and JM. Manuscript writing: All authors. All authors contributed to the article and approved the submitted version.

FUNDING

This work was supported by the National Natural Science Foundation of China (grant number 11875320).

ACKNOWLEDGMENTS

We would like to thank the native English speaking scientists Richard Lipkin, PhD of Liwen Bianji, Edanz Group China for editing our manuscript.

REFERENCES

1. Mehta MP, Tsao MN, Whelan TJ, Morris DE, Hayman JA, Flickinger JC, et al. The American Society for Therapeutic Radiology and Oncology (ASTRO) Evidence- Based Review of the Role of Radiosurgery for Brain Metastasis. *Int J Radiat Oncol Biol Phys* (2005) 63:37–46. doi: 10.1016/j.ijrobp.2005.05.023
2. Franchino F, Rudà R, Soffietti R. Mechanisms and Therapy for Cancer Metastasis to the Brain. *Front Oncol* (2018) 8:161. doi: 10.3389/fonc.2018.00161
3. Yamamoto M, Serizawa T, Shuto T, Akabane A, Higuchi Y, Kawagishi J, et al. Stereotactic Radiosurgery for Patients With Multiple Brain Metastases (JLGK0901): A Multi-Institutional Prospective Observational Study. *Lancet Oncol* (2014) 15:387–95. doi: 10.1016/S1470-2045(14)70221-9
4. Shuto T, Akabane A, Yamamoto M, Serizawa T, Higuchi Y, Sato Y, et al. Multiinstitutional Prospective Observational Study of Stereotactic Radiosurgery for Patients With Multiple Brain Metastases From non-Small Cell Lung Cancer (JLGK0901 Study-NSCLC). *J Neurosurg* (2018) 129 (Suppl1):86–94. doi: 10.3171/2018.7.GKS181378
5. Alongi F, Fiorentino A, Navarria P, Bello L, Scorsetti M. Stereotactic Radiosurgery for Patients With Brain Metastases. *Lancet Oncol* (2014) 15 (7):e246–7. doi: 10.1016/S1470-2045(14)70151-2
6. Otto K. Volumetric Modulated Arc Therapy: IMRT in a Single Gantry Arc. *Med Phys* (2008) 35(1):310–7. doi: 10.1118/1.2818738
7. Clark GM, Popple RA, Young PE, Fiveash JB. Feasibility of Single-Isocenter Volumetric Modulated Arc Radiosurgery for Treatment of Multiple Brain Metastases. *Int J Radiat Oncol Biol Phys* (2010) 76(1):296–302. doi: 10.1016/j.ijrobp.2009.05.029
8. Stanhope C, Chang Z, Wang Z, et al. Physics Considerations for Single-Isocenter, Volumetric Modulated Arc Radiosurgery for Treatment of Multiple Intracranial Targets. *Pract Radiat Oncol* (2016) 6:207–13. doi: 10.1016/j.prro.2015.10.010
9. Morrison J, Hood R, Yin FF, Salama JK, Kirkpatrick J, Adamson J. Is a Single Isocenter Sufficient for Volumetric Modulated Arc Therapy Radiosurgery When Multiple Itracranial Metastases are Spatially Dispersed? *Med Dosim* (2016) Winter; 41(4):285–9. doi: 10.1016/j.meddos.2016.06.007

10. Ballangrud Å, Kuo LC, Happersett L, Lim SB, Beal K, Yamada Y, et al. Institutional Experience With SRS VMAT Planning for Multiple Cranial Metastases. *J Appl Clin Med Phys* (2018) 19(2):176–83. doi: 10.1002/acm2.12284
11. Ruggieri R, Naccarato S, Mazzola R, Ricchetti F, Corradini S, Fiorentino A, et al. Linac-Based VMAT Radiosurgery for Multiple Brain Lesions: Comparison Between a Conventional Multi-Isocenter Approach and a New Dedicated Mono-Isocenter Technique. *Radiat Oncol* (2018) 13(1):38. doi: 10.1186/s13014-018-0985-2
12. Roper J, Chanyavanich V, Betzel G, Switchenko J, Dhabaan A. Single-Isocenter Multiple-Target Stereotactic Radiosurgery: Risk of Compromised Coverage. *Int J Radiat Oncol Biol Phys* (2015) 93(3):540. doi: 10.1016/j.ijrobp.2015.07.2262
13. Faught AM, Trager M, Yin FF, Kirkpatrick J, Adamson J. Re-Examining TG-142 Recommendations in Light of Modern Techniques for Linear Accelerator Based Radiosurgery. *Med Phys* (2016) 43(10):5437. doi: 10.1118/1.4962471
14. Chang J. A Statistical Model for Analyzing the Rotational Error of Single Isocenter for Multiple Targets Technique. *Med Phys* (2017) 44(6):2115–23. doi: 10.1002/mp.12262
15. Miao J, Xu Y, Tian Y, Liu Z, Dai J. A Study of Nonuniform CTV to PTV Margin Expansion Incorporating Both Rotational and Translational Uncertainties. *J Appl Clin Med Phys* (2019) 20(12):78–86. doi: 10.1002/acm2.12763
16. Kang J, Ford EC, Smith K, Wong J, McNutt TR. A Method for Optimizing LINAC Treatment Geometry for Volumetric Modulated Arc Therapy of Multiple Brain Metastases. *Med Phys* (2010) 37(8):4146–54. doi: 10.1118/1.3455286
17. Wu Q, Snyder KC, Liu C, Huang Y, Zhao B, Chetty IJ, et al. Optimization of Treatment Geometry to Reduce Normal Brain Dose in Radiosurgery of Multiple Brain Metastases With Single-Isocenter Volumetric Modulated Arc Therapy. *Sci Rep* (2016) 6:34511. doi: 10.1038/srep34511
18. International Commission on Radiation Units and Measurements. Prescribing, Recording, and Reporting Photon-Beam Intensity-Modulated Radiation Therapy (IMRT). ICRU Report 83. In: *J ICRU*. Oxford University Press (2010). doi: 10.1093/jicru
19. International Commission on Radiation Units and Measurements. Prescribing, Recording, and eporting of Stereotactic Treatments With Small Photon Beams. ICRU Report 91. In: *J ICRU*. Oxford University Press (2014).
20. Paddick I. A Simple Scoring Ratio to Index the Conformity of Radiosurgical Treat- Ment Plans. *Tech note J Neurosurg* (2000) 93 Suppl 3:219–22. doi: 10.3171/jns.2000.93.supplement_3.0219
21. Yuchao M, Jianping X, Nan B, Yingjie X, Yuan T, Hongmei Z, et al. Whole-Brain Irradiation With Simultaneous Integrated Boost by Helical Tomotherapy for Multiple Brain Metastases: Dosimetric and Clinical Analyses. *Chin J Radiat Oncol* (2018) 27(5):435–40. doi: 10.3760/cma.j.issn.1004-4221.2018.05.001

Conflict of Interest: The authors declare that the research was conducted in the absence of any commercial or financial relationships that could be construed as a potential conflict of interest.

frontiers in Oncology

ORIGINAL RESEARCH
published: 25 November 2021
doi: 10.3389/fonc.2021.760631

A Prospective Phase II Study of Simultaneous Modulated Accelerated Radiotherapy Concurrently With CDDP/S1 for Esophageal Squamous Cell Carcinoma in the Elderly

SuPing Guo[1,2,3†], FangJie Liu[1,2,3,4†], Hui Liu[1,2,3,4], YingJia Wu[1,2,3], XuHui Zhang[1,2,3], WenFeng Ye[2,3,5], GuangYu Luo[2,3,6], QiWen Li[1,2,3,4], NaiBin Chen[1,2,3,4], Nan Hu[1,2,3,4], Bin Wang[1,2,3], Jun Zhang[1,2,3], MaoSheng Lin[1,2,3], HuiXia Feng[1,2,3] and Bo Qiu[1,2,3,4*]*

[1] Department of Radiation Oncology, Sun Yat-Sen University Cancer Center, Guangzhou, China, [2] State Key Laboratory of Oncology in South China, Guangzhou, China, [3] Collaborative Innovation Center for Cancer Medicine, Guangzhou, China, [4] Guangdong Association Study of Thoracic Oncology, Guangzhou, China, [5] Department of Clinical Nutrition, Sun Yat-Sen University Cancer Center, Guangzhou, China, [6] Department of Endoscopy, Sun Yat-Sen University Cancer Center, Guangzhou, China

Background: To explore the efficacy and toxicity of simultaneous modulated accelerated radiotherapy (SMART) concurrently with cisplatin (CDDP) and S1 (tegafur/gimeracil/oteracil) in elderly patients with esophageal squamous cell carcinoma (ESCC).

Methods: This single-arm, phase II study enrolled pathologically confirmed, stage II–IVa ESCC of 70–80 years old and Eastern Cooperative Oncology Group performance status (ECOG PS) 0–2. Patients received SMART (64 Gy to gross tumor volume and 48 Gy to clinical target volume in 30 fractions) with concurrent CDDP (day 1 of each week) and S1 (days 1–14, 22–35). The primary endpoint was objective response rate (ORR). The secondary endpoints included progression-free survival (PFS), overall survival (OS) and toxicities.

Results: Thirty-seven eligible patients were analyzed with median follow-up of 25.7 months for all and 46.1 months for survivors. The ORR was 88.9%. Patients with baseline weight loss <5% (p=0.050) and nutritional risk index (NRI) ≥105.2 (p=0.023) had better tumor response. Median PFS was 13.8 months with 2-year PFS of 37.5%. Median OS was 27.7 months with 2-year OS of 57.5%. OS was significantly associated with ECOG PS (p=0.005), stage (p=0.014), gross tumor volume (p=0.004), baseline NRI (p=0.036), baseline C-reactive protein (CRP) level (p=0.003) and tumor response (p=0.000). CRP level (p=0.016) and tumor response (p=0.021) were independently prognostic of OS. ≥grade 3 anemia, neutropenia and thrombocytopenia occurred in 2.7%, 10.8% and 13.5% of patients; ≥grade 3 esophagitis and pneumonitis occurred in 18.9% and 2.7% of patient, respectively.

OPEN ACCESS

Edited by:
Francesco Cellini, Fondazione Policlinico A. Gemelli IRCCS, Italy

Reviewed by:
Brígida Ferreira, University of Lisbon, Portugal
Fabiana Gregucci, Ospedale Generale Regionale Francesco Miulli, Italy

***Correspondence:**
Bo Qiu
qiubo@sysucc.org.cn
HuiXia Feng
fenghx@sysucc.org.cn

†These authors have contributed equally to this work and share first authorship

Specialty section:
This article was submitted to Radiation Oncology, a section of the journal Frontiers in Oncology

Received: *18 August 2021*
Accepted: *05 November 2021*
Published: *25 November 2021*

Citation:
Guo S, Liu F, Liu H, Wu Y, Zhang X, Ye W, Luo G, Li Q, Chen N, Hu N, Wang B, Zhang J, Lin M, Feng H and Qiu B (2021) A Prospective Phase II Study of Simultaneous Modulated Accelerated Radiotherapy Concurrently With CDDP/S1 for Esophageal Squamous Cell Carcinoma in the Elderly. Front. Oncol. 11:760631. doi: 10.3389/fonc.2021.760631

Conclusion: SMART concurrently with CDDP/S1 yielded satisfactory response rate, survival outcome and tolerable treatment-related toxicities in elderly patients with ESCC. Further studies are warranted to validate the results.

Keywords: chemoradiotherapy, esophageal cancer, elderly patients, treatment-related toxicity, survival outcome

INTRODUCTION

Esophageal cancer is the sixth leading cause of cancer death worldwide (1). Approximately 30% of patients diagnosed as esophageal cancer are over 70 years' old (2), so there is an urgent need to optimize the treatment strategy in elderly. Although RTOG8501 has established the role of concurrent chemoradiotherapy (CCRT) in locally advanced esophageal cancer, only 23% of the subjects in the clinical trial were over 70 years old (3). Given that the risk of ≥grade 4 side effects was 10% in the concurrent chemoradiotherapy group, significantly higher than that in the radiotherapy alone group, the concurrent treatment mode is more inclined to younger patients with better general conditions. Elderly patients have greater risk of serious treatment-related toxicities due to less physiologic reserve or more comorbidities, therefore are less likely to receive multimodality treatment compared with younger patients (4). The efficacy and tolerance of CCRT for esophageal cancer in the elderly have not been fully studied, with most of the available researches were retrospective studies or prospective studies with small sample sizes (5–8). How to balance treatment efficacy and safety remains a challenging topic.

Tumor response and locoregional control are vital for the relief of tumor-associated symptoms and the improvement of quality of life in elderly patients. Since most of the local failures after radiotherapy occurred in the location of gross tumor volume (GTV), advanced radiation technique might safely improve the local control by increasing the dose to GTV (9). Simultaneous modulated accelerated radiotherapy (SMART) simultaneously delivers a higher dose per fraction to gross tumor and a relatively lower dose to the elective regions. Dosimetry analysis showed that the SMART plan could increase the dose of GTV from 50.4 Gy to 64.8 Gy while keeping a similar dose to the normal tissue compared with IMRT plan (10). Clinical study also supported the efficacy and safety of SMART at a dose of 59.92 Gy to gross tumor and 50.40 Gy to elective regions in 28 fractions concurrently with paclitaxel and nedaplatin for unresectable esophageal cancer (11). Therefore, we hypothesized that SMART can effectively protect normal tissues while increasing the dose of GTV for esophageal cancer, offering an effective and safety choice for elderly patient.

Cisplatin (CDDP)/5-fluorouracil (5-FU) is one of the most common chemotherapy regimens used concurrently with radiotherapy for esophageal cancer. The use of CDDP/5-FU regimen in elderly patients is limited by its high incidence of adverse effects (7). S1 is an oral 5-FU derivate composed of tegafur, gimeracil and oteracil. It also acts as a RT sensitizer. Studies have shown that S1 has superior efficacy and lower risk of toxicities than 5-Fu (12, 13). In clinical studies, RT concurrently with CDDP/S1 achieved promising response rates of 64.4–89.7% with modest toxicities in non-age-selected esophageal cancer (14, 15). Based on its modest toxicities in esophageal cancer, we hypothesized that CDDP/S1 might be a feasible concurrent chemotherapy regimen for elderly patients.

Although SMART and CDDP/S1 showed promising results in esophageal cancer, the evidence in elderly patients is still very limited. Therefore, we carried out this prospective, phase II trial to explore the efficacy and toxicity of SMART concurrently with CDDP/S1 for elderly patients with esophageal squamous cell carcinoma (ESCC).

MATERIALS AND METHODS

Study Design and Participants

This was a single-arm, phase II study. Eligibility criteria included pathologically confirmed ESCC; stage II–IVa (AJCC TNM staging system, 7th edition) confirmed by endoscopic ultrasonography, CT imaging, bone scan and/or PET scan; aging 70 to 80; ECOG performance status of 0–2; Charlson score ≤4; weight loss ≤15% within the past 6 months; forced expiratory volume in 1s≥1L; adequate bone marrow, hepatic and renal functions; and ability to provide informed consent. Patients with prior chemotherapy, radiotherapy or biological therapy were excluded. This study was approved by the review board of our center and conducted according to the Declaration of Helsinki. Written informed consent was obtained from all participants.

Treatment

Patients were immobilized using a vacuum bag in the supine position, and underwent a planning CT scan with 5-mm-thick slices. Four dimensional CT was performed to account for respiratory motion. GTV was contoured as visible primary tumors and positive lymph nodes based on endoscopy, CT and/or positron emission tomography (PET) scans. Clinical target volume (CTV) included GTV plus a lateral margin of 0.5–1.0 cm, a longitudinal margin of 3–4 cm and elective lymph nodes regions. The planning target volume for GTV (PTV-GTV) and CTV (PTV-CTV) covered the GTV and CTV with a 0.5 cm margin (10), respectively. SMART technique was used, and treatment plans were generated by the Monaco treatment planning system (Elekta). Radiation was delivered with 6-MV photons by a linear accelerator. The prescribed doses were 64 Gy for PTV-GTV (2.1 Gy/fraction) and 48 Gy for PTV-CTV (1.6 Gy/fraction) in 30 fractions. It was required that 95% of the PTV receive the prescribed dose. Dose constraints for normal structures included: mean lung dose <20 Gy and the total lung volumes

irradiated above 20 Gy (V20) <30%; V40 of the heart <30%; maximum dose of spinal cord dose ≤45 Gy; D0.5cc of the small bowl ≤45 Gy; maximum dose of the stomach <54 Gy; and V18 of the kidney <30%. In case of grade 4 myelosuppression, or ≥grade 3 nonhematologic toxicities that lasted longer than one week, RT was stopped until the toxicities resolved to ≤grade 2. For patients with a break ≥2 weeks, a new plan for a dose boost to PTV-GTV would be given at clinical discretion.

CDDP (25mg/m2) was delivered intravenously on day 1 of each week of RT, and S1 (40 mg/m2, bid) was delivered orally on days 1–14 and 22–35 during RT. For patients who could not swallow S1 capsule, the powder of S1 would be administered through the tube. Chemotherapy administration could be interrupted in case of adverse effects. Then a dose adjustment on weekly basis was needed when the adverse effects resolved.

Routine nutritional support was performed from the start of CCRT, including oral nutritional supplements, enteral nutrition *via* nasogastric tube or percutaneous endoscopic gastrostomy, and/or parenteral nutrition.

Evaluation

Patient history, physical examination, complete blood count, serum chemistries, endoscopy, chest/upper abdomen CT, chest magnetic resonance imaging (MRI), bone scan and/or PET scan were obtained before CCRT. Nutritional risk index (NRI) was calculated as: 1.519 × serum albumin level (g/L) + 41.7 × (present/usual weight). Neutrophil-lymphocyte ratio (NLR) was calculated as: the absolute neutrophils count/the absolute lymphocyte count. Charlson score was used for the evaluation of comorbid condition (16). Complete blood count (CBC) and serum chemistries were obtained weekly during CCRT. Objective response was assessed by endoscopy, chest/upper abdomen CT and chest MRI two months after CCRT according the tri-modality criteria (17). Assessment of disease by endoscopy, chest/upper abdomen CT and chest MR were first performed two months after CCRT, and then every 3-4 months for the first 2 years, every 6 months for years 3 to 5, and yearly thereafter. Bone scan or PET scan were performed when the patient was suspected for distant progression. Treatment related toxicities were graded by the Common Terminology Criteria for Adverse Events version 4.0 (CTCAE 4.0) from the start of radiotherapy until 2 months afterward. In particular, pneumonitis was observed from the start until one year after radiotherapy. The maximum observable toxicities were recorded.

Statistical Analysis

The primary endpoint of this study was objective response rate (ORR). ORR was defined as the percentage of patients who achieved partial or complete remission two months after CCRT (17). We assumed that the ORR could be improved from 60% according to previous published data to 80% in the current study. Enrollment of 36 patients was required to yield 80% power to detect an expected improvement based on a one-sided 0.025 level test. Considering the rate of dropout as 10%, planned enrollment was 40 patients.

The secondary endpoints included overall survival (OS), progression-free survival (PFS), loco-regional recurrence-free survival (LRFS), distant metastasis-free survival (DMFS) and toxicities. Endpoints of OS, locoregional recurrence and distant metastasis were measured from the start of CCRT. Correlation between clinical variables and tumor response was performed by the Chi-square test. Survival analyses were performed using the Kaplan-Meier method. Correlation between clinical variables and survival was performed using Cox proportional hazards model. Variables with a p-value <0.05 in univariate analysis were included in the multivariate model. The statistical analysis was performed using SPSS 24.0. A p-value <0.05 was considered statistically significant.

RESULTS

Patients

Between July 2015 and June 2018, 42 patients with stage II–IVa ESCC were enrolled in this study. Five patients were excluded from analyses because of distant metastasis before treatment (n=2), inappropriate histology (n=1) or patient withdrawal (n=2). Thirty-seven patients were included in the current analyses (**Figure 1**). The characteristics of the analyzed patients are detailed in **Table 1**. At the time of last follow-up (June 20, 2020), 16 patients (43.2%) were alive and 21 patients (56.8%) were dead. Median follow-up time was 25.7 months (range, 1.1-59.0 months) for all and 46.1 months (range, 19.5-59.0 months) for living patients.

Treatment Compliance

Treatment compliance is detailed in **Table 2**. Of the 37 patients, 22 patients (59.5%) completed the planned RT as planned. Other than that, there were 13 patients (35.1%) who completed RT with a break ≥7days due to persistent grade 3 esophagitis (n=6), grade 3 fatigue (n=5) or weight loss ≥10% during treatment (n=2). Two patients (5.4%) discontinued treatment and received a radiation dose < 50 Gy due to grade 5 sepsis (n=1) or grade 3 pneumonitis (n=1). The median treatment duration was 43 days (range, 39-134 days) for those who completed RT.

Thirty-two patients (86.5%) completed ≥4 weeks of CDDP, and 27 (73.0%) completed 4 weeks of S1. The reasons for dose modification included myelosuppression (thrombocytopenia in 4 patients, neutropenia in 3 patients and both in 1 patient), gastrointestinal toxicities (n=5) and decline in nutrition status (n=2).

Enteral nutrition during CCRT was performed *via* oral supplements, nasogastric tube and percutaneous endoscopic gastrostomy in 21 (56.8%), 7 (18.9%) and 9 (24.3%) patients respectively.

Response to CCRT and Survival

Thirty-six (36/37) patients were assessed for response two months after the end of CCRT (one patient died during CRT due to septic shock). There were 22 (59.5%) with complete remission (CR) of disease, 10 (27.0%) with partial remission (12) and 4 (10.8%) with progressive disease (PD). Progressive disease occurred in distant sites in three patient and in locoregional site in one patient. The objective response (CR+PR) rate was 88.9% (32/36). Gross tumor

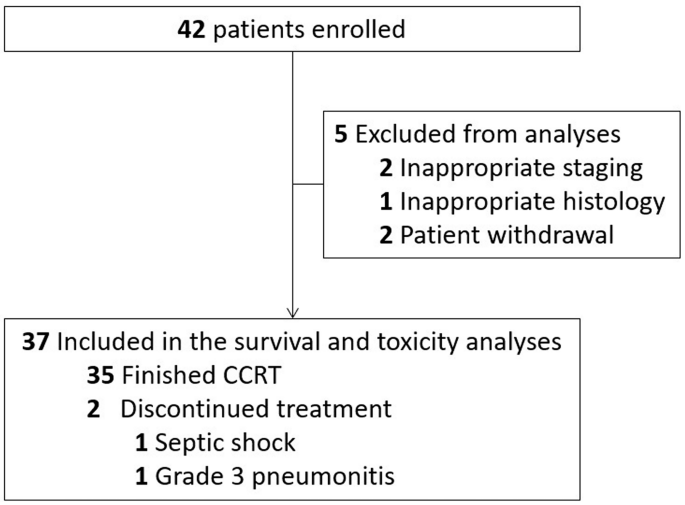

FIGURE 1 | Trial profile. CCRT, Concurrent chemoradiotherapy.

volume change two months after the therapy is shown in **Supplementary Figure 1**. Gross tumor reduction >70% was achieved in all patients with PR. The correlation between clinical variables and tumor response was explored (**Table 3**). Patients with baseline weight loss <5% (p=0.050) and baseline NRI ≥105.2 (p=0.023) tended to have better tumor response two months after CCRT.

Twenty-four (64.9%) of 37 patients had disease progression or died at last follow-up. Median PFS was 13.8 months (95% CI, 9.3-18.4 months), with 1-year, 2-year and 3-year PFS rates of 59.5% (95% CI, 43.6-75.4%), 37.5% (95% CI, 21.8-53.2%) and 34.4% (95% CI, 18.9-49.9%), respectively (**Figure 2A**). Twenty-one (56.8%) died at last follow-up. The estimated median OS was 27.7 months (95% CI, 15.8-39.7 months), with 1-year, 2-year and 3-year OS rates of 70.3% (95% CI, 55.6-85.0%), 57.5% (95% CI, 40.8-74.2%) and 42.6% (95% CI, 25.0-60.2%), respectively (**Figure 2B**).

As shown in **Table 4**, in univariable analysis, median OS was significantly correlated with ECOG performance score (2 *vs* 0-1, 1.1 *vs* 27.7 months, p=0.005), stage (III-IVa *vs* II, 22.1 months *vs* not reached [NR], p=0.014), pre-treatment GTV volume (≥60.5 *vs* <60.5 cm3, 16.5 months *vs* NR, p=0.004), baseline NRI (≥105.2 *vs* <105.2, 16.5 months *vs* NR, p=0.036), baseline CRP level (≥10 *vs* <10mg/L, 13.5 months *vs* NR, p=0.003) and tumor response (non-CR *vs* CR, 13.5 months *vs* NR, p=0.000). OS showed no significant difference between patients who completed RT as planned and those who completed RT with break ≥7 days (27.7 *vs* 34.1 months, p=0.787). In multivariable analysis, baseline CRP level (p=0.016) and tumor response (p=0.021) were independently prognostic of OS (**Figure 3**).

Failure Patterns

At the time of analysis, 8 patients (21.6%) developed loco-regional recurrence. 2-year LRFS was 64.4% (95%CI, 44.2-84.6%). Thirteen patients (35.1%) developed distant metastasis. 2-year DMFS was 59.1% (95%CI, 40.7-77.5%). The failure pattern is detailed in **Supplementary Figure 2**. Distant metastasis was the main cause of treatment failure with lungs being the most common involved site.

Toxicities

Treatment related toxicities are listed in **Table 5**. ≥Grade 3 hematologic toxicities included anemia in 1 (2.7%) patient, neutropenia in 4 (10.8%) patients and thrombocytopenia in 5 (13.5%) patients. Grade 3 non-hematologic toxicities included esophagitis in 7 (18.9%) patients, pneumonitis in 1 (2.7%) patient, gastrointestinal toxicity in 1 (2.7%) patient, fatigue in 1 (2.7%) patient and bleeding in 1 (2.7%) patient. No grade 4 non-hematologic toxicities were developed. Grade 5 sepsis occurred in 1 (2.7%) patient.

DISCUSSION

The treatment for ESCC in elderly patients remains challenging due to the decreased physiologic reserve, increased prevalence of cardiopulmonary comorbidities, and increased risk of treatment-related toxicities in this population. The current study prospectively assessed the efficacy and toxicity of SMART concurrently with CDDP/S1 in 37 elderly patients with ESCC. Thirty-five (35/37, 94.6%) patients completed the SMART, while approximately one third of them experienced a treatment break ≥7days. The ORR was 88.9%, beyond the assumption goal of 60%. The median OS and PFS was 27.7 and 13.8 months respectively. Toxicities were acceptable with ≥grade 3 esophagitis in 7 (18.9%) patients and pneumonitis in 1 (2.7%) patient. Grade 4 side effects included neutropenia in 1 (2.7%) patient and thrombocytopenia in 3 (8.1%) patients. Treatment-related death occurred in 1 (2.7%) patient due to septic shock.

TABLE 1 | Baseline characteristics (n = 37).

Characteristics	n (%)
Age (years)	
Median (Range)	73 (70–77)
Sex	
Female	10 (27.0)
Male	27 (73.0)
ECOG performance status	
0-1	35 (94.6)
2	2 (5.4)
Charlson score	
0	28 (75.7)
1	6 (16.2)
2	2 (5.4)
3	1 (2.7)
Percent weight loss at diagnosis[#]	
<5%	25 (67.6)
≥5%	12 (32.4)
Primary tumor location	
Cervical	4 (10.8)
Proximal third	8 (21.6)
Middle third	21 (56.8)
Distal third	3 (8.1)
Multiple origin	1 (2.7)
Primary tumor length (mm)*	
Median (Range)	58 (12–125)
cTNM stage	
II	10 (27.0)
III	21 (56.8)
IVa	6 (16.2)
GTV volume (cm^3)	
Median (Range)	60.5 (7.5-176.8)
Baseline NRI	
Median (Range)	105.2 (95.4-111.6)
Baseline NLR	
Median (Range)	2.56 (1.10-5.42)
Baseline HGB	
Median (Range)	129 (98–152)
Baseline CRP	
<10mg/L	27 (73.0)
≥10mg/L	10 (27.0)

*ECOG PS, Eastern Cooperative Oncology Group (ECOG) performance status; GTV, gross tumor volume; NRI, nutritional risk index; NLR, neutrophil-lymphocyte ratio; HGB, hemoglobin; CRP, C-reactive protein. [#]Percent weight loss at diagnosis was defined as the percentage of weight loss in the past three months before diagnosis (18). *Primary tumor length was the endoscopically measured tumor length.*

TABLE 2 | Treatment compliance (n = 37).

RT compliance (n, %)	
Completion of RT as planned	22 (59.5)
Completion of RT with break of 7–80 days	12 (32.4)
Completion of RT with break ≥80 days	1 (2.7%)
Discontinue RT	2 (5.4)
RT dose received by PTV-GTV (n, %)	
64 Gy	35 (84.6)
<64 Gy	2 (5.4)
RT durations (days, n = 35)	
Median	43
Range	39-134
CDDP delivery (weeks)	
2	7 (18.9)
3	7 (18.9)
4	18 (48.7)
5	4 (10.8)
6	1 (2.7)
S1 delivery (weeks)	
1	1 (2.7)
2	5 (13.5)
3	4 (10.8)
4	27 (73.0)
Enteral nutrition	
Oral supplements	21 (56.8%)
Nasogastric tube	7 (18.9%)
Percutaneous endoscopic gastrostomy	9 (24.3%)

RT, radiotherapy.

TABLE 3 | Correlation between tumor response and clinical variables (n = 36).

Variables	p value
Sex (male *vs*. female)	0.301
Age (≥73 *vs*. <73 yrs)	0.318
ECOG performance status (2 *vs*. 0-1)	0.263
Charlson score (0-1 *vs*. 2-3)	0.304
Percent weight loss at diagnosis *(≥5% *vs*. <5%)	**0.050**
Stage (III, IVa *vs*. II)	0.056
GTV volume (≥60.5 *vs*. <60.5cm^3)	0.067
Baseline NRI (≥105.2 *vs*. <105.2)	**0.023**
Baseline NLR (≥2.56 *vs*. <2.56)	0.497
Baseline HGB (≥129 *vs*. <129g/L)	0.478
Baseline CRP (≥10 *vs*. <10mg/L)	0.908
Completion of RT (Completion of RT as planned *vs*. completion of RT with break ≥7days *vs*. Discontinue RT)	0.554

*ECOG PS, Eastern Cooperative Oncology Group (ECOG) performance status; GTV, gross tumor volume; NRI, nutritional risk index; NLR, neutrophil-lymphocyte ratio; HGB, hemoglobin; CRP, C-reactive protein. *Percent weight loss at diagnosis was defined as the percentage of weight loss in the past three months before diagnosis (18).*
The bold values mean these p-values are statistically significant (p<0.05).

Some studies have evaluated the efficacy and safety of definitive CCRT in elderly patients and indicated that CCRT was a feasible strategy (5–8, 19–24). More information details were shown in **Table 6**. These studies delivered RT at doses ranging from 50 to 60Gy. The RT technique included 2D, 3D and IMRT. Concurrent chemotherapy regimen included CDDP/carboplatin plus 5-fluorouracil (5-FU), CDDP plus paclitaxel, CDDP plus capecitabine and single-agent regimen. The ORR ranged from to 56.7 to 84%. The median OS ranged from 9 to 35 months, with 2-year OS rate of 27 to 78%. Small sample size, different inclusion criteria, different RT technique/dose, and diverse chemotherapy regimen might account for the difference in survival outcomes. To the best of our knowledge, our study is the first prospective study assessing SMART concurrently with CDDP/S1 in elderly patients. Wang et al. retrospectively evaluated the feasibility and efficacy of CCRT with CDDP/S1 for elderly ESCC patients (21). The radiation dose was lower than ours (54 *vs.* 64 Gy). The chemotherapy regimens were similar except that CDDP was delivered as a three-months manner in their study. We achieved a higher ORR (88.9 *vs.* 84.0%) and OS (27.7 *vs.* 18.2 months) possibly due to the higher radiation dose.

Despite emerging evidence of CCRT for elderly patients with ESCC, the optimal treatment strategy remains to be elucidated. The first question is the selection of proper concurrent chemotherapeutic drugs. Previous study showed CDDP and 5-FU concurrently with CCRT might not be an appropriate regimen

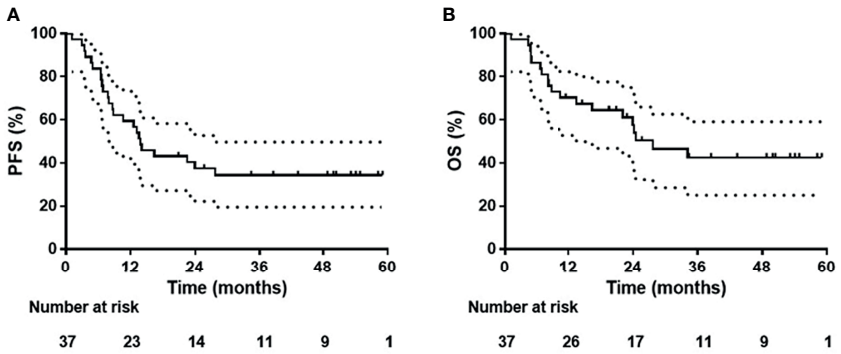

FIGURE 2 | **(A)** Progression-free survival and **(B)** overall survival curves for 37 patients.

TABLE 4 | Univariable and multivariable analysis of prognostic factors for overall survival.

Variables	Univariable analysis		Multivariable analysis	
	HR, 95% CI	p value	HR, 95% CI	p value
Sex (male *vs*. female)	3.376, (0.980-11.626)	0.054		
Age (≥73 *vs*. <73 yrs)	1.028, (0.414-2.549)	0.953		
ECOG performance status (2 *vs*. 0-1)	9.774, (1.958-48.801)	**0.005**	4.036, (0.365-44.661)	0.255
Charlson score (0-1 *vs*. 2-3)	0.506, (0.067-3.796)	0.508		
Percent weight loss at diagnosis* (≥5% *vs*. <5%)	2.206 (0.920-5.287)	0.076		
Stage (III, IVa *vs*. II)	12.555, (1.669-94.463)	**0.014**	3.977, (0.398-39.734)	0.240
GTV volume (≥60.5 *vs*. <60.5cm^3)	4.022, (1.547-10.460)	**0.004**	1.149, (0.352-3.746)	0.818
Baseline NRI (≥105.2 *vs*. <105.2)	0.377, (0.151-0.938)	**0.036**	0.918, (0.252-3.345)	0.936
Baseline NLR (≥2.56 *vs*. <2.56)	1.157, (0.490-2.732)	0.739		
Baseline HGB (≥129 *vs*. <129g/L)	1.318, (0.553-3.137)	0.533		
Baseline CRP (≥10 *vs*. <10mg/L)	3.981, (1.588-9.977)	**0.003**	1.020, (1.004-1.037)	**0.016**
Completion of RT (Completion of RT as planned *vs*. completion of RT with break ≥7days)	1.143, (0.435-3.005)	0.787		
Tumor response (non-CR *vs*. CR)	6.632, (2.978-14.772)	**0.000**	4.088, (1.236-13.518)	**0.021**

*ECOG PS, Eastern Cooperative Oncology Group (ECOG) performance status; GTV, gross tumor volume; NRI, nutritional risk index; NLR, neutrophil-lymphocyte ratio; HGB, hemoglobin; CRP, C-reactive protein. *Percent weight loss at diagnosis was defined as the percentage of weight loss in the past three months before diagnosis (18).*
The bold values mean these p-values are statistically significant (p < 0.05).

for elderly patients because of frequent treatment discontinuation (57.6%) and substantial grade 3 hematological toxicities (7). S1, an oral fluoropyrimidine, showed several advantages over 5-FU when used as a radiosensitizer (13). It could prolong the half-life of 5-FU in plasma. The oral and daily delivery method shortens hospitalization and makes dose modification convenient. Several studies showed platinum/S1 concurrently with CCRT exhibited encouraging efficacy and manageable toxicity in non-age-selected esophageal cancer, with myelosuppression being the most common adverse effect (14, 15, 25). In a prospective study evaluating CCRT with nedaplatin/S1 in stage II/III esophageal cancer, CR was achieved in 80% of 20 patients, and the 3-year OS was 58.0% (25). Grade 3-4 neutropenia, thrombocytopenia and anemia occurred in 18%, 12% and 6% of patients, respectively. In another phase II study of CCRT with CDDP/S1 in 116 patients with stage II-IVa esophageal cancer, the median PFS and OS were 14.4 and 27.6 months respectively (14). Grade 3-4 neutropenia thrombocytopenia and anemia occurred in 37.9%, 13.8% and 9.5% of patients. The survival data of these studies seemed to be better than that using CCRT concurrent with CDDP/5-FU, with a median OS of 13-17.5 months (3, 26). Based on the above evidence, we chose CDDP/S1 as concurrent regimen in elderly patients. Considering the decreased reserve in this less-fit population, CDDP was delivered in a weekly manner. Compared with the above studies in non-age-selected patients, our study showed similar survival outcomes and hematological toxicities in elderly patients. It is noteworthy that about one third of patients needed chemotherapy dose reduction mostly due to hematological toxicities in our study. The weekly delivered CDDP and daily delivered S1 allowed for in-time modification of drug dose, which was important for elderly patients with decreased bone marrow reserve. The suboptimal compliance to chemotherapy in the current study indicates that a modified chemotherapy regimen, such as single-agent chemotherapy, might be better-tolerated in elderly patients.

The more frequent chemotherapy dose reduction in elderly patients was concerned to affect the response rate and locoregional control. Therefore, intensifying the radiation dose to compensate for the inadequate concurrent drug delivery might be an option to increase treatment efficacy. At the same

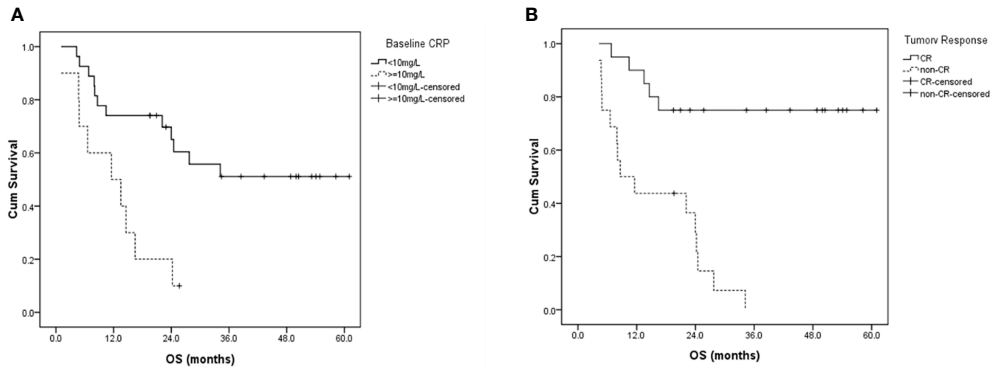

FIGURE 3 | Overall survival curves for patients with **(A)** different baseline CRP levels, and **(B)** different tumor responses two months after radiotherapy. CRP, C-reactive protein; CR, complete response; OS, overall survival.

TABLE 5 | Treatment related toxicities (n = 37).

Toxicity	Grade, No. (n/37%)				
	1	2	3	4	5
Non-hematologic					
Esophagitis	10 (27.0)	20 (54.1)	7 (18.9)	0	0
Pneumonitis	24 (64.9)	2 (5.4)	1 (2.7)	0	0
Gastrointestinal	14 (37.8)	9 (24.3)	1 (2.7)	0	0
Arrhythmia	2 (5.4)	1 (2.7)	0	0	0
Fatigue	7 (18.9)	3 (8.1)	1 (2.7)	0	0
Skin	8 (21.6)	3 (8.1)	0	0	0
Weight loss	3 (8.1)	1 (2.7)	0	0	0
Bleeding	2 (5.4)	0	1 (2.7)	0	0
Sepsis	0	0	0	0	1 (2.7)
Hematologic					
Anemia	12 (32.4)	18 (48.6)	1 (2.7)	0	0
Neutropenia	6 (16.2)	8 (21.6)	3 (8.1)	1 (2.7)	0
Thrombocytopenia	7 (18.9)	10 (27.0)	2 (5.4)	3 (8.1)	0
ALT elevation	3 (8.1)	0	0	0	0
AST elevation	2 (5.4)	0	0	0	0
Creatinine elevation	1 (2.7)	2 (5.4)	0	0	0

Toxicities were graded by CTCAE version 4.0.
ALT, alanine aminotransferase; AST, aspartate aminotransferase.

time, treatment-related toxicities must be considered when escalating RT dose. A population-based analysis included 2553 elderly patients (>65 years) with esophageal cancer treated with either 3-dimensional radiotherapy (3DCRT) or IMRT (27). The use of IMRT was associated with lower cardiac mortality and all-cause mortality compared with 3DCRT. In the current study, we used SMART technique to deliver an escalated dose of 64 Gy to gross tumor with a fraction dose of 2.13 Gy. The relatively high biological effective dose may explain the promising response rate and loco-regional control. Meanwhile, ≥grade 3 pneumonitis occurred in 1 (2.7%) patient and no cardiopulmonary cause death was observed with median follow-up of 25.7 months. These results suggested that dose intensification *via* SMART could be a good choice for the treatment of elderly patients with ESCC, which enables improvement in tumor response and better preservation of organ function. Longer follow up was needed for a better understanding of late toxicities.

General health condition of elderly patients needed special attention before the delivery of CCRT. Nutrition status and systemic inflammatory response have been reported as prognostic factors independent of age, performance status and clinical stage in patients with esophageal cancer (28–30). NRI, calculated by serum albumin and weight, is an objective and simple tool for assessment of nutrition risk. This index has been proposed for the evaluation of nutrition status in patients with various chronic disease (31). Our study showed that patients with baseline weight loss <5% and baseline NRI ≥105.2 tended to have better tumor response two months after CCRT. Baseline NRI was also predictive of OS. This was consistent with the results from non-age-selected population. Inflammation factors were reported to correlate with survival outcome in various cancer types including esophageal cancer (29). We explored the potential role of inflammation-based prognostic factors including CRP and NLR on OS. Baseline CRP level was found to be independently prognostic of OS. These results suggest

TABLE 6 | Previous studies of radiotherapy for elderly patients with esophageal cancer.

Study	Study nature	N	Age	Stage	Treatment group	Radiation technique	Radiation therapy dose prescription	Chemotherapy regimens	Median OS (mo)	2-year OS rate (%)	ORR (%)	≥3 grade esophagitis (%)	≥3 grade pneumonitis (%)
Takeuchi (7)	Retrospective	33	≥71	II–III	CCRT	–	60 Gy/30 fractions	CDDP/5-FU	14.7	47*	63.6 (CRR)	9.1	–
Tougeron (5)	Retrospective	109	≥70	I-IV	CCRT	–	50–55 Gy (1.8 or 2 Gy/day)	CDDP/5-FU or CDDP +irinotecan	15.2	35.5	57.8 (CRR)	–	–
Rochigneux (6)	Retrospective	58	≥75	IIB-IIIC	CCRT	3D-CRT	The mean dose was 50.9 Gy (range, 27–72 Gy)	CDDP or CDDP/5-FU or 5-FU	14.5	25.9	–	–	–
Zhang (24)	Retrospective	128	≥65	I-IV	CCRT RT alone	3D-CRT or IMRT	60 Gy (range, 46–70 Gy)/25–35 fractions	Docetaxel +CDDP or CDDP/5-FU	22 13	55* 42*	69.9 47.3	5.5 3.6	2.7 1.8
Servagi-Vernat (23)	Prospective phase II single-arm study	30	≥75	II-III	CCRT	–	50 Gy/25 fractions	CDDP or oxaliplatin	14.5	28*	73.3	–	–
Li (22)	Retrospective	116	≥70	I-IV	CCRT sCRT RT alone	3D-CRT or IMRT	The median dose was 60Gy (range, 20-70 Gy)/ 1.8-2Gy per fraction	Docetaxel or CDDP/5-FU or carboplatin +paclitaxel or doxifluridine	22.3 18.0 12.4	50* 38* 30*	- - -	25 16.7 13.3	0 0 0
Song (8)	Retrospective	82	≥70	I-IV	CCRT	3D-CRT	60 Gy/30 fractions	Paclitaxel+CDDP	26.9	–	69.1	8.5	–
Wang (21)	Retrospective	56	≥70	II-IV	CCRT	–	54 Gy/27–30 fractions	CDDP/S1	18.2	44*	84	14.3	3.6
Chen (20)	Retrospective	90	≥65	IIb-III	CCRT RT alone	3D-CRT	56.0–59.4 Gy/30–33 fractions	CDDP/S1	30.6 18.7	78* 20*	73.5 51.2	26.5 14.6	6.1 9.8
Huang (19)	Retrospective	271	≥65	I-IV	RT alone single-agent-based CCRT double-agent-based CCRT	2D-RT, or 3D-CRT or IMRT	The mean dose was 58.4 ± 6.4 Gy (range, 40-74 Gy)	Single agents: 5-FU, platinum, and docetaxel Double agents: platinum combined with 5-FU or paclitaxel or docetaxel	15.6 28.8 27.8	39 59 57	60.3 67.2 82.1	20.4 (G2-3) 32.1 (G2-3) 42.7 (G2-3)	0.9 (G2-3) 3.6 (G2-3) 3.2 G2-3)
Our study	Prospective phase II Study	37	70-80	II–IVa	CCRT	SMART	64 Gy/30 fractions	CDDP/S1	27.7	57.5	88.9	18.9	2.7

**Estimating from the survival curve.*

3D-CRT, 3D conformal radiotherapy; 5-FU, 5-fluorouracil; CCRT, concurrent chemoradiotherapy; CDDP, cisplatin; CRR, complete response rate; IMRT, intensity modulated radiotherapy; ORR, objective response rate; OS, overall survival; RT, radiotherapy; sCRT, sequential chemoradiotherapy; SMART, simultaneous modulated accelerated radiation therapy.

that the baseline assessment of nutritional and inflammation status using routine clinical variables could predict survival in elderly patients, and serves an important basis for the individualized anti-cancer and supportive therapy. It's unclear how the dynamic changes of these factors during CCRT influence clinical outcomes and it remains to be further investigated in the future.

As indicated in the multivariate analysis for OS, tumor response two months after CCRT was prognostic of OS. It motivates to assess tumor response as early as possible to adjust the treatment accordingly. Alternative treatment approaches, such as immunotherapy could be investigated for patients that have a poor response to the initial treatment protocol. Advanced disease stage and large GTV volume adversely affects the objective tumor response with marginal significance (**Table 3**). They were also significantly associated with overall survival in univariate analysis. These results were in line with previous studies on esophageal cancer (32, 33).

The analysis of treatment compliance revealed that treatment break was common in CCRT for elderly patients who are more susceptible to treatment toxicities due to the decreased physiologic reserve (8, 21). In our study, about one third of patients had a break ≥7 days during RT due to toxicities. From radiobiologic

perspective, prolonging overall treatment time results in decreased tumor control probability and is therefore not desirable. Nevertheless, for elderly patient, a planned treatment break might help reduce treatment-related morbidity and maintain good general condition. Univariable analysis in our cohort showed that delayed and normal timed patients did not show a difference in OS. The relatively high radiation dose compensating for tumor repopulation during the break might explain the result of univariable analysis. It also implies that maintaining good general condition was as important as treatment consistency in this less-fit population.

In conclusion, our study showed that the SMART concurrently with CDDP/S1 yielded satisfactory response rate, survival outcomes and tolerable treatment-related toxicities in elderly patients with ESCC. Baseline CRP and tumor response were prognostic of overall survival. This study was limited by the relatively small number of patients and single-arm design. Randomized studies with larger sample size are warranted to further evaluate the efficacy and toxicity of this treatment approach.

DATA AVAILABILITY STATEMENT

The raw data supporting the conclusions of this article will be made available by the authors, without undue reservation.

ETHICS STATEMENT

The studies involving human participants were reviewed and approved by Sun Yat-Sen University Cancer Center IRB, Sun Yat-Sen University. The patients/participants provided their written informed consent to participate in this study.

AUTHOR CONTRIBUTIONS

Study conception and design: SG, FL, HL, HF, and BQ. Literature review: YW. Data acquisition: YW, FL, SG, XZ, WY, GL, QL, and HF. Statistical analysis: NC, NH, HL, and BW. Data interpretation: NC, JZ, and ML. Manuscript preparation: SG, FL, HL, HF, and BQ. Manuscript review: All authors. All authors contributed to the article and approved the submitted version.

SUPPLEMENTARY MATERIAL

The Supplementary Material for this article can be found online at: https://www.frontiersin.org/articles/10.3389/fonc.2021.760631/full#supplementary-material.

REFERENCES

1. Torre LA, Bray F, Siegel RL, Ferlay J, Lortet-Tieulent J, Jemal A. Global Cancer Statistics, 2012. *CA Cancer J Clin* (2015) 65(2):87–108. doi: 10.3322/caac.21262
2. National Cancer Institute. *Cancer Statistics: SEER Stat Fact Sheets: Esophagus*. Available at: http://seer.cancer.gov/statfacts/html/esoph.html.
3. Cooper JS, Guo MD, Herskovic A, Macdonald JS, Martenson JA Jr, Al-Sarraf M, et al. Chemoradiotherapy of Locally Advanced Esophageal Cancer: Long-Term Follow-Up of a Prospective Randomized Trial (RTOG 85-01). Radiation Therapy Oncology Group. *JAMA* (1999) 281(17):1623–7. doi: 10.1001/jama.281.17.1623
4. Steyerberg EW, Neville B, Weeks JC, Earle CC. Referral Patterns, Treatment Choices, and Outcomes in Locoregional Esophageal Cancer: A Population-Based Analysis of Elderly Patients. *J Clin Oncol* (2007) 25(17):2389–96. doi: 10.1200/jco.2006.09.7931
5. Tougeron D, Di Fiore F, Thureau S, Berbera N, Iwanicki-Caron I, Hamidou H, et al. Safety and Outcome of Definitive Chemoradiotherapy in Elderly Patients With Oesophageal Cancer. *Br J Cancer* (2008) 99(10):1586–92. doi: 10.1038/sj.bjc.6604749
6. Rochigneux P, Resbeut M, Rousseau F, Bories E, Raoul JL, Poizat F, et al. Radio(chemo)therapy in Elderly Patients With Esophageal Cancer: A Feasible Treatment With an Outcome Consistent With Younger Patients. *Front Oncol* (2014) 4:100. doi: 10.3389/fonc.2014.00100
7. Takeuchi S, Ohtsu A, Doi T, Kojima T, Minashi K, Mera K, et al. A Retrospective Study of Definitive Chemoradiotherapy for Elderly Patients With Esophageal Cancer. *Am J Clin Oncol* (2007) 30(6):607–11. doi: 10.1097/COC.0b013e3180ca7c84
8. Song T, Zhang X, Fang M, Wu S. Concurrent Chemoradiotherapy Using Paclitaxel Plus Cisplatin in the Treatment of Elderly Patients With Esophageal Cancer. *Onco Targets Ther* (2015) 8:3087–94. doi: 10.2147/ott.s92537
9. Settle SH, Bucci MK, Palmer MB, Liu H, Liengsawangwong R, Guerrero TM, et al. PET/CT Fusion With Treatment Planning CT (TP CT) Shows Predominant Pattern of Locoregional Failure in Esophageal Patients Treated With Chemoradiation (CRT) Is in GTV. *Int J Radiat OncolBiolPhys* (2008) 72(1 Supplement):S72–S3. doi: 10.1016/j.ijrobp.2008.06.931
10. Welsh J, Palmer MB, Ajani JA, Liao Z, Swisher SG, Hofstetter WL, et al. Esophageal Cancer Dose Escalation Using a Simultaneous Integrated Boost Technique. *Int J Radiat Oncol Biol Phys* (2012) 82(1):468–74. doi: 10.1016/j.ijrobp.2010.10.023
11. Li C, Ni W, Wang X, Zhou Z, Deng W, Chang X, et al. A Phase I/II Radiation Dose Escalation Trial Using Simultaneous Integrated Boost Technique With Elective Nodal Irradiation and Concurrent Chemotherapy for Unresectable Esophageal Cancer. *Radiat Oncol (Lond Engl)* (2019) 14(1):48. doi: 10.1186/s13014-019-1249-5
12. Harada K, Kawaguchi S, Supriatno, Kawashima Y, Yoshida H, Sato M. S-1, an Oral Fluoropyrimidine Anti-Cancer Agent, Enhanced Radiosensitivity in a Human Oral Cancer Cell Line *In Vivo* and *In Vitro*: Involvement Possibility of Inhibition of Survival Signal, Akt/PKB. *Cancer Lett* (2005) 226(2):161–8. doi: 10.1016/j.canlet.2004.12.048
13. Boku N, Yamamoto S, Fukuda H, Shirao K, Doi T, Sawaki A, et al. Fluorouracil Versus Combination of Irinotecan Plus Cisplatin Versus S-1 in Metastatic Gastric Cancer: A Randomised Phase 3 Study. *Lancet Oncol* (2009) 10(11):1063–9. doi: 10.1016/s1470-2045(09)70259-1
14. Iwase H, Shimada M, Tsuzuki T, Hirashima N, Okeya M, Hibino Y, et al. Concurrent Chemoradiotherapy With a Novel Fluoropyrimidine, S-1, and Cisplatin for Locally Advanced Esophageal Cancer: Long-Term Results of a Phase II Trial. *Oncology* (2013) 84(6):342–9. doi: 10.1159/000348383
15. Chang H, Shin SK, Cho BC, Lee CG, Kim CB, Kim DJ, et al. A Prospective Phase II Trial of S-1 and Cisplatin-Based Chemoradiotherapy for Locoregionally Advanced Esophageal Cancer. *Cancer Chemother Pharmacol* (2014) 73(4):665–71. doi: 10.1007/s00280-013-2371-y
16. Charlson ME, Pompei P, Ales KL, MacKenzie CR. A New Method of Classifying Prognostic Comorbidity in Longitudinal Studies: Development and Validation. *J Chronic Dis* (1987) 40(5):373–83. doi: 10.1016/0021-9681(87)90171-8
17. Qiu B, Wang D, Yang H, Xie W, Liang Y, Cai P, et al. Combined Modalities of Magnetic Resonance Imaging, Endoscopy and Computed Tomography in the Evaluation of Tumor Responses to Definitive Chemoradiotherapy in Esophageal Squamous Cell Carcinoma. *Radiother Oncol J Eur Soc Ther Radiol Oncol* (2016) 121(2):239–45. doi: 10.1016/j.radonc.2016.09.017
18. Rojer AG, Kruizenga HM, Trappenburg MC, Reijnierse EM, Sipilä S, Narici MV, et al. The Prevalence of Malnutrition According to the New ESPEN

Definition in Four Diverse Populations. *Clin Nutr (Edinburgh Scotland)* (2016) 35(3):758–62. doi: 10.1016/j.clnu.2015.06.005
19. Huang C, Zhu Y, Li Q, Zhang W, Liu H, Zhang W, et al. Feasibility and Efficiency of Concurrent Chemoradiotherapy With a Single Agent or Double Agents *vs* Radiotherapy Alone for Elderly Patients With Esophageal Squamous Cell Carcinoma: Experience of Two Centers. *Cancer Med* (2019) 8(1):28–39. doi: 10.1002/cam4.1788
20. Chen F, Luo H, Xing L, Liang N, Xie J, Zhang J. Feasibility and Efficiency of Concurrent Chemoradiotherapy With Capecitabine and Cisplatin Versus Radiotherapy Alone for Elderly Patients With Locally Advanced Esophageal Squamous Cell Carcinoma: Experience of Two Centers. *Thorac Cancer* (2018) 9(1):59–65. doi: 10.1111/1759-7714.12536
21. Wang H, Li G, Chen L, Duan Y, Zou C, Hu C. Definitive Concurrent Chemoradiotherapy With S-1 and Cisplatin in Elderly Esophageal Squamous Cell Carcinoma Patients. *J Thorac Dis* (2017) 9(3):646–54. doi: 10.21037/jtd.2017.03.105
22. Li X, Zhao LJ, Liu NB, Zhang WC, Pang QS, Wang P, et al. Feasibility and Efficacy of Concurrent Chemoradiotherapy in Elderly Patients With Esophageal Squamous Cell Carcinoma: A Respective Study of 116 Cases From a Single Institution. *Asian Pacific J Cancer Prev APJCP* (2015) 16 (4):1463–9. doi: 10.7314/apjcp.2015.16.4.1463
23. Servagi-Vernat S, Créhange G, Roullet B, Guimas V, Maingon P, Puyraveau M, et al. Phase II Study of a Platinum-Based Adapted Chemotherapy Regimen Combined With Radiotherapy in Patients 75 Years and Older With Esophageal Cancer. *Drugs Aging* (2015) 32(6):487–93. doi: 10.1007/s40266-015-0275-8
24. Zhang P, Xi M, Zhao L, Shen JX, Li QQ, He LR, et al. Is There a Benefit in Receiving Concurrent Chemoradiotherapy for Elderly Patients With Inoperable Thoracic Esophageal Squamous Cell Carcinoma? *PLoS One* (2014) 9(8):e105270. doi: 10.1371/journal.pone.0105270
25. Tsuda T, Inaba H, Miyazaki A, Izawa N, Hirakawa M, Watanabe Y, et al. Prospective Study of Definitive Chemoradiotherapy With S-1 and Nedaplatin in Patients With Stage II/III (non-T4) Esophageal Cancer. *Esophagus* (2011) 8 (1):45–51. doi: 10.1007/s10388-011-0261-0
26. Conroy T, Galais MP, Raoul JL, Bouché O, Gourgou-Bourgade S, Douillard JY, et al. Definitive Chemoradiotherapy With FOLFOX Versus Fluorouracil and Cisplatin in Patients With Oesophageal Cancer (PRODIGE5/ACCORD17): Final Results of a Randomised, Phase 2/3 Trial. *Lancet Oncol* (2014) 15(3):305–14. doi: 10.1016/s1470-2045(14)70028-2
27. Lin SH, Zhang N, Godby J, Wang J, Marsh GD, Liao Z, et al. Radiation Modality Use and Cardiopulmonary Mortality Risk in Elderly Patients With Esophageal Cancer. *Cancer* (2016) 122(6):917–28. doi: 10.1002/cncr.29857
28. Rietveld SCM, Witvliet-van Nierop JE, Ottens-Oussoren K, van der Peet DL, de van der Schueren MAE. The Prediction of Deterioration of Nutritional Status During Chemoradiation Therapy in Patients With Esophageal Cancer. *Nutr Cancer* (2018) 70(2):229–35. doi: 10.1080/01635581.2018.1412481
29. Wu CC, Li SH, Lu HI, Lo CM, Wang YM, Chou SY, et al. Inflammation-Based Prognostic Scores Predict the Prognosis of Locally Advanced Cervical Esophageal Squamous Cell Carcinoma Patients Receiving Curative Concurrent Chemoradiotherapy: A Propensity Score-Matched Analysis. *PeerJ* (2018) 6:e5655. doi: 10.7717/peerj.5655
30. Clavier JB, Antoni D, Atlani D, Ben Abdelghani M, Schumacher C, Dufour P, et al. Baseline Nutritional Status Is Prognostic Factor After Definitive Radiochemotherapy for Esophageal Cancer. *Dis Esophagus* (2014) 27 (6):560–7. doi: 10.1111/j.1442-2050.2012.01441.x
31. Bo Y, Wang K, Liu Y, You J, Cui H, Zhu Y, et al. The Geriatric Nutritional Risk Index Predicts Survival in Elderly Esophageal Squamous Cell Carcinoma Patients With Radiotherapy. *PLoS One* (2016) 11(5):e0155903. doi: 10.1371/journal.pone.0155903
32. Lin FC, Chang WL, Chiang NJ, Lin MY, Chung TJ, Pao TH, et al. Radiation Dose Escalation can Improve Local Disease Control and Survival Among Esophageal Cancer Patients With Large Primary Tumor Volume Receiving Definitive Chemoradiotherapy. *PLoS One* (2020) 15(8):e0237114. doi: 10.1371/journal.pone.0237114
33. Chen J, Lin Y, Cai W, Su T, Wang B, Li J, et al. A New Clinical Staging System for Esophageal Cancer to Predict Survival After Definitive Chemoradiation or Radiotherapy. *Dis Esophagus* (2018) 31(11). doi: 10.1093/dote/doy043

Conflict of Interest: The authors declare that the research was conducted in the absence of any commercial or financial relationships that could be construed as a potential conflict of interest.

frontiers in Oncology

CASE REPORT
published: 26 November 2021
doi: 10.3389/fonc.2021.780581

Reirradiation of Whole Brain for Recurrent Brain Metastases: A Case Report of Lung Cancer With 12-Year Survival

*Minmin Li, Yanbo Song, Longhao Li, Jian Qin, Hongbin Deng and Tao Zhang**

Department of Oncology, The First Affiliated Hospital of Chongqing Medical University, Chongqing, China

OPEN ACCESS

Edited by:
Francesco Cellini, Fondazione Policlinico A. Gemelli (IRCCS), Italy

Reviewed by:
Francesco Ricchetti, Sacro Cuore Don Calabria Hospital, Italy
Alba Fiorentino, Ospedale Generale Regionale Francesco Miulli, Italy

***Correspondence:**
Tao Zhang
tumorzzt@163.com

Specialty section:
This article was submitted to Radiation Oncology, a section of the journal Frontiers in Oncology

Received: *21 September 2021*
Accepted: *05 November 2021*
Published: *26 November 2021*

Citation:
Li M, Song Y, Li L, Qin J, Deng H and Zhang T (2021) Reirradiation of Whole Brain for Recurrent Brain Metastases: A Case Report of Lung Cancer With 12-Year Survival. Front. Oncol. 11:780581. doi: 10.3389/fonc.2021.780581

Whole brain radiotherapy (WBRT) for brain metastases (BMs) was considered to be dose limited. Reirradiation of WBRT for recurrent BM has always been challenged. Here, we report a patient with multiple BMs of non-small-cell lung cancer (NSCLC), who received two courses of WBRT at the interval of 5 years with the cumulative administration dose for whole brain as 70 Gy and a boost for the local site as 30 Gy. Furthermore, after experiencing relapse in the brain, he underwent extra gamma knife (GK) radiotherapy for local brain metastasis for the third time after 5 years. The overall survival was 12 years since he was initially diagnosed with NSCLC with multiple brain metastases. Meanwhile, each time of radiotherapy brought a good tumor response to brain metastasis. Outstandingly, during the whole survival, he had a good quality of life (QoL) with Karnofsky Performance Score (KPS) above 80. Even after the last GK was executed, he had just a mild neurocognitive defect. In conclusion, with the cautious evaluation of a patient, we suggest that reirradiation of WBRT could be a choice, and the cumulative radiation dose of the brain may be individually modified.

Keywords: reirradiation, whole brain radiotherapy, lung cancer, brain metastasis, long survival

INTRODUCTION

Brain metastases (BMs) occur in 40% of patients with systemic cancer, among which lung cancer is the most common primary tumor (1). Radiation therapy is the cornerstone of modern brain metastases treatment (2), and whole brain radiotherapy (WBRT) is the standard option for multiple BMs. As a result of advances in systemic therapy management, there shows greater rates of recurrence of BMs, as patients with lung cancer have been living longer.

The management of recurrent cranial metastatic disease previously treated with WBRT represents a challenge owing to the potential high risk of radionecrosis and neurocognitive deterioration, especially when choosing reirradiation of WBRT (3). The reported data on the topic of retreatment with WBRT is fractured and without a clear consensus (4, 5).

In this report, we presented a case of a patient with multiple BMs of NSCLC who underwent repetitive WBRT treatment during the course of the disease. The cumulative administration dose for the whole brain was 70 Gy, and a boost for the local site was 30 Gy. Meanwhile, during the whole survival, he had a good quality of life (QoL) and mild neurocognitive defects. Then, we discussed how we chose the strategy of reirradiation for brain metastasis.

CASE PRESENTATION

A 42-year-old Chinese man presented with cough, sputum, and facial paralysis in May 2006. The fibrobronchoscope demonstrated adenocarcinoma at the site of the inferior lobe of the left lung. At the same time, the initial magnetic resonance imaging (MRI) showed that the tumor had already invaded the brain with multiple intracranial metastases. The clinical staging was stage IV (cT4bN2M1 IVb), so surgery was not indicated. After careful evaluation, we suggested a combination of chemotherapy and radiotherapy as the optimal therapy for him. After one cycle of Gemcitabine and Cisplatin (GP) chemotherapy has been completed, the patient underwent radiotherapy for the primary site with a total dose of 70 Gy in 35 fractions, using the two-dimensional radiotherapy (2DRT) technique. The WBRT with a dose of 40 Gy in 20 fractions was delivered initially using 2DRT with two opposing lateral fields and a rotated collimator to fit the whole brain to shield the lens. Subsequently, we measured the depth and size of metastatic sites on diagnostic CT and marked them on the body. Then, a boost plan that employed an anterior field and a lateral field with a 45° wedge was delivered for intracranial metastatic sites with 10 Gy in five fractions based on these marks and measurements. After that, he was treated with three cycles of TP (Paclitaxel and Cisplatin) chemotherapy. After the treatment, the symptoms alleviated apparently, and the serological tumor markers decreased apparently. The radiographic tumor response was evaluated as a complete remission (CR). In addition, he had no prolonged fatigue and/or neurocognitive defects. It is a pity that because it has been a long time, he could not supply his medical information in details.

Without regular follow-up, the complete radiological remission lasted almost 5 years; in July 2011, the patient experienced the first intracranial relapse of multiple lesions, located in the right temporal lobe, parietal lobe, occipital lobe, and the left frontal lobe regions (**Figures 1A, B**), which had already received a boost of radiotherapy in 2006. He was found to have disturbance of consciousness by his family. The routine scan of the whole body showed that extracranial lesions were stable. Even though the patient's epidermal growth factor receptor (EGFR) mutation status was unknown, he chose to accept erlotinib 150 mg daily. Meanwhile, he received

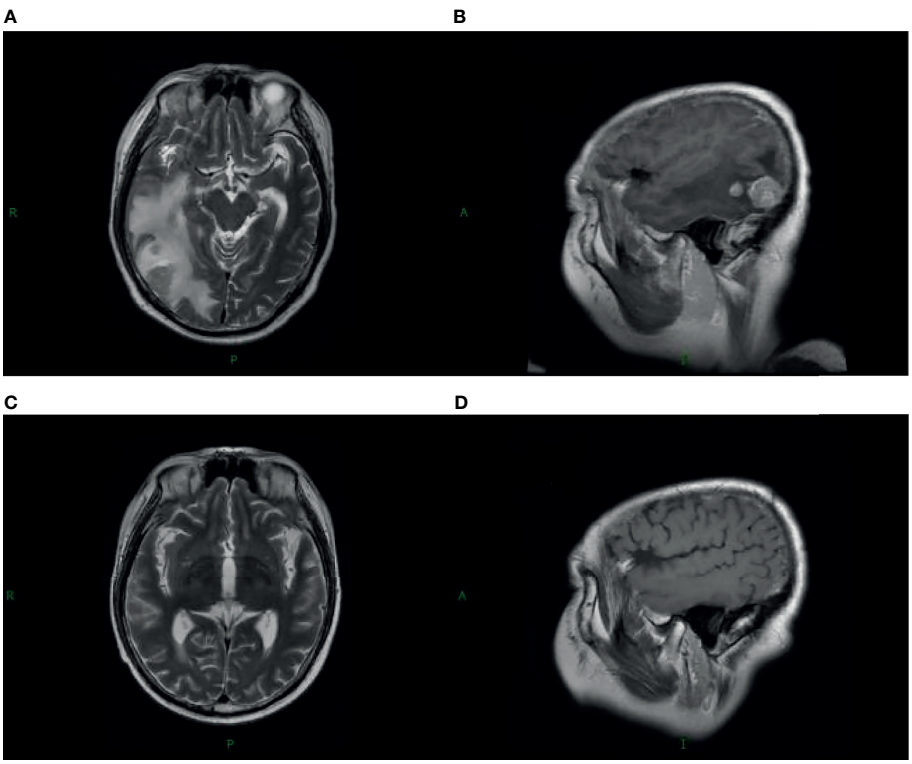

FIGURE 1 | Magnetic resonance imaging (MRI) with contrast enhancement of brain metastasis. **(A, B)** July 2011, before radiotherapy on brain. **(C, D)** September 2011, after radiotherapy on the brain.

reirradiation of the whole brain with a dose of 30 Gy in 15 fractions adopting three-dimensional radiotherapy (3DRT). The patient was immobilized with a thermoplastic mask. We contoured the target volume on the fusion images of CT/MRI and delivered a single isocenter coplanar intensity-modulated radiation therapy (IMRT) boost plan with a dose of 20 Gy in 10 fractions for metastatic intracranial tumors. Then, four cycles of nimustine (125 mg per 3 weeks) and maintenance erlotinib were followed. A follow-up MRI scan in September 2011 revealed that metastatic brain lesions regressed significantly (**Figures 1C, D**).

There were no signs of progression until January 2016, when a relapse was located on the left parieto-temporal lobe (**Figures 2A–C**). Then, GK radiotherapy was performed focusing on the intracranial single lesion of the patient, which was executed at the Third Military Medical University Hospital, China, with an 18-mm collimator. The central dose of the target was 25.4 Gy, and the isodose line of 14 Gy (55% of the central dose) covered the whole tumor. The tumor response of this patient was a partial response (PR) at initial treatment, but just after 3 months, other new intracranial lesions have been observed in the frontal lobe (**Figures 3A–D**). Due to tumor progression in such a short time after radiotherapy, we chose chemotherapy with nimustine (125 mg per 4 weeks) as the palliative treatment modality. From then, recurrent pulmonary infection bothered the patient, and he eventually died of respiratory failure in August 2018.

Outstandingly, during the whole survival, the patient had a good QoL with Karnofsky Performance Score (KPS) above 80. Even after the last GK was executed, he had just a mild neurocognitive defect in March 2018 after neuropsychological testing including 13 questionnaires in the Department of Geriatrics (**File 1**). Together with the brain MRI (slight necrosis and cerebromalacia), we found that the reirradiation of the whole brain did not bring severe neurocognitive defects as we worried before. It is noteworthy that no serious toxicity was observed throughout the entire survival, although the administered dose was far beyond the limits.

DISCUSSION

Brain metastasis management is a complicated task. In this case, we chose WBRT as the first-line therapy, as it is the conventional option for multiple BMs. Generally accepted treatment for WBRT is 30 Gy in 10 fractions (6, 7). Additional radiation doses may be executed depending on the patient prognosis. Because this patient was diagnosed initially at 43 years old, we finally chose WBRT with a dose of 40 Gy in 20 fractions and a boost for intracranial metastatic sites with 10 Gy in 5 fractions, considering his life expectancy.

Treatment should be decided individually, and the appropriate patient selection is very important to benefit from reirradiation. It is most essential to evaluate the prognosis of patients with BMs. The prognostic index that has now become the most prominent is the diagnosis-specific Graded Prognostic Assessment (DS-GPA) (8). As defined by DS-GPA classes, our patient is a male of younger age (<65 years) with a good KPS (KPS >70), control of primary disease, and absence of extracranial metastases. Theoretically, even though the EGFR mutation status was unknown, he was supposed to deserve a better prognosis. Thus, when he had a brain relapse, we chose a positive strategy for him.

For recurrent cranial metastatic disease, the optimal treatment option is not clear. There is an increasing number of reports on the topic of reirradiation with WBRT, but still no clear consensus has been reached. Radiotherapy oncologists agreed that several factors must be considered simultaneously in the process of selecting patients (9, 10), including previous treatment details, such as dose, fractionation, volume, and the interval between the two irradiations, and the current patients' condition, such as the cranial lesions' number, location, and size, patient's performance score, the status of extracranial disease, and patients' life expectancy. One of the earliest, large retrospective cohorts of patients undergoing repeat WBRT was conducted by Cooper et al. in 1990 (11). He concluded that reirradiation with WBRT for cerebral metastases is a viable option for patients who

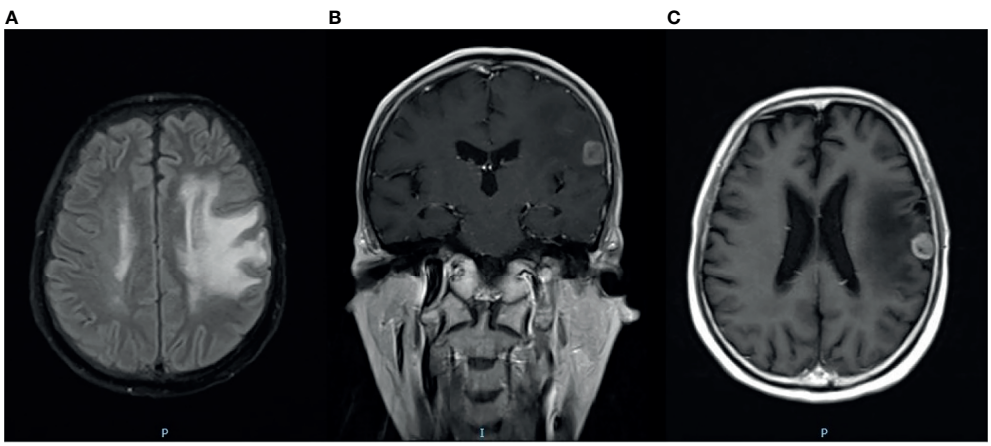

FIGURE 2 | Magnetic resonance imaging (MRI) with contrast enhancement of brain metastasis. **(A–C)** January 2016, before GK radiotherapy on the brain.

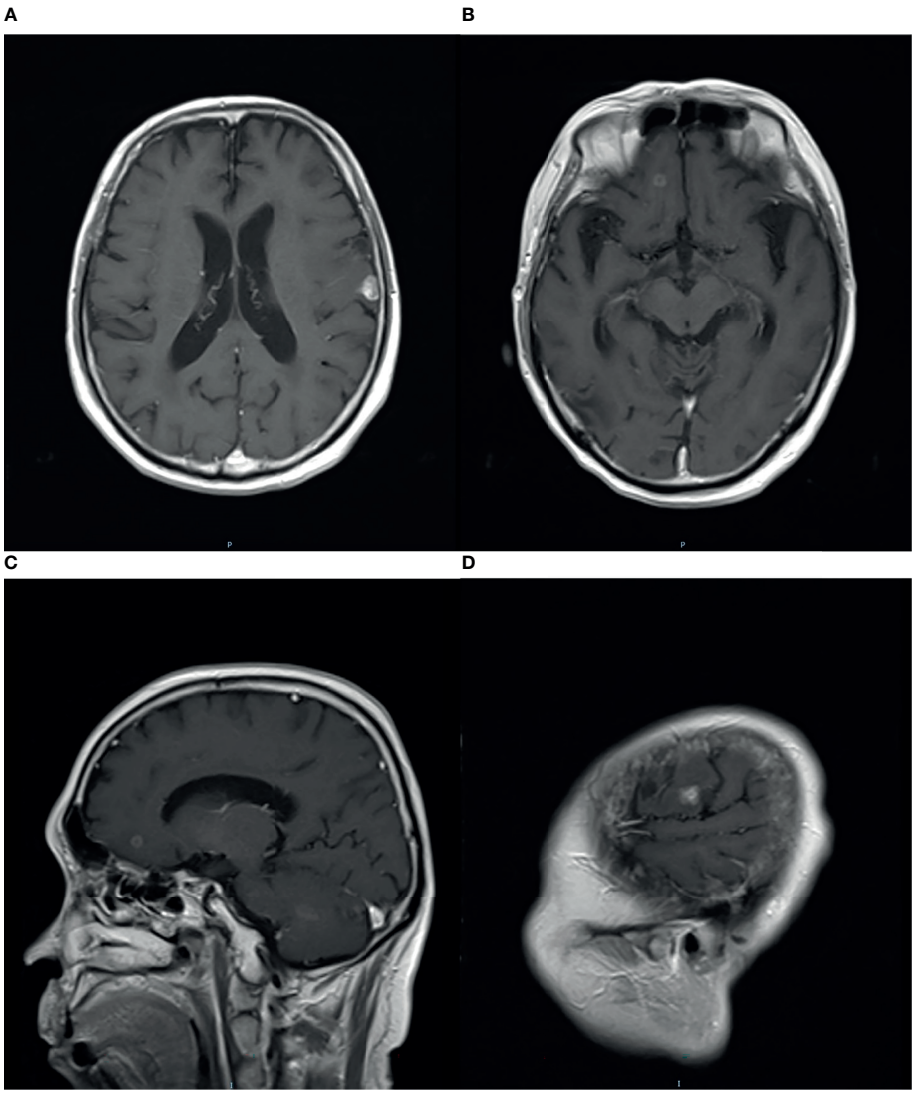

FIGURE 3 | Magnetic resonance imaging (MRI) with contrast enhancement of brain metastasis. **(A–D)** April 2016, after GK radiotherapy on the brain, new intracranial lesions have been observed.

experience cranial relapse more than 4 months after a satisfactory response to initial WBRT. Meanwhile, those patients also stayed in a good general condition when they experienced the cranial relapse. After reirradiation of WBRT, most patients had better survival outcomes and resolution of neurological symptoms. This conclusion was further supported by more studies. Researchers found that stable extracranial disease was associated with improved survival in patients undergoing reirradiation of WBRT (3, 12, 13). What is more, patients with higher KPS scores had a significantly better prognosis after reirradiation with WBRT (14, 15). In this case, our patient is a male of younger age (<65 years) with a good KPS (KPS >70), control of primary disease, and absence of extracranial metastases. Thus, when he had brain relapse, we chose reirradiation of WBRT for him with a dose of 30 Gy in 15 fractions and a boost for intracranial metastatic sites with 20 Gy in 10 fractions.

Except for the response ratio and survival benefits, the potential toxicity of reirradiation with WBRT is another significant consideration in choosing this treatment option for patients. However, few studies have reported severe toxicities from reirradiation with WBRT till now (4, 5). Radiation-induced brain injury was generally classified into three phases: acute, early-delayed, and late-delayed injury (16), among which we cared about most was the late-delayed injury, commonly observed from 6 months to several years after radiation therapy, because it is usually irreversible and progressive (17). Previous studies reported that cognitive deficiency was one of the most frequent consequences of radiation-induced late-delayed injury (18), occurring in 50%–90% of brain tumor survivors, and

it could directly decline the quality of life of the long-term survivors (19). Currently, our knowledge on the mechanisms underlying radiation-induced brain injury is still limited, but it is believed that high radiation doses are responsible for permanent injury, especially the biologically effective dose (BED) (20). What is worth our attention in this case report is that this patient got the cumulative administration dose for the whole brain as high as 70 Gy and a boost for a local site as 30 Gy, without calculating the definite dose of the GK. The $BED_{cumulative}$ of this case is approximately 166.7 Gy ($\alpha/\beta = 3$) or 200 Gy ($\alpha/\beta = 2$) in total. Even as the total BED is far beyond the conventional limits, this patient ultimately benefited from the repeated radiation of the whole brain and had a good quality of life with just a mild neurocognitive defect. As mentioned above, a break of more than 6 months till the second treatment would be a factor in clinics, as it may allow tissues to recover from occult injury. In this patient, the time interval between two WBRT was as long as 5 years. This could better help to explain his outcomes. Certainly, this time interval was usually accepted in the spinal cord, while rare data were shown in the brain. Considering the similarity in morphological and biological characteristics between the spinal cord and brain, we made this recommendation. What could help us better in the future is that choosing the WBRT technique, no matter for initial or repeated treatment with hippocampal avoidance, could be beneficial to protect neurocognitive function (21).

In fact, during the past decades, some developments have surged into the area of treating multiple BMs. The remarkable expansion of stereotactic radiosurgery (SRS) has been administered to patients with BMs, which was historically been utilized for some benign lesions. SRS is supposed to be particularly suitable for metastatic tumors because most are well-circumscribed. Kann et al. (22) reported that the overall utilization rate for SRS rose from 9.8% to 25.6% from 2004 to 2014. The most widely accepted technique of SRS is GK, while various innovations in linear accelerator (Linac)-based systems are now being well-used worldwide. For a long time, the upper limit of SRS alone without WBRT is generally considered to be four lesions. However, more and more studies have demonstrated that the number could not be the limitation. A trend for patients with ≥5 tumors to be considered for SRS alone is already apparently accepted early in this century (23). The prospective observational JLGK0901 study clearly showed the non-inferiority of SRS with GK for those with 5–10 BMs versus patients with 2–4, no matter in terms of overall survival (OS) or most secondary endpoints (24). Before this, the team of Yamamoto has presented two patients with more than 10 BMs who accepted treatment of GK alone and had a good outcome in the follow-up (25). Meanwhile, due to the technological advancement of Linac, there was a continuous increasing interest in SRS Linac-based applications. In the 1980s, several studies showed similar results in terms of accuracy between 4–10 MV Linac-based SRS and GK (26, 27). Alongi compared the two approaches for BMs in multiple dimensions and found that there were no differences in terms of local progression-free survival, survival rates, toxicity, and cost effectiveness. Even if GK remains superior in terms of deep isotropic dose fall-off out of the target, the integration of IGRT tools for SRS Linac-based treatment guaranteed the option of a frameless SRS safe and reliable similar to GK. Magnetic-resonance-guided radiotherapy (MRgRT) marks the beginning of a new era further (28). Due to the lack of device in this case, we chose WBRT to reirradiate, while a number of retrospective studies have documented re-SRS to be safe and effective (29, 30). Especially with the Linac-based SRS, whether with the non-coplanar mono-isocenter (HyperArc^{TM}) technique or the multiple non-coplanar arcs technique, they were demonstrated to improve survival outcomes (31, 32).

In summary, the case report showed that reirradiation of WBRT for patients with multiple BMs even as high cumulative dose still can contribute to good survival and showed slight neurocognitive defects. Therefore, careful selection of the appropriate patient for reirradiation will be needed, and new strategies for BMs would be a better indication. All of these could help to make a proper therapeutic choice.

CONCLUSION

Management of BMs has changed substantially in the past 5–10 years, with varied treatments that have a greater focus on disease control and mitigating the effects of treatment, especially on the role of reirradiation of BMs. However, in reality, lots of departments could not afford the new and expensive equipment so that WBRT is still the cornerstone of modern brain metastases treatment. We report the administration of >70 Gy cumulative activity of WBRT without serious toxicity. This case underscores the therapeutic potential of WBRT therapy in metastatic disease and interindividual dose-tolerance variability. This, to our knowledge, represents a high reported value of reirradiation with whole brain radiotherapy for recurrent brain metastases. In an individual attempt to palliate metastatic disease, the high cumulative activity of radiotherapy should not preclude the patient from repeat treatment.

DATA AVAILABILITY STATEMENT

The raw data supporting the conclusions of this article will be made available by the authors, without undue reservation.

ETHICS STATEMENT

Written informed consent was obtained from the individual(s) for the publication of any potentially identifiable images or data included in this article.

AUTHOR CONTRIBUTIONS

ML and TZ conceived and wrote the article. LL and HD managed this patient in clinics. YS did the radiation plan of this patient. JQ collected information of follow-up about this patient. All authors contributed to the article and approved the submitted version.

FUNDING

This study was supported by The Project on Science and Technology Situation in Yuzhong District, Chongqing (No. 20190101) without any involvement in writing the manuscript.

SUPPLEMENTARY MATERIAL

The Supplementary Material for this article can be found online at: https://www.frontiersin.org/articles/10.3389/fonc.2021.780581/full#supplementary-material

REFERENCES

1. Hocht S, Wiegel T, Hinkelbein W. Reirradiation for Recurrent Brain Metastases: An Overview. *Front Radiat Ther Oncol* (1999) 33:327–31. doi: 10.1159/000061215
2. Patchell RA. The Management of Brain Metastases. *Cancer Treat Rev* (2003) 29:533–40. doi: 10.1016/S0305-7372(03)00105-1
3. Son CH, Jimenez R, Niemierko A, Loeffler JS, Oh KS, Shih HA. Outcomes After Whole Brain Reirradiation in Patients With Brain Metastases. *Int J Radiat Oncol Biol Phys* (2012) 82:e167–72. doi: 10.1016/j.ijrobp.2011.03.020
4. Akiba T, Kunieda E, Kogawa A, Komatsu T, Tamai Y, Ohizumi Y. Re-Irradiation for Metastatic Brain Tumors With Whole-Brain Radiotherapy. *Jap J Clin Oncol* (2012) 42:264–9. doi: 10.1093/jjco/hys007
5. Hazuka MB, Kinzie JJ. Brain Metastases: Results and Effects of Re-Irradiation. *Int J Radiat Oncol Biol Phys* (1988) 15:433–7. doi: 10.1016/S0360-3016(98)90026-8
6. Komarnicky LT, Phillips TL, Martz K, Asbell S, Isaacson S, Urtasun R. A Randomized Phase III Protocol for the Evaluation of Misonidazole Combined With Radiation in the Treatment of Patients With Brain Metastases (RTOG-7916). *Int J Radiat Oncol Biol Phys* (1991) 20:53–8. doi: 10.1016/0360-3016(91)90137-S
7. Murray KJ, Scott C, Greenberg HM, Emami B, Seider M, Vora NL, et al. A Randomized Phase III Study of Accelerated Hyperfractionation Versus Standard in Patients With Unresected Brain Metastases: A Report of the Radiation Therapy Oncology Group (RTOG) 9104. *Int J Radiat Oncol Biol Phys* (1997) 39:571–4. doi: 10.1016/S0360-3016(97)00341-6
8. Sperduto PW, Kased N, Roberge D, Xu Z, Shanley R, Luo X, et al. Summary Report on the Graded Prognostic Assessment: An Accurate and Facile Diagnosis Specific Tool to Estimate Survival for Patients With Brain Metastases. *J Clin Oncol* (2012) 30(4):419–25. doi: 10.1200/JCO.2011.38.0527
9. Bahl A, Kumar M, Sharma DN, Basu KSJ, Jaura MS, Rath GK, et al. Reirradiation for Progressive Brain Metastases. *J Cancer Res Ther* (2009) 5:161–164.4. Ammirati M, Cobbs CS. doi: 10.4103/0973-1482.57120
10. Ammirati M, Cobbs CS, Linskey ME, Paleologos NA, Ryken TC, Burri SH, et al. The Role of Retreatment in the Management of Recurrent/Progressive Brain Metastases: A Systematic Review and Evidence-Based Clinical Practice Guideline. *J Neurooncol* (2010) 96:85–96. doi: 10.1007/s11060-009-0055-6
11. Cooper JS, Steinfeld AD, Lerch IA. Cerebral Metastases: Value of Reirradiation in Selected Patients. *Radiology* (1990) 174(Pt 1):883–5. doi: 10.1148/radiology.174.3.2305074
12. Sadikov E, Bezjak A, Yi QL, Wells W, Dawson L, Millar BA, et al. Value of Whole Brain Re-Irradiation for Brain Metastases—Single Centre Experience. *Clin Oncol* (2007) 19:532–8. 32. doi: 10.1016/j.clon.2007.06.001
13. Scharp M, Hauswald H, Bischof M, Debus J, Combs SE. Re-Irradiation in the Treatment of Patients With Cerebral Metastases of Solid Tumors: Retrospective Analysis. *Radiat Oncol* (2014) 9:4. 33. doi: 10.1186/1748-717X-9-4
14. Aktan M, Koc M, Kanyilmaz G, Tezcan Y. Outcomes of Reirradiation in the Treatment of Patients With Multiple Brain Metastases of Solid Tumors: A Retrospective Analysis. *Ann Transl Med* (2015) 3:325. 30. doi: 10.3978/j.issn.2305-5839.2015.12.21
15. Guo S, Balagamwala EH, Reddy C, Elson P, Suh JH, Chao ST. Clinical and Radiographic Outcomes From Repeat Whole-Brain Radiation Therapy for Brain Metastases in the Age of Stereotactic Radiosurgery. *Am J Clin Oncol* (2016) 39:288–93. doi: 10.1097/COC.0000000000000051
16. Phillips TL, Scott CB, Leibel SA, Rotman M, Weigensberg IJ. Results of a Randomized Comparison of Radiotherapy and Bromodeoxyuridine With Radiotherapy Alone for Brain Metastases: Report of RTOG Trial 89-05. *Int J Radiat Oncol Biol Phys* (1995) 33:339–48. doi: 10.1016/0360-3016(95)00168-X
17. Schultheiss TE, Stephens LJC. Permanent Radiation Myelopathy. *Br J Radiol* (1992) 65(777):737–53. doi: 10.1259/0007-1285-65-777-737
18. Warrington JP, Csiszar A, Mitschelen M, Lee YW, Sonntag WE. Whole Brain Radiation-Induced Impairments in Learning and Mem-Ory Are Time-Sensitive and Reversible by Systemic Hypoxia. *PloS One* (2012) 7(1):e30444.
19. Meyers CA, Brown PD. Role and Relevance of Neurocognitive Assessment in Clinical Trials of Patients With CNS Tumors. *J Clin Oncol* (2006) 24(8):1305–9. 45. doi: 10.1200/JCO.2005.04.6086
20. Mayer R, Sminia P. Reirradiation Tolerance of the Human Brain. *Int J Radiat Oncol Biol Phys* (2008) 70(5):1350–60. doi: 10.1016/j.ijrobp.2007.08.015
21. Giaj Levra N, Sicignano G, Fiorentino A, Fersino S, Ricchetti F, Mazzola R, et al. Whole Brain Radiotherapy With Hippocampal Avoidance and Simultaneous Integrated Boost for Brain Metastases: A Dosimetric Volumetric-Modulated Arc Therapy Study. *Radiol Med* (2016) 121(1):60–9. doi: 10.1007/s11547-015-0563-8
22. Kann BH, Park HS, Johnson SB, Chiang VL, Yu JB. Changing Practice Patterns and Disparities in the United States. *J Natl Compr Canc Netw* (2017) 15:1494–502. doi: 10.6004/jnccn.2017.7003
23. Knisely JPS, Yamamoto M, Gross CP. Radiosurgery Alone for Five or More Brain Metastases: Expert Opinion Survey. *J Neuorosurg* (2010) 113(Suppl):84–9. doi: 10.3171/2010.8.GKS10999
24. Yamamoto M, Serizawa T, Higuchi Y, Sato Y, Kawagishi J, Yamanaka K, et al. A Multi-Institutional Pro-Spective Observational Study of Stereotactic Radiosurgery for Patients With Multiple Brain Metastases (JLGK0901 Study Update): Irradiation-Related Complications and Long-Term Maintenance of Mini-Mental State Examination Scores. *Int J Radiat Oncol Biol Phys* (2017) 99:31–40. doi: 10.1016/j.ijrobp.2017.04.037
25. Yamamoto M, Ide M, Jimbo M, Aiba M, Ito M, Hirai H, et al. Gamma Knife Radiosurgery With Numerous Target Points for Intracranially Disseminated Metastases: Early Experience in Three Patients and Experimental Analysis of Whole Brain Irradiation Doses. In: D Kondziolka, editor. *Radiosurgery 1997*, vol. 2 . Basel: Karger (1998). p. 94–109.
26. Betti OO, Derechinsky VE. Hyperselective Encephalic Irradiation With a Linear Accelerator. *Acta Neurochir* (1984) 33(Suppl.):385–90. doi: 10.1007/978-3-7091-8726-5_60
27. Winston KR, Lutz W. Linear Accelerator as a Neurosurgical Tool for Stereotactic Radiosurgery. *Neurosurgery* (1987) 22(3):454–64.
28. Corradini1 S, Alongi F, Andratschke N, Belka C, Boldrini L, Cellini F, et al. MR-Guidance in Clinical Reality: Current Treatment Challenges and Future Perspectives. *Radiat Oncol* (2019) 14:92. doi: 10.1186/s13014-019-1308-y
29. Kim DH, Schultheiss TE, Radany EH, Badie B, Pezner RD. Clinical Outcomes of Patients Treated With a Second Course of Stereotactic Radio-Surgery for Locally or Regionally Recurrent Brain Metastases After Prior Stereotactic Radiosurgery. *J Neurooncol* (2013) 115:37–43. doi: 10.1007/s11060-013-1191-6
30. McKay WH, McTyre ER, Okoukoni C, Sullivan NKA, Ruiz J, Munley MT, et al. Repeat Stereotactic Radiosurgery as Salvage Therapy for Locally Recurrent Brain Metastases Previously Treated With Radiosurgery. *J Neurosurg* (2017) 127:148–56. doi: 10.3171/2016.5.JNS153051
31. Nicosia L, Figlia V, Mazzola R, Napoli G, Giaj-Levra N, Ricchetti F, et al. Repeated Stereotactic Radiosurgery (SRS) Using a Non-Coplanar Mono-Isocenter (Hyperarc™) Technique Versus Upfront Whole-Brain Radiotherapy (WBRT): A Matched-Pair Analysis. *Clin Exp Metastasis* (2020) 37(1):77–83. doi: 10.1007/s10585-019-10004-3
32. Ruggieri R, Naccarato S, Mazzola R, Ricchetti F, Corradini S, Fiorentino A, et al. Linac-Based Radiosurgery for Multiple Brain Metastases: Comparison Between Two Mono-Isocenter Techniques With Multiple

Non-Coplanar Arcs. *Radiother Oncol* (2019) 132:70–8. doi: 10.1016/j.radonc.2018.11.014

Conflict of Interest: The authors declare that the research was conducted in the absence of any commercial or financial relationships that could be construed as a potential conflict of interest.

Publisher's Note: All claims expressed in this article are solely those of the authors and do not necessarily represent those of their affiliated organizations, or those of the publisher, the editors and the reviewers. Any product that may be evaluated in this article, or claim that may be made by its manufacturer, is not guaranteed or endorsed by the publisher.

frontiers in Oncology

ORIGINAL RESEARCH
published: 14 December 2021
doi: 10.3389/fonc.2021.760090

Clinical Values and Markers of Radiation-Induced Liver Disease for Hepatocellular Carcinoma With Portal Vein Tumor Thrombus Treated With Stereotactic Body Radiotherapy

Jun Jia, Jing Sun, Xuezhang Duan and Wengang Li**

Radiation Oncology Department, The Fifth Medical Center of Chinese People's Liberation Army (PLA) General Hospital, Beijing, China

OPEN ACCESS

Edited by:
Nicola Silvestris, University of Bari Aldo Moro, Italy

Reviewed by:
Francesco Cuccia, Sacro Cuore Don Calabria Hospital, Italy
Christiane Matuschek, University Hospital of Düsseldorf, Germany

***Correspondence:**
Wengang Li
doctor302@163.com
Xuezhang Duan
duanxuezhang2006@163.com

Specialty section:
This article was submitted to Radiation Oncology, a section of the journal Frontiers in Oncology

Received: *17 August 2021*
Accepted: *08 November 2021*
Published: *14 December 2021*

Citation:
Jia J, Sun J, Duan X and Li W (2021) Clinical Values and Markers of Radiation-Induced Liver Disease for Hepatocellular Carcinoma With Portal Vein Tumor Thrombus Treated With Stereotactic Body Radiotherapy. Front. Oncol. 11:760090. doi: 10.3389/fonc.2021.760090

Background: Information about radiation-induced liver disease (RILD) in hepatocellular carcinoma (HCC) patients preexisting hepatitis B cirrhosis with portal vein tumor thrombus (PVTT) extended to the main portal vein treated with stereotactic body radiotherapy (SBRT) is still inadequate and the predictive markers for RILD have not been cleared in these patients. The aim of the study is to identify factors that can be used to predict RILD and to evaluate the influence of RILD in these patients.

Methods: In our study, 59 patients were analyzed and evaluated from December 2015 to June 2019, according to the entry criteria. After treatment, 59 patients were followed up within the first month and then every 3 months. Hematology test, tumor markers, three-phasic CT scan of the lungs, and CT or MRI scan of the liver were performed at each follow up.

Results: Median overall survival time was 10.7 months (range, 5.8 to 14.9). RILD appeared in 17 of the 59 patients (28.8%) at the 3rd month after SBRT. In the univariate analysis, not only the CP score class (A or B) but also each different pretreatment CP score ($p < 0.05$) was a significant predictive factor of RILD. More RILD cases were detected with the increase of CP score. The recovery rate decreased as the baseline CP score increased ($p < 0.05$). It was found that the overall survival time was affected by only baseline CP score and RILD ($p < 0.05$).

Conclusions: The development of RILD has a dependency on the CP score in these patients. CP scores before treatment and RILD are significantly associated with overall survival. SBRT is an effective and safe method for patients with CP ≤ B7. For patients with CP-B8, liver function should be monitored more frequently. It is not safe enough for the SBRT treatment in CP-B9 patients.

Keywords: HCC, SBRT, PVTT, RILD, radiation-induced liver disease

INTRODUCTION

Hepatocellular carcinoma (HCC) is a kind of tumor with very high malignancy. The incidence of HCC ranked 6th among all types of cancer worldwide. It has ranked third in the causes of cancer-related death in China up to now (1, 2). The first choice of treatment for small HCC is surgical resection. However, when being diagnosed many patients are unsuitable or hard for resection or other local treatments, especially the cases with macrovascular invasion (MVI) (3, 4). The most common form of MVI in HCC is portal vein tumor thrombus (PVTT), patients with which have a very short survival time, with an incidence ranging from 44 to 62.2%, and the prognosis for patients with PVTT remains poor till now (5). The treatment of HCC with extensive portal vein involvement remains disputed and intricate. In previous studies, patients with PVTT presented in the main or contralateral branch of portal vein had no survival benefits from surgical resection, whose survival times were generally even shorter (6). Treatments of HCC with PVTT extended to the main portal vein are multidisciplinary and include surgery, intervention such as trans-arterial chemoembolization (TACE), radiotherapy, tyrosine kinase inhibitors (TKIs), and programmed cell death protein 1 inhibitors (PD-1) (7, 8).

It can be learned from previous studies that in the cases of PVTT extended to the main portal vein, radiotherapy (RT) was often considered as a secondary treatment that might be effective (9, 10). Stereotactic body radiotherapy (SBRT), as an emerging technology, delivers high doses of radiation to the target in a few fractions, coupled with a high degree of accuracy in target delineation, which takes advantage of the advancements in precise radiation dose delivery, respiratory motion management, and precise image guidance (11–13). Nowadays, for the small HCC patients who are not qualified for surgery or other local treatments, SBRT has already been adopted as an effective treatment (14). By now, few studies have explored the efficacy and risk of SBRT for the treatment of PVTT involving the main trunk. Among the treatments of HCC patients in our center, SBRT is adopted for the patients who have unresectable HCC with PVTT now.

Meanwhile, side effects must be considered and managed in the use of SBRT. Because of limited effective treatments to cure various kinds of side effects, radiation-induced liver disease (RILD) is so important in the use of SBRT that more attention should be drawn to it. So, determining predictive factors for RILD seems important in clinical work. For some kinds of tumors, a few studies have found that dose-volumetric parameters were predictive factors of RILD (12, 15, 16). In addition, some clinical factors were related to the occurrence and development of RILD have been reported (13, 15–17). But the research is even less about RILD in patients with HCC, especially patients with PVTT extended to the main portal vein who were treated with SBRT. Many factors may increase the risk of RILD. In China, the main cause of liver cancer is hepatitis B cirrhosis. In clinical work, the great majority of patients with HCC in China have been preexisting hepatitis B, which also affects the occurrence and development of RILD (12). Information about RILD in HCC patients preexisting hepatitis B cirrhosis with PVTT presented in the main portal vein treated with SBRT remains inadequate.

The purpose of the study is to investigate suitable markers that affect RILD in patients who have been preexisting hepatitis B cirrhosis with PVTT presented in the main portal vein who are treated with SBRT and we followed the methods of Kim et al., 2018 (18).

DATA AND METHODS

Ethics Statement

This study was approved by the Institutional Review Board of The Fifth Medical Center of PLA General Hospital and was conducted in accordance with the Declaration of Helsinki and internationally accepted ethical guidelines. All patients signed written informed consent for their information to be stored in the hospital databases and used for research.

Clinical Data

From December 2015 to June 2019, 59 HCC patients with PVTT treated by SBRT in the Fifth Medical Center of PLA General Hospital were finally enrolled. The inclusion criteria were as follows: primary HCC with hepatitis B cirrhosis, pretreatment Child-Pugh (CP) class A or B with good performance status (0 or 1 score), HCC with PVTT presented in the main portal vein at the time of diagnosis, no evidence of extrahepatic metastasis, the follow-up studies ≥ 3 months, no other treatments were performed before SBRT, no other local treatment was taken within 3 months after SBRT, more than 700 cc of uninvolved liver.

Therapeutic Method

Target tracking was provided by 4 to 6 golden fiducials implanted before receiving SBRT treatment (CyberKnife, Accuray, USA). Dynamic respiration tracking and fiducial tracking were applied simultaneously in the treatment. CT localization: A plain CT scan was done one week after implantation. Except for benchmark images, the additional images were chosen based on patients' conditions, and these images were enhanced CT scans, magnetic resonance imaging (MRI), positron emission tomography-computed tomography (PET-CT), or hepatic arteriography, etc. SBRT treatment plan design: The gross tumor volume (GTV) represented the tumor thrombosis visualized on the contrast-enhanced CT or MRI. The gross tumor volume (GTV) and organs at risk (normal liver, kidneys, esophagus, stomach, duodenum, bowel, and spinal cord) were contoured by an oncologist and the planning target volume (PTV) was expanded 3–5 mm around the GTV, which contoured 100% of GTV (14). All plans were designed by G4 CyberKnife MultiPlan (Version 4.0.2). A total dose of 49-54Gy was delivered in 7–9 fractions (49Gy/7f, 48Gy/8f, or 54Gy/9f). The normal tissue dose was within the normal radiotherapy tolerance dose (TG-101).

Follow-Up

Liver function assessment and routine blood examination were all done before treatment. After SBRT, the patients were followed up and liver function was examined within 1 month and then every 3 months until the death or necessary.

Evaluation of RILD

The liver toxicity reaction evaluation is based on the definition of RILD, of which there are two types: classic RILD and non-classic RILD. Non-classic RILD occurs in patients with underlying chronic hepatic diseases. So, we refer to the non-classic RILD definition which is divided into elevated liver transaminases increased by more than fivefold compared to normal levels, or worsening of Child-Pugh (CP) score by 2 or more within 3 months after SBRT. Meanwhile, a decrease of CP score or normalization of hepatic enzymes within 6 months could be defined as recovery from RILD (19). CP score was recorded at the beginning of SBRT within 1 week. The clinical data analyzed were age, gender, CP score, alpha fetoprotein (AFP), aspartate aminotransferase (AST), and alanine aminotransferase (ALT). Dose-volumetric data analyzed were SBRT dose and dose per fraction. Liver function, coagulation function, and routine blood tests were examined regularly during the SBRT procedure to evaluate acute toxicity every 3-5 days. After treatment, all patients were followed up within 1 month, and then every 3 months.

Statistical Methods

SPSS 26.0 software was used to perform statistical analyses. Differences between groups were compared according to the Chi-square test, or Student *t* test. The overall survival (OS) was calculated from the diagnosis to the date of either death or the last follow-up visit. Cox regression analysis was used to predict the effective markers for survival time. P-values less than 0.05 were considered to indicate statistically significant differences.

RESULTS

Patient Characteristics

Baseline characteristics of the patients are summarized in **Table 1**. The follow-up time of the patients is 14.9 months. According to the admission criteria for this study, 59 patients were analyzed and evaluated. Overall survival time was defined as the time from diagnosis to death. The median overall survival time was 10.7 months (range, 5.8 to 14.9). The median age was 57 years old (range, 33 to 74). RILD was observed in 17 of the 59 patients (28.8%) in the 3rd month after the end of SBRT. An increase of CP score by 2 appeared in 13 of the 17 patients (76.5%). A liver transaminases increase by more than fivefold compared to normal levels appeared in 4 of the 17 patients (23.5%). By definition, CP Class A includes CP scores 5 and 6, and CP Class B includes CP scores 7, 8, and 9. Of all the patients, 27 were in CP Class A and 32 were in Class B. The number of initial AFP increased (> 10 ng/ml) was 53, the initial ALT increase (> 35 U/ml) was 31 and the initial AST increase (> 40 U/ml) was 26. A total of 48 patients (81.4%) received tyrosine kinase inhibitors (TKIs) (23 Sorafenib, 25 Lenvatinib) after SBRT. There were 2 (4.7%) patients that received programmed cell death protein 1 inhibitors (PD-1) alone after SBRT, 5 patients (11.6%) that received SBRT alone,7 (11.9%) patients that received both PD-1 inhibitors and TKIs after SBRT, and 23 (38.9%) patients that received TACE when progression happened after SBRT.

TABLE 1 | Baseline characteristics of the patients.

Characteristics	No. of patients (n = 59)
Age (years)	
Median	57
Range	33-74
Sex	
Male	45
Female	14
RILD	
yes	17
no	42
Child-Pugh class	
A	27
B	32
Child-Pugh score	
5	14
6	13
7	16
8	14
9	2
Radiation dose (Gy)	
Median	48
Range	45-49
Fraction	8
Median	7-9
Range	
Treatment after SBRT	
TKIs alone	41
PD-1 alone	2
TKIs and PD-1	7
TACE	23
Baseline marker levels	
AFP>10ng/ml	53
ALT>35U/L	31
AST>40U/L	26
Overall Survival	10.7
Median	5.8-14.9
Range	

Markers of RILD

In the univariate analysis, not only CP score class (A or B) but also different pretreatment CP score ($p < 0.05$) is the significant predictive factor of RILD. By analyzing, it is found that age, gender, baseline AST, baseline ALT, baseline AFP, SBRT dose, and dose per fraction do not have an obvious correlation to RILD (**Table 2**). Different scores are found to be significantly associated with RILD ($p < 0.05$). From the data analyzed separately, compared with CP-A5 patients, the incidence of RILD in CP-A6 patients and CP-B7 patients does not increase statistically, while the increase of the incidence of RILD in CP-B8 and CP-B9 patients has statistical significance. For the incidence of RILD, the CP-B7 patients may be a watershed in the treatment

TABLE 2 | Patient characteristics in relation to the risk of RILD.

Variable	RILD (n=17)	Non-RILD (n=42)	p value
Sex			0.518
Male	12	33	
Female	5	9	
Age (year)	57 (42-69)	57 (33-73)	0.881
CP score			0.047
5	1	13	
6	2	11	
7	5	11	
8	7	7	
9	2	0	
CP score class			0.009
A	3	24	
B	14	18	
Radiation dose (Gy)			
Median	48	49	0.102
Range	45-49	45-49	
Fraction			
Median	8	8	0.197
Range	7-9	7-9	
Baseline markers			
AFP	43 (128 ± 49.991)	14 (40 ± 10.680)	0.179
ALT	45 (51.176 ± 5.757)	32 (45.615 ± 6.074)	0.919
AST	54 (48.471 ± 3.988)	54.5 (40.154 ± 6.270)	0.584
Overall survival			
Median	7.8	9.4	≤0.001
Range	4.7-9.2	4.7-12.5	
Recovery			
Yes	6		
No	11		

of the patients who have been preexisting hepatitis B cirrhosis with PVTT extended to the main portal vein [CP score 6 (CP-A6): 95% confidence interval (CI), -0.407–0.243; p=0.613] [CP score 7 (CP-B7): 95% CI, -0.550–0.068; p=0.123] [CP score 8 (CP-B8): 95% CI, -0.747–0.110; p=0.009] [CP score 9(CP-B9): 95% CI, -1.566–0.291; p=0.005] (**Table 3**).

RILD and CP Score

The occurrence of RILD is correlated with the baseline CP score, especially the CP > B7 patients. The incidence of RILD after SBRT is 7.14% (1 of 14 patients) in CP-A5 patients, 15.38% (2 of 13 patients) in CP-A6 patients, 31.25% (5 of 16 patients) in CP-B7 patients, 50.00% (7 of 14 patients) in CP-B8 patients, and 100.00% (2 of 2 patients) in CP-B9 patients. The incidence of RILD increases clearly above CP-A6, and it has statistical significance above CP-B7. The recovery rate decreases as baseline CP score increases. The recovery rate is 100.00% (1 of 1 patients) in CP-A5 patients, 50.00% (1 of 2 patients) in CP-A6 patients, 40.00% (2 of 5 patients) in CP-B7 patients, 28.57% (2 of 7 patients) in CP-B8 patients, and 0.00% (0 of 2 patients) in CP-B9 patients. The recovery rate decreases evidently in patients above CP-B7 (**Figure 1** and **Table 4**).

Changes of Liver Function

We examined patients' liver function and calculated CP scores at the 3rd and 6th months after SBRT (**Figure 2** and **Table 5**). With the increase of CP score stage, the variance of CP score after SBRT became larger. The change in CP score is 0.64, 0.15, 0.63, 0.64, and 1.5 points in patients with CP-A5, CP-A6, CP-B7, CP-B8, and CP-B9 at the 3rd month, respectively. The change in CP score is -0.21, 0.16, 0.12, 0.29, and 0.5 points in patients with CP-A5, CP-A6, CP-B7, CP-B8, and CP-B9 at the 6th month compared to those at the 3rd month, respectively. We can see that in the 6th month, with the increase of baseline CP score, the change range of CP score also increases. There was 1 patient with CP-B9 who died within 6 months because of hepatic failure.

TABLE 3 | Each different score in relation to the risk of RILD.

Variable	95%CI	*p* value
Child-Pugh score		
5	–	–
6	-0.407–0.243	0.613
7	-0.550–0.068	0.123
8	-0.747–0.110	0.009
9	-1.566–0.291	0.005

Investigation of Survival Time

In the Cox regression analysis, the overall survival time is affected by baseline CP score and RILD. The relationship between age, baseline ALT/AST/AFP, and survival time is not statistically significant (p>0.05) (**Table 6**). For these patients treated with SBRT, with the increase of baseline CP score, the survival time decreases significantly. And for the patients with similar basic characteristics, the occurrence of RILD affects the survival time. This means that once RILD occurs, survival may be impaired. For patients with low CP scores and without RILD, the survival time is longer (CP-A6: hazard ratio (HR), 0.003; 95% CI, 0.000 to 0.107; p = 0.001) (CP-B7: HR, 0.009; 95% CI, 0.000 to 0.208; p = 0.003) (CP-B8: HR, 0.023; 95% CI, 0.001 to 0.372; p = 0.008) (CP-B9: HR, 0.094; 95% CI, 0.004 to 0.645; p = 0.022) (RILD: HR, 1.007; 95% CI, 0.347 to 2.880; p = 0.04) (**Figure 3** and **Table 6**). Of the 17 RILD patients, 1 (5.88%) died of RILD within 6 months after SBRT. Death related to RILD occurred only in patients with CP-B9.

Possible Effects of Follow-Up Treatment

Overall survival time is 10.93 months for those who received TKIs after SBRT, 9.78 months for those receiving PD-1 inhibitors after SBRT, and 11.94 months for those who received TACE after SBRT when progression happened. Although the overall survival time is not statistically significant in this study, we can still find some trends. The use of systemic therapy may help improve survival under the premise of fully considering the possible toxic reactions.

DISCUSSION

For HCC patients, in addition to the malignant degree of the tumor, the survival time is also affected by the degree of liver cirrhosis. The more severe the liver cirrhosis is, the worse the liver function is, and the worse tolerance to various anti-tumor treatment methods is. In China, the main cause of liver cirrhosis is hepatitis B cirrhosis. In addition, for patients with PVTT, the

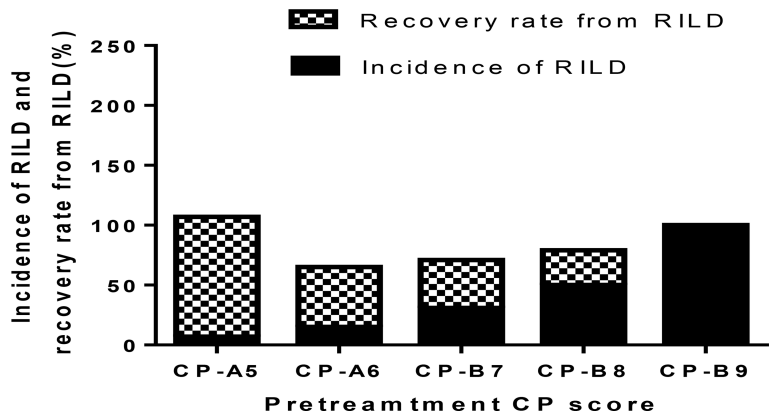

FIGURE 1 | The incidence of RILD and recovery rate after SBRT in different CP scores.

TABLE 4 | Incidence and recovery rate.

	Incidence rate of RILD (%)	Recovery rate from RILD (%)
CP-A5	7.14	100.00
CP-A6	15.38	50.00
CP-B7	31.25	40.00
CP-B8	50.00	28.57
CP-B9	100.00	0.00

pressure of the portal vein increases, and the incidence of liver failure and gastrointestinal bleeding increases significantly. Previous studies have shown that when the cancer thrombus existed in the main portal vein, the median survival time was only 5.6 months, especially in patients with liver function grade B, whose median survival time was less than 3 months (20). It can be concluded from the above that if there is a main portal vein tumor thrombus in hepatitis B related HCC patients, there is a great challenge in the anti-tumor treatment, as such patients have short survival periods, limited treatment options, and a high risk of hepatic failure. Therefore, we consider that for such patients, the implementation of SBRT for portal vein tumor thrombus may open up a new situation. In present studies, the patients with PVTT, especially involving the main trunk, were unsuitable for surgery or TACE due to the failure in prolonging the survival time, while traditional radiotherapy might improve the risk of hepatic failure. In recent years, SBRT has emerged to be a critical treatment for such patients. But the risk of RILD for SBRT is still uncertain for those patients. So, markers to predict RILD need to be established to help us to avoid the occurrence of RILD as far as possible. In some literatures, RILD is divided into "classic" and "non-classic" types (19). Classic RILD typically occurs at about 1 month after the completion of radiotherapy. Some previous studies showed that non-classic RILD was discovered in patients with underlying chronic liver disease, so RILD is defined as the non-classic in our study (15, 21, 22). In our study, RILD was found in 17 of the enrolled 59 patients. The results showed that CP score before treatment was significantly associated with the occurrence of RILD. Compared with CP-A5 patients, the incidence of RILD in CP-A6 patients and CP-B7 patients did not increase statistically, while the increase of the

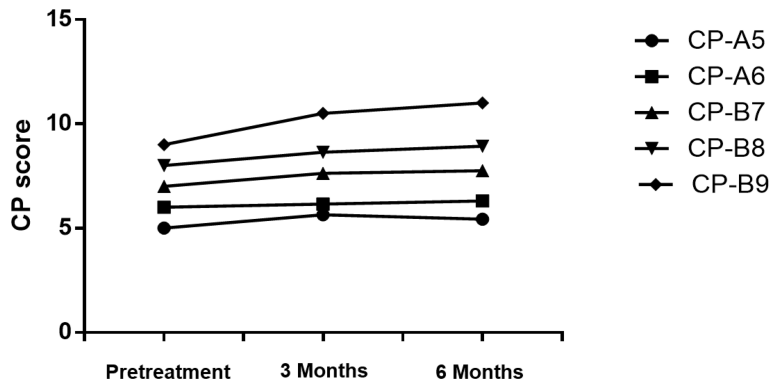

FIGURE 2 | The change of CP score at the 3rd and 6th month.

TABLE 5 | Variance of CP score.

	Pretreatment	3 Months	6 Months
CP-A5	5	5.64	5.43
CP-A6	6	6.15	6.31
CP-B7	7	7.63	7.75
CP-B8	8	8.64	8.93
CP-B9	9	10.5	11

TABLE 6 | Analysis of overall survival.

Variable	HR	95%CI	p value
Age	1.011	0.951-1.075	0.726
AST	1.006	0.987-1.025	0.568
ALT	0.998	0.979-1.018	0.851
AFP	1.0002	0.999-1.004	0.155
Child-Pugh score			0.024
5			
6	0.003	0.000-0.107	0.001
7	0.009	0.000-0.208	0.003
8	0.023	0.001-0.372	0.008
9	0.049	0.004-0.645	0.022
RILD	1.007	0.347-2.880	0.04

incidence of RILD in CP-B8 and CP-B9 patients had statistical significance. Previously, some studies also reported that ALT and AST were important factors to predict RILD (17, 23), but we did not find the relevance in our study. According to Kimura T et al. (23), the incidence rate of RILD was higher in the CP class B than class. A. Jung J et al. (17) have found that the marker related to grade 3 liver toxicity or greater was CP score. We followed the methods of Kim et al. to find more information about RILD in HCC patients preexisting hepatitis B cirrhosis with PVTT extended to the main portal vein treated with SBRT (18). In our study, we chose a group of patients who were prone to radiation injury, as all the patients enrolled had hepatitis B cirrhosis. The patients with different CP scores do not have the same liver function in clinical work. We analyzed the relation of the incidence rate of RILD and CP score. The probability of RILD is related to the stage of CP score ($p < 0.05$) (**Table 3**). This suggests that for patients in our study, especially in cases of CP class B, there may be differences in the development of RILD. For the incidence of RILD, the CP-B7 patients may be a watershed in the treatment of these patients. Some studies have reported that the liver function of patients with CP-A6 may be inferior to that of CP-A5 patients because of fibrosis (24, 25). So, there are reasons to believe that CP > B7 patients have a higher probability of RILD than others. Patients with different CP scores have different risk probabilities. There may be differences between CP-A5, CP-A6, and CP-B7, but perhaps due to the number of cases, there is no statistical difference in our study.

The recovery rate from RILD is examined and the dynamic changes of CP score after SBRT are described. The recovery rate is 100% in CP-A5 patients. It is moderate in CP-A6 (50%) and CP-B7 (40%) patients. The recovery rate is clearly lower in CP ≥ B8 patients: 28.57% in CP-B8 patients and 0% in CP-B9 patients (**Figure 1** and **Table 4**). That RILD is not safe enough in CP-B9 patients can be concluded due to the high possibility of RILD and low recovery rate from it. For the CP-B8 patients, treatment should be evaluated carefully because the risk of RILD is high and liver function should be assessed more frequently because the recovery rate is clearly lower than the CP < B8 patients. Several other studies also supported that it was not safe enough in CP ≥ B8 patients during the treatment of SBRT. Nabavizadeh N. suggested that only CP ≤ B7 patients may be suitable for SBRT because of the moderate liver toxicity (26). Another study has reported that CP ≥ B8 is associated with serious liver toxicity or death ($p = 0.030$) (23). We can conclude that in our study, for the patients with PVTT extended to the main portal vein, more attention should be given during and after the treatment of SBRT in CP ≥ B8 patients.

It is obvious that SBRT could affect liver function. However, few studies about it have been done. Wo JY et al. have reported that decline in CP classification in HCC patients is the most important and common change after SBRT (27). In this study, we evaluate CP score and liver function at the 3rd and 6th months after SBRT. In patients with CP-A5, CP-B7, and CP-B8, the CP score changes by 0.5-1 point at the 3rd month. However, different from the other two groups, the scores of CP-A5 patients dropped at the 6th month. So, we find that the change in function of the liver is more clear in CP ≥ B7 patients than it in CP < B7 patients. But for the CP-B9 patients, the CP score changes by 1.5 points at the 3rd month. The CP class evolves from class B to C (**Figure 2** and **Table 5**). The results show that the CP-A5 and CP-A6 patients with PVTT extended to the main portal vein are safe, in contrast, as they can tolerate the liver toxicity caused by SBRT. In the patients with CP-B7, it is neccessary to monitor liver function carefully to avoid RILD as far as possible. In patients with CP-B8, more methods should be tried to adjust dose per fraction and total dose and monitor liver function more frequently. In patients with CP-B9, it is not safe enough for the SBRT treatment.

The results show that CP score before treatment and RILD are significantly associated with overall survival. Previously, Xu ZY et al. (16) and Son SH et al. (28) have shown that the overall survival time could be shorted by RILD. It can be concluded in our study, the overall survival is also related to RILD statistically for the hepatitis B patients with PVTT extended to the main portal vein. Especially in the patients with poor baseline liver function (CP ≥ B8, especially B9), RILD seems an important factor that can influence overall survival time. The correlation between initial CP score and survival time is obvious too. Patients with different scores have different survival times. It was reported by Kimura T et al. that CP ≥ B8 patients were more probably subjected to severe liver toxicity and the death rate was rising (23). In some other research, the CP-B7 patients had a longer survival time and less toxicity caused by radiotherapy than CP ≥ B8 patients (29). In the light of these studies, CP ≥ B8 patients might have irreversible damage of liver function, thus the survival time could be shorted. Therefore, once RILD occurs, it is hard for these patients to reverse the damage. For these patients treated with SBRT, with the increase of baseline CP score, the survival time decreases significantly. And for the

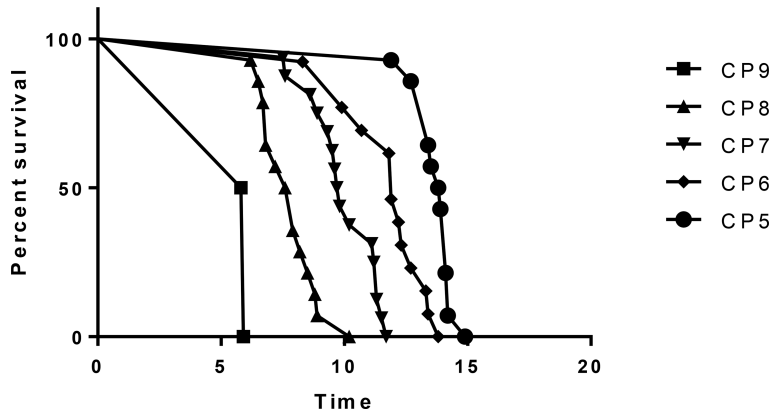

FIGURE 3 | Overall survival in different CP scores.

patients with similar basic characteristics, the occurrence of RILD affects the survival time. The survival time of patients with poor liver function is shorter as we know. While the occurrence of RILD means that these patients have poor tolerance to SBRT. So, it is not hard to understand the impact of these two factors on survival time.

Our study also has some limitations. First, it is a retrospective study. Second, the number of cases is relatively small, because we include only HCC patients who have been preexisting hepatitis B cirrhosis with PVTT extended to the main portal vein treated by SBRT. More CP-B Class patients need to be treated with SBRT to find more markers to reduce the incidence of RILD for clinicians. Further prospective investigation is needed to clarify more relationships between liver function, RILD, and survival time. Due to the small number of cases and the lack of previous experience, the combined therapy of TKIs, PD-1 inhibitors, and SBRT failed to show a clear survival advantage, statistically. If there is no contraindication, TACE is still a better choice for patients with tumor progression after SBRT. After we have accumulated the experience of treatment, multidisciplinary treatment needs to be proven to be the direction of the future in more prospective investigations.

CONCLUSION

CP score is closely related to the development of RILD in patients who have been preexisting hepatitis B cirrhosis with PVTT extended to the main portal vein. CP score before treatment and RILD are significantly associated with overall survival. SBRT is a safe and effective treatment for patients with CP ≤ B7. For patients with CP-B8, more methods should be tried to adjust dose per fraction and total dose and monitor liver function more frequently. It is not safe enough for the SBRT treatment in CP-B9 patients. The use of systemic therapy may help improve survival under the premise of fully considering the possible toxic reactions.

DATA AVAILABILITY STATEMENT

The original contributions presented in the study are included in the article/s **Supplementary Material**. Further inquiries can be directed to the corresponding author.

ETHICS STATEMENT

This study was approved by the Institutional Review Board of The Fifth Medical Center of PLA General Hospital and was conducted in accordance with the Declaration of Helsinki and internationally accepted ethical guidelines. All patients signed written informed consent for their information to be stored in the hospital databases and used for research.

AUTHOR CONTRIBUTIONS

Data analysis and interpretation, and drafting and revision of the manuscript for critically important intellectual content JJ, data acquisition JS, manuscript preparation JJ, and provision of final approval of the version to be published WL and XD. All authors have read and approved the final version.

FUNDING

This study protocol was supported by a grant from the National Natural Science Foundation of China 81972856.

SUPPLEMENTARY MATERIAL

The Supplementary Material for this article can be found online at: https://www.frontiersin.org/articles/10.3389/fonc.2021.760090/full#supplementary-material

REFERENCES

1. Siegel RL, Miller KD, Jemal A. Cancer Statistics, 2020. *CA Cancer J Clin* (2020) 70(1):7–30. doi: 10.3322/caac.21590
2. Chen W, Zheng R, Baade PD, Jemal A, Zeng H, Bray F, et al. Cancer Statistics in China, 2015. *CA Cancer J Clin* (2016) 66(2):115–32.
3. Kudo M, Izumi N, Kubo S, Kokudo N, Sakamoto M, Shiina S, et al. Report of the 20th Nationwide Follow-Up Survey of Primary Liver Cancer in Japan. *Hepatol Res* (2020) 50(1):15–46. doi: 10.1111/hepr.13438
4. Roayaie S, Blume IN, Thung SN, Guido M, Fiel M-I, Hiotis S, et al. A System of Classifying Microvascular Invasion to Predict Outcome After Resection in Patients With Hepatocellular Carcinoma. *Gastroenterology* (2009) 137 (3):850–5. doi: 10.1053/j.gastro.2009.06.003
5. Zhang Z-M, Lai ECH, Zhang C, Yu H-W, Liu Z, Wan B-J, et al. The Strategies for Treating Primary Hepatocellular Carcinoma With Portal Vein Tumor Thrombus. *Int J Surg* (2015) 20:8–16. doi: 10.1016/j.ijsu.2015.05.009
6. Katagiri S, Yamamoto M. Multidisciplinary Treatments for Hepatocellular Carcinoma With Major Portal Vein Tumor Thrombus. *Surg Today* (2014) 44 (2):219–26. doi: 10.1007/s00595-013-0585-6
7. Cheng S, Chen M, Cai J, Sun J, Guo R, Bi X, et al. Chinese Expert Consensus on Multidisciplinary Diagnosis and Treatment of Hepatocellular Carcinoma With Portal Vein Tumor Thrombus (2018 Edition). *Liver Cancer* (2020) 9 (1):28–40. doi: 10.1159/000503685
8. Kokudo T, Hasegawa K, Matsuyama Y, Takayama T, Izumi N, Kadoya M, et al. Survival Benefit of Liver Resection for Hepatocellular Carcinoma Associated With Portal Vein Invasion. *J Hepatol* (2016) 65(5):938–43. doi: 10.1016/j.jhep.2016.05.044
9. Sheu JC, Huang GT, Chen DS, Sung JL, Yang PM, Wei TC, et al. Small Hepatocellular Carcinoma: Intratumor Ethanol Treatment Using New Needle and Guidance Systems. *Radiology* (1987) 163:43–8. doi: 10.1148/radiology.163.1.3029806
10. Ikeda K, Kumada H, Saitoh S, Arase Y, Chayama K. Effect of Repeated Transcatheter Arterial Embolization on the Survival Time in Patients With Hepatocellular Carcinoma: An Analysis by the Cox Proportional Hazard Model. *Cancer* (1991) 68:2150–4. doi: 10.1002/1097-0142(19911115)68:10<2150::AID-CNCR2820681011>3.0.CO;2-F
11. Cui TM, Liu Y, Wang JB, Liu LX. Adverse Effects of Immune-Checkpoint Inhibitors in Hepatocellular Carcinoma. *Onco Targets Ther* (2020) 13:11725–40. doi: 10.2147/OTT.S279858
12. Li Z, Dong Y, Fan M, Yin Y, Zhu J, Li B, et al. Analysis of Hepatitis B Virus Reactivation After Radiotherapy in Patients With Hepatocellular Carcinoma Using the Lyman NTCP Model. *Technol Cancer Res Treat* (2019) 18:1533033819875136. doi: 10.1177/1533033819875136
13. Nicosia L, Cuccia F, Mazzola R, Figlia V, Alongi F. Stereotactic Body Radiotherapy (SBRT) can Delay Polymetastatic Conversion in Patients Affected by Liver Oligometastases. *J Cancer Res Clin Oncol* (2020) 146(6). doi: 10.1007/s00432-020-03223-9
14. Zhang T, Sun J, He W, Li H, Piao J, Xu H, et al. Stereotactic Body Radiation Therapy as an Effective and Safe Treatment for Small Hepatocellular Carcinoma. *BMC Cancer* (2018) 18(1):451. doi: 10.1186/s12885-018-4359-9
15. Son SH, Choi BO, Mi RR, Kang YN, Ji SJ, Si HB, et al. Stereotactic Body Radio-Therapy for Patients With Unresectable Primary Hepatocellular Carcinoma: Dose-Volumetric Parameters Predicting the Hepatic Complication. *Int J Radiat Oncol Biol Phys* (2010) 78:1073–80. doi: 10.1016/j.ijrobp.2009.09.009
16. Xu ZY, Liang SX, Zhu J, Zhu XD, Zhao JD, Lu HJ, et al. Prediction of Radiation-Induced Liver Disease by Lyman Normal-Tissue Complication Probability Model in Three-Dimensional Conformal Radiation Therapy for Primary Liver Carcinoma. *Int J Radiat Oncol Biol Phys* (2006) 65(1):189–95. doi: 10.1016/j.ijrobp.2005.11.034
17. Jung J, Yoon SM, Kim SY, Cho B, Park J-H, Kim SS, et al. Radiation-Induced Liver Disease After Stereotactic Body Radiotherapy for Small Hepatocellular Carcinoma: Clinical and Dose-Volumetric Parameters. *Radiat Oncol* (2013) 8:249. doi: 10.1186/1748-717X-8-249
18. Jun BG, Kim YD, Cheon GJ, Kim ES, Jwa E, Kim SG, et al. Clinical Significance of Radiation-Induced Liver Disease After Stereotactic Body Radiation Therapy for Hepatocellular Carcinoma. *Korean J Intern Med* (2018) 33(6):1093–102. doi: 10.3904/kjim.2016.412
19. Doi H, Shiomi H, Masai N, Tatsumi D, Igura T, Imai Y, et al. Threshold Doses and Prediction of Visually Apparent Liver Dysfunction After Stereotactic Body Radiation Therapy in Cirrhotic and Normal Livers Using Magnetic Resonance Imaging. *J Radiat Res* (2016) 57(3):294–300. doi: 10.1093/jrr/rrw008
20. Yamamoto Y, Ikoma H, Morimura R, Shoda K, Konishi H, Murayama Y, et al. Post-Hepatectomy Survival in Advanced Hepatocellular Carcinoma With Portal Vein Tumor Thrombosis. *World J Gastroenterol* (2015) 21(1):246–53. doi: 10.3748/wjg.v21.i1.246
21. Pablo MS, Sylvia N, Dawson LA. Radiation-Induced Liver Toxicity. *Semin Radiat Oncol* (2017) 27(4):350–7. doi: 10.1093/jrr/rrw008
22. Gkika E, Schultheiss M, Bettinger D, Maruschke L, Neeff HP, Schulenburg M, et al. Excellent Local Control and Tolerance Profile After Stereotactic Body Radiotherapy of Advanced Hepatocellular Carcinoma. *Radiat Oncol* (2017) 12 (1):116. doi: 10.1186/s13014-017-0851-7
23. Kimura T, Takeda A, Sanuki N, Ariyoshi K, Yamaguchi T, Imagumbai T, et al. Multicenter Prospective Study of Stereotactic Body Radiotherapy for Previously Untreated Solitary Primary Hepatocellular Carcinoma: The STRSPH Study. *Hepatol Res* (2020). doi: 10.1016/j.semradonc.2017.04.002
24. Okajima C, Arii S, Tanaka S, Matsumura S, Ban D, Ochiai T, et al. Prognostic Role of Child-Pugh Score 5 and 6 in Hepatocellular Carcinoma Patients Who Underwent Curative Hepatic Resection. *Am J Surg* (2015) 209:199–205. doi: 10.1016/j.amjsurg.2014.03.009
25. Chiu J, Tang YF, Yao TJ, Wong A, Wong H, Leung R, et al. The Use of Single-Agent Sorafenib in the Treatment of Advanced Hepatocellular Carcinoma Patients With Underlying Child-Pugh B Liver Cirrhosis: A Retrospective Analysis of Efficacy, Safety, and Survival Benefits. *Cancer* (2012) 118 (21):5293–301. doi: 10.1002/cncr.27543
26. Nabavizadeh N, Jahangiri Y, Rahmani R, Tomozawa Y, Geeratikun Y, Chen Y, et al. Thermal Ablation *Versus* Stereotactic Body Radiotherapy Following Transarterial Chemoembolization for Inoperable Hepatocellular Carcinoma: A Propensity Score Weighted Analysis. *AJR Am J Roentgenol* (2020). doi: 10.2214/AJR.20.24117
27. Wo JY, Dawson LA, Zhu AX, Hong TS. An Emerging Role for Radiation Therapy in the Treatment of Hepatocellular Carcinoma and Intrahepatic Cholangiocarcinoma. *Surg Oncol Clin N Am* (2014) 23(2):353–68. doi: 10.1016/j.soc.2013.10.007
28. Son SH, Jang HS, Jo IY, Choi B, Jang J, Yoon S. Significance of an Increase in the Child-Pugh Score After Radiotherapy in Patients With Unresectable Hepatocellular Carcinoma. *Radiat Oncol* (2014) 9:101. doi: 10.1186/1748-717X-9-101
29. Culleton S, Jiang H, Haddad CR, Kim J, Brierley J, Brade A, et al. Outcomes Following Definitive Stereotactic Body Radiotherapy for Patients With Child-Pugh B or C Hepatocellular Carcinoma. *Radiother Oncol* (2014) 111:412–7. doi: 10.1016/j.radonc.2014.05.002

Conflict of Interest: The authors declare that the research was conducted in the absence of any commercial or financial relationships that could be construed as a potential conflict of interest.

frontiers in Oncology

ORIGINAL RESEARCH
published: 25 January 2022
doi: 10.3389/fonc.2022.766066

First-Line Tyrosine Kinase Inhibitors Combined With Local Consolidative Radiation Therapy for Elderly Patients With Oligometastatic Non-Small Cell Lung Cancer Harboring EGFR Activating Mutations

*Xiaolong Hu[1], Hongqi Li[2], Xiaoli Kang[2], Xuan Wang[2], Haifeng Pang[2], Chen Liu[2], Jianchun Zhang[1] and Yingjie Wang[2]**

[1] Department of Radiation Oncology, Beijing Geriatric Hospital, Beijing, China, [2] Department of Radiation Oncology, Air Force General Hospital, Beijing, China

OPEN ACCESS

Edited by:
Nicola Silvestris,
University of Bari Aldo Moro, Italy

Reviewed by:
Francesco Ricchetti,
Sacro Cuore Don Calabria Hospital (IRCCS), Italy
Anil Tibdewal,
Tata Memorial Hospital, India

***Correspondence:**
Yingjie Wang
wangyj9999@126.com

Specialty section:
This article was submitted to Radiation Oncology, a section of the journal Frontiers in Oncology

Received: 28 August 2021
Accepted: 03 January 2022
Published: 25 January 2022

Citation:
Hu X, Li H, Kang X, Wang X, Pang H, Liu C, Zhang J and Wang Y (2022) First-Line Tyrosine Kinase Inhibitors Combined With Local Consolidative Radiation Therapy for Elderly Patients With Oligometastatic Non-Small Cell Lung Cancer Harboring EGFR Activating Mutations. Front. Oncol. 12:766066. doi: 10.3389/fonc.2022.766066

Objective: The aim of this study was to investigate the efficacy and safety of combined applications of local consolidative radiation therapy (LCRT) and first-line tyrosine kinase inhibitors (TKIs) for the treatment of primary tumors and oligometastatic sites in oligometastatic NSCLC harboring Epidermal Growth Factor Receptor (EGFR) activating mutations.

Patients and Methods: Elderly patients with oligometastatic NSCLC (≤5 metastases) harboring EGFR activating mutations at the time of diagnosis were identified. They were treated with first-line TKIs alone or in combination with LCRT. Progression-free survival (PFS) and overall survival (OS) were estimated through the Kaplan–Meier method.

Results: A total of 122 elderly patients were enrolled between February 2010 and January 2018. Among them, 41.0% (n = 50) received TKIs combined with LCRT (TKIs + LCRT group), whereas 59.0% (n = 72) received TKIs monotherapy (TKIs alone group). Patients were followed up for a median length of 34 months (ranging from 7.0 to 64 months). The median PFS in TKIs + LCRT group was 17 months (95%CI: 15.37–18.63), which was significantly longer than that of the TKIs-alone group (12 months; 95%CI: 11.05–12.95) ($p < 0.001$). Median OS in TKIs + LCRT group was 38 months (95%CI: 35.61–40.39), while that of the TKIs-alone group was 29 months (95%CI: 26.86–31.14) ($p < 0.001$). Multivariate analyses revealed that LCRT, one to two metastases, and good ECOG PS were independent predictors for better PFS ($p < 0.001$, $p = 0.004$, and $p = 0.027$). Moreover, LCRT, good ECOG PS, and T_{1-2} stage were independent predictors for better OS ($p < 0.001$, $p = 0.007$ and $p = 0.007$). Most of the patients suffered from grade 1 to 2 toxicities, and treatment-related deaths were not recorded.

Conclusion: First-line TKIs combined with LCRT may improve survival outcomes for elderly patients with oligometastatic NSCLC harboring EGFR activating mutations. This approach was not associated with much toxicity, therefore, it can be used for the treatment of elderly patients with oligometastatic disease.

Keywords: EGFR mutant NSCLC, local consolidation radiation, residual disease, oligometastatic, elderly patients

INTRODUCTION

The prevalence of non-small cell lung cancer (NSCLC) among elderly people has been increasing. Approximately 50% of NSCLC patients present with distant metastases at the time of diagnosis (1). In advanced NSCLC patients with sensitizing EGFR mutations, EGFR-TKIs have been found to effectively improve clinical outcomes, relative to cytotoxic chemotherapies (2–5). However, within 9–12 months of treatment, most patients develop resistance to EGFR-TKIs (6, 7). In 1995, Hellman proposed the concept of "oligometastasis", which is the transition stage between local primary tumors and extensive metastasis. Several randomized clinical trials have evaluated the efficacy of different treatments for patients with oligometastatic NSCLC (8–10). However, available treatments are not effective for geriatric patients with NSCLC harboring EGFR mutations, without T790M-mediated resistance to their initial EGFR inhibitor. Unlike younger patients, elderly patients are often administered with less aggressive treatments, possibly due to resistance to EGFR-TKIs. Therefore, there is a need to develop treatment options that can suppress tumor progression among elderly patients. A combination of local consolidation therapy and EGFR-TKIs in patients with oligometastatic NSCLC harboring EGFR activating mutations significantly prolonged PFS and overall survival (OS), relative to TKIs alone (11). Currently, the efficacy and safety of combined local consolidative radiation therapy (LCRT) and first-line EGFR-TKIs in elderly patients with oligometastatic NSCLC harboring EGFR activating mutations have not been clearly defined. In this study, we tested the hypothesis that elderly patients with oligometastatic NSCLC harboring EGFR mutations may benefit from combined treatments of LCRT and first-line EGFR-TKIs.

MATERIALS AND METHODS

Patients

Stage IV EGFR-mutant NSCLC patients with oligometastatic disease within 1 month of diagnosis at the Beijing Geriatric Hospital and Air Force General Hospital were retrospectively analyzed between January, 2010 and February, 2018. The inclusion criteria were: 65 years or older (elderly), pathologically confirmed NSCLC harboring EGFR-sensitizing mutations, patients with synchronous oligometastatic disease (≤5 metastases) confirmed by comprehensive imaging examinations (namely, brain magnetic resonance imaging (MRI) + whole-body positron emission tomography computed tomography (PET-CT) or brain MRI + thoracic/abdominal/pelvic CT, and bone scan when necessary), Eastern Cooperative Oncology Group Performance Status (ECOG PS) score of 2 or less, after initial treatment with first-line EGFR-TKIs, the primary tumor and all metastases were stable.

Treatment responses were assessed 6–8 weeks after treatment with first-line TKIs, in accordance with response evaluation criteria for solid tumors, Revised RECIST guidelines (version 1.1). The EGFR-TKIs used in this study were gefitinib (250 mg daily) and erlotinib (150 mg daily). Patients that responded well to first-line TKIs followed by treatment with local consolidative radiation therapy (LCRT) to primary tumor and all oligometastatic sites were designated as the TKIs + LCRT group. Patients treated with first-line TKIs alone were designated as the TKIs-alone group. Progression-free survival was defined as the time from initiation of TKIs treatment to progression or death from any cause. Overall survival was defined as the duration between the date of TKIs initiation and date of death.

Local Consolidative Radiation Therapy Procedure

The application of local consolidative radiation therapy was decided by a multidisciplinary team (namely, oncologists, radiation oncologists, radiologists, orthopedic surgeons, neurosurgeons, cardiologists, respiratory physicians, and geriatricians) at each center. Clinical assessment included the evaluation of factors such as age, cardiopulmonary functions, underlying diseases, pathological fracture risk, nutritional status, central nervous system symptoms, and risk–benefit ratio. The local consolidative radiation therapy regimen was determined by radiation oncologists based on general conditions, tumor locations, tumor sizes, tumor boundary, pulmonary functions, bone marrow, hepatic, and renal functions.

The primary tumor was subjected to hypofractionated radiotherapy (70 Gy in 10–15 fractions, the biologically effective dose was 103–119 Gy) or conventional fractionated radiotherapy (70 Gy in 30–35 fractions, the biologically effective dose was 84.0–86.3 Gy). Vertebral metastases were treated with conventional fractionated radiotherapy (30 Gy in 10 fractions or 40 Gy in 20 fractions), isolated brain metastases were treated with gamma knife radiosurgery (50% Isodose line 22 Gy/1f), multiple brain metastases were treated with conventional fractionated radiotherapy (60 Gy in 20 fractions to brain metastases) or conventional fractionated radiotherapy plus whole-brain radiation therapy (50 Gy in 20 fractions to brain metastases plus WBRT 40 Gy in 20 fractions). Liver metastases were managed *via* hypofractionated radiotherapy (65 Gy in 20 fractions or 60 Gy in 15 fractions). Contralateral lung metastases were treated with gamma knife radiosurgery (70% Isodose line70–78 Gy/10–14 f),

hypofractionated radiotherapy (70 Gy in 15 fractions or 60 Gy in 15 fractions) or conventional fractionated radiotherapy (60 Gy in 20 fractions). Non-regional lymph node metastases were controlled by conventional fractionated radiotherapy (70 Gy in 30–35 fractions or 60 Gy in 30 fractions).

Toxicity Assessment

Acute and long-term toxicities were defined before and after 90 days using the Common Terminology Criteria for Adverse Events (CTCAE) version 5 in accordance with the National Cancer Institute (NCI). TKIs-related acute toxicities included skin rash, diarrhea, pneumonitis, neutropenia, fatigue, vomiting, and elevated ALT levels. Radiotherapy-related acute toxicities included pneumonia, fatigue, thrombocytopenia, anemia, leukopenia, dermatitis, and esophagitis.

Statistical Analysis

Statistical analyses were performed using the IBM Statistical Package for Social Sciences (SPSS) software 25 (SPSS Inc., Chicago, IL, USA), and GraphPad Prism 7 version 7.04 (GraphPad Software, Inc., La Jolla, California USA). Normally distributed quantitative data are expressed as mean and standard deviation (M ± SD). Categorical variables are presented in percentages and frequency distributions. Kaplan–Meier analysis with the log-rank test was used to calculate and analyze survival curves. A Cox proportional hazards model was used for univariate and multivariate analyses to assess possible prognostic factors and calculate survival hazard ratios (HRs) for PFS and OS at 95% confidence intervals (95%CI). The significant parameters identified in univariate analyses ($p < 0.05$) were incorporated into multivariate Cox regression analysis to determine the independent prognostic factors. A two-sided $p < 0.05$ was considered statistically significant.

RESULTS

Patient Characteristics

A total of 122 patients with oligometastatic NSCLC (≤5 metastases) harboring the EGFR sensitizing mutation and treated with first line TKIs without progression were enrolled between February 2010 and January 2018 (**Figure 1**). **Table 1** shows the general clinical characteristics for the enrolled patients. The patients had a median age of 72.5 years, with 39.3% (n = 48) of them being older than 75 years. Majority of the patients (n = 102, 83.6%) had adenocarcinoma histology, 4.9% (n = 6) had squamous cell carcinoma, 54.9% (n = 67) had Exon 21 L858R mutations, 59% (n = 72) were present or former smokers, 80.3% (n = 98) had underlying diseases, 63.9% (n = 78) had hypertension, 39.3% (n = 48) had diabetes, 28.7% (n = 35) had chronic obstructive pulmonary disease (COPD), 52.5% (n = 64) had ECOG PS 0 or 1, 46.7% (n = 57) had N_{0-1} stage, while 51.6% (n = 63) had T_{1-2} stage. Most of the patients (77.9%, n = 95) received gefitinib as first-line treatment. Regarding the quantity of oligometastatic lesions in the 122 patients, 55.7% (n = 68) had one to two metastases, with 8 patients having the brain as the only site for metastases. Moreover, 44.3% (n = 54) of the patients had three to five metastases. With respect to oligometastatic sites, 50.8% (n = 62) patients had brain metastases, 48.3% (n = 59) had bone metastases, 34.4% (n = 42) had contralateral lung metastases, 28.7% (n = 35) had adrenal metastases, 7.4% (n = 9) had liver metastases, while 6.60% (n = 8) had non-regional lymph nodes metastases.

Overall, 41% (n = 50) of the patients received local consolidative radiation therapy to primary tumor and all oligometastatic sites (**Table 2**). Thirty two patients in the TKIS + LCRT group received hypofractionated radiotherapy (BED_{10} ≥100 Gy) for the primary tumor (**Table 3**), 4 patients received gamma knife radiosurgery for isolated brain metastases, 13 patients received conventional radiotherapy plus whole-brain radiation therapy, 8 patients received gamma knife radiosurgery for contralateral lung metastases, 4 patients received hypofractionated radiotherapy for adrenal metastases, while 2 patients received hypofractionated radiotherapy for liver metastases.

Survival Outcomes

The median length of follow-up time was 34 months (range, 7.0–64 months). The median progression free survival (mPFS) time in the TKIs + LCRT group was 17 months, while that of the TKIs-alone group was 12 months ($p < 0.001$). The median overall survival (mOS) time in the TKIs + LCRT group was 38 months, while that of the TKIs-alone group was 29 months ($p < 0.001$) (**Figure 2**). The mPFS in the entire study population was 13 months, while mOS was 34 months (95%CI: 30.3–37.7).

Univariate and Multivariate Analyses of PFS and OS

Univariate analysis revealed that LCRT for primary tumor and all oligometastatic sites resulted in better PFS (HR = 0.30, $p < 0.001$). A similar observation was made for one to two metastases (HR = 0.49, $p < 0.001$), and good ECOG PS (HR = 0.68, $p = 0.035$). Multivariate analysis revealed that LCRT for primary tumor and all oligometastatic sites was an independent predictive factor for better PFS (HR = 0.32, 95%CI: 0.20–0.51, $p < 0.001$). This was the case for one to two metastases (HR = 0.57, 95%CI: 0.39–0.83, $p = 0.004$), and good ECOG PS (HR = 0.67, 95%CI: 0.46–0.96, $p = 0.027$) (**Table 4**).

Univariate analysis showed that patients who received LCRT to primary tumor and all oligometastatic sites were associated with better OS (HR = 0.48, $p < 0.001$), T_{1-2} stage (HR = 0.60, $p = 0.008$), good ECOG PS (HR = 0.46, $p < 0.001$), second-line treatment (HR = 0.67, $p = 0.045$), and presented with one to two metastases (HR = 0.62, $p = 0.016$). Multivariate analysis showed that patients that received LCRT to primary tumor and all oligometastatic sites was an independent prognostic factor for better OS (HR = 0.41, 95%CI: 0.27–0.63, $p < 0.001$), good ECOG PS (HR = 0.54, 95%CI: 0.34–0.85, $p = 0.007$), and T_{1-2} stage (HR = 0.56, 95%CI: 0.37–0.85, $p = 0.007$) (**Table 5** and **Figure 3**).

In the TKIs + LCRT group, clinical factors for primary tumor, BED ≥100 Gy, were associated with better OS and PFS in univariate analyses ($p = 0.004$ and $p = 0.031$, respectively) (**Figure 4**). However, multivariate analysis revealed that the difference was not significant ($p = 0.19$ and $p = 0.61$, respectively).

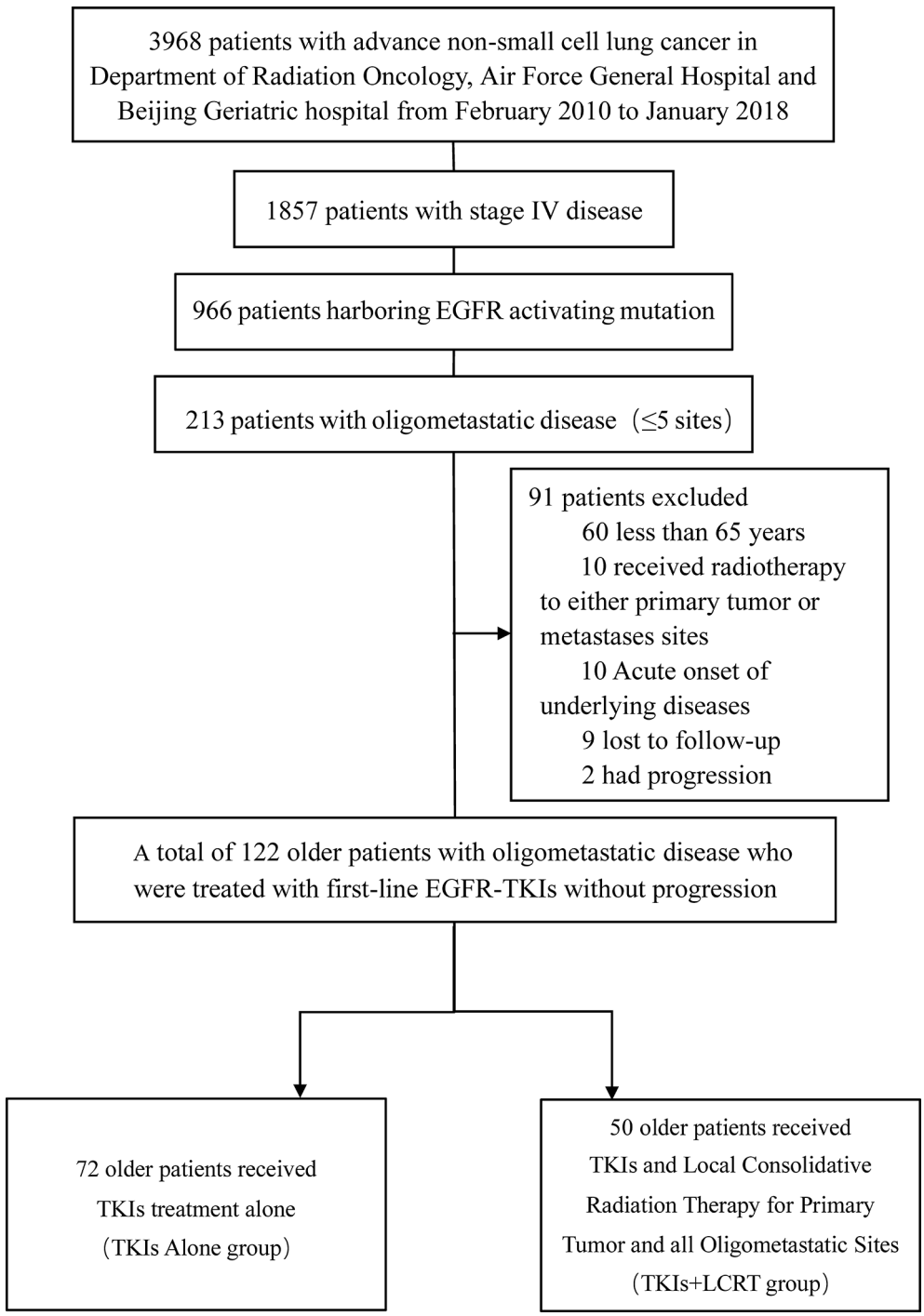

FIGURE 1 | Flowchart showing selection process for patients. EGFR, Epidermal Growth Factor Receptor; TKIs, Tyrosine Kinase Inhibitors; LCRT, Local Consolidative Radiation Therapy.

Toxicity

For non-hematological adverse effects during EGFR-TKIs therapy, the most common events were skin rash, diarrhea, fatigue, nausea, vomiting, increased ALT levels, and pneumonitis. Most of the patients presented with grade 1–2 toxicities. Incidences of >grade 3 skin rash was 4.9% (n = 6). For radiotherapy-related acute side effects, most of the patients exhibited grade 1–2 toxicity, with very few patients exhibiting grade 3 toxicities. The incidence of grade 1–2

TABLE 1 | Baseline patient characteristics.

Characteristics	N	No. of Patients (%)
Gender		
Male	41	33.6%
Female	81	66.4%
Age		
65–75	74	60.7%
>75	48	39.3%
EOCG performance status		
0–1	64	52.5%
2	58	47.5%
Histology		
Adenocarcinoma	102	83.6%
Adenosquamous	9	7.4%
Squamous cell	6	4.9%
NSCLC	5	4.1%
EGFR mutation		
Exon 19 deletion	55	45.1%
Exon 21 L858R	67	54.9%
Smoking status		
Nonsmoker	50	41.0%
Present or former smoker	72	59.0%
Smoking Index		
<600	71	58.2%
≥600	51	41.8%
Comorbidity		
No	24	19.7%
Yes	98	80.3%
Comorbidity type		
Hypertension	78	63.9%
Diabetes	48	39.3%
COPD	35	28.7%
CHD	30	24.6%
Atrial Fibrillation	21	17.2%
N stage		
N0–1	57	46.7%
N2–3	65	53.3%
T stage		
T1–2	63	51.6%
T3–4	59	48.4%
Second-line treatment		
No	58	47.5%
Yes	64	52.5%
No. of metastases		
1–2	68	55.7%
3–5	54	44.3%
Metastasis location		
Brain	62	50.8%
Bone	59	48.3%
Lung	42	34.4%
Adrenal	35	28.7%
Liver	9	7.40%
Non-region lymph nodes	8	6.60%
PET-CT		
No	37	30.3%
Yes	85	69.7%
LCRT for both PT and OS		
No	72	59.0%
Yes	50	41.0%

NSCLC, non-small cell lung cancer; Smoking Index, number of cigarettes smoked per day × years of smoking; ECOG PS, Eastern Cooperative Oncology Group Performance Status; COPD, Chronic Obstructive Pulmonary Disease; CHD, Coronary Heart Disease; CNS, Central Nervous System; BED, Biological Effective Dose; PET-CT, Positron Emission Tomography Computed Tomography; PT, Primary Tumor; OS, Oligometastatic Sites; LCRT, Local Consolidative Radiation Therapy; EGFR, Epidermal Growth Factor Receptor.

TABLE 2 | Patients characteristics of tkis alone group and LCRT + TKIs group.

Characteristics	TKIs Alone (n = 72) No. (%)	LCRT + TKIs (n = 50) No. (%)
Gender		
Male	24 (33.3%)	17 (34.0%)
Female	48 (66.7%)	33 (66.0%)
Age		
65–75	47 (65.3%)	27 (54.0%)
>75	25 (34.7%)	23 (46.0%)
EOCG performance status		
0–1	39 (54.2%)	25 (50.0%)
2	33 (45.8%)	25 (50.0%)
Histology		
Adenocarcinoma	72 (80.6%)	44 (88.0%)
Nonadenocarcinoma	14 (19.4%)	6 (12.0%)
EGFR mutation		
Exon 19 deletion	32 (44.4%)	23 (46.0%)
Exon 21 L858R	40 (55.6%)	27 (54.0%)
Smoking status		
Nonsmoker	34 (47.2%)	16 (32.0%)
Present or former smoker	38 (52.8%)	34 (68.0%)
Smoking Index		
<600	47 (65.3%)	24 (48.0%)
≥600	25 (34.7%)	26 (52.0%)
Comorbidity		
No	31 (43.1%)	19 (38.0%)
Yes	41 (56.9%)	31 (62.0%)
N stage		
N0–1	38 (52.8%)	19 (38.0%)
N2–3	34 (47.2%)	31 (62.0%)
T stage		
T1–2	41 (56.9%)	22 (44.0%)
T3–4	31 (43.1%)	28 (56.0%)
Second-line treatment		
No	34 (47.2%)	24 (48.0%)
Yes	38 (52.8%)	26 (52.0%)
No. of metastases		
1–2	38 (52.8%)	30 (60.0%)
3–5	34 (47.2%)	20 (40.0%)
Metastasis location		
Brain		
No	36 (50%)	24 (48.0%)
Yes	36 (50%)	26 (52.0%)
Bone		
No	32 (44.4%)	31 (62.0%)
Yes	40 (55.6%)	19 (38.0%)
Lung		
No	44 (61.1%)	36 (72.0%)
Yes	28 (38.9%)	14 (28.0%)
Adrenal		
No	49 (68.1%)	38 (76.0%)
Yes	23 (31.9%)	12 (24.0%)
Liver		
No	66 (91.7%)	47 (94.0%)
Yes	6 (8.3%)	3 (6.0%)
Non-region lymph nodes		
No	66 (91.7%)	48 (96.0%)
Yes	6 (8.3%)	2 (4.0%)
PET-CT		
No	25 (34.7%)	12 (24.0%)
Yes	47 (65.3%)	38 (76.0%)

NSCLC, non-small cell lung cancer; Smoking Index, number of cigarettes smoked per day × years of smoking; ECOG PS, Eastern Cooperative Oncology Group Performance Status; TKIs, Tyrosine Kinase Inhibitors; EGFR, Epidermal Growth Factor Receptor; PET-CT, Positron Emission Tomography Computed Tomography; LCRT, Local Consolidative Radiation Therapy.

radiation pneumonitis in the TKIs + LCRT group was 26% (n = 13), while grade 3 pneumonia (n = 3, 6%) was only found in COPD patients. Two patients treated with head gamma knife (22 Gy/1 f) were subjected to asymptomatic radiation necrosis.

DISCUSSION

Clinical incidence for metastatic NSCLC among NSCLC patients is approximately 50%. Metastatic NSCLC is more common in

TABLE 3 | Local radiation therapy for primary tumor and oligometastatic sites mode.

Sites of Disease/Treatment Regimen	Patients	No. of Patients (%)
Primary tumor and region lymph nodes	50	
Dt 70 Gy/10 f	10	20.0%
Dt 70 Gy/15 f	22	44.0%
Dt 70 Gy/30–35 f	18	36.0%
Metastasis location		
Brain	26	
Dt 50% Isodose line 22 Gy/1 f*	4	15.4%
Dt 60 Gy/20 f	9	34.6%
Dt 50 Gy/20 f + WBRT	13	50.0%
Bone	19	
Dt 30 Gy/10 f	10	52.6.%
Dt 40 Gy/20 f	9	47.4%
Lung	14	
Dt 70% Isodose line70–78 Gy/10–14 f#	8	57.2%
Dt 70 Gy/15 f	1	7.1%
Dt 60 Gy/15 f	2	14.3%
Dt 60 Gy/20 f	3	21.4%
Adrenal	12	
Dt 70 Gy/10–15 f	4	33.3%
Dt 60 Gy/20 f	7	58.3%
Dt 45 Gy/15 f	1	8.40%
Liver	3	
Dt 65 Gy/20 f	1	33.3%
Dt 60 Gy/15 f	2	66.7%
Non-region lymph nodes	2	
Dt 70 Gy/30–35 f	1	50.0%
Dt 60 Gy/30 f	1	50.0%

Dt, Dose of Target; WBRT, Whole Brain Radiation Therapy.
**The Head Gamma Knife.*
#*The Body Gamma Knife.*

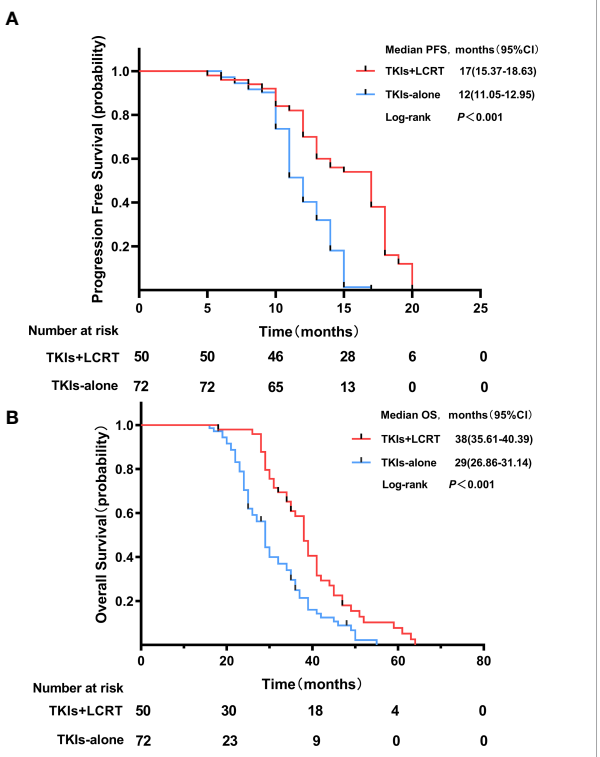

FIGURE 2 | Progression free survival **(A)** and overall survival **(B)** of patients treated with TKIs + LCRT or TKIs alone for oligometastatic NSCLC harboring EGFR activating mutations.

older patients than in younger patients (12). This is because, in elderly patients, the disease is at a more advanced stage at the time of diagnosis. In this study, the median age for the 1,857 metastatic NSCLC patients at the time of diagnosis was 63.5 years. Approximately 20–50% of advanced NSCLC patients were oligometastatic NSCLC (13). There is no universally accepted definition of oligometastases. However, recent studies have described oligometastases as 3–5 metastases (8–10). PET-CT has an excellent sensitivity in detecting distant and occult metastases. Detection of oligometastatic disease can be more accurate when combined with brain MRI (14, 15). Approximately, 70% of patients (n = 85) received PET-CT examinations. This enabled precise determination of clinical stages of oligometastatic NSCLC. Few clinical trials have included elderly patients with advanced tumors. Therefore, it can be difficult to choose appropriate therapeutic approaches for elderly patients with advanced tumors, leading to insufficient and inappropriate treatment (16). Apart from surgery and chemotherapy, radiotherapy is one of the most important methods for cancer treatment. Very elderly patients have been shown to tolerate radiotherapy, both in definitive and palliative settings (17, 18). Schmid et al. (19) reported that adoption of novel treatment approaches for the elderly population is lagging. This study was retrospective in nature, therefore, based on clinical records, we concluded that elderly patients treated with TKIs alone at the time did not receive radiation therapy because of: fear and anxiety regarding radiotherapy; lack of radiotherapy information resources; concerns regarding acute and long-term side effects; lack of symptoms of pain and a low willingness for radiation treatment.

NSCLC patients with EGFR activating mutations and who are treated with TKIs exhibit longer PFS and higher response rates, compared to those with EGFR mutation-negative tumors treated with conventional chemotherapies (20, 21). Elderly patients and patients with poor PS have been shown to have similar clinical benefits as younger and fitter patients, therefore, they should be offered targeted treatments in case of oncogenic driver alterations (22). However, within a year, majority of the patients eventually progress, primarily due to acquired resistance in the EGFR kinase domain. Elderly patients treated with TKIs and LCRT exhibited longer mPFS and mOS, relative to those treated with TKIs alone (17 vs.12 months, p <0.001; 38 vs. 29 months, p <0.001, respectively). Multivariate analysis showed that LCRT constitutes one of the independent favorable prognostic factors for PFS (HR = 0.32, 95%CI: 0.20–0.51, p <0.001), and OS (HR = 0.41, 95%CI: 0.27–0.63, p <0.001). These results are in accordance with recent studies, which reported that among 231 patients with EGFR mutant stage IV NSCLC, mPFS and mOS were significantly longer for the local consolidation therapy (surgery or radiotherapy) plus TKIs group than the TKIs monotherapy group (23).

Traditionally, local radiotherapy is considered to be a palliative care for elderly patients with advanced metastatic

TABLE 4 | Factors associated with progress free survival in univariate and multivariate analyses.

Variable	Univariable			Multivariable		
	HR	95%CI	*P*	HR	95%CI	*P*
Gender						
Male vs. Female	0.97	0.67–1.41	0.871			
Age						
65–75 vs. >75	0.78	0.55–1.14	0.792			
EOCG performance status						
0–1 vs. 2	0.68	0.47–0.97	***0.035***	0.67	0.46–0.96	***0.027***
Histology						
Adenocarcinoma vs. Nonadenocarcinoma	0.93	0.57–1.49	0.750			
EGFR mutation						
Exon 19 deletion vs. Exon 21 L858R	1.05	0.74–1.51	0.776			
Smoking status						
Present or former smoker vs. Nonsmoker	1.09	0.75–1.55	0.682			
Smoking Index						
≥600 vs.<600	1.02	0.71–1.46	0.924			
Comorbidity						
Yes vs. No	1.16	0.81–1.67	0.413			
T stage						
T1–2 vs. T3–4	0.84	0.59–1.21	0.348			
N stage						
N0–1 vs. N2–3	0.97	0.68–1.40	0.900			
CNS metastases						
Yes vs. No	1.10	0.77–1.56	0.623			
No. of metastases						
1–2 vs. 3–5	0.49	0.33–0.71	***<0.001***	0.57	0.39–0.83	***0.004***
LCRT for both PT and OS						
Yes vs. No	0.30	0.19–0.48	***<0.001***	0.32	0.20–0.51	***<0.001***

NSCLC, non-small cell lung cancer; Smoking Index, number of cigarettes smoked per day × years of smoking; ECOG PS, Eastern Cooperative Oncology Group Performance Status; CNS, Central Nervous System; EGFR, Epidermal Growth Factor Receptor; PT, Primary Tumor; OS, Oligometastatic Sites; LCRT, Local Consolidative Radiation Therapy.
The bold values indicate significant P values.

tumors. However, treatment goals and strategies have changed from palliative care to improvement of PFS and OS. This is attributed to the introduction of the concept of oligometastatic disease. A retrospective study found that in EGFR mutant oligometastatic NSCLC patients, administration of EGFR-TKIs with local consolidation radiation therapy resulted in significantly longer mPFS, compared to TKIs monotherapy (36 vs.14 months, p = 0.0024) (24). A phase 2 randomized trial involving 29 patients reported significant benefits in PFS with addition of consolidative radiotherapy to maintenance chemotherapy for patients with oligometastatic NSCLC (9.7 vs. 3.5 months) (25). Studies have reported that patients with EGFR-positive NSCLC are more likely to develop brain metastases (26, 27). In this study, 50.8% of the patients (n = 62) had brain metastases. Survival analysis did not reveal statistically significant differences in survival probabilities between patients with or without brain metastases (p = 0.342). However, in the subgroup with brain metastases, OS was significantly improved by LCRT for brain metastases (38 vs. 25 months, HR = 0.38, 95% CI: 0.21–0.69, p = 0.001).

Significant comorbidities can limit life expectancy, decreasing potential survival benefits from cancer treatment (28, 29). In this research, 80.3% of the elderly patients (n = 98) had underlying diseases. Only three patients died of acute myocardial infarction, with no tumor progression. Survival analysis showed that there was no evident effect of comorbidities on prognostic outcomes (HR = 1.23, 95%CI: 0.83–1.82, p = 0.300). This may be relevant in relation to how underlying diseases are controlled. In oligometastatic NSCLC, a good quality of life, a small number of metastatic sites, a small primary lung mass size and local consolidation therapy are favorable prognostic factors (30, 31). In this study, good ECOG PS (HR = 0.54, 95%CI: 0.34–0.85, p = 0.007) was established to be an independent favorable prognostic factor for OS and PFS, consistent with a previous study by Sheu et al. (32). A good physical score indicated that the quality of life was satisfactory, nutritional intake was sufficient, and body immune function played a partial role. This ensured treatment continuity as the disease progressed. Moreover, we found that one to two metastases (HR = 0.57, 95%CI: 0.39–0.83, p = 0.004) were independent prognostic factors for better PFS. This implies that patients with a small number of metastatic sites have a relatively low probability for widespread metastatic disease from localized diffusion. Survival analysis revealed that LCRT to primary tumor and all oligometastatic sites is an independent favorable prognostic factor for OS and PFS, in tandem with findings from previous studies (8, 33). A study reported a high local control rate in hypofractionated radiotherapy (BED_{10} ≥100 Gy) lesions (34). In this study, 64% (n = 32) of the patients in the TKIS + LCRT group were subjected to hypofractionated radiotherapy (BED_{10} ≥100 Gy) for primary tumor. In subgroup survival analysis (TKIs + LCRT group), patients who received BED_{10} ≥100 Gy for primary tumor exhibited

TABLE 5 | Factors associated with overall survival in univariate and multivariate analyses.

Variable	Univariable			Multivariable		
	HR	95%CI	*P*	HR	95%CI	*P*
Gender						
Male vs. Female	0.90	0.61–1.34	0.612			
Age						
65–75 vs. >75	0.79	0.53–1.16	0.224			
EOCG performance status						
0–1 vs. 2	0.46	0.33–0.72	***<0.001***	0.54	0.34–0.85	***0.007***
Histology						
Adenocarcinoma vs. Nonadenocarcinoma	0.88	0.52–1.48	0.620			
EGFR mutation						
Exon 19 deletion vs. Exon 21 L858R	0.99	0.68–1.46	0.999			
Smoking status						
Present or former smoker vs. Nonsmoker	1.38	0.93–2.02	0.115			
Smoking Index						
≥600 vs.<600	1.06	0.72–1.55	0.777			
Second-line treatment						
Yes vs. No	0.67	0.45–0.99	***0.045***	0.95	0.63–1.46	0.833
Comorbidity						
Yes vs. No	1.23	0.83–1.82	0.300			
T stage						
T1–2 vs. T3–4	0.60	0.41–0.87	***0.008***	0.56	0.37–0.85	***0.007***
N stage						
N0–1 vs. N2–3	0.80	0.54–1.18	0.258			
CNS metastases						
Yes vs. No	1.20	0.82–1.76	0.342			
No. of metastases						
1–2 vs. 3–5	0.62	0.42–0.92	***0.016***	0.86	0.57–1.29	0.458
LCRT for both PT and OS						
Yes vs. No	0.48	0.32–0.72	***<0.001***	0.41	0.27–0.63	***<0.001***

NSCLC, non-small cell lung cancer; Smoking Index, number of cigarettes smoked per day × years of smoking; ECOG PS, Eastern Cooperative Oncology Group Performance Status; CNS, Central Nervous System; EGFR, Epidermal Growth Factor Receptor; PT, Primary Tumor; OS, Oligometastatic Sites; LCRT, Local Consolidative Radiation Therapy.
The bold values indicate significant P values.

significantly better survival benefits in OS (39 vs. 31 months, p = 0.004), and PFS (17 vs. 13 months, p = 0.031). This shows that a high local control rate for primary tumor can translate into a survival benefit for elderly patients with oligometastases. Herrera et al. reported that by performing stereotactic body radiation therapy (SBRT) to the local tumor, the body can activate systemic anti-tumor immune effects, enhancing cellular immunity (35).

SRS (Gamma Knife, CyberKnife, and standard linear accelerator) for the intracranial oligometastatic disease has shown promising results. SBRT, a non-surgical alternative for oligometastatic disease, is associated with low reported toxicity and impact on the quality of life. Compared to conventional radiotherapy, SRS and SBRT have numerous advantages that increase the probability of local control while maintaining the risk of normal tissue toxicity at acceptable levels (36). Cuccia et al. (37) reported that 61 elderly patients (median age 82 years) with 90 oligometastases were treated with SBRT with a median BED10 100 Gy (range, 48–180 Gy). Local control rates at 1- and 2-years were 98.8 and 88.2%, respectively, and there were no grade 2 or higher adverse events. In this study, most patients received SBRT, stereotactic radiosurgery (SRS), or hypofractionated radiotherapy, while some patients received conventional fractionated radiotherapy. When the primary tumor was close to the esophagus or in combination with severe chronic obstructive pulmonary disease, the primary tumor was treated with conventional fractionated radiotherapy (70 Gy in 30 or 35 fractions). Most of the patients experienced grade 1–2 radiation-related esophagitis, while none of the patients developed grade 3–4 esophagitis. Vertebral metastases were treated with 30 Gy in 10 fractions or 40 Gy in 20 fractions, since the planning target volume (PTV) encompasses the entire vertebra. Meanwhile, metastasis of superficial lymph nodes was treated with conventional fractionated radiotherapy to reduce incidences of severe radiation dermatitis.

In the FLAURA study, osimertinib showed superior clinical outcomes, compared to standard EGFR-TKIs in EGFR-mutated NSCLC (38). Osimertinib became a preferred first-line treatment modality in previously untreated advanced NSCLC harboring EGFR activating mutations. Zeng et al. (39) reported that 108 patients treated with osimertinib later developed oligometastatic disease. They also reported that for 14 patients who received local consolidation therapy, mPFS was significantly longer than for the osimertinib alone group (NR vs. 12.8 months, p = 0.01), and were independently associated with prolonged PFS (HR = 0.29, 95%CI: 0.12–0.68, p = 0.004). In this study, most of the patients (77.9%) received gefitinib as first-line treatment, while only 7 patients received osimertinib as subsequent

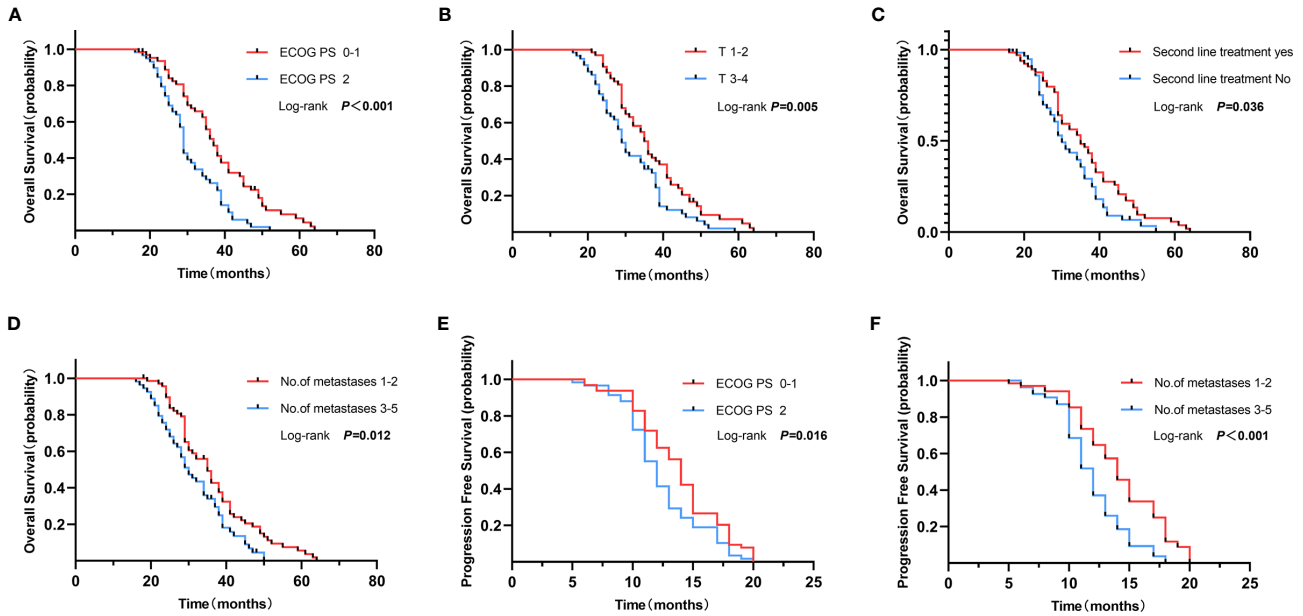

FIGURE 3 | Overall survival of ECOG PS 0–1 vs. 2 **(A)**, T_{1-2} vs. T_{3-4} **(B)**, Second line treatment yes vs. no **(C)** and no. of metastases 1–2 vs. 3–5 **(D)**. Progression free survival of ECOG PS 0–1 vs. 2 **(E)**, and no. of metastases 1–2 vs. 3–5 **(F)**.

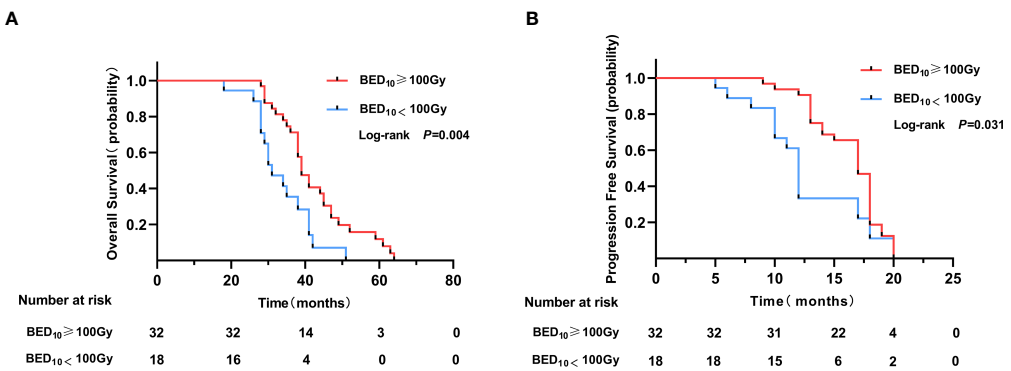

FIGURE 4 | Overall survival and progression free survival of primary tumors treated with BED_{10} ≥100 Gy **(A)** or BED_{10} <100 Gy **(B)** in the TKIs + LCRT group.

treatment. This may be attributed to clinical guidelines, heavy cost of treatment, individual treatment strategies, and family treatment wishes. Approximately 50% of patients in both groups did not receive any second line treatment, including next-generation TKIs. This was attributed to reluctance to accept intensive chemotherapy and cost implications. For instance, before November 2018, the cost of osimertinib was mostly met by households through out-of-pocket expenditure. However, with the cost of osimertinib being covered by health insurance, more EGFR-mutated NSCLC patients received osimertinib as the first-line treatment. In this study, after initial first-line TKIs treatment, 72 patients in the TKIs alone group were not subjected to any radiotherapy in case there was no progression. Fourteen (19.4%) patients with symptomatic brain metastases received palliative radiotherapy (WBRT 40 Gy in 20 fractions or WBRT 30 Gy in 10 fractions). Twelve (16.7%) patients received local radiotherapy for palliation of painful bone metastases (30 Gy in 10 fractions or 40 Gy in 20 fractions).

This study had several limitations. i. The sample size was small, making it difficult to detect statistical differences in some subgroups. ii. It is a retrospective study, and the patients were from two centers. Patients from the Beijing Geriatric Hospital were older than those from the Air Force General Hospital (median age 73 vs. 68 years). Moreover, patients from the Beijing Geriatric Hospital had more comorbidities, compared to those from the Air Force General Hospital. Therefore, the

center spends more time dealing with comorbidities before performing LCRT. Segmentation plans and doses of LCRT were also different in the two centers. Aggressive treatment approaches were performed at the Air Force General Hospital. iii. Elderly patients were not evaluated by comprehensive geriatric assessment (CGA) and did not further clarify which type of oligometastatic NSCLC benefited more from LCRT.

CONCLUSION

LCRT for primary tumor and all oligometastatic sites in elderly patients with oligometastatic NSCLC harboring EGFR activating mutations during first-line EGFR-TKIs treatment may improve their survival outcomes with tolerable toxicity. This is a potential treatment approach for elderly patients with oligometastatic disease.

DATA AVAILABILITY STATEMENT

The datasets used and/or analyzed during the current study are available from the corresponding author on reasonable request. Requests to access these datasets should be directed to: xiaodaigua903@163.com.

ETHICS STATEMENT

The studies involving human participants were reviewed and approved by The Ethics Committee of Beijing Geriatric Hospital.

AUTHOR CONTRIBUTIONS

Conception and design: YW, and XH. Administrative support: JZ. Provision of study materials or patients: CL and YW. Data collection and assembly: XH, HL, and HP. Data analysis and interpretation: XH, HL, and XK. Manuscript writing: All authors. All authors contributed to the article and approved the submitted version.

FUNDING

This work was supported by Beijing Geriatric Hospital Special Fund for Geriatrics Research (2020bjlnyy-q-1).

REFERENCES

1. Bunn PA Jr, Dimou A. Systemic Therapy for Elderly Patients With Advanced Non-Small-Cell Lung Cancers. *J Clin Oncol* (2018) 36(25):2571–4. doi: 10.1200/JCO.2018.79.2457
2. Mok TS, Wu YL, Thongprasert S, Yang CH, Chu DT, Saijo N, et al. Gefitinib or Carboplatin-Paclitaxel in Pulmonary Adenocarcinoma. *N Engl J Med* (2009) 361(10):947–57. doi: 10.1056/NEJMoa0810699
3. Rosell R, Carcereny E, Gervais R, Vergnenegre A, Massuti B, Felip E, et al. Erlotinib Versus Standard Chemotherapy as First-Line Treatment for European Patients With Advanced EGFR Mutation-Positive Non-Small-Cell Lung Cancer (EURTAC): A Multicenter, Open-Label, Randomised Phase 3 Trial. *Lancet Oncol* (2012) 13(3):239–46. doi: 10.1016/S1470-2045(11)70393-X
4. Wu YL, Lu S, Lu Y, Zhou J, Shi YK, Sriuranpong V, et al. Results of PROFILE 1029, a Phase III Comparison of First Line Crizotinib Versus Chemotherapy in East Asian Patients With ALK-Positive Advanced Non-Small Cell Lung Cancer. *J Thorac Oncol* (2018) 13(10):1539–48. doi: 10.1016/j.jtho.2018.06.012
5. Wu YL, Cheng Y, Zhou X, Lee KH, Nakagawa K, Niho S, et al. Dacomitinib Versus Gefitinib as First-Line Treatment for Patients With EGFR-Mutation-Positive Non-Small-Cell Lung Cancer (ARCHER 1050): A Randomised, Open-Label, Phase 3 Trial. *Lancet Oncol* (2017) 18(11):1454–66. doi: 10.1016/S1470-2045(17)30608-3
6. Pao W, Miller VA, Politi KA, Riely GJ, Somwar R, Zakowski MF, et al. Acquired Resistance of Lung Adenocarcinomas to Gefitinib or Erlotinib Is Associated With a Second Mutation in the EGFR Kinase Domain. *PLoS Med* (2005) 2(3):e73. doi: 10.1371/journal.pmed.0020073
7. Cortot AB, Jänne PA. Molecular Mechanisms of Resistance in Epidermal Growth Factor Receptor-Mutant Lung Adenocarcinomas. *Eur Respir Rev* (2014) 23(133):356–66. doi: 10.1183/09059180.00004614
8. Gomez DR, Blumenschein GRJr, Lee JJ, Hernandez M, Ye R, Camidge DR, et al. Local Consolidative Therapy Versus Maintenance Therapy or Observation for Patients With Oligometastatic Non-Small-Cell Lung Cancer Without Progression After First-Line Systemic Therapy: A Multicenter, Randomized, Controlled, Phase 2 Study. *Lancet Oncol* (2016) 17(12):1672–82. doi: 10.1016/S1470-2045(16)30532-0
9. Iyengar P, Wardak Z, Gerber DE, Tumati V, Ahn C, Hughes RS, et al. Consolidative Radiotherapy for Limited Metastatic Non-Small-Cell Lung Cancer: A Phase 2 Randomized Clinical Trial. *JAMA Oncol* (2018) 4(1): e173501. doi: 10.1001/jamaoncol.2017.3501
10. Palma DA, Olson R, Harrow S, Gaede S, Louie AV, Haasbeek C, et al. Stereotactic Ablative Radiotherapy Versus Standard of Care Palliative Treatment in Patients With Oligometastatic Cancers (SABR-COMET): A Randomized, Phase 2, Open-Label Trial. *Lancet* (2019) 393(10185):2051–8. doi: 10.1016/S0140-6736(18)32487-5
11. Xu Q, Zhou F, Liu H, Jiang T, Li X, Xu Y, et al. Consolidative Local Ablative Therapy Improves the Survival of Patients With Synchronous Oligometastatic NSCLC Harboring EGFR Activating Mutation Treated With First-Line EGFR-TKIs. *J Thorac Oncol* (2018) 13(9):1383–92. doi: 10.1016/j.jtho.2018.05.019
12. Ouyang WW, Su SF, Ma Z, Hu YX, Lu B, Li QS, et al. Prognosis of Non-Small Cell Lung Cancer Patients With Bone Oligometastases Treated Concurrently With Thoracic Three-Dimensional Radiotherapy and Chemotherapy. *Radiat Oncol* (2014) 9:147. doi: 10.1186/1748-717X-9-147
13. Bergsma DP, Salama JK, Singh DP, Chmura SJ, Milano MT. Radiotherapy for Oligometastatic Lung Cancer. *Front Oncol* (2017) 7:210. doi: 10.3389/fonc.2017.00210
14. Juan O, Popat S. Ablative Therapy for Oligometastatic Non-Small Cell Lung Cancer. *Clin Lung Cancer* (2017) 18(6):595–606. doi: 10.1016/j.cllc.2017.03.002
15. Lardinois D, Weder W, Hany TF, Kamel EM, Korom S, Seifert B, et al. Staging of Non-Small-Cell Lung Cancer With Integrated Positron-Emission Tomography and Computed Tomography. *N Engl J Med* (2003) 348 (25):2500–7. doi: 10.1056/NEJMoa022136
16. Hutchins LF, Unger JM, Crowley JJ, Coltman CAJr, Albain KS. Underrepresentation of Patients 65 Years of Age or Older in Cancer-Treatment Trials. *N Engl J Med* (1999) 341(27):2061–7. doi: 10.1056/NEJM199912303412706
17. Watanabe K, Katsui K, Sugiyama S, Yoshio K, Kuroda M, Hiraki T, et al. Lung Stereotactic Body Radiation Therapy for Elderly Patients Aged ≥ 80 Years With Pathologically Proven Early-Stage Non-Small Cell Lung Cancer: A Retrospective Cohort Study. *Radiat Oncol* (2021) 16(1):39. doi: 10.1186/s13014-021-01769-7
18. Nieder C, Kämpe TA. Patient-Reported Symptoms and Performance Status Before Palliative Radiotherapy in Geriatric Cancer Patients (Octogenarians).

Tech Innov Patient Support Radiat Oncol (2017) 1:8–12. doi: 10.1016/j.tipsro.2016.12.002
19. Schmid S, Suipyte J, Herrmann C, Mousavi M, Hitz F, Früh M. Does Progress Achieved in the Treatment of Patients With Metastatic Non-Small-Cell Lung Cancer Reach the Elderly Population? A Cohort Study From a Cancer Centre From Eastern Switzerland. *Eur J Cancer Care (Engl)* (2020) 29(2):e13206. doi: 10.1111/ecc.13206
20. Planchard D, Popat S, Kerr K, Novello S, Smit EF, Faivre-Finn C, et al. Metastatic Non-Small Cell Lung Cancer: ESMO Clinical Practice Guidelines for Diagnosis, Treatment and Follow-Up. *Ann Oncol* (2018) 29(Suppl 4): iv192–237. doi: 10.1093/annonc/mdy275
21. Rosell R, Carcereny E, Gervais R, Vergnenegre A, Massuti B, Felip E, et al. Erlotinib Versus Standard Chemotherapy as First-Line Treatment for European Patients With Advanced EGFR Mutation-Positive Non-Small-Cell Lung Cancer (EURTAC): A Multicentre, Open-Label, Randomized Phase 3 Trial. *Lancet Oncol* (2012) 13(3):239–46. doi: 10.1016/S1470-2045(11)70393-X
22. Wu YL, Zhou C, Hu CP, Feng J, Lu S, Huang Y, et al. Afatinib Versus Cisplatin Plus Gemcitabine for First-Line Treatment of Asian Patients With Advanced Non-Small-Cell Lung Cancer Harboring EGFR Mutations (LUX-Lung 6): An Open-Label, Randomized Phase 3 Trial. *Lancet Oncol* (2014) 15(2):213–22. doi: 10.1016/S1470-2045(13)70604-1
23. Hu F, Xu J, Zhang B, Li C, Nie W, Gu P, et al. Efficacy of Local Consolidative Therapy for Oligometastatic Lung Adenocarcinoma Patients Harboring Epidermal Growth Factor Receptor Mutations. *Clin Lung Cancer* (2019) 20 (1):e81–90. doi: 10.1016/j.cllc.2018.09.010
24. Elamin YY, Gomez DR, Antonoff MB, Robichaux JP, Tran H, Shorter MK, et al. Local Consolidation Therapy (LCT) After First Line Tyrosine Kinase Inhibitor (TKIS) for Patients With EGFR Mutant Metastatic Non-Small-Cell Lung Cancer (NSCLC). *Clin Lung Cancer* (2019) 20(1):43–7. doi: 10.1016/j.cllc.2018.09.015
25. Chan OSH, Lam KC, Li JYC, Choi FPT, Wong CYH, Chang ATY, et al. ATOM: A Phase II Study to Assess Efficacy of Preemptive Local Ablative Therapy to Residual Oligometastases of NSCLC After EGFR TKIS. *Lung Cancer* (2020) 142:41–6. doi: 10.1016/j.lungcan.2020.02.002
26. Fujita Y, Kinoshita M, Ozaki T, Takano K, Kunimasa K, Kimura M, et al. The Impact of EGFR Mutation Status and Single Brain Metastasis on the Survival of Non-Small-Cell Lung Cancer Patients With Brain Metastases. *Neurooncol Adv* (2020) 2(1):vdaa064. doi: 10.1093/noajnl/vdaa064
27. Baek MY, Ahn HK, Park KR, Park HS, Kang SM, Park I, et al. Epidermal Growth Factor Receptor Mutation and Pattern of Brain Metastasis in Patients With Non-Small Cell Lung Cancer. *Korean J Intern Med* (2018) 33(1):168–75. doi: 10.3904/kjim.2015.158
28. Read WL, Tierney RM, Page NC, Costas I, Govindan R, Spitznagel EL, et al. Differential Prognostic Impact of Comorbidity. *J Clin Oncol* (2004) 22 (15):3099–103. doi: 10.1200/JCO.2004.08.040
29. Piccirillo JF, Tierney RM, Costas I, Grove L, Spitznagel ELJr. Prognostic Importance of Comorbidity in a Hospital-Based Cancer Registry. *JAMA* (2004) 291(20):2441–7. doi: 10.1001/jama.291.20.2441
30. Guo T, Ni J, Yang X, Li Y, Li Y, Zou L, et al. Pattern of Recurrence Analysis in Metastatic EGFR-Mutant NSCLC Treated With Osimertinib: Implications for Consolidative Stereotactic Body Radiation Therapy. *Int J Radiat Oncol Biol Phys* (2020) 107(1):62–71. doi: 10.1016/j.ijrobp.2019.12.042
31. Zhang JT, Liu SY, Yan HH, Wu YL, Nie Q, Zhong WZ. Recursive Partitioning Analysis of Patients With Oligometastatic Non-Small Cell Lung Cancer: A Retrospective Study. *BMC Cancer* (2019) 19(1):1051. doi: 10.1186/s12885-019-6216-x
32. Sheu T, Heymach JV, Swisher SG, Rao G, Weinberg JS, Mehran R, et al. Propensity Score-Matched Analysis of Comprehensive Local Therapy for Oligometastatic Non-Small Cell Lung Cancer That did Not Progress After Front-Line Chemotherapy. *Int J Radiat Oncol Biol Phys* (2014) 90(4):850–7. doi: 10.1016/j.ijrobp.2014.07.012
33. Gomez DR, Tang C, Zhang J, Blumenschein GR Jr, Hernandez M, Lee JJ, et al. Local Consolidative Therapy Vs. Maintenance Therapy or Observation for Patients With Oligometastatic Non-Small-Cell Lung Cancer: Long-Term Results of a Multi-Institutional, Phase II, Randomized Study. *J Clin Oncol* (2019) 37(18):1558–65. doi: 10.1200/JCO.19.00201
34. Arcidiacono F, Aristei C, Marchionni A, Italiani M, Fulcheri CPL, Saldi S, et al. Stereotactic Body Radiotherapy for Adrenal Oligometastasis in Lung Cancer Patients. *Br J Radiol* (2020) 93(1115):20200645. doi: 10.1259/bjr.20200645
35. Herrera FG, Bourhis J, Coukos G. Radiotherapy Combination Opportunities Leveraging Immunity for the Next Oncology Practice. *CA Cancer J Clin* (2017) 67(1):65–85. doi: 10.3322/caac.21358
36. Chen H, Louie AV, Higginson DS, Palma DA, Colaco R, Sahgal A. Stereotactic Radiosurgery and Stereotactic Body Radiotherapy in the Management of Oligometastatic Disease. *Clin Oncol (R Coll Radiol)* (2020) 32(11):713–27. doi: 10.1016/j.clon.2020.06.018
37. Cuccia F, Mazzola R, Pastorello E, Figlia V, Giaj-Levra N, Nicosia L, et al. SBRT for Elderly Oligometastatic Patients as a Feasible, Safe and Effective Treatment Opportunity. *Clin Exp Metastasis* (2021) 38(5):475–81. doi: 10.1007/s10585-021-10122-x
38. Soria JC, Ohe Y, Vansteenkiste J, Reungwetwattana T, Chewaskulyong B, Lee KH, et al. Osimertinib in Untreated EGFR-Mutated Advanced Non-Small-Cell Lung Cancer. *N Engl J Med* (2018) 378(2):113–25. doi: 10.1056/NEJMoa1713137
39. Zeng Y, Ni J, Yu F, Zhou Y, Zhao Y, Li S, et al. The Value of Local Consolidative Therapy in Osimertinib-Treated Non-Small Cell Lung Cancer With Oligo-Residual Disease. *Radiat Oncol* (2020) 15(1):207. doi: 10.1186/s13014-020-01651-y

Conflict of Interest: The authors declare that the research was conducted in the absence of any commercial or financial relationships that could be construed as a potential conflict of interest.

frontiers in Oncology

SYSTEMATIC REVIEW
published: 03 February 2022
doi: 10.3389/fonc.2022.796657

Efficacy and Safety of ^{225}Ac-PSMA-617-Targeted Alpha Therapy in Metastatic Castration-Resistant Prostate Cancer: A Systematic Review and Meta-Analysis

Jiao Ma[1], *Lanying Li*[1], *Taiping Liao*[1], *Weidong Gong*[1] *and Chunyin Zhang*[1,2,3]*

[1] Department of Nuclear Medicine, The Affiliated Hospital of Southwest Medical University, Luzhou, China, [2] Nuclear Medicine and Molecular Imaging Key Laboratory of Sichuan Province, Luzhou, China, [3] Academician (expert) Workstation of Sichuan Province, Luzhou, China

OPEN ACCESS

Edited by:
Milly Buwenge,
University of Bologna, Italy

Reviewed by:
Ekaterina Laukhtina,
I.M. Sechenov First Moscow State Medical University, Russia
Felice Crocetto,
Federico II University Hospital, Italy

***Correspondence:**
Chunyin Zhang
zhangchunyin345@sina.com

Specialty section:
This article was submitted to Radiation Oncology, a section of the journal Frontiers in Oncology

Received: *17 October 2021*
Accepted: *10 January 2022*
Published: *03 February 2022*

Citation:
Ma J, Li L, Liao T, Gong W and Zhang C (2022) Efficacy and Safety of ^{225}Ac-PSMA-617-Targeted Alpha Therapy in Metastatic Castration-Resistant Prostate Cancer: A Systematic Review and Meta-Analysis. Front. Oncol. 12:796657. doi: 10.3389/fonc.2022.796657

Objective: To conduct a meta-analysis of the efficacy and safety of ^{225}Ac-PSMA-617 in the treatment of metastatic castration-resistant prostate cancer based on existing clinical evidence.

Methods: Search for retrospective studies about ^{225}Ac-PSMA-617 in the treatment of metastatic castration-resistant prostate cancer from establishment to July 2021 in PubMed and EMBASE. The primary endpoint was ^{225}Ac-PSMA-617 biochemical response evaluation criteria after treatment [any prostate specific antigen (PSA) decrease and PSA decrease >50% from baseline] to evaluate the treatment effect. Secondary endpoints included assessment of overall survival (OS), progression-free survival (PFS), molecular response, and toxicity for all studies. Two researchers conducted literature screening, data extraction and quality evaluation according to the inclusion and exclusion criteria. Use stata16.0 software for analysis, fixed-effects model for data merging and forest plots for display.

Results: A total of 6 retrospective studies, namely, 201 patients, were included in the final analysis. The pooled proportions of patients with decreased PSA and PSA decreased by more than 50% were 87.0% (95% confidence interval, 0.820 to 0.920) and 66.1% (95% confidence interval, 0.596 to 0.726), respectively. The pooled proportions of OS and PFS were 12.5 months (95%CI: 6.2–18.8 months) and 9.1 months (95%CI: 2.6–15.7 months). The patients showing molecular responses were 54% (95% confidence interval: 25–84%). In all studies, the most common side effect of ^{225}Ac-PSMA-617 TAT was xerostomia, with any degree of xerostomia occurring in 77.1% (155 out of 201), and grade III only accounted for 3.0%. The second was 30.3% (61 out of 201) anemia of any degree, and grade III accounts for 7.5% (15 out of 201). Grade III leukopenia and thrombocytopenia were 4.5% (9 out of 201) and 5.5% (11 out of 201), respectively. Only 6 (3.0%) of 201 patients had Grade III nephrotoxicity.

Conclusion: ^{225}Ac-PSMA-617 is an effective and safe treatment option for mCRPC patients, and the toxicity caused by it is relatively low. However, future randomized controlled trials and prospective trials are required in the future to judge the therapeutic effects and survival benefits compared with existing clinical treatments.

Systematic Review Registration: PROSPERO: CRD42021281967.

Keywords: ^{225}Ac-PSMA-617, α nuclide therapy, metastatic castration-resistant prostate cancer, meta-analysis, systematic review

INTRODUCTION

Prostate cancer is one of the most common malignant tumors in men around the world. According to the latest report of global cancer statistics in 2020, the incidence and mortality rates of prostate cancer rank the 2nd and 5th among malignant tumors in men around the world (1). At present, the main treatment methods for prostate cancer include radical surgical resection, radiotherapy, chemotherapy, local radiotherapy, androgen deprivation therapy, targeted therapy, and immunotherapy. As the condition of the patient progresses, the efficacy of these therapies will gradually decrease or even be completely ineffective (2). For advanced prostate cancer, androgen deprivation therapy has an effective effect. In the stage of metastatic emasculation-sensitive prostate cancer (mCSPC), combination therapy can improve survival rate than ADT alone (3). But there is still a lack of consensus on the best treatment options. Studies have shown that compared with docetaxel, androgen receptor axis targeting (ARAT) drugs may better improve the outcome of OS. However, the best treatment option remains to be determined (4). Most patients will become castration resistant after a period of 1 to 2 years of androgen sensitivity. The emergence of a state of castration resistance will lead to rapid progress of the disease, accelerate the metastasis of prostate cancer, and eventually progress to metastatic castration-resistant prostate cancer, leading to the ineffectiveness of chemotherapy and castration treatment. This is also the main cause of death in prostate cancer patients (5). Drugs such as abiraterone acetate, enzalutamide, carbachol, and apalutamide have good treatments for patients with mCRPC.In addition, olaparib and rucaparib can be used to treat mCRPC with BRCA gene mutations. Pembrolizumab is the first PD-1 inhibitor approved to treat prostate cancer. However, these drugs have unclear resistance mechanisms, and most patients will develop congenital or acquired resistance after treatment. The first α nuclide radiopharmaceutical approved by the US FDA for clinical treatment, ^{223}Ra-dichloride, is suitable for the treatment of patients with CRPC with symptomatic bone metastases and no known visceral metastases. In order to improve the clinical symptoms, overall survival (OS) and quality of life of patients, new drugs are being studied and are developing rapidly. However, the demand for effective treatments for mCRPC has not yet been met. We still lack effective treatments to treat patients at this stage of the disease. Therefore, there is an urgent need to find a new method with high efficiency, safety and low recurrence rate to treat mCRPC.

In recent years, radionuclide-labeled prostate-specific membrane antigen ligands have been used in the diagnosis and treatment of prostate cancer, and have achieved promising results. Prostate-specific membrane antigen is a membrane glycoprotein that is overexpressed on prostate cancer cells. Compared with normal prostate tissue, its expression level in prostate cancer tissue has increased by about 100–1,000 times. There is a direct correlation between androgen independence, metastasis, and disease progression, making PSMA an ideal target for diagnosis and treatment. ^{177}Lu-PSMA-617, which emits beta rays, has shown good effectiveness, safety, and easy availability for mCRPC, and has high clinical value and application prospects (6, 7). However, most patients still tolerate ^{177}Lu treatment or their condition continues to progress after ^{177}Lu and this treatment is contraindicated for patients with diffuse red bone marrow infiltration (8).

The half-life of ^{225}Ac is 10.0 d and the decay can produce 6 daughter nuclides, and each decay process releases 4 alpha particles, 2 beta particles and 2 gamma photons (9). Compared with ^{177}Lu, ^{225}Ac ray has higher energy, shorter range, and stronger killing effect on tumor cells. In addition, ^{225}Ac-PSMA-617 also has the advantage of targeting any metastatic tissue, and it has a good application prospect for small tumors, scattered cancers and micrometastasis (10). At present, ^{225}Ac-PSMA-617 for mCRPC has been gradually undergoing clinical trials in multiple centers to evaluate its efficacy and safety. However, due to the small sample size, population heterogeneity and different results, there are few systematic reviews or meta-analysis studies on the efficacy and safety of ^{225}Ac-PSMA-617 targeted therapy for mCRPC in the published literature. This study will meta-analyze the current published clinical studies on the treatment of mCRPC with ^{225}Ac-PSMA-617, in the hopes of providing evidence-based medicine for the efficacy and safety of ^{225}Ac-PSMA-617 in the treatment of mCRPC.

MATERIALS AND METHODS

This systematic review followed the Preferred Reporting Items for Systematic Reviews and Meta-Analysis (PRISMA) guidelines (11). The registration number on PROSPERO is: CRD42021281967.

Search Strategy

Articles were searched in PubMed and Embase for articles published until July 2021 about ^{225}Ac-PSMA-617 in the

treatment of metastatic castration-resistant prostate cancer. The search keywords were as follows: [prostate* neoplasm* (Mesh) OR prostate cancer] AND [Actinium-225 (Mesh) OR 225Ac OR 225Actinium OR Ac-225]. All retrospective studies were searched and appropriate data were included for analysis. If the article meets the research criteria, the full text will be searched. If there were duplications (patient data from the same trial or institution), only the most complete, up-to-date and relevant studies were selected.

Study Selection and Quality Assessment

We only selected studies that meet the following criteria: Participants (P) were no less than 10 people who had been diagnosed as mCRPC through ^{68}Ga-PSMA-11 PET/CT. Interventions (I) were completed at least 1 cycle of ^{225}Ac-PSMA-617 treatment; If data came from the same study group, the study with the highest number of patients will be included. The main outcome endpoint (O) was any decrease in PSA and Greater than 50% PSA decline. The type of study (S) included in the article was retrospective research. Exclusion criteria include: mCRPC patients suffering from severe leukopenia, low platelets, renal failure, and those who cannot tolerate ^{225}Ac-PSMA-617 treatment in the terminal stage of cancer; Patients with hormone-sensitive prostate cancer receive ^{225}Ac-PSMA-617 targeted radiotherapy; Repeated studies, meta-analysis, reviews, case reports, brief communications, abstracts, letters to the editor. The Newcastle–Ottawa Scale (NOS) scale was used to evaluate the literature methodological quality of the selected studies. The quality scale was divided into three categories: selectivity (1 to 4 points), comparability (1 to 2 points), and results (1 to 3 points). According to the scores from these three aspects, the quality of the literatures with NOS ≥6 points was better (**Table 1**).

Data Extraction

Two researchers independently conducted a literature search and extracted data. If there was a dispute, this was discussed and resolved with a third person. The basic research data extracted included: author name, publication year, patient demographics, Gleason score, Eastern Cancer Cooperation Group performance score, and baseline level (**Table 2**). Observation indicators included tumor markers (PSA), number of ^{225}Ac-PSMA-617 treatment cycles, follow-up interval, dose and drug activity, and primary outcome endpoint was biochemical response. Secondary outcome endpoints included overall survival (OS), progression-free survival (PFS), molecular reactions, and toxicity (**Tables 3–5**).

TABLE 1 | Quality assessment of the included studies based on the Newcastle–Ottawa Scale.

NO.	Author and year	Selection	Comparability	Outcome	Score
1	Kratochwil et al. (12)	3	1	3	7
2	Sathekge et al. (13)	3	1	3	7
3	van der Doelen et al. (14)	3	1	3	7
4	Satapathy et al. (15)	3	1	2	6
5	Feuerecker et al. (16)	2	1	3	6
6	Sen et al. (17)	3	1	3	7

TABLE 2 | Basic characteristics of the included studies.

Author and year	Patients (n)	Age (yr) (Median, Range)	Baseline PSA (ng/ml) (Median)	GS	ECOG
Kratochwil et al. (12)	40	70	169	NR	0–1 (80%) ≥2 (20%)
Sathekge et al. (13)	73	69 (45–85)	57.2	8 (6–10)	0–1 (82%) 2–3 (18%)
van der Doelen et al. (14)	13	71 (64–77)	878 (203–1611)	≥8 6 (46.2%)	0 (23.1%) 1–2 (76.9%)
Satapathy et al. (15)	11	68 (57–81)	158 (35–840)	8 (7–9)	0–1 (64%) 2 (36%)
Feuerecker et al. (16)	26	72.5 (63–75.8)	331 (142–682)	8 (7–9)	1 (0-1)
Sen et al. (17)	38	68 (53–84)	NR	7≤ (10.5%) ≥8 (89.5%)	≤2 (100%)

Author and year	Doce-taxel	Enzaluta-mide	Previous treatment (%) Abiraterone-cetate	Cabazit-axel	^{223}Ra-Cl$_3$	Olaparib	^{177}Lu-PSMA	Site of metastases at baseline
Kratochwil et al. (12)	70%	60%	85%	17.5%	22.5%	NR	NR	Skeletal:97.5%;liver:22; lung:22.5%;brain:5%; others: 7.5%
Sathekge et al. (13)	NR	1%	1%	NR	NR	NR	14%	skeletal:90%;Isolated lymph node: 10%; liver:5%;lung:3%;brain:1%
van der Doelen et al. (14)	100%	76.9%	84.6%	61.5%	30.8%	63.6%	15.4%	skeletal:100%;Lymph node: 77%;visceral: 62%
Satapathy et al. (15)	91%	36%	64%	27%	NR	NR	46%	skeletal: 100%; Lymph node: 82%;
Feuerecker et al. (16)	96%	85%	88%	54%	23%	NR	100%	skeletal:100%;Lymph node:88%;liver:19%; lung:23%; others: 19%
Sen et al. (17)	100%	34%	63%	10.50%	5.20%	10.50%	23.6%	skeletal:47%;Lymph node:34%;lung:11%; liver:8%

NR, not reported; PSA, prostate-specific antigen; ECOG, Eastern Cooperative Oncology Group; GS, Gleason score.

TABLE 3 | The treatment characteristics of the included studies.

Author and year	Patients Analyzed for PSA Decline (n)	Dose	Cycles of Therapy (Median, Range)	Follow-Up (wk)	Any PSA Decline (%)	PSA Decline >50%
Kratochwil et al. (12)	38	100 KBq/kgBW	1–3	8	33/38 (87)	24/38 (63)
Sathekge et al. (13)	73	4–8 MBq/cycle	3 (1–8)	8	60/73 (83)	51/73 (70)
van der Doelen et al. (14)	13	6–8 MBq/cycle	3 (1–4)	8	NR	9/13 (69)
Satapathy et al. (15)	11	100 KBq/kgBW	2 (1–4)	8–12	NR	5/11 (46)
Feuerecker et al. (16)	26	9 MBq/cycle	2 (1–6)	8	23/26 (88)	17/26 (65)
Sen et al. (17)	38	100 KBq/kgBW	2 (2–5)	8	33/38 (87)	25/38 (66)

NR, not reported; BW, body weight; PSA, prostate-specific antigen.

TABLE 4 | The treatment characteristics of the included studies.

Author and Year	Patients (n)	Molecular Response n/N (%)	OS (Months) (Median, Range)	PFS (Months) (Median, Range)	Treatment Related Deaths, n/N (%)
Kratochwil et al. (12)	40	NR	>12.0 (NR)	7.0 (NR)	NR
Sathekge et al. (13)	73	21/73 (29)	18 (16.2–19.9)	15.2 (13.1–17.4)	NR
van der Doelen et al. (14)	13	6/7 (86)	8.5 (NR)	5.5 (NR)	NR
Satapathy et al. (15)	11	NR	NR	NR	3/11 (27)
Feuerecker et al. (16)	26	NR	7 (4.5–12.1)	3.5 (1.8–11.2)	NR
Sen et al. (17)	38	17/38 (45)	12 (9.1–14.9)	8 (5.3–10.6)	NR

NR, not reported; OS, overall survival; PFS, progression-free survival.

TABLE 5 | Treatment-related toxicity of the included studies.

Author and Year	Patients (n)	Hematological Toxicity n/N (%) Any grade Grade ≥3	Nephrotoxicity n/N (%) Any grade Grade ≥3	Xerostomia, n/N (%) Any grade Grade ≥3	Other Manifestation
Kratochwil et al. (12)	40	NR	NR	19/40 (47.5) NR	NR
Sathekge et al. (13)	73	① 27/73 (37) 5/73 (7) ② 9/73 (12) 2/73 (3) ③ 7/73 (10) 1/73 (1)	23/73 (32) 5/73 (7)	62/73 (85) 0/73 (0)	Grade1/2 nause 15/73 (21) Anorexia 23/73 (32), Constipation 19/73 (26), Fatigue 37/73 (51), Weightloss 28/73 (38), Hypoalbuminemia 14/73 (19), Dysuria 13/73 (18), xerophthalmia 4/73 (6)
Van der Doelen et al. (14)	13	① 0/13 (0) / ② 0/13 (0) / ③ 0/13 (0) /	0/13 (0) /	3/13 (100) 0/13 (0)	swallowing, speech, dysgeusia 13/13 (100)
Satapathy et al. (15)	11	① 8/11 (73) 1/11 (9) ② 5/11 (46) 0/11 (0) ③ 5/11 (46) 2/11 (18)	1/11 (9) 1/11 (9)	8/11 (73) 1/11 (9)	Grade1/2 nausea 2/11 (18), Constipation 2/11 (18), Fatigue 3/11 (27), Weightloss 2/11 (18), Anorexia 3/11 (27)
Feuerecker et al. (16)	26	①15/26 (58) 9/26 (35) ②13/26 (50) 7/26 (27) ③14/26 (54) 5/26 (19)	5/26 (19) 0/26(0)	26/26 (100) 0/26(0)	Grade1 fatigue 12/26 (36), Weightloss 3/26 (12), anorexia 8/26 (31)
Sen et al. (17)	38	①11/20 0/20 ②3/38 0/38 ③4/38 3/38	NR	37/38 (97) 5/38()	Weightloss 21/38 (55), Grade IV Hearing loss 2/38 (), Gradel/2 nausea 9/38,

① Anemia; ② leucopenia; ③ Thrombocytopenia; NR, not reported.

The biochemical response was evaluated according to the criteria defined by the Prostate Cancer Clinical Trials Working Group 3 (PCWG3) (18). Patients with greater than 50% PSA decline from baseline were defined as a biochemically significant response, and any decrease in PSA level was recorded. The molecular response was scanned on ^{68}Ga-PSMA PET/CT, evaluated according to adjusted PERSIST 1.0 (19), and the proportion of patients with complete response (CR) and partial response (PR) was combined as the molecular response rate. PFS was defined as the time from the first dose of ^{225}Ac-PSMA-617 to the first evidence of progression or death or the end of the study period; OS was defined as the time from the first dose of ^{225}Ac-PSMA-617 to death from any cause. Toxicity was defined according to the Common Terminology Standard for Adverse Events Version 5.0 (CTCAE 5.0) (20).

Statistical Analyses

Stata16.0 was used for meta-analysis. The main endpoint was to evaluate the treatment effect through the biochemical response evaluation standard after ^{225}Ac-PSMA-617 treatment (any decrease in PSA and greater than 50% PSA decline). Secondary endpoints included OS, PFS, molecular reactions, and toxicity, and drawing forest maps for analysis. I^2 statistic was used for heterogeneity test. If there was no significant heterogeneity among studies (I^2 ≤50%, P <0.10), a fixed effect model was used to merge data. If there was significant heterogeneity among the studies (I^2 >50%, P ≥0.10), the random effect model was used to merge the data. The funnel chart and Egger test were used to evaluate the publication bias of the biochemical response after ^{225}Ac-PSMA-617 treatment, and P ≤0.05 was considered statistically significant.

RESULTS

A Systematic Review of Literature

According to the prescribed search strategy, a total of 176 related articles were first checked out. A total of 64 duplicate articles were excluded. A total of 99 articles were excluded by reading titles and abstracts, namely, 43 reviews, 22 preclinical studies, 9 radiochemistry, 8 case reports and brief communications, and 8 dosimetry and imaging related articles, 5 other alpha nuclide therapies and not related to ^{225}Ac-PSMA treatment, 2 meta-analysis, 1 ^{225}Ac-PSMA resistance gene sequencing, and 1 ^{225}Ac-PSMA-I&T treatment. After further reading the full text, and according to the inclusion and exclusion criteria designed in this study, 7 articles were excluded. An article by Sathekge et al. (21) reported about ^{225}Ac-PSMA-617 in chemotherapy-naive patients. Two articles by Kratochwil et al. (22, 23), first discussed about only 2 patients, and the other on a dose escalation study of ^{225}Ac-PSMA-617. A prospective study was also done by Yadav et al. (24). Three articles reported using ^{225}Ac-PSMA-617/^{177}Lu-PSMA-617 tandem treatment (25–27). Finally, a total of 6 articles were included (12–17), as shown in **Figure 1**.

Any PSA Decline

A total of 4 articles (12, 13, 16, 17) were included in the analysis. Among 201 patients, 175 patients were evaluated with a decline of PSA level, and 149 patients had any decline of PSA. The result of heterogeneity analysis showed that there was no significant heterogeneity (I^2 = 0.0%, P = 0.948), so the fixed effect model was used to merge the PSA reduction rate. The result of meta-analysis showed that the pooled rate of PSA decline after treatment with ^{225}Ac-PSMA-617 was 0.870 (95%CI: 0.820–0.920), as shown in **Figure 2**.

Greater Than 50% PSA Decline

A total of 6 articles (12–17) were included in the analysis. Among 201 patients, 199 patients were evaluated, and 131 patients had PSA >50% decline. The results of heterogeneity analysis showed that there was no significant heterogeneity (I^2 = 0.0%, P = 0.771), so the fixed effect model was used to merge the PSA reduction rate of greater than 50%.The forest plot indicated (**Figure 3**) that the pooled rate of greater than 50% PSA decline was 0.661 (95% CI: 0.596–0.726).

Survival

OS and PFS were reported in 5 studies (12–14, 16, 17). But in only 3 studies,137 patients, the median of OS and PFS and 95% confidence interval were reported (13, 16, 17). The pooled estimates of median OS and PFS were 12.5 months (95%CI: 6.2–18.8 months) and 9.1 months (95%CI: 2.6–15.7 months).

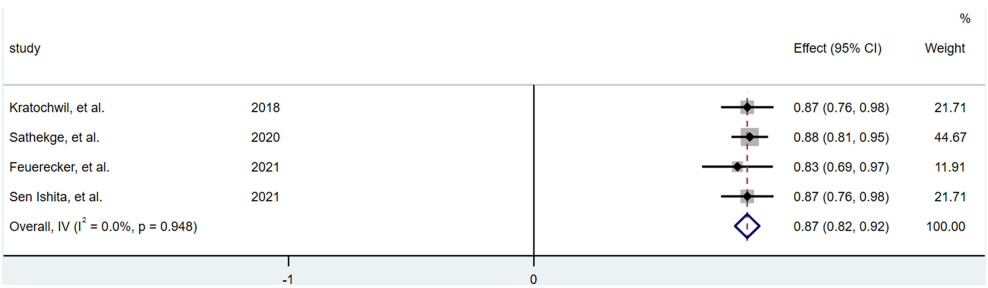

FIGURE 1 | Flowchart of literature screening.

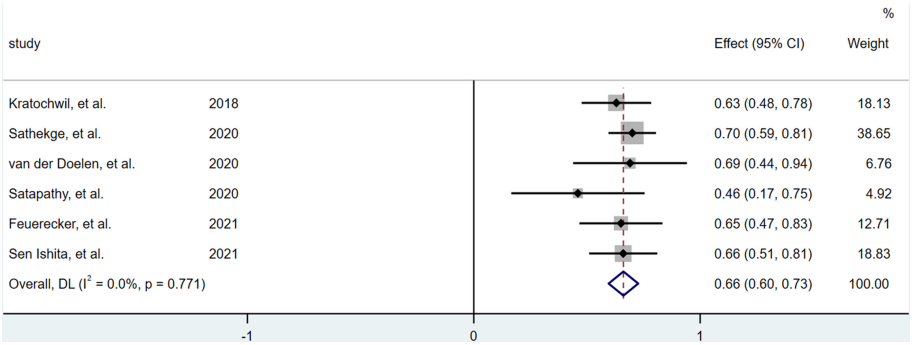

FIGURE 2 | Forest plot for any PSA decline after treatment.

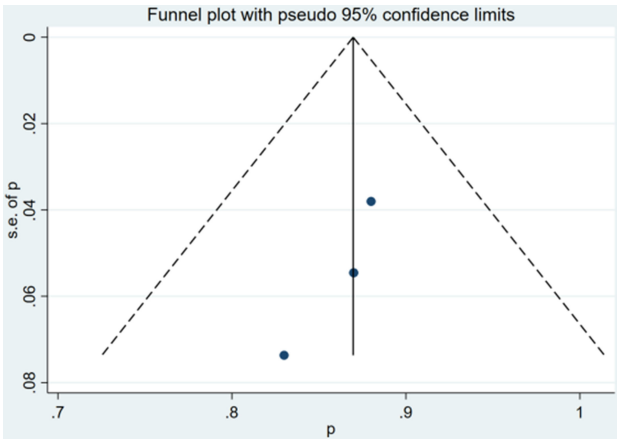

FIGURE 3 | Forest plot for >50% PSA decline after treatment.

Molecular Response

The molecular response was evaluated according to the adjusted PERSIST 1.0, and the complete reaction (CR) and partial reaction (PP) were combined as molecular response. There were 3 studies that met the evaluation requirements (13, 14, 17), namely, 124 patients, and the pooled proportion of patients with molecular response was 54% (95%CI: 25–84%).

Toxicity

According to the Common Terminology Standard for Adverse Events Version 5.0 (CTCAE 5.0), the toxicity of ^{225}Ac-PSMA-617 TAT was analyzed in 6 studies. Xerostomia was the most common side effect. Xerostomia of any degree accounted for 77.1% (155 out of 201 people), and only 6 people had grade III xerostomia, occurring in 3.0%. Then anemia was 30.3% (61 out of 201 people), and grade III anemia was 7.5% (15 out of 201 people). Leukopenia and thrombocytopenia of any degree were 14.9 (30 out of 201); grade III leukopenia and thrombocytopenia were 4.5% (9 out of 201) and 5.5% (11 out of 201). Only 6 (3.0%) of 201 patients had Grade III nephrotoxicity. Other adverse reactions included weight loss 26.9% (54 out of 201), fatigue 25.9% (52 out of 201), anorexia 16.9% (34 out of 201), nausea 12.9% (26 out of 201), and constipation 10.4% (21 out of 201). In addition, in the study of Sathekge (13), 4 patients had symptoms of xerophthalmia, and the study of Sen (17) reported 2 patients with hearing loss. Among the evaluable patients, treatment-related deaths were reported in only one study (15), and 3 of 11 patients had treatment-related deaths.

Risk of Bias

The qualitative and quantitative evaluation of publication bias used funnel chart and Egger test (**Figures 4**, **5**). The results of any PSA decline indicated that there was no significant publication bias (P = 0.081). The Egger test result of greater than 50% PSA decline suggested that there was no significant publication bias (P = 0.105).

DISCUSSION

Currently, ^{225}Ac-PSMA-617 targeted therapy for prostate cancer is undergoing trials in different countries. ^{225}Ac has shown

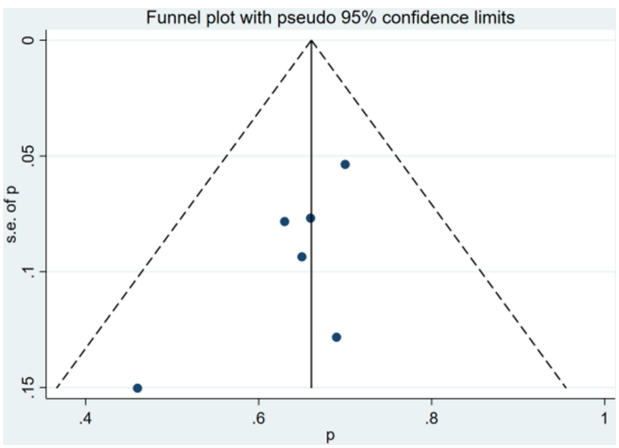

FIGURE 4 | Funnel plot for any PSA decline after treatment.

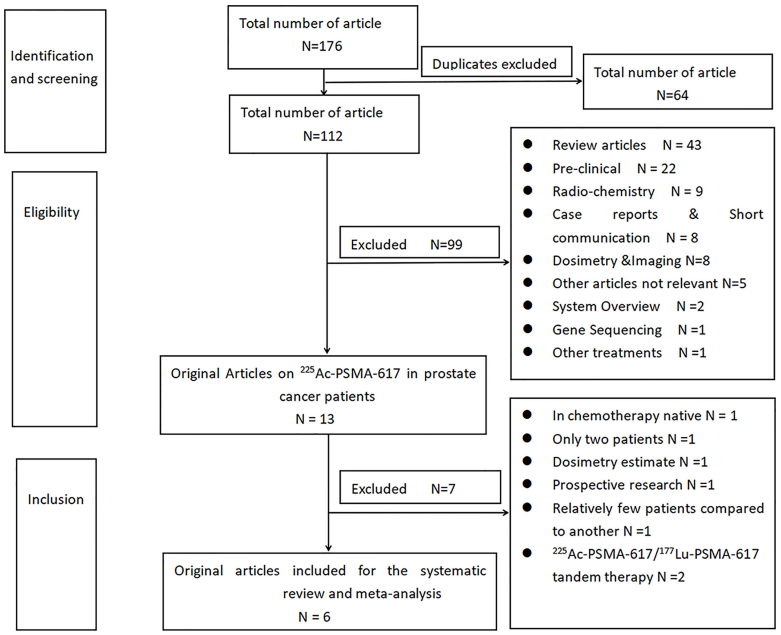

FIGURE 5 | Funnel plot for >50% PSA decline after treatment.

encouraging effect in the study of mCRPC patients, but since most of the trials are small samples and mostly retrospective, there are only few systematic reviews of ^{225}Ac-PSMA-617 TAT. This meta-analysis evaluated the efficacy and safety of ^{225}Ac-PSMA-617 TAT in mCRPC patients from retrospective studies published so far. The results showed that ^{225}Ac targeted therapy for prostate cancer patients had a significant therapeutic effect and low toxicity. More than 80% of patients had any PSA decline, and more than 60% of patients had greater than 50% PSA decline. All patients who received this treatment had previously received second/third-line treatments such as abilaterol, enzalutamide, apalutamide or ^{177}Lu-PSMA-617 and all failed. With ^{225}Ac as a rescue treatment attempt, the results showed that OS and PFS were 12.5 months and 9.1 months. Approximately 54% of patients had complete or partial molecular reactions. After the failure of previous androgen receptor inhibitor (ARPI) treatment of prostate cancer, treatment with abiraterone or enzalutamide had an OS of 4 months, and cabazitaxel OS was 13–14 months. In contrast, the OS treated with ^{177}Lu was 15.3 months (28). This study showed that the OS of ^{225}Ac treatment of prostate cancer was better than the standard second-line/third-line treatment. Another study reported that giving ^{177}Lu before docetaxel treatment produced a better PSA response than after docetaxel treatment (29). In a meta-analysis of randomized controlled trials in patients with mCRPC, the benefits and harms of eight third-line (L3) treatments for prostate cancer were evaluated. Compared with treatment with abiraterone, enzalutamide, mitoxantrone or cabazitaxel, PSMA PRLT resulted in a higher rate of PSA decline and a 1.1-fold increase in PFS (30). Although it was a preliminary study, it had shown the great potential of targeted radionuclide therapy. The decrease of PSA reflected the killing ability of cells during the treatment, and the progression-free survival reflected the comprehensive effects of cell killing and regeneration during the treatment cycle. The overall survival rate reflected the comprehensive effect of progression-free survival and treatment. The decline in PSA cannot predict OS and PFS. On the contrary, when PSA progressed, it indicated shorter OS and PFS (12, 24). These results had important implications for the extensive terminal stages of cancer, especially for patients with mCRPC. Among clinical relevant toxic reactions, xerostomia was the most common adverse reaction. More than 70% of patients had different degrees of xerostomia, but most were mild and transient. Significant treatment-related toxicities were only seen in a few patients. Grade III anemia, leukopenia, thrombocytopenia, and nephrotoxicity were only seen in 7.5, 4.5, 5.5, and 3.0% of the patients. In addition, toxicities such as nausea, fatigue, dysgeusia, indigestion, and constipation could be observed. Only 3 treatment-related deaths were reported in one article (15).

In the treatment of mCRPC, health-related quality of life is an important parameter to evaluate the subjective experience of the disease and its treatment. Most patients with mCRPC have bone metastases, which can lead to a significant incidence of bone pain and bone-related events. In addition, there will be a lot of general symptoms, such as fatigue, anorexia, bladder and intestinal disorders, nausea, vomiting, and sleep disturbances. Treatment-related adverse reactions may aggravate the deterioration of the quality of life of these patients. In this case, any new therapeutic drug not only needs to prove its survival benefit, but also needs to prove its impact on the quality of life of the patient. ^{225}Ac-PSMA-617 treatment significantly improved

health-related quality of life. Examples include physical symptoms such as pain, difficulty urinating, fatigue, and limited physical activity. In the van der Doelen, Feuerecker, and Sen studies, the European Organization for Cancer Research and Treatment (EORTC-QLQ30) quality of life questionnaire was used to evaluate patients (31). In the questionnaire assessment of van der Doelen and Sen, compared with baseline, pain was significantly improved, the use of analgesics was reduced, and the responses to analgesics were also improved. In addition, Sen et al. used the Standard Pain Numerical Scale (NPS) and Brief pain Inventory Questionnaire (BPI) for multidimensional pain assessment (32). Eight weeks after the second dose of ^{225}Ac-PSMA-617 treatment, the NPS score dropped from baseline 5 points to 1 point. BPI measures the interference of pain on general activities, sleep, and mood, and had a significant improvement compared with baseline. The NCCN-FACT-FPSI-17 (version 2.0) (FACIT.org, Ponte Vedra, Florida, USA) questionnaire was used by Satapathy for evaluation (33), and the results showed that pain had also been significantly improved. For other aspects, van der Doelen showed greater improvement in fatigue and dyspnea; Satapathy showed significant improvement in dysuria, bone pain, fatigue and physical activity limitation; Feuerecker showed improvement in social function; Sen Showed significant improvement in fatigue, insomnia and constipation compared with baseline.

The PERCIST is only standardized for ^{18}F-FDG PET/CT imaging. The complete and partial molecular responses observed on ^{68}GA-PSMA PET/CT scans are still controversial. Therefore, it is challenging to accurately assess the treatment response of mCRPC patients. Velez et al. (34) showed that PERCIST 1.0 could provide important prognostic information for mCRPC patients receiving systemic chemotherapy, especially when combined with PSA treatment response criteria. More large-scale trials are needed to test the accuracy of ^{68}GA-PSMA PET/CT in the evaluation of treatment response. In addition, the choice of treatment regimen and dosage is empirical. Most studies use 100 KBq/kg, and the treatment cycle ranges from 1 to 8 cycles. However, the effect of this targeted therapy is related to the expression level of PSMA. Although the expression of PSMA is closely related to hormone resistance and disease progression, the expression of PSMA in different metastases is heterogeneous. Moreover, the interaction between systemic therapy and PSMA expression has not been studied clearly (35), so the individualized treatment plan and dose selection for patients still need to be explored continuously. The current study inclusion criteria are all patients with positive PSMA expression, and the results showed a good treatment effect. However, for patients with lack or low expression of PSMA, whether these patients can still benefit from PSMA RLT, and how to choose a reasonable and effective combination treatment plan still needs continuous follow-up research.

This study also has certain limitations. All included studies were single-arm retrospective observational studies, the sample size of the trial was small, and the risk of bias was high. In addition, these trials were heterogeneous in terms of research design, other diseases, the course of prostate cancer, previous treatments, and the degree of PSMA expression. The follow-up time was short, and there were few studies on the comprehensive evaluation of molecular response and survival, which limited the accuracy of observation and evaluation of these indicators.

CONCLUSION

^{225}Ac-PSMA-617 is an effective and safe treatment option for mCRPC patients, and the treatment-related side effects caused by it are relatively low. However, 225Ac-PSMA-617 is in the clinical trial stage, and the efficacy and safety of its treatment plan still need to be evaluated in a high-quality, multi-center and prospective multi-arm randomized controlled trial.

DATA AVAILABILITY STATEMENT

The original contributions presented in the study are included in the article/supplementary material. Further inquiries can be directed to the corresponding author.

AUTHOR CONTRIBUTIONS

JM, LL, and CZ contributed to conception and design of the study. JM organized the database. JM, LL, and TL performed the statistical analysis. JM wrote the first draft of the manuscript. LL, TL, and WG wrote sections of the manuscript. All authors listed have made a substantial, direct, and intellectual contribution to the work and approved it for publication.

REFERENCES

1. Cao W, Chen HD, Yu YW, Li N, Chen WQ. Changing Profiles of Cancer Burden Worldwide and in China: A Secondary Analysis of the Global Cancer Statistics 2020. *Chin Med J (Engl)* (2021) 134(7):783–91. doi: 10.1097/CM9.0000000000001474
2. Parker C, Castro E, Fizazi K, Heidenreich A, Ost P, Procopio G, et al. Prostate Cancer: ESMO Clinical Practice Guidelines for Diagnosis, Treatment and Follow-Up. *Ann Oncol* (2020) 31(9):1119–34. doi: 10.1016/j.annonc.2020.06.011
3. Iacovelli R, Ciccarese C, Schinzari G, Maiorano BA, Rossi E, Pierconti F, et al. Going Towards a Precise Definition of the Therapeutic Management of *De-Novo* Metastatic Castration Sensitive Prostate Cancer Patients: How Prognostic Classification Impact Treatment Decisions. *Crit Rev Oncol Hematol* (2019) 139:83–6. doi: 10.1016/j.critrevonc.2019.05.005
4. Ferro M, Lucarelli G, Crocetto F, Dolce P, Verde A, La Civita E, et al. First-Line Systemic Therapy for Metastatic Castration-Sensitive Prostate Cancer: An Updated Systematic Review With Novel Findings. *Crit Rev Oncol Hematol* (2020) 157:103198. doi: 10.1016/j.critrevonc.2020.103198
5. Rozet F, Mongiat-Artus P, Hennequin C, Beauval JB, Beuzeboc P, Cormier L, et al. Corrigendum to "French ccAFU Guidelines-Update 2020-2022: Prostate Cancer" [Prog. Urol 30 (12 S) (2020), Pp S136-S251]. *Prog Urol* (2021) 31(6):381–2. doi: 10.1016/j.purol.2021.04.001
6. Mayor N, Sathianathen NJ, Buteau J, Koschel S, Antón Juanilla M, Kapoor J, et al. Prostate-Specific Membrane Antigen Theranostics in Advanced Prostate

Cancer: An Evolving Option. *BJU Int* (2020) 126(5):525–35. doi: 10.1111/bju.15143
7. Wen JN, Cheng C, Chen R. New Progress of (177)Lu-PSMA-617 in the Treatment of Metastatic Castration-Resistant Prostate Cancer. *Acad J Second Military Med Univ* (2021) 42(04):377–84. doi: 10.16781/j.0258-879x.2021.04.0377
8. Kratochwil C, Giesel FL, Stefanova M, Benešová M, Bronzel M, Afshar-Oromieh A, et al. PSMA-Targeted Radionuclide Therapy of Metastatic Castration-Resistant Prostate Cancer With 177Lu-Labeled PSMA-617. *J Nucl Med* (2016) 57(8):1170–6. doi: 10.2967/jnumed.115.171397
9. Francesconi LC, McDevitt MR, Morris MJ, Lewis JS. α-Emitters for Radiotherapy: From Basic Radiochemistry to Clinical Studies-Part 1. *J Nucl Med* (2018) 59(6):878–84. doi: 10.2967/jnumed.116.186338
10. Yang MD, Fan X, Qin SS. Application of Alpha Nuclide in Precision Medicine for Malignant Tumors. *Chin J Nucl Med Mol Imaging* (2020) 40(11):693–7. doi: 10.3760/cma.j.cn321828-20191008-00217
11. Moher D, Liberati A, Tetzlaff J, Altman DGPRISMA Group. Preferred Reporting Items for Systematic Reviews and Meta-Analyses: The PRISMA Statement. *PloS Med* (2009) 6(7):e1000097. doi: 10.1371/journal.pmed.1000097
12. Kratochwil C, Bruchertseifer F, Rathke H, Hohenfellner M, Giesel FL, Haberkorn U, et al. Targeted α-Therapy of Metastatic Castration-Resistant Prostate Cancer With 225Ac-PSMA-617: Swimmer-Plot Analysis Suggests Efficacy Regarding Duration of Tumor Control. *J Nucl Med* (2018) 59(5):795–802. doi: 10.2967/jnumed.117.203539
13. Sathekge M, Bruchertseifer F, Vorster M, Lawal IO, Knoesen O, Mahapane J, et al. Predictors of Overall and Disease-Free Survival in Metastatic Castration-Resistant Prostate Cancer Patients Receiving 225ac-PSMA-617 Radioligand Therapy. *J Nucl Med* (2020) 61(1):62–9. doi: 10.2967/jnumed.119.229229
14. van der Doelen MJ, Mehra N, van Oort IM, Looijen-Salamon MG, Janssen MJR, Custers JAE, et al. Clinical Outcomes and Molecular Profiling of Advanced Metastatic Castration-Resistant Prostate Cancer Patients Treated With 225Ac-PSMA-617 Targeted Alpha-Radiation Therapy [Published Online Ahead of Print, 2020 Dec 19]. *Urol Oncol* (2020) 39(10):729.e7–16. doi: 10.1016/j.urolonc.2020.12.002
15. Satapathy S, Mittal BR, Sood A, Das CK, Singh SK, Mavuduru RS, et al. Health-Related Quality-Of-Life Outcomes With Actinium-225-Prostate-Specific Membrane Antigen-617 Therapy in Patients With Heavily Pretreated Metastatic Castration-Resistant Prostate Cancer. *Indian J Nucl Med* (2020) 35(4):299–304. doi: 10.4103/ijnm.IJNM_130_20
16. Feuerecker B, Tauber R, Knorr K, Heck M, Beheshti A, Seidl C, et al. Activity and Adverse Events of Actinium-225-PSMA-617 in Advanced Metastatic Castration-Resistant Prostate Cancer After Failure of Lutetium-177-PSMA. *Eur Urol* (2021) 79(3):343–50. doi: 10.1016/j.eururo.2020.11.013
17. Sen I, Thakral P, Tiwari P, Pant V, Das SS, Manda D, et al. Therapeutic Efficacy of 225Ac-PSMA-617 Targeted Alpha Therapy in Patients of Metastatic Castrate Resistant Prostate Cancer After Taxane-Based Chemotherapy. *Ann Nucl Med* (2021) 35(7):794–810. doi: 10.1007/s12149-021-01617-4
18. Scher HI, Morris MJ, Stadler WM, Higano C, Basch E, Fizazi K, et al. Trial Design and Objectives for Castration-Resistant Prostate Cancer: Updated Recommendations From the Prostate Cancer Clinical Trials Working Group 3. *J Clin Oncol* (2016) 34(12):1402–18. doi: 10.1200/JCO.2015.64.2702
19. Seitz AK, Rauscher I, Haller B, Krönke M, Luther S, Heck MM, et al. Preliminary Results on Response Assessment Using 68Ga-HBED-CC-PSMA PET/CT in Patients With Metastatic Prostate Cancer Undergoing Docetaxel Chemotherapy. *Eur J Nucl Med Mol Imaging* (2018) 45(4):602–12. doi: 10.1007/s00259-017-3887-x
20. Freites-Martinez A, Santana N, Arias-Santiago S, Viera A. Using the Common Terminology Criteria for Adverse Events (CTCAE - Version 5.0) to Evaluate the Severity of Adverse Events of Anticancer Therapies. CTCAE Versión 5.0. Evaluación De La Gravedad De Los Eventos Adversos Dermatológicos De Las Terapias Antineoplásicas. *Actas Dermosifiliogr (Engl Ed)* (2021) 112(1):90–2. doi: 10.1016/j.ad.2019.05.009
21. Sathekge M, Bruchertseifer F, Knoesen O, Reyneke F, Lawal I, Lengana T, et al. 225Ac-PSMA-617 in Chemotherapy-Naive Patients With Advanced Prostate Cancer: A Pilot Study [Published Correction Appears in Eur J Nucl Med Mol Imaging. 2019 Jun 26]. *Eur J Nucl Med Mol Imaging* (2019) 46(1):129–38. doi: 10.1007/s00259-018-4167-0
22. Kratochwil C, Bruchertseifer F, Giesel FL, Weis M, Verburg FA, Mottaghy F, et al. 225Ac-PSMA-617 for PSMA-Targeted α-Radiation Therapy of Metastatic Castration-Resistant Prostate Cancer. *J Nucl Med* (2016) 57(12):1941–4. doi: 10.2967/jnumed.116.178673
23. Kratochwil C, Bruchertseifer F, Rathke H, Bronzel M, Apostolidis C, Weichert W, et al. Targeted α-Therapy of Metastatic Castration-Resistant Prostate Cancer With 225Ac-PSMA-617: Dosimetry Estimate and Empiric Dose Finding. *J Nucl Med* (2017) 58(10):1624–31. doi: 10.2967/jnumed.117.191395
24. Yadav MP, Ballal S, Sahoo RK, Tripathi M, Seth A, Bal C. Efficacy and Safety of 225Ac-PSMA-617 Targeted Alpha Therapy in Metastatic Castration-Resistant Prostate Cancer Patients. *Theranostics* (2020) 10(20):9364–77. doi: 10.7150/thno.48107
25. Rosar F, Krause J, Bartholomä M, Maus S, Stemler T, Hierlmeier I, et al. Efficacy and Safety of [225Ac]Ac-PSMA-617 Augmented [177lu]Lu-PSMA-617 Radioligand Therapy in Patients With Highly Advanced mCRPC With Poor Prognosis. *Pharmaceutics* (2021) 13(5):722. doi: 10.3390/pharmaceutics13050722
26. Rosar F, Hau F, Bartholomä M, Maus S, Stemler T, Linxweiler J, et al. Molecular Imaging and Biochemical Response Assessment After a Single Cycle of [225Ac]Ac-PSMA-617/[177lu]Lu-PSMA-617 Tandem Therapy in mCRPC Patients Who Have Progressed on [177Lu]Lu-PSMA-617 Monotherapy. *Theranostics* (2021) 11(9):4050–60. doi: 10.7150/thno.56211
27. Khreish F, Ebert N, Ries M, Maus S, Rosar F, Bohnenberger H, et al. 225Ac-PSMA-617/177lu-PSMA-617 Tandem Therapy of Metastatic Castration-Resistant Prostate Cancer: Pilot Experience. *Eur J Nucl Med Mol Imaging* (2020) 47(3):721–8. doi: 10.1007/s00259-019-04612-0
28. Sartor O, de Bono J, Chi KN, Fizazi K, Herrmann K, Rahbar K, et al. Lutetium-177-PSMA-617 for Metastatic Castration-Resistant Prostate Cancer. *N Engl J Med* (2021) 385(12):1091–103. doi: 10.1056/NEJMoa2107322
29. Meyrick D, Gallyamov M, Sabarimurugan S, Falzone N, Lenzo N. Real-World Data Analysis of Efficacy and Survival After Lutetium-177 Labelled PSMA Ligand Therapy in Metastatic Castration-Resistant Prostate Cancer. *Target Oncol* (2021) 16(3):369–80. doi: 10.1007/s11523-021-00801-w
30. von Eyben FE, Kairemo K, Paller C, Hoffmann MA, Paganelli G, Virgolini I. 177Lu-PSMA Radioligand Therapy Is Favorable as Third-Line Treatment of Patients With Metastatic Castration-Resistant Prostate Cancer. A Systematic Review and Network Meta-Analysis of Randomized Controlled Trials. *Biomedicines* (2021) 9(8):1042. doi: 10.3390/biomedicines9081042
31. Aaronson NK, Ahmedzai S, Bergman B, Bullinger M, Cull A, Duez NJ, et al. The European Organization for Research and Treatment of Cancer QLQ-C30: A Quality-of-Life Instrument for Use in International Clinical Trials in Oncology. *J Natl Cancer Inst* (1993) 85(5):365–76. doi: 10.1093/jnci/85.5.365
32. Cleeland CS, Ryan KM. Pain Assessment: Global Use of the Brief Pain Inventory. *Ann Acad Med Singap* (1994) 23(2):129–38.
33. Victorson DE, Beaumont JL, Rosenbloom SK, Shevrin D, Cella D. Efficient Assessment of the Most Important Symptoms in Advanced Prostate Cancer: The NCCN/FACT-P Symptom Index. *Psychooncology* (2011) 20(9):977–83. doi: 10.1002/pon.1817
34. Velez EM, Desai B, Ji L, Quinn DI, Colletti PM, Jadvar H. Comparative Prognostic Implication of Treatment Response Assessments in mCRPC: PERCIST 1.0, RECIST 1.1, and PSA Response Criteria. *Theranostics* (2020) 10(7):3254–62. doi: 10.7150/thno.39838
35. Afshar-Oromieh A, Debus N, Uhrig M, Hope TA, Evans MJ, Holland-Letz T, et al. Impact of Long-Term Androgen Deprivation Therapy on PSMA Ligand PET/CT in Patients With Castration-Sensitive Prostate Cancer. *Eur J Nucl Med Mol Imaging* (2018) 45(12):2045–54. doi: 10.1007/s00259-018-4079-z

Conflict of Interest: The authors declare that the research was conducted in the absence of any commercial or financial relationships that could be construed as a potential conflict of interest.

Publisher's Note: All claims expressed in this article are solely those of the authors and do not necessarily represent those of their affiliated organizations, or those of the publisher, the editors and the reviewers. Any product that may be evaluated in this article, or claim that may be made by its manufacturer, is not guaranteed or endorsed by the publisher.

frontiers in Oncology

ORIGINAL RESEARCH
published: 16 February 2022
doi: 10.3389/fonc.2022.805051

Proton Therapy for Primary Bone Malignancy of the Pelvic and Lumbar Region – Data From the Prospective Registries ProReg and KiProReg

Rasin Worawongsakul[1,2,3], Theresa Steinmeier[1,3], Yi-Lan Lin[1,3], Sebastian Bauer[3,4,5], Jendrik Hardes[3,5,6], Stefanie Hecker-Nolting[7], Uta Dirksen[3,5,8] and Beate Timmermann[1,3,5]*

[1] Department of Particle Therapy, University Hospital Essen, West German Proton Therapy Centre Essen, Essen, Germany, [2] Radiation Oncology Unit, Department of Diagnostic and Therapeutic Radiology, Ramathibodi Hospital, Mahidol University, Bangkok, Thailand, [3] West German Cancer Centre Network, Essen, Germany, [4] Department of Medical Oncology, Sarcoma Center, West German Cancer Center, University of Duisburg-Essen, Essen, Germany, [5] German Cancer Consortium (DKTK), Essen, Germany, [6] Department of Orthopedic Oncology, University Hospital Essen, Essen, Germany, [7] Pediatrics 5 (Oncology, Hematology, Immunology), Klinikum Stuttgart Olgahospital, Stuttgart, Germany, [8] Pediatrics III (Hematology, Oncology, Immunology, Cardiology, Pulmonology), University Hospital Essen, Essen, Germany

OPEN ACCESS

Edited by:
Francesco Cellini, Università Cattolica del Sacro Cuore, Italy

Reviewed by:
Sebastian Dorin Asaftei, Ospedale Città della Salute e della Scienza, Italy
Luc Ollivier, Institut de Cancérologie de l'Ouest, France

****Correspondence:***
Rasin Worawongsakul
rasin.wor@mahidol.ac.th

Specialty section:
This article was submitted to Radiation Oncology, a section of the journal Frontiers in Oncology

Received: *29 October 2021*
Accepted: *11 January 2022*
Published: *16 February 2022*

Citation:
Worawongsakul R, Steinmeier T, Lin Y-L, Bauer S, Hardes J, Hecker-Nolting S, Dirksen U and Timmermann B (2022) Proton Therapy for Primary Bone Malignancy of the Pelvic and Lumbar Region – Data From the Prospective Registries ProReg and KiProReg. Front. Oncol. 12:805051. doi: 10.3389/fonc.2022.805051

Purpose/Objective(s): Multimodality treatments together with local proton therapy (PT) are commonly used in unresectable primary bone malignancies in order to provide better tumor control rate while maintaining good feasibility. The aim of this study is to provide data on outcome of PT for the challenging cohort of pelvic and lumbar bone tumors.

Methods and Materials: This retrospective study includes all patients with primary bone malignancy of the pelvis and lumbar spine receiving PT in our institution between May 2013 and December 2019 enrolled in the prospective registries KiProReg and ProReg collecting information on demographics, treatment, tumor characteristics, toxicities, and outcome.

Results: Eighty-one patients were enrolled with a median age of 19.7 years (1.3–85.8). The median follow-up time was 27.5 months (1.2–83.2). The majority of patients was male (64.2%), ECOG status of 0–1 (75.2%), underwent only biopsy (50.6%), received chemotherapy (69.1%) and was assigned for definite PT (70.4%). The predominant tumor characteristics were as follows: Ewing's sarcoma histology (58%), negative nodal involvement (97.5%) and no metastasis at diagnosis (81.5%). Median maximal diameter of tumor was 8 cm (1.4–20). LC, EFS and OS rate were 76.5, 60, and 88.1% at two years and 72.9, 45.7, and 68.9% at three years, respectively. Age over 20 years was a significant negative factor for LC, EFS, and OS. Metastatic disease at initial diagnosis affected OS and ECOG status of 2–4 affected EFS only. Regarding 17 relapsed cases (21%), isolated distant relapse was the most common failure (46.9%) followed by local failure (40.6%). Eleven out of 14 evaluable patients relapsed within high-dose region of radiotherapy. Acute grade 3–4 toxicity was found in 41 patients (50.6%) and all toxicities were manageable. Late grade 3 toxicity was reported in 7 patients (10.4%) without any of

grade 4. Most common higher grade acute and late side effects concerned hematologic and musculoskeletal toxicity.

Conclusion: Proton therapy resulted in good oncological outcomes when being part of the multimodality treatment for pelvic and lumbar primary bone malignancies. However, distant metastases and local failures within the high-dose region of radiotherapy are still a common issue. Acute and late toxicities of combined therapy were acceptable.

Keywords: Proton therapy, bone malignancy, bone tumor, sarcoma, pelvic, lumbar

INTRODUCTION

Primary bone malignancy is a rare malignant disease (1, 2). Resection is still the main curative local treatment for bone tumors (3), but not all patients are suitable for total tumor removal with adequate margins, especially for tumors of difficult locations as pelvis and lumbar spine (4, 5). Due to the close proximity to important normal structures, complete surgery of the tumor in these regions can cause unacceptable morbidity to patients. However, worse survival rates have been reported in patients not having total resection (3, 5, 6). Thus, radiotherapy will play a major role in these patients to improve local control and survival rates. However, high doses of radiotherapy are needed due to the radioresistant nature of bone tumor potentially leading to relevant toxicity (7–10). One way to minimize this risk for treatment complication is the use of proton therapy (PT). While proton passes through the body of a patient, it releases kinetic energy in the certain depth without any dose exposure to normal tissue distal to this area. The peak of kinetic energy deposited in tissue is called Bragg peak. Due to this physical advantage, PT offers the chance to increasing RT doses while lowering the burden to the surrounding normal tissues (11, 12).

While clinical data on proton therapy in primary bone malignancy of the pelvic and lumbar area is still limited, this study provides clinical tumor outcome, toxicity and pattern of failure after treatment with proton therapy from our prospective registries embedded in a large interdisciplinary sarcoma center and the national study framework.

MATERIALS AND METHODS

Patient Selection

Patients from both the prospective ProReg (Registry number: DRKS00004384) and KiProReg registries (Registry number: DRKS00005363) with primary diagnosis of Ewing's sarcoma, chondrosarcoma, chordoma, osteosarcoma, and osteoblastoma with tumor locations of the pelvis and lumbar spine who started proton treatment in our institution between May 1, 2013 and December 31, 2019 were included in this analysis. Approval of the local ethics committee for ProReg (12-5143-BO) and for KiProReg (13-5544-BO) had been obtained. All patients had signed informed consent for enrollment into the respective registry. Database covered data collection on demographics, treatment, tumor characteristics, survival and toxicities.

General Treatment Approach

All the files of the patients were discussed in a multidisciplinary tumor board with regard to the appropriate treatment decision including surgical approach for each patient before starting PT. The treatment was applied according to the recommendation from the tumor board and European treatment protocols such as the EURO-EWING for Ewing's sarcoma and the EURAMOS for osteosarcoma, respectively. In addition, patients with chordoma and chondrosarcoma were treated according to in-house standard of practice (SOP) (13). In these protocols, wide or marginal resection was recommended for patients if the risk of surgery was manageable and acceptable post-operative morbidity was expected. For histologies such as Ewing's sarcoma, high-graded chondrosarcoma and osteosarcoma, chemotherapy was given to patients according to the protocol. If gross total tumor resection with oncologically appropriate surgical margins could not be achieved or poor response to chemotherapy was reported, radiotherapy was introduced. Therefore, adjuvant radiotherapy was still considered for chordoma and chondrosarcoma patients who achieved gross total (R0 or R1) resection. The radiation dose and volume depended on the extent of resection, histopathology and timing of radiotherapy.

Radiotherapy Concept

Patients were set-up either in supine or prone position depending on dorsal or ventral location of tumor. Immobilization was assured with individually customized vacuum casts. In pelvic tumors, bladder filling protocol, either *via* drinking or suprapubic cystostomy (the latter particularly for pediatric patients), were considered case by case in accordance with the location of tumor. All patients with lumbar tumors were planned for treatment with empty bladder. After performing planning CT with internal or external planning MRI, import and matching of diagnostic MRI at first diagnosis and during course of treatment to the Raysearch (RaySearch Laboratories, Stockholm, Sweden) planning system were done for target volume delineation. GTV1 was contoured according to the initial tumor volume and defined as the tumor bed after adaptation to any geometrical changes. Gross residual tumor at the time of PT was contoured as GTV2. CTV1 was generated from tumor bed plus a CTV margin depending on histology: 1.5–2 cm for Ewing's sarcoma, 1 cm for chordoma and

chondrosarcoma, 2 cm for osteosarcoma and 0.5–2 cm for osteoblastoma. The next level of prescription dose was defined differently according to histology. Whereas CTV2 of chordoma, chondrosarcoma and osteosarcoma was GTV2 (CTV2 = GTV2), CTV2 of Ewing's sarcoma was tumor bed (CTV2 = Tumor bed). No CTV2 was defined for osteoblastoma. Subsequently, additional boost to GTV2 as CTV3 was considered for Ewing's sarcoma patients with gross residual disease (see **Supplementary 1**). Safety PTV margin of 5 mm was used in the pelvic and lumbar location of tumor.

The dose of proton therapy was calculated taking into account the RBE expressed in Gy (RBE), which equals the absorbed dose in Gray of protons multiplied by 1.1. Thus, dose constraints for plan evaluation were all determined in Gy (RBE). Proton treatment can be planned either sequentially boost, which we used homogenous dose and reduced volume for the boost in the later phase, or simultaneous integrated boost (SIB), which we boost to high-risk region simultaneously by using heterogenous dose distribution. Equivalent biological dose was calculated for SIB planning to provide same radiobiological effect as sequential treatment. Dose to organ at risks (OARs) was determined as a maximal dose of 50 Gy (RBE) to spinal cord, maximal dose of 66 Gy (RBE) and mean dose of 55 Gy (RBE) to caudal sac, mean dose 45 Gy (RBE) to femoral heads in adults and 26 Gy (RBE) in children, mean dose of 50 Gy (RBE) to penile bulb and mean dose of testis of 3 Gy. Volume of bowel exposure to a dose of 45 Gy (RBE) or more should be kept below 195 ml. Mean dose of kidneys should be kept below 18 Gy and volume exposure to a radiation dose of 15 Gy or higher should be kept below 65% for one side or below 20–25% for both sides. Volume of bladder and rectum receiving doses of more than 50 Gy should be kept below 60% and 50%, respectively. Whole involved vertebras were covered with at least 20–30 Gy in case of pre-puberty patients to stop bone growth symmetrically and reduce scoliosis in the future.

Staging and Follow-up

For all patients, relevant staging information was requested before treatment. Information included initial, postoperative and recent MRI imaging, surgery reports, general medical report, neurological status, blood count, lung and bone screening and additional investigations if appropriate like rectoscopy, or for bladder and kidney function. All of the patients had clinical base-line evaluation before starting PT. Weekly clinical assessments were performed in all patients during proton therapy. Blood count was requested and performed on a regular basis if chemotherapy was applied or if the field of PT was considered to potentially affect bone marrow. After completion of treatment, all patients should have personal appointment at the institution at 90 days after PT and then yearly on basis. If they were not able or willing to have their check-up in person, written inquiries by questionnaires and telephone interviews were performed. At the same time points, all relevant medical documents and imaging including reports were requested. During COVID-19 pandemic, appointments by telephone without personal visits were suggested.

Pattern of Failure Evaluation

Pattern failure was also reported within the registries. In case of local recurrence, the MRI at time of progression was imported and fused with planning CT in Raysearch planning system. Local failure pattern was scored according to Dawson et al. (14). High-dose region recurrence was defined if local tumor progression of more than 20% in size or relapse was situated with more than 95% volume inside 95% of total cumulative prescription dose. Lower-dose region recurrence was defined if more than 95% volume of relapsed tumor was covered by 95% of the prescription dose for CTV1. Local failure was considered "marginal" if 20 to 95% of recurrent tumor volume was within 95% of the dose to CTV1. If image data at time of progression was not available, it was specifically requested. If finally only report was available, local recurrence was registered but not scored according to type of local recurrence.

Toxicity Evaluation

All toxicities were assessed and graded prospectively according to the Common Terminology Criteria for Adverse Events (CTCAE) version 4.0. All patients were evaluated before the start of PT, weekly during PT and then as explained above. Higher-grade toxicities were defined as CTCAE grade 3 or higher. Whereas acute toxicities were defined as any adverse events occurring during PT and before 3 months after completion of PT, late toxicities were defined as any adverse event occurring since 3 months after completion of PT.

Statistics

This study analyzed data retrospectively. Qualitative data were presented as frequency and percentage, quantitative data was reported as median and range. Follow-up time was calculated from first diagnosis to last contact of patient or death. Overall survival (OS—time from diagnosis to dead of any cause) was the primary objective. Both local control (LC—time from diagnosis to local recurrence or progression) and event-free survival (EFS—time from diagnosis to any event) were the secondary objectives for this study. They were all analyzed with the Kaplan–Meier Method. Any recurrence or death of any cause was defined as an event. After univariate analysis with log-rank test, multivariate analysis for factors which have or tend to have effect on local control, EFS and OS was conducted with Cox regression test, respectively.

All statistical analyses were performed in 95% confidence interval (5% alpha risk) using IBM SPSS Statistics version 27.

RESULTS

Eighty-one patients were eligible for this study. Characteristics of patients are displayed in **Table 1**. Median and mean age were 19.7 and 30.5 years (1.3–85.8 years). The majority of patients were male (64.2%) with good ECOG performance status of 0-1 (71.6%) treated with curative intent (97.5%). The most common histopathology was Ewing's sarcoma family tumor (58%), followed by chordoma (24.7%), chondrosarcoma (7.4%),

TABLE 1 | Patient Demographics, Tumor and Treatment Characteristics.

	N (%)
Number of patients (%)	81 (100)
Mean age at diagnosis (years)	30.5
Median age at diagnosis (years)	19.7
(range)	(1.3–85.8)
≤20 years (n)	42 (51.9)
>20 years (n)	39 (48.1)
Sex	
Female	29 (35.8)
Male	52 (64.2)
ECOG performance status	
0–1	58 (71.6)
2	9 (11.1)
3	11 (13.6)
4	1 (1.2)
Unknown	2 (2.5)
Location of tumor	
Pelvis and sacrum	68 (84)
Lumbar	13 (16)
Histology	
Ewing's sarcoma	47 (58)
Chordoma	20 (24.7)
Chondrosarcoma	6 (7.4)
Osteosarcoma	6 (7.4)
Osteoblastoma	2 (2.5)
Tumor size (median in cm)	8.00
(range)	(1.4–20)
N staging	
N0	79 (97.5)
N+	2 (2.5)
M staging	
M0	66 (81.5)
M+, Lung only	7 (8.6)
M+, Non-Lung	2 (2.5)
Combined	6 (7.4)
Surgery	
Biopsy only	41 (50.6)
R0 resection	12 (14.8)
R1 Resection	3 (3.7)
R2 Resection	19 (23.5)
Rx resection	6 (7.4)
Chemotherapy	
No	25 (30.9)
Any chemotherapy	56 (69.1)
Any concurrent	43 (53.1)
Any before PT	55 (67.9)
Any after PT	45 (55.6)
PT Timing	
First RT course	79 (97.5)
Re-irradiation	2 (2.5)
Location of PT	
Primary tumor	70 (86.4)
Recurrence tumor	7 (8.6)
Primary and metastatic sites	4 (5)
Indication of PT	
Definite	57 (70.4)
Adjuvant	18 (22.2)
Pre-operative	6 (7.4)
Median radiation dose	59.4
(range)	(45–74)
Definite	59.4 (50.4–74)
Adjuvant	55 (45–74)
Pre-operative	50.4 (45–54)
Technique of PT	
Sequential	66 (81.5)
SIB	15 (18.5)
Median interval (range):	
From surgery to PT	147.5 (34–519)
From PT to Surgery	69.5 (20–153)

PT, Proton therapy; SIB, Simultaneous integrated boost.

osteosarcoma (7.4%) and osteoblastoma (2.5%). Tumors were located either in pelvic and sacral sites (84%) or the lumbar region (16%). The median tumor size was 8 cm (1.4 – 20 cm). The majority of patients did not have any nodal involvement (97.5%) or other metastatic disease at time of diagnosis (81.5%). Nodal involvement was found in only 2 patients and all of them were diagnosed with Ewing's sarcoma.

With regard to the surgical approach, the majority of patients underwent only biopsy (50.6%), in 14.8% R0-resection was achieved, whereas in 3.7% R1-resection and in 23.5% R2-resection was confirmed, respectively. Six patients who underwent total resection, resection status could not be categorized either R0 or R1 (Rx). In the present cohort, more than half of the patients received concurrent chemotherapy (53.1%) and even more (69.1%) received some chemotherapy at any time. Regarding all patients in this cohort, 67.9% had chemotherapy before receiving PT and 55.6% received chemotherapy following PT. Despite neoadjuvant chemotherapy, only 12 patients received definite surgery. In eleven of them pathological reports were available. While seven patients of them showed good response (more than 90% necrosis of tumor), in four patients response to chemotherapy was poor. Whereas all patients diagnosed with Ewing's sarcoma and osteosarcoma were treated with chemotherapy according to the respective protocol, none of the chordoma patients or any osteoblastoma patients received any chemotherapy. In chondrosarcoma, however, half of the patients who had high-graded chondrosarcoma with a higher risk for distant metastasis received chemotherapy as part of the multimodality treatment.

With regard to radiotherapy, most patients had 1st course radiotherapy treatment (97.5%) with curative intent. Approximately 86.4% of patients received radiotherapy only at primary lesion for the first course of treatment at initial diagnosis, 5% at both primary and metastatic sites and 8.6% at primary location after recurrence. In 70.4% of the cohort, radiotherapy was given as definite local therapy. Postoperative radiotherapy was given in 22.2% and pre-operative radiotherapy in 7.4% of the patients, respectively. Prescription doses differed according to histopathology, extent of resection and timing of radiotherapy. Median radiotherapy dose of 59.4 Gy in Ewing's sarcoma, 74 Gy in chordoma, 69.3 Gy in chondrosarcoma, 70 Gy in osteosarcoma and 54 Gy in osteoblastoma were applied (see **Supplementary 2**). Sixty-six patients (81.5%) were treated with sequential cone-down technique and 15 patients (18.5%) were treated with SIB technique (**Table 1**).

Median time from surgery to radiotherapy was 147.5 days (34–519) for post-operative treatment, and median time from radiotherapy to surgery was 69.5 days (20–153) for pre-operative radiotherapy, respectively.

Survival

Median follow-up time for all 81 patients in this cohort was 27.5 months (12–83.2 months). Two-year and 3-year OS for all patients in this cohort were 88.1 and 68.9%, respectively. While 2-year and 3-year EFS were 60 and 45.7%, 2-year and 3-year LC were 76.5 and 72.9%, respectively (**Figure 1**). Regarding non-metastatic patients, 2-year and 3-year OS were 89.1 and 77.4%. EFS rates at 2 and 3 years were 60.2 and 48.5%, whereas LC rates at 2 and 3 years were 72.9 and 68.8%, respectively.

Within univariate analysis for the whole cohort (**Supplementary 3**), age older than 20 years displayed an impact on LC and EFS and metastatic disease impacted on OS (**Figure 2**). Furthermore, ECOG performance status of 0–1, tumor of 10 cm in size or lower and any resection of tumor showed borderline significance with regard to superior EFS. Nodal metastases tended to have impact on survival. Accordingly, those factors were analyzed also within multivariate analysis except for nodal metastasis due to very low number of patients on nodal positive arm (n = 2). Within the multivariate testing, age older than 20 years had a significant detrimental effect on LC (HR 8.77, p <0.01), EFS (HR 4.37, p <0.01) and OS (HR 4.8, p = 0.02), respectively. Furthermore, metastatic patients had significantly inferior OS (HR 3.72 p = 0.02) and worse performance ECOG status, scored 2–4, had significantly poorer EFS (HR 2.38, p = 0.04 (**Table 2**). However, we also analyzed correlation between local relapse and surgical status. Whereas, 11 of 41 (26.8%) patients who underwent only biopsy developed local relapse, six of forty patients who underwent any surgery (15%) also experienced local relapse. Anyway, no statistical significant difference was observed between both groups and even in patients who achieved R0-resection, two of twelve patients (16.7%) still experienced local relapse.

Ewing's sarcoma patients represented the largest subgroup in this cohort (n = 47 patients) and were analyzed separately. The results of both 2-year and 3-year LC were 80.2%. Whereas, 2- and 3-year EFS were 61.7 and 50.1%, OS rate at 2 and 3 years were 88.7 and 67.7%, respectively (**Figure 3**). Tumor larger than 10 cm showed negative impact on LC and EFS. While, patient older than 20 years showed poorer EFS rate and patient with nodal metastasis had impact on survival, radiotherapy at primary as initial treatment showed better EFS and OS than radiation after recurrence (**Supplementary 4**). Nodal metastasis was not included for the further multivariate analysis due to the same reason as mentioned before. As a result of multivariate analysis, only significant adverse effect on EFS was found for older age (>20 years of age) (HR 4.51, p <0.01), Tumor of more than 10 cm (HR 4.16, p = 0.02) and radiation for recurrence versus initial therapy (HR 7.59, p <0.01). However, none of the factors showed any significant effect on LC or OS (**Supplementary 5**).

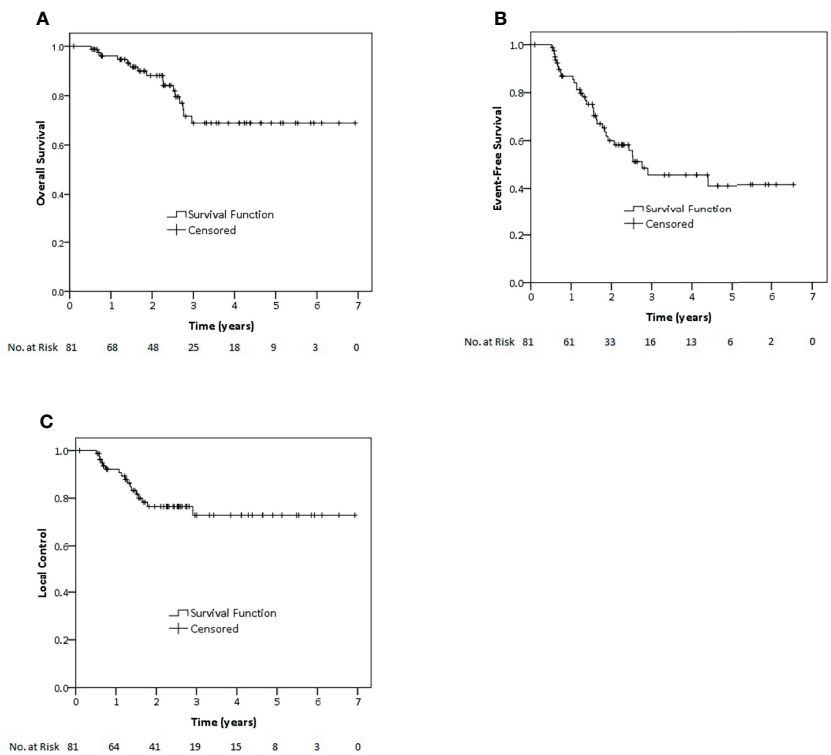

FIGURE 1 | Kaplan–Meier estimates of overall survival **(A)**, event-free survival **(B)** and local control **(C)** rates for all patients of this study.

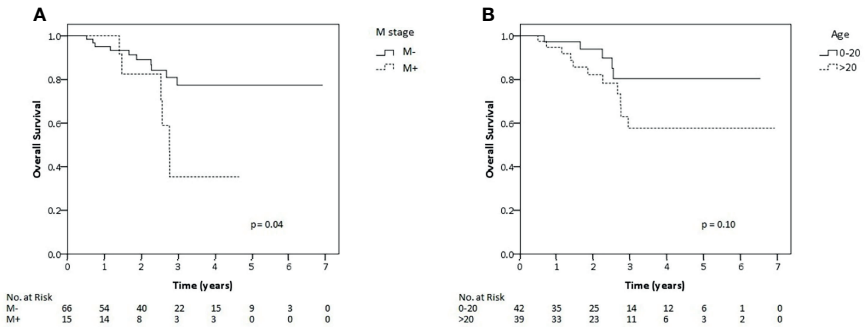

FIGURE 2 | Kaplan–Meier estimates of overall survival rates for all patients of this study according to metastatic status **(A)** and age **(B)**.

TABLE 2 | Multivariate analysis of all patients.

Factors	Local control		EFS		OS	
	HR (95% CI)	p-value	HR (95% CI)	p-value	HR (95% CI)	p-value
Age ≤20 vs >20	**8.77 (1.99–38.66)**	**<0.01**	**4.37 (1.95–9.8)**	**<0.01**	**4.8 (1.31–17.6)**	**0.02**
Performance status 0–1 vs 2–4	2.16 (0.7–6.72)	0.18	**2.38 (1.06–5.34)**	**0.04**	2.26 (0.68–7.55)	0.19
Tumor size ≤10 vs >10 cm	1.18 (0.37–3.78)	0.78	1.54 (0.67–3.53)	0.31	1.91 (0.55–6.59)	0.31
M staging M0 vs M1	0.35 (0.04–2.93)	0.33	1.4 (0.53–3.69)	0.5	**3.72 (1.21–11.44)**	**0.02**
Surgery No resection vs any resection	0.82 (0.28–2.4)	0.71	0.65 (0.31–1.37)	0.25	0.88 (0.28–2.8)	0.83

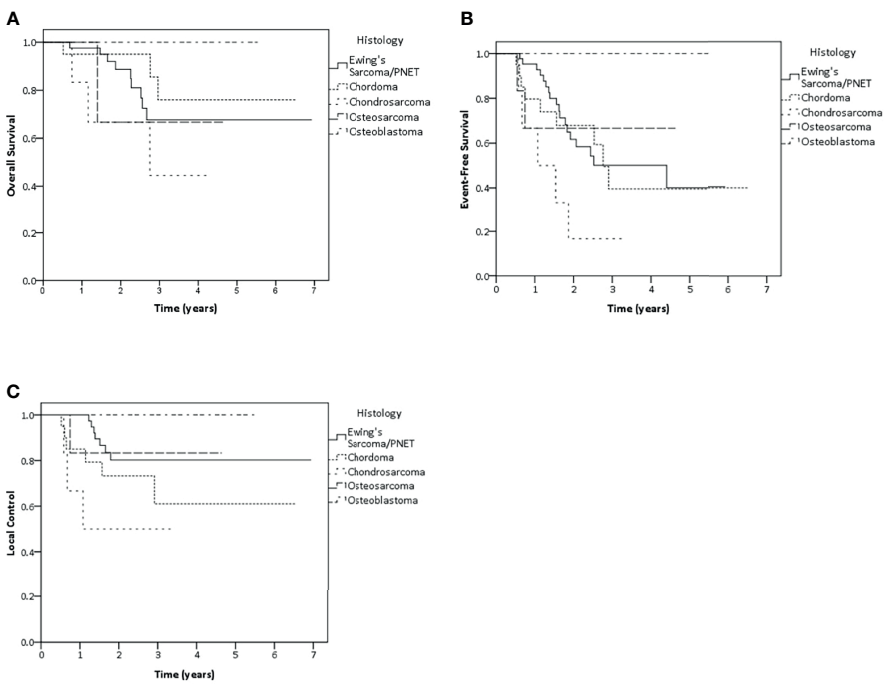

FIGURE 3 | Kaplan–Meier estimates of overall survival **(A)**, event-free survival **(B)** and local control **(C)** rates according to histology.

Concerning other histology, 2-year and 3-year LC rate were 73.2 and 61% in chordoma group. Whereas both 2-year and 3-year LC rate were 50% in chondrosarcoma patients, 83.3% LC rate in osteosarcoma patients and 100% LC rate in osteoblastoma patients were found in both 2 and 3 years (**Figure 3**).

Pattern of Failure

During follow-up, 32 patients experienced progressive disease. The most common cause of progression was distant failure in 15 patients (46.9%), followed by local failure in 13 patients (40.6%) and combined local and distant failure in 4 patients (12.5%), respectively.

Median time to local relapse was 14.7 months (6.2–34.9). Out of the 17 patients experiencing local relapse with or without distant metastasis, in 14 all required information for matching of relapse imaging data with RT plan was available. Eleven (64.7%) had progression or relapse in the high-dose region of PT. Two patients had local failure within the lower dose region and 1 patient had marginal failure of tumor. The later patient unfortunately experienced synchronous extensive metastatic failure, too.

Toxicity

During the course of PT, overall higher-grade acute toxicity was documented in 41 patients (**Table 3**). The most common acute higher-grade toxicity was hematologic toxicity, occurring in 34 patients out of 72 patients having blood counts on a regularly basis. In 15 patients, higher-grade gastrointestinal toxicity, and in 7 higher-grade skin toxicity occurred. Regarding hematologic toxicity, all concerned 34 patients with higher-grade toxicity received chemotherapy before or concurrent to proton treatment. The most common type of hematologic toxicity was leukopenia occurring as grade 3 or 4 in 33 patients. One patient presented with ileostomy before the beginning of the radiotherapy session, which was defined as non-radiotherapy-related grade 4 gastrointestinal toxicity. Three patients needed unplanned hospitalization for reasons other than receiving chemotherapy (due to febrile neutropenia, accident, and hematoma of left knee of unknown cause, respectively). Five patients had more than three days of treatment interruption, either due to toxicity or to machine issues.

TABLE 3 | Acute toxicity report for all patients.

System	N	Grading of toxicity (N)				
		Grade 0	Grade 1	Grade 2	Grade 3	Grade 4
General	81	15	40	24	2	0
Skin	81	2	22	50	7	0
GI	81	41	23	12	4	1
GU	79	52	14	11	2	0
Musculoskeletal	81	60	17	2	2	0
Psychology	31	27	4	0	0	0
Neuro	31	18	10	3	0	0
Hematology	72	14	11	13	18	16
Overall	81	0	8	32	24	17

GI, gastro-intestinal; GU, Genito-urinary.

After radiotherapy, data on late toxicity (**Table 4**) during follow-up was available for 67 patients (82.7%) so far. Higher-grade toxicities were found in seven out of 67 patients (10.4%). The most common toxicity was found regarding the musculoskeletal system for three patients (bone pain in 2, bone deformity in 1).

DISCUSSION

Due to the rarity of primary malignant bone tumors, data on RT are sparse, particularly with regard to modern RT technologies. This study was performed in retrospective manner to provide clinical data of 81 patients treated with modern PT, focusing on primary bone malignancy located in the pelvic and lumbar region. In general, RT for bone tumors is challenging due to the need for high doses at delicate sites. Principally, PT can provide some benefits due to the advantage of physical characteristics in order to spare normal tissue. However, clinical data for proton therapy treatment is still limited today.

When compared to other studies, our patient cohort seems to display unfavorable risk factors. All patients included in this analysis had tumors located in the pelvic and lumbar region, which is known to have worse prognosis when compared to those in the extremities (15–18). Furthermore, majority of our patients had large tumor size which also understood as a negative predicting factor (5, 15) and complete tumor resection was not considered feasible. Some patients also had nodal or distant metastatic disease at diagnosis which considered as high-risk in sarcoma patients. So, chemotherapy and relatively high doses of radiation for treatment were required in majority of patients in this cohort.

Still, the results of the survival analysis were satisfactory in this study. Overall, the results of our study were similar or even somewhat superior when compared to other studies despite the particularly unfavorable cohort we had investigated. Systematic review outcomes of primary pelvic bone sarcoma from 2018 showed 5-year LC of 81.7% and 5-year OS of 55% (19). In addition, Kerr, et al. (2019) studied the treatment outcomes of primary spinal bone malignant tumor and reported 5-year OS in different histological types of primary bone tumor. The best

TABLE 4 | Late toxicity report for all patients.

System	N (%)	Grading of toxicity (N)				
		Grade 0	Grade 1	Grade 2	Grade 3	Grade 4
General	65 (80.2)	31	16	16	2	0
Skin	64 (79)	26	25	13	0	0
GI	65 (80.2)	50	9	4	2	0
GU	62 (76.5)	45	10	6	1	0
Musculoskeletal	66 (81.5)	44	10	9	3	0
Psychology	47 (58)	38	5	4	0	0
Neuro	48 (59.3)	41	5	2	1	0
Hematology	0	0	0	0	0	0
Overall	67 (82.7)	12	19	29	7	0

GI, gastro-intestinal; GU, Genito-urinary.

prognosis was observed in chordoma patients with 5-year OS of 70%, followed by chondrosarcoma with 5-year OS of 69% and Ewing's sarcoma with 5-year OS of 62%. The most unfavorable outcome was reported for osteosarcoma, with only 38% survival rates at 5 years (5). When comparing our study with some surgical series, the results are still very much alike. Laitinen et al. reported 5-year LC and 5-year disease-specific survival (DSS) of 58 and 70.2%, respectively, and 10-year DSS of 62.9% (6). Another surgical series from 2016 reported on patients very high local control and survival at 5 years of 91.3 and 84.4%, respectively (20). However, this surgical series included only 23 patients with some of them having had only benign tumors. Tumor sizes were small and could be resected totally. While in 17 patients (73.9%) negative margins could be achieved, six had contaminated margins; adjuvant radiotherapy was given to seven patients in that study. Supposedly, this was the reason why this study reported favorable treatment outcomes.

Due to Ewing's sarcoma patients being the largest subgroup in this study, we also analyzed outcomes for Ewing's sarcoma treatment separately. Therefore, local control and survival results are comparable to former series reporting 5-year OS of 50.3–73% and 5-year LC of 72–88% (7, 21–23). Only one report from Japan, in which multimodality treatment combined with proton therapy was used, showed substantially higher survival rate at 3 years of 92% and a high local control rate of 89.7% (24). Among all 35 non-metastatic Ewing's sarcoma patients in the Japanese study, five had initially unresectable tumor of more than 8 cm and therefore had to receive higher radiotherapy dose. Whereas one of them received 59.4 Gy, the other four patients received even 64.8 Gy. None of the patients received doses in excess of 59.4 Gy encountered local relapsed of the disease. In our present study, the median total dose for Ewing sarcomas was 59.4 Gy, but in the majority of our cases the tumor was unresectable and had maximal diameter of more than 8 cm tumor. In addition, it included metastatic patients. This could explain the slightly superior treatment results of the Japanese study.

Regarding the outcome of osteosarcomas, our study resulted in high local control and survival rates with LC of 83.3% and both EFS and OS of 66.7% similarly at 2 years and 3 years even though this study had only one patient who underwent gross total surgery. These results are superior when compared to previous reports of pelvic osteosarcoma treated with photons (10, 25). When looking at previous proton therapy studies, findings are comparable (26). However, the number of patients with osteosarcoma in our study was limited and the median follow-up time for osteosarcomas was still limited with 16.4 months (9.3–55.6 months).

We also analyzed the factors potentially influencing on oncological outcome. Older patients have poor prognosis in all oncological outcomes. This negative impact of higher age has already been described in other studies indicating that younger patients have better survival after treatment particularly in Ewing's sarcoma comprising the largest group in our analysis (5, 9, 16, 23). However, there is no definite cut-off level of age and a variety of cut-off levels were used in different studies. In our analysis, we used an age of 20 (young adult) as cut-off. However, we have to acknowledge that in patients of 20 years and more had a higher proportion of pelvic tumor sites (27), while younger cut-off level showed no significant impact on survival in the whole cohort patients. Besides higher age, also metastatic disease showed negative impact on survival in our study. This negative impact on survival outcome was observed across all sarcomas (28–31). Interestingly, also poor performance status was associated with decreased EFS. However, surgery did not show significant better local control or survival in our cohort which might because of insufficient number of patients in subgroup analysis. Among Ewing's sarcoma patients alone, patients who were older than 20 years and tumor larger than 10 cm had worse prognosis for EFS. In accordance with our findings, the negative impact of older age and tumor size on survival has been revealed in other historical studies already (15, 16, 31). However, 8 cm of size which was used in many previous studies and TNM staging did not display any significant impact in our study. Radiotherapy given to the primary tumor for the first course of treatment showed better EFS in Ewing's sarcoma patients when compared to patients who had radiotherapy at time of recurrence or when irradiated for metastatic sites which considered as higher risk disease. Surprisingly, none of the factors impacting on EFS appeared to affect overall survival. However, observation time may be too short to display the effect of the EFS on overall survival.

This study reported on 32 patients having relapsed. The most common pattern was isolated distant failure. However, local failure concerned more than half of all patients with or without dissemination. These results reflect the need for effective local therapy despite the high risk for dissemination for the majority of bone tumors. When highlighting the results of local PT, pattern of relapse with regard to high dose volume seems of particular importance. Our data suggest that the predominant site of failure was inside the high-dose region of PT. Only one patient experienced marginal failure but having synchronous widespread metastasis. Therefore, it is difficult to distinguish local marginal relapse from metastatic disease in this patient. This might be explained by the well-known radio-resistance of primary bone malignant tumors. It may be required to explore even higher dose or hypofractionation in the future to overcome of this radio-resistant nature. Presently, several studies are going to address dose escalation particularly in Ewing tumors with bulky residual disease (32).

Regarding toxicity profile, acute grades 3-4 toxicity were reported in 41 patients. The most common toxicity was hematological toxicity, which is not surprising as 69% of patients in this cohort received chemotherapy. All acute toxicity was manageable. Only three patients needed short-term hospitalization apart from receiving chemotherapy and only 2 patients had more than 3 days of PT interruption due to any toxicity-related. Furthermore, late toxicity of any higher grade was observed in only seven patients but not exceeding grade 3. Even though some data were missing, we still gathered about 82.7% of toxicity reports displaying a low rate of late toxicity so far. Two patients had undefined pain and bone pain, respectively. One patient treated osteosarcoma with total resection and adjuvant PT at age of 17 developed bone

deformity, one patient had neuromotor problems, one patient had urinary incontinence and the last two patients had chronic diarrhea and fecal incontinence, respectively. Despite, one-third of patients received high dose radiotherapy of almost 70 Gy, low rate of late toxicity can be observed. This finding supports the idea of dose escalation of PT in this region can be well-tolerated.

It has to be acknowledged, that this analysis is limited due to its retrospective nature even if data collection within the registry was performed prospectively. Furthermore, selection bias cannot be excluded as the trial was not generated in a randomized fashion against other local therapies. Patients' characteristics were also somewhat heterogeneous and difficult to compare because of the unbalanced nature of the data. In addition, some follow-up data were missing and could not be obtained. For surgical status, the recorded data did not distinguish between R0 or R1 status in some of patients who underwent gross total resection. Another limitation is the relatively small number of patients in our study particularly making statistical analyses difficult. We also have to acknowledge the limited follow-up periods. The median follow-up of this study was 27.5 months, and further investigation after longer follow-up will have to be done. Overall, longer follow-up and a greater number of patients is desirable to provide better evidence in the future.

CONCLUSION

Multimodality treatment of pelvic and lumbar primary bone malignancy combined with proton therapy provided high local control and overall survival rates in a high-risk population despite limited extent of surgery for most of the patients. Isolated distant metastasis was the major cause of failure. However, local recurrence was occurring in more than half of the patients, predominantly situated within the high-dose radiotherapy region suggesting to further exploring dose escalation concepts for subcohorts of high-risk patients. Proton therapy was well feasible on a short term even when combined with chemotherapy and applied to typically large volumes. Therefore, not surprising, hematological toxicity was the most common acute toxicity followed by gastrointestinal toxicity. However, late toxicity has to be considered when applying locally intensive therapy. In our study, late complications were reported in less than 10% of our patients but after limited follow-up time and concerned predominantly musculoskeletal issues.

DATA AVAILABILITY STATEMENT

The original contributions presented in the study are included in the article/**Supplementary Material**. Further inquiries can be directed to the corresponding author.

ETHICS STATEMENT

The studies involving human participants were reviewed and approved by the Ethik-Kommission der Medizinischen Fakultät der Universität Duisburg-Essen. Written informed consent to participate in this study was provided by the participants' legal guardian/next of kin.

AUTHOR CONTRIBUTIONS

RW, TS, and BT contributed to conception and design of the study. RW, TS organized the database. RW performed the statistical analysis. RW wrote the first draft of the manuscript. RW, TS and BT edited the final manuscript. All authors listed have made a substantial, direct, and intellectual contribution to the work and approved it for publication.

SUPPLEMENTARY MATERIAL

The Supplementary Material for this article can be found online at: https://www.frontiersin.org/articles/10.3389/fonc.2022.805051/full#supplementary-material

REFERENCES

1. Stiller CA, Trama A, Serraino D, Rossi S, Navarro C, Chirlaque MD, et al. Descriptive Epidemiology of Sarcomas in Europe: Report From the RARECARE Project. *Eur J Cancer (Oxford England: 1990)* (2013) 49 (3):684–95. doi: 10.1016/j.ejca.2012.09.011
2. Howlader N, Noone AM, Krapcho M, Miller D, Brest A, Yu M, et al. *SEER Cancer Statistics Review, 1975-2018*. Bethesda, MD: National Cancer Institute (2021). Available at: https://seer.cancer.gov/csr/1975_2018.
3. Mukherjee D, Chaichana KL, Parker SL, Gokaslan ZL, McGirt MJ. Association of Surgical Resection and Survival in Patients With Malignant Primary Osseous Spinal Neoplasms From the Surveillance, Epidemiology, and End Results (SEER) Database. *Eur Spine J* (2013) 22(6):1375–82. doi: 10.1007/s00586-012-2621-4
4. Han I, Lee YM, Cho HS, Oh JH, Lee SH, Kim HS. Outcome After Surgical Treatment of Pelvic Sarcomas. *Clinics Orthop Surg* (2010) 2(3):160–6. doi: 10.4055/cios.2010.2.3.160
5. Kerr DL, Dial BL, Lazarides AL, Catanzano AA, Lane WO, Blazer DG 3rd, et al. Epidemiologic and Survival Trends in Adult Primary Bone Tumors of the Spine. *Spine J* (2019) 19(12):1941–9. doi: 10.1016/j.spinee.2019.07.003
6. Laitinen MK, Parry MC, Albergo JI, Umathi VS, Jeys LM, Grimer RJ. Resection of the Ilium in Patients With a Sarcoma: Should the Pelvic Ring be Reconstructed? *Bone Joint J* (2017) 99-b(4):538–43. doi: 10.1302/0301-620x.99b4.Bjj-2016-0147.R1
7. Andreou D, Ranft A, Gosheger G, Timmermann B, Ladenstein R, Hartmann W, et al. Which Factors Are Associated With Local Control and Survival of Patients With Localized Pelvic Ewing's Sarcoma? A Retrospective Analysis of Data From the Euro-EWING99 Trial. *Clin Orthop Related Res* (2020) 478(2):290–302. doi: 10.1097/corr.0000000000000962
8. De Amorim Bernstein K, DeLaney T. Chordomas and Chondrosarcomas-The Role of Radiation Therapy. *J Surg Oncol* (2016) 114(5):564–9. doi: 10.1002/jso.24368
9. Jian BJ, Bloch OG, Yang I, Han SJ, Aranda D, Tihan T, et al. Adjuvant Radiation Therapy and Chondroid Chordoma Subtype are Associated With A Lower Tumor Recurrence Rate of Cranial Chordoma. *J Neuro-Oncol* (2010) 98(1):101–8. doi: 10.1007/s11060-009-0068-1

10. DeLaney TF, Park L, Goldberg SI, Hug EB, Liebsch NJ, Munzenrider JE, et al. Radiotherapy for Local Control of Osteosarcoma. *Int J Radiat Oncol Biol Phys* (2005) 61(2):492–8. doi: 10.1016/j.ijrobp.2004.05.051
11. Wilson RR. Radiological Use of Fast Protons. *Radiology* (1946) 47(5):487–91. doi: 10.1148/47.5.487
12. Cotter SE, Herrup DA, Friedmann A, Macdonald SM, Pieretti RV, Robinson G, et al. Proton Radiotherapy for Pediatric Bladder/Prostate Rhabdomyosarcoma: Clinical Outcomes and Dosimetry Compared to Intensity-Modulated Radiation Therapy. *Int J Radiat Oncol Biol Phys* (2011) 81(5):1367–73. doi: 10.1016/j.ijrobp.2010.07.1989
13. Weber DC, Rutz HP, Pedroni ES, Bolsi A, Timmermann B, Verwey J, et al. Results of Spot-Scanning Proton Radiation Therapy for Chordoma and Chondrosarcoma of the Skull Base: The Paul Scherrer Institut Experience. *Int J Radiat Oncol Biol Phys* (2005) 63(2):401–9. doi: 10.1016/j.ijrobp.2005.02.023
14. Dawson LA, Anzai Y, Marsh L, Martel MK, Paulino A, Ship JA, et al. Patterns of Local-Regional Recurrence Following Parotid-Sparing Conformal and Segmental Intensity-Modulated Radiotherapy for Head and Neck Cancer. *Int J Radiat Oncol Biol Phys* (2000) 46(5):1117–26. doi: 10.1016/s0360-3016(99)00550-7
15. Bosma SE, Ayu O, Fiocco M, Gelderblom H, Dijkstra PDS. Prognostic Factors for Survival in Ewing Sarcoma: A Systematic Review. *Surg Oncol* (2018) 27(4):603–10. doi: 10.1016/j.suronc.2018.07.016
16. Cotterill SJ, Ahrens S, Paulussen M, Jürgens HF, Voûte PA, Gadner H, et al. Prognostic Factors in Ewing's Tumor of Bone: Analysis of 975 Patients From the European Intergroup Cooperative Ewing's Sarcoma Study Group. *J Clin Oncol* (2000) 18(17):3108–14. doi: 10.1200/jco.2000.18.17.3108
17. Donaldson SS, Torrey M, Link MP, Glicksman A, Gilula L, Laurie F, et al. A Multidisciplinary Study Investigating Radiotherapy in Ewing's Sarcoma: End Results of POG 8346. Pediatric Oncology Group. *Int J Radiat Oncol Biol Phys* (1998) 42(1):125–35. doi: 10.1016/s0360-3016(98)00191-6
18. Bielack SS, Kempf-Bielack B, Delling G, Exner GU, Flege S, Helmke K, et al. Prognostic Factors in High-Grade Osteosarcoma of the Extremities or Trunk: An Analysis of 1,702 Patients Treated on Neoadjuvant Cooperative Osteosarcoma Study Group Protocols. *J Clin Oncol* (2002) 20(3):776–90. doi: 10.1200/jco.2002.20.3.776
19. Wilson RJ, Freeman THJr., Halpern JL, Schwartz HS, Holt GE. Surgical Outcomes After Limb-Sparing Resection and Reconstruction for Pelvic Sarcoma: A Systematic Review. *JBJS Rev* (2018) 6(4):e10. doi: 10.2106/jbjs.Rvw.17.00072
20. Sciubba DM, de la Garza Ramos R, Goodwin CR, Xu R, Bydon A, Witham TF, et al. Total En Bloc Spondylectomy for Locally Aggressive and Primary Malignant Tumors of the Lumbar Spine. *Eur Spine J* (2016) 25(12):4080–7. doi: 10.1007/s00586-016-4641-y
21. Yock TI, Krailo M, Fryer CJ, Donaldson SS, Miser JS, Chen Z, et al. Local Control in Pelvic Ewing Sarcoma: Analysis From INT-0091–A Report From the Children's Oncology Group. *J Clin Oncol* (2006) 24(24):3838–43. doi: 10.1200/jco.2006.05.9188
22. Ahmed SK, Robinson SI, Arndt CAS, Petersen IA, Haddock MG, Rose PS, et al. Pelvis Ewing Sarcoma: Local Control and Survival in the Modern Era. *Pediatr Blood Cancer* (2017) 64(9). doi: 10.1002/pbc.26504
23. Chen L, Long C, Liu J, Xing F, Duan X. Characteristics and Prognosis of Pelvic Ewing Sarcoma: A SEER Population-Based Study. *PeerJ* (2019) 7:e7710. doi: 10.7717/peerj.7710
24. Uezono H, Indelicato DJ, Rotondo RL, Mailhot Vega RB, Bradfield SM, Morris CG, et al. Treatment Outcomes After Proton Therapy for Ewing Sarcoma of the Pelvis. *Int J Radiat Oncol Biol Phys* (2020) 107(5):974–81. doi: 10.1016/j.ijrobp.2020.04.043
25. Parry MC, Laitinen M, Albergo J, Jeys L, Carter S, Gaston CL, et al. Osteosarcoma of the Pelvis. *Bone Joint J* (2016) 98-b(4):555–63. doi: 10.1302/0301-620x.98b4.36583
26. Ciernik IF, Niemierko A, Harmon DC, Kobayashi W, Chen YL, Yock TI, et al. Proton-Based Radiotherapy for Unresectable or Incompletely Resected Osteosarcoma. *Cancer* (2011) 117(19):4522–30. doi: 10.1002/cncr.26037
27. Worch J, Ranft A, DuBois SG, Paulussen M, Juergens H, Dirksen U. Age Dependency of Primary Tumor Sites and Metastases in Patients With Ewing Sarcoma. *Pediatr Blood Cancer* (2018) 65(9):e27251. doi: 10.1002/pbc.27251
28. Ferguson JL, Turner SP. Bone Cancer: Diagnosis and Treatment Principles. *Am Family Phys* (2018) 98(4):205–13.
29. Strotman PK, Reif TJ, Kliethermes SA, Sandhu JK, Nystrom LM. Dedifferentiated Chondrosarcoma: A Survival Analysis of 159 Cases From the SEER Database (2001-2011). *J Surg Oncol* (2017) 116(2):252–7. doi: 10.1002/jso.24650
30. Sawamura C, Springfield DS, Marcus KJ, Perez-Atayde AR, Gebhardt MC. Factors Predicting Local Recurrence, Metastasis, and Survival in Pediatric Soft Tissue Sarcoma in Extremities. *Clin Orthopaedics Related Res* (2010) 468(11):3019–27. doi: 10.1007/s11999-010-1398-1
31. Shi J, Yang J, Ma X, Wang X. Risk Factors for Metastasis and Poor Prognosis of Ewing Sarcoma: A Population Based Study. *J Orthopaedic Surg Res* (2020) 15(1):88. doi: 10.1186/s13018-020-01607-8
32. Laskar S, Sinha S, Chatterjee A, Khanna NR, Puri A, Gulia A, et al. Radiotherapy Dose Escalation in Unresectable Ewing's Sarcoma/PNET: Final Results of a Phase III Randomized Controlled Trial. *Int J Radiat Oncol Biol Phys* (2019) 105(1, Supplement):S62. doi: 10.1016/j.ijrobp.2019.06.504

Conflict of Interest: The authors declare that the research was conducted in the absence of any commercial or financial relationships that could be construed as a potential conflict of interest.

frontiers in Oncology

HYPOTHESIS AND THEORY
published: 23 February 2022
doi: 10.3389/fonc.2022.809279

A Novel Radiotherapeutic Approach to Treat Bulky Metastases Even From Cutaneous Squamous Cell Carcinoma: Its Rationale and a Look at the Reliability of the Linear-Quadratic Model to Explain Its Radiobiological Effects

Gianluca Ferini[1†], Paolo Castorina[2,3,4†], Vito Valenti[1], Salvatore Ivan Illari[5], Ilias Sachpazidis[6,7], Luigi Castorina[1], Maurizio Marrale[8,9‡] and Stefano Pergolizzi[10‡]*

[1] Department of Radiation Oncology, REM Radioterapia srl, Viagrande, Italy, [2] Istituto Oncologico del Mediterraneo, Viagrande, Italy, [3] Faculty of Mathematics and Physics, Charles University, Prague, Czechia, [4] Istituto Nazionale Fisica Nucleare, Catania, Italy, [5] Department of Radiation Oncology, Fondazione IOM, Viagrande, Italy, [6] Department of Radiation Oncology, Division of Medical Physics, Medical Centre, Faculty of Medicine, University of Freiburg, Freiburg, Germany, [7] Department of Research & Development, Medical Innovation and Technology P. C., Mesolongi, Greece, [8] Department of Physics and Chemistry, "Emilio Segrè" ATeN Center, University of Palermo, Palermo, Italy, [9] Istituto Nazionale di Fisica Nucleare (INFN), Sezione di Catania, Catania, Italy, [10] Dipartimento di Scienze Biomediche, Odontoiatriche e delle Immagini Morfologiche e Funzionali Università di Messina, Messina, Italy

Introduction: Metastatic cutaneous squamous cell carcinoma (cSCC) is a very rare condition. The lack of definition of an oligometastatic subgroup means that there is no consensus for its treatment, unlike the mucosal head and neck counterpart. Like the latter, the cutaneous form is able to develop bulky tumor masses. When this happens, the classic care approach is just for palliative intent due to a likely unfavorable benefit–risk balance typical of aggressive treatments. Here we proposed a novel radiotherapy (RT) technique to treat bulky metastases from cSCC in the context of an overall limited tumor burden and tried to explain its clinical outcome by the currently available mathematical radiobiological and *ad hoc* developed models.

Methods: We treated a case of facial cSCC with three metastases: two of them by classic stereotactic RT and the other by lattice RT supported by metabolic imaging (^{18}F-FDG PET) due to its excessively large dimensions. For the latter lesion, we compared four treatment plans with different RT techniques in order to define the best approach in terms of normal tissue complication probability (NTCP) and tumor control probability (TCP). Moreover, we developed an *ad hoc* mathematical radiobiological model that could fit better with the characteristics of heterogeneity of this bulky metastasis for which, indeed, a segmentation of normoxic, hypoxic, and necrotic subvolumes might have been assumed.

OPEN ACCESS

Edited by:
Francesco Cellini, Università Cattolica del Sacro Cuore, Italy

Reviewed by:
Stefania Manfrida, Agostino Gemelli University Polyclinic (IRCCS), Italy
Liliana Belgioia, Università di Genova, Italy
Giorgio Russo, National Research Council, Italy

****Correspondence:***
Vito Valenti
vito.valenti@grupposamed.com

[†]These authors share first authorship

[‡]These authors share last authorship

Specialty section:
This article was submitted to Radiation Oncology, a section of the journal Frontiers in Oncology

Received: *04 November 2021*
Accepted: *26 January 2022*
Published: *23 February 2022*

Citation:
Ferini G, Castorina P, Valenti V, Illari SI, Sachpazidis I, Castorina L, Marrale M and Pergolizzi S (2022) A Novel Radiotherapeutic Approach to Treat Bulky Metastases Even From Cutaneous Squamous Cell Carcinoma: Its Rationale and a Look at the Reliability of the Linear-Quadratic Model to Explain Its Radiobiological Effects. Front. Oncol. 12:809279. doi: 10.3389/fonc.2022.809279

Results: We observed a clinical complete response in all three disease sites; the bulky metastasis actually regressed more rapidly than the other two treated by stereotactic RT. For the large lesion, NTCP predictions were good for all four different plans but even significantly better for the lattice RT plan. Neither the classic TCP nor the *ad hoc* developed radiobiological models could be totally adequate to explain the reported outcome. This finding might support a key role of the host immune system.

Conclusions: PET-guided lattice RT might be safe and effective for the treatment of bulky lesions from cSCC. There might be some need for complex mathematical radiobiological models that are able to take into account any immune system's role in order to explain the possible mechanisms of the tumor response to radiation and the relevant key points to enhance it.

Keywords: lattice radiotherapy, tumor control probability (TCP), normal tissue complication probability (NTCP), spatially fractionated radiation therapy, immunotherapy, metabolic tumor volume, bulky tumors, cutaneous squamous cell carcinoma

INTRODUCTION

The main aim of reporting this experience is to inform insiders about the possibility to safely and aggressively irradiate difficult-to-treat bulky tumors, even large metastases from cutaneous squamous cell carcinoma (cSCC), with a particular radiotherapeutic option. An interpretation of its clinical results is provided, as well as of its ambiguities, likely needing new radiobiological investigations.

Facial cSCC is one of the most frequent skin cancers, especially among elderly patients who most commonly report a history of prolonged occupational exposure to ultraviolet radiation from sunlight (1). It is able to develop disfiguring and ulcerating bulky lesions and regional lymph nodes and, occasionally, distant metastases through the bloodstream (2). Oligometastatic status was described for the mucosal counterpart of the head and neck squamous cell carcinoma (HNSCC), but not for its cutaneous form (3). However, these two variants are often grouped together in some cancer registries (4, 5) and share some chemo- and immunotherapy regimens in locally advanced/metastatic stages (6). The rarity of the metastatic disease and the low risk of cancer-specific death for cSCC (7) do not allow to rule out the existence of an oligometastatic stage whereby radiotherapy (RT) could be employed with a curative purpose, as it has been successfully done for other metastatic cancers by adopting the stereotactic approach (8–10). Moving from a low palliative radiation dose prescription toward a higher radical one causes some concerns about normal tissue tolerance, especially for the treatment of bulky tumors. Spatially fractionated RT (SFRT), specifically lattice RT, overcomes such an issue by delivering a highly heterogeneous radiation dose to large targets in order to spare the neighboring organs at risk (OARs) (11). Such a peculiar dose delivery method could face the typical non-homogeneous tumor growth by selecting the hypoxic regions to be boosted for overcoming their relative radioresistance (12). In these scenarios, choosing the best dose prescription could be very difficult for the radiation oncologist who must strike a balance between an optimal tumor control probability (TCP) and an acceptable NTCP (13). Actually, the classic RT protocols can be unable to achieve a clinical complete response (cCR), likely due to a radiation dose insufficient to eradicate any residual cancer cell (14). Tumor behavior may be described by mathematical models, as regards both the initial cancer cell proliferation and the repopulation dynamics following the oncologic treatments. Some of these models, including the popular linear-quadratic (LQ) one, can assist the radiation oncologist in the radiobiological determination of dose escalation to improve TCP, as well as of the most suitable fraction size and interval to avoid normal tissue damage (15).

Here we report a case of metastatic facial cSCC with three separate distant lesions, two of which were radically treated with stereotactic body RT (SBRT) and the remaining one with lattice RT (**Figure 1**). For the latter case, we present four different treatment plans that are inter-compared by dose volume histograms (DVHs). Furthermore, in order to evaluate the effectiveness of each plan, TCP values according to Poisson's model as well as NTCP distributions according to the Lyman–Kutcher–Burman (LKB) model were calculated. Furthermore, we developed a numerical analysis based on the cell regrowth model to try to explain some aspects of the observed clinical outcome taking also into account the tumor heterogeneity.

CASE PRESENTATION

A 75-year-old patient with no significant comorbidities was submitted to surgical removal of a growing reddish and hard skin nodule located on the inner canthus of the left eye in December 2017. The histology report showed a moderately differentiated cSCC, which was totally resected with negative margins (R0). No adjuvant therapies were deemed necessary since it was an early-stage cancer. Long-term follow-up was negative up to February 2021, when the patient required medical attention due to the appearance of a suspicious red, painful, and

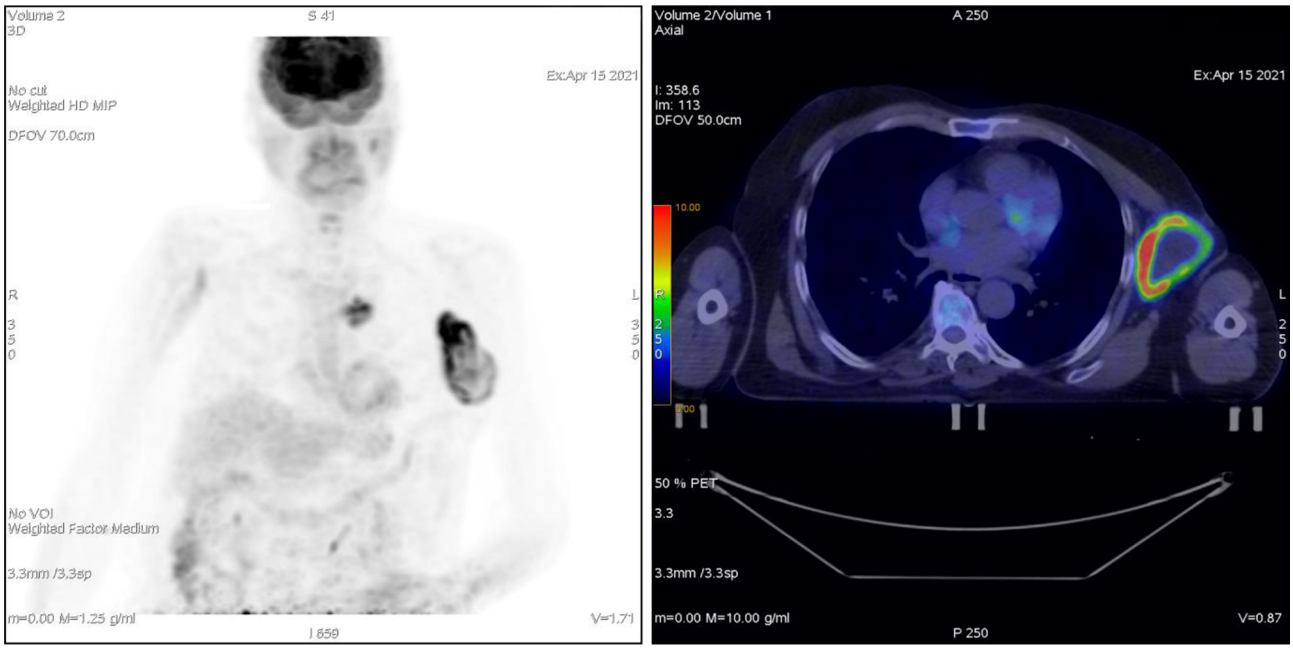

FIGURE 1 | Patient ^{18}F-FDG PET at presentation.

semi-soft lump in the left axilla. The nature of such a lesion was then clarified by means of a needle biopsy, which found the same histology of the previous facial tumor. A complete head and neck clinical workup (i.e., physical and fiber-optic examination) allowed us to exclude a mucosal origin. A contrast-enhanced CT scan showed that the palpable axillary lump was just the tip of an inhomogeneous bulky lesion with a semi-fluid core [maximum diameter was 10.4 cm, volume 171.3 cm^3, Hounsfield units range −115 to 24.4 (± 17.3)] and revealed two further lesions: one was lymphadenopathy of 2-cm diameter located at the II left Robbins level of the neck and the other was a painless metastasis of 3.5-cm diameter at the second left sternocostal joint. An ^{18}F-FDG PET confirmed the three sites of metastatic disease. The axillary bulky lesion had a highly inhomogeneous radioactive tracer distribution due to the presence of a "photopenic area" (SUVmean 0.9) in the inner region, corresponding to the low-density area [Hounsfield units range −100 to 22.9 (± 13.8)] on the CT image: such characteristics suggested a necrotic core, surrounded by a super-avid actively proliferating thick ring, in a way that we were able to segment two subvolumes for this lesion (**Figure 1**). We attributed such differences to a heterogeneous oxygen landscape within the tumor. Consequently, we named three concentric subvolumes (**Figure 2**): the innermost was the "necrotic core" (86.8 cm^3), the outermost was the "normoxic subvolume" (71.5 cm^3), and the transitional mid-layer was arbitrarily established as the "hypoxic subvolume" (13 cm^3) in an analogous way as previously done by Tubin et al. (16). The latter volume was derived from a 2-mm isometric expansion of the clinically detected necrotic area from which then a ring-shaped subvolume has been subtracted. We considered the disease as in oligometastatic status and proposed an aggressive treatment, keeping us away from a purely palliative intent. The two smallest lesions were treated with SBRT for a total dose of 30 Gy in five consecutive daily fractions of 6 Gy. We deemed the bulky axillary lesion as not approachable by SBRT due to its exceeding size. Therefore, we decided to treat this lesion with SFRT by using a single-shot dose of 15 Gy precisely conformed to five small vertices, followed by 30 Gy in 10 daily fractions of 3 Gy delivered to the entire gross volume. The patient completed the RT schedule in 17 days in total (from April 21 to May 7) with no toxicity. An ^{18}F-FDG PET was performed 1 month later for a very early assessment of tumor response to treatment: according to the PERCIST criteria (17), the neck node was stable, sternocostal metastasis had a partial response (PR), and the bulky axillary lesion had a complete response. The co-registered CT scan documented stable disease for the lymphadenopathy, a slight increase in the skeletal lesion (still fitting the RECIST criteria for stable disease), and a smaller residual liquid-like axillary mass without any solid component all around (**Figure 3**). Five weeks after completion of RT, the patient started systemic treatment with cemiplimab (350 mg i.v. q3weeks administered by intravenous infusion over 30 min). After 15 weeks from the start of cemiplimab (20 weeks after the end of RT), an ^{18}F-FDG PET/CT was performed for a new assessment of tumor response, showing a complete response in both neck node and sternocostal metastases; the axillary lesion maintained a complete absence of pathological metabolism. On a co-registered CT scan, a further reduction in the size of the axillary mass was detected (from the initial size mm 70 × 46 ×

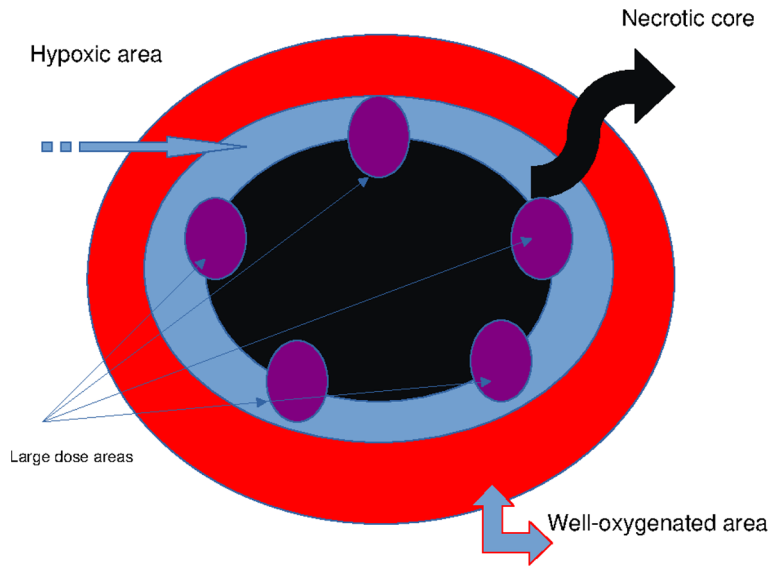

FIGURE 2 | Schematic representation of the axillary GTV: necrotic core (black), mitotic area (red), whole hypoxic area (blue), and vertices targeted by large dose boost (purple). GTV, gross tumor volume.

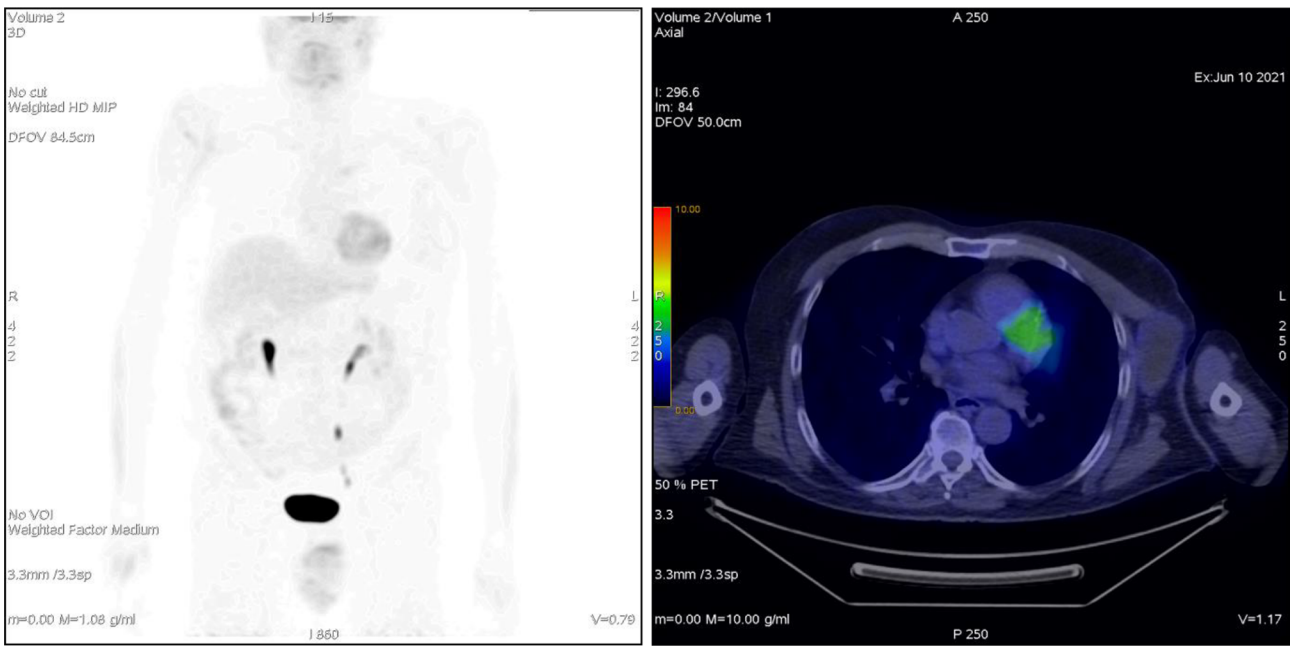

FIGURE 3 | Patient ^{18}F-FDG PET 1 month after treatment.

104 to mm 52 × 35 × 83) (**Figure 4**). At the last follow-up, October 29, 2021 (after 25 weeks from the end of irradiation), the patient developed no treatment-related toxicity and complete pain relief in the axillary site. Cemiplimab was well-tolerated. The patient's timeline is shown in **Figure 5**.

METHODS

Target Volume Definition

A neck and thorax 1.25-mm thickness slice CT simulation without contrast medium was performed after modeling a

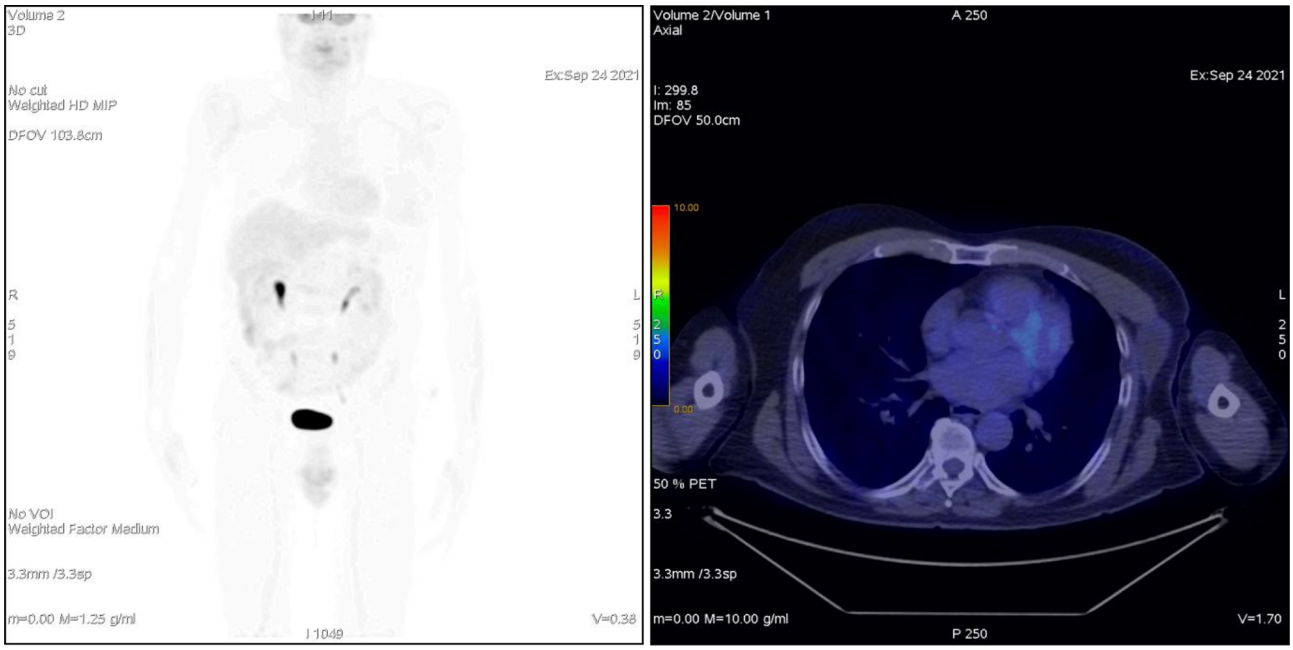

FIGURE 4 | Patient ^{18}F-FDG PET at 4.5 months after treatment.

thermoplastic mask on the patient for immobilization of the head, neck, and shoulders in a reproducible setup. Regarding the metabolic imaging, PET/CT scans were acquired with a GE Discovery five-ring PET tomography 50 min after i.v. of 185 MBq of ^{18}F-FDG and processed with software Q Clear. Thanks to this software, it was possible to calculate not only the SUVmax and the SUVmean but also the metabolic tumor volume (MTV) and the total lesion glycolysis (TLG = MTV × SUVmean).

For the left axillary site, the gross tumor volume (GTV) was the entire bulky lesion as defined on the CT scan. We contoured three concentric subvolumes: the innermost was the "necrotic core" (86.8 cm^3), the outermost the "normoxic subvolume" (71.5 cm^3), and the transitional mid-layer was arbitrarily established as the "hypoxic subvolume" (13 cm^3) (**Figure 6**). The vertices were five spheres of 1-cm diameter, astride the boundary between the metabolically active external ring and the necrotic core, that is, where a transitional hypoxic zone may be assumed. The other two GTVs (neck lymph node and sternocostal joint) were defined on the CT images with the support of an ^{18}F-FDG PET. Three clinical target volumes (CTVs) were created by an isometric expansion of 0.5 cm for each GTV in order to target also the subclinical disease around the macroscopic one.

Treatment Planning

For the axillary bulky lesion, three couple of plans were generated using Treatment Planning Software Eclipse® (version 13.7.14 powered by Varian) in a Volumetric Modulated Arc Therapy (VMAT) technique; the treatment unit used for this work was a Novalis-TrueBeam STx linear accelerator equipped with a high-definition multi-leaf collimator (MLC) and an X-ray image guidance system including a six degrees of freedom robotic couch (ExacTrac, BrainLab®, Munich, Germany). The high-dose vertex volume was arbitrarily configured using five spherical high-dose vertices with a diameter of 1.0 cm placed within the GTV and with at least 2.0 cm of separation (center to center). The optimized monoisocentric plan resulted in at least 99% of the prescribed dose covering 100% of each vertex volume (D100vertex ≥ 14.85 Gy).

Each couple of plans was made a planned sum.

The four plans were named as follows:

Plan A: 30 Gy in 10 daily fractions of 3 Gy each to the CTV (**Figure 7**), every time summed up to one of the following three.
Plan B: 15 Gy to the GTV in one fraction (**Figure 8**).
Plan C: 15 Gy to the hypoxic ring in one fraction (**Figure 9**).
Plan D: 15 Gy to the vertices in one shot (**Figures 10**, **11**).

For each plan, 2 half coplanar arcs (0°–179° CW/CCW) were used with jaw tracking technique, i.e., a specific technique that was provided by the Varian TrueBeam series (Varian, Crawley, UK), where the jaw can track the aperture of the MLC to reduce the leakage and transmission and thus reduce doses to normal tissues around the tumor.

For the other two disease sites, the above equipment and procedure were used for delivering an SBRT treatment with a dose of 30 Gy in five daily fractions of 6 Gy each.

The algorithm used for the plans was Anisotropic Analytical Algorithm (AAA version 13.7.14).

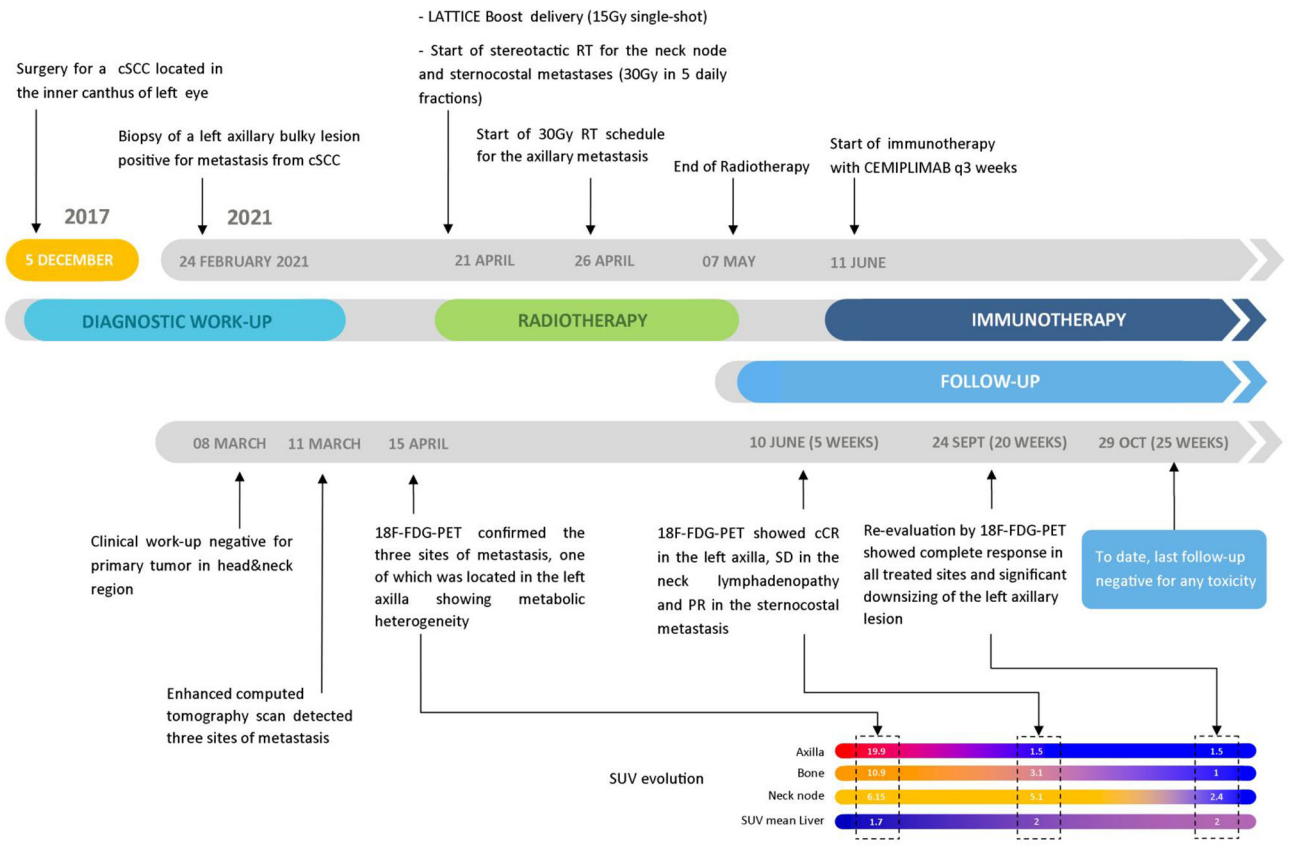

FIGURE 5 | Patient's timeline from the beginning of the disease to the last follow-up accompanied by the SUV evolution of the ^{18}F-FDG PET scans through the various steps.

Numerical Analysis

Computational analyses were performed in order to evaluate the ability of tumor control and the risk for OARs for the various plans considered.

In particular, two independent analyses were carried out: 1) calculation of the TCP using Poisson's model (empirical model) and the NTCP adopting the LKB model; 2) *ad hoc* developed radiobiological model considering the different regions present within the tumor.

Tumor Control Probability and Normal Tissue Complication Probability Modeling

Structure sets and calculated three-dimensional (3D)-dose matrices of the RT plans were exported as DICOM files.

In order to calculate the TCP and NTCP values, the equivalent dose in 2 Gy per fraction, EQD_2, was evaluated using the following expression:

$$EQD_2 = D\left(\frac{d + \alpha/\beta}{2 + \alpha/\beta}\right)$$

where D is the total dose in Gy, d is the dose per fraction, and α/β is the ratio of linear to quadratic cell killing probability according to the LQ model. In particular, for a tumor, the value of α/β=10.5Gy was used (18), and the values of α/β=8.8Gy (19) and α/β=3.5Gy (20) were adopted for the skin and chest wall, respectively. Since the spatial resolutions of the various plans considered were not identical, all plans were re-sampled to the highest resolution ($1.5 \times 1.5 \times 1.5$ mm^3).

TCP was calculated based on the LQ Poisson's model (21, 22) through the use of the pyradiobiology software (23, 24). The values of the parameters TCD50 and γ are those for head and neck squamous cells, at 51.77 Gy and 2.28, respectively (25).

For NTCP calculation for the skin and chest wall, the LKB model was applied (26). The parameters adopted for these calculations are n = 0.1, m = 0.21, and TD50 = 68.00 Gy for the case of pathological fracture of the chest wall and n = 0.1, m = 0.12, and TD50 = 70.00 Gy for the case of necrosis/ulceration of the skin (27).

Ad Hoc Radiobiological Model

The above-described analysis does not completely take into account the heterogeneity of the tumor region, and, therefore, the reliability of TCP values is limited. For this reason, a numerical radiobiological model able to consider various aspects of the complexity of the system was provided.

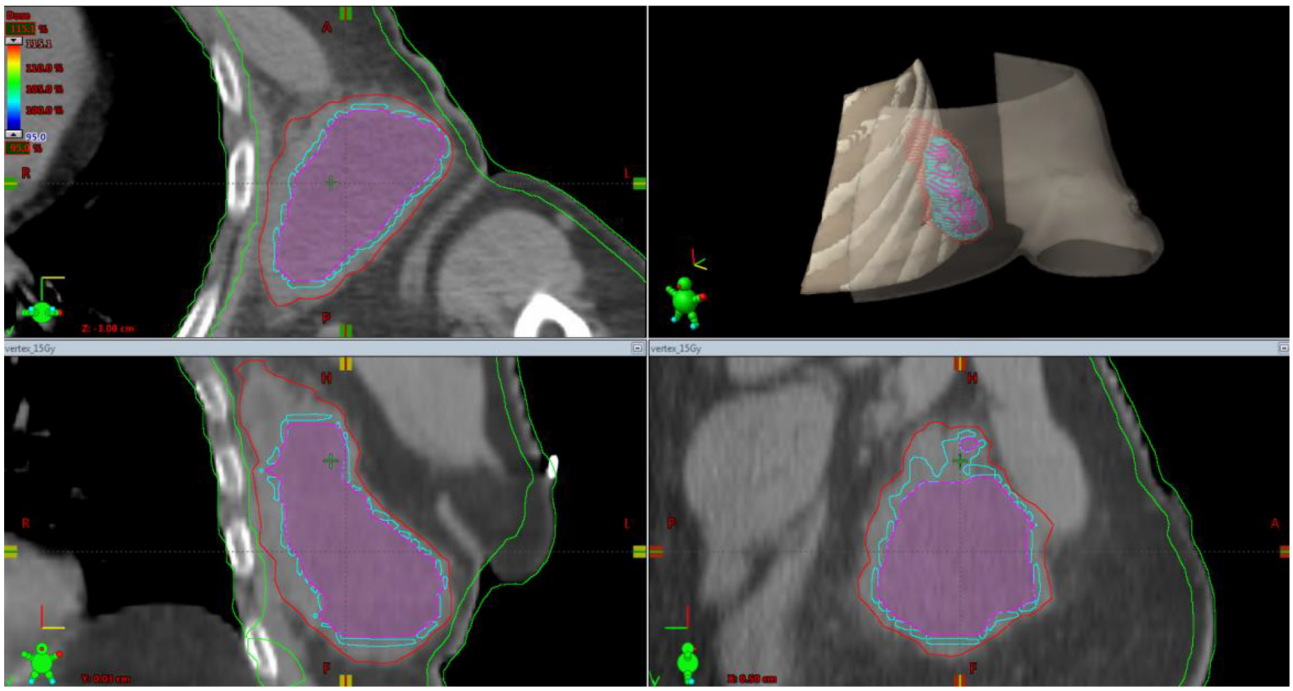

FIGURE 6 | Simulation CT scan images in the axial (top left), coronal (lower left), sagittal (lower right) planes. In the top right picture, a 3D rendering of the spatial relations of target subvolumes with the skin and chest wall (portions included in the NTCP calculation) is shown. The purple line encloses the necrotic subvolume, the light-blue one represents the hypoxic ring, the red line contains the gross tumor volume, and the green lines are for OARs, i.e., chest wall and skin. NTCP, normal tissue complication probability; OARs, organs at risk.

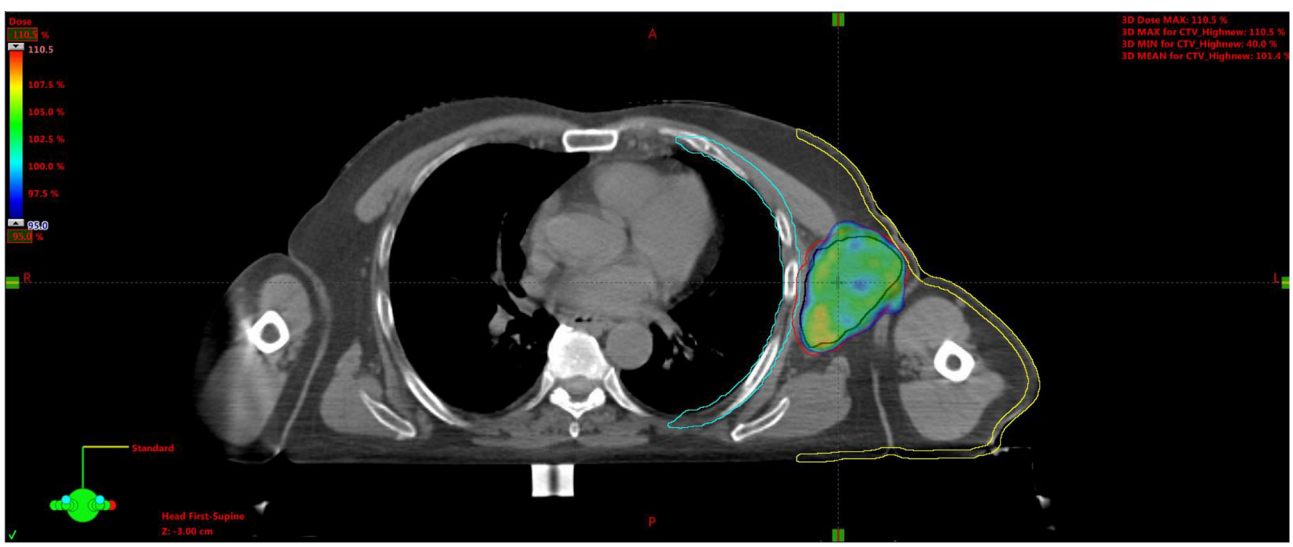

FIGURE 7 | Plan A: 30 Gy to the entire CTV. Black line is for GTV, red for CTV, light-blue for the chest wall, and yellow for the skin. CTV, clinical target volume; GTV, gross tumor volume.

The proposed analytic method proposed to analyze the different radiobiological treatments is based on the following points:

I. Tumor spheroid approximation since the volumes of the cell subpopulations are more relevant than their shapes;
II. The radiation effect is described by the LQ model;

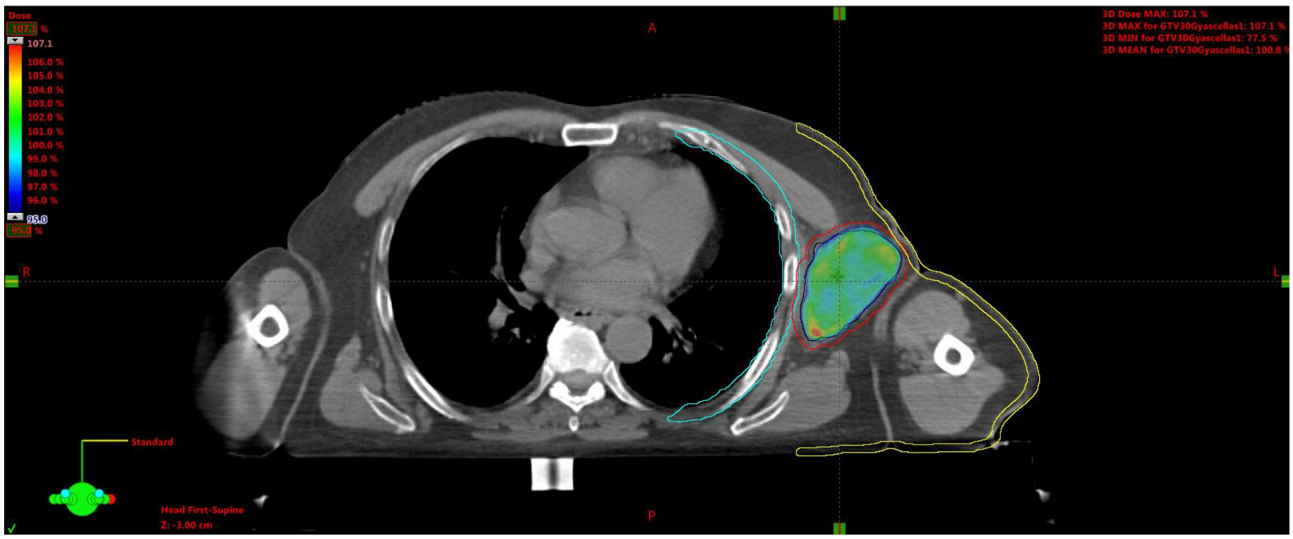

FIGURE 8 | Plan B: 15 Gy to the GTV. GTV, gross tumor volume.

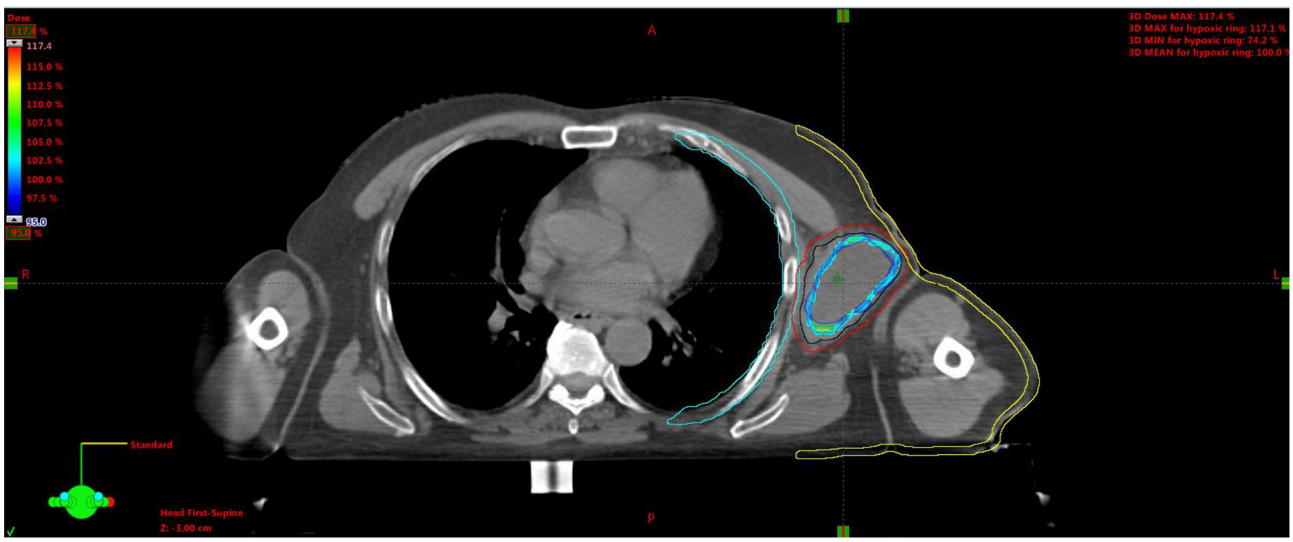

FIGURE 9 | Plan C: 15 Gy to the hypoxic ring (light-blue area).

III. The radioresistance of the hypoxic area is taken into account by the oxygen enhancement ratio (OER) approach;
IV. The vertices are localized in partial overlap with the necrotic and hypoxic volumes;
V. The effects of the initial large dose (15 Gy) on the normoxic and hypoxic cells is described by average doses;
VI. 10 daily doses of 3 Gy follow the initial treatment.

The detail of the calculations is reported in **Supplementary Material 1**, and the final results compare (see *Discussion*) different methods of delivery of the large initial dose.

RESULTS

The effectiveness in tumor control and damage to healthy tissues was evaluated for the four different RT approaches by means of the two numerical studies mentioned above.

The analysis was performed *via* the pyradiobiology software, which calculates the TCP using Poisson's model, and the NTCP adopting the LKB model. The results are reported in (**Table 1**).

From this analysis, it is evident that NTCP for the chest wall for Plan D (lattice) is comparable to that for Plan A (30 Gy in 10

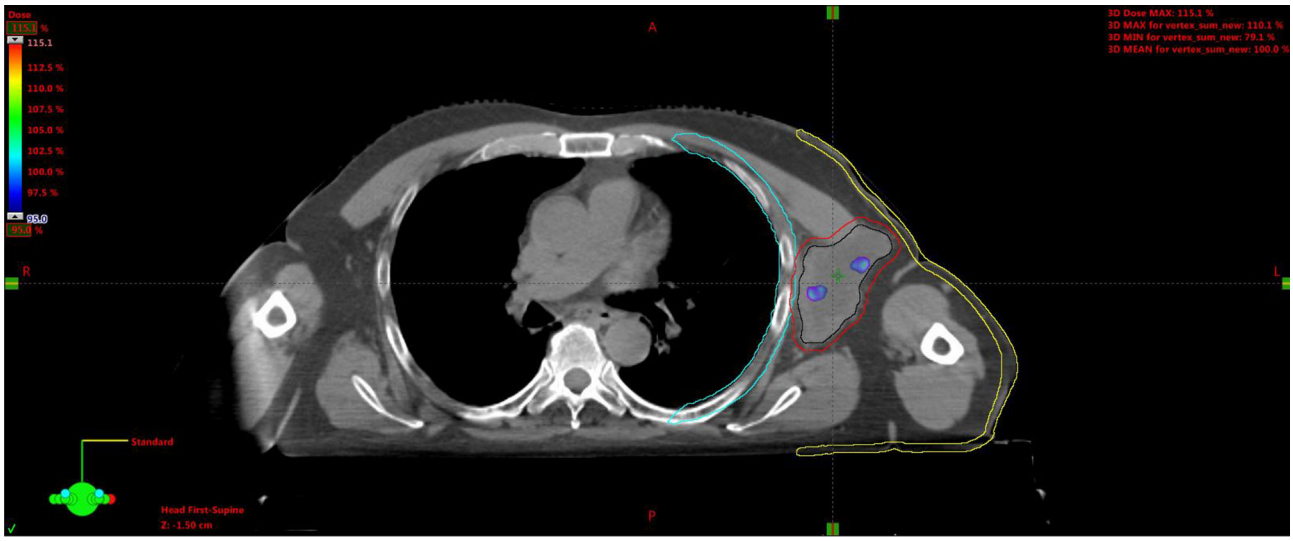

FIGURE 10 | Plan D: 15 Gy to the vertices (red circles).

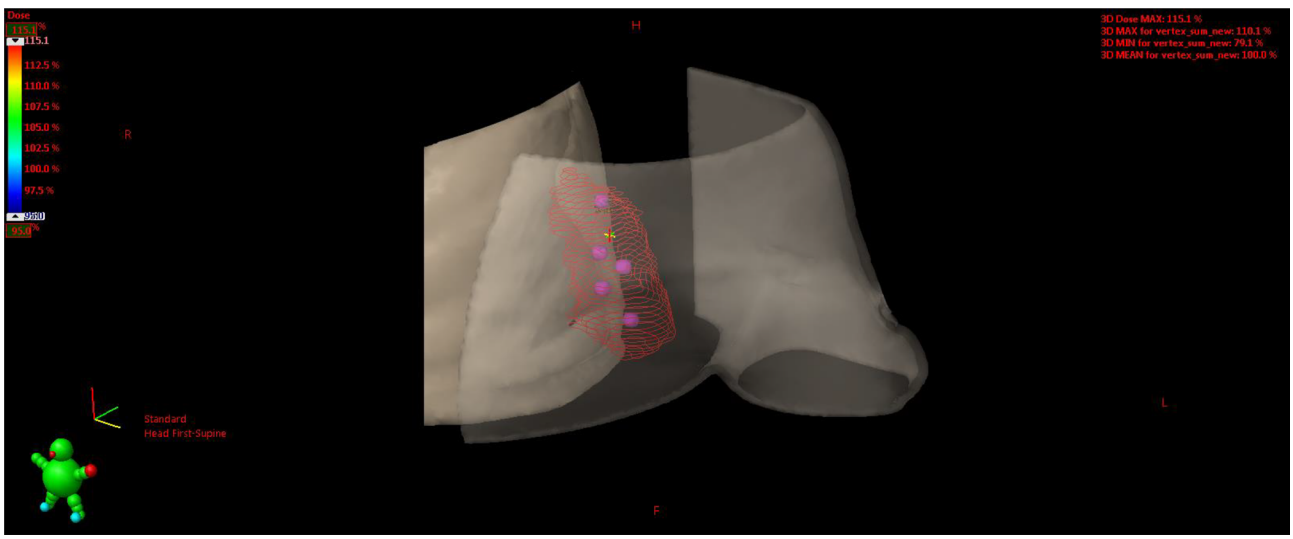

FIGURE 11 | 3D rendering of vertices within the GTV enclosed between the skin and chest wall. GTV, gross tumor volume.

fractions), and it is an order of magnitude smaller than that for Plan C (which is a combination of SBRT-PATHY as employed by Tubin et al. and a sequential palliative 30-Gy dose in 10 fractions of 3 Gy/day to the entire tumor volume) and 2 orders of magnitude smaller than that for Plan B (a single dose of 15 Gy homogeneously delivered to the entire tumor volume followed by 30 Gy in 10 fractions of 3 Gy/day).

Analogous behavior is observed for NTCP values related to skin exposure. Therefore, the lattice configuration of irradiation allows sparing healthy tissues better than hypoxic ring irradiation (Plan C) and entire volume irradiation (Plan B).

Regarding TCP analysis, Plan B is characterized by a high value (i.e., 87%), and this is related to the total volume irradiation with preliminary 15-Gy exposure, whereas in the case of Plan C (hypoxic ring irradiation), this probability is more than halved, and in the case of lattice irradiation (Plan D actually delivered to the patient), it is equal to about 3%. In order to consider also the heterogeneity of the tumor regions and to further model the response of this tumor to the RT procedure chosen, plans C and D were compared by means of an *ad hoc* developed radiobiological model, providing the respective cancer cell survival probability (CCSP) predictions. For such models, we used the α, β, and α/β values for cSCC suggested by van Leeuwen

TABLE 1 | TCP values for tumor cells and NTCP values evaluated for the chest wall and skin.

	TCP Tumor	NTCP Chest Wall	NTCP Skin
Plan A	0.030	0.00040	$2.0 * 10^{-9}$
Plan B	0.870	0.020	0.000015
Plan C	0.400	0.0076	0.000013
Plan D	0.032	0.00047	$2.3 * 10^{-9}$

Plan A: 30 Gy/10 fractions to GTV. Plan B: 15 Gy/1 fraction to GTV. Plan C: 15 Gy/1 fraction to "hypoxic ring." Plan D: 15 Gy/1 fraction to 5 vertices.
TCP, tumor control probability; NTCP, normal tissue complication probability; GTV, gross tumor volume.

et al. (28). The numerical analysis in **Supplementary Material 1** carried out a detailed quantitative comparison between methods C and D, by evaluating the survival fraction before and after the standard treatment for the normoxic and hypoxic subpopulations. The results are reported in **Tables S2**, **S3** (**Supplementary Material 1**) where you can observe that the initial radiation dose of 15 Gy delivered to the whole hypoxic area (model C), rather than to the vertices (model D), gives a smaller survival probability, i.e., a better tumor control, but with a very large average dose (Dmean_normoxic_subvolume equal to 10.44 Gy for Plan C and to 4.3 Gy for Plan D) distributed in the nearby normoxic area.

DISCUSSION

Background and Radiobiological Issues

This case report presents a novel technique to treat bulky tumors, generally treated with palliative-only RT. The peculiarity of the RT technique here presented is mainly linked to the ability to deliver high radiation doses to small areas of the GTV, so that radiation oncologists can treat with a higher total dose the GTV as compared to other techniques using lower homogeneous radiation doses due to the close proximity of OARs. Furthermore, as regards the treatment planning, this is no more difficult than the other volumetric plans; it is likely more time-consuming because the radiation oncologist has to choose the vertex positioning within the GTV and to co-register PET/CT images with simulation CT images. Finally, the time to deliver radiation doses to the vertices is no different than that of other modulated/stereotactic techniques. The palliative radiation approach could not achieve a satisfying TCP, thus adversely affecting the patient survival chances. This issue is particularly relevant when a large mass develops in the context of an overall limited tumor burden, as in the present case, where it is reasonable to expect a better outcome than a multimetastatic setting (29–32). Currently, the oligometastatic disease is effectively treated by stereotactic RT, that is, with an approximately homogeneous radiation dose delivered to the entire tumor volume (33). Such an approach would appear to allow a deferral in the use of aggressive chemotherapy regimens even among those patients affected by oligometastatic mucosal HNSCC (34). The advanced and/or metastatic cSCC counterpart may be treated with targeted therapies, but such a consideration does not rule out a key role for ablative RT (35, 36), not yet extensively tested due to the low rate of metastatic disease (37). However, bulky masses could not be treated with high-dose stereotactic RT without exceeding the normal tissue tolerance (38). Alternative solutions to deliver ablative radiation doses are under study, and SFRT is among them (39). Such a method is supposed to trigger a killing bystander effect (**Figure 2**) on the underdosed tumor subvolumes (40). Bulky tumors are characterized by a heterogeneous oxygen supply that generates an alternation of well-oxygenated proliferating areas and hypoxic "dormant" areas. Notoriously, tumor hypoxia represents the main obstacle to the full effectiveness of RT (41). For a given dose, such a condition increases the cancer cell survival fraction both *in vitro* and *in vivo*. This issue may occur for two reasons: 1) due to a spatial limit of oxygen diffusion to cells that are more distantly located from newly formed vessels during disordered neoangiogenic sprouting or 2) to a transient mechanic occlusion of such capillaries because of endothelial cell abnormalities, starving harder the innermost cells. Both phenomena determine a significant reduction in the partial pressure of oxygen (pO_2) that, for the aforesaid reasons, is inhomogeneous within the tumor tissue. Considering that the oxygen path is mostly stopped at a depth from the vessel of 100–200 μm, it explains how, beyond this threshold, cell cascades culminating in necrosis may be triggered (42). Thus, it is not infrequent to find a necrotic core surrounded by a vital cell ring. It is reasonable to assume that between normoxic and necrotic areas, hypoxic cell clones exist. These cells, for example, through—but not only—the hypoxia-inducible factor 1α (HIF-1α) signaling pathway, develop a metabolic adaptation to hypoxia and survive (43). They may be not actively proliferating but still viable and able to escape from the radiation effects. In fact, oxygen enhances free radical formation and fixes chemical damages induced by ionizing radiations, especially double-strand DNA breaks. The variability of cell survival rate at different levels of pO_2 is summarized by the OER parameter. Therefore, oxygen deprivation, by increasing tumor cell survival, could impair oncologic outcomes, such as local control (LC) and, consequently, also overall survival (OS). Indeed, the clearance of normoxic cells by radiation could recruit previously hypoxic cells to be exposed to a better promitotic pO_2, thus enhancing their proliferative and metastatic potential. Such cell behavior is at the root of radiation dose fractionation in clinical practice. In fact, the tumor redox landscape constantly changes in parallel with variations in cellular density (44). However, total removal of all cells is not always achievable. This applies especially to bulky tumors whose absolute number of hypoxic cells may be very high. In this scenario, another issue becomes evident: as expected, the unintended dose delivered to nearby healthy tissues (OARs) increases when the target volume increases due

to a deleterious dose–volume effect (45). Then, radiation oncologists face daily this dose-limiting factor associated with a poor radiosensitivity of the hypoxic components. To counteract the depletion of tumor oxygen, various strategies such as the use of radiosensitizers have been tested to improve the therapeutic ratio of radiation dose. Unfortunately, practical results have not always confirmed the theoretical assumptions, likely because the topic is even more complex (46). Regarding the dose fraction size, it is known that large ones could overcome hypoxia-related radioresistance, but these could not be easily deliverable in a uniform manner to the entire tumor due to the aforementioned dose–volume effect that puts a strain on the tolerance of neighboring OARs. A compromise solution could be to deliver a high radiation dose/fraction solely in some tumor subvolumes, namely, the hypoxic ones. This is the actual basis for oxygen-guided RT. This novel concept is based on the detection of hypoxic subvolumes within tumor tissue for a selective radiation boost while limiting the unnecessarily escalated dose to well-oxygenated and radiosensitive ones. Such a pattern of radiation dose delivery is shared with another treatment strategy, the SFRT, basically known in two main forms: the GRID and the lattice one (39). These two differ by a more rigorously geometric arrangement of high-dose regions in the first respect to the second one. Both treatments were created as non-oxygen guided. We believe that an SFRT technique based on hypoxia tracking could enhance the synergy between high radiation dose, able to eradicate hypoxic clones, and the subsequently elicited radiobiological effects, which could promote tumor regression also in low-dose regions as well as distantly in non-targeted lesions (11). However, cell interactions against the background of the host immune system are not fully known and, consequently, not purposely engageable to lead an antitumor response. On the other hand, by adopting an *in silico* model to explain the interaction (that is, the killing effect) between radiation dose and hypoxic cells, the radical dose to eliminate them all, even after taking into account the time between a fraction and the next one, could be approximately predicted (12).

Clinical Implications and Perspectives

In clinical practice, the finding of bulky tumors is not uncommon. A large part of them sometimes presents a necrotic core, detectable as a deeper hypodense region on CT scans (47, 48) or as photopenic on ^{18}F-FDG PET images (49). The most common approach used in these cases, especially when these masses are metastases, is to treat the total volume with a homogeneous palliative dose, so as not to exceed the tolerance of OARs at the boundary with the target periphery. Clearly, such a strategy is unable to produce a durable LC and, subsequently, could address the need for re-treatment, obviously not without serious concerns regarding toxicities. Conversely, a uniform high-dose delivery could be not deliverable without a hazardous dose–volume effect. Hence, the radiation oncologist is often forced to settle for the first option. To circumvent these risks, recently, Tubin et al. proposed an unconventional irradiation technique for partially treating inhomogeneous bulky tumors (SBRT-PATHY): to deliver a high radiation dose to hypoxic areas with a sharp dose fall-off toward the outside of the tumor in order to spare the normoxic portion and, above all, the peripheral microenvironment for evoking immune radiobiological effects (bystander and abscopal) (50). This strategy achieved great clinical results in terms of tumor volume regression with no additional toxicity as compared to conventional palliative treatment (16). In this technique, the low-dose region represented by the normoxic peripheral tumor ring acts as a "buffer" between the high-dose hypoxic rim and the adjacent OARs to spare. However, further clinical trials with a larger sample size are needed prior to translating these preliminary results to routine clinical practice. In fact, partially uncovering some tumor subvolumes could be at least controversial or even hazardous from the radiation oncologist's point of view. The concern about the difficulty in precisely mapping the hypoxic areas for selective irradiation could deter the implementation of this strategy. After all, the spatial resolution of current clinical imaging could be unable to detect all minor hypoxic regions. The consequence of missing out on the required radiation dose to one of these areas may be poor tumor control. For this reason, an alternative to SBRT-PATHY could be to selectively boost detectable hypoxic areas while maintaining a low effective dose in the remaining normoxic areas. Such an approach could balance the need for a booster dose in radioresistant hypoxic regions with the need to cover the overall tumor volume with an adequate radiation dose to hamper a rapid tumor regrowth while preserving nearby normal tissues. This strategy is calling for a mathematical model that can help to determine the required radiation dose to overcome hypoxic radioresistance. For this purpose, we have chosen a single dose of 15 Gy because this dose size has proven to be more effective in terms of tumor regression when compared to lower doses (51). Moreover, the single shot allowed us to bypass the redistribution in tumor oxygenation, following each radiation dose in fractionated schedules. In fact, the tumor oxygen map constantly evolves after radiation due to the recovery from vaso-occlusive events in tumor vessels on the one hand and to the prothrombotic effect associated with the swelling of irradiated tumor endothelial cells on the other (52). Among the non-invasive techniques currently available for measuring oxygen levels in tumor tissues, we find optical methods, those based on NMR, and nuclear medicine techniques. PET/CT has several advantages: a good intrinsic resolution, a 3D representation of the tumor, the possibility of making semiquantitative evaluations of the hypoxic tumor load, the ease of execution, the reproducibility of the data, and above all the highest diagnostic specificity in the characterization of the hypoxic tissue (53). A large number of PET tracers have now been developed for the identification of hypoxia. ^{18}F-fluoromisonidazole is the most studied PET tracer for hypoxia imaging, but the accumulation of the tracer in the hypoxic tissues is rather slow, and the tumor/background ratio is still quite low. Therefore, only a few radiopharmacies produce specific tracers for hypoxia, and procurement is very difficult. ^{18}F-FDG is the most widely used PET tracer in oncology, as cancer cells usually show an increase in their metabolism and in particular in

glycolysis, even in conditions of aerobiosis (Warburg effect). The increase in the expression of glucose transporters and glycolytic enzymes can also be activated by hypoxia, through the factor HIF-1α (anaerobic glycolysis, the Pasteur effect) (53). Apart from the constitutive photopenia of large tumor necrosis, the uptake of FDG under both normal and reduced oxygen pressure conditions obviously makes FDG non-specific for hypoxia. However, FDG-PET/CT proved to be a good tool in staging patients with cSCC as well (54). Other studies have reported nodal involvement sensitivities ranging between 91% and 100% and change in management in 6.25%–40% of patients (55–57). A recent study in node-positive cSCC patients calculated the positive and negative predictive values for nodal detection in preoperative FDG-PET/CT as 91.1% and 66.7%, respectively (56). As a consequence of this, the use of such an imaging to study and characterize the tumor disease in our patient was appropriate.

Mathematical Radiobiological Models: A Call For New Ones?

Taking into account the different dose prescriptions and a more and more detrimental dose–volume effect as the irradiated volume increases, Plan A would have an excellent NTCP but the worst TCP. Conversely, Plan B would be likely characterized by an excellent TCP and a not negligible NTCP for the chest wall (2%) when compared to plans C and D (58) and at the expense of the target dose coverage as evidenced by the cumulative DVH shown in **Figure S1** of **Supplementary Material 2** (see the smoother slope of the orange curve nearby the dose prescription value). As these outcomes do not fit a radical and safe curative purpose, we developed an *ad hoc* mathematical radiobiological model only for plans C and D in order to further investigate their respective CCSPs. Interestingly, the numerical results about the cell survival rate according to the LQ model show a strong reduction of the subpopulation volumes, although with a TCP that could be small for a large clonogenic number (see **Tables S2**, **S3** on the cell survival fraction). This means that the LQ model could not be able to explain the reported cCR after lattice RT delivery. Such a finding supports our assumption about immune intervention even more. After all, the involvement of immune response, specifically the recruitment of effector immune cells at the distant disease sites, needed to be adduced to explain the abscopal effect reported in a case with multiple nodules of cSCC, of which only one was irradiated (59). As Plan A employed a palliative dose by definition and Plan B a not safely deliverable uniform high dose, respectively, we deemed it useless to provide CCSP for them. Conversely, we elaborated NTCP for the skin and chest wall for all four dose prescriptions, purposely rescaled in EQD2 (Equivalent Dose in 2 Gy/Fx) value. As evidenced by cumulative EQD2-DVHs in **Supplementary Material 2**, the volume of the skin and chest wall for Plan D was constantly lower than that for Plans B and C at each dose level. In other terms, the addition of vertices dose has an almost negligible effect over the two OARs when compared to the other two plans. This was particularly evident at the highest dose levels, as inferred from the differential DVHs. However, all plans have a very-low near-zero risk of damage for both the chest wall and skin. Indeed, as a more detailed examination shows, the near-zero risk of Plan D is of another order of magnitude in comparison with that of Plans B and C, e.g., up to 10,000 times smaller for the skin. In fact, on the NTCP curve, the value of risk for Plan D is just beyond that of Plan A and significantly distant from that of Plans B and C, which, conversely, are closer to the curve section with the greatest slope that indicates a very real danger for the chest wall and skin. Also regarding the chest wall, the largest volume to be boosted in Plan B entails a low but significant risk (≈2%) when compared to the risks of Plans C and D. This means that Plan D is a more precautionary method of radiation delivery. Such a finding could be mainly useful in case of the need for re-treatment or treatment of neighboring metachronous metastases. Moreover, it has to be emphasized that NTCP predictions are largely influenced by the amount of OAR volume under investigation. We considered a very large portion of the skin and chest wall, namely, the one approximately exposed to at least 2 Gy because no dose is without sequelae. Thus, in the NTCP simulation, the risk prediction related to the highest doses could be underrated if such doses are computed as scattered in a very large volume rather than as concentrated in a small one. Starting from these considerations, the lattice approach could be even more advantageous than it appears in this particular case. The flexibility for high-dose vertices positioning permits to maximize tumor control without threatening the surrounding healthy tissues. This assumption can be valid also for other tumor histology and high-risk locations. Of particular note, the lattice dose delivery permitted a more rapid tumor response than the other two disease sites treated with classic stereotactic RT.

Advantages From This Preliminary Experience

As cSCC is prevalent among very elderly and frail patients, our SFRT solution could be valuable also for the treatment of primary bulky lesions in those cases not eligible for radical surgery due to a high anesthetic risk or technical complexity (60). In this patient setting, the treatment option here presented could be safer and more tolerable than the multi-drug systemic therapies investigated in currently ongoing trials (61). Besides, such immuno- and chemotherapeutic agents may struggle to penetrate within hypo-vascularized hypoxic tumor subdomains with a consequent decline in LC. Also, well-established drug protocols, like the one here used, based on cemiplimab, are not without serious concerns about toxicities and still have a poor overall response rate (62). To improve the latter, a combination of cemiplimab with hypofractionated RT has been already tested with encouraging results (63).

Limitations

We are fully aware that this study has several limitations. First of all, one swallow does not make a summer: a case report does not allow to draw any definitive conclusions. Secondly, all the numerical analyses are based on the estimated number of cells contained in each voxel, in a way that their computation is, of course, largely approximate. Thirdly, the failure to use clinical imaging that was specifically devoted to accurately distinguishing the different subvolumes (normoxic, hypoxic, and necrotic ones) represents another weakness. In any case, in this regard, on the

basis of ^{18}F-FDG tracer distribution, it is reasonable to assume that a transitional layer populated by oxygen-starved cells rings an innermost photopenic area due to necrosis. Fourthly, the whole procedure of target contouring, particularly the choice of vertex number, size, dose, and positioning, was strictly operator-dependent and this could undermine the reproducibility of the result. Fifthly, the role of lattice RT in achieving the reported results may be overestimated due to the use of cemiplimab following the RT course, although it must be emphasized that the cCR in the bulky axillary lesion was documented already prior to the drug administration. However, we did not just present our successful approach but even tried to provide a reliable scientific insight, in agreement with the currently available mathematical radiobiological models. It is indeed worth stressing that the LQ model predicted a very small value of TCP for the delivered plan (3%), but nevertheless, we observed a very positive outcome: actually, there is the possibility that we described just one of the three cases out of 100 with tumor control. Further investigations on large series with similar tumors should be performed in order to confirm the reliability of this model in describing this type of RT planning.

Final Considerations

To the best of our knowledge, this is the first report about lattice RT in which the vertex positioning was based on the ^{18}F-FDG PET-detected metabolic heterogeneity within a large tumor mass as a surrogate of its oxygen landscape and whose clinical outcome was attempted to be explained either by the currently available mathematical radiobiological models or an *ad hoc* developed one. Neither the first nor the second could be sufficient to exhaustively explain the reported outcome, likely calling for more complex radiobiological models.

The list of successful lattice RT applications now includes bulky cSCCs.

CONCLUSIONS

Lattice RT might be safe and effective for the treatment of bulky locally advanced or metastatic cSCCs. Large trials are needed to draw up tailored RT for difficult-to-treat cancer patients, and wide investigations are needed to deeply evaluate the effectiveness of the lattice RT. Moreover, more theoretical analyses with existent and/or novel radiobiological models could be useful to explain lattice RT effects, also taking into account the reaction of the host immune system to this particular radiation dose delivery.

DATA AVAILABILITY STATEMENT

The original contributions presented in the study are included in the article/**Supplementary Material**. Further inquiries can be directed to the corresponding author.

ETHICS STATEMENT

Ethical approval was not provided for this study on human participants because ethical approval was waived in view of the retrospective nature of the study, and all the procedures being performed were part of the routine care. This research study was conducted retrospectively from data obtained for clinical purposes and is in accordance with the local legislation and institutional requirements. The patients/participants provided their written informed consent to participate in this study.

AUTHOR CONTRIBUTIONS

All authors contributed equally to the paper. GF and PC shared the first authorship. MM and SP shared the last authorship.

SUPPLEMENTARY MATERIAL

The Supplementary Material for this article can be found online at: https://www.frontiersin.org/articles/10.3389/fonc.2022.809279/full#supplementary-material

REFERENCES

1. Ferini G, Molino L, Bottalico L, De Lucia P, Garofalo F. A Small Case Series About Safety and Effectiveness of a Hypofractionated Electron Beam Radiotherapy Schedule in Five Fractions for Facial Non Melanoma Skin Cancer Among Frail and Elderly Patients. *Rep Pract Oncol Radiother* (2021) 26(1):66–72. doi: 10.5603/RPOR.a2021.0013
2. Cherpelis BS, Marcusen C, Lang PG. Prognostic Factors for Metastasis in Squamous Cell Carcinoma of the Skin. *Dermatol Surg* (2002) 28(3):268–73. doi: 10.1046/j.1524-4725.2002.01169.x
3. Vincent AG, Wang W, Shokri T, Ducic Y. Treatment of Oligometastatic Disease in Squamous Cell Carcinoma of the Head and Neck. *Laryngoscope* (2021) 131(5):E1476–80. doi: 10.1002/lary.29115
4. Green AC, Olsen CM. Cutaneous Squamous Cell Carcinoma: An Epidemiological Review. *Br J Dermatol* (2017) 177(2):373–81. doi: 10.1111/bjd.15324
5. AIRTUM Working Group, Busco S, Buzzoni C, Mallone S, Trama A, Castaing M, et al. Italian Cancer Figures–Report 2015: The Burden of Rare Cancers in Italy. *Epidemiol Prev* (2016) 40(1 Suppl 2):1–120. doi: 10.19191/EP16.1S2.P001.035
6. Available at: https://www.nccn.org/professionals/physician_gls/pdf/squamous.pdf.
7. Schmults CD, Karia PS, Carter JB, Han J, Qureshi AA. Factors Predictive of Recurrence and Death From Cutaneous Squamous Cell Carcinoma: A 10-Year, Single-Institution Cohort Study. *JAMA Dermatol* (2013) 149(5):541–7. doi: 10.1001/jamadermatol.2013.2139
8. Cacciola A, Parisi S, Tamburella C, Lillo S, Ferini G, Molino L, et al. Stereotactic Body Radiation Therapy and Radiofrequency Ablation for the Treatment of Liver Metastases: How and When? *Rep Pract Oncol Radiother* (2020) 25(3):299–306. doi: 10.1016/j.rpor.2020.02.010
9. Pontoriero A, Iatì G, Cacciola A, Conti A, Brogna A, Siragusa C, et al. Stereotactic Body Radiation Therapy With Simultaneous Integrated Boost in Patients With Spinal Metastases. *Technol Cancer Res Treat* (2020) 19:1533033820904447. doi: 10.1177/1533033820904447

10. D'Angelillo RM, Ingrosso G, Ravo V, Triggiani L, Magli A, Mazzeo E, et al. Consensus Statements on Ablative Radiotherapy for Oligometastatic Prostate Cancer: A Position Paper of Italian Association of Radiotherapy and Clinical Oncology (AIRO). *Crit Rev Oncol Hematol* (2019) 138:24–8. doi: 10.1016/j.critrevonc.2019.03.014
11. Ferini G, Valenti V, Tripoli A, Illari SI, Molino L, Parisi S, et al. Lattice or Oxygen-Guided Radiotherapy: What If They Converge? Possible Future Directions in the Era of Immunotherapy. *Cancers (Basel)* (2021) 13 (13):3290. doi: 10.3390/cancers13133290
12. Castorina P, Castorina L, Ferini G. Non-Homogeneous Tumor Growth and Its Implications for Radiotherapy: A Phenomenological Approach. *J Pers Med* (2021) 11(6):527. doi: 10.3390/jpm11060527
13. Warkentin B, Stavrev P, Stavreva N, Field C, Fallone BG. A TCP-NTCP Estimation Module Using DVHs and Known Radiobiological Models and Parameter Sets. *J Appl Clin Med Phys* (2004) 5(1):50–63. doi: 10.1120/jacmp.v5i1.1970
14. Vadalà RE, Santacaterina A, Sindoni A, Platania A, Arcudi A, Ferini G, et al. Stereotactic Body Radiotherapy in Non-Operable Lung Cancer Patients. *Clin Transl Oncol* (2016) 18(11):1158–9. doi: 10.1007/s12094-016-1552-7
15. Bentzen SM, Joiner MC. The Linear-Quadratic Approach in Clinical Practice. In: MC Joiner, A van der Kogel, editors. *Basic Clin. Radiobiol*, *4th ed*. London: Hodder Arnold (2009).
16. Tubin S, Khan MK, Salerno G, Mourad WF, Yan W, Jeremic B. Mono-Institutional Phase 2 Study of Innovative Stereotactic Body RadioTherapy Targeting PArtial Tumor HYpoxic (SBRT-PATHY) Clonogenic Cells in Unresectable Bulky Non-Small Cell Lung Cancer: Profound Non-Targeted Effects by Sparing Peri-Tumoral Immune Microenvironment. *Radiat Oncol* (2019) 14(1):212. doi: 10.1186/s13014-019-1410-1
17. Kishikawa T, Suzuki M, Takemoto N, Fukusumi T, Michiba T, Hanamoto A, et al. Response Evaluation Criteria in Solid Tumors (RECIST) and PET Response Criteria in Solid Tumors (PERCIST) for Response Evaluation of the Neck After Chemoradiotherapy in Head and Neck Squamous Cell Carcinoma. *Head Neck* (2021) 43(4):1184–93. doi: 10.1002/hed.26583
18. Stuschke M, Thames HD. Fractionation Sensitivities and Dose-Control Relations of Head and Neck Carcinomas: Analysis of the Randomized Hyperfractionation Trials. *Radiother Oncol* (1999) 51(2):113–21. doi: 10.1016/s0167-8140(99)00042-0
19. Turesson I, Thames HD. Repair Capacity and Kinetics of Human Skin During Fractionated Radiotherapy: Erythema, Desquamation, and Telangiectasia After 3 and 5 Year's Follow-Up. *Radiother Oncol* (1989) 15(2):169–88. doi: 10.1016/0167-8140(89)90131-x
20. Bentzen SM, Overgaard M, Thames HD. Fractionation Sensitivity of a Functional Endpoint: Impaired Shoulder Movement After Post-Mastectomy Radiotherapy. *Int J Radiat Oncol Biol Phys* (1989) 17(3):531–7. doi: 10.1016/0360-3016(89)90103-x
21. Munro TR, Gilbert CW. The Relation Between Tumour Lethal Doses and the Radiosensitivity of Tumour Cells. *Br J Radiol* (1961) 34:246–51. doi: 10.1259/0007-1285-34-400-246
22. Brahme A, Agren AK. Optimal Dose Distribution for Eradication of Heterogeneous Tumours. *Acta Oncol* (1987) 26(5):377–85. doi: 10.3109/02841868709104364
23. Available at: https://www.sachpazidis.com/software-projects/pyradiobiology/.
24. Spohn SKB, Sachpazidis I, Wiehle R, Thomann B, Sigle A, Bronsert P, et al. Influence of Urethra Sparing on Tumor Control Probability and Normal Tissue Complication Probability in Focal Dose Escalated Hypofractionated Radiotherapy: A Planning Study Based on Histopathology Reference. *Front Oncol* (2021) 11:652678. doi: 10.3389/fonc.2021.652678
25. Okunieff P, Morgan D, Niemierko A, Suit HD. Radiation Dose-Response of Human Tumors. *Int J Radiat Oncol Biol Phys* (1995) 32(4):1227–37. doi: 10.1016/0360-3016(94)00475-z
26. Semenenko VA, Li XA. Lyman-Kutcher-Burman NTCP Model Parameters for Radiation Pneumonitis and Xerostomia Based on Combined Analysis of Published Clinical Data. *Phys Med Biol* (2008) 53(3):737–55. doi: 10.1088/0031-9155/53/3/014
27. Emami B, Lyman J, Brown A, Coia L, Goitein M, Munzenrider JE, et al. Tolerance of Normal Tissue to Therapeutic Irradiation. *Int J Radiat Oncol Biol Phys* (1991) 21(1):109–22. doi: 10.1016/0360-3016(91)90171-y
28. van Leeuwen CM, Oei AL, Crezee J, Bel A, Franken NAP, Stalpers LJA, et al. The Alfa and Beta of Tumours: A Review of Parameters of the Linear-Quadratic Model, Derived From Clinical Radiotherapy Studies. *Radiat Oncol* (2018) 13(1):96. doi: 10.1186/s13014-018-1040-z
29. Zhang Y, Schoenhals J, Christie A, Mohamad O, Wang C, Bowman I, et al. Stereotactic Ablative Radiation Therapy (SAbR) Used to Defer Systemic Therapy in Oligometastatic Renal Cell Cancer. *Int J Radiat Oncol Biol Phys* (2019) 105(2):367–75. doi: 10.1016/j.ijrobp.2019.07.023
30. Zhang B, Leech M. A Review of Stereotactic Body Radiation Therapy in the Management of Oligometastatic Prostate Cancer. *Anticancer Res* (2020) 40 (5):2419–28. doi: 10.21873/anticanres.14211
31. Zhao Y, Li J, Li D, Wang Z, Zhao J, Wu X, et al. Tumor Biology and Multidisciplinary Strategies of Oligometastasis in Gastrointestinal Cancers. *Semin Cancer Biol* (2020) 60:334–43. doi: 10.1016/j.semcancer.2019.08.026
32. Zhou Y, Yu F, Zhao Y, Zeng Y, Yang X, Chu L, et al. A Narrative Review of Evolving Roles of Radiotherapy in Advanced Non-Small Cell Lung Cancer: From Palliative Care to Active Player. *Transl Lung Cancer Res* (2020) 9 (6):2479–93. doi: 10.21037/tlcr-20-1145
33. Zayed S, Correa RJM, Palma DA. Radiation in the Treatment of Oligometastatic and Oligoprogressive Disease: Rationale, Recent Data, and Research Questions. *Cancer J* (2020) 26(2):156–65. doi: 10.1097/PPO.0000000000000436
34. Bonomo P, Greto D, Desideri I, Loi M, Di Cataldo V, Orlandi E, et al. Clinical Outcome of Stereotactic Body Radiotherapy for Lung-Only Oligometastatic Head and Neck Squamous Cell Carcinoma: Is the Deferral of Systemic Therapy a Potential Goal? *Oral Oncol* (2019) 93:1–7. doi: 10.1016/j.oraloncology.2019.04.006
35. Zhou J, Liu R, Luo C, Zhou X, Xia K, Chen X, et al. MiR-20a Inhibits Cutaneous Squamous Cell Carcinoma Metastasis and Proliferation by Directly Targeting LIMK1. *Cancer Biol Ther* (2014) 15(10):1340–9. doi: 10.4161/cbt.29821
36. Zilberg C, Lee MW, Kraitsek S, Ashford B, Ranson M, Shannon K, et al. Is High-Risk Cutaneous Squamous Cell Carcinoma of the Head and Neck a Suitable Candidate for Current Targeted Therapies? *J Clin Pathol* (2020) 73 (1):17–22. doi: 10.1136/jclinpath-2019-206038
37. Karia PS, Han J, Schmults CD. Cutaneous Squamous Cell Carcinoma: Estimated Incidence of Disease, Nodal Metastasis, and Deaths From Disease in the United States, 2012. *J Am Acad Dermatol* (2013) 68(6):957–66. doi: 10.1016/j.jaad.2012.11.037
38. Bujold A, Massey CA, Kim JJ, Brierley J, Cho C, Wong RK, et al. Sequential Phase I and II Trials of Stereotactic Body Radiotherapy for Locally Advanced Hepatocellular Carcinoma. *J Clin Oncol* (2013) 31(13):1631–9. doi: 10.1200/JCO.2012.44.1659
39. Billena C, Khan AJ. A Current Review of Spatial Fractionation: Back to the Future? *Int J Radiat Oncol Biol Phys* (2019) 104(1):177–87. doi: 10.1016/j.ijrobp.2019.01.073
40. Pellizzon ACA. Lattice Radiation Therapy - Its Concept and Impact in the Immunomodulation Cancer Treatment Era. *Rev Assoc Med Bras (1992)* (2020) 66(6):728–31. doi: 10.1590/1806-9282.66.6.728
41. Rockwell S, Dobrucki IT, Kim EY, Marrison ST, Vu VT. Hypoxia and Radiation Therapy: Past History, Ongoing Research, and Future Promise. *Curr Mol Med* (2009) 9(4):442–58. doi: 10.2174/156652409788167087
42. Small W. Perez and Brady's Principles and Practice of Radiation Oncology. *JAMA* (2009) 301:2046. doi: 10.1001/jama.2009.718
43. Lee SH, Golinska M, Griffiths JR. HIF-1-Independent Mechanisms Regulating Metabolic Adaptation in Hypoxic Cancer Cells. *Cells* (2021) 10(9):2371. doi: 10.3390/cells10092371
44. Hall EJ, Giaccia AJ. *Radiobiology for the Radiologist*. Philadelphia, PA, USA: Wolters Kluwer Health/Lippincott Williams & Wilkins (2012).
45. Li Q, Chen J, Zhu B, Jiang M, Liu W, Lu E, et al. Dose Volume Effect of Acute Diarrhea in Post-Operative Radiation for Gynecologic Cancer. *Rev Invest Clin* (2017) 69(6):329–35. doi: 10.24875/RIC.17002373
46. Eschwège F, Sancho-Garnier H, Chassagne D, Brisgand D, Guerra M, Malaise EP, et al. Results of a European Randomized Trial of Etanidazole Combined With Radiotherapy in Head and Neck Carcinomas. *Int J Radiat Oncol Biol Phys* (1997) 39(2):275–81. doi: 10.1016/s0360-3016(97)00327-1

47. Miyake H, Hori Y, Dono S, Mori H. Low Attenuation Intratumoral Matrix: CT and Pathologic Correlation. *J Comput Assist Tomogr* (2000) 24(5):761–72. doi: 10.1097/00004728-200009000-00018
48. Shan X, Wang D, Chen J, Xiao X, Jiang Y, Wang Y, et al. Necrosis Degree Displayed in Computed Tomography Images Correlated With Hypoxia and Angiogenesis in Breast Cancer. *J Comput Assist Tomogr* (2013) 37(1):22–8. doi: 10.1097/RCT.0b013e318279abd1
49. Ashley Cox R, Akhurst T, Bressel M, MacManus M, Ball D. Survival and Central Photopenia Detected by Fluorine-18 Fluoro-Deoxy-Glucose Positron Emission Tomography (FDG-PET) in Patients With Locoregional Non-Small Cell Lung Cancer Treated With Radiotherapy. *Radiother Oncol* (2017) 124 (1):25–30. doi: 10.1016/j.radonc.2017.06.004
50. Tubin S, Popper HH, Brcic L. Novel Stereotactic Body Radiation Therapy (SBRT)-Based Partial Tumor Irradiation Targeting Hypoxic Segment of Bulky Tumors (SBRT-PATHY): Improvement of the Radiotherapy Outcome by Exploiting the Bystander and Abscopal Effects. *Radiat Oncol* (2019) 14(1):21. doi: 10.1186/s13014-019-1227-y
51. Mohiuddin M, Fujita M, Regine WF, Megooni AS, Ibbott GS, Ahmed MM. High-Dose Spatially-Fractionated Radiation (GRID): A New Paradigm in the Management of Advanced Cancers. *Int J Radiat Oncol Biol Phys* (1999) 45 (3):721–7. doi: 10.1016/s0360-3016(99)00170-4
52. Brat DJ, Van Meir EG. Vaso-Occlusive and Prothrombotic Mechanisms Associated With Tumor Hypoxia, Necrosis, and Accelerated Growth in Glioblastoma. *Lab Invest* (2004) 84(4):397–405. doi: 10.1038/labinvest.3700070
53. Lopci E, Grassi I, Chiti A, Nanni C, Cicoria G, Toschi L, et al. PET Radiopharmaceuticals for Imaging of Tumor Hypoxia: A Review of the Evidence. *Am J Nucl Med Mol Imaging* (2014) 4(4):365–84.
54. Mahajan S, Barker CA, Sing B, Pandit-Taskar N. Clinical Value of 18F-FDG-PET/CT in Staging Cutaneous Squamous Cell Carcinoma. *Nucl Med Commun* (2019) 40(7):744–51. doi: 10.1097/MNM.0000000000001029
55. Fujiwara M, Suzuki T, Takiguchi T, Fukamizu H, Tokura Y. Evaluation of Positron Emission Tomography Imaging to Detect Lymph Node Metastases in Patients With High-Risk Cutaneous Squamous Cell Carcinoma. *J Dermatol* (2016) 43:1314–20. doi: 10.1111/1346-8138.13403
56. Hirshoren N, Olayos E, Herschtal A, Kumar ASR, Gyorki DE. Preoperative Positron Emission Tomography for Node-Positive Head and Neck Cutaneous Squamous Cell Carcinoma. *Otolaryngol Head Neck Surg* (2018) 158:122–6. doi: 10.1177/0194599817731735
57. Supriya M, Suat-Chin N, Sizeland A. Use of Positron Emission Tomography Scanning in Metastatic Head and Neck Cutaneous Squamous Cell Cancer: Does it Add to Patient Management? *Am J Otolaryngol* (2014) 35:347–52. doi: 10.1016/j.amjoto.2014.01.006
58. Bongers EM, Haasbeek CJ, Lagerwaard FJ, Slotman BJ, Senan S. Incidence and Risk Factors for Chest Wall Toxicity After Risk-Adapted Stereotactic Radiotherapy for Early-Stage Lung Cancer. *J Thorac Oncol* (2011) 6 (12):2052–7. doi: 10.1097/JTO.0b013e3182307e74
59. Bellia SR, Feliciani G, Duca MD, Monti M, Turri V, Sarnelli A, et al. Clinical Evidence of Abscopal Effect in Cutaneous Squamous Cell Carcinoma Treated With Diffusing Alpha Emitters Radiation Therapy: A Case Report. *J Contemp Brachytherapy* (2019) 11(5):449–57. doi: 10.5114/jcb.2019.88138
60. Lupon E, Lellouch AG, Deilhes F, Chaput B, Berthier C. Reconstruction of a Dorsal Thoracic Wall Defect With a Dorsal Intercostal Artery Perforator Flap After Removal of a Bulky Cutaneous Squamous Cell Carcinoma: A Case Report. *J Med Case Rep* (2019) 13(1):294. doi: 10.1186/s13256-019-2226-1
61. Lin C, Ballah T, Nottage M, Hay K, Chua B, Kenny L, et al. A Prospective Study Investigating the Efficacy and Toxicity of Definitive ChemoRadiation and ImmunOtherapy (CRIO) in Locally and/or Regionally Advanced Unresectable Cutaneous Squamous Cell Carcinoma. *Radiat Oncol* (2021) 16 (1):69. doi: 10.1186/s13014-021-01795-5
62. Migden MR, Khushalani NI, Chang ALS, Lewis KD, Schmults CD, Hernandez-Aya L, et al. Cemiplimab in Locally Advanced Cutaneous Squamous Cell Carcinoma: Results From an Open-Label, Phase 2, Single-Arm Trial. *Lancet Oncol* (2020) 21(2):294–305. doi: 10.1016/S1470-2045(19)30728-4
63. Papadopoulos KP, Johnson ML, Lockhart AC, Moore K, Falchook GS, Formenti SC, et al. First-In-Human Study of Cemiplimab Alone or In Combination With Radiotherapy and/or Low-Dose Cyclophosphamide in Patients With Advanced Malignancies. *Clin Cancer Res* (2020) 26(5):1025–33. doi: 10.1158/1078-0432.CCR-19-2609

Conflict of Interest: IS is co-founder of the company Medical Innovation and Technology P.C.

The remaining authors declare that the research was conducted in the absence of any commercial or financial relationships that could be construed as a potential conflict of interest.

frontiers | Frontiers in Oncology

ORIGINAL RESEARCH
published: 12 May 2022
doi: 10.3389/fonc.2022.801743

MRI-Based Radiomics Features to Predict Treatment Response to Neoadjuvant Chemotherapy in Locally Advanced Rectal Cancer: A Single Center, Prospective Study

Bi-Yun Chen[1†], Hui Xie[1†], Yuan Li[2], Xin-Hua Jiang[1], Lang Xiong[1], Xiao-Feng Tang[3], Xiao-Feng Lin[1], Li Li[1] and Pei-Qiang Cai[1*]*

[1] Department of Medical Imaging, Collaborative Innovation Center for Cancer Medicine, State Key Laboratory of Oncology in South China, Sun Yat-sen University Cancer Center, Guangzhou, China, [2] Department of Colorectal, Collaborative Innovation Center for Cancer Medicine, State Key Laboratory of Oncology in South China, Sun Yat-sen University Cancer Center, Guangzhou, China, [3] Department of Ultrasound, Collaborative Innovation Center for Cancer Medicine, State Key Laboratory of Oncology in South China, Sun Yat-sen University Cancer Center, Guangzhou, China

OPEN ACCESS

Edited by:
Rosario Mazzola, Sacro Cuore Don Calabria Hospital (IRCCS), Italy
Reviewed by:
Massimo Galia, University of Palermo, Italy
Damiano Caruso, Sapienza University of Rome, Italy

***Correspondence:**
Pei-Qiang Cai
caipq@sysucc.org.cn
Li Li
lil@sysucc.org.cn

[†]These authors share first authorship

Specialty section:
This article was submitted to Radiation Oncology, a section of the journal Frontiers in Oncology

Received: *25 October 2021*
Accepted: *31 March 2022*
Published: *12 May 2022*

Citation:
Chen B-Y, Xie H, Li Y, Jiang X-H, Xiong L, Tang X-F, Lin X-F, Li L and Cai P-Q (2022) MRI-Based Radiomics Features to Predict Treatment Response to Neoadjuvant Chemotherapy in Locally Advanced Rectal Cancer: A Single Center, Prospective Study. Front. Oncol. 12:801743. doi: 10.3389/fonc.2022.801743

This is a prospective, single center study aimed to evaluate the predictive power of peritumor and intratumor radiomics features assessed using T2 weight image (T2WI) of baseline magnetic resonance imaging (MRI) in evaluating pathological good response to NAC in patients with LARC (including Tany N+ or T3/4a Nany but not T4b). In total, 137 patients with LARC received NAC between April 2014 and August 2020. All patients were undergoing contrast-enhanced MRI and 129 patients contained small field of view (sFOV) sequence which were performed prior to treatment. The tumor regression grade standard was based on pathological response. The training and validation sets (n=91 vs. n=46) were established by random allocation of the patients. Receiver operating characteristic curve (ROC) analysis was applied to estimate the performance of different models based on clinical characteristics and radiomics features obtained from MRI, including peritumor and intratumor features, in predicting treatment response; these effects were calculated using the area under the curve (AUC). The performance and agreement of the nomogram were estimated using calibration plots. In total, 24 patients (17.52%) achieved a complete or near-complete response. For the individual radiomics model in the validation set, the performance of peritumor radiomics model in predicting treatment response yield an AUC of 0.838, while that of intratumor radiomics model is 0.805, which show no statically significant difference between then(P>0.05). The traditional and selective clinical features model shows a poor predictive ability in treatment response (AUC=0.596 and 0.521) in validation set. The AUC of combined radiomics model was improved compared to that of the individual radiomics models in the validation sets (AUC=0.844). The combined clinic-radiomics model yield the highest AUC (0.871) in the validation set, although it did not

improve the performance of the radiomics model for predicting treatment response statically (P>0.05). Good agreement and discrimination were observed in the nomogram predictions. Both peritumor and intratumor radiomics features performed similarly in predicting a good response to NAC in patients with LARC. The clinic-radiomics model showed the best performance in predicting treatment response.

Keywords: rectal cancer, treatment response, neoadjuvant chemotherapy, nomogram, magnetic resonance imaging radiomics

INTRODUCTION

Rectal cancer is one of the most common malignant neoplasms and the second leading cancer-related cause of death worldwide (1). Locally advanced rectal cancer (LARC) accounts for approximately 70% of newly diagnosed rectal cancer cases annually, which is defined as T3-4Nany or TanyN+, regardless the status of the CRM (2). Following neoadjuvant fluorouracil-based chemoradiotherapy (CRT), total mesorectal excision (TME) and adjuvant chemotherapy are the recommended standard treatments for LARC before. However, several large prospective trials, including RAPIDO (3), PRODIGE 23 (4) have brought neoadjuvant chemotherapy to the fore as a new standard to LARC. Furthermore, recent results indicated that, compared to nCRT, neoadjuvant chemotherapy (NAC) showed no statistically significant difference in terms of 3-year local recurrence (8.3% vs 7.0%~ 8.0%), disease-free survival (DFS) (73.5% vs 72.9%~77.2%), and overall survival (OS) (90.7% vs 89.1%~91.3%) between the three arms (5). Even Habr-Gama and colleagues suggest the 'wait and watch' strategy for patients with LARC with a clinical complete response (cCR) after neoadjuvant chemoradiotherapy (nCRT) (5). Although the rate of pathological complete response (pCR) in the CRT group was higher than that in the NAC group, higher toxicity and more postoperative complications were observed in patients who received only radiotherapy (6, 7). Predicting patients who could achieved CR undervent NAC before operation is of great clinically meaning. It may indicates that the specific patients could avoid the unnecessary radiotherapy (8).

However, pCR (pathology complete response) can only be confirmed in the resected specimens after surgery.Magnetic resonance imaging (MRI) has merged as a dominant method of pelvic imaging in rectal cancer for its superb soft tissue contrast between tumor and other soft tissue (9). Besides, MRI is particular accurate in assessing the distance between the tumor and the mesorectal fascia with sensitivity and specificity up to 94% and 76% respectively (10). Furthermore, 3.0T MRI scanner perform better than the 1.5T MRI in the visual assessment of the complete response patients of rectal cancer (10). In spatially and temporally heterogeneous solid cancers, invasive biopsies specimens cannot reflect the overall characteristics of the tumor, which limits the use of invasive biopsy based molecular assays but gives huge potential for medical imaging (11). Radiomics, as a new term, was first proposed by Lambin et al. in 2012 (12). Radiomics can convert traditional radiological images into data that can be further analysis. The workflow includes multi-steps: images acquisition, image segmentation, features extraction and selection, model construction and validation. The aim of radiomics is to translate medical images into quantitative data, which may reveal a deeper information of the tumor (13). With its ability to perform high-throughput extraction of image features derived from radiographic images, radiomics can provide a non-invasive method of describing intra-tumoral heterogeneity (12). Previous studies (14–18) have estimated the predictive performance of magnetic resonance imaging (MRI) or computed tomography (CT) features to evaluate tumor treatment response. In these studies, most examinations were focused on LARC after nCRT, which is of little significance for making decisions regarding NAC. In addition, previous radiomics studies of LARC focused on the intertumoral region alone, and information regarding peritumoral radiomics features was overlooked. Recently, in other cancers, the peritumoral area has been used to predict the treatment response. For example, Khorram et al. (19) used combined peri- and intratumoral radiomics models to predict the response to chemotherapy in lung adenocarcinoma and indicated that radiomic features extracted within the nodule and border (from the baseline CT scan) performed well in predicting treatment response in association with time to progress (TTP) and overall survival (OS). Hu et al. (20) showed that, in patients with esophageal squamous cell carcinoma, a model combining intra- and peritumoral radiomics showed good performance in predicting pCR following NAC (0.852 (95% CI, 0.753-0.951). At present, to the best of our knowledge, only a few studies have focused on peritumor radiomics research, and its role in predicting treatment response to NAC has not been definitively demonstrated. Therefore, we aimed to establish the model based on radiomics of the intratumor and peritumor to predict the efficacy of NAC in LARC. Prediction of good response to NAC can reduce radiotherapy-related toxicity and the economic burden of the patients. Our findings, if confirmed, may help identify good response patients and lower the overtreatment rate.

MATERIALS AND METHODS

Patient Population

The study was approved by the Ethical Committee of the Sun Yat-sen University Cancer Center. This was a secondary analysis based on prospective research data (Approval no. 5010-2014-013). The ethical principles of the Declaration of Helsinki were followed in conducting work involving human participants enrolled in this study. Informed consent was obtained from

each patient prior to treatment and participation. The study cohort was enrolled between April 2014 and August 2020. The patients were recruited based on the following inclusion criteria: (1) pathologically confirmed single primary rectal cancer; (2) clinical diagnosis of LARC (defined as the tumor invading the muscularized layer of the intestinal wall with positive peripheral lymph node metastasis (T2 N+) or primary tumor invading the subserosa regardless of the status of the lymph node (T3-4aNany); (3) no distant metastasis; (4) initial pretreatment MRI of the pelvis; (5) no other malignant cancers; (6) no anti-cancer treatment in other clinical centers; (7) an Eastern Cooperative Oncology Group score of 0–1; (8) age between 18 and 75 years. The exclusion criteria were as follows: (1) preoperative staging evaluating whether the tumor had invaded the surrounding tissues or organs (T4b); (2) severe hypertension with poor control; (3) history of viral infection, including human immunodeficiency virus or chronic hepatitis B or C; (4) arrhythmia requiring antiarrhythmic treatment (except *via* blockers or digoxin), myocardial ischemia (i.e., myocardial infarction in the last 6 months), or symptomatic coronary artery disease with heart failure exceeding New York Heart Association level II criteria; and (5) a history of pelvic or abdominal radiotherapy to exclude the influence of other serious diseases and treatment history on the treatment outcomes. The patient selection process for this study is summarized in **Figure 1**. A total of 302 eligible patients were

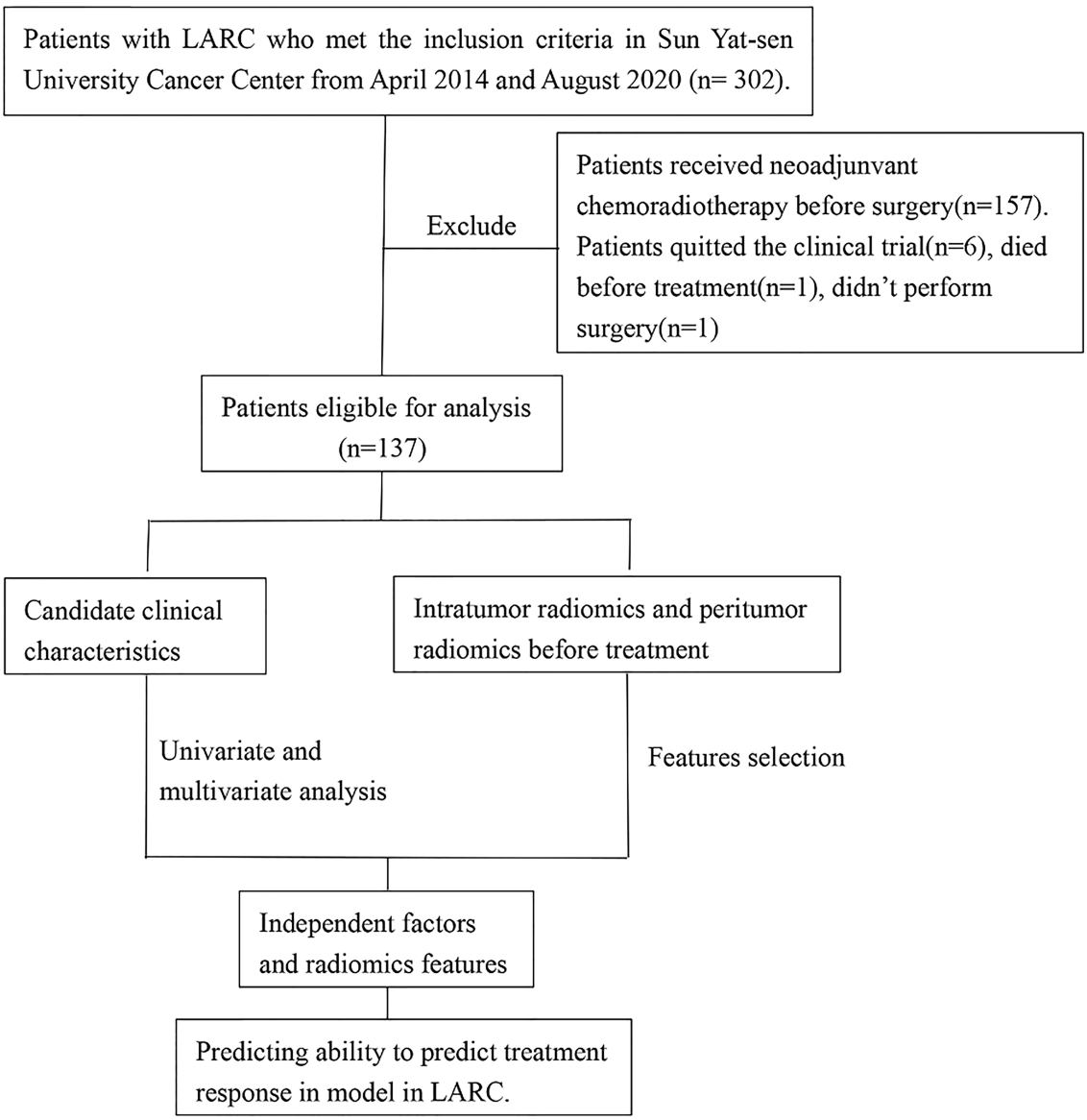

FIGURE 1 | Flow chart of the study.

recruited from April 2014 and August 2020. Of these, a further 165 patients were ineligible and were excluded, including 157 patients received CRT, 6 patients quitted the clinical trial, 1 patient died before treatment and 1 patient didn't perform surgery, and finally data collection could be complete on a total 137 participants (83 men and 54 women).

The following variables were obtained from patient medical charts: age, sex, body mass index (BMI), history of smoking, initial carcinoembryonic antigen (CEA) and carbohydrate antigen 19-9 (CA19-9) levels (as determined by MRI), the date and cycle of chemotherapy, surgery date, and tumor regression grade (TRG). Blood samples were collected from all patients within one week of treatment. In addition, the date of the baseline MRI, clinical T and N staging, the distance from the tumor to the anal edge, the long and short diameter of the tumor, the status of mesorectal fascia (MRF) invasion, and extramural vascular invasion as determined by MRI were obtained.

Neoadjuvant Chemotherapy and Pathological Assessment

The chemotherapy regimen implemented within the current study was the CapeOx plan (oxaliplatin 30 mg/m^2, day 1; capecitabine 850–1,000 mg/m^2, bid, days 1–14). There were breaks of three weeks between cycles. The total number of cycles ranged between two and four. Upon completion of chemotherapy, TME surgery was performed.

Two experienced gastrointestinal cancer pathologists (Dr. Xi and Dr. Wu) with 8 and 12 years of diagnosis experience, respectively, reviewed and evaluated all resected specimens. Clinical and MRI data were also evaluated by these pathologists. TRG was evaluated based on the TRG system proposed by Mandard et al. (21) TRG was quantitated in five grades: TRG1 (complete regression) showed absence of residual cancer and fibrosis extending through the different layers of the bowel wall; TRG2 was characterized by the presence of rare residual cancer cell scattered through the fibrosis; TRG3 was characterized by an increase in the number of residual cancer cells, but fibrosis still predominated; TRG4 showed residual cancer outgrowing fibrosis; and TRG 5 was characterized by absence of regressive changes. Considering that a good response to NAC can lead to avoiding radiotherapy and that poor responders may need further treatment or assess other treatment options, patients were divided into two response groups: good responders (TRG 1–2 disease, no or rare tumor cells remaining) and poor responders (TRG 3–5 disease, moderate to extensive residual cancer cells). A consensus was reached in cases involving uncertainties in evaluating the pathology specimens.

MRI and Image Evaluation

Patients underwent rectal MRI prior to NAC. The time from the MRI to the start of therapy was less than 2 weeks. Response: thank you very much for your question. All the MRI examinations were performed without bowel preparation, endorectal gel or spasmolytic drugs. Pretreatment MRI was performed using a 3.0 T MR scanner (Trio Tim, Siemens Healthcare, Malvern, PA, USA; Achicva 781-278, Philips, Cambridge, MA, USA) using two elements of the body matrix coil as well as two elements of the spine matrix coil, or was performed using a 3.0 T system (Discovery 750, 750 W, SIGNA Pioneer GE Healthcare, Chicago, IL, USA; uMR 780, United Imaging, Shanghai, China) equipped with an eight-channel phased-array body coil in the supine position. A conventional rectal MRI protocol including diffusion-weighted imaging (DWI) and axial, coronal, and sagittal T2W images was implemented in all patients. Contrast-enhanced sequences were obtained. Detailed MRI protocol were list in **Table 1**.

The features of tumor location, MRF, and extramural venous invasion (EMVI) were evaluated by two radiologists (Dr. Cai and Dr. Li with 12 and 16 years of experience respectively in rectal cancer imaging), and the double-blind principle was applied. The rectum extends from the anal verge (AV) to a distance 15 cm cranially and can be divided into upper rectum (10.1-15cm from AV), mid rectum (5.1-10cm from AV) and lower rectum (0 to 5 cm from AV). The MRF positive was defined that the distance was less than 1mm from the tumor to mesorectal fascia. The extramural venous invasion was assess based on the EMVI scoring system raised by Smith et al. (22). Score 0-2 was defined EMVI negative and score 3-4 was defined EMVI positive.

Tumor Segmentation

All regions of interest (ROIs) were manually evaluated *via* the T2 Weighted image (T2WI) in each slice of the MRI for 3D segmentation. The ROI 1 is the segmentation for the whole tumor and ROI 2 was the segmentation for the tumor bed, which was defined the area that the tumor invaded to the mesorectal. Image segmentation was performed using the open-source software ITK-SNAP (version 3.8.0, www.itksnap.org/; developed at the University of Pennsylvania and the University of North Carolina at Chapel Hill). Digital imaging and communications in medicine images were obtained prior to

TABLE 1 | Detailed MRI protol.

MRI protocol			
Sequences	**FOV (cm)**	**Slice gap**	**Slice sapcing**
Axis T2WI without fat suppress, small FOV, thin layer, The upper bound included the entire sacral promontory, and the lower bound included the entire anus, area larger than 320*256	20	3	0.5
Axis T1WI without fat suppress, small FOV, thin layer, Turbo spin echo (TSE)	30-40	5	1
Axis DWI with fat suppress, b=800	30-40	5	1
Axis contrast-enhanced LAVA sequences with fat suppress	30-40	4	-2 ov

treatment. Small field of view, high-resolution axial T2W sequence is a priority for segmentation. If this sequence could not be obtained, the T2W sequence best displaying the tumor was used for segmentation (including coronal, sagittal, or large field images of the non-high-resolution axial).

Radiomics Feature Extraction

ROI segmentation was used for radiomics feature extraction. Radiomics feature extraction was performed using the "PyRadiomics" package in Python (version 3.0, Wilmington, DE, USA; https://pyradiomics.readthedoc s.io/). Features extracted from the volume of the entire tumor were defined as intertumoral features. Based on the whole tumor, peritumor features were acquired by expanding 5 mm from the border of the tumor to the tumor bed. The process of intratumor and peritumor ROI segmentation is shown in **Figure 2**.

To avoid data heterogeneity bias, all MRI data were subjected to imaging normalization (the intensity of the image was scaled to 0–100) and resampled to the same resolution (1mm×1mm×1 mm) before feature extraction. For each ROI, six feature classes [251 first order statistics, and texture classes (including 336 gray level cooccurrence matrix, 224 gray level run length matrix, 224 gray level size zone matrix, 196 gray level dependence matrix, and 70 neighboring gray tone difference matrix)] were calculated, which resulted in a total of 1301 radiomics features for each scan. The file for the extraction process is included in the **Supplementary Material**.

Feature Selection

The selection process was as follows to screen valuable features and reduce redundant, irrelevant features. First, it was necessary to perform standard scaling of the extracted features. Second, the inter-reader agreement was estimated using the interclass coefficient (ICC) between features extracted from the two segmentations. Only features with an ICC >0.70 were selected for the feature selection process. Third, after conducting Pearson correlation, univariate analysis, and the application of the least absolute shrinkage and selection operator (LASSO) algorithm, the most useful predictive parameters were selected to construct the delta-radiomics signature. Finally, multivariate logistic regression was used to generate the prediction model. The workflow of the radiomics model construction was showed in **Figure 3**.

Statistical Analysis

X^2 or Fisher's exact tests were used for comparing categorical variables, while the Kruskal–Wallis test was used to compare numeric variables. A receiver operating characteristic curve (ROC) analysis was performed to estimate the predictive performance of different models, which was calculated as the area under the curve (AUC). Calibration curve were evaluated using calibration and decision curves. Univariate and multivariate logistic analyses were performed to clarify the relationship between clinical parameters and pCR. Statistical significance was defined as a two-tailed p-value of <0.05. Python (version 3.7) and R statistical software (version 3.3.3; Vienna, Austria) were used for graphical depiction and statistical analysis, respectively.

RESULTS

Clinical Characteristics

The clinical characteristics of the enrolled patients are summarized in **Table 2**. In total, 137 patients were recruited in this study. Participants were randomly divided into training (n=91) and validation sets (n=46). The mean age of the patients was 57 (range: 30–77) years; 83 (60.1%) were men, and 55 (39.8%) were women. There was no statistically significant difference in the good response rate between the training and validation cohorts (16.5% vs. 19.5%, p=0.834). Except for maximal lymphnode (max LN), statistically significant differences were not observed in all clinical

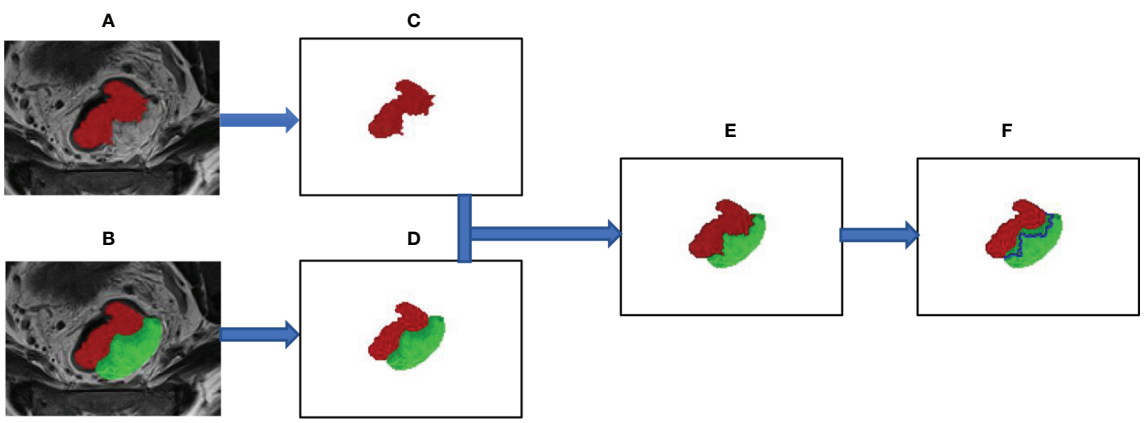

FIGURE 2 | The segmentation process of the region of interest for intratumor and peritumor. **(A)** The whole tumor was manually segmented on axial T2-weighted images and labeled as "intratumor" area (the red area). **(B)** Manually outline the area of the tumor bed (the green area), which is defined as the mesorectal area that the tumor has invaded. **(C)** Show the outline of the entire tumor. **(D–F)** The edge link to the "tumor bed" of "tumor" was dilated by 5 mm and subtracted to obtain the "peritumor" tissues (the blue area).

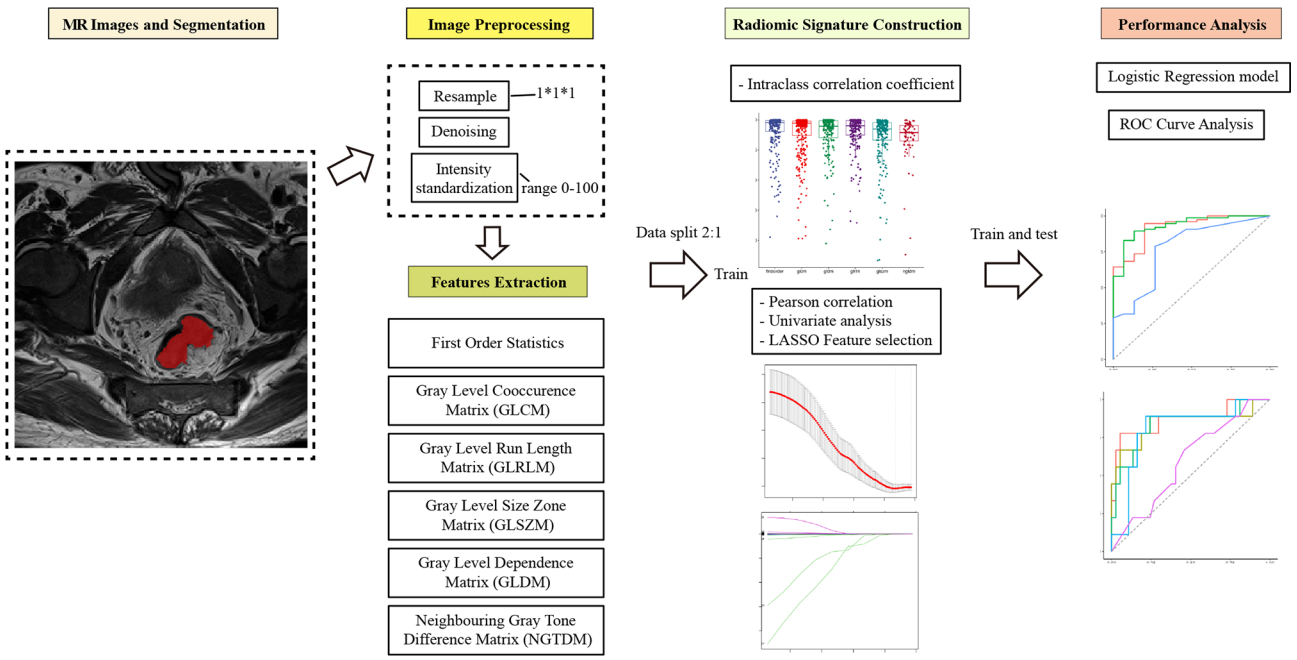

FIGURE 3 | The workflow of the radiomics model construction.

features when comparing the training and validation cohorts. mulivariate factor analysis revealed that the CEA level, T stage, and tumor invasion circumference (TIC) were relative to TRG ($p<0.05$). (**Table 3**).

Feature Selection and Radiomics Signature Construction

In total, 1,301 radiomics features were retrieved from intratumor and peritumor images conducted *via* T2WI. We performed Pearson correlation and univariate analyses to screen the correlative features and eliminate features with low reproducibility. LASSO analysis was then used to select the features from among the screened features (**Supplementary Figure 1**). Finally, following backward elimination, 9 and 10 features were selected from the peritumor and intratumor images, respectively (**Table 4**). The remaining features are listed in **Supplementary Table 1**.

Eventually, the traditional clinical characteristics, selective clinical characteristics and radiomics signature were used to constructed the predictive model, including the traditional clinical model (including T and N stage), selective clinical model (including T stage, CEA level, TIC), intratumor radiomics model, peritumor radiomics model, combined radiomics model (including intra-peritumor radiomics) and clinic-radiomics model (selective clinical characteristics combined intra-peritumor radiomics).

Models Performance

The traditional clinical model yields an AUC of 0.677 (95% confidence interval [CI] 0.527–0.827) in training set and an AUC of 0.701 (95% CI 0.565-0.837) in validation set. When considering the selective clinical model, the results suggest that the AUC in the training set is 0.775 (95% CI 0.637-0.913) and that is 0.596 (95% CI 0.637-0.913) in validation set. In the training cohort, intratumor radiomics features model yielded an AUC of 0.932, whereas that of the peritumor model was 0.921. Furthermore, the two models yielded an AUC of 0.805 and 0.838, respectively, in the validation set (**Table 5**).

Compared to selective clinical model and the intratumor radiomics model individually, the combined selective clinic-intratumor radiomics model achieved the highest AUC (0.940, 95% CI 0.882–0.997) in the training set, whereas the AUC value is 0.781(95% CI 0.603–0.959) in the validation set. Besides, The AUC of the selective clinic-peritumor radiomics model for training set is 0.932 (95% CI 0.871–0.992) and that of the validation set is 0.844 (0.667-1.000), which is statistically significantly higher than that of the selective clinical model ($p=0.025$) (**Table 6**).

The AUC of the combined radiomics model was 0.949 (95% CI 0.887–0.998) in the training cohort and 0.844 (95% CI 0.650–1) in the validation cohort, which was higher than that of the individual radiomics model. Compared to the combined radiomics model, the combined clinic-radiomics model, improved the AUC from 0.844 to 0.871 in the validation set (**Table 7**).

The nomogram of clinics-intratumor and clinics-peritumor for predicting good response as well as the calibration curve are presented in **Figures 4**, **5** respectively. The nomogram showed good performance in predicting the response to NAC. Good discrimination and good calibration for the probability of TRG were observed in the validation set with respect to clinics-

TABLE 2 | Clinical characteristics of patients in the training and validation set.

Characteristics	Training (N = 91)	Validation (N = 46)	*P*
Gender			0.54
Male	53	30	
Female	38	16	
Age			0.90
<60	49	26	
≥60	42	20	
BMI			0.64
<18.5	8	6	
18.5-24	56	25	
>24	27	15	
Smoking			0.28
no	74	33	
yes	17	13	
Family history			0.85
no	72	35	
yes	19	11	
HB (g/l)			0.78
<120	15	6	
≥120	76	40	
CEA (ng/ml)			0.99
<5	56	28	
≥5	35	18	
CA19-9 (u/ml)			0.53
<35	82	39	
≥35	9	7	
T stage			0.42
T3a	28	13	
T3b	24	16	
T3c	4	0	
T4a	35	17	
Distance (cm)			0.55
≤5	14	8	
5.1-10	65	29	
>10	12	9	
TIC			0.69
1/4	1	1	
2/4	26	11	
3/4	41	25	
4/4	23	9	
MRF			0.64
negative	77	32	
positive	14	14	
EMVI			0.45
negative	72	32	
positive	19	14	
LN metastasis			0.20
negative	63	26	
positive	28	20	
max LN (mm)			0.04*
<5	48	15	
≥5	43	31	
TRG			0.83
0	76	37	
1	15	9	

*$p < 0.05$.

peritumor radiomics, with an AUC of 0.838. However, in the validation set, our nomogram for the clinics-intratumor models did not achieve better discriminatory efficiency than that of the peritumor models. The nomogram of the clinic-radiomics model showed good discrimination in predicting treatment response in the validation set as well (**Figures 6 A–E**).

DISCUSSION

Pretreatment prediction of good treatment response is of great significance in pre-therapeutic decision-making. These models demonstrated that the performance of the radiomics signature model in predicting treatment response was far superior to that of the traditional or selective clinical features model. In addition, we found that peritumor radiomics model performed as well as intratumor radiomics model in predicting good treatment response after NAC. The combined clinic-radiomics model showed superior performance in predicting treatment response.

MRI is the image modality of choice when dealing with the primary staging and restaging after treatment in LARC. Although high-resolution MRI is recommended for T and N staging in patients with rectal cancer, the accuracy of staging is still unsatisfactory (18). The main challenge of MRI in assessment of pretreatment T stage is that differentiating early RC (T1-T2) from LARC (12). The study of Detering et al. showed that the accuracy of T stage of early RC evaluated by MRI is poor, with a 54% agreement to pathology (23). For the total T category, the sensitivity, specificity and accuracy of MRI assessment are 87%, 75% and 85% (24). In the assessment of N staging, a poor accuracy of 69% was observed in Detering's study. Radiomics, which were obtained from the primary image of tumor, reflect number of characteristics, not only the shape and location, but also the tumor heterogeneity. Due to the lower accuracy of the staging of RC, it may lead to the poor performance in predicting the prognosis or the treatment response in rectal cancer. This hypothesis is consisted with our findings. Our study revealed that radiomics model has higher predictive performance than clinical model, no matter the traditional or the selective model, suggesting that radiomics could be a practical image biomarker for patients with LARC in predicting treatment response. However, lack of the standard protocol for MRI acquisition and uncertainties in tumor segmentation adversely limit the clinical application of radiomics.

Previous studies have identified that pretreatment T2W images play an important role in predicting treatment response (15, 16) in patients with LARC. However, these studies focused on patients with LARC who received nCRT. The rate of pCR to nCRT was higher than that to NAC in patients with LARC (6). In consideration of individual therapy strategies, screening patients who are likely to achieve a good response to NAC is important to avoid over-treatment. Moreover, most previous studies on radiomics in patients with LARC concentrated on whole tumor features in patients treated with nCRT. Palmisano and colleagues (25) analyzed the apparent diffusion coefficient (ADC) and imaging *via* DWI and T2WI before, during, and after nCRT in patients with LARC and demonstrated that changes in the ADC value and tumor volume at different times could help identify pCR. Shaish et al. (26) reported that T2WI radiomics could be used to predict pCR, neoadjuvant rectal scores, and TRG in patients with LARC receiving nCRT. Furthermore, Petresc et al. (27) reported that T2WI radiomics showed good predictive performance for LARC non-response. In our research, we proposed a pretreatment MRI-based peri- and intratumor

TABLE 3 | Univariate and multivariate analyses of the clinical characteristics.

Characteristics	univariate			Multivariate		
	HR	CI 95%	P	HR	CI 95%	P
Gender						
Male						
Female	1.27	0.41-3.90	0.67			
Age						
<60						
≥60	1.03	0.33-3.13	0.97			
BMI						
<18.5						
18.5-24	1.34	0.20-26.63	0.80			
>24	1.59	0.21-33.19	0.69			
Smoking						
Yes						
No	0.63	0.09-2.60	0.56			
Family history						
yes						
no	2.21	0.61-7.34	0.20			
HB (g/l)						
<120						
≥120	0.75	0.20-3.64	0.69			
CEA (ng/ml)						
<5						
≥5	0.20	0.03-0.79	0.04*	0.23	0.03-1.05	0.08**
CA19-9(u/ml)						
<35						
≥35	0.28	0.02-1.52	0.23			
T stage						
T3a						
T3b	0.19	0.03-0.86	0.05*	0.23	0.03-1.15	0.10
T3c	0.70	0.03-6.42	0.77	0.83	0.03-12.02	0.89
T4a	0.20	0.04-0.76	0.03*	0.25	0.05-1.09	0.08**
LN metastasis						
positive						
negative	1.15	0.33-3.64	0.81			
Distance (cm)						
≤5						
5.1-10	1.22	0.28-8.56	0.81			
>15	1.20	0.13-11.54	0.87			
TIC						
≤2/4						
3/4	0.22	0.05-0.76	0.02*	0.26	0.06-1.02	0.06**
4/4	0.19	0.03-0.86	0.05*	0.53	0.06-3.39	0.52
MRF						
positive						
nagative	1.48	0.30-5.62	0.59			
MRF invasion						
Tumor						
LN	0.70	0.15-2.57	0.61			
tumor deposit	1.23	0.06-9.45	0.86			
other	2.45	0.11-28.1	0.48			
EMVI						
positive						
negative	0.94	0.20-3.40	0.93			
max LN (mm)						
<5						
≥5	0.97	0.31-2.97	0.96			

*$p < 0.05$; **$p < 0.1$.

features model combining clinical and radiomic features to predict a favorable response to NAC in patients with LARC. Interestingly, the model combining intratumor and clinical features did not show statistically significant improvement in the predictive performance compared to that of the radiomics model. The reason for this may be that the radiomics model yielded good performance in predicting treatment responses in patients with LARC, and the partial clinical characteristics were reflected in the radiomics. Although prediction performance varied in the validation cohort, the model incorporating

TABLE 4 | Numbers of features that remained after each selection step for radiomics signature construction.

Feature selection steps	Peritumor Features	Intratumor Features
Before selection	1301	1301
ICC	1275	1143
Pearson correlation	345	336
Univariate analysis	56	37
LASSO	14	16
Backward elimination	9	10

ICC, interclass correlation coefficient; LASSO, least absolute shrinkage and selection operator.

TABLE 5 | The AUC value of clinical characteristics and radiomics model.

variable	Training			
	AUC	**95% CI**	**PI**	**P2**
R1	0.921	0.852-0.990	reference	0.751
R2	0.932	0.870-0.995	0.751	reference
Clinis	0.775	0.637-0.913	0.066	0.044
T+N	0.677	0.527-0.827	< 0.001*	< 0.001*
variable			**Validation**	
	AUC	**95% CI**	**PI**	**P2**
R1	0.838	0.661-1.000	reference	0.583
R2	0.805	0.633-0.976	0.583	reference
clinics	0.596	0.396-0.796	0.079	0.125
T+N	0.521	0.279-0.763	0.024*	0.047*

R1, stand for peritumor radiomics; R2, stand for intratumor radiomics. T, T stage; N, N stage; CEA, carcinoembryonic antigen; Clinics, combined the selective clinical characterisitics, including CEA、Tstage and TIC.
**P < 0.05.*

TABLE 6 | The AUC of selective clinical model compared to radiomics model.

variable	Training			Validation		
	AUC	**95%CI**	**P**	**AUC**	**95%CI**	**P**
R1+clinics	0.932	0.871-0.992	reference	0.844	0.667-1.000	reference
R1	0.921	0.852-0.990	0.400	0.838	0.661-1.000	0.781
clinics	0.775	0.637-0.913	0.040	0.596	0.396-0.796	0.025*
R2+clinics	0.940	0.882-0.997	reference	0.781	0.603-0.959	reference
R2	0.932	0.870-0.995	0.392	0.805	0.633-0.976	0.360
clinics	0.775	0.637-0.913	0.030	0.775	0.637-0.913	0.180

**p < 0.05.*

TABLE 7 | The AUC of radiomics model and clinics model.

variable	Training			Validation		
	AUC	**95%CI**	**P**	**AUC**	**95%CI**	**P**
R1+R2+clinics	0.961	0.922-0.999		0.871	0.706-1.000	
R1+R2	0.949	0.887-0.998	0.547	0.844	0.650-1.000	0.353
R1	0.921	0.852-0.990	0.322	0.838	0.661-1.000	0.789
R2	0.932	0.870-0.995	0.445	0.805	0.633-0.977	0.588
clinics	0.775	0.637-0.913	0.010*	0.596	0.396-0.796	0.001*

**p < 0.05.*

peritumor features performed as well as that incorporating intratumor features in predicting good treatment response.

To our knowledge, this is the first study to evaluate the performance of a model including both peritumor and intratumor radiomics features in predicting a good response to NAC in LARC. Delli Pizzi et al. (28) reported that a model combining primary staging and radiomics, including information on tumor cores and borders, performed best in

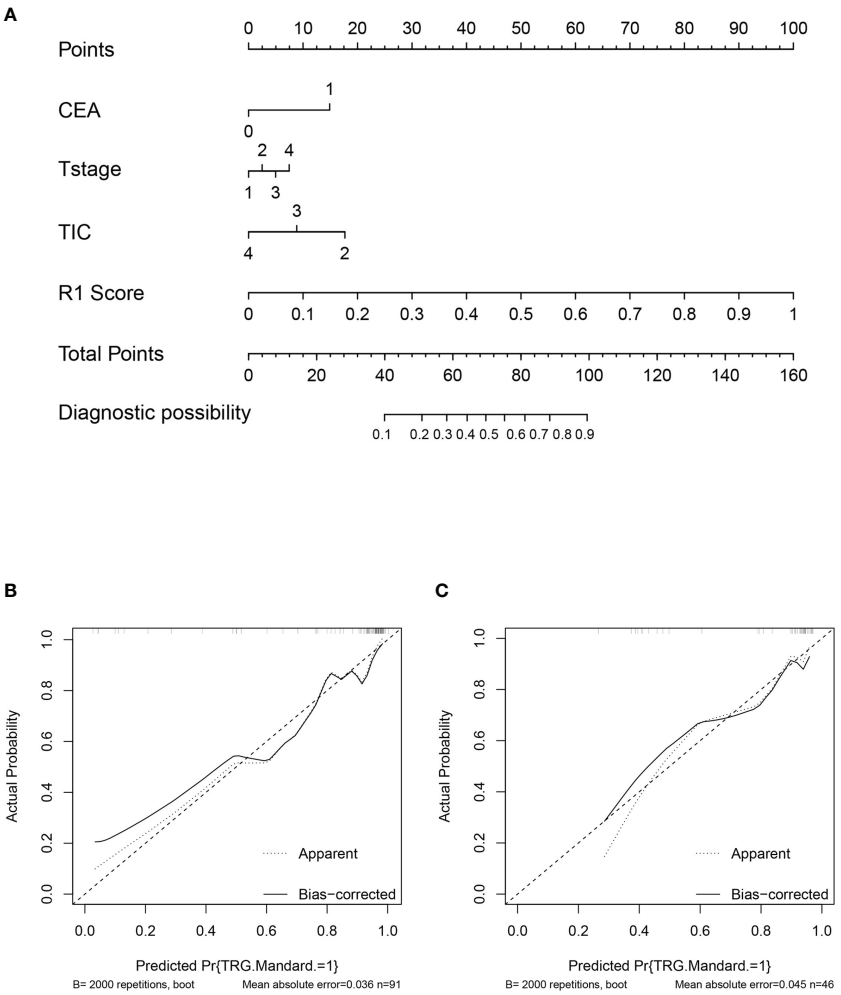

FIGURE 4 | Nomogram based on the clinical characteristics and peritumor radiomics features in the prediction of response to neoadjuvant chemotherapy in locally advanced rectal cancer (LARC). **(A)** Nomogram based on peritumor radiomics clinical features. **(B)** The calibration curve for peritumor radiomics and clinical features in predicting treatment response for LARC in the training set. **(C)** The calibration curve for peritumor radiomics and clinical features in predicting treatment response for LARC in the validation set.

predicting the response to CRT. In that study, they included 72 patients with LARC who received nCRT for analysis, and those with TRGs of 1 or 2 were defined as good responders (this was the definition within our study as well). For image feature analysis, machine-learning approaches were adopted to establish the model. Models evaluating tumor core and tumor border radiomics and clinical features yielded AUC values of 0.689 and 0.541, respectively; the combined model improved the AUC to 0.793 ($z=4.00$, $p=5.6\times10^{-5}$). The tumor border model performed poorly in predicting treatment response. However, in our study, the model combining peri- and intratumor radiomics features did not improve the AUC significantly compared to the individual radiomics models. This may be because of differences between the treatment program and image processing. In contrast, a study by Hu et al. (20) found that the performance of the peritumor model was better than that of the intratumor model in predicting treatment response within the training set among patients with esophageal squamous cell carcinoma; the performance of the two models was similar in the test set as well. Our results showed that there were no significant differences in performance between peritumor and intratumor radiomics models, which was in agreement with the study conducted by Hu et al. (20). Li and colleagues (29) constructed a multimodal model to predict good treatment response in patients with LARC receiving NAC, including CT, HR-T2WI, DCE-T1WI, and ADC and demonstrated that the HR-T2WI model showed the best performance. However, in that study, the authors did not include peritumor information. Braman and colleagues (30) observed that a model combining intra- and peritumor radiomic features showed good performance in predicting pCR to NAC based on pretreatment breast DCE-MRI and suggested that the radiomic feature performance for predicting response was associated with

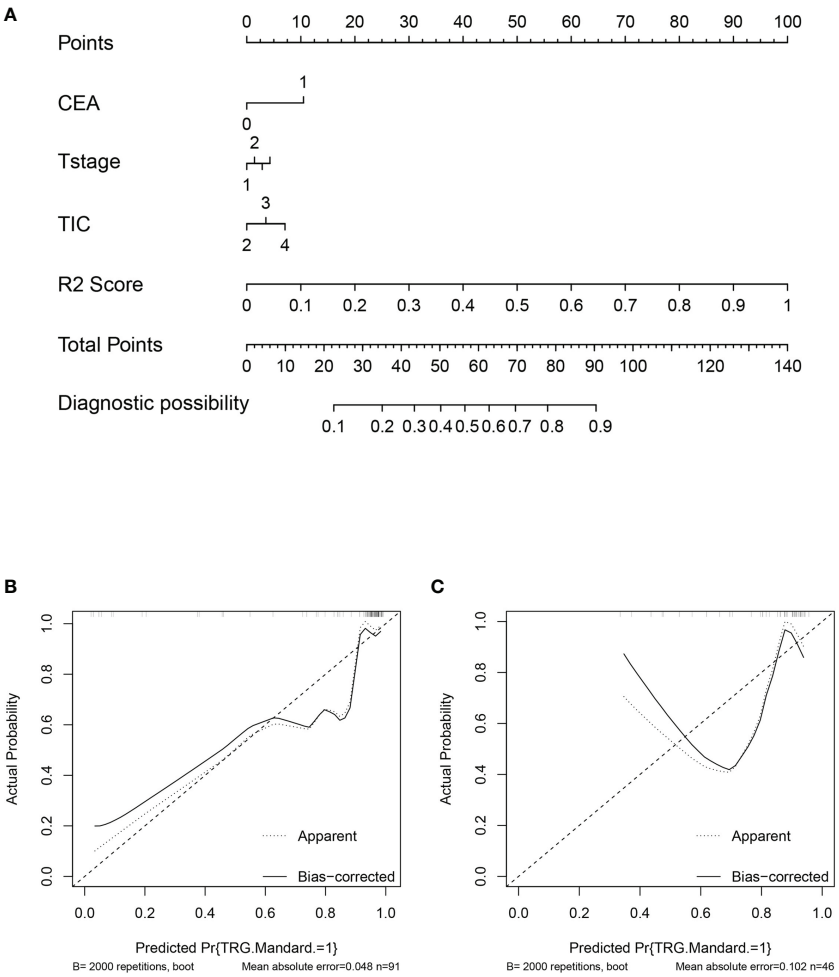

FIGURE 5 | Nomogram based on the clinical characteristics and intratumor radiomics features in the prediction of response to neoadjuvant chemotherapy in locally advanced rectal cancer (LARC). **(A)** Nomogram based on clinical features and intratumor radiomics. **(B)** The calibration curve for intratumor radiomics and clinical features in predicting treatment response for LARC in the training set. **(C)** The calibration curve for intratumor radiomics and clinical features in predicting treatment response for LARC in the validation set.

breast tumor receptor subtypes. Furthermore, Wu and colleagues (22) identified that the enhancement patterns of the tumor-adjacent tissue obtained *via* DCE-MRI might be related to the signaling pathways involved in tumor necrosis as well as a worse prognosis in patients with breast cancer. Thus, peritumor imaging features contain overlooked information related to treatment response. Combining intra-peritumor radiomics features and clinical characteristics can thus be expected to improve prediction performance.

Peritumor characteristics were associated with treatment response, which may be related to the peritumor stroma, lymphocyte infiltration, and immune microenvironment. This suggests that the stroma in rectal cancer contains important information concerning the prognosis and treatment response. Various studies have also revealed that the response to chemo- or radiotherapy may be related to stoma cells or lymphocytes in other malignant neoplasms (31). Our results demonstrate that a peritumor radiomics model performs similarly to an intratumor radiomics model in predicting treatment response. This indicates that peritumor tissue might contain components that influence the treatment response and implies the importance of predictive information within peritumor radiomics features.

Limitations

Our study proved that combining peri- and intratumor radiomics could predict a good response to NAC. However, our study has several limitations. First, because of the single-center design, small sample design study, selection bias is inevitable during patient recruitment. Besides, lack of standard protocol of acquisition of image also leads to selection bias. Second, Evaluating the peritumor area relies on experienced radiologists and requires substantial time and effort. The variability between the inter-reader may lead to poor reproducibility. Third, we only analyzed the impact of peritumor features on neoadjuvant treatment

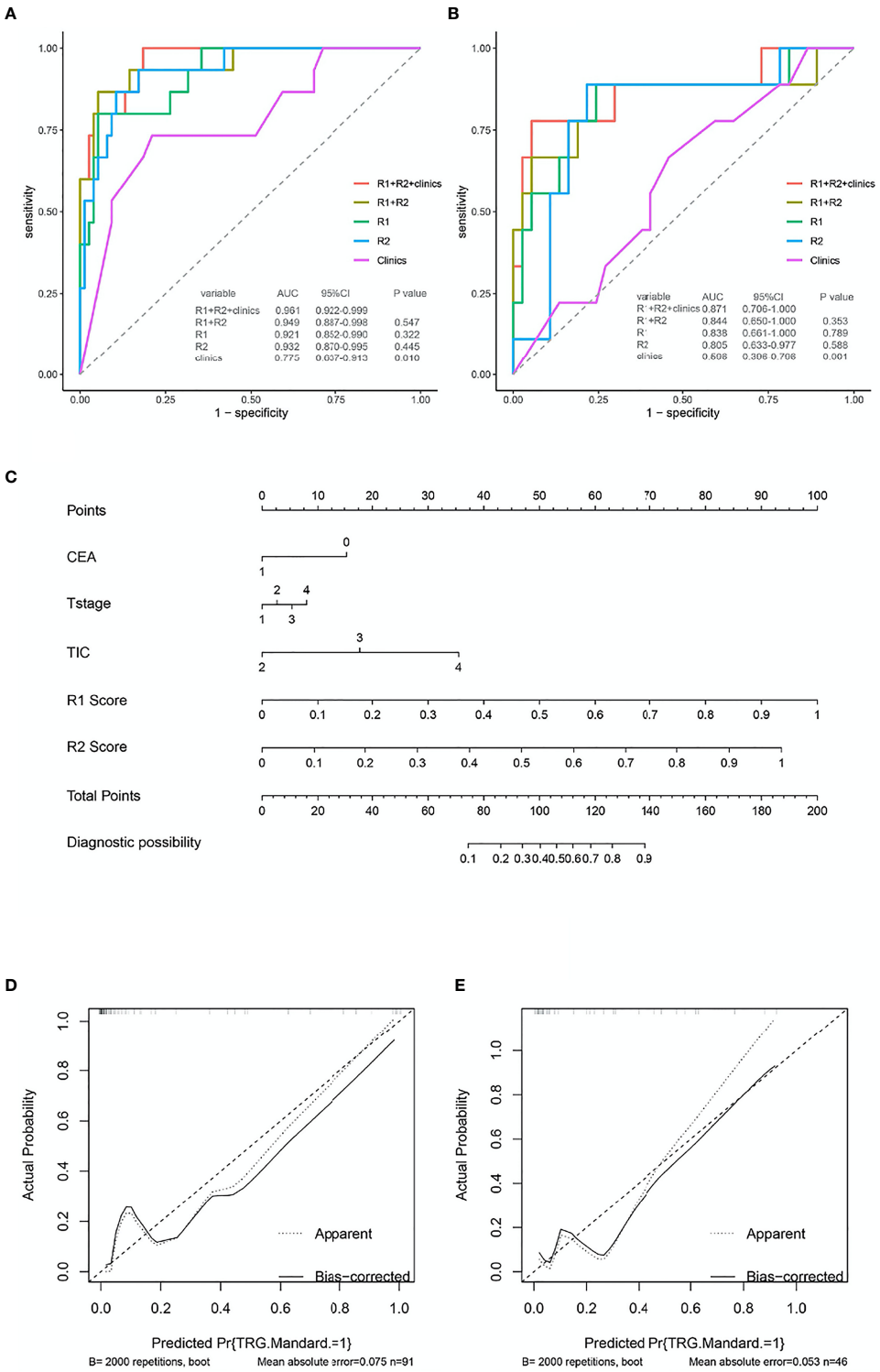

FIGURE 6 | ROC and nomogram based on the clinical characteristics and intra-peritumor radiomics features in the prediction of response to neoadjuvant chemotherapy in locally advanced rectal cancer (LARC). **(A)** The receiver operating characteristic curve (ROC) for different models in predicting treatment response for LARC in the training set.**(B)** The ROC for different models in predicting treatment response for LARC in the validation set. **(C)** Nomogram based on the clinical characteristics and combined-radiomics features in the prediction of response to neoadjuvant chemotherapy in locally advanced rectal cancer (LARC). **(D, E)** The calibration curve for the models in predicting treatment response for LARC in the training set and validation set.

response at the theoretical level and have not further confirmed these findings at the molecular level. Thus, it is impossible to clarify the pathophysiological process underlying the impact of the tumor perimeter on neoadjuvant treatment response.

CONCLUSIONS

Our study demonstrated that peritumor radiomics features contained important information related to a favorable response to NAC. We found that a model combining the clinical characteristics and intra-peritumor radiomics features could improve predictive capability in terms of identifying a good response to NAC in patients with LARC. Predictive models are commonly used in precision medicine. The results of our study inform future research directions and, if confirmed, will inform medical guidelines and optimal clinical decision-making in personalized medicine.

DATA AVAILABILITY STATEMENT

The original contributions presented in the study are included in the article/**Supplementary Material**. Further inquiries can be directed to the corresponding authors.

ETHICS STATEMENT

The study design was approved by the ethics committee of the Sun Yat-sen University Cancer Center (Approval no. B2021-157-01).

AUTHOR CONTRIBUTIONS

B-YC designed the study. YL, X-HJ, LX, and X-FL organized the data. HJ and HX analyzed and visualized the data. B-YC drafted the article. X-FT, P-QC, and LL revised the paper. All authors contributed to the article and approved the submitted version.

FUNDING

This work was supported by The Youth Fund Project of Guangdong Basic and Applied Basic Research Fund Regional Joint Fund (2020A1515110939).

ACKNOWLEDGMENTS

We thank Han-Jiao for the radiomics feature extraction.

SUPPLEMENTARY MATERIAL

The Supplementary Material for this article can be found online at: https://www.frontiersin.org/articles/10.3389/fonc.2022.801743/full#supplementary-material

Supplementary Figure 1 | Texture feature selection using the least absolute shrinkage and selection operator binary logistic regression model. **(A, B)** Selection of peritumor radiomics. **(C, D)** Selection of intratumor radiomics.

REFERENCES

1. Sung H, Ferlay J, Siegel RL, Laversanne M, Soerjomataram I, Jemal A, et al. Global Cancer Statistics 2020: GLOBOCAN Estimates of Incidence and Mortality Worldwide for 36 Cancers in 185 Countries. *CA Cancer J Clin* (2021) 71(3):209–49. doi: 10.3322/caac.21660
2. Liu Z, Zhang XY, Shi YJ, Wang L, Zhu HT, Tang Z, et al. Radiomics Analysis for Evaluation of Pathological Complete Response to Neoadjuvant Chemoradiotherapy in Locally Advanced Rectal Cancer. *Clin Cancer Res* (2017) 23(23):7253–62. doi: 10.1158/1078-0432.CCR-17-1038
3. Bahadoer RR, Dijkstra EA, van Etten B, Marijnen CAM, Putter H, Kranenbarg EM, et al. Short-Course Radiotherapy Followed by Chemotherapy Before Total Mesorectal Excision (TME) Versus Preoperative Chemoradiotherapy, TME, and Optional Adjuvant Chemotherapy in Locally Advanced Rectal Cancer (RAPIDO): A Randomised, Open-Label, Phase 3 Trial. *Lancet Oncol* (2021) 22(1):29–42. doi: 10.1016/S1470-2045(20)30555-6
4. Giunta EF, Bregni G, Pretta A, Deleporte A, Liberale G, Bali AM, et al. Total Neoadjuvant Therapy for Rectal Cancer: Making Sense of the Results From the RAPIDO and PRODIGE 23 Trials. *Cancer Treat Rev* (2021) 96:102177. doi: 10.1016/j.ctrv.2021.102177
5. Habr-Gama A, Perez RO, Nadalin W, Sabbaga J, Ribeiro U Jr, Silva e Sousa AH Jr, et al. Operative Versus Nonoperative Treatment for Stage 0 Distal Rectal Cancer Following Chemoradiation Therapy: Long-Term Results. *Ann Surg* (2004) 240(4):711–717; discussion 717-718. doi: 10.1097/01.sla.0000141194.27992.32
6. Deng Y, Chi P, Lan P, Wang L, Chen W, Cui L, et al. Modified FOLFOX6 With or Without Radiation Versus Fluorouracil and Leucovorin With Radiation in Neoadjuvant Treatment of Locally Advanced Rectal Cancer: Initial Results of the Chinese FOWARC Multicenter, Open-Label, Randomized Three-Arm Phase III Trial. *J Clin Oncol* (2016) 34(27):3300–7. doi: 10.1200/JCO.2016.66.6198
7. Deng Y, Chi P, Lan P, Wang L, Chen W, Cui L, et alNeoadjuvant Modified FOLFOX6 With or Without Radiation Versus Fluorouracil Plus Radiation for Locally Advanced Rectal Cancer: Final Results of the Chinese FOWARC Trial. *J Clin Oncol* (2019) 37(34):3223–3. doi: 10.1200/JCO.18.02309.
8. Ogura A, Uehara K, Aiba T, Sando M, Tanaka A, Ohara N, et al. Indications for Neoadjuvant Treatment Based on Risk Factors for Poor Prognosis Before and After Neoadjuvant Chemotherapy Alone in Patients With Locally Advanced Rectal Cancer. *Eur J Surg Oncol* (2021) 47(5):1005–11. doi: 10.1016/j.ejso.2020.10.038
9. Torkzad MR, Pahlman L, and Glimelius B. Magnetic Resonance Imaging (MRI) in Rectal Cancer: A Comprehensive Review. *Insights Imaging* (2010) 1 (4):245–67. doi: 10.1007/s13244-010-0037-4
10. Caruso D, Zerunian M, De Santis D, Biondi T, Paolantonio P, Rengo M, et al. Magnetic Resonance of Rectal Cancer Response to Therapy: An Image Quality Comparison Between 3.0 and 1.5 Tesla. *BioMed Res Int* (2020) 2020:9842732. doi: 10.1155/2020/9842732
11. Caruso D, Polici M, Zerunian M, Pucciarelli F, Guido G, Polidori T, et al. Radiomics in Oncology, Part 1: Technical Principles and Gastrointestinal Application in CT and MRI. *Cancers (Basel)* (2021) 13(11):2522. doi: 10.3390/cancers13112522
12. Lambin P, Rios-Velazquez E, Leijenaar R, Carvalho S, van Stiphout RG, Granton P, et al. Radiomics: Extracting More Information From Medical Images Using Advanced Feature Analysis. *Eur J Cancer* (2012) 48(4):441–6. doi: 10.1016/j.ejca.2011.11.036
13. Coppola F, Giannini V, Gabelloni M, Panic J, Defeudis A, Lo Monaco S, et al. Radiomics and Magnetic Resonance Imaging of Rectal Cancer: From Engineering to Clinical Practice. *Diagnostics (Basel)* (2021) 11(5):756. doi: 10.3390/diagnostics11050756

14. Bulens P, Couwenberg A, Intven M, Debucquoy A, Vandecaveye V, Van Cutsem E, et al. Predicting the Tumor Response to Chemoradiotherapy for Rectal Cancer: Model Development and External Validation Using MRI Radiomics. *Radiother Oncol* (2020) 142:246–52. doi: 10.1016/j.radonc.2019.07.033
15. Chen H, Shi L, Nguyen KNB, Monjazeb AM, Matsukuma KE, Loehfelm TW, et al. MRI Radiomics for Prediction of Tumor Response and Downstaging in Rectal Cancer Patients After Preoperative Chemoradiation. *Adv Radiat Oncol* (2020) 5(6):1286–95. doi: 10.1016/j.adro.2020.04.016
16. Horvat N, Veeraraghavan H, Khan M, Blazic I, Zheng J, Capanu M, et al. MR Imaging of Rectal Cancer: Radiomics Analysis to Assess Treatment Response After Neoadjuvant Therapy. *Radiology* (2018) 287(3):833–43. doi: 10.1148/radiol.2018172300
17. Li Z, Ma X, Shen F, Lu H, Xia Y, and Lu J. Evaluating Treatment Response to Neoadjuvant Chemoradiotherapy in Rectal Cancer Using Various MRI-Based Radiomics Models. *BMC Med Imaging* (2021) 21(1):30. doi: 10.1186/s12880-021-00560-0
18. Wan L, Peng W, Zou S, Ye F, Geng Y, and Ouyang H. MRI-Based Delta-Radiomics are Predictive of Pathological Complete Response After Neoadjuvant Chemoradiotherapy in Locally Advanced Rectal Cancer. *Acad Radiol* (2021) 28(Suppl 1):S95–S104. doi: 10.1016/j.acra.2020.10.026
19. Khorrami M, Khunger M, Zagouras A, Patil P, Thawani R, Bera K, et al. Combination of Peri- and Intratumoral Radiomic Features on Baseline CT Scans Predicts Response to Chemotherapy in Lung Adenocarcinoma. *Radiol Artif Intell* (2019) 1(2):e180012. doi: 10.1148/ryai.2019180012
20. Hu Y, Xie C, Yang H, Ho JWK, Wen J, Han L, et al. Assessment of Intratumoral and Peritumoral Computed Tomography Radiomics for Predicting Pathological Complete Response to Neoadjuvant Chemoradiation in Patients With Esophageal Squamous Cell Carcinoma. *JAMA Netw Open* (2020) 3(9):e2015927. doi: 10.1001/jamanetworkopen.2020.15927
21. Mandard AM, Dalibard F, Mandard JC, Marnay J, Henry-Amar M, Petiot JF, et al. Pathologic Assessment of Tumor Regression After Preoperative Chemoradiotherapy of Esophageal Carcinoma. *Cancer* (1994) 73(11):2680–6. doi: 10.1002/1097-0142(19940601)73:11<2680::aid-cncr2820731105>3.0.co;2-c
22. Smith NJ, Barbachano Y, Norman AR, Swift RI, Abulafi AM, and Brown G. Prognostic Significance of Magnetic Resonance Imaging-Detected Extramural Vascular Invasion in Rectal Cancer. *Br J Surg* (2008) 95(2):229–36. doi: 10.1002/bjs.5917
23. Detering R, van Oostendorp SE, Meyer VM, van Dieren S, Bos ACRK, Dekker JWT, et al. MRI Ct1-2 Rectal Cancer Staging Accuracy: A Population-Based Study. *Br J Surg* (2020) 107(10):1372–82. doi: 10.1002/bjs.11590
24. Arya S, Sen S, Engineer R, Saklani A, and Pandey T. Imaging and Management of Rectal Cancer. *Semin Ultrasound CT MR* (2020) 41(2):183–206. doi: 10.1053/j.sult.2020.01.001
25. Palmisano A, Di Chiara A, Esposito A, Rancoita PMV, Fiorino C, Passoni P, et al. MRI Prediction of Pathological Response in Locally Advanced Rectal Cancer: When Apparent Diffusion Coefficient Radiomics Meets Conventional Volumetry. *Clin Radiol* (2020) 75(10):798.e1–.e11. doi: 10.1016/j.crad.2020.06.023
26. Shaish H, Aukerman A, Vanguri R, Spinelli A, Armenta Zhang P, Jambawalikar S, et al. Radiomics of MRI for Pretreatment Prediction of Pathologic Complete Response, Tumor Regression Grade, and Neoadjuvant Rectal Score in Patients With Locally Advanced Rectal Cancer Undergoing Neoadjuvant Chemoradiation: An International Multicenter Study. *Eur Radiol* (2020) 30(11):6263–73. doi: 10.1007/s00330-020-06968-6
27. Petresc B, Lebovici A, Caraiani C, Feier DS, Graur F, and Buruian MM. Pre-Treatment T2-WI Based Radiomics Features for Prediction of Locally Advanced Rectal Cancer Non-Response to Neoadjuvant Chemoradiotherapy: A Preliminary Study. *Cancers (Basel)* (2020) 12(7):1984. doi: 10.3390/cancers12071894
28. Delli Pizzi A, Chiarelli AM, Chiacchiaretta P, d'Annibale M, Croce P, Rosa C, et al. MRI-Based Clinical-Radiomics Model Predicts Tumor Response Before Treatment in Locally Advanced Rectal Cancer. *Sci Rep* (2021) 11(1):5379. doi: 10.1038/s41598-021-84816-3
29. Li ZY, Wang XD, Li M, Liu XJ, Ye Z, Song B, et al. Multi-Modal Radiomics Model to Predict Treatment Response to Neoadjuvant Chemotherapy for Locally Advanced Rectal Cancer. *World J Gastroenterol* (2020) 26(19):2388–402. doi: 10.3748/wjg.v26.i19.2388
30. Braman NM, Etesami M, Prasanna P, Dubchuk C, Gilmore H, Tiwari P, et al. Intratumoral and Peritumoral Radiomics for the Pretreatment Prediction of Pathological Complete Response to Neoadjuvant Chemotherapy Based on Breast DCE-MRI. *Breast Cancer Res* (2017) 19(1):57. doi: 10.1186/s13058-017-0846-1
31. Post AEM, Smid M, Nagelkerke A, Martens JWM, Bussink J, Sweep FCGJ, et al. Interferon-Stimulated Genes Are Involved in Cross-Resistance to Radiotherapy in Tamoxifen-Resistant Breast Cancer. *Clin Cancer Res* (2018) 24(14):3397–408. doi: 10.1158/1078-0432.CCR-17-2551

Conflict of Interest: The authors declare that the research was conducted in the absence of any commercial or financial relationships that could be construed as a potential conflict of interest.

frontiers | Frontiers in Oncology

ORIGINAL RESEARCH
published: 27 May 2022
doi: 10.3389/fonc.2022.785350

Survival Is Worse in Patients Completing Immunotherapy Prior to SBRT/SRS Compared to Those Receiving It Concurrently or After

*Susan Woody[1], Aparna Hegde[1,2], Hyder Arastu[1], M. Sean Peach[1], Nitika Sharma[3], Paul Walker[4,5] and Andrew W. Ju[1]**

[1] Department of Radiation Oncology, Brody School of Medicine at East Carolina University, Greenville, NC, United States, [2] Department of Hematology and Oncology, University of Alabama at Birmingham School of Medicine, Birmingham, AL, United States, [3] Anne Arundel Medical Center's DeCesaris Cancer Institute, Annapolis Oncology Center, Annapolis, MD, United States, [4] Brody School of Medicine at East Carolina University, Greenville, NC, United States, [5] Circulogene, Birmingham, AL, United States

OPEN ACCESS

Edited by:
Francesco Cellini,
Università Cattolica del Sacro Cuore, Italy

Reviewed by:
Asal Rahimi,
University of Texas Southwestern Medical Center, United States
Charles B. Simone,
Memorial Sloan Kettering Cancer Center, United States

***Correspondence:**
Andrew W. Ju
jua@ecu.edu

Specialty section:
This article was submitted to Radiation Oncology, a section of the journal Frontiers in Oncology

Received: 29 September 2021
Accepted: 21 April 2022
Published: 27 May 2022

Citation:
Woody S, Hegde A, Arastu H, Peach MS, Sharma N, Walker P and Ju AW (2022) Survival Is Worse in Patients Completing Immunotherapy Prior to SBRT/SRS Compared to Those Receiving It Concurrently or After. Front. Oncol. 12:785350. doi: 10.3389/fonc.2022.785350

Purpose/Objectives: The abscopal effect could theoretically be potentiated when combined with immunomodulating drugs through increased antigen production. The optimal dosing and schedule of radiotherapy with immunotherapy are unknown, although they are actively investigated in laboratory and clinical models. Clinical data in patients treated for metastatic disease with both modalities may guide future studies.

Materials and Methods: This is a single-institution retrospective review of all patients treated with stereotactic body radiotherapy (SBRT)/stereotactic radiosurgery (SRS) and immunomodulating therapy within 6 months before or after SBRT/SRS for metastatic cancer. Clinical and tumor characteristics were recorded, as well as SBRT/SRS details, immunotherapy details, and survival. Log-rank tests on Kaplan–Meier curves for overall survival (OS) that were calculated from the end of SBRT/SRS were used in univariate analysis and Cox proportional hazards regression for multivariate analysis.

Results: A total of 125 patients were identified who met the inclusion criteria; 70 received SBRT, and 57 received SRS. Eighty-three patients were treated for non-small cell lung cancer, 7 patients for small cell lung cancer, and 35 patients for other cancers, with the most common one being melanoma. Fifty-three percent of patients received nivolumab, 29% pembrolizumab, 13% atezolizumab, 5% other. Twenty percent received immunotherapy before SBRT/SRS, 39% during SBRT/SRS, 41% after. Eighty-six patients had died by the time of the analysis; the median OS for the whole cohort was 9.7 months. Patients who had completed immunotherapy prior to SBRT/SRS had worse OS than those who received concurrent therapy or immunotherapy after SBRT/SRS, with a difference in median OS of 3.6 months vs. 13.0 months ($p = 0.010$) that was retained on multivariate analysis ($p = 0.011$). There was no significant difference in OS between patients receiving SRS vs. SBRT ($p = 0.20$), sex ($p = 0.53$), age >62 years ($p = 0.76$), or lung primary vs. others ($p = 0.73$) on univariate or multivariate analysis. When comparing

before/concurrent to after/concurrent administration, there is a difference in survival with after/concurrent survival of 8.181 months and before survival of 13.010 months, but this was not significant (p = 0.25).

Conclusions: OS appears to be worse in patients who complete immunotherapy prior to SBRT/SRS compared to those receiving it concurrently or after. The design of this retrospective review may be prone to lead time bias, although the difference in median survival is longer than the 6-month window before SBRT/SRS and could only account for part of this difference. Further analysis into causes of death and toxicity and prospective studies are needed to confirm the results of this analysis.

Keywords: SBRT, SRS, immunotherapy, abscopal effect, radiation

INTRODUCTION

Cancer remains a leading cause of death in developed countries. One therapeutic technique that has yet to be optimized is the combination of local radiation therapy and immunotherapy, which is thought to have a synergistic effect (1–4). Since 1953, radiation therapy has been found to aid antitumor activity outside of the irradiated site in a phenomenon known as the abscopal effect (5–8). The exact mechanism behind the abscopal effect is unknown, but current research suggests that local radiation generates tumor-specific antigens that are processed and presented to T cells for systemic antitumor activity (2, 6, 8, 9). However, the inability to predict when the abscopal effect will happen had led to clinical limitations. In addition, the posited idea of antigen generation by radiation may be limited by modulators of the immune system including program cell death protein-1 (PD-1) and program cell death protein ligand-1 (PD-L1) (6, 8–10). For instance, Park et al. (10) showed that the abscopal effect induced by stereotactic ablative radiotherapy (SABR) was minimized by PD-1 in preclinical mouse models of melanoma and renal cell carcinoma. New immunotherapy medications that target immune modulators such as PD-1 and PD-L1 have led to a new interest in the abscopal effect with radiation. For instance, Smilowitz et al. (11) showed in 2016 that combining radiation therapy with immune checkpoint inhibitors improved outcomes in a mouse model of intracerebral melanoma. As such, it is thought that immune checkpoint inhibitors present a way to circumvent the immunosuppressive components that limit the influence of abscopal effects.

There remain a lot of unknowns about the relationship between immunotherapy and the abscopal effect. In particular, the optimal sequence of immunotherapy with radiation remains unknown (12). Specifically, is immunotherapy best to give before, concurrently, or after localized radiation? Various studies have indicated that the optimal sequence remains unknown (12).

To analyze the optimal sequence, we conducted a retrospective review at our institution of the best time to administer immunotherapy targeting PD-1 and PD-L1 with localized radiation. A preclinical study in 2014 suggested that concurrent delivery of radiation with PD-L1 antagonism was better than subsequent administration of immunotherapy (13). Initial experience at our hospital also suggested similar results with the use of PD-1 inhibitors and stereotactic body radiotherapy (SBRT) or stereotactic radiosurgery (SRS) (14). Our hypothesis was that administering immunotherapy concurrently with SBRT (i.e., a sandwiched approach) would produce the best improvement in overall survival (OS) compared to administering immunotherapy before SBRT/SRS or after SBRT/SRS.

MATERIALS AND METHODS

We conducted a single-center retrospective chart review for this study. The study was conducted with institutional review board (IRB) approval under UMC IRB 15-001726.

Patient Selection

Patients were selected for review if they had received PD-1 or PD-L1 immunotherapy and SBRT/SRS within 6 months of each other from January 1, 2014, to December 31, 2019. This was initially established from an institutional lung database, but we expanded our data set to include cancers other than lung (14).

Patient Data Collection

The selected patients' charts were reviewed to collect the following information: age, gender, date of birth, date of cancer diagnosis, cancer pathology, cancer stage at diagnosis, any metastasis that existed at the time of immunotherapy administration, site of radiation treatment, type of radiation treatment (SBRT vs. SRS), date(s) of radiation treatment, fractionation or dose of radiation treatment, immunotherapy drug used, immunotherapy dates of treatment, the date it was decided to start immunotherapy, failure or progression following immunotherapy, if a patient was alive or deceased, and date last known alive or date of death. If the patient was still alive on December 31, 2019, this date was chosen as his or her last known alive/death date.

Patients were then classified into one of three categories as to when they received their immunotherapy relative to their radiation treatment: before radiation, after radiation, or sandwiched with radiation treatment. To encompass patients who may experience the abscopal effect, only patients who

received immunotherapy concurrently, 6 months before, or 6 months after radiation treatment were included in the study. This time frame was based on discussions with multiple clinicians at our site and the time frame they would use to combine radiation with immunotherapy to induce the abscopal effect, although reports of the abscopal effect lasting up to 12 months have been reported (15). Some patients received multiple rounds of immunotherapy and radiation treatment during their cancer care between the 2014 and 2019 time frame. Since this study's hypothesis focused on the sandwiched radiation to immunotherapy effect, if a patient received immunotherapy sandwiched with radiation, then this was the prioritized time frame used for this study. In such cases where a patient received multiple courses of immunotherapy concurrently with radiation, then the immunotherapy course closest to radiation was used. If a patient did not receive radiation and immunotherapy concurrently, then the most recent course of radiation/immunotherapy was used.

Data Analysis

Our primary endpoint was OS as calculated from the end of SBRT/SRS to a patient's last known alive date. Significance was defined as a p-value <0.05. All statistical analyses were performed using MedCalc Statistical Software (v20.013, Acacialaan 22, B-8400 Ostend Belgium). Kaplan–Meier survival analysis was conducted using the log-rank test. Multivariate analysis was performed using Cox multiple regression analysis.

RESULTS

Patient Demographics

In total, we found 125 patients who fit our inclusion criteria, and the results are summarized in **Table 1**. There were 56% men and 44% women. Ninety (72%) patients had lung cancer with adenocarcinoma (47.2% patients), squamous cell carcinoma (19.2%), or small cell carcinoma (5.6%). Thirty-five (28%) patients had other histological cancers including 9 patients with melanoma (7.2%). About 55% received SBRT, and 45% received SRS. In this study, 54.4% of the patients received nivolumab, 31.2% received pembrolizumab, 12.8% received atezolizumab, and 0.8% received avelumab or durvalumab as immunotherapy.

Primary Endpoint

We calculated OS from the end of radiation therapy to the patient's last known alive date or his/her death. We found that the OS of patients receiving immunotherapy before radiation was 3.285 months compared to 13.010 months for patients who received immunotherapy concurrently or after radiation (p = 0.014). The curve can be seen in **Figure 1** and results in **Table 2**. This difference in OS was maintained on multivariate analysis accounting for patient age (p = 0.76), sex (0.53), cancer type (lung vs. non-lung) (0.73), and modality of radiation (SBRT/SRS) (p = 0.20) as seen in **Table 3**. In comparison, the median OS from SBRT/SRS was not significantly different in other comparisons. For patients who received immunotherapy before/concurrently with radiation, OS was 8.181 months compared to 12.682 months for those patients who received immunotherapy after radiation (p = 0.33). For patients who received immunotherapy concurrently with radiation, OS was 13.010 months vs. 8.641 months for those who received it before or after radiation (p = 0.46).

Due to the potential for lead time bias in our calculation, we also calculated OS starting from the end of all SBRT/immunotherapy treatment and starting from the decision to treat with immunotherapy. These results are noted in **Figures 2**, **3**, respectively. OS as calculated from the end of treatment of either radiation or immunotherapy was longer for those who received immunotherapy concurrently/after at 9.331 months compared to those who received immunotherapy before radiation at 3.088 months, but that result was not significant (p = 0.064). This difference in OS between these cohorts is not present when OS is calculated from the decision to start immunotherapy. Those who received immunotherapy before survived 10.02 months compared to 12.65 months for those who received immunotherapy concurrently or after radiation (p = 0.81). These can be seen in **Figure 3** and **Table 4**.

We tested the difference between immunotherapy given before radiation vs. being given concurrently/after radiation at a shortened interval between immunotherapy and radiation of 3 months and 1 month, respectively. Within 3 months, the OS for

TABLE 1 | Patient demographics including sex, cancer type (divided into subclassifications for lung cancer), type of radiation therapy, timing of immunotherapy, and exact immunotherapy used.

DEMOGRAPHICS (n = 125)	
Men	70 (56%)
Women	55 (44%)
Lung cancer	90 (72.0%)
• Adenocarcinoma	59 (47.2%)
• Squamous cell	24 (19.2%)
• Small cell	7 (5.6%)
Non-lung cancer	35 (28.0%)
• Melanoma	9 (7.2%)
• Poorly differentiated	4 (3.2%)
• Head and neck	3 (2.4%)
• Neuroendocrine	2 (1.6%)
• Thymic	2 (1.6%)
• Other (1 case of each)	15 (16%)
TYPE OF THERAPY	
SBRT	68 (54.4%)
SRS	57 (45.6%)
TIMING OF IMMUNOTHERAPY	
Before	26 (20.8%)
After	51 (40.8%)
During	48 (38.4%)
IMMUNOTHERAPY	
Nivolumab (PD-1)	68 (54.4%)
Pembrolizumab (PD-1)	39 (31.2%)
Atezolizumab (PD-L1)	16 (12.8%)
Avelumab (PD-L1)	1 (0.8%)
Durvalumab (PD-L1)	1 (0.8%)

SBRT, Stereotactic Body Radiotherapy; SRS, Stereotactic Radiosurgery.

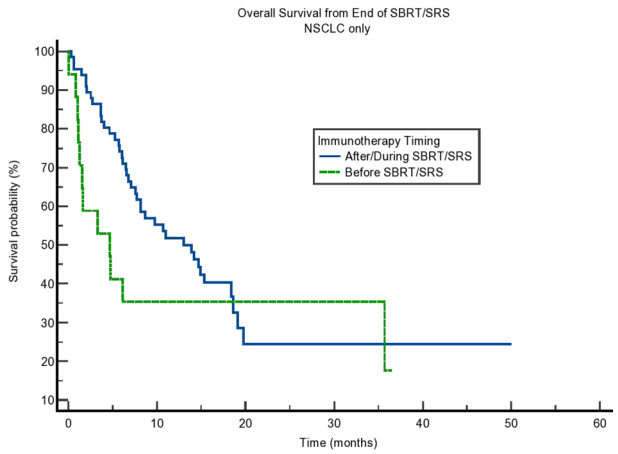

FIGURE 1 | Kaplan–Meier curve showing overall survival (OS) from the end of stereotactic body radiotherapy (SBRT)/stereotactic radiosurgery (SRS). Comparing immunotherapy when given during/after SBRT/SRS compared to before SBRT/SRS. p = 0.014.

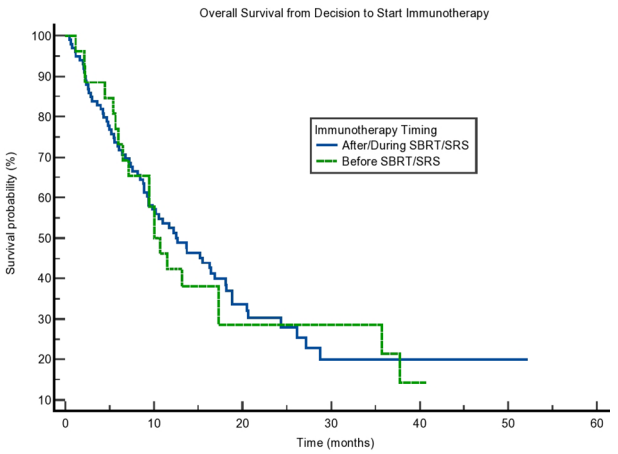

FIGURE 2 | Kaplan–Meier curve showing overall survival (OS) from the end of treatment. OS separated based on immunotherapy given during/after stereotactic body radiotherapy (SBRT)/stereotactic radiosurgery (SRS) compared to before SBRT/SRS. p = 0.064.

TABLE 2 | Median OS from SBRT in months as calculated from the end of radiation treatment.

Immunotherapy	Median OS from SBRT (months)	p-value
Before*	3.285	0.014
Concurrent/After*	13.010	
Before/Concurrent	8.181	0.33
After	12.682	
Concurrent	13.010	0.46
Before/After	8.641	

**Indicates significance. OS, Overall Survival; SBRT, Stereotactic Body Radiotherapy.*

TABLE 3 | Multivariate analysis results showing that immunotherapy timing remained significant when accounting for age, sex, type of cancer (lung vs. other), and type of radiation treatment.

Multivariate Analysis	p-value
Immunotherapy Timing (Before vs. During/After)	0.0
Age > or <62 years	0.76
Gender	0.53
Lung Cancer vs. Non lung cancer	0.73
SBRT vs. SRS	0.20

SBRT, Stereotactic Body Radiotherapy; SRS, Stereotactic Radiosurgery.

patients who received immunotherapy before radiation was 1.971 months compared to 9.725 months for those who received it concurrently or after radiation. This difference was smaller at 1 month with an OS of 3.285 months for those who received immunotherapy before radiation compared to 9.593 months for those who received immunotherapy concurrently or after radiation. Of note, the differences in OS at 3 months (p = 0.17) and 1 month (p = 0.57) were not statistically significant.

We also calculated the difference in OS of those with non-small cell lung cancer (NSCLC), as this group comprised most of our population. Interestingly, although the difference in OS was present, it was not statistically significant (p = 0.16). The results can be seen in **Figure 4**. Finally, we tested SBRT/SRS comparisons of survival. While SBRT had a trend toward a difference in OS, there was a statistical difference in terms of SRS patients. This can be seen in **Table 5**. This result is intriguing and opens the possibility of studying SRS timing with immunotherapy in more detail.

DISCUSSION

Based on our analysis, we see that the OS was significantly greater for those patients receiving immunotherapy concurrently or after radiation compared to those who received immunotherapy prior to radiation. This contrasts with previous preliminary data we had that suggested that immunotherapy sandwiched between SBRT/SRS was more beneficial, but the data were more limited in that abstract (14). A recently published phase 2 trial also showed improvement for patients who received pembrolizumab after SBRT for NSCLC (16). However, results did not meet significance as defined by the trial and were influenced by patients with PD-L1-positive tumors. Therefore, the data on how to combine therapies are still inconclusive. With respect to OS based on the decision to start immunotherapy, our results were not significant. We suspect that this may also be confounded due to differing times between the decision to start immunotherapy and the patient actually receiving immunotherapy, but this is a valuable clinical decision point. As such, the applicability of our results to clinical decision-making remains limited.

Our data expand on existing knowledge about the optimal timing of radiation therapy and immunotherapy. Secondary review of the KEYNOTE-001 trial suggested that receiving pembrolizumab after radiation promoted greater progression-free survival and OS for NSCLC. This was for any amount of

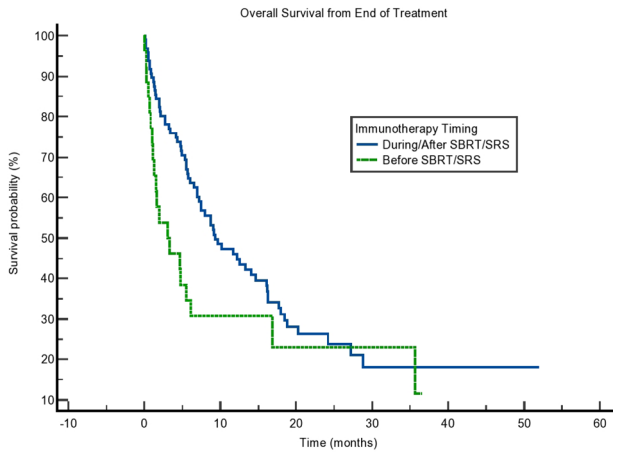

FIGURE 3 | Kaplan–Meier curve showing overall survival (OS) from the decision to start immunotherapy. OS based on immunotherapy given during/after stereotactic body radiotherapy (SBRT)/stereotactic radiosurgery (SRS) compared to before SBRT/SRS. p = 0.81.

TABLE 4 | Median OS as calculated from the end of treatment (immunotherapy or radiation) or decision to start immunotherapy.

Endpoint for OS	Immunotherapy Timing	Median OS from SBRT (months)	p-value
End of treatment	Before	3.088	0.064
	Concurrent/After	9.331	
Decision to start immunotherapy	Before	10.02	0.91
	Concurrent/After	12.65	

OS, Overall survival; SBRT, Stereotactic Body Radiotherapy.

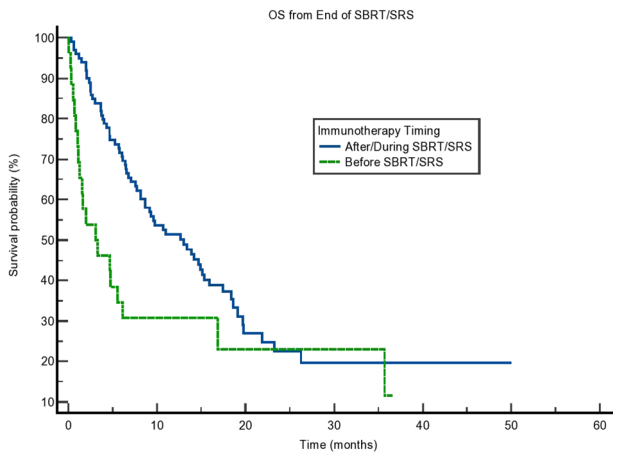

FIGURE 4 | Kaplan–Meier curve showing overall survival (OS) from the end of stereotactic body radiotherapy (SBRT)/stereotactic radiosurgery (SRS) for non-small cell lung cancer (NSCLC) patients only. OS based on immunotherapy given during/after SBRT/SRS compared to before SBRT/SRS. p = 0.16.

TABLE 5 | Median OS as calculated from the end of radiation treatment based on the type of radiation.

Type of Radiation	Immunotherapy Timing	Median OS from SBRT (months)	p-value
SBRT	Before	6.538	0.64
	Concurrent/After	12.583	
SRS	Before*	3.088	0.0098
	Concurrent/After*	9.593	

**Indicates significance. OS, Overall survival; SBRT, Stereotactic Body Radiotherapy; SRS, Stereotactic Radiosurgery.*

time prior to pembrolizumab treatment (17). A year later, a phase 1 trial that treated urothelial carcinoma with radiotherapy and pembrolizumab demonstrated that the sandwiched approach was more effective than immunotherapy after radiation (18). Interestingly, our results also show that either a sandwiched approach of immunotherapy and radiation or providing immunotherapy after radiation shows benefit.

Of note, there are several limitations to our study. As mentioned above, external application is limited clinically because there is no significant difference in OS in the timing of immunotherapy/radiation when analyzed from the decision to start immunotherapy. While the end of radiation is a usable point in a retrospective review, its use as a clinical decision point is not feasible.

Additionally, as a retrospective review, we attempt to limit inherent differences in the groups of selections. However, the OS of those patients who received immunotherapy prior to SBRT/SRS was significantly lower than those who received immunotherapy concurrently or after. This suggests a difference in the groups outside of the parameters chosen for inclusion and exclusion in the study.

Furthermore, our study has analyzed several different types of cancer in addition to combining SBRT and SRS, and this leads to concerns over its applicability. Overall, our results show the need for clinical trials with robust methodology that specifies sequencing of immunotherapy and radiation and does so for a particular cancer. Chemotherapy regimens are currently delineated for specific cancers, and the same approach should be applied when using immunotherapy and radiation.

Our results raise more questions about determining the optimal sequence for radiation and immunotherapy. There needs to be a wider collection of retrospective data combined with randomized trials to determine what sequence is best for what cancer. In addition to the timing of SBRT/SRS with immunotherapy, there is a need to optimize other portions of SBRT/SRS and immunotherapy administration including the optimal dose of radiation and fractionation. Overall, more data are needed to elucidate the optimal timing of immunotherapy with SBRT/SRS. There are several studies currently exploring this topic (2–4), and it is important that the full benefit of this combination is understood to improve clinical care.

DATA AVAILABILITY STATEMENT

The raw data supporting the conclusions of this article will be made available by the authors without undue reservation.

ETHICS STATEMENT

The studies involving human participants were reviewed and approved by UMC IRB 15-001726. Written informed consent for participation was not required for this study in accordance with the national legislation and the institutional requirements.

AUTHOR CONTRIBUTIONS

AH, AJ, HA, PW, and NS aided in designing the study. SW and AH collected the data for the retrospective review. SW, AJ, and MP contributed to the statistical analysis and wrote the first draft of the article. All authors contributed to article revision and read and approved the submitted version.

REFERENCES

1. USCS Data Visualizations - CDC. Centers for Disease Control and Prevention. Available at: https://gis.cdc.gov/Cancer/USCS/DataViz.html (Accessed May 1, 2021).
2. Lubas MJ, Kumar SS. The Combined Use of SBRT and Immunotherapy-A Literature Review. *Curr Oncol Rep* (2020) 22(12):117. doi: 10.1007/s11912-020-00986-9
3. Tuyaerts S, Van Nuffel AMT, Naert E, Van Dam PA, Vuylsteke P, De Caluwé A, et al. PRIMMO Study Protocol: A Phase II Study Combining PD-1 Blockade, Radiation and Immunomodulation to Tackle Cervical and Uterine Cancer. *BMC Cancer* (2019) 19(1):506. doi: 10.1186/s12885-019-5676-3
4. Bozorgmehr F, Hommertgen A, Krisam J, Lasitschka F, Kuon J, Maenz M, et al. Fostering Efficacy of Anti-PD-1-Treatment: Nivolumab Plus Radiotherapy in Advanced Non-Small Cell Lung Cancer - Study Protocol of the FORCE Trial. *BMC Cancer* (2019) 19(1):1074. doi: 10.1186/s12885-019-6205-0
5. Abuodeh Y, Venkat P, Kim S. Systematic Review of Case Reports on the Abscopal Effect. *Curr Probl Cancer* (2016) 40(1):25–37. doi: 10.1016/j.currproblcancer.2015.10.001
6. Buchwald ZS, Wynne J, Nasti TH, Zhu S, Mourad WF, Yan W, et al. Radiation, Immune Checkpoint Blockade and the Abscopal Effect: A Critical Review on Timing, Dose and Fractionation. *Front Oncol* (2018) 8:612. doi: 10.3389/fonc.2018.00612
7. Cushman TR, Gomez D, Kumar R, Likacheva A, Chang JY, Cadena AP, et al. Combining Radiation Plus Immunotherapy to Improve Systemic Immune Response. *J Thorac Dis* (2018) 10(Suppl 3):S468–79. doi: 10.21037/jtd.2018.01.130
8. Ngwa W, Irabor OC, Schoenfeld JD, Hesser J, Demaria S, Formenti SC. Using Immunotherapy to Boost the Abscopal Effect. *Nat Rev Cancer* (2018) 18(5):313–22. doi: 10.1038/nrc.2018.6
9. Chen D, Verma V, Patel RR, Barsoumian HB, Cortez MA, Welsh JW. Absolute Lymphocyte Count Predicts Abscopal Responses and Outcomes in Patients Receiving Combined Immunotherapy and Radiation Therapy: Analysis of 3 Phase 1/2 Trials. *Int J Radiat Oncol Biol Phys* (2020) 108(1):196–203. doi: 10.1016/j.ijrobp.2020.01.032
10. Park SS, Dong H, Liu X, Harrington SM, Krco CJ, Grams MP, et al. PD-1 Restrains Radiotherapy-Induced Abscopal Effect. *Cancer Immunol Res* (2015) 3(6):610–9. doi: 10.1158/2326-6066.CIR-14-0138
11. Smilowitz HM, Micca PL, Sasso D, Wu Q, Dyment N, Xue C, et al. Increasing Radiation Dose Improves Immunotherapy Outcome and Prolongation of Tumor Dormancy in a Subgroup of Mice Treated for Advanced Intracerebral Melanoma. *Cancer Immunol Immunother* (2016) 65(2):127–39. doi: 10.1007/s00262-015-1772-7
12. Turgeon GA, Weickhardt A, Azad AA, Solomon B, Siva S. Radiotherapy and Immunotherapy: A Synergistic Effect in Cancer Care. *Med J Aust* (2019) 210(1):47–53. doi: 10.5694/mja2.12046
13. Breen WG, Leventakos K, Dong H, Merrell KW. Radiation and Immunotherapy: Emerging Mechanisms of Synergy. *J Thorac Dis* (2020) 12(11):7011–23. doi: 10.21037/jtd-2019-cptn-07
14. Pinnamaneni R, Hegde AP, Cherukuri SD, Arastu HH, Bowling M, Leinweber C, et al. Sequence of Stereotactic Ablative Radiotherapy and Immune Checkpoint Blockade in the Treatment of Metastatic Lung Cancer. *J Clin Oncol* (2017) 35(15_suppl):e20665–5. doi: 10.1200/JCO.2017.35.15_suppl.e20665
15. Golden EB, Chhabra A, Chachoua A, Adams S, Donach M, Fenton-Kerimian M, et al. Local Radiotherapy and Granulocyte-Macrophage Colony-Stimulating Factor to Generate Abscopal Responses in Patients With Metastatic Solid Tumours: A Proof-Of-Principle Trial. *Lancet Oncol* (2015) 16(7):795–803. doi: 10.1016/S1470-2045(15)00054-6
16. Theelen WSME, Peulen HMU, Lalezari F, van der Noort V, de Vries JF, Aerts JGJV, et al. Effect of Pembrolizumab After Stereotactic Body Radiotherapy vs Pembrolizumab Alone on Tumor Response in Patients With Advanced Non-Small Cell Lung Cancer: Results of the PEMBRO-RT Phase 2 Randomized Clinical Trial. *JAMA Oncol* (2019) 5(9):1276–82. doi: 10.1001/jamaoncol.2019.1478
17. Shaverdian N, Lisberg AE, Bornazyan K, Veruttipong D, Goldman JW, Formenti SC, et al. Previous Radiotherapy and the Clinical Activity and Toxicity of Pembrolizumab in the Treatment of non-Small-Cell Lung Cancer: A Secondary Analysis of the KEYNOTE-001 Phase 1 Trial. *Lancet Oncol* (2017) 18(7):895–903. doi: 10.1016/S1470-2045(17)30380-7
18. Sundahl N, Vandekerkhove G, Decaestecker K, Meireson A, De Visschere P, Fonteyne V, et al. Randomized Phase 1 Trial of Pembrolizumab With Sequential Versus Concomitant Stereotactic Body Radiotherapy in Metastatic Urothelial Carcinoma. *Eur Urol* (2019) 75(5):707–11. doi: 10.1016/j.eururo.2019.01.009

Conflict of Interest: Author PW was employed by Circulogene, Birmingham, AL, United States.

The remaining authors declare that the research was conducted in the absence of any commercial or financial relationships that could be construed as a potential conflict of interest.

frontiers | Frontiers in Oncology

ORIGINAL RESEARCH
published: 01 June 2022
doi: 10.3389/fonc.2022.829812

Modulation of Peripheral Immune Cell Subpopulations After RapidArc/Moderate Hypofractionated Radiotherapy for Localized Prostate Cancer: Findings and Comparison With 3D Conformal/Conventional Fractionation Treatment

Fiorella D'Auria[1†], Teodora Statuto[2†], Luciana Rago[3], Antonietta Montagna[3], Giovanni Castaldo[3], Irene Schirò[3], Anna Zeccola[3], Teresa Virgilio[3], Gabriella Bianchino[1], Antonio Traficante[1], Alessandro Sgambato[4], Vincenzo Fusco[3], Luciana Valvano[2‡] and Giovanni Calice[5‡]*

[1] Laboratory of Clinical Pathology, Centro di Riferimento Oncologico della Basilicata (IRCCS-CROB), Rionero in Vulture, Italy, [2] Laboratory of Clinical Research and Advanced Diagnostics, Centro di Riferimento Oncologico della Basilicata (IRCCS-CROB), Rionero in Vulture, Italy, [3] Radiotherapy Unit, Centro di Riferimento Oncologico della Basilicata (IRCCS-CROB), Rionero in Vulture, Italy, [4] Scientific Direction, Centro di Riferimento Oncologico della Basilicata (IRCCS-CROB), Rionero in Vulture, Italy, [5] Laboratory of Preclinical and Translational Research, Centro di Riferimento Oncologico della Basilicata (IRCCS-CROB), Rionero in Vulture, Italy

Radiotherapy (RT) is an important therapeutic option in patients with localized prostate cancer (PC). Unfortunately, radiation treatment causes a decrease in peripheral lymphocytes and, consequently, influences the patients' immune status. Our aim was to study changes in peripheral blood immune cell subpopulations after RT and during 6 months' follow-up in 2 groups of PC patients irradiated with different techniques and dose fractions with curative intent. We also investigated the presence of correlation between immune cell modulation and genitourinary or gastrointestinal toxicity. We enrolled 44 patients treated with curative RT (RapidArc/hypofractionation regimen or 3D conformal/conventional fractionation) for localized PC. Total white blood cell (WBC), absolute lymphocyte counts (ALCs), and peripheral immune cell subpopulations were analyzed at baseline, at the end of RT, and 3 and 6 months after the end of RT. WBC and ALC greatly decreased at the end of RT with a trend to recover at 6 months' follow-up in the hypofractionation group but not in the conventional one. Furthermore, B, total T, T CD4+, T CD8+, and NK cell values dropped significantly in both groups at the end of RT, with a minor decrease detectable in the hypofractionation group for B, total T, and T CD4+ lymphocytes with respect to the other technique/fractionation group. Double-negative T (DNT), double-positive T (DPT), and NKT cells significantly decreased at the end of RT with a slight tendency to recover values during follow-up, particularly in the hypofractionation group. No correlation with genitourinary or gastrointestinal toxicity was found. In this

OPEN ACCESS

Edited by:
Francesco Cellini, Radioterapia Oncologica ed Ematologia, Italy

Reviewed by:
Maria Helena Ornellas, Universidade Estadual do Rio de Janeiro, Brazil
Maurizio Valeriani, Sapienza University of Rome, Italy

***Correspondence:**
Fiorella D'Auria
fiore.dauria@virgilio.it
orcid.org/0000-0002-3030-1651

†These authors have contributed equally to this work and share first authorship

‡These authors have contributed equally to this work and share last authorship

Specialty section:
This article was submitted to Radiation Oncology, a section of the journal Frontiers in Oncology

Received: *06 December 2021*
Accepted: *21 April 2022*
Published: *01 June 2022*

Citation:
D'Auria F, Statuto T, Rago L, Montagna A, Castaldo G, Schirò I, Zeccola A, Virgilio T, Bianchino G, Traficante A, Sgambato A, Fusco V, Valvano L and Calice G (2022) Modulation of Peripheral Immune Cell Subpopulations After Rapid Arc/Moderate Hypofractionated Radiotherapy for Localized Prostate Cancer: Findings and Comparison With 3D Conformal/Conventional Fractionation Treatment. Front. Oncol. 12:829812. doi: 10.3389/fonc.2022.829812

study, we showed, for the first time, the effects of RapidArc/moderate hypofractionation RT on immune cell subsets in patients treated for localized PC. Due to the growing interest in minority T-cell subpopulations for immunotherapy, we also reported longitudinal monitoring of the effects of RT on DNT, DPT, and NKT, which was never studied before. Our preliminary data highlight the importance of considering the effects of different RT techniques/fractionation regimens on peripheral immune cells, in the era of RT and immunotherapy combination.

Keywords: prostate cancer, radiotherapy, conventional fractionation, peripheral immune cells, toxicity, hypofractionation

INTRODUCTION

Prostate cancer is the second most frequently diagnosed malignancy in men worldwide (1). Radiotherapy (RT) is an important treatment modality in patients with localized prostate cancer (2). Conventionally, RT is delivered using single doses of 1.8–2.0 Gray (Gy) and a total dose range from 76 to 80 Gy (3). After Brenner and Hall (4) showed that prostatic cancers appear more sensitive to changes in fractionation than most other cancers, as they contain a low proportion of proliferating cells and an α/β value of 1.5, several trials have evaluated the suitability of hypofractionated RT confirming its clinical efficacy and the economic and logistic advantages (5–10).

Unfortunately, during whole-pelvis radiotherapy (WPRT), radiation impairs radiosensitive tissues such as bone marrow (11). The resulting decrease in peripheral leukocyte count, particularly lymphocytes, has been widely reported in literature (12–16). Several authors (17–24) have yet to observe, in different types of cancer, the changes of lymphocyte subpopulations after RT. In particular, Lissoni et al. (17) evidenced that in patients affected by uterine tumors that underwent WPRT, T lymphocyte, CD4+, CD8+, and natural killer (NK) cell mean absolute values significantly decreased but with different behavior. In breast cancer patients, differential effects of RT with and without adjuvant chemotherapy were shown on lymphocyte counts and lymphocyte subpopulation composition (18). Prostate cancer patients treated with carbon ion radiotherapy (CIR) (22) experienced a gradual decrease of CD19+ cells and an increase of CD4+ cells during RT. These variations, together with those of CD3+ and CD8+ counts, can be predictive of outcome for prostate cancer patients after CIR (22). Eckert et al. (23) observed in 18 patients affected by prostate cancer that during the course of standard RT (70–78 Gy) combined (in 83.3% of the cases) with anti-hormonal therapy, percentage of T cells, CD8+ and naïve CD4+ T cells, and B cells decreased while regulatory T and NK cells increased. A further study on a group of 33 prostate cancer patients (24) investigated the different effects of definitive or salvage RT on peripheral lymphocyte subsets. The authors found that they cause similar effects and, in particular, that B lymphocytes are more sensitive to both type of RT with respect to T and NK cells.

Moreover, Yuan and Wang (25) found that T, B, and NK lymphocytes reacted differently to different RT regimens in breast cancer patients.

In addition to the well-known CD4+ T helper and CD8+ T cytotoxic populations, other smaller subgroups of T cells exist in peripheral blood: regulatory T cells (Tregs), a subset of CD4+ T cells with immune suppression functions (26); NKT cells, a subset of T lymphocytes that expresses NK markers (27); and double-negative T (DNT) cells, a subset of T lymphocytes negative for CD4, CD8, and NK cell markers. DNT cells are involved in immune response regulation (28, 29).

The other rare T-cell population present in peripheral blood is CD4+ CD8+ double-positive T (DPT). Its function is controversial, with studies reporting a cytotoxic or suppressive role for these cells (30, 31).

We studied changes of peripheral blood immune cell subpopulations after RT and during 6 months' follow-up, in a group of PC patients undergoing RapidArc and moderate hypofractionated RT with curative intent. The RT immune effects in these patients were compared with those in a second small group of PC patients treated with 3D conformal/conventional fractionation RT.

MATERIALS AND METHODS

Study Characteristics

Forty-four male patients candidate to curative RT for localized prostate cancer (median age, 76; range, 54–91), who had not received chemotherapy, were prospectively enrolled into our single-institute study that was examined and approved by the local ethics committee (Comitato Etico Unico Regionale per la Basilicata). All the enrolled patients gave their informed consent prior to their inclusion in the study. Thirty-two patients (hypoF group) underwent moderate hypofractionation using volumetric arc intensity modulated radiation therapy technique (RapidArc, RA), with a daily dose/fraction of 3.1 Gy and a total dose to the planned target volume (PTV) of 62 Gy. Twelve patients (standard group) underwent conventional daily fractionation of 2 Gy using a 3D conformal technique (3D-CRT) and a total prescription dose to PTV of 78 Gy (**Table 1**). Patients were selected for the technique in a casual manner, based on the instrumentation availability. During the study, according to our institutional standards, the 3D-CRT has no longer been used for the treatment of this type of patients, in favor of RA. This resulted in the small number of patients in the standard group.

Twenty-four (54.5%) patients received hormone therapy, 8 (66.6%) in the standard group and 16 (50%) in the hypoF group.

Treatment Characteristics

The patients were simulated using Combifix (CIVCO, Orange City, IA, USA) and treated by RA RT with Trilogy Linac (Varian Medical System, Palo Alto, CA, USA) and for 3D conformal RT with Clinac 2100 (Varian Medical System, Palo Alto, CA, USA).

The clinical target volume (CTV) was composed of the prostate gland with or without the seminal vesicles. The corresponding PTV was defined as CTV + 8 mm margin in each direction, with the exception of the posterior direction.

Planning Parameters

The planning object was to cover 95% of each PTV with at least 95% of the prescribed dose and Dmax < 107%. For RA RT, the organ at risk (OAR) planning objectives were as follows: V43.4 Gy < 50%, V51 Gy < 40%, and V59.5 Gy < 25% for the rectum; V51 Gy < 35% for the bladder; Dmean < 45 Gy for the femoral heads; 410 cc < 45 Gy, 740 cc < 30 Gy, and 1,050 cc < 15 Gy for the intestinal cavity. The beam energy used to perform the treatment plans was equal to 6 MV.

For 3D conformal RT, OAR objectives were as follows: V46.5 Gy < 50% and V64.5 Gy < 15% for the rectum; V46.5 Gy < 50% and V64.5 < 20% for the bladder; 410 cc < 45 Gy, 740 cc < 30 Gy, and 1,050 cc < 15 Gy for the intestinal cavity. The beam energy used to perform the treatment plans was equal to 15 MV.

Flow Cytometry

For flow cytometry analysis, peripheral blood samples were collected before RT (t0), at the end of RT (t1), which is the day when the RT planning was completed, and at follow-up time of 3 (t2) and 6 months (t3) after the end of RT for each patient.

TABLE 1 | Patients' characteristics.

Characteristics	Observed values (n = 44 patients)
Median age (range)	76 (54–91)
Stage	
T2a	1
T2b	13
T2c	12
T3a	18
Gleason	
6 (3 + 3)	13
7 (3 + 4)	13
7 (4 + 3)	5
8 (4 + 4)	13
Initial PSA (ng/ml, median, range)	9.73 (0.046–48)
Risk class	
Low	15
Intermediate	16
High	13
Prescription dose to PTV and dose/fraction of 3D conformal RT (Gy)	78; 2.0
Prescription dose to PTV and dose/fraction of RA RT (Gy)	62; 3.1

PTV, planned target volume; RA, RapidArc irradiation technique.

At the same time points, absolute counts of white blood cells (WBCs) and lymphocytes (ALC) were determined with a Beckman Coulter DXH800.

The peripheral blood immune cell subpopulations of total T cells (CD3+), T helper cells (CD3+ CD4+), T cytotoxic cells (CD3+ CD8+), regulatory T cells (Tregs) (CD4+ CD25+ CD127low/-), DNT cells (CD3+ CD4- CD8- CD16- CD56-), DPT cells (CD3+ CD4+ CD8+), NKT cells (CD3+ CD16+ CD56+), NK cells (CD3- CD16+ CD56+), and B cells (CD19+) were analyzed by a FACSCanto II flow cytometer (BD Biosciences), as previously reported (32). In brief, fluorescence-labeled antibodies (BD Biosciences) were mixed with 100 µl of peripheral blood and incubated for 15 min in the dark. The antibody combinations were CD3-FITC/CD16CD56-PE/CD45-PerCP/CD8-PE-Cy7/CD4-APC/CD19-APC-Cy7; CD127-PE/CD4-PerCP/CD25-PE-Cy7/CD45-APC-Cy7. For each combination, 50,000 to 100,000 CD45-positive cells were analyzed. Each immune cell subpopulation was indicated as the percentage of the total lymphocyte population, gated using CD45 and SSC data. The absolute number of each cell subpopulation was obtained using the percentage and the ALC values (data summarized in **Table 2**).

Statistical Analysis

We evaluated, at every time point, the possible relationship between the clinical covariates and the variation of lymphocyte subpopulations by the linear regression model. We applied a false discovery rate (FDR) approach and the Benjamini–Hochberg method for multiple comparisons correction.

We have checked the normal distribution of immune cell subpopulation values by Shapiro–Wilk's normality method. Since not all data had a normal course, we chose to represent them by median and interquartile range (IQR) and to apply the non-parametric statistical Kruskal–Wallis test and Wilcoxon test. Statistical significance was considered on a 0.05 cutoff. All the statistical analyses were performed by R software and CRAN packages (33); customized images were processed by the ggpubr package (34).

RESULTS

Considering the entire group of patients (44), the absolute values of WBC, of lymphocytes, and of all the peripheral immune cell subpopulations (total T, B, NK, Tregs, T CD4+, and T CD8+) displayed significant variations (p-value < 0.001) during the 4 time points considered (**Figures 1**, **2**). Percentages of total T, B, NK, Tregs, and T CD4 cells significantly changed (p-value < 0.05) during the four time points considered, too (**Figure 3**). RT significantly affected the absolute values of the three small T-cell populations of DNT, DPT, and NKT, as shown in **Figure 4** (p-value < 0.05).

When comparing the two groups of patients (hypoF and standard), at 6 months' follow-up time (t3), the hypoF group showed significantly higher absolute values of total T (linear regression model, adjusted p-value: 0.03) and T CD4+ cells (adjusted p-value: 0.005) than the standard group. We observed this difference between the two groups also for the

TABLE 2 | Cell populations' values at baseline (μl^{-1}, median, range).

	RA/hypofractionation RT group (*n* = 32)	3D conformal/conventional fractionation RT group (*n* = 12)
WBC	7,285 (3,340–13,770)	6,835 (5,100–9,700)
ALC	2,150 (800–4,000)	2,100 (1,200–3,300)
B cells	134.6 (25.9–439.4)	137.1 (35.1–260.7)
NK cells	314.5 (104.4–948.5)	506.1 (200–1,120.6)
Total T cells	1,490.8 (575.2–3,104.3)	1,431.1 (868.8–2,039.4)
T CD4+ cells	987 (409.7–1,716.8)	851.8 (542.1–1,531.2)
T CD8+ cells	537.6 (75.2–1,842.6)	419.4 (231.6–792)
Regulatory T cells	37.1 (6.8–88.2)	34.5 (8.7–57.2)
DNT cells	30.8 (0.14–262.5)	39.2 (20.8–80.6)
DPT cells	13.8 (0.08–56.7)	11.9 (3.2–97.3)
NKT cells	128.4 (3.2–453.8)	99.2 (47.9–564.6)

RA, RapidArc irradiation technique; WBC, white blood cell; ALC, absolute lymphocyte count; NK, natural killer; DNT, double-negative T; DPT, double-positive T.

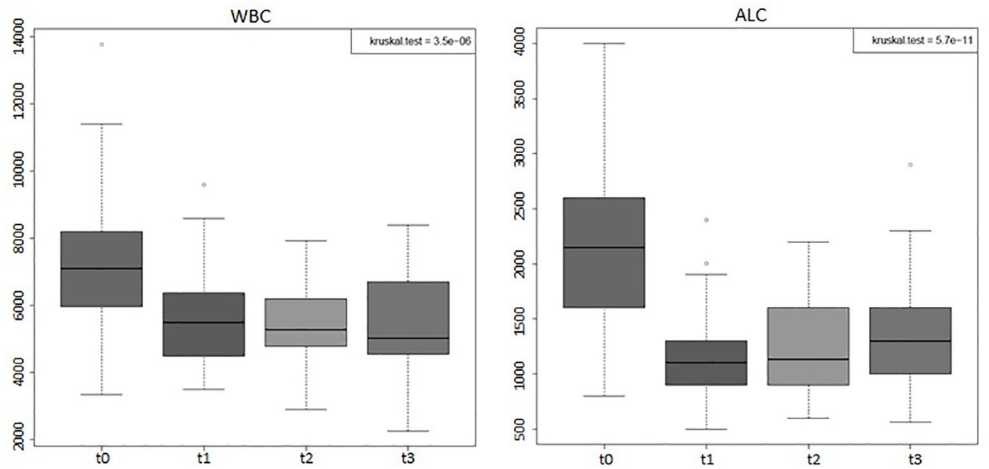

FIGURE 1 | Boxplots of the absolute white blood counts (WBCs) and absolute lymphocyte counts (ALCs) of the entire group of prostate cancer patients (44) who underwent curative RT. The data shown evidenced variations statistically significant during the four time points considered (Kruskal–Wallis test, p-value < 0.001). t0: before RT; t1: end of RT; t2: 3 months after RT; t3: 6 months after RT. All values are expressed as cells/μl.

absolute values of B cells (adjusted p-value: 0.014) but, in particular, at the end of RT (t1). Treg values were also higher in the hypoF group with respect to the standard one at the t2 time point (adjusted p-value: 0.03). No statistically significant differences, in terms of WBC, ALC, or peripheral immune cell subpopulations, were found when comparing patients who received hormone therapy with those who did not (data not shown).

As shown in **Figure 5**, ALC dropped significantly in both groups at the end of RT (t0 vs. t1, standard: adjusted p-value: 0.0042; hypoF: adjusted p-value: 5.18e-06). At t3, ALC (median: 1,450/μl, IQR: 1,885–1,099/μl) partially recovered with respect to t1 (median: 1,200/μl, IQR: 1,300–900/μl) in the hypoF group (adjusted p-value: 0.0094), but not in the standard one in which we did not observe any statistically significant difference at t1 (median: 1000/μl, IQR: 1,150–875/μl) with respect to t3 (median: 1,000/μl, IQR: 1,350–875/μl) (adjusted p-value: 0.418). For B cells also, as depicted in **Figure 6A**, there was a significant decrease at the end of RT (t1) with respect to the basal values (t0), in both groups (t0 vs. t1, standard: adjusted p-value: 0.00097; hypoF: adjusted p-value: 1.49e-07). This subpopulation, in the hypoF group, at t3 was 88.8% (median: 120/μl, IQR: 174–73/μl) of the t0 value (median: 135/μl, IQR: 251–97/μl). In the standard group, instead, at t3, the B-cell absolute value was still 48.2% (median: 66/μl, IQR: 97–30/μl) of the t0 value (median: 137/μl, IQR: 198–95/μl). Total T cells (t0 vs. t1, standard: adjusted p-value: 0.00097; hypoF: adjusted p-value: 1.49e-07) and subpopulations of T CD4+ (t0 vs. t1, standard: adjusted p-value: 0.00097; hypoF: adjusted p-value: 1.88e-07) and T CD8+ (t0 vs. t1, standard: adjusted p-value: 0.0015; hypoF: adjusted p-value: 5.21e-07) also decreased significantly at t1 with respect to t0 in both groups (**Figures 6B–D**). The values of these three peripheral immune cell populations partially recovered at t3 with respect to t1 only in the hypoF group (statistically significant only for T CD8+ cells, adjusted p-value: 0.0091) (**Figures 6B–D**). As regards the NK lymphocyte population, there was a great difference in values, but not statistically significant, before the beginning of RT between the two groups of patients, not detected for ALC or for the other

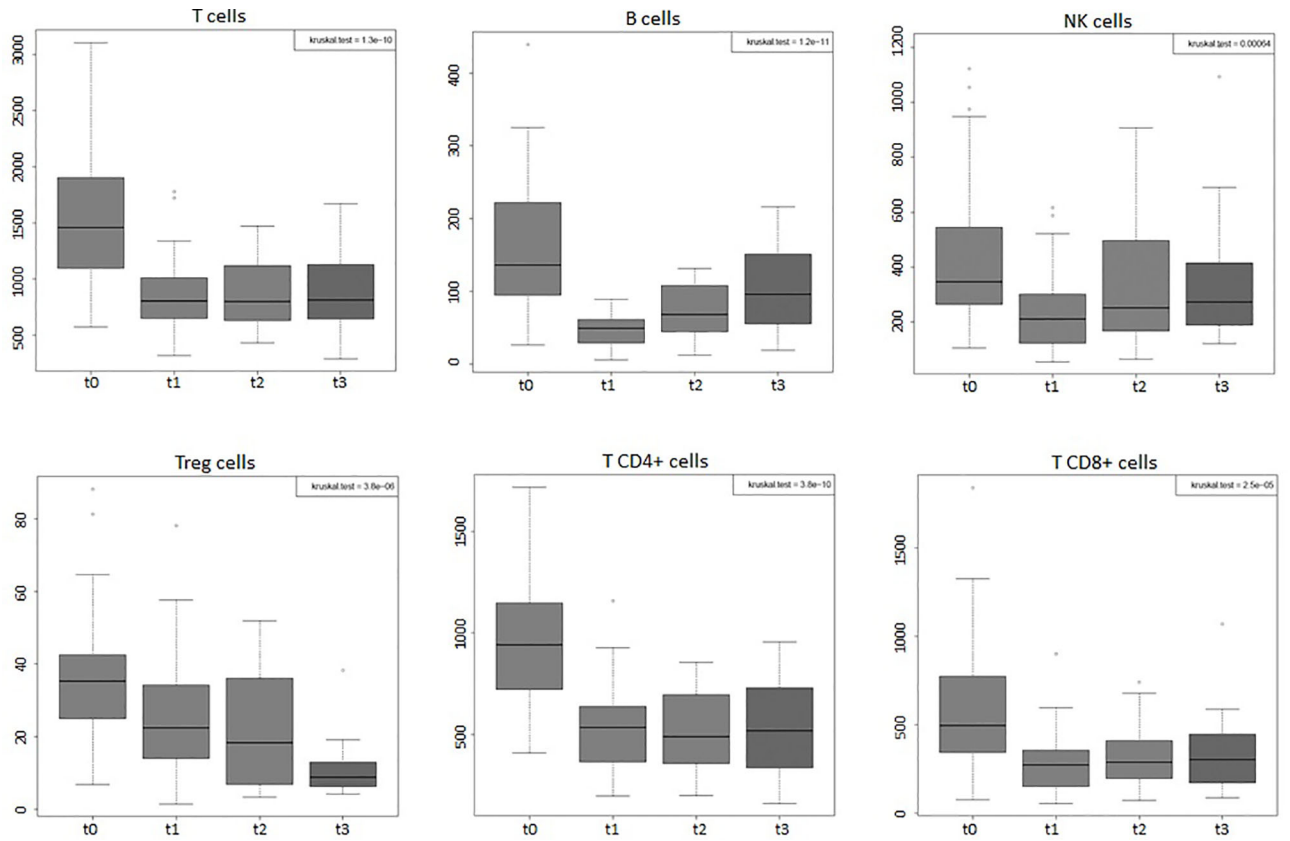

FIGURE 2 | Boxplots of the absolute values of total T, B, NK, Tregs, T CD4, and T CD8 cells of the entire group of prostate cancer patients (44) undergoing curative RT. The data shown evidenced variations statistically significant during the four time points considered (Kruskal–Wallis test, p-value < 0.001). t0: before RT; t1: end of RT; t2: 3 months after RT; t3: 6 months after RT. All values are expressed as cells/μl.

immune cell subpopulations. At the end of RT, the NK cell absolute values significantly dropped in both groups of patients (t0 vs. t1, standard: adjusted p-value: 0.0055; hypoF: adjusted p-value: 5.24e-07), and during follow-up, such values partially recovered only in the hypoF group (**Figure 6E**). We found no significant difference in Treg lymphocyte absolute values between the two groups (data not available for all patients and all time points) during the 4 time points considered. As shown in **Figure 6F**, their values were lower at 6 months' follow-up (t3) than at the end of RT (t1).

As regards DNT cells (**Figure 7A**), in the hypoF group, we found that their values decreased significantly following RT (t1) (t0 vs. t1, adjusted p-value: 0.00079). During follow-up time points, we observed a statistically significant increase in values (t1 vs. t3, adjusted p-value: 0.0073). We observed the same trend of the DNT values (**Figure 7A**) also in the standard group at the end of RT (t0 vs. t1, adjusted p-value: 0.0087), with an increase in values (not statistically significant) during follow-up time. For the immune cell population of DPT (**Figure 7B**), in the hypoF group, we observed a reduction of values at t1 (t0 vs. t1, adjusted p-value; 0.028) and a recovery of values (t1 vs. t2, adjusted p-value: 0.037). In the standard group, DPT values dropped down significantly at t1 (t0 vs. t1, adjusted p-value: 0.038), and they remained almost stable during follow-up (**Figure 7B**). NKT cells decreased in the hypoF group at the end of RT but not significantly, probably due to large variability in baseline values. In the standard group, we registered a statistically significant reduction of NKT values at t1 with respect to t0 (adjusted p-value: 0.0058) (**Figure 7C**).

Considering the entire group of patients enrolled, the median follow-up time was 18 months (range, 6–36 months), in particular 28 months (range, 6–36 months) for the standard group and 18 months (range, 6–36 months) for the hypoF group. Biochemical free-survival (BFS) was 97.7% (100% for the standard group and 96.8% for the hypoF group) as only one patient, in the hypoF group, relapsed 6 months after the end of RT.

As regards genitourinary (GU) and gastrointestinal (GI) toxicity (35), we did not find any significant difference between the two techniques/fractionation regimens, as also none of the immune cell subpopulations, ALC, or WBC values correlated to acute or late GU or GI toxicity. We registered, instead, a significantly higher number of late Grade 1 leukopenias (35) at t3 time points in the standard group with respect to the hypoF

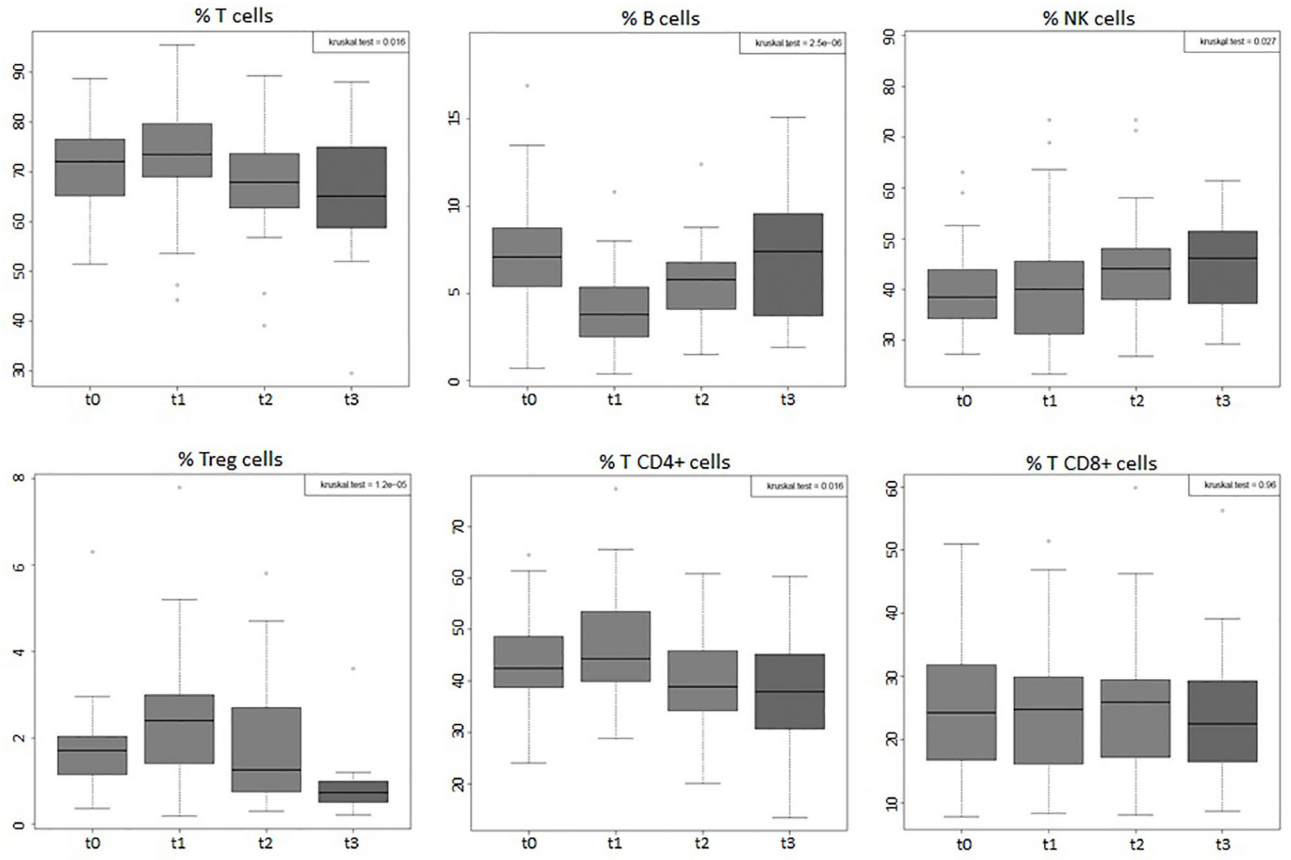

FIGURE 3 | Boxplots of the percentages, among total lymphocytes, of total T, B, NK, Tregs, T CD4, and T CD8 cells of the entire group of prostate cancer patients (44) undergoing curative RT. The data shown evidenced variations statistically significant during the four time points considered (Kruskal–Wallis test, p-value < 0.05), except for T CD8+ cells that did not undergo significant changes. t0: before RT; t1: end of RT; t2: 3 months after RT; t3: 6 months after RT.

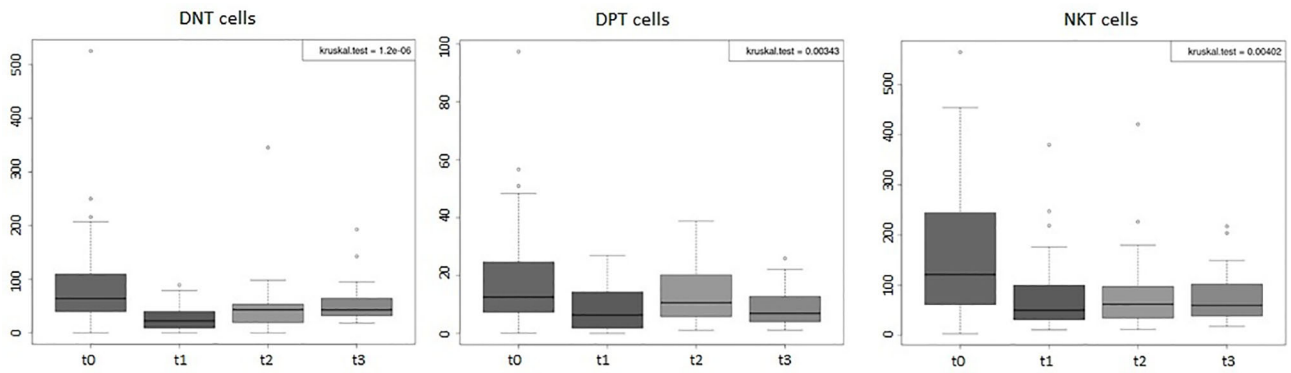

FIGURE 4 | Boxplots of the absolute values of double-negative T (DNT), double-positive T (DPT), and NKT cells of the entire group of prostate cancer patients (44) undergoing curative RT. The data shown evidenced variations statistically significant during the four time points considered (Kruskal–Wallis test, p-value < 0.005). t0: before RT; t1: end of RT; t2: 3 months after RT; t3: 6 months after RT. All values are expressed as cells/μl.

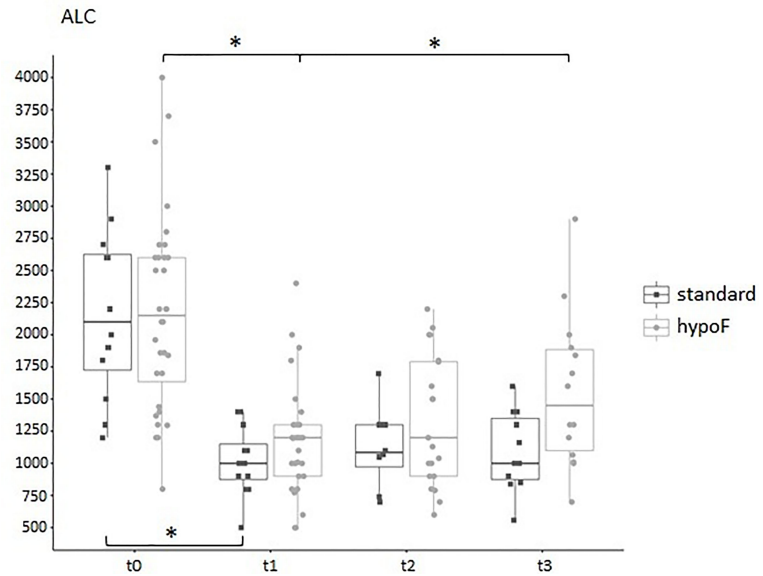

FIGURE 5 | Boxplot of the absolute lymphocyte counts, expressed as cells/μl, in standard (n = 12) and hypoF (n = 32) RT groups of patients during the four time points considered. Statistically significant differences were marked (Wilcoxon test, *adjusted p-value < 0.01).

group (81.8% vs. 21.4%, linear regression model, adjusted p-value: 0.0065). All toxicity data are reported in **Table 3**.

DISCUSSION

Leukopenia and lymphopenia are two side effects of WPRT, well known by radiation oncologists and well documented in literature (15, 17, 36, 37). The purpose of our study was to compare the modulation of peripheral immune cell subpopulation values by two different RT technique/fractionated regimens commonly used to treat localized prostate cancer patients. We found that WBCs, and particularly ALCs, are significantly affected by RT and greatly decreased at the end of the treatment. Sanguineti et al. (38) have recently reported a WBC count depression in prostate cancer patients following RT treatment in moderate hypofractionation with respect to conventional fractionation. In our study, ALC values showed a trend to recover 6 months after the end of RT in the hypoF group but not in the standard group, in which the number of Grade 1 leukopenias was significantly higher at this time point. Hematologic toxicity, in particular lymphopenia, in this setting of patients was also found to be prolonged and not negligible by Cozzarini et al. (37), who, anyway, did not find differences among 3 different intensity modulated radiation therapy (IMRT) modalities (Helical Tomotherapy, RA, Static Field-IMRT). The same authors showed that a higher risk of acute or late lymphopenia was associated with higher bone marrow volumes receiving ≥40 Gy (V40) (15). With regard to the different immune cell subpopulations, we found less toxicity of the RA/hypofractionation technique for B cells at t1 and for total T and T CD4+ at t3 with respect to conformal/conventional fractionation RT. The B-cell population was the only one that decreased in both percentage (**Figure 3**) and absolute (**Figure 2**) values after RT and appeared to be mostly affected at the end of RT with both technique/fractionation regimens (**Figure 6A**). This finding is in line with previous studies that documented the effects of RT on lymphocyte subpopulation composition, and in particular on B cells, in breast cancer patients (18, 25) and in patients undergoing pelvis RT (17, 19, 20), particularly for prostate cancer (21–24). Since they mature in the bone marrow (39), in fact, B cells are the most vulnerable to RT directed towards the pelvis bones. Moreover, we found that B cells display the highest rate of recovery 6 months after the end of RT (t3) (89% and 48% of the baseline values in the hypoF and standard group, respectively) with respect to the other lymphocyte subpopulations. Three and six months after the end of RT, total T, T CD4+, T CD8+, and NK lymphocytes, in fact, tended to have almost the same absolute values observed at the end of RT in the standard group and showed a limited recovery in the hypoF group. The only exception was the Treg population that displayed lower absolute values at the follow-up time of 6 months with respect to the end of RT in both groups. A previous study (23) conducted on 18 PC patients who underwent normofractionated RT reported that the percentage of total T cells, T CD8+, and T CD4+ decreased during RT, while Treg and NK cells increased. The proportion of NK and total T cells remained significantly altered at 3 months' follow-up. They did not investigate the absolute values of the single immune population in the peripheral blood.

Changes in immune cell subpopulations, in particular T lymphocytes, following RT is currently a topic of interest. In

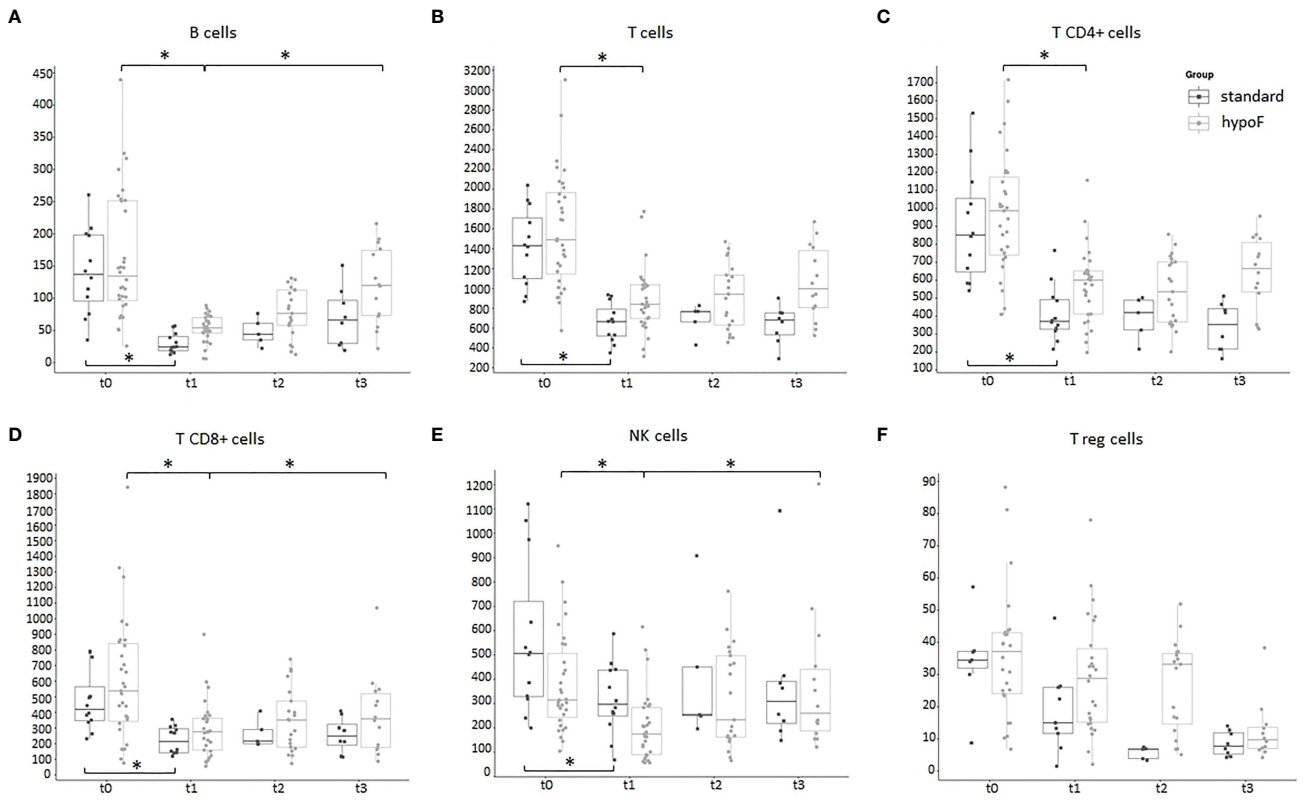

FIGURE 6 | Boxplots of the peripheral immune cell subpopulation values, expressed as cells/μl, in standard (n = 12) and hypoF (n = 32) RT groups during the four time points considered. **(A)** CD19+ B cells; **(B)** CD3+CD16-CD56- T cells; **(C)** CD4+CD3+ T helper cells; **(D)** CD8+CD3+ T cytotoxic cells; **(E)** CD3-CD16+CD56+ NK cells; **(F)** CD4+CD25+CD127- T reg cells. Statistically significant differences were marked (Wilcoxon test, *adjusted p-value < 0.01).

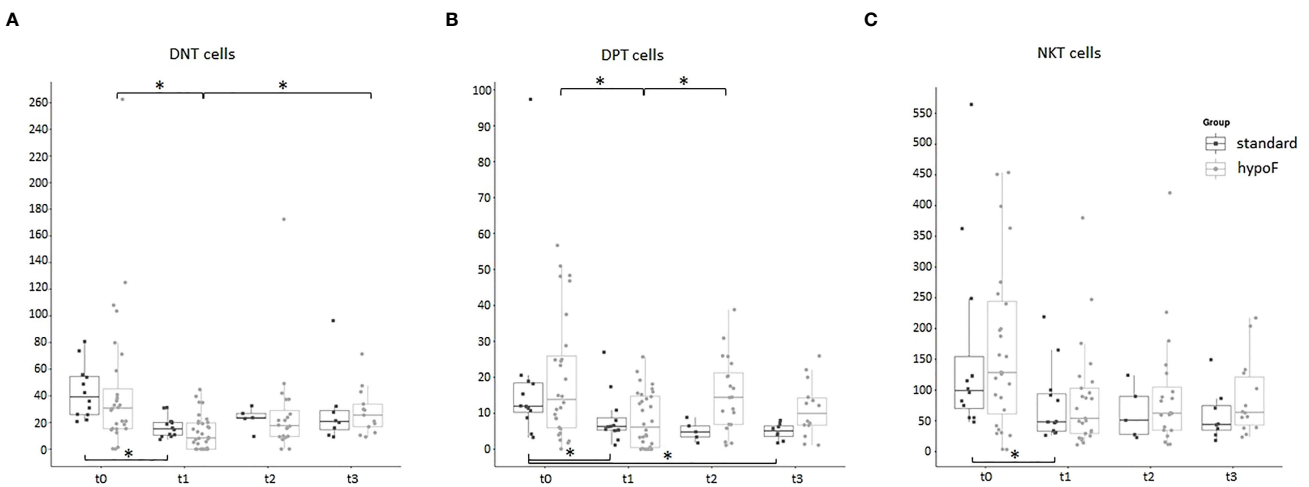

FIGURE 7 | Boxplots of the 3 small T-cell population values, expressed as cells/μl, in standard (n = 12) and hypoF (n = 32) RT groups during the four time points considered. **(A)** CD3+CD4-CD8-CD16-CD56- double-negative T cells (DNT); **(B)** CD3+CD8+CD4+ double-positive T cells (DPT); **(C)** CD3+CD16+CD56+ NKT cells. Statistically significant differences were marked (Wilcoxon test, *adjusted p-value < 0.05).

TABLE 3 | Toxicity data.

	RA/hypofractionation RT group (*n* = 32)		3D conformal/conventional fractionation RT group (*n* = 12)	
	Grade 1	**Grade 2**	**Grade 1**	**Grade 2**
Acute toxicity				
Genitourinary	9 (20.4%)	2 (4.5%)	6 (13.6%)	2 (4.5%)
Gastrointestinal	11 (25%)	3 (6.8%)	6 (13.6%)	3 (6.8%)
Hematological (lymphopenia)	4 (9%)	4 (9%)	4 (9%)	1 (2.3%)
Late toxicity				
Genitourinary	9 (20.4%)	0	1 (2.3%)	0
Gastrointestinal	3 (6.8%)	1 (2.3%)	1 (2.3%)	1 (2.3%)
Hematological (lymphopenia)	0	1 (2.3%)	3 (6.8%)	1 (2.3%)

RA, RapidArc irradiation technique; RT, radiotherapy.

this context, a recent meta-analysis by Wang et al. summarized the effects of RT in different types of tumor, concluding that during the first month of RT, the values of T lymphocytes undergo an evident reduction due to apoptosis (40).

Our study is the first to perform a longitudinal monitoring of the effects of RT on small populations of T lymphocytes DNT, DPT, and NKT.

These populations have already been previously studied in the cancer setting. Two different groups reported a significant decrease in peripheral DNT cells, respectively, in metastatic melanoma and multiple myeloma patients compared to healthy controls (41, 42). DPT cells with cytotoxic potential were found in great numbers in pleural effusion in human breast cancer patients and were described to play a suppressive role in colorectal cancer (31). NKT-like cell values were also reduced in colorectal cancer (27). Regarding DNT, in both groups, we found a significant decrease in values at the end of RT treatment. DNT values then tend to increase during 6 months' follow-up. The DPT cells also dropped down significantly in both groups at the t1 time point, but then remained almost stable during follow-up in the standard group while they have an increase in the hypoF group. The NKT cell values, after the decrease observed at the end of RT, remained stable up to 6 months after the end of RT.

To the best of our knowledge, this is the first study to discuss the effects of RapidArc/moderate hypofractionation curative RT on immune cell subsets in patients treated for localized prostate cancer. Furthermore, we also tried to compare these effects with those due to 3D conformal/conventional fractionation RT, albeit in a limited number of patients.

In the future, we intend to also elucidate the possible correlation between changes in immune cell populations and irradiated volumes as well as other RT parameters.

In conclusion, our preliminary findings, obtained in a small subset of prostate cancer patients, suggest a lower hematologic and immunologic toxicity of the RA/hypofractionation technique with respect to conformal/conventional fractionation RT in terms of ALC as well as of the different peripheral immune cell subpopulations, which play several roles in innate and adaptive immunity. In the era of personalized medicine, it is challenging to study the different RT effects on immune system cells, particularly in those clinical settings in which there is a possibility to combine RT with immunotherapy.

DATA AVAILABILITY STATEMENT

The datasets presented in this article are not readily available because of the participants' identifiable data. Requests to access the datasets should be directed to fiore.dauria@virgilio.it.

ETHICS STATEMENT

The studies involving human participants were reviewed and approved by Comitato Etico Unico Regionale per la Basilicata. The patients/participants provided their written informed consent to participate in this study.

AUTHOR CONTRIBUTIONS

Design of the work: LR and VF. Statistical analysis: GCal. Investigation and interpretation of data: FD'A, TS, and LV. Acquisition of data: GB and AT. Acquisition of data and organization of the database: AM, GCas, IS, AZ, and TV. Writing—original draft: FD'A and LR. Writing—review and editing: AS and GCal. All authors contributed to the article and approved the submitted version.

REFERENCES

1. Jemal A, Jemal A, Bray F, Center MM, Ferlay J, Ward E, Forman D. Global Cancer Statistics. *CA Cancer J Clin* (2011) 61:69–90. doi: 10.3322/caac.20107
2. Pollack A, Zagars GK, Starkschall G, Antolak JA, Lee JJ, Huang E, et al. Prostate Cancer Radiation Dose Response: Results of the M.D. Anderson Phase III Randomized Trial. *Int J Radiat Oncol Biol Phys* (2002) 53:1097–105. doi: 10.1016/S0360-3016(02)02829-8
3. Mangoni M, Desideri I, Detti B, Bonomo P, Greto D, Paiar F, et al. Hypofractionation in Prostate Cancer: Radiobiological Basis and Clinical Appliance. *BioMed Res Int* (2014) 2014:781340. doi: 10.1155/2014/781340

4. Brenner DJ, Hall EJ. Fractionation and Protraction for Radiotherapy of Prostate Carcinoma. *Int J Radiat Oncol Biol Phys* (1999) 43:1095–101. doi: 10.1016/S0360-3016(98)00438-6
5. Yeoh EE, Botten RJ, Butters J, Di Matteo AC, Holloway RH, Fowler J. Hypofractionated Versus Conventionally Fractionated Radiotherapy for Prostate Carcinoma: Final Results of a Phase III Randomized Trial. *Int J Radiat Oncol Biol Phys* (2011) 81:1271–8. doi: 10.1016/j.ijrobp.2010.07.1984
6. Arcangeli G, Saracino B, Arcangeli S, Gomellini S, Petrongari MG, Sanguineti G, et al. Moderate Hypofractionation in High-Risk, Organ-Confined Prostate Cancer: Final Results of a Phase III Randomized Trial. *J Clin Oncol* (2017) 35:1891–7. doi: 10.1200/JCO.2016.70.4189
7. Pollack A, Walker G, Horwitz EM, Price R, Feigenberg S, Konski AA, et al. Randomized Trial of Hypofractionated External-Beam Radiotherapy for Prostate Cancer. *J Clin Oncol* (2013) 31:3860–8. doi: 10.1200/JCO.2013.51.1972
8. Catton CN, Lukka H, Gu CS, Martin JM, Supiot S, Chung PWM, et al. Randomized Trial of a Hypofractionated Radiation Regimen for the Treatment of Localized Prostate Cancer. *J Clin Oncol* (2017) 35:1884–90. doi: 10.1200/JCO.2016.71.7397
9. Lee WR, Dignam JJ, Amin MB, Bruner DW, Low D, Swanson GP, et al. Randomized Phase III non-Inferiority Study Comparing Two Radiotherapy Fractionation Schedules in Patients With Low-Risk Prostate Cancer. *J Clin Oncol* (2016) 34:2325–32. doi: 10.1200/JCO.2016.67.0448
10. Incrocci L, Wortel RC, Alemayehu WG, Aluwini S, Schimmel E, Krol S, et al. Hypofractionated Versus Conventionally Fractionated Radiotherapy for Patients With Localized Prostate Cancer (HYPRO): Final Efficacy Results From a Randomized, Multicenter, Open-Label, Phase 3 Trial. *Lancet Oncol* (2016) 17:1061–9. doi: 10.1016/S1470-2045(16)30070-5
11. Hall EJ, Giaccia AJ. *Radiobiology for the Radiologist. 6th ed*. Philadelphia: Lippincot Williams & Wilkins (2006).
12. Blomgren H, Edsmyr F, Näslund I, Petrini B, Wasserman J. Distribution of Lymphocyte Subsets Following Radiation Therapy Directed to Different Body Regions. *Clin Oncol* (1983) 9:289–98.
13. Raben M, Walach N, Galili U, Schlesinger M. The Effect of Radiation Therapy on Lymphocyte Subpopulations in Cancer Patients. *Cancer* (1976) 37:1417–21. doi: 10.1002/1097-0142(197603)37:3<1417::AID-CNCR2820370324>3.0.CO;2-N
14. Rand RJ, Jenkins DM, Bulmer R. T and B Lymphocytes Sub-Populations Following Radiotherapy for Invasive Squamous Cell Carcinoma of the Uterine Cervix. *Clin Exp Immunol* (1978) 33:159–65. PMID: 309370
15. Sini C, Fiorino C, Perna L, Noris Chiorda B, Deantoni CL, Bianchi M, et al. Dose-Volume Effects for Pelvic Bone Marrow in Predicting Hematological Toxicity in Prostate Cancer Radiotherapy With Pelvic Node Irradiation. *Radiother Oncol* (2016) 118:79–84. doi: 10.1016/j.radonc.2015.11.020
16. Mell LK, Kochanski JD, Roeske JC, Haslam JJ, Mehta N, Yamada SD, et al. Dosimetric Predictors of Acute Hematologic Toxicity in Cervical Cancer Patients Treated With Concurrent Cisplatin and Intensity-Modulated Pelvic Radiotherapy. *Int J Radiat Oncol Biol Phys* (2006) 66:1356–65. doi: 10.1016/j.ijrobp.2006.03.018
17. Lissoni P, Meregalli S, Bonetto E, Mancuso M, Brivio F, Colciago M, et al. Radiotherapy-Induced Lymphocytopenia: Changes in Total Lymphocyte Count and in Lymphocyte Subpopulations Under Pelvic Irradiation in Gynecologic Neoplasms. *J Biol Regul Homeost Agents* (2005) 19:153–8.
18. Sage EK, Schmid TE, Sedelmayr M, Gehrmann M, Geinitz H, Duma MN, et al. Comparative Analysis of the Effects of Radiotherapy After Adjuvant Chemotherapy on the Composition of Lymphocyte Subpopulations in Breast Cancer Patients. *Radiother Oncol* (2016) 118:176–80. doi: 10.1016/j.radonc.2015.11.016
19. Louagie H, Van Eijkeren M, Philippe J, Thierens H, de Ridder L. Changes in Peripheral Blood Lymphocyte Subsets in Patients Undergoing Radiotherapy. *Int J Radiat Biol* (1999) 75:767–71. doi: 10.1080/095530099140113
20. Belka C, Ottinger H, Kreuzfelder E, Weinmann M, Lindemann M, Lepple-Wienhues A, et al. Impact of Localized Radiotherapy on Blood Immune Cells Counts and Function in Humans. *Radiother Oncol* (1999) 50:199–204. doi: 10.1016/S0167-8140(98)00130-3
21. Johnke RM, Edwards JM, Kovacs CJ, Evans MJ, Daly BM, Karlsson U, et al. Response of T Lymphocyte Populations in Prostate Cancer Patients Undergoing Radiotherapy: Influence of Neoajuvant Total Androgen Suppression. *Anticancer Res* (2005) 25:3159–66.
22. Yang ZR, Zhao N, Meng J, Shi ZL, Li BX, Wu XW, et al. Peripheral Lymphocyte Subset Variation Predicts Prostate Cancer Carbon Ion Radiotherapy Outcomes. *Oncotarget* (2016) 7:26422–35. doi: 10.18632/oncotarget.8389
23. Eckert F, Schaedle P, Zips D, Schmid-Horch B, Rammensee HG, Gani C, et al. Impact of Curative Radiotherapy on the Immune Status of Patients With Localized Prostate Cancer. *Oncoimmunology* (2018) 7:e1496881. doi: 10.1080/2162402X.2018.1496881
24. Sage EK, Schmid TE, Geinitz H, Gehrmann M, Sedelmayr M, Duma MN, et al. Effects of Definitive and Salvage Radiotherapy on the Distribution of Lymphocyte Subpopulations in Prostate Cancer Patients. *Strahlenther Onkol* (2017) 193:648–55. doi: 10.1007/s00066-017-1144-7
25. Yuan C, Wang Q. Comparative Analysis of the Effect of Different Radiotherapy Regimens on Lymphocyte and its Subpopulations in Breast Cancer Patients. *Clin Transl Oncol* (2018) 20:1219–25. doi: 10.1007/s12094-018-1851-2
26. Sakaguchi S, Wing K, Miyara M. Regulatory T Cells – a Brief History and Perspective. *Eur J Immunol* (2007) 37(Suppl 1):S116–23. doi: 10.1002/eji.200737593
27. Krijgsman D, de Vries NL, Skovbo A, Andersen MN, Swets M, Bastiaannet E, et al. Characterization of Circulating T-, NK-, and NKT Cell Subsets in Patients With Colorectal Cancer: The Peripheral Blood Immune Cell Profile. *Cancer Immonol Immunother* (2019) 68:1011–24. doi: 10.1007/s00262-019-02343-7
28. Zhang ZX, Young K, Zhang L. CD3+CD4-CD8- Alphabeta-TCR+ T Cell as Immune Regulatory Cell. *J Mol Med (Berl)* (2001) 79:419–27. doi: 10.1007/s001090100238
29. Yang L, Zhu Y, Tian D, Wang S, Guo J, Sun G, et al. Transcriptome Landscape of Double Negative T Cells by Single-Cell RNA Sequencing. *J Autoimmun* (2021) 121:102653. doi: 10.1016/j.jaut.2021.102653
30. Nascimbeni M, Shin EC, Chiriboga L, Kleiner DE, Rehermann B. Peripheral CD4(+)CD8(+) T Cells are Differentiated Effector Memory Cells With Antiviral Functions. *Blood* (2004) 104:478–86. doi: 10.1182/blood-2003-12-4395
31. Overgaard NH, Jung JW, Steptoe RJ, Wells JW. CD4+/CD8+ Double-Positive T Cells: More Than Just a Developmental Stage? *J Leukoc Biol* (2015) 97:31–8. doi: 10.1189/jlb.1RU0814-382
32. D'Auria F, Valvano L, Rago L, Statuto T, Calice G, D'Arena G, et al. Monoclonal B-Cell Lymphocytosis and Prostate Cancer: Incidence and Effects of Radiotherapy. *J Investig Med* (2019) 67:779–82. doi: 10.1136/jim-2018-000902
33. R Core Team. *R: A Language and Environment for Statistical Computing*. R Foundation for Statistical Computing, Vienna, Austria (2021). Available at: https://www.R-project.org/.
34. Kassambara A. *ggpubr: 'ggplot2' Based Publication Ready Plots* (2019). Available at: https://CRAN.R-project.org/package=ggpubr.
35. US Department of Health and Human Services. *Common Terminology Criteria for Adverse Events (CTCAE). Version 5.0*. (2017).
36. Pinkawa M, Djukic V, Klotz J, Petz D, Piroth MD, Holy R, et al. Hematologic Changes During Prostate Cancer Radiation Therapy are Dependent on the Treatment Volume. *Future Oncol* (2014) 10:835–43. doi: 10.2217/fon.13.237
37. Cozzarini C, Noris Chiorda B, Sini C, Fiorino C, Briganti A, Montorsi F, et al. Hematologic Toxicity in Patients Treated With Postprostatectomy Whole-Pelvis Irradiation With Different Intensity Modulated Radiation Therapy Techniques is Not Negligible and is Prolonged: Preliminary Results of a Longitudinal, Observational Study. *Int J Radiat Oncol Biol Phys* (2016) 95:690–5. doi: 10.1016/j.ijrobp.2016.01.022
38. Sanguineti G, Giannarelli D, Petrongari MG, Arcangeli S, Sangiovanni A, Saracino B, et al. Leukotoxicity After Moderately Hypofractionated Radiotherapy Versus Conventionally Fractionated Dose Escalated Radiotherapy for Localized Prostate Cancer: A Secondary Analysis From a Randomized Study. *Radiat Oncol* (2019) 14:23. doi: 10.1186/s13014-019-1223-2
39. Cooper MD. The Early History of B Cells. *Nat Rev Immunol* (2015) 15:191–7. doi: 10.1038/nri3801
40. Wang Q, Li S, Qiao S, Zheng Z, Duan X, Zhu X, et al. Changes in T Lymphocyte Subsets in Different Tumors Before and After Radiotherapy: A Meta-Analysis. *Front Immunol* (2021) 12:648652. doi: 10.3389/fimmu.2021.648652

41. De Tullio G, Strippoli S, Angarano R, De Fazio V, Sgherza N, Negri A, et al. αβ-Double Negative CD4/CD8 (CD56) T Cells (DNTs) in Metastatic Melanoma: Basal Frequency and Behavior During Ipilimumab Treatment. Preliminary Evaluations. *J Transl Med* (2015) 13:O10. doi: 10.1186/1479-5876-13-S1-O10
42. Feyler S, von Lilienfeld-Toal M, Jarmin S, Marles L, Rawstron A, Ashcroft AJ, et al. CD4(+)CD25(+)FoxP3(+) Regulatory T Cells Are Increased Whilst CD3(+)CD4(-)CD8(-)alphabetaTCR(+) Double Negative T Cells are Decreased in the Peripheral Blood of Patients With Multiple Myeloma Which Correlates With Disease Burden. *Br J Haematol* (2009) 144:686–95. doi: 10.1111/j.1365-2141.2008.07530.x

Conflict of Interest: The authors declare that the research was conducted in the absence of any commercial or financial relationships that could be construed as a potential conflict of interest.

Publisher's Note: All claims expressed in this article are solely those of the authors and do not necessarily represent those of their affiliated organizations, or those of the publisher, the editors and the reviewers. Any product that may be evaluated in this article, or claim that may be made by its manufacturer, is not guaranteed or endorsed by the publisher.

frontiers | Frontiers in Oncology

ORIGINAL RESEARCH
published: 22 June 2022
doi: 10.3389/fonc.2022.832343

Predicting Chemo-Radiotherapy Sensitivity With Concordant Survival Benefit in Non-Small Cell Lung Cancer *via* Computed Tomography Derived Radiomic Features

Yixin Liu[1,2†], Haitao Qi[3†], Chunni Wang[3], Jiaxing Deng[3], Yilong Tan[3], Lin Lin[3], Zhirou Cui[3], Jin Li[1] and Lishuang Qi[3*]*

[1] College of Intelligent Systems Science and Engineering, Harbin Engineering University, Harbin, China, [2] Basic Medicine College, Harbin Medical University, Harbin, China, [3] College of Bioinformatics Science and Technology, Harbin Medical University, Harbin, China

OPEN ACCESS

Edited by:
Francesco Cellini,
Radioterapia Oncologica ed Ematologia, Italy

Reviewed by:
Chang Zou,
Jinan University, China
Yee Ung,
University of Toronto, Canada

***Correspondence:**
Jin Li
lijin@hrbeu.edu.cn
Lishuang Qi
qilishuang7@ems.hrbmu.edu.cn

[†]These authors have contributed equally to this work

Specialty section:
This article was submitted to Radiation Oncology, a section of the journal Frontiers in Oncology

Received: 09 December 2021
Accepted: 17 May 2022
Published: 22 June 2022

Citation:
Liu Y, Qi H, Wang C, Deng J, Tan Y, Lin L, Cui Z, Li J and Qi L (2022) Predicting Chemo-Radiotherapy Sensitivity With Concordant Survival Benefit in Non-Small Cell Lung Cancer via Computed Tomography Derived Radiomic Features. Front. Oncol. 12:832343. doi: 10.3389/fonc.2022.832343

Background: To identify a computed tomography (CT) derived radiomic signature for the options of concurrent chemo-radiotherapy (CCR) in patients with non-small cell lung cancer (NSCLC).

Methods: A total of 226 patients with NSCLC receiving CCR were enrolled from public dataset, and allocated to discovery and validation sets based on patient identification number. Using CT images of 153 patients in the discovery dataset, we pre-selected a list of radiomic features significantly associated with 5-year survival rate and adopted the least absolute shrinkage and selection operator regression to establish a predictive radiomic signature for CCR treatment. We performed transcriptomic analyzes of the signature, and evaluated its association with molecular lesions and immune landscapes in a dataset with matched CT images and transcriptome data. Furthermore, we identified CCR resistant genes positively correlated with resistant scores of radiomic signature and screened essential resistant genes for NSCLC using genome-scale CRIPSR data. Finally, we combined DrugBank and Genomics of Drug Sensitivity in Cancer databases to excavate candidate therapeutic agents for patients with CCR resistance, and validated them using the Connectivity Map dataset.

Results: The radiomic signature consisting of nine features was established, and then validated in the dataset of 73 patients receiving CCR log-rank P = 0.0005, which could distinguish patients into resistance and sensitivity groups, respectively, with significantly different 5-year survival rate. Furthermore, the novel proposed radiomic nomogram significantly improved the predictive performance (concordance indexes) of clinicopathological factors. Transcriptomic analyzes linked our signature with important tumor biological processes (e.g. glycolysis/glucoseogenesis, ribosome). Then, we identified 36 essential resistant genes, and constructed a gene-agent network including 10 essential resistant genes and 35 candidate therapeutic agents, and excavated AT-

7519 as the therapeutic agent for patients with CCR resistance. The therapeutic efficacy of AT-7519 was validated that significantly more resistant genes were down-regulated induced by AT-7519, and the degree gradually increased with the enhanced doses.

Conclusions: This study illustrated that radiomic signature could non-invasively predict therapeutic efficacy of patients with NSCLC receiving CCR, and indicated that patients with CCR resistance might benefit from AT-7519 or CCR treatment combined with AT-7519.

Keywords: computed tomography, non-small cell lung cancer, concurrent chemo-radiotherapy, radiomic signature, candidate therapeutic agents

INTRODUCTION

Lung cancer was the first most commonly diagnosed cancer (1), with non-small cell lung cancer (NSCLC) accounting for 80% to 85% of cases (2). More than 30% of patients with NSCLC have locally advanced and unresectable disease, and the 5-year survival rate is less than 15% (3). International guidelines recommend concurrent chemo-radiotherapy (CCR) as a standard first-line treatment option for locally advanced stage NSCLC patients (4). However, the prognosis achieved with CCR remains unsatisfactory with the 5-year survival rate of less than 25% (5, 6). Therefore, it is imperative to develop a clinically feasible signature to stratify patients who might benefit from CCR treatment, avoiding these side effects of unnecessary treatment.

Currently, most predictive signatures for CCR therapeutic efficacy were constructed based on molecular characterization using genomic and proteomic technologies (7–9). However, these techniques are limited due to tumors are spatially and temporally heterogeneous, which could not provide a complete characterization of the tumor (10). In contrast, medical imaging can be used to non-invasively and cost-effectively visualize the characteristics of entire tumor, providing dynamic information that can be used to monitor the occurrence and development of tumors (11, 12). Currently, computed tomography (CT), which is the most commonly used imaging modality in oncology, especially lung cancer, allows non-invasive detection of tissue density and describes tumor spatial heterogeneity (12).

Radiomics converts medical images into high-throughput quantitative features; this is a new field that could be the vanguard of precision medicine (10, 13), which offers the possibility to minimize adverse effects and optimize the efficacy of treatments (14). Current, most researchers firstly developed prognostic signatures (15–17) for patients not receiving CCR and then demonstrated that only the high-risk patients predicted by the signatures showed significantly survival benefit after CCR treatment. Obviously, such prognostic signatures were just able to identify patients with poor prognosis who need CCR treatment, but unable to identify patients who might be sensitive to treatment. In order to provide support in patient management and achieve maximum clinical benefit, the development of CT derived radiomic signature for predicting the patients sensitive to CCR need to be assessed to predict the therapeutic efficacy of CCR treatment.

In this study, using CT images of patients, we develop a non-invasive radiomic signature for patients with locally advanced stage NSCLC receiving CCR, which might help to accurately predict therapeutic efficacy for CCR treatment with improved 5-year survival rate. Subsequently, based on the dataset with matched CT images and gene expression profiles, we characterized the underlying functional pathways reflected by the radiomic features in the signature and tentatively captured the potentially beneficial agents required for the treatment of patients with CCR resistance based on cancer cell lines dataset.

MATERIALS AND METHODS

Data Sources

In this study, the NSCLC-Radiomics (NR) dataset (10) with DICOM CT scans was downloaded from The Cancer Imaging Archive (TCIA, https://www.cancerimagingarchive.net/, 2020), including 422 patients previously treated with CCR or radiotherapy. The inclusion criteria of the samples for CCR treatment planning were as follows: 1) available treatment-naive CT scans; 2) confirmed NSCLC; 3) patients treated with CCR; 4) available survival information. Finally, 226 patients with locally advanced stage NSCLC receiving CCR were preselected and divided into discovery (n = 153) and validation (n = 73) datasets based on patient identification number (pid), that is, the 153 patients whose pid wasn't divisible by 3 were used as a discovery dataset to develop a radiomic signature for CCR treatment, and the remaining 73 patients were assigned to the validation dataset. These details and applications of the analyzed datasets are displayed in **Table 1** and **Supplementary Figure S1**.

NSCLC-Radiogenomics (NRG) dataset (18) with DICOM CT scans and matched gene expression profiles were downloaded from TCIA, including 67 NSCLC patients treated with different therapeutic strategies, which was used to understand the biological processes linked to the radiomic signature.

Genome-wide CRISPR screening of NSCLC cells (n = 87) was downloaded from the DepMap portal (https://depmap.org/portal/download/; 2019). Dependency scores for around 17,000 candidate genes were calculated using the CERES algorithm (19). Essential genes for NSCLC were defined as the genes with a CERES score of <−1 across 75% of NSCLC cell lines. The DrugBank database (https://go.drugbank.com/) was used to identify therapeutic agents targeting essential genes.

Genomics of Drug Sensitivity in Cancer dataset (20) (GDSC, https://www.cancerrxgene.org, release-8.2), which contains responses to 345 anticancer agents across 917 cancer cell lines,

TABLE 1 | Baseline clinical characteristics of patients in the analyzed datasets.

	Discovery dataset (*n* = 153)	Validation dataset (*n* = 73)
Age (years)		
≤ 65	78 (51.0%)	35 (47.9%)
> 65	70 (45.8%)	34 (46.6%)
Gender		
Female	54 (35.3%)	28 (38.4%)
Male	99 (64.7%)	45 (61.6%)
TNM stage		
I	–	–
II	–	–
III	153 (100%)	73 (100%)
T stage		
T1	20 (13.1%)	20 (27.4%)
T2	68 (44.4%)	24 (32.9%)
T3	21 (13.7%)	10 (13.7%)
T4	41 (26.8%)	19 (26.0%)
N stage		
N0	–	–
N1	–	–
N2	97 (63.4%)	44 (60.3%)
N3	56 (36.6%)	29 (39.7%)
Histologic subtype		
ADC	18 (11.8%)	11 (15.1%)
SCC	53 (34.6%)	22 (30.1%)
LCC	53 (34.6%)	23 (31.5%)
NOS	22 (14.4%)	13 (17.8%)
Average survival (Month)	28.65	34.78

ADC, Adenocarcinoma; SCC, Squamous cell carcinoma; LCC, Large-cell lung carcinoma; NOS, Not otherwise specified subtype.

with gene expression profiles and half-maximal inhibitory concentrations (IC_{50}) values of cell lines were used to identify potential therapeutic agents.

Gene expression profiles of 27 samples treated with different concentrations (0.01 - 10 μM) of AT-7519 for 24 hours and the corresponding 124 untreated control samples were downloaded from Connectivity Map dataset (21) (CMap, https://clue.io/data/CMap2020#LINCS2020), including 12,328 genes. These samples were derived from A549 and HCC515 NSCLC cell lines. The samples treated with AT-7519 were divided into three dose groups: Low (dose < 1 μM), Middle (1 < dose < 10 μM) and High (dose = 10 μM), which was used to validate therapeutic efficacy of AT-7519.

Image Segmentation and Radiomic Feature Extraction

The regions of interest (ROI) of CT scans in the NR and NRG datasets were publicly available. In general, the three-dimensional radiomic features that enabled quantification of the tumor characteristics were divided into ten groups according to the following: I) Tumor intensity, II) Shape, III) Texture, IV) wavelet filters, V) Laplacian of Gaussian filters, VI) Logarithm filters, VII) Square filters, VIII) Exponential filters, IX) Gradient filters and X) Squareroot filters features. For the NR and NRG datasets, radiomic feature extraction was performed for each CT scan with ROIs using free and open-source PyRadiomics (v2.2.0) libraries. An extraction intensity bin width was set at 25 HU and the slice thicknesses of all scans were interpolated to a voxel size of 1×1×1 mm^3. The quantitative values of 1781 radiomic features (**Supplementary Table S1**) were calculated according to feature definitions in the PyRadiomics documentation (https://pyradiomics.readthedocs.io/en/latest/index.html) by the Imaging Biomarker Standardization Initiative (22).

Construction of the Radiomic Signature for CCR Treatment

In the discovery dataset, radiomic features whose quantitative values were significantly associated with the 5-year survival rate were identified as CCR-associated features. Based on the CCR-associated features, we adopted the least absolute shrinkage and selection operator (LASSO) regression (23) using "glmnet" R package to establish an optimal predictive model, and defined it as a predictive radiomic signature for CCR treatment. "Cox" was set as the family in the model. Ten-fold cross-validation was performed using cv.glmnet function to select lambda minimum to give the minimum cross-validated error. The resistant score of the signature for each patient was calculated *via* a linear combination of features in the signature that were weighted by their respective coefficients as follows:

$$\text{Risk} \quad \text{score} = \sum_{i=1}^{n} w_i FeatureValue_i \quad i \in \quad n$$

where i represents the *i-th* feature in the signature; w_i represents the weight of the *i-th* feature derived from LASSO model; $FeatureValue_i$ represents the quantitative value of the *i-th* feature; and n represents the number of features contained in the signature.

The median value of resistant scores of the radiomic signature in the discovery dataset was used as the cut-off value for dividing

patients into the resistance (≧ Median) and sensitivity (< Median) groups.

Statistics Analyzes

The 5-year survival rate of the patients was used as the end point of interest. Patients with more than 5 years follow-up were censored at 5 years because deaths occurring past five years were not likely to be related to CCR treatment. Survival curves were estimated using the Kaplan-Meier method and statistically compared using the log-rank test (24). To analyze the associations between the different influencing factors and the 5-year survival rate of the patients, a univariate Cox regression model was used, and to test the independent association of the radiomic signature with the 5-year survival rate after adjusting for the clinical parameters recorded in the data, a multivariate Cox regression model was used. Hazard ratio (HR) and 95% confidence interval (CI) were generated using the Cox proportional hazards models, and the concordance index (C-index) (25) was also used to estimate the predictive performance of clinical factors. Time-dependent receiver operating characteristic curve (ROC) analysis (26) and the area under the curve (AUC) were performed to evaluate the radiomic signature's performance in predicting the 1-, 3- and 5-year survival rates.

To assess the complementary effect of the radiomic signature on the clinical model in predicting the therapeutic efficacy in patients with NSCLC receiving CCR treatment, a radiomic nomogram was constructed using multivariate linear regression analysis ("rms" R package). Additionally, the predictive performance of the radiomic nomogram was evaluated based on C-index, calibration curve, and the decision curve analysis. The net reclassification improvement (NRI) (27) index was determined to quantify the radiomic signature's incremental improvement using the "nricens" R package.

Spearman's rank correlation was applied to investigate the association between the radiomic signature and clinical parameters. The "clusterProfiler" R package was used to conduct the functional enrichment analysis of the genes that were correlated with the radiomic features based on the current Kyoto Encyclopaedia of Genes and Genomes (KEGG) database, wherein a hypergeometric test was employed.

ESTIMATE (28) was introduced to estimate the immune score for a given sample by performing ssGSEA (29), based on its mRNA expression profiles using an "estimate" R package. The ssGSEA was also utilized to quantify the relative infiltration levels of 28 immune cell types in the tumor microenvironment by using a "GSVA" R package. The relative infiltration levels of each immune cell type were represented by an enrichment score in the ssGSEA analysis.

Student's *t*-test was used to examine the intergroup difference by comparing samples treated with potential therapeutic agents and the corresponding untreated control samples. Binomial distribution was used to examine the difference in the distribution of the down-regulated and up-regulated resistance genes induced by the potential therapeutic agents.

Statistical analyzes were performed using R, version 3.5.3; *P* values were adjusted using the Benjamini-Hochberg procedure for multiple tests to control the false discovery rate (FDR). Statistical significance was defined as two-sided $P<0.05$ or FDR<0.05 for multiple tests.

RESULT

Construction and Validation of a Radiomic Signature for CCR Treatment

Figure 1 describes the flowchart of this study. In the discovery dataset, comprising 153 patients with NSCLC receiving CCR, we extracted 398 CCR-associated radiomic features which were potentially significantly associated with 5-year survival rate (Univariate Cox regression, $P < 0.05$). The CCR-associated features were selected as inputs for LASSO regression to generate a radiomic signature consisting of nine weighted features (denoted as CCR-9RS, **Figure 2A** and **Table 2**). The weighted sum of these nine radiomic features gave a resistant score for each sample (**Supplementary Table S2**). Using the median value (0.6241) of the 153 samples as the cut-off value, the patients were divided into resistance and sensitivity groups, respectively, with significantly 5-year survival rate differences (resistance vs. sensitivity = 77: 76, log-rank P = 2.38E-06, HR = 2.33, 95% CI: 1.63-3.34, C-index = 0.61, **Figure 2B**) in the discovery dataset. The time-dependent ROC curve of CCR-9RS in predicting the 1-, 3-, and 5-year survival rates were shown in **Figure 2C**, and the area under the curve (AUC) was 0.69, 0.73, and 0.74, respectively. In the multivariate Cox regression model, CCR-9RS remained significantly associated with the 5-year survival rate (P = 7.40E-06, HR = 2.45, 95% CI: 1.66-3.62, **Figure 2D**) after adjusting for TNM stage, age, gender and histologic subtype.

The predictive performance of CCR-9RS was validated in the validation dataset, consisting of 73 patients with NSCLC receiving CCR. According to the trained cut-off (0.6241) of CCR-9RS, the 35 patients were classified into the resistance group, and exhibited significantly shorter 5-year survival rate than the 38 patients classified into the sensitivity group (log-rank P = 0.0005, HR = 2.52, 95% CIs: 1.47-4.30, C-index = 0.61, **Figure 3A**). The time-dependent ROC curve confirmed that CCR-9RS had a good performance for predicting 1-, 3- and 5-year survival rates in the validation dataset (**Figure 3B**). Multivariate Cox analysis revealed that 5-year survival rate was independently predicted by CCR-9RS after adjusting for the clinical factors in validation dataset (**Figure 3C**). Additionally, in order to exclude the influence of the not otherwise specified (NOS) subtype of NSCLC, CCR-9RS was also validated in the patients with clarifying histologic subtypes (Adenocarcinoma, Squamous cell carcinoma and Large-cell lung carcinoma) in the discovery dataset (n = 131, log-rank P = 4.81E-05, HR = 2.19, 95% CI: 1.49-3.22, C-index = 0.60, **Supplementary Figure S2A**) and validation dataset (n = 60, log-rank P = 0.0013, HR = 2.55, 95% CI: 1.42-4.61, C-index = 0.62, **Supplementary Figure S2B**), respectively.

Incremental Value of CCR-9RS

To further investigate whether CCR-9RS could provide incremental value for therapeutic evaluation of patients with

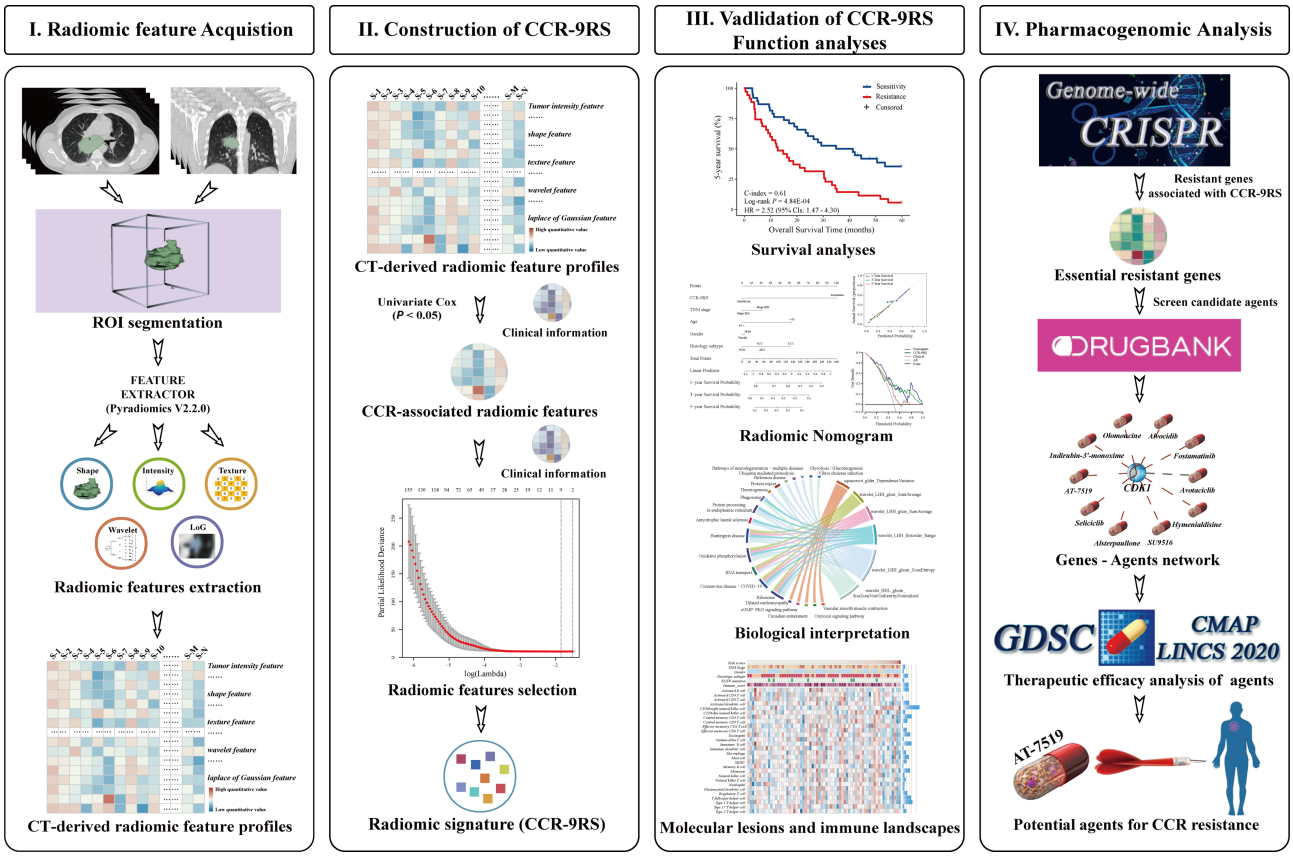

FIGURE 1 | Flowchart of developing and validating of a radiomic signature derived from computer tomography (CT) for the patients with NSCLC receiving CCR treatment.

NSCLC receiving CCR, we generated a radiomic nomogram (**Figure 4A**) that incorporated clinical factors (TNM stage, age, gender and histologic subtype) and CCR-9RS. The radiomic nomogram showed a significantly higher C-index relative to that of the clinical nomogram (**Supplementary Figure S3A**) and CCR-9RS alone based on the NRI index ($P < 0.05$, **Supplementary Figures S3B, C**) in the discovery dataset (C-index = 0.65, **Table 3**) and validation dataset (C-index = 0.66, **Table 3**). The calibration curves corresponding to the radiomic nomogram at 1-, 3-, and 5-year survival rates 7 showed good agreement between the estimations and the clinical outcomes in the discovery (**Figure 4B**) and validation datasets (**Figure 4C**). Furthermore, the decision curve analysis showed that the radiomic nomogram exhibited superior performance compared with the clinical nomogram across the majority of the range of reasonable threshold probabilities in the discovery (**Figure 4D**) and validation datasets (**Figure 4E**).

Biological Function of CCR-9RS

The biological basis of CCR-9RS was evaluated in the independent NRG dataset (n = 67) with matched CT images and gene expression profiles. Using Spearman's rank correlation analysis, we identified the significantly correlated genes of each feature in CCR-9RS ($P < 0.05$) and performed functional enrichment analysis for these correlated genes. It was observed that 6 of the 9 features were significantly enriched in 20 functional pathways (hypergeometric test, FDR < 0.05; **Figure 5A** and **Supplementary Table S3**), including "glycolysis/glucoseogenesis" (30), "ribosome" (31) and other functional pathways related to CCR treatment resistance. For example, we observed that "wavelet_HHL_glszm_SizeZoneNonUniformityNormalized" showed a strong positive correlation with genes enriched in "ribosome", "glycolysis/glucoseogenesis" (**Supplementary Table S3**). The feature measures the variability of size zone volumes throughout the image, and a higher value of this feature represents a higher level of tumor heterogeneity, which might reflect the high glycolysis ability of a tumor with high CCR resistant capability (30, 32).

We also investigated the association of CCR-9RS with the molecular lesions (EGFR mutation, KRAS mutation and ALK translocation) and immune landscapes based on Spearman's rank correlation analysis (**Figure 5B**). The resistant scores of CCR-9RS were not observed to be significantly associated with EGFR mutation ($P = 0.3685$), KRAS mutation ($P = 0.8272$) and ALK translocation ($P = 0.6256$). The result indicated that

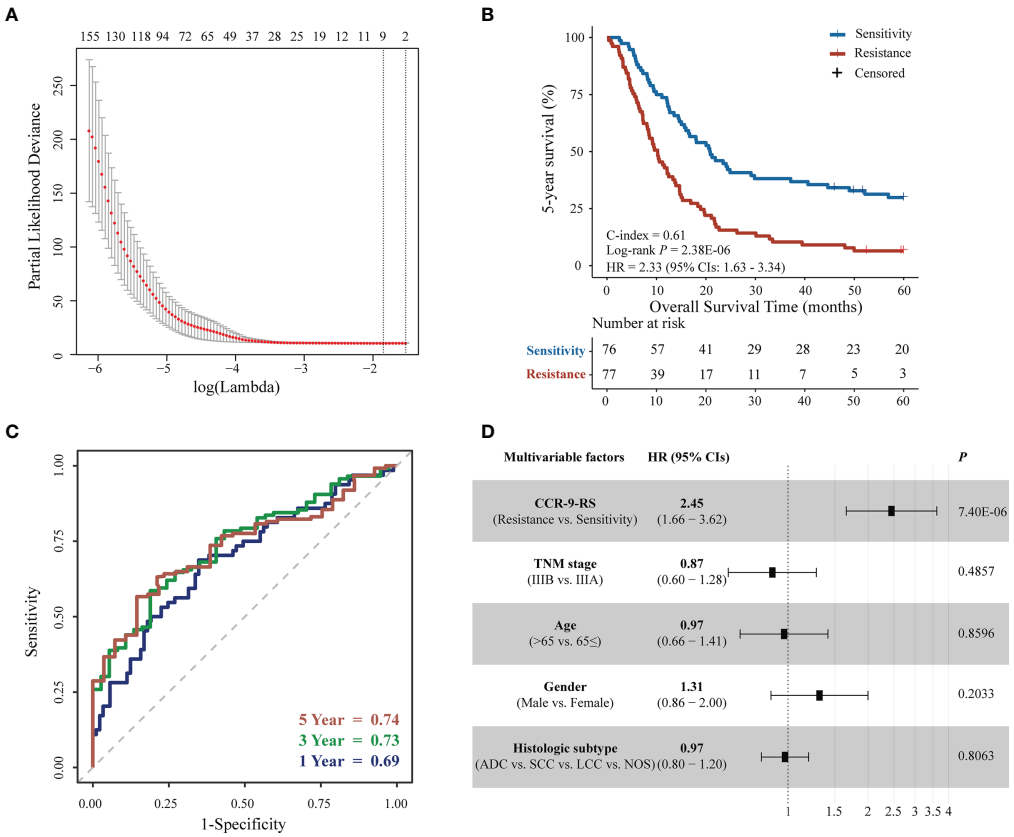

FIGURE 2 | Feature selection and survival analyzes for patients with NSCLC receiving CCR in the discovery dataset. **(A)** Tuning parameter (λ) selection in the least absolute shrinkage and selection operator (LASSO) Cox model used a 10-fold cross-validation *via* minimum criteria. The area under the receiver operating characteristic (AUC) curve was plotted versus log(λ). **(B)** Kaplan–Meier curves of the 5-year survival rate for 153 patients. **(C)** Time-dependent receiver operating characteristic curve (ROC) of CCR-9RS in predicting the 1-, 3- and 5-year survival rates. **(D)** Multivariate Cox analyzes of CCR-9RS after adjusting for clinical factors.

patients with CCR resistance might not benefit from the currently molecular-targeted therapies. Furthermore, we observed that patients with CCR resistance exhibited marginally significantly negatively correlated with immune scores (29) (*Rho* = -0.2222, *P* = 0.0707), and significantly negatively correlated with some immune cells (28), such as Activated dendritic cell (*Rho* = -0.2488, *P* = 0.0423), Activated B cells (*Rho* = -0.2387, P = 0.0517) and Central memory CD4 T cell (*Rho* = -0.2968, *P* = 0.0147). The result suggested that patients with CCR resistance had lower infiltration levels predicted by CCR-9RS, who might also not benefit from immunotherapy.

Identification of Potential Therapeutic Agents for Patients Resistant to CCR Treatment

To further screen candidate therapeutic agents for patients resistant to CCR treatment, we first identified 470 resistant

TABLE 2 | Composition of CCR-9RS.

Radiomic feature name	HR	*P*-value	C-index
squareroot_gldm_DependenceVariance	1.06	0.0011	0.58
wavelet_LHH_glcm_JointAverage	1.10	0.0067	0.55
wavelet_LHH_glcm_SumAverage	1.05	0.0067	0.55
wavelet_LHH_firstorder_Range	1.01	0.0053	0.55
wavelet_LHH_glszm_ZoneEntropy	1.67	0.0051	0.56
wavelet_LLH_glrlm_LongRunHighGrayLevelEmphasis	1.01	0.0005	0.57
wavelet_LLH_glszm_SizeZoneNonUniformity	1.01	0.0002	0.58
wavelet_HHH_glszm_SizeZoneNonUniformity	1.02	2.91E-05	0.56
wavelet_HHL_glszm_SizeZoneNonUniformityNormalized	5370.36	0.0042	0.57

HR and P-value are the statistics calculated using a univariate Cox regression model. HR represents the risk coefficient of the quantitative values for the feature; P-value represents the significance of the quantitative values for radiomic feature.

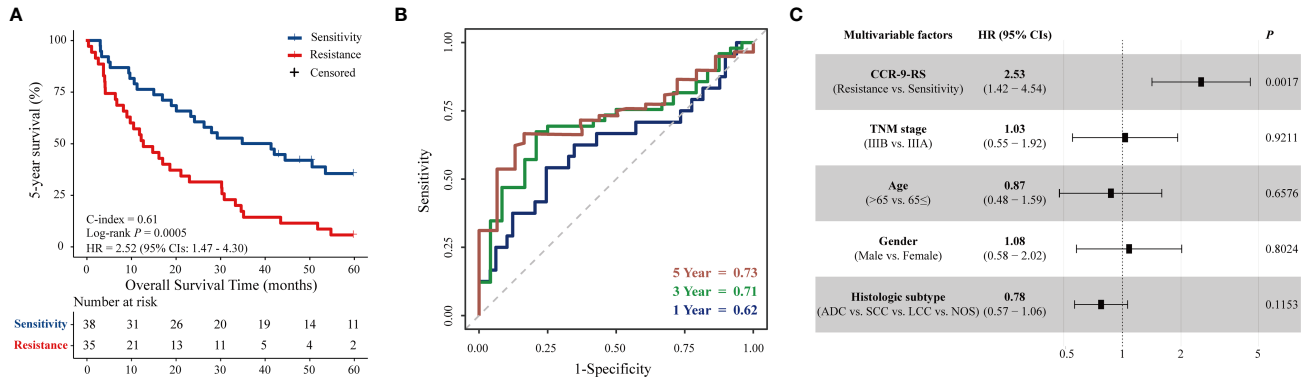

FIGURE 3 | Validation of CCR-9RS. **(A)** Kaplan–Meier curves of 5-year survival rate for patients in the validation dataset (n = 73). **(B)** Time-dependent receiver operating characteristic curve (ROC) of CCR-9RS in predicting 1-, 3- and 5-year survival rates in the validation dataset. **(C)** Multivariate Cox analyzes of CCR-9RS after adjusting for clinical factors in the validation dataset.

genes responsible for their resistance, whose expression values were significantly positively associated with the resistant scores of CCR-9RS in the NRG dataset (Spearman's rank correlation, $Rho > 0$ and $P < 0.05$, **Figure 6A**). Second, we investigated genome-wide CRISPR-based loss-of-function screens derived from DepMap to pinpoint 689 essential genes for maintaining survival in 87 NSCLC cell lines and found 36 resistant genes to be essential genes for NSCLC. The correlations among ;the 36 resistant genes is displayed in **Supplementary Figure S4**. Therefore, the 36 essential resistant genes could be the potential targets of patients with CCR resistance. Third, taking advantage of the DrugBank database, we extracted 35 candidate therapeutic agents targeting 10 essential resistant genes and constructed a gene-agent network (**Figure 6B**). Finally, we input the 35 candidate therapeutic agents of gene-agent network into the GDSC cancer cell line dataset, and searched for 4 overlapped therapeutic agents (Seliciclib, AT-7519, Vinorelbine and Vinblastine) with completely IC_{50} values

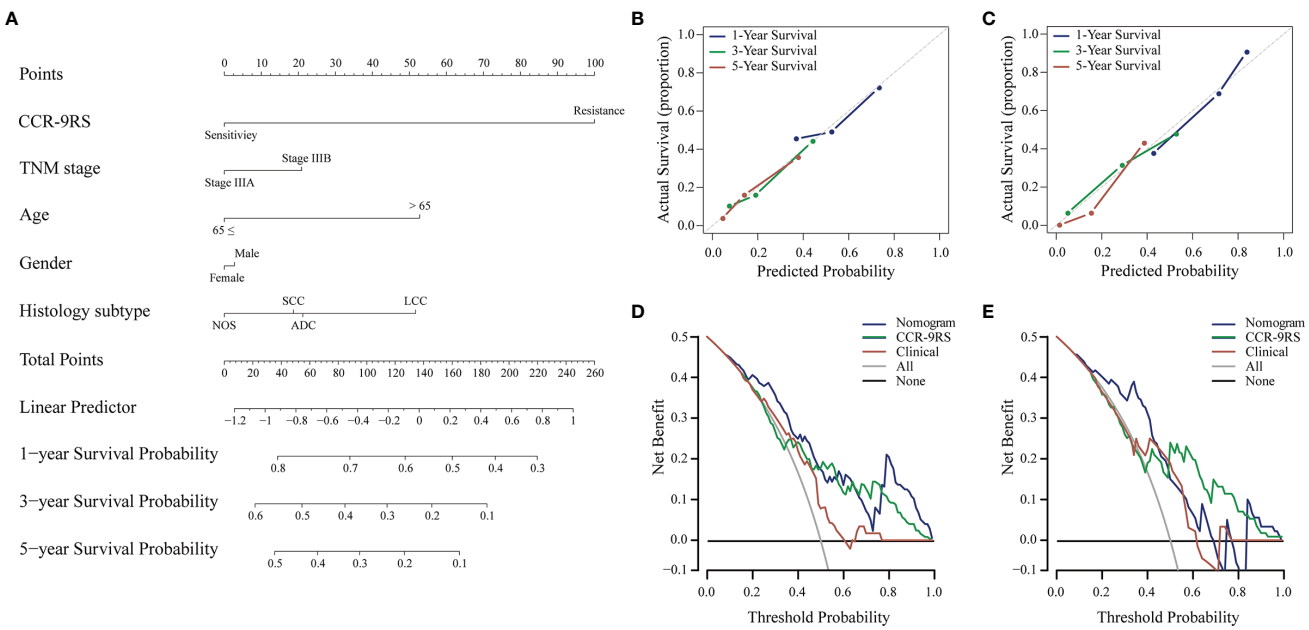

FIGURE 4 | Radiomic nomogram and its performance for patients with NSCLC receiving CCR treatment. **(A)** Survival radiomic nomogram that incorporated with CCR-9RS and the clinical factors trained in the discovery cohort (n=153). The points of CCR-9RS and the clinical factors were obtained based on the top 'points' bar (scale: 0–100). The total point was calculated by summing the two points, and a line was drawn downward to the survival axes to determine the likelihood of 1-, 3-, or 5-year survival rate. **(B, C)** Calibration curves for the radiomic nomogram in the discovery and validation datasets; the diagonal gray line represents an ideal evaluation. **(D, E)** Decision curves for the radiomic nomogram in the discovery and validation datasets.

TABLE 3 | Performances of different models.

	C-index (95% CIs)	
	Discovery dataset	**Validation dataset**
Radomic nomogram	0.65 (0.60 - 0.71)	0.66 (0.59 - 0.74)
CCR-9RS	0.61 (0.57 - 0.65)	0.61 (0.55 - 0.68)
Clinical nomogram	0.57 (0.51 - 0.63)	0.58 (0.50 - 0.66)

corresponding to two essential resistant genes (*CDK1* and *TUBB*). Using Spearman's rank correlation analysis, we found that only the IC_{50} value of AT-7519 therapeutic agent was significantly negatively associated with the mRNA expression of the target gene (*CDK1*) in the GDSC dataset (*Rho* = -0.1548, *P* = 5.86E-06, **Figure 6C**). Therefore, AT-7519 was selected as a candidate therapeutic agent for the patients resistant to CCR treatment.

Finally, using the CMap dataset, we collected 27 samples treated with AT-7519 and the corresponding 124 untreated control samples to tentatively validate the therapeutic efficacy of AT-7519 for samples with CCR resistance. The detailed information of cell line samples treated with AT-7519 have been described in the **Supplementary Table S4**. Among the 341 resistant genes measured in the CMap dataset, we found that 183 resistant genes were significantly differently expressed between the AT-7519-treated and control groups (Student's *t*-test, FDR < 0.05). Herein, 124 of the 183 resistance genes were significantly down-regulated induced by AT-7519, including the targeted *CDK1* gene of AT-7519 (Student's *t*-test, *P* = 0.0046, **Supplementary Figure S5**), and showed a significant difference in the resistance genes distribution of the down-regulated induced (67.76%) and up-regulated induced (32.24%) by binomial distribution (*P* = 1.76E-06, **Figure 6D**). Furthermore, we divided the samples treated with AT-7519 into three dose groups: Low (*n* = 15), Middle (*n* = 8) and High (*n* = 4), and found that significantly more resistant genes (Low, 59; Middle, 93; High, 118, **Figure 6E**) were down-regulated induced by AT-7519, and the degree was gradually increased with the enhanced doses.

DISCUSSION

Radiomics is an emerging technique that converts traditional medical images into high-dimensional features, and has been widely applied in early diagnosis, prognosis and therapeutic efficacy evaluation, guiding clinicians develop individualized treatment plans for patients. In this study, we established a CT derived radiomic signature (CCR-9RS), which is the predictor of the therapeutic efficacy in patients with locally advanced stage NSCLC receiving CCR treatment. The radiomic signature successfully stratified NSCLC patients into the resistance and sensitivity groups with significantly different 5-year survival rate when they receiving CCR treatment. The combination of clinical factors with the radiomic signature in a radiomic nomogram could significantly improve the predictive performance of the clinical evaluation system in the discovery and validation datasets. These results indicated that CCR-9RS could provide additional predictive information for patients within the same clinical factors, and it will be worthwhile to develop this signature as a non-invasive predictive tool for clinical application.

Additionally, we tentatively estimated the predictive performance of CCR-9RS in early stage (stage I-II) NSCLC patients receiving radiotherapy, which is a guideline-

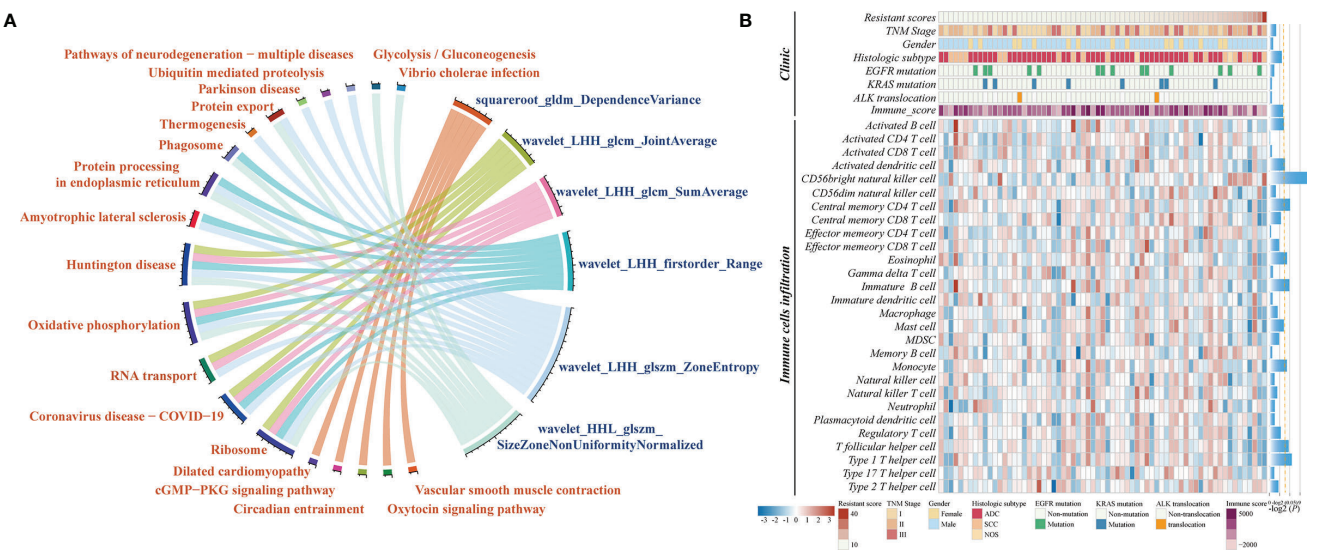

FIGURE 5 | Molecular characteristics associated with CCR-9RS in NSCLC. **(A)** Gene-enrichment analysis of correlated genes with 6 radiomic features in CCR-9RS based on the Kyoto Encyclopedia of Genes and Genomes (KEGG) database in the NRG (NSCLC-Radiogenomics) dataset. **(B)** Molecular lesions and immune landscapes along with the resistant scores calculated by CCR-9RS. The correlation was estimated by Spearman rank correlation. The histogram on the right represents the significantly correlation with the resistant scores of CCR-9RS; the orange-dotted line represents *P* = 0.05.

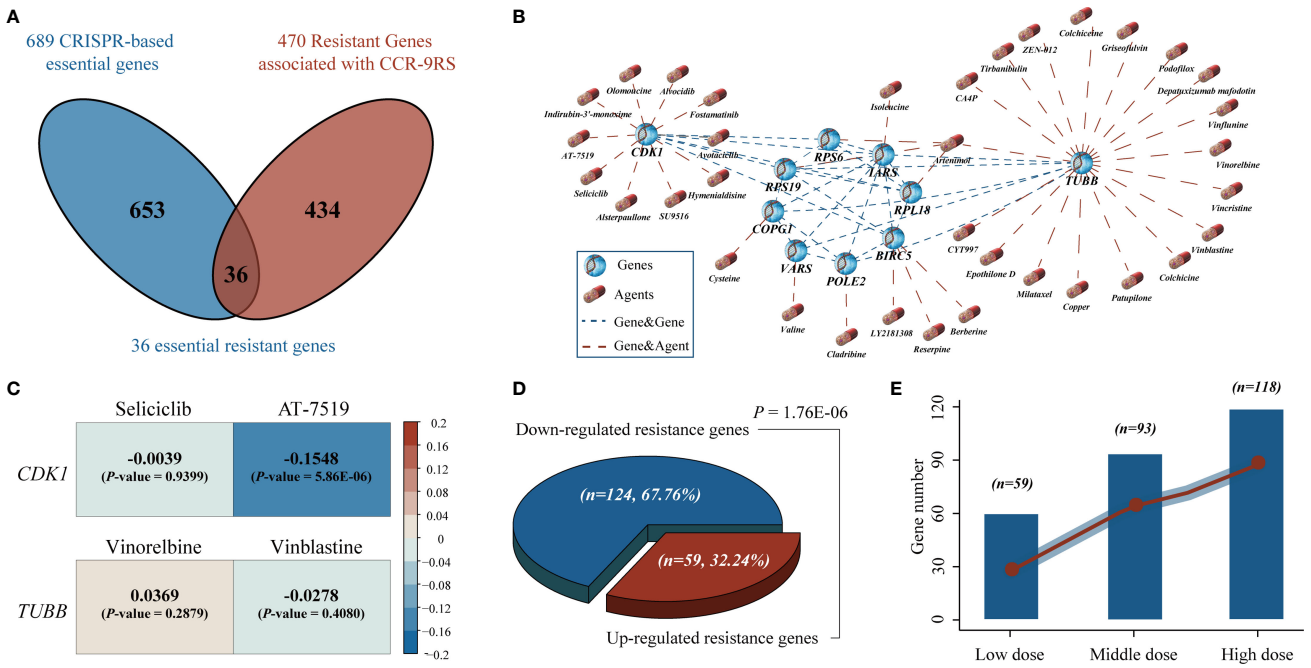

FIGURE 6 | Identification of potential therapeutic agents for the patients resistant to CCR treatment. **(A)** Venn diagram of the resistant genes identified in tumor tissues (NSCLC-Radiogenomics dataset) and essential genes identified by CRISPR dataset. The blue circle represents the essential genes screened by CRISPR dataset and the red circle represents the resistant genes significantly positively associated with the resistant scores of the CCR-9RS in the NSCLC-Radiogenomics dataset. **(B)** A gene-agent network of essential resistant genes and candidate therapeutic agents using DrugBank database. The blue dotted line represents the significantly correlated essential resistant genes (Pearson correlation, FDR < 0.05, **Figure S4**) and the red dotted line represents the candidate therapeutic agents targeting essential resistant genes in DrugBank database. **(C)** The correlation analysis of four overlapped therapeutic agents corresponding to two essential resistant genes using GDSC cancer cell line dataset. **(D)** Binomial distribution for the down-regulated and up-regulated resistance genes induced by AT-7519. **(E)** The number of down-regulated resistance genes induced by AT-7519 in three dose groups (left to right: Low, Middle and High).

recommended treatment for some early stage patients, based on the hypothesis that patients who were resistant to CCR should be resistant to both chemotherapy and radiotherapy. Here, we collected 93 stage I and 40 stage II NSCLC patients receiving radiotherapy in the NR dataset, and found that the resistance patients predicted by CCR-9RS also had significantly shorter 5-year survival rate than the predicted sensitivity patients (resistance vs. sensitivity = 55 vs. 78, log-rank $P = 0.0138$, HR = 1.61, 95% CI: 1.10-2.35, C-index = 0.57, **Supplementary Figure S6A**) when they receiving radiotherapy only. The time-dependent ROC curve confirmed the good performance of CCR-9RS in predicting 1-, 3- and 5-year survival rates of patients receiving radiotherapy (**Supplementary Figure S6B**). Multivariate Cox analysis revealed that 5-year survival rate was independently predicted by CCR-9RS after adjusting for the clinical factors in the radiotherapy dataset (**Supplementary Figure S6C**). This result indicated that CCR-9RS might also predict the efficacy of radiotherapy for early stage NSCLC patients, which needs further validation.

The underlying biological progression of the radiomic signature for CCR treatment is favorable for clinical application. Therefore, we first revealed that several known cancer-related functional processes, including "glycolysis/glucoseogenesis", "ribosome" and other functional pathways related to CCR resistance, might be reflected by radiomic features in CCR-9RS. Next, we found that patients with CCR sensitivity were characterized by a higher immune score and levels of some immune cell infiltration (such as Activated dendritic cell and Activated B cells), providing evidence that patients sensitive to CCR treatment with higher infiltration levels might benefit from CCR treatment in the molecular mechanism. In contrast, patients with CCR resistance might not benefit from targeted therapy or immunotherapy, which requires further analysis of the benefit from other therapeutic agents.

In order to further screen potential therapeutic agents for the patients with CCR resistance, we first identified resistant genes significantly positively associated with the resistant scores of CCR-9RS in the tumor tissues (NRG dataset). Thereafter, *via* the leveraging the genome-scale CRIPSR data, we pre-selected a set of essential resistant genes, which could be the potential targets of the patients with CCR resistance. Then, we extracted candidate therapeutic agents targeting essential resistant genes and constructed a gene-agent network using the DrugBank database. Finally, we identified AT-7519 as a therapeutic agent for samples with CCR resistance in GDSC dataset. Furthermore, we tentatively validated the therapeutic efficacy of AT-7519 for samples with CCR resistance using the CMap dataset that significantly more resistant genes, positively correlated with the resistant scores of CCR-9RS, were down-regulated induced by AT-7519, and the degree was gradually increased with the enhanced doses of AT-

7519. The results suggest that the patients with CCR resistance might benefit from AT-7519 or CCR treatment combined with AT-7519. We additionally explored the underlying correlation of AT-7519 and immunetherapy, and found that AT-7519 induced significant increases in the expression levels of 17 immune inhibitor/checkpoint genes (33) in CMap dataset (Student's t-test, $P < 0.05$, **Supplementary Figure S7**), such as *CTLA4* (P = 0.0002), *PDCD1* (P = 0.0298) and *IDO1* (*P* = 6.61E-06). The correlation between AT-7519 and immunotherapy has not been mentioned yet, which merits further exploration. AT-7519 is an ATP competitive CDK inhibitor with effective anti-proliferative activity and has been undertaken or are undergoing the phase I and II clinical trials in a variety of solid tumors, including colorectal cancer (34), cervical cancer (35) and ovarian cancer (36). Therefore, AT-7519 would be a practical therapeutic agent for NSCLC patients with CCR resistance, because the conventional drug in new use can avoid the time-consuming and expensive procedure of new drug development (37).

This study still had some limitations. First, as a single-center retrospective study, the predictive estimation of CCR-9RS still need to be further validated in multicenter clinical trial studies. Second, our study indicated that the NSCLC patients with CCR resistance might benefit from AT-7519 or CCR treatment combined with AT-7519, which should be further validated in the phase of clinical development for cancer treatment.

In conclusion, the radiomic signature developed in this study could be applied to identify patients with NSCLC, who might benefit from CCR treatment prior to treatment, thus allowing clinicians to monitor the progress of patients. Furthermore, AT-7519 was captured as a potentially therapeutic agent for NSCLC patients with CCR resistance, which is worth exploring in future studies.

DATA AVAILABILITY STATEMENT

The datasets for this study can be found in the NSCLC-Radiomics and NSCLC-Radiogenomics datasets (TCIA, https://www.cancerimagingarchive.net/, 2020), the Genome-wide CRISPR (https://depmap.org/portal/download/; 2019), the GDSC dataset (https://www.cancerrxgene.org, release-8.2) and the CMap dataset (https://clue.io/data/CMap2020#LINCS2020).

ETHICS STATEMENT

All data in this study source from public data sets. The patients/participants provided their written informed consent to participate in this study.

AUTHOR CONTRIBUTIONS

Experiment conceiving, LQ and JL. Manuscript writing, LQ and YL. Results interpretation, JL, LQ, and YL. Experimental design and execution, YL and HQ. Image collection, reading, and interpretation, HQ and CW. Data collection and analysis, HQ, CW, YT, JD, LL, and ZC. Manuscript editing, all authors. All authors contributed to the article and approved the submitted version.

FUNDING

This work was supported by the National Natural Science Foundation of China (no. 81872396 and 61773134) and the National Undergraduate Innovation and Entrepreneurship Training Program (no. 202110226018).

ACKNOWLEDGMENTS

The authors thank Professor Zheng Guo (College of Bioinformatics Science and Technology, Harbin Medical University, Harbin, China) for providing significant insights.

SUPPLEMENTARY MATERIAL

The Supplementary Material for this article can be found online at: https://www.frontiersin.org/articles/10.3389/fonc.2022.832343/full#supplementary-material

REFERENCES

1. Siegel RL, Miller KD, Fuchs HE, Jemal A. Cancer Statistics, 2021. *CA Cancer J Clin* (2021) 71(1):7–33. doi: 10.3322/caac.21654
2. Bade BC, Dela Cruz CS. Lung Cancer 2020: Epidemiology, Etiology, and Prevention. *Clin Chest Med* (2020) 41(1):1–24. doi: 10.1016/j.ccm.2019.10.001
3. Postmus PE, Kerr KM, Oudkerk M, Senan S, Waller DA, Vansteenkiste J, et al. Early and Locally Advanced Non-Small-Cell Lung Cancer (NSCLC): ESMO Clinical Practice Guidelines for Diagnosis, Treatment and Follow-Up. *Ann Oncol* (2017) 28(suppl_4):iv1–iv21. doi: 10.1093/annonc/mdx222
4. Hennequin C, Favaudon V, Balosso J, Marty M, Maylin C. [Radio-Chemotherapy Combinations: From Biology to Clinics]. *Bull Cancer* (1994) 81(12):1005–13.
5. O'Rourke N, Macbeth F. Is Concurrent Chemoradiation the Standard of Care for Locally Advanced Non-Small Cell Lung Cancer? A Review of Guidelines and Evidence. *Clin Oncol (R Coll Radiol)* (2010) 22(5):347–55. doi: 10.1016/j.clon.2010.03.007
6. Liu WJ, Du Y, Wen R, Yang M, Xu J. Drug Resistance to Targeted Therapeutic Strategies in non-Small Cell Lung Cancer. *Pharmacol Ther* (2020) 206:107438. doi: 10.1016/j.pharmthera.2019.107438
7. Qi L, Li Y, Qin Y, Shi G, Li T, Wang J, et al. An Individualised Signature for Predicting Response With Concordant Survival Benefit for Lung Adenocarcinoma Patients Receiving Platinum-Based Chemotherapy. *Br J Cancer* (2016) 115(12):1513–9. doi: 10.1038/bjc.2016.370
8. Van Laar RK. Genomic Signatures for Predicting Survival and Adjuvant Chemotherapy Benefit in Patients With non-Small-Cell Lung Cancer. *BMC Med Genomics* (2012) 5:30. doi: 10.1186/1755-8794-5-30
9. Yu P, Tong L, Song Y, Qu H, Chen Y. Systematic Profiling of Invasion-Related Gene Signature Predicts Prognostic Features of Lung Adenocarcinoma. *J Cell Mol Med* (2021) 25(13):6388-6402. doi: 10.1111/jcmm.16619
10. Aerts HJ, Velazquez ER, Leijenaar RT, Parmar C, Grossmann P, Carvalho S, et al. Decoding Tumour Phenotype by Noninvasive Imaging Using a Quantitative Radiomics Approach. *Nat Commun* (2014) 5:4006. doi: 10.1038/ncomms5006

11. Aerts HJ. The Potential of Radiomic-Based Phenotyping in Precision Medicine: A Review. *JAMA Oncol* (2016) 2(12):1636–42. doi: 10.1001/jamaoncol.2016.2631
12. Seijo LM, Peled N, Ajona D, Boeri M, Field JK, Sozzi G, et al. Biomarkers in Lung Cancer Screening: Achievements, Promises, and Challenges. *J Thorac Oncol* (2019) 14(3):343–57. doi: 10.1016/j.jtho.2018.11.023
13. Lambin P, Leijenaar RTH, Deist TM, Peerlings J, de Jong EEC, van Timmeren J, et al. Radiomics: The Bridge Between Medical Imaging and Personalized Medicine. *Nat Rev Clin Oncol* (2017) 14(12):749–62. doi: 10.1038/nrclinonc.2017.141
14. Trebeschi S, Drago SG, Birkbak NJ, Kurilova I, Calin AM, Delli Pizzi A, et al. Predicting Response to Cancer Immunotherapy Using Noninvasive Radiomic Biomarkers. *Ann Oncol* (2019) 30(6):998–1004. doi: 10.1093/annonc/mdz108
15. Vaidya P, Bera K, Gupta A, Wang X, Corredor G, Fu P, et al. CT Derived Radiomic Score for Predicting the Added Benefit of Adjuvant Chemotherapy Following Surgery in Stage I, II Resectable Non-Small Cell Lung Cancer: A Retrospective Multi-Cohort Study for Outcome Prediction. *Lancet Digit Health* (2020) 2(3):e116–28. doi: 10.1016/s2589-7500(20)30002-9
16. Sun C, Tian X, Liu Z, Li W, Li P, Chen J, et al. Radiomic Analysis for Pretreatment Prediction of Response to Neoadjuvant Chemotherapy in Locally Advanced Cervical Cancer: A Multicentre Study. *EBioMedicine* (2019) 46:160–9. doi: 10.1016/j.ebiom.2019.07.049
17. Xie D, Wang TT, Huang SJ, Deng JJ, Ren YJ, Yang Y, et al. Radiomics Nomogram for Prediction Disease-Free Survival and Adjuvant Chemotherapy Benefits in Patients With Resected Stage I Lung Adenocarcinoma. *Transl Lung Cancer Res* (2020) 9(4):1112–23. doi: 10.21037/tlcr-19-577
18. Bakr S, Gevaert O, Echegaray S, Ayers K, Zhou M, Shafiq M, et al. A Radiogenomic Dataset of Non-Small Cell Lung Cancer. *Sci Data* (2018) 5:180202. doi: 10.1038/sdata.2018.202
19. Meyers RM, Bryan JG, McFarland JM, Weir BA, Sizemore AE, Xu H, et al. Computational Correction of Copy Number Effect Improves Specificity of CRISPR-Cas9 Essentiality Screens in Cancer Cells. *Nat Genet* (2017) 49 (12):1779–84. doi: 10.1038/ng.3984
20. Yang W, Soares J, Greninger P, Edelman EJ, Lightfoot H, Forbes S, et al. Genomics of Drug Sensitivity in Cancer (GDSC): A Resource for Therapeutic Biomarker Discovery in Cancer Cells. *Nucleic Acids Res* (2013) 41:D955–61. doi: 10.1093/nar/gks1111
21. Lamb J, Crawford ED, Peck D, Modell JW, Blat IC, Wrobel MJ, et al. The Connectivity Map: Using Gene-Expression Signatures to Connect Small Molecules, Genes, and Disease. *Science* (2006) 313(5795):1929–35. doi: 10.1126/science.1132939
22. Zwanenburg A, Vallieres M, Abdalah MA, Aerts H, Andrearczyk V, Apte A, et al. The Image Biomarker Standardization Initiative: Standardized Quantitative Radiomics for High-Throughput Image-Based Phenotyping. *Radiology* (2020) 295(2):328–38. doi: 10.1148/radiol.2020191145
23. Tibshirani R. The Lasso Method for Variable Selection in the Cox Model. *Stat Med* (1997) 16(4):385–95. doi: 10.1002/(sici)1097-0258(19970228)16:4<385::aid-sim380>3.0.co;2-3
24. Bland JM, Altman DG. The Logrank Test. *BMJ* (2004) 328(7447):1073. doi: 10.1136/bmj.328.7447.1073
25. Harrell FEJr., Lee KL, Mark DB. Multivariable Prognostic Models: Issues in Developing Models, Evaluating Assumptions and Adequacy, and Measuring and Reducing Errors. *Stat Med* (1996) 15(4):361–87. doi: 10.1002/(SICI)1097-0258(19960229)15:4<361::AID-SIM168>3.0.CO;2-4
26. Heagerty PJ, Lumley T, Pepe MS. Time-Dependent ROC Curves for Censored Survival Data and a Diagnostic Marker. *Biometrics* (2000) 56(2):337–44. doi: 10.1111/j.0006-341x.2000.00337.x
27. Pencina MJ, D'Agostino SR RB, D'Agostino RBJr., Vasan RS. Evaluating the Added Predictive Ability of a New Marker: From Area Under the ROC Curve to Reclassification and Beyond. *Stat Med* (2008) 27(2):157–72. doi: 10.1002/sim.2929
28. Yoshihara K, Shahmoradgoli M, Martinez E, Vegesna R, Kim H, Torres-Garcia W, et al. Inferring Tumour Purity and Stromal and Immune Cell Admixture From Expression Data. *Nat Commun* (2013) 4:2612. doi: 10.1038/ncomms3612
29. Subramanian A, Tamayo P, Mootha VK, Mukherjee S, Ebert BL, Gillette MA, et al. Gene Set Enrichment Analysis: A Knowledge-Based Approach for Interpreting Genome-Wide Expression Profiles. *Proc Natl Acad Sci U S A* (2005) 102(43):15545–50. doi: 10.1073/pnas.0506580102
30. Jeong H, Kim S, Hong BJ, Lee CJ, Kim YE, Bok S, et al. Tumor-Associated Macrophages Enhance Tumor Hypoxia and Aerobic Glycolysis. *Cancer Res* (2019) 79(4):795–806. doi: 10.1158/0008-5472.CAN-18-2545
31. Ruan Y, Sun L, Hao Y, Wang L, Xu J, Zhang W, et al. Ribosomal RACK1 Promotes Chemoresistance and Growth in Human Hepatocellular Carcinoma. *J Clin Invest* (2012) 122(7):2554–66. doi: 10.1172/JCI58488
32. Ye M, Wang S, Wan T, Jiang R, Qiu Y, Pei L, et al. Combined Inhibitions of Glycolysis and AKT/autophagy Can Overcome Resistance to EGFR-Targeted Therapy of Lung Cancer. *J Cancer* (2017) 8(18):3774–84. doi: 10.7150/jca.21035
33. Ayers M, Lunceford J, Nebozhyn M, Murphy E, Loboda A, Kaufman DR, et al. IFN-Gamma-Related mRNA Profile Predicts Clinical Response to PD-1 Blockade. *J Clin Invest* (2017) 127(8):2930–40. doi: 10.1172/JCI91190
34. Do KT, O'Sullivan Coyne G, Hays JL, Supko JG, Liu SV, Beebe K, et al. Phase 1 Study of the HSP90 Inhibitor Onalespib in Combination With AT7519, a Pan-CDK Inhibitor, in Patients With Advanced Solid Tumors. *Cancer Chemother Pharmacol* (2020) 86(6):815–27. doi: 10.1007/s00280-020-04176-z
35. Xi C, Wang L, Yu J, Ye H, Cao L, Gong Z. Inhibition of Cyclin-Dependent Kinases by AT7519 is Effective to Overcome Chemoresistance in Colon and Cervical Cancer. *Biochem Biophys Res Commun* (2019) 513(3):589–93. doi: 10.1016/j.bbrc.2019.04.014
36. Wang L, Chen Y, Li H, Xu Q, Liu R. The Cyclin-Dependent Kinase Inhibitor AT7519 Augments Cisplatin's Efficacy in Ovarian Cancer *via* Multiple Oncogenic Signaling Pathways. *Fundam Clin Pharmacol* (2022) 36(1):81–8. doi: 10.1111/fcp.12709
37. Mandal R, Becker S, Strebhardt K. Targeting CDK9 for Anti-Cancer Therapeutics. *Cancers (Basel)* (2021) 13(9):2181. doi: 10.3390/cancers13092181

Conflict of Interest: The authors declare that the research was conducted in the absence of any commercial or financial relationships that could be construed as a potential conflict of interest.

frontiers | Frontiers in Oncology

TYPE Original Research
PUBLISHED 13 September 2022
DOI 10.3389/fonc.2022.774816

OPEN ACCESS

EDITED BY
Nicola Silvestris,
University of Messina, Italy

REVIEWED BY
Dat Vo,
University of Texas Southwestern Medical Center, United States
Junqiang Chen,
Fujian Cancer Hospital and Fujian Medical University Cancer Hospital, China

*CORRESPONDENCE
Fen Zhao
zhaofen1029@126.com
Minghuan Li
sdlmh2014@163.com

†These authors have contributed equally to this work

SPECIALTY SECTION
This article was submitted to Radiation Oncology, a section of the journal Frontiers in Oncology

RECEIVED 13 September 2021
ACCEPTED 15 August 2022
PUBLISHED 13 September 2022

CITATION
Zhu L, Zhao Z, Liu A, Wang X, Geng X, Nie Y, Zhao F and Li M (2022) Lymph node metastasis is not associated with survival in patients with clinical stage T4 esophageal squamous cell carcinoma undergoing definitive radiotherapy or chemoradiotherapy. *Front. Oncol.* 12:774816. doi: 10.3389/fonc.2022.774816

Lymph node metastasis is not associated with survival in patients with clinical stage T4 esophageal squamous cell carcinoma undergoing definitive radiotherapy or chemoradiotherapy

Liqiong Zhu[1,2,3†], Zongxing Zhao[3†], Ao Liu[2,4], Xin Wang[5], Xiaotao Geng[6], Yu Nie[1,2], Fen Zhao[2*†] and Minghuan Li[2*†]

[1]Department of Clinical Medicine, Shandong First Medical University and Shandong Academy of Medical Sciences, Jinan, China, [2]Department of Radiation Oncology, Shandong Cancer Hospital and Institute, Shandong First Medical University and Shandong Academy of Medical Sciences, Jinan, China, [3]Department of Radiation Oncology, Liaocheng People's Hospital, Liaocheng, China, [4]School of Medicine, Shandong University, Jinan, China, [5]National Cancer Center/Cancer Hospital, Chinese Academy of Medical Sciences (CAMS) and Peking Union Medical College (PUMC), Beijing, China, [6]Department of Radiation Oncology, Weifang People's Hospital, Weifang, China

Background: Clinical T4 stage (cT4) esophageal tumors are difficult to be surgically resected, and definitive radiotherapy (RT) or chemoradiotherapy (dCRT) remains the main treatment. The study aims to analyze the association between the status of lymph node (LN) metastasis and survival outcomes in the cT4 stage esophageal squamous cell carcinoma (ESCC) patients that underwent treatment with dCRT or RT.

Methods: This retrospective study analyzed the clinical data of 555 ESCC patients treated with dCRT or RT at the Shandong Cancer Hospital and the Liaocheng People's Hospital from 2010 to 2017. Kaplan–Meier and Cox regression analyses was performed to determine the relationship between LN metastasis and survival outcomes of cT4 and non-cT4 ESCC patients. The chi-square test was used to evaluate the differences in the local and distal recurrence patterns in the ESCC patients belonging to various clinical T stages.

Results: The 3-year survival rates for patients with non-cT4 ESCC and cT4 ESCC were 47.9% and 30.8%, respectively. The overall survival (OS) and progression-free survival (PFS) rates were strongly associated with the status of LN metastasis in the entire cohort (all $P < 0.001$) and the non-cT4 group (all $P < 0.001$) but not in the cT4 group. The local recurrence rates were 60.7% for the cT4 ESCC patients and 45.1% for the non-cT4 ESCC patients ($P < 0.001$). Multivariate analysis showed that clinical N stage ($P = 0.002$), LN size ($P = 0.007$), and abdominal LN involvement ($P = 0.011$) were independent

predictors of favorable OS in the non-cT4 group. However, clinical N stage (P = 0.824), LN size (P = 0.383), and abdominal LN involvement (P = 0.337) did not show any significant correlation with OS in the cT4 ESCC patients.

Conclusions: Our data demonstrated that the status of LN metastasis did not correlate with OS in the cT4 ESCC patients that received dCRT or RT. Furthermore, the prevalence of local recurrence was higher in the cT4 ESCC patients.

KEYWORDS

esophageal carcinoma, cT4 disease, tumor recurrence, prognosis, patient survival

Introduction

Esophageal carcinoma (EC) is the sixth leading cause of cancer-related mortality worldwide (1). Esophageal squamous cell carcinoma (ESCC) is the main EC type in Asia and South America, whereas esophageal adenocarcinoma is the most frequent type of EC in Europe and the USA (2). The low survival rate of ESCC patients is primarily attributed to diagnosis in the advanced stages (3). The clinical T4 (cT4) EC tumors are characterized by tumor invasion into the adjacent anatomical structures. Despite significant advances in the surgical techniques, cT4 ESCC is considered inoperable. Currently, definitive chemoradiotherapy (dCRT) or radiotherapy (RT) is the standard therapy for ESCC patients who refuse surgery or are ineligible for surgical resection (4, 5). It is a clinical challenge to determine the clinical target volume (CTV) of elective nodal irradiation (ENI) or involved-field radiotherapy (IFRT) Furthermore, the optimal RT strategy for EC patients at different clinical T stages is unclear.

The number of metastatic lymph node (LN) is associated with survival of ESCC patients that have undergone surgery (6, 7). However, the effect of LN metastasis status on the survival for the non-surgical ESCC patients remains unclear, especially those in the cT4 stage. In order to provide clinical information to individualized RT strategies for different cT stages, we investigated the relationship between the status of LN metastasis and the survival outcomes in the cT4 and non-cT4 ESCC patients.

Methods

Patients

The clinical data of 555 patients with ESCC without distant metastasis who were treated with dCRT or RT at the Shandong Cancer Hospital and the Liaocheng People's Hospital between April 2010 and December 2017 was analyzed retrospectively. The pre-treatment staging was based on data from the physical examinations, barium swallow test, tissue biopsy, and imaging data from endoscopic ultrasonography, contrast-enhanced computed tomography (CT), and/or 18F-fluorodeoxyglucose imaging (18F-FDG). Tumor staging was performed by three experienced radiologists based on the guidelines from the American Joint Committee on Cancer (AJCC) Cancer Staging Manual (Eighth edition) (8). This study included ESCC patients with the cT2–4 stages that were classified into the following three groups: (1) Total (cT4+non-cT4) group; (2) cT4 group, and (3) non-cT4 group. Patients with metastatic LNs > 2 cm showed higher rates of tumor recurrence and poor treatment response (9). The extent of LN involvement was classified into three groups based on the number of anatomical positions (cervical, thoracic, and abdomen) involved. Then, the relationship between patient survival and the status of LN metastasis was analyzed. The status of LN metastasis was based on multiple characteristics, namely, (1) the number of metastatic LNs: cN0, cN1, cN2 and cN3; (2) the extent of LN metastasis: cN0, involvement of one anatomical region, involvement of two anatomical regions, and involvement of three anatomical regions; (3) LN size: cN0, ≤2 cm, and >2 cm; (4) abdominal LN involvement: cN0, with or without abdominal LN involvement. This study was approved by the Medical Ethics Committees of the Shandong Cancer Hospital and the Liaocheng People's Hospital.

Criteria for LN metastasis and cT4 stage

In this study, the cT4a stage was defined as tumor invasion into the pleura, pericardium, azygos vein, diaphragm, or the peritoneum. The cT4b stage was defined as tumor invasion into additional surrounding structures such as the aorta, the vertebral

body, and the trachea (10). Patients with cT4 stage demonstrated loss of fat plane between the primary tumor and the adjacent mediastinal structures (11). Tracheobronchial invasion was defined as a tumor protrusion into the lumen of the trachea or the bronchus on the CT scans. Aortic invasion was defined as > 90 degree contact between the aorta and the tumor or loss of fat plane in the triangular space between the esophagus, spine, and the aorta on the CT scans (12).

Regional LNs were defined as those in the periesophageal tissue from the upper esophageal sphincter to the adventitia of the celiac artery as previously described (10). LN metastasis was confirmed as positive if the short axis diameter of the LNs was >10 mm or if the short axis diameter of the paraesophageal, tracheoesophageal sulcus, pericardial angle, or the abdominal LNs was > 5 mm in the CT or magnetic resonance imaging (MRI) scans. LNs were considered as metastatic if they demonstrated a round shape, hypoechoic pattern, and visible borders in the endoscopic ultrasonography, or demonstrated high maximum standardized FDG uptake. The diagnostic accuracy of CT in the cT4 esophageal cancer patients was 80%. In this study, CT examination was used to diagnose all the patients with cT4 ESCC.

Treatment details

The gross tumor volume (GTV) was delineated on the 3-dimensional (3D) planning system by the supervising radiation oncologist using data from the CT/MRI fusion scans, diagnostic CT scans, and endoscopic ultrasonography scans. The GTV included all the visible macroscopic esophageal lesions and the clinically positive LNs. The CTV included 3–5 cm cephalic and caudal margins of the primary tumor, 0.8–1.0 cm radial margins, and the regional high-risk LNs. The CTV for IFI included the clinically positive lymph nodes with metastasis and the CTV for ENI included regional high-risk LNs. Most patients were treated with ENI in our study. The organs at risk, including the heart, spinal cord, and the lungs, were outlined. All the patients received a total dose of 50.4–66 Gy in 28–33 fractions (1.8/2.0-Gy fractions once daily, 5 days a week). All the patients received 3D-conformal or intensity-modulated RT. In this study, 309 patients received concurrent platinum-based chemotherapy and 246 patients received definitive RT alone due to advanced age, complications, or refusal to receive chemotherapy. All the patients underwent dCRT received at least 2 cycles of chemotherapy (a combination of platinum and 5-fluorouracil or platinum and taxanes or other commonly used protocols).

Follow up

The patients were examined 1-month after treatment completion, every 3 months for the first 2 years, and every 6 months until loss of follow-up or death. Each follow-up assessment included a physical examination, blood test, esophageal endoscopy, enhanced CT scans, and the barium swallow test. The patients who missed their follow-up schedule were sent reminders by phone. Patients with suspected recurrence were subjected to histology or cytology testing. Local recurrence was defined as recurring tumor at the primary tumor site or the regional LNs. Recurrence at any other site was defined as distant recurrence. Overall survival (OS) and progression-free survival (PFS) were calculated from the day of pathologic diagnosis until an event or censorship.

Statistical analysis

The statistical analysis in this study was performed using the SPSS version 24.0 software (SPSS, Chicago, IL, USA). Survival analysis was performed using the Kaplan–Meier method. The chi-square test was used to compare the differences in local recurrence and distant recurrence between the cT4 and non-cT4 patients with ESCC. Log-rank tests and Cox proportional risk regression models were used to assess the relationship between patient survival and the clinical factors. A two-sided p-value <0.05 was considered statistically significant.

Results

Patient characteristics

This retrospective study analyzed the clinical data of 555 ESCC patients that were treated between April 2010 and December 2017 at the Shandong Cancer Hospital (n=406) and the Liaocheng People's Hospital (n=149). Among these, 107 (19.3%) patients were diagnosed with the cT4 stage disease and 448 (80.7%) patients were diagnosed with the non-cT4 stage disease. The median follow-up time was 41.5 months. The median age at diagnosis was 66 years (range: 38–90 years) and included 421 (75.9%) males and 134 (24.1%) females. Furthermore, 309 (55.7%) patients received dCRT and 246 (44.3%) patients received definitive RT alone. LN metastasis was diagnosed in 394 (71.0%) patients. Moreover, 161 (29.0%), 211 (38.0%), 152 (27.4%), and 31 (5.6%) patients were classified as cN0, cN1, cN2, and cN3, respectively. The detailed characteristics of the included patients are listed in Table 1.

10.3389/fonc.2022.774816

TABLE 1 Total group (cT2-4) patients' characteristics of prognostic factors.

Variables	Total Group (T2/T3/T4)	non-cT4 Group (T2/T3)	cT4 Group	P Value
All	555	448 (80.7%)	107 (19.3%)	
Age (years)				**0.020**
≤60 years	143 (25.8%)	106 (23.7%)	37 (34.5%)	
> 60 years	412 (74.2%)	342 (76.3%)	70 (65.5%)	
Sex, n (%)				0.142
Female	134 (24.1%)	114 (25.4%)	20 (18.6%)	
Male	421 (75.9%)	334 (74.6%)	87 (81.4%)	
Smoking, n (%)				0.879
Never	263 (47.4%)	213 (47.5%)	50 (46.7%)	
Ever	292 (52.6%)	235 (52.5%)	57 (53.3%)	
Drinking, n (%)				**0.031**
Never	311 (56.0%)	261 (58.3%)	50 (46.7%)	
Ever	244 (44.0%)	187 (41.7%)	57 (53.2%)	
Tumor location, n (%)				0.762
Cervical Upper	243 (43.8%)	199 (44.4%)	44 (41.1%)	
Middle	190 (34.2%)	153 (34.2%)	37 (34.6%)	
Lower	122 (22.0%)	96 (21.4%)	26 (24.3%)	
Treatment regimen, n (%)				0.757
RT alone	246 (44.3%)	200 (44.6%)	46 (42.9%)	
CRT	309 (55.7%)	248 (55.3%)	61 (57.1%)	
RT dose, n (%)				**0.044**
≤60 Gy	397 (71.5%)	312 (69.6%)	85 (79.5%)	
> 60 Gy	158 (28.5%)	136 (30.3%)	22 (20.5%)	
Clinical cN				0.380
cN0	161 (29.0%)	135 (30.1%)	26 (24.3%)	
cN1	211 (38.0%)	168 (37.5%)	43 (40.2%)	
cN2	152 (27.4%)	123 (27.5%)	29 (27.1%)	
cN3	31 (5.6%)	22 (4.9%)	9 (8.4%)	
Extent of LNs				0.667
0	161 (29.0%)	135 (30.1%)	26 (24.3%)	
1 region	258 (46.5%)	202 (45.1%)	54 (50.4%)	
2 regions	112 (20.2%)	90 (20.1%)	22 (20.6%)	
3 regions	24 (4.3%)	21 (4.7%)	5 (4.7%)	
Size of LNs				0.104
0	161 (29.0%)	135 (30.1%)	26 (24.3%)	
≤ 2 cm	329 (59.3%)	268 (59.8%)	63 (58.9%)	
>2 cm	65 (11.7%)	45 (10.1%)	18 (16.8%)	
Abdominal region-involved				0.490
N0	161 (29.0%)	135 (30.2%)	26 (24.3%)	
Without	322 (59.0%)	255 (56.9%)	66 (61.7%)	
With	72 (13.0%)	58 (12.9%)	15 (14.0%)	

LNs, lymph nodes; RT, chemoradiotherapy; CRT, chemoradiotherapy; cT4, clinical T4; Bold values indicates a statistically difference in statistical analysis.

Recurrence patterns in cT4 ESCC patients compared to the non-cT4 ESCC patients

The follow-up showed that the prevalence of local recurrence was 48.1% (267 cases), the prevalence of distant recurrence was 22.8% (127 cases) in all the included ESCC patients, and 7.6% (42 cases) both in. The relationship between the clinical T stages and the tumor recurrence patterns is shown in Table 2. Local recurrence was significantly higher in patients with cT4 disease compared to those with non-cT4 ESCC (60.7% vs. 45.1%; P <0.001). However, distant recurrence rates were

TABLE 2 Correlation between cT stage and patterns of failure.

Patterns of failure	cT4	non-cT4	P value
LR			**<0.001**
yes	65 (60.7%)	202 (45.1%)	
no	42 (39.3%)	246 (54.9%)	
M			0.368
yes	28 (26.2%)	99 (22.1%)	
no	79 (73.8%)	349 (77.9%)	

LR, local recurrence; M, metastases; cT4, clinical T4; Bold values indicates a statistically difference in statistical analysis.

statistically insignificant between cT4 ESCC and non-cT4 ESCC patients (26.2% vs. 22.1%; $P = 0.368$).

Survival

The 1-, 3-, and 5-year OS rates for all the included patients in this study were 80.9%, 44.8%, and 33.3%, respectively. The median survival time was 30.2 months (range: 1.7-82.2 months). The 3-year OS rates in all patients with cN0, cN1, cN2, and cN3 disease were 56.9%, 46.2%, 37.8%, and 0%, respectively. The median OS rates in all patients with cN0, cN1, cN2, and cN3 disease were 46.0, 31.0, 26.0, and 11.0 months, respectively.

Effect of lymph node metastasis status on the survival outcomes

Kaplan–Meier survival analysis demonstrated that factors such as N stage (cN0, cN1, cN2 and cN3), extent of LN metastasis (cN0, 1 region, 2 regions, and 3 regions), size of the LNs (cN0, 2cm, and ≥ 2cm), and abdominal LN metastasis (cN0, with or without abdominal involvement) showed significant correlation with OS and PFS in the total (cT4+non-cT4) group (all $P < 0.001$; Figure 1).

We then investigated the effect of the LN metastasis status on the survival outcomes in different clinical T stages. The advanced N stage, larger LNs, extent of LN metastasis, and presence of abdominal LN metastasis showed significant correlation with poor OS and PFS in the non-cT4 group (all $P < 0.001$; Figure 2).

However, in patients with cT4 disease, OS and PFS did not show significant association with the N stage ($P = 0.059$ and $P = 0.121$; Figures 3A, B), LN size ($P = 0.430$ and $P = 0.650$; Figures 3E, F), and the abdominal LN involvement ($P = 0.399$ and $P = 0.547$; Figures 3G, H). Although the extent of LN metastasis showed a significant association with the OS of cT4 group patients ($P = 0.034$; Figure 3C), the Kaplan-Meier curve analysis showed the survival curves of patients in cN0, 1, 2, and 3 anatomic regions were crossed. Furthermore, there was no significant association between the extent of LN metastasis and

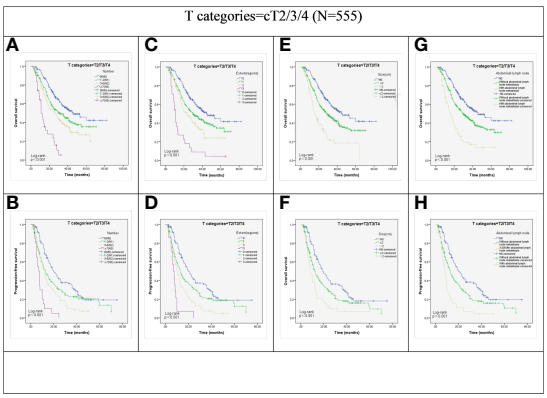

FIGURE 1
Kaplan-Meier representations of OS and PFS with respect to the N stage **(A, B)**, lymph node extent **(C, D)**, lymph node size **(E, F)**, and abdominal lymph node **(G, H)** in cT2/3/4 patients (N=555). P values were all less than 0.001.

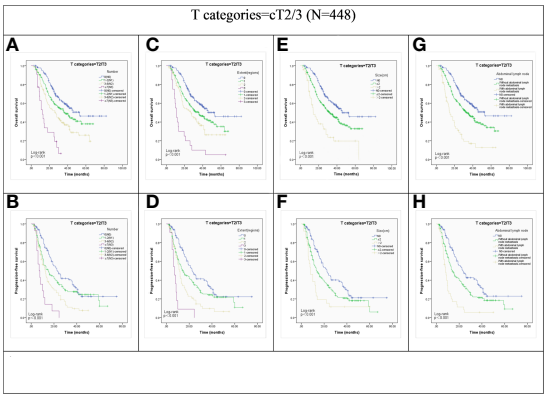

FIGURE 2
Kaplan-Meier representations of OS and PFS with respect to the N stage **(A, B)**, lymph node extent **(C, D)**, lymph node size **(E, F)**, and abdominal lymph node **(G, H)** in cT2/3 patients (N=448). P values were all less than 0.001.

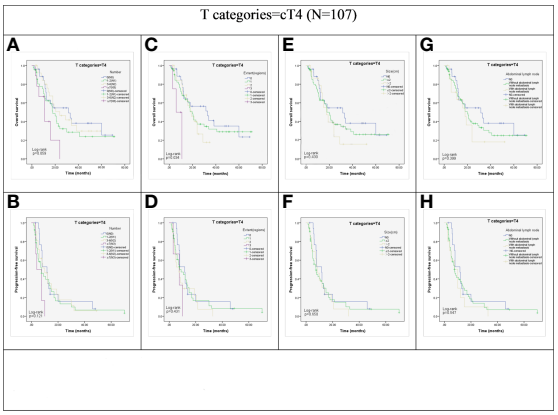

FIGURE 3
Kaplan-Meier representations of OS and PFS with respect to the N stage ((**A**) p=0.059; (**B**) p=0.121), lymph node extent (**C**, p=0.034; (**D**) p=0.431), lymph node size ((**E**), p=0.430; (**F**), p=0.650), and abdominal lymph node ((**G**), p=0.399; (**H**), p=0.547) in cT4 patients (N=107).

progression-free survival (PFS) in the cT4 group (P = 0.431; Figure 3D).

Prognostic factors

Univariate analysis was performed to identify clinical factors associated with prognostic prediction in the total (cT4+non-cT4) group, the non-cT4 group and the cT4 groups. Then, factors with P-values < 0.2 were included in the multivariate analysis and the results are shown in Table 3. Of note, the lymph node metastasis status as a prognostic factor differed among the total group, non-cT4 and cT4 ESCC group. The clinical N stage (hazard ratio [HR], 1.534; 95% CI, 1.189–1.980; P = 0.001), LN ≥2 cm (HR, 1.502; 95% CI, 1.060–2.129; P = 0.022), and abdominal LN metastasis (HR, 1.462; 95% CI, 1.026–2.085; P = 0.036) were independent predictors of favorable OS for the total group. Furthermore, clinical N stage (HR, 1.599; 95% CI, 1.195–2.140; P = 0.002), LN ≥2 cm (HR, 1.737; 95% CI, 1.167–2.587; P = 0.007), and abdominal LN involvement (HR, 1.681; 95% CI, 1.126–2.512; P = 0.011) were independent predictors of favorable OS in patients with non-cT4 disease. However, none of these node-related factors were independent predictors of OS in patients with cT4 ESCC.

Discussion

This study investigated the association between LN metastasis and survival outcomes in ESCC patients who underwent RT and the prognostic differences between ESCC patients belonging to the cT4 and non-cT4 stages. The study cohort of ESCC patients was categorized into sub-groups based on multiple criteria such as the number of metastatic LNs according to the AJCC recommendations, the size of LNs, and others. The results of this study highlighted significant differences in the survival outcomes of ESCC patients based on the metastatic LN status.

Tumor staging is essential for determining the optimal treatment strategy for the EC patients. Previous studies reported the association between the number of metastatic LNs and the survival outcomes of ESCC patients that underwent esophagectomy (13, 14). This study investigated the correlation between the number of metastatic LNs and the survival outcomes of ESCC patients receiving RT according to the AJCC guidelines for EC. The results showed significant differences in the survival outcomes between the cT4 and the non-cT4 ESCC patients. Our data demonstrated that the advanced N stage non-cT4 patients were associated with worse OS and PFS. However, we did not observe the association between N stages and the survival outcomes in the cT4 ESCC patients. Furthermore, the prognostic value of N staging based on the number of metastatic LNs is a matter of debate for EC patients that underwent surgery (15–17). Therefore, in the clinic, other LN staging strategies have been used for the ESCC patients.

The size of LNs is one of the factors used for N staging in the non-surgically treated patients with head and neck tumors. It has been demonstrated that the size of LNs correlates with treatment outcomes and prognostic prediction in EC patients treated surgically (18–20). Furthermore, in our previous study regarding ESCC patients treated with RT, the objective response rates (ORRs) of patients with metastatic LNs > 2cm were significantly worse compared to those with metastatic LNs ≤ 2 cm (P = 0.038) (9). In ESCC, the size of LNs shows significant prognostic value and positive correlation with the extra-nodal spread (21, 22). Therefore, we evaluated the relationship between LN metastasis status and the survival outcomes using the size of LNs in patients with ESCC at different cT stages as a parameter. We observed significant differences in the OS and PFS rates of patients belonging to the N0, LN ≤ 2cm, LN > 2cm categories in the non-cT4 ESCC group. However, it was not observed that the correlation between the size of LNs and the survival outcomes had significant differences in the cT4 ESCC group.

The frequency of cross-regional LN metastasis is high in ESCC because of the abundant lymphatic channels in the lamina propria and submucosa of the esophagus. Several studies have investigated the association between the anatomical regions of LN metastasis and the survival outcomes of patients with ESCC, and recommend the extent of lymph node metastases as the basis for N staging (15, 23, 24). Our results demonstrated that the OS and PFS rates varied significantly in regard to the various extent (1,2,3 anatomical regions involved) of LN metastasis in the non-cT4 group. However, the various extent of LN

10.3389/fonc.2022.774816

TABLE 3 Cox regression of OS for total group (cT2/3/4), non-T4 group(cT2/3) and cT4 group ESCC patients.

Variables	Total Group (cT2/T3/T4)				non-T4 Group (cT2/T3)				cT4 Group			
	Univariate analysis		Multivariate analysis		Univariate analysis		Multivariate analysis		Univariate analysis		Multivariate analysis	
	HR (95% CI)	P value	HR (95% CI)	P value	HR (95% CI)	P value	HR (95% CI)	P value	HR (95% CI)	P value	HR (95% CI)	P value
Sex												
Female	1				1				1			
Male	1.342 (1.015-1.774)	**0.039**		NS	1.272 (0.937-1.727)	**0.123**		NS	1.478 (0.731-2.989)	0.277		
Age												
≤60 years	1				1				1			
> 60 years	1.073 (0.828-1.390)	0.594			1.159 (0.856-1.571)	0.340			0.999 (0.602-1.658)	0.996		
Smoking												
Never	1				1				1		1	
Ever	1.348 (1.073-1.694)	**0.010**		NS	1.239 (0.958-1.603)	**0.102**		**NS**	1.829 (1.107-3.022)	**0.018**	1.829 (1.107-3.022)	**0.018**
Drinking												
Never	1		1		1		1		1			
Ever	1.440 (1.149-1.803)	**0.002**	1.424 (1.134-1.789)	**0.002**	1.315 (1.019-1.698)	**0.035**	1.334(1.031-1.726)	**0.028**	1.736 (1.049-2.872)	**0.032**		**NS**
Tumor location		**<0.001**		**0.001**		**<0.001**		**0.007**		**0.105**		**NS**
Cervical/ Upper	1		1		1		1		1			
Middle	1.483 (1.146-1.945)	**0.003**	1.391 (1.063-1.820)	**0.016**	1.514 (1.123-2.040)	**0.006**	1.362 (1.003-1.848)	**0.048**	1.347 (0.759-2.391)	0.308		
Lower	2.238 (1.681-2.980)	**<0.001**	1.818 (1.323-2.499)	**<0.001**	2.292 (1.658-3.169)	**<0.001**	1.774 (1.240-2.540)	**0.002**	1.950 (1.053-3.611)	**0.034**		
RT dose												
≤60 Gy	1				1				1			
>60 Gy	0.723 (0.557-0.939)	**0.015**		NS	0.770 (0.578-1.025)	**0.073**		NS	0.624 (0.318-1.225)	**0.171**		**NS**
Treatment regimen												
RT alone	1		1		1		1		1			
CRT	0.854(0.680-1.071)	**0.171**	0.744 (0.589-0.940)	**0.013**	0.806 (0.624-1.041)	**0.099**	0.689(0.528-0.898)	**0.006**	0.989 (0.599-1.634)	0.967		
Clinical N stage												
cN0-1	1		1		1		1		1			
cN2-3	1.733(1.324-2.267)	**<0.001**	1.534(1.189-1.980)	**0.001**	1.911(1.474-2.276)	**<0.001**	1.599(1.195-2.140)	**0.002**	1.060(0.637-1.762)	0.824		
Extent of LNs												
0-1 region	1				1				1			
2-3 regions	1.791(1.403-2.302)	**<0.001**		NS	1.871(1.419-2.468)	**<0.001**		NS	1.506(0.859-2.642)	**0.153**		**NS**
Size of LNs												
≤ 2 cm	1		1		1		1		1			
>2 cm	2.160(1.566-2.979)	**<0.001**	1.502(1.060-2.129)	**0.022**	2.415(1.668-3.495)	**<0.001**	1.737(1.167-2.587)	**0.007**	1.336(0.696-2.564)	0.383		
Abdominal region-involved												

(Continued)

TABLE 3 Continued

Variables	Total Group (cT2/T3/T4)				non-T4 Group (cT2/T3)				cT4 Group			
	Univariate analysis		Multivariate analysis		Univariate analysis		Multivariate analysis		Univariate analysis		Multivariate analysis	
	HR (95% CI)	P value	HR (95% CI)	P value	HR (95% CI)	P value	HR (95% CI)	P value	HR (95% CI)	P value	HR (95% CI)	P value
NO	1		1		1		1		1			
YES	2.411(1.784-3.258)	**<0.001**	1.462(1.026-2.085)	**0.036**	2.753(1.967-3.853)	**<0.001**	1.681(1.126-2.512)	**0.011**	1.392(0.709-2.737)	0.337		

LNs, lymph nodes; CI, confidence interval; CRT, chemoradiotherapy; RT, radiotherapy; HR, hazard ratio; NS, non-significant. Bold values indicate a statistically difference in statistical analysis.

metastasis was not associated with survival prediction in the ESCC patients of the cT4 group.

Abdominal LN metastasis was considered as distant metastasis in the 6th edition of the AJCC/UICC TNM staging guidelines and as regional metastasis in the 7th and 8th editions of AJCC/UICC TNM staging guidelines. Rutegard et al. (25) retrospectively analyzed 446 patients with stage III or IV EC that underwent surgical resection and demonstrated that the disease-specific mortality and OS rates of patients with celiac LN metastasis were comparable to those of patients with metastasis to the distant organs. Therefore, in this study, we stratified the ESCC patients into groups according to the presence of metastatic lesions in the abdominal LNs, which included LNs in the paracardial, left gastric artery, common hepatic artery, splenic artery, and the celiac trunk. Our results showed significant differences in the OS and PFS rates between non-cT4 patients with or without abdominal LN metastasis (all $P < 0.001$), but the differences in OS ($P = 0.399$) and PFS ($P = 0.547$) rates were not statistically significant between cT4 patients with or without abdominal LN metastasis.

Local recurrence was predominant among the ESCC patients in this study. Moreover, the prevalence of local recurrence was significantly higher in patients with cT4 ESCC compared to the patients with non-cT4 ESCC. Welsh et al. (26) reported that the T stage of patients with EC undergoing dCRT was associated with local control, and the local control rate in patients with T3 and T4 tumors was significantly lower than that of patients with T1 and T2 tumors (25% vs. 71%). Another study also confirmed more frequent local recurrence at the primary tumor site compared to the LNs in the EC patients receiving dCRT (27). Our data was consistent with results of the previously reported findings (26–28) and showed that local recurrence was more frequent than distant recurrence (outfield of the planning target volume recurrence) in EC patients treated with RT, and advanced T-stages were associated with poor local tumor control. Our preliminary data showed that the median PFS for primary progression in the cT4 ESCC patients was 7.63 months (range: 1.5-70 months) and 8.5 months (range: 2–32.87 months) for patients with distant metastasis. This suggested that local recurrence often preceded distant recurrence among the cT4 ESCC patients treated with RT. The effect of T stage may mask the impact of LN metastasis on the survival outcomes of the cT4 ESCC patients. Therefore, local control should be prioritized over irradiating distant LNs in such patients. Hence, local salvage treatments such as re-RT or salvage esophagectomy may be beneficial for ESCC patients with advanced T staging.

The CTV coverage for elective nodal irradiation (ENI) and involved-field radiotherapy (IFRT) is not clear in the advanced T-stage ESCC patients. Several studies have reported that ENI prevented regional LN recurrence but did not improve OS and local control of ESCC patients (29–31). Moreover, regional LN failure was not common in ESCC patients that received ENI or IFRT (32, 33). Our findings showed that the pre-treatment LN metastasis status did not correlate with the survival outcomes of cT4 ESCC patients. Therefore, we postulate that prophylactic LN irradiation may not significantly improve survival. Furthermore, IFRT was associated with reduced lung, esophagus and hematological toxicity, thereby enabling a higher number of EC patients to tolerate RT and chemotherapy (29). Because of the advanced disease stage and high local recurrence rates, involved-field irradiation (IFI) may be more beneficial for the cT4 ESCC patients.

This study has several limitations. First, this was a retrospective study that included patients with significantly different treatment plans including radiation doses and chemotherapy regimens. Second, LN metastasis in the study cohort was assessed by the non-invasive pre-processing staging methods such as endoscopic ultrasonography (EUS), computed tomography (CT), and fluorodeoxyglucose-positron emission tomography (FDG-PET) rather than histopathology methods. Third, the competitive risk model may be better at estimating the impacts of local and distal recurrence on LN metastasis and survival.

Conclusions

The status of LN metastasis characteristics such as the number of metastatic LNs, size of the metastatic LNs, and

abdominal LN metastasis was associated with the survival prediction of patients with non-cT4 ESCC who have received radiotherapy. However, LN metastasis status was not associated with the survival outcomes of patients with cT4 ESCC. Our results suggested that the treatment strategy for cT4 ESCC patients may be different from the treatment strategy for the non-cT4 ESCC patients and may require strengthening the local control of the primary lesions for cT4 ESCC patients. Future prospective and randomized clinical trials are required to validate the feasibility and efficacy of high radiation doses and IFRT in patients with non-cT4 ESCC.

Data availability statement

The original contributions presented in the study are included in the article/supplementary material. Further inquiries can be directed to the corresponding authors.

Author contributions

LZ, ZZ, FZ and ML analyzed the data and drafted the manuscript. AL, XW, XG, and YN participated in data collection. All authors read and approved the final manuscript.

Funding

This study was supported by the Natural Science Foundation of China (Grant No NSFC 82172677).

Acknowledgments

The authors would such as to express their great thanks to the Natural Science Foundation of China.

Conflict of interest

The authors declare that the research was conducted in the absence of any commercial or financial relationships that could be construed as a potential conflict of interest.

Publisher's note

References

1. Siegel RL, Miller KD, Jemal A. Cancer statistics, 2020. *CA Cancer J Clin* (2020) 70(1):7–30. doi: 10.3322/caac.21590

2. Edgren G, Adami HO, Weiderpass E, Nyren O. A global assessment of the oesophageal adenocarcinoma epidemic. *Gut* (2013) 62(10):1406–14. doi: 10.1136/gutjnl-2012-302412

3. Ferlay J, Soerjomataram I, Dikshit R, Eser S, Mathers C, Rebelo M, et al. Cancer incidence and mortality worldwide: sources, methods and major patterns in GLOBOCAN 2012. *Int J Cancer* (2015) 136(5):E359–86. doi: 10.1002/ijc.29210

4. Ajani JA, D'Amico TA, Almhanna K, Bentrem DJ, Besh S, Chao J, et al. Nccn guidelines insights: Esophageal and esophagogastric junction cancers, version 1.2015. *J Natl Compr Canc Netw* (2015) 13:194–227. doi: 10.6004/jnccn.2015.0028

5. Kuwano H, Nishimura Y, Oyama T, Kato H, Kitagawa Y, Kusano M, et al. Guidelines for diagnosis and treatment of carcinoma of the esophagus April 2012 edited by the Japan esophageal society. *Esophagus* (2015) 12:1–30. doi: 10.1007/s10388-014-0465-1

6. Ohtsu A, Boku N, Muro K, Chin K, Muto M, Yoshida S, et al. Definitive chemoradiotherapy for T4 and/or M1 lymph node squamous cell carcinoma of the esophagus. *J Clin Oncol* (1999) 17:2915–21. doi: 10.1200/jco.1999.17.9.2915

7. Jingu K, Umezawa R, Matsushita H, Sugawara T, Kubozono M, Yamamoto T, et al. Chemoradiotherapy for T4 and/or M1 lymph node esophageal cancer: experience since 2000 at a high-volume center in Japan. *Int J Clin Oncol* (2015) 21(2):276–82. doi: 10.1007/s10147-015-0896-2

8. Rice TW, Patil DT, Blackstone EH. 8th edition AJCC/UICC staging of cancers of the esophagus and esophagogastric junction: application to clinical practice. *Ann Cardiothoracic Surg* (2017) 6(2):119–30. doi: 10.21037/acs.2017.03.14

9. Zhao Z, Zhang Y, Wang X, Wang P, Geng X, Zhu L, et al. The prognostic significance of metastatic nodal size in non-surgical patients with esophageal squamous cell carcinoma. *Front Oncol* (2020) 10:523. doi: 10.3389/fonc.2020.00523

10. Donohoe CL, Phillips AW. Cancer of the esophagus and esophagogastric junction: an 8(th) edition staging primer. *J Thorac Dis* (2017) 9(3):E282–E4. doi: 10.21037/jtd.2017.03.39

11. Kim TJ, Kim HY, Lee KW, Kim MS. Multimodality assessment of esophageal cancer: preoperative staging and monitoring of response to therapy. *Radiographics* (2009) 29:403–21. doi: 10.1148/rg.292085106

12. Makino T, Yamasaki M, Miyazaki Y, Wada N, Takahashi T, Kurokawa Y, et al. Utility of initial induction chemotherapy with 5-fluorouracil, cisplatin, and docetaxel (DCF) for T4 esophageal cancer: a propensity score-matched analysis. *Dis Esophagus* (2018) 31(4). doi: 10.1093/dote/dox130

13. Mariette C, Piessen G, Briez N, Triboulet JP. The number of metastatic lymph nodes and the ratio between metastatic and examined lymph nodes are independent prognostic factors in esophageal cancer regardless of neoadjuvant chemoradiation or lymphadenectomy extent. *Ann Surg* (2008) 247(2):365–71. doi: 10.1097/SLA.0b013e31815aaadf

14. Gu Y, Swisher SG, Ajani JA, Correa AM, Hofstetter WL, Liao Z, et al. The number of lymph nodes with metastasis predicts survival in patients with esophageal or esophagogastric junction adenocarcinoma who receive preoperative chemoradiation. *Cancer* (2006) 106(5):1017–25. doi: 10.1002/cncr.21693

15. Peng J, Wang WP, Dong T, Cai J, Ni PZ, Chen LQ. Refining the nodal staging for esophageal squamous cell carcinoma based on lymph node stations. *Ann Thorac Surg* (2016) 101(1):280–6. doi: 10.1016/j.athoracsur.2015.06.081

16. Yamasaki M, Miyata H, Miyazaki Y, Takahashi T, Kurokawa Y, Nakajima K, et al. Evaluation of the nodal status in the 7th edition of the UICC-TNM classification for esophageal squamous cell carcinoma: proposed modifications for improved survival stratification : impact of lymph node metastases on overall survival after esophagectomy. *Ann Surg Oncol* (2014) 21(9):2850–6. doi: 10.1245/s10434-014-3696-4

17. Ning ZH, Wang ZG, Chen J, Li XD, Chen LJ, Xu B, et al. Proposed modification of nodal staging as an alternative to the seventh edition of the American joint committee on cancer tumor-Node-Metastasis staging system improves the prognostic prediction in the resected esophageal squamous-cell carcinoma. *J Thorac Oncol* (2015) 10(7):1091–8. doi: 10.1097/JTO.0000000000000580

18. Bollschweiler E, Besch S, Drebber U, Schroder W, Monig SP, Vallbohmer D, et al. Influence of neoadjuvant chemoradiation on the number and size of analyzed lymph nodes in esophageal cancer. *Ann Surg Oncol* (2010) 17(12):3187–94. doi: 10.1245/s10434-010-1196-8

19. Dhar DK. The prognostic significance of lymph node size in patients with squamous esophageal cancer. *Ann Surg Oncol* (2002) 9(10):1010–6. doi: 10.1245/aso.2002.03.090

20. Mine S, Watanabe M, Imamura Y, Okamura A, Kurogochi T, Sano T. Clinical significance of the pre-therapeutic nodal size in patients undergoing neo-adjuvant treatment followed by esophagectomy for esophageal squamous cell carcinoma. *World J Surg* (2017) 41(1):184–90. doi: 10.1007/s00268-016-3675-y

21. Wang ZW, Zhang W, Dong W, Li BS, Mu DB, Huang W, et al. Pathological analysis of extracapsular extension of metastatic lymph node and its potential impact on nodal clinical target volume in the radiotherapy of esophageal squamous cell carcinoma. *Neoplasma* (2014) 61(3):324–30. doi: 10.4149/neo_2014_042

22. Metzger R, Bollschweiler E, Drebber U, Monig SP, Schroder W, Alakus H, et al. Neoadjuvant chemoradiotherapy for esophageal cancer: impact on extracapsular lymph node involvement. *World J Gastroenterol* (2010) 16(16):1986–92. doi: 10.3748/wjg.v16.i16.1986

23. Hu K, Kang N, Liu Y, Guo D, Jing W, Lu J, et al. Proposed revision of n categories to the 8th edition of the AJCC-TNM staging system for non-surgical esophageal squamous cell cancer. *Cancer Sci* (2019) 110(2):717–25. doi: 10.1111/cas.13891

24. Xu QR, Zhuge XP, Zhang HL, Ping YM, Chen LQ. The n-classification for esophageal cancer staging: should it be based on number, distance, or extent of the lymph node metastasis? *World J Surg* (2011) 35(6):1303–10. doi: 10.1007/s00268-011-1015-9

25. Rutegard M, Lagergren P, Johar A, Rouvelas I, Lagergren J. The prognostic role of coeliac node metastasis after resection for distal oesophageal cancer. *Sci Rep* (2017) 7:43744. doi: 10.1038/srep43744

26. Welsh J, Settle SH, Amini A, Xiao L, Suzuki A, Hayashi Y, et al. Failure patterns in patients with esophageal cancer treated with definitive chemoradiation. *Cancer* (2012) 118(10):2632–40. doi: 10.1002/cncr.26586

27. Versteijne E, van Laarhoven HW, van Hooft JE, van Os RM, Geijsen ED, van Berge Henegouwen MI, et al. Definitive chemoradiation for patients with inoperable and/or unresectable esophageal cancer: locoregional recurrence pattern. *Dis Esophagus* (2015) 28(5):453–9. doi: 10.1111/dote.12215

28. Amini A, Ajani J, Komaki R, Allen PK, Minsky BD, Blum M, et al. Factors associated with local-regional failure after definitive chemoradiation for locally advanced esophageal cancer. *Ann Surg Oncol* (2014) 21(1):306–14. doi: 10.1245/s10434-013-3303-0

29. Yamashita H, Takenaka R, Omori M, Imae T, Okuma K, Ohtomo K, et al. Involved-field radiotherapy (IFRT) versus elective nodal irradiation (ENI) in combination with concurrent chemotherapy for 239 esophageal cancers: a single institutional retrospective study. *Radiat Oncol* (2015) 10:171. doi: 10.1186/s13014-015-0482-9

30. Yamashita H, Okuma K, Wakui R, Kobayashi-Shibata S, Ohtomo K, Nakagawa K. Details of recurrence sites after elective nodal irradiation (ENI) using 3D-conformal radiotherapy (3D-CRT) combined with chemotherapy for thoracic esophageal squamous cell carcinoma–a retrospective analysis. *Radiother Oncol* (2011) 98(2):255–60. doi: 10.1016/j.radonc.2010.10.021

31. Cheng YJ, Jing SW, Zhu LL, Wang J, Wang L, Liu Q, et al. Comparison of elective nodal irradiation and involved-field irradiation in esophageal squamous cell carcinoma: a meta-analysis. *J Radiat Res* (2018) 59(5):604–15. doi: 10.1093/jrr/rry055

32. Zhao KL, Ma JB, Liu G, Wu KL, Shi XH, Jiang GL. Three-dimensional conformal radiation therapy for esophageal squamous cell carcinoma: is elective nodal irradiation necessary? *Int J Radiat Oncol Biol Phys* (2010) 76(2):446–51. doi: 10.1016/j.ijrobp.2009.02.078

33. Morota M, Gomi K, Kozuka T, Chin K, Matsuura M, Oguchi M, et al. Late toxicity after definitive concurrent chemoradiotherapy for thoracic esophageal carcinoma. *Int J Radiat Oncol Biol Phys* (2009) 75(1):122–8. doi: 10.1016/j.ijrobp.2008.10.075

Advantages of publishing in Frontiers

OPEN ACCESS
Articles are free to read for greatest visibility and readership

FAST PUBLICATION
Around 90 days from submission to decision

HIGH QUALITY PEER-REVIEW
Rigorous, collaborative, and constructive peer-review

TRANSPARENT PEER-REVIEW
Editors and reviewers acknowledged by name on published articles

Frontiers
Avenue du Tribunal-Fédéral 34
1005 Lausanne | Switzerland

Visit us: www.frontiersin.org
Contact us: frontiersin.org/about/contact

REPRODUCIBILITY OF RESEARCH
Support open data and methods to enhance research reproducibility

DIGITAL PUBLISHING
Articles designed for optimal readership across devices

FOLLOW US
@frontiersin

IMPACT METRICS
Advanced article metrics track visibility across digital media

EXTENSIVE PROMOTION
Marketing and promotion of impactful research

LOOP RESEARCH NETWORK
Our network increases your article's readership